

Woody and agricultural biomass torrefaction : experimental study and modelling of solid conversion and volatile species release based on biomass extracted macromolecular components

María González Martínez

▶ **To cite this version:**

María González Martínez. Woody and agricultural biomass torrefaction : experimental study and modelling of solid conversion and volatile species release based on biomass extracted macromolecular components. Chemical and Process Engineering. Institut National Polytechnique de Toulouse - INPT, 2018. English. ⟨NNT : 2018INPT0091⟩. ⟨tel-04227859⟩

HAL Id: tel-04227859

https://theses.hal.science/tel-04227859v1

Submitted on 4 Oct 2023

HAL is a multi-disciplinary open access archive for the deposit and dissemination of scientific research documents, whether they are published or not. The documents may come from teaching and research institutions in France or abroad, or from public or private research centers.

L'archive ouverte pluridisciplinaire **HAL**, est destinée au dépôt et à la diffusion de documents scientifiques de niveau recherche, publiés ou non, émanant des établissements d'enseignement et de recherche français ou étrangers, des laboratoires publics ou privés.



HAL Authorization



THÈSE

En vue de l'obtention du

DOCTORAT DE L'UNIVERSITÉ DE TOULOUSE

Délivré par :

Institut National Polytechnique de Toulouse (Toulouse INP)

Discipline ou spécialité :

Génie des Procédés et de l'Environnement

Présentée et soutenue par :

MME MARIA GONZALEZ MARTINEZ

le vendredi 12 octobre 2018

Titre :

Woody and agricultural biomass torrefaction : experimental study and modelling of solid conversion and volatile species release based on biomass extracted macromolecular components

---

Ecole doctorale :

Mécanique, Energétique, Génie civil, Procédés (MEGeP)

Unité de recherche :

Laboratoire de génie chimique (LGC)

Directeur(s) de Thèse :

M. CHRISTOPHE GOURDON

MME XUAN-MI MEYER

Rapporteurs :

M. MATHIEU PETRISSANS, UNIVERSITE DE LORRAINE

MME SYLVIA LARSSON, UNIVERSITY OF AGRICULTURAL SCIENCES

Membre(s) du jury :

M. GERARD MORTHA, INPG, Président

MME XUAN-MI MEYER, TOULOUSE INP, Membre

M. CHRISTOPHE GOURDON, TOULOUSE INP, Membre

MME CAPUCINE DUPONT, UNIVERSITE LYON I, Membre

Woody and agricultural biomass torrefaction: experimental study and modelling of solid conversion and volatile species release based on biomass extracted macromolecular components

---

Torréfaction de biomasses forestières et agricoles : étude expérimentale et modélisation de la conversion du solide et de la production d'espèces volatiles à partir des composants macromoléculaires extraits de la biomasse

JURY

Pr. **Christophe Gourdon,** Directeur de thèse

Pr. **Xuan-mi Meyer,** Co-directeur de thèse

Pr. **Mathieu Pétrissans,** Rapporteur

Pr. **Sylvia Larsson,** Rapporteur

Dr. HDR **Capucine Dupont,** Examinateur

Pr. **Gérard Mortha,** Examinateur

Pr. **Pascal Floquet**, Invité

Dr. **Sylvie Valin,** Invitée

Dr. **Tarja Tamminen**, Invitée

Dr. **Denilson da Silva Perez**, Invité

This work presented in this thesis was carried out at the Laboratory of Bioresources Preparation (LPB), CEA Grenoble (France), in collaboration with the Laboratory of Chemical Engineering (LGC), INP Toulouse/CNRS (France).

This project has received funding from the European Union's Horizon 2020 research and innovation program under grant agreement No 637020–MOBILE FLIP.

The future belongs to those
who believe in the beauty of their dreams.

Eleanor Roosevelt

Para los que creen en el futuro
de Chandrexa de Queixa
y del rural europeo.

For those who believe in the future
of European rural areas.

Acknowledgements

I would like to thank all the people involved in this thesis, each one in our communication language. Thank you for understanding it and for the length of this section, you were many people interacting with this work during these last three years…

Tout d'abord, merci beaucoup Capucine, pour ton accompagnement tout au long de la thèse, pour ma formation scientifique et pour m'avoir offert l'opportunité de découvrir de plus près le monde de l'enseignement. Merci pour ta confiance pour me laisser être moteur de ces travaux depuis le premier jour. Merci aussi pour m'intégrer dans Mobile Flip dès la minute zéro et pour partager ta profonde connaissance du sujet avec moi. Enfin merci pour les moments partagés !

Je voudrais remercier de tout cœur mes directeurs de thèse, Christophe Gourdon et Xuan Meyer, pour votre accompagnement et votre écoute attentive de mon travail et mes questions. Merci pour me permettre de rester attachée au monde du génie chimique avec la participation aux conférences et au LGC. Xuan, merci pour ton aide précieuse sur le modèle et l'exploitation des résultats ; Christophe, merci pour ton regard critique, et toujours pratique, sur mon travail.

I would like to specially thank the members of the jury for the time dedicated to review this work and your valuable contributions. Thank you for your venue and participation in the thesis defense.

I acknowledge the financial support of the European H2020 Mobile Flip project. The project was a valuable work group which became a wonderful scientific family through these three years. It was a pleasure for me to be part of the Mobile Flip adventure! Thank you for listening to my view-point of the project about the role of the mobile units to fight against fires in the South of Europe. In this sense, I sincerely thank Tarja Tamminen for her support and for many interesting discussions during project meetings. Thank you all (Sylvia, Gunnar, David, Matthieu, Simon, Denilson, Riitta, Hanne, Kimmo, Finn, Electra…) for all wonderful moments together (such as discovering the pleasure of the sauna + Finnish lake under the sunset, dancing Finnish music, hiking in Finnish and Swedish beautiful forests, as well as along Greek coasts, etc.). Thank you also for the nice and fruitful project meetings (and DTMs!) in Thessaloniki, Umeå, Paris and Orilampi.

I would like to thank again Tarja Tamminen and Capucine Dupont, for the idea of the scientific visit to VTT in April 2017. It was an exciting experience, rich in scientific work about Py-GC/MS but also rich in personal moments shared in your nice team, thank you all! And I sincerely thank Taina, for your patience, all I could learn with you and the articles written together. *Kiitos!*

Je remercie aussi la patience et le travail de Denilson Da Silva Perez, ainsi que de Rodolf et Audrey (FCBA Grenoble): sans vous, les fractions extraites n'auraient jamais vu le jour. Merci pour tant de discussions sur la caractérisation des biomasses, les résultats de la thèse, le projet Mobile Flip… enfin *obrigada per tudo!* C'était aussi un grand plaisir de travailler avec Gérard Mortha (Pagora, INP Grenoble), avec qui j'ai appris énormément de choses sur la cellulose. Merci

aussi de votre soutien pour l'interprétation des résultats et les articles. Merci aussi à Chamseddine pour les linters de coton et son enthousiasme. Un énorme merci aussi à Pascal Floquet (LGC, INP Toulouse), pour m'aider à aller si loin avec l'ACP.

Je tiens à remercier à l'INP Grenoble pour m'avoir permis de participer en tant qu'intervenante aux cours, qui ont renforcé mon goût pour l'enseignement. Merci aux élèves aussi !

Je remercie le CEA Grenoble, qui m'a permis de réaliser cette thèse au Laboratoire de Préparation des Bioresources. Un grand merci à notre super chef de labo Muriel, pour tout son soutien pendant cette thèse, sa disponibilité avec un sourire et sa reconnaissance de mon travail. Merci à toute l'équipe biomasse pour les moments partagés, depuis les repas de Noël en musique (même galicienne) à la première gazéification de Giroflé, en passant par les moments pause-café, repas, présentations, discussions scientifiques ou philosophiques (Thierry Chataing, Guillaume), des idées randos (Françoise, Serge), etc. Merci de votre accueil et de me faire sentir partie intégrante de l'équipe. Merci à Maguelone pour son aide sur l'ATG, sur les macros et sur tant d'autres choses, toujours avec le sourire ; à Snoopy pour sa patience pour réparer mon creuset ; à Thierry Melkior, Gilles et Estéban, pour leur soutien sur la torréfaction sous vapeur d'eau (et à Gilles pour avoir découvert et aimé la Galice); à Guillaume pour l'aide sur les bilans des sucres ; à Sylvie et Morgane pour les conférences ensemble ; à Hélène pour mille et une analyses ; à Séb : merci mille fois, parce que cette thèse est aussi en partie à toi : sans ATG-GC/MS du tonnerre, pas de thèse ! Merci aussi à Clément, pour les bons moments (Fête de la Science, brevets, pauses…) ; à Marion, pour garder un contact qui nous remonte le moral avec de bonnes rigolades ; à Timothée et Elvira pour vos précieux travaux sur la torréfaction au labo ; à Hiwot pour les calibrations de la GC/MS et l'opportunité d'encadrer une stagiaire ; aux stagiaires et thésards de ces dernières années, y muchas gracias Carolina, por hacerme sonreir tantas veces. Merci aussi à Maïté pour avoir été là au début de l'aventure, m'encourager toujours et rester à côté même depuis loin.

Je veux également remercier les scientifiques rencontrés en conférence qui se sont intéressé à mon travail, pour en savoir plus et/ou donner leur regard : Pascal Fongarland (LGPC), Jean-Michel Commandré (Cirad), Sylvain Salvador, Elsa Weiss (Mines d'Albi), François-Xavier Collard (SUN), Annabelle Couvert (ENSCR)… Merci aussi au CODEGEPRA et à la DRT du CEA Grenoble pour les prix de la meilleure présentation et poster lors des Journées Scientifiques de ces dernières années.

I would like to thank interesting discussions and critical opinions about my work from specialists in biomass during conferences these last years: Andrés Anca-Couce (TU Graz, Austria), Joan Manyà (UniZar, Spain), the team from Sagrario Betrán (UBurgos, Spain), Phil Westmoreland (NCSU, USA), Darren McAvoy (Utah State University, USA), Franco Berruti (University of Western Ontario, Canada)... I would also specially thank Karla Dussan (ECN) and Stephen Dooley (TCD, Ireland) for their interest in my data for further torrefaction modelling, thanks to WasteEng 2018!

Cette thèse n'aurait jamais croisé ma route sans le lien établi par Florian, merci à toi pour cela ! Et pour les moments partagés, depuis mon arrivée à Rennes, ainsi qu'à Aurélia. Merci à vous, et à Euphrasie et Maxime, puis Maxime, Benjamin, d'être venus partager des moments avec nous.

Le sport a été pour moi un support indispensable pendant cette thèse. Je voudrais remercier en particulier les maîtres-nageurs Julien et Thierry du CN Sassenage pour avoir accompli mon rêve d'apprendre à nager dans les règles de l'art, et à Antonella, je me suis bien éclatée à la piscine avec vous, merci ! D'autre part, un énorme merci aussi au groupe de badminton des lundis et jeudis midis à Sassenage : Pascale, Linda, Christine, Fred, Jerôme, Christophe… et à mes partenaires de doubles (Isa) et mixtes (Marc). J'ai vraiment pris du plaisir à jouer avec vous, merci beaucoup de votre soutien pendant la thèse et merci de tant de super moments ensemble.

Me gustaría agradecer el haber llegado hasta aquí a los que me incitaron a dar lo mejor de mí en cada momento de mi formación y a descubrir mi pasión por la ciencia, en particular la química, y la ingeniería: Carolina Varela (CEIP Chandrexa de Queixa), D. Juan, José Luis Guede, Cristina Iglesias (Josefinas, Ourense), D. Rafael Boullón, Pedro, Mercedes, Hortensia, Almudena, Elisa, Afonso Monxardín (IES As Lagoas, Ourense), Jorge Lázaro (EHU, Bilbao), Isabel y Alicia Iborra, Maria Sancho, Silvia Álvarez, Jaime Primo, José García Antón (ETSII-UPV, Valencia)…

Quiero agradecer también la colaboración de Luis Míguez en el artículo de la valorización de las biomasas de Galicia. Gracias por tu ojo de buen biólogo para comprender mejor mis resultados.

Por último, me gustaría agradecer a mi familia, así como a Ana, Iria e Ima, por acompañarme en cada momento de esta tesis, aun estando lejos. Gracias a mis abuelas, por haberme enseñado tanto y porque sin ellas no sería como soy. Gracias mi abuelo Flaminio, por seguir los avances de la ciencia y creer conmigo en el potencial de Chandrexa. Gracias a Avi, por escucharme tantas veces; siempre estarás en mi corazón y en cada mariposa que vuele sobre la biomasa del mundo. Gracias a mi madre y a mi hermana Belén, por entenderme a menudo y esperar que vuelva, y a mi padre, por haber intentado entender y seguir esta tesis conmigo, desde el Tandy y sin ser científico. Gracias a vosotros también por la recogida de las biomasas de Chandrexa y por creer en el proyecto de las unidades móviles para acabar con los incendios en nuestros montes. Gracias por vuestro apoyo y por todas las veces que pude volver a casa y cambiar de aires ayudando en el súper o paseando por el lugar más bonito del mundo para nosotros: Chandrexa de Queixa.

Y muchas gracias a Dimitri, por tantos momentos compartidos durante estos años, por entender mi implicación en este trabajo, por haber soportado tantos kilómetros a recorrer cada fin de semana y por haberme hecho descubrir lugares tan maravillosos. ¡Sigamos adelante construyendo juntos en este mundo!

Thank you all!

Merci à vous tous !

¡Gracias a todos vosotros!

Graciñas a todos vós!

Abstract

Nowadays, there is an increasing awareness on the importance of biomass waste as a renewable source of energy, materials and chemicals. In this context, the European project MOBILE FLIP aims at developing and demonstrating mobile conversion processes suitable with various underexploited agro- and forest based biomass resources in order to produce energy carriers, materials and chemicals. One of these processes is torrefaction, which consists in a mild thermal treatment, occurring typically between 200 and 300°C during a few tens of minutes in a default-oxygen atmosphere. The solid product obtained has thermal and processing properties closer to coal, and thus is suitable as fuel for combustion or gasification. During torrefaction, condensable coproducts are released, that may also be source of "green" chemicals. It is therefore crucial to characterize them to optimize the torrefaction process and design industrial units.

Up to now, only few works have been focused on characterizing and modelling both solid and condensable species during torrefaction versus operating conditions and feedstock type. Furthermore, these studies typically include a reduced number of biomasses. Cellulose, hemicellulose and lignin, which constitute biomass macromolecular composition, are determining properties to predict biomass behaviour during torrefaction. However, torrefaction tests on these constituents are rare and always based on commercial compounds, which were proved as little representative of the native biomass.

The objective of this study is to analyse the influence of biomass characteristics, mainly represented by the macromolecular composition in cellulose, hemicellulose and lignin, on the global behaviour of biomass in torrefaction, both in terms of solid mass loss and of production profiles of the volatile species released, in function of the operating conditions.

14 biomasses from the main biomass families (deciduous wood, coniferous wood, agricultural by-products and herbaceous crops) were selected for this study. An optimized extraction procedure was proposed to recover cellulose, hemicellulose and lignin fractions from 5 reference biomasses. Experiments were performed on a thermogravimetric analyzer coupled to a gas chromatography mass spectrometer device through a heated storage loop system (TGA-GC/MS). Solid degradation kinetics and volatile release profiles were followed during torrefaction experiments combining non-isothermal (200 to 300°C at 3°C/min) and isothermal (300°C, 30 min) conditions, ensuring the chemical regime thanks to the appropriate operating conditions.

The results obtained with the raw materials demonstrated that biomass macromolecular composition is a main factor influencing biomass behavior in torrefaction. Consequently, the heterogeneity of the resource results in a diverse behavior in torrefaction, particularly in the case of agricultural biomasses. The results with the extracted components evidenced their very different behavior compared to the commercial compounds, particularly in the case of cellulose. This suggests that a limitation could be induced by the common use in literature of commercial components for torrefaction modelling. The impact on the characterization of macromolecular components was also shown to be prevailing in their behavior in torrefaction, especially in the case of hemicellulose sugar composition and cellulose crystallinity. Furthermore, differences in release kinetics of volatile species during torrefaction were observed, even for volatiles belonging to the same chemical family (acids, furans, ketones). Derived from these results, a torrefaction model based on the additive contribution of extracted cellulose, hemicelluloses and lignin to the global behavior of biomass in torrefaction was proposed, and this for the 5 representative biomasses.

Résumé

Il existe aujourd'hui une prise de conscience croissante visant à considérer les résidus de biomasse comme source potentielle d'énergie, de matériaux et de produits chimiques. Dans ce contexte, le projet européen Mobile Flip vise à développer des unités mobiles de conversion de biomasse pour la valorisation de ressources agricoles et forestières non exploitées. L'une des technologies proposées est la torréfaction, traitement thermique doux entre 200 et 300°C pendant quelques minutes et en défaut d'oxygène. Le solide torréfié présente des propriétés proches de celles du charbon et convient à la combustion ou à la gazéification. En même temps, des matières volatiles sont relâchées, dont des espèces condensables potentiellement à haute valeur ajoutée en chimie. Il est donc crucial de caractériser le solide torréfié et les espèces volatiles afin d'optimiser le procédé jusqu'à l'échelle industrielle.

Jusqu'à présent, peu de travaux ont simultanément cherché à caractériser et à modéliser le comportement du solide et des espèces volatiles produites en torréfaction en fonction des conditions opératoires et du type de biomasse. De plus, ces travaux portaient sur un nombre réduit de biomasses. La composition macromoléculaire de la biomasse en cellulose, hémicelluloses et lignine impacte de manière déterminante les produits de torréfaction. Cependant, les essais de torréfaction avec ces constituants sont peu nombreux et généralement réalisés avec des composants commerciaux peu représentatifs de la biomasse brute.

L'objectif de ces travaux de thèse est d'étudier l'influence des caractéristiques de la biomasse, principalement représentée par sa composition en cellulose, hémicellulose et lignine, sur le comportement global de la biomasse en torréfaction, tant en termes de perte de masse du solide que de production d'espèces volatiles, en fonction des conditions opératoires.

14 représentants des principales familles de biomasse (bois feuillus, bois résineux, sous-produits agricoles et plantes herbacées) ont été sélectionnés pour cette étude. Une procédure d'extraction optimisée a été proposée pour obtenir des fractions de cellulose, hémicellulose et lignine de 5 biomasses de référence. Les données expérimentales ont été obtenues en utilisant une thermobalance couplée à une chromatographie gazeuse et une spectrométrie de masse via un système de boucles de stockage chauffées (ATG-GC/MS). La cinétique de dégradation du solide et les profils de formation des espèces volatiles ont été étudiés au cours des expériences de torréfaction incluant une partie non-isotherme (200 à 300°C, 3°C/min) suivie d'une partie isotherme (300°C, 30 min), dans des conditions expérimentales assurant le régime chimique.

Les résultats obtenus avec les biomasses brutes montrent que la composition macromoléculaire de la biomasse est un facteur clé influant sur son comportement en torréfaction. Par conséquent, l'hétérogénéité de la ressource se traduit par une diversité de comportements en torréfaction, en particulier pour les biomasses agricoles. Il a été observé un comportement très différent pour les composants extraits comparés aux composants commerciaux, particulièrement dans le cas de la cellulose. Ceci montre que l'usage commun de composants commerciaux pour bâtir les modèles de torréfaction n'est pas pertinent. L'impact des caractéristiques des composants macromoléculaires sur le comportement en torréfaction a été aussi mis en évidence, particulièrement en ce qui concerne la composition en sucres des hémicelluloses et la cristallinité de la cellulose. En outre, des différences de profils de production des espèces volatiles ont été observées, même pour des composés de même nature chimique. A partir de ces résultats, un modèle de torréfaction basé sur la contribution additive de la cellulose, des hémicelluloses et de la lignine extraites est proposé pour décrire le comportement global de la biomasse en torréfaction, et ceci pour les 5 biomasses de référence.

Table of contents

INTRODUCTION 1
I. CONTEXT OF THE STUDY 7
1. Lignocellulosic biomass 7
1.1. Definition 7
1.2. Classification 7
1.3. Available potential 8
1.4. Structure 9
1.5. Composition 11
1.5.1. Elemental composition 11
1.5.2. Macromolecular composition 11
1.5.2.1. Cellulose 12
1.5.2.2. Hemicelluloses 12
1.5.2.3. Lignin 15
1.5.2.4. Extractives 16
1.5.2.5. Ash 16
1.5.3. Interactions between macromolecular components 17
1.6. Biomass properties 19
1.6.1. Moisture 19
1.6.2. Density/volumetric weight 19
1.6.3. Thermal properties 19
1.7. Biomass conversion 20
2. Torrefaction 22
2.1. Definition 22
2.2. History 22
2.3. Torrefaction products 22
2.3.1. Torrefied solid 23
2.3.1.1. Hydrophobicity 24
2.3.1.2. Energy densification 24
2.3.1.3. Flowability 24
2.3.1.4. Grindability 24
2.3.2. Gaseous species 25
2.4. Torrefaction technologies 26
3. Objective of the work 28
II. STATE-OF-THE-ART OF BIOMASS TORREFACTION 31
1. Torrefaction products 31
1.1. Torrefied solid 31

1.2. Gaseous products ... 31
1.2.1. Permanent gases ... 32
1.2.2. Condensable products ... 32
2. Influence of the operating conditions ... 35
2.1. Temperature and residence time ... 35
2.2. Heating rate ... 35
2.3. Atmosphere and pressure ... 36
3. Phenomenology in biomass torrefaction ... 37
3.1. Physical phenomena ... 37
3.2. Chemical phenomena ... 38
3.2.1. Cellulose ... 41
3.2.2. Hemicelluloses ... 43
3.2.3. Lignin ... 45
3.3. Characteristic time analysis ... 48
4. Modelling of biomass torrefaction ... 48
5. Conclusion and approach ... 53
III. MATERIALS AND METHODS ... 57
1. Raw materials ... 57
1.1. Raw biomasses ... 57
1.2. Extracted macromolecular components from reference biomass ... 62
1.2.1. Extraction procedure ... 62
1.2.2. Cellulose ... 64
1.2.2.1. « Cellulose II » fraction ... 64
1.2.2.2. « DMSO residue » fraction ... 65
1.2.3. Hemicelluloses ... 66
1.2.3.1. « Hemicelluloses 1 » fraction ... 66
1.2.2.3. « Hemicelluloses 2 » fraction ... 67
1.2.4. Lignin ... 68
1.3. Mixtures of extracted macromolecular components from reference biomasses ... 69
1.4. Commercial compounds ... 70
2. Experimental set-up ... 70
2.1. Study of solid mass loss in thermobalance ... 71
2.2. Study of the volatile species release in GC/MS ... 72
2.3. Coupling TGA-GC/MS by a heated storage loop system ... 73
3. Definition of the experimental conditions ... 74
3.1. Characteristic time calculations ... 74
3.1.1. Torrefaction regimes with temperature and particle size ... 74
3.1.2. Torrefaction regimes with temperature and bed thickness ... 75

3.2. Preliminary experiments with commercial xylan from beech 76
4. Data treatment 78
4.1. Solid transformation (TGA) 78
4.2. Volatile species release (GC/MS) 79
4.2.1. Identification 79
4.2.2. Semi-quantification 82
4.2.2. Quantification 82
4.2.2.1. Calibration of volatile species in GC/MS 82
4.2.2.2. Volatile species production 82
4.3. Uncertainty estimation 84
4.4. Principal Component Analysis 84
5. Conclusion 86
IV. RESULTS AND DISCUSSION 89
1. Raw biomasses 89
1.1. Raw biomasses 89
1.1.1. Solid mass loss kinetics during torrefaction 89
1.1.2. Volatile species release 93
2. Extracted macromolecular components from the reference biomasses 100
2.1. Cellulose 100
2.1.1. «Cellulose II» fraction 101
2.1.1.1. Solid transformation 101
2.1.1.2. Volatile species release 104
2.1.2. «DMSO residue» fraction 108
2.1.2.1. Solid transformation 108
2.1.2.2. Volatile species release 110
2.2. Hemicelluloses 113
2.2.1. «Hemicelluloses 1» fraction 113
2.2.1.1. Solid transformation 113
2.2.1.2. Volatile species release 116
2.2.2. «Hemicelluloses 2» fraction 121
2.2.2.1. Solid transformation 122
2.2.2.2. Volatile species release 123
2.3. Lignin 127
2.3.1. Solid transformation 127
2.3.2. Volatile species release 129
2.4. Mixtures of extracted macromolecular components from the reference biomasses 135
2.4.1. Ternary mixtures 135

2.4.1.1. Solid transformation 135
2.4.1.2. Volatile species release 136
2.4.2. Binary mixtures for beech 140
2.4.2.1. Solid transformation 141
2.4.2.2. Volatile species release 143
3. Synthesis of the results 148
3.1. Solid kinetics 148
3.2. Volatile species release 150
V. MODELLING 157
1. Principal Component Analysis 157
1.1. Key parameters in biomass characterization 157
1.1.1. PCA on macromolecular and elemental composition 157
1.1.2. PCA on biomass elemental composition 160
1.1.3. PCA on macromolecular and elemental composition for 12 selected biomasses 162
1.2. Solid transformation 163
1.2.1. PCA of the solid transformation during the non-isothermal torrefaction step 163
1.2.2. PCA of the solid transformation during the isothermal torrefaction step 165
1.3. Volatile species production 167
1.3.1. PCA on beech data 167
1.3.2. PCA on raw biomasses 170
a) All biomasses 170
b) Deciduous wood (ash wood, beech, poplar, willow) 172
c) Coniferous wood (Pine, pine forest residues, scot pine bark) and grape seed cake 173
d) Agricultural biomasses and herbaceous crops 174
1.4. Conclusions of the PCA 176
2. Torrefaction model 177
2.1. Nocquet's model and commercial compounds 177
2.2. First-level model 179
2.2.1. Representation of the first-level model 179
2.2.2. Comparison of the simplified additive model and the experimental data 183
2.2.2.1. Comparison of the torrefaction model and the raw biomass 183
2.2.2.2. Comparison of the torrefaction model prediction, the ternary mixtures and the extracted fraction experiments 186
2.2.1.3. Attempt of representation of interactions between macromolecular components 188
2.3. Second-level model 189
2.3.1. Sugar mass balances 190

2.3.1.1. DMSO fraction composition ... 190
2.3.1.2. Hemicelluloses composition ... 192
.3.2. Reconstruction of the complementary fractions ... 195
2.3.2.1. « Cellulose I » ... 195
2.3.2.2. Total « hemicelluloses » ... 196
2.3.3. Representation of the second-level model ... 197
2.3.3.1. Comparison with the first-level additive model and the raw biomass ... 198
2.3.3.2. Attempt of accounting with interactions between macromolecular components ... 200
2.4. Extrapolation of the torrefaction model ... 201
2.5. Conclusion ... 204
Conclusions and outlook ... 207
Conclusions ... 207
Outlook ... 213
Bibliography ... 217
Annex ... 235
I. Complementary raw biomasses ... 235
1. Introduction ... 235
2. Geographical context ... 237
2.1. Description of the vegetal cover ... 237
2.2. Incurrence in forest fires ... 238
3. Biomass characterization ... 238
4. Behavior in torrefaction ... 241
4.1. Solid kinetics ... 241
4.2. Volatile species release ... 244
5. Conclusions ... 248
II. Characterization methods ... 249
III. Cellulose size-exclusion chromatography characterizations ... 250
IV. Calculations for the characteristic time analysis in torrefaction ... 255
1. Bed-scale analysis ... 255
2. Particle-scale analysis ... 256
3. Calculations and discussion ... 257
4. Sensitivity analysis of parameters involved ... 259
V. Leakage tests of the storage loops ... 260
VI. Uncertainty estimation ... 261
1. Uncertainty in solid degradation ... 261
2. Uncertainty in volatile species detection and quantification ... 262
VII. Calibration of volatile species in GC/MS ... 264

VIII. Py-GC/MS ... 266
1. Influence of step duration in fractionated Py-GC/MS of lignocellulosic biomass ... 266
1. Introduction ... 266
2. Material and methods ... 268
2.1. Biomass description ... 268
2.2. Py-GC/MS experiments ... 269
3. Results and discussion ... 270
3.1. Effect of residence time on volatile species formation ... 270
3.2. Volatile species identified ... 273
4. Conclusions ... 280
2. Detailed structural elucidation of different lignocellulosic biomass types using optimized temperature and time profiles in Py-GC/MS ... 281
1. Introduction ... 281
2. Material and methods ... 283
2.1. Biomass description ... 283
2.2. Py-GC/MS experiments ... 283
3. Results and discussion ... 285
3.1. Analysis of the volatile species released per biomass ... 285
3.2. Detailed analysis of volatile species per detected chemical compound ... 287
Conclusions ... 297
IX. Influence of the polymerization degree in the starting degradation temperature of cellulose in torrefaction ... 298

Nomenclature

m_i	Remaining solid mass at temperature T_i	mg
m_0	Initial mass of the solid sample (t_0 or T_0 = 200°C)	mg
t_{torref}	Characteristic time of torrefaction	s
K_{torref}	Kinetic constant for torrefaction	s^{-1}
R	Universal gas constant	8.314 J mol^{-1} K^{-1}
T	Temperature of torrefaction	K
t_{rad}	Characteristic time of external radiation	s
ρ_{bed}	Volumetric weight of the bed	Kg m^{-3}
cp_{bed}	Mass heat capacity of the bed	KJ Kg^{-1} K^{-1}
L_c	Characteristic length	m
ω	Emissivity	-
σ	Stefan-Boltzmann constant	$5.6703 \cdot 10^{-8}$W m^{-2} $^{-4}$
T_g	Gas temperature (considered at torrefaction temperature)	K
T_{bed}	Bed temperature (wood considered at ambient temperature)	298 K
t_{cond}	Characteristic time of internal conduction	s
λ_{bed}	Thermal conductivity of the bed	W m^{-1} K^{-1}
t_{conv}	Characteristic time of external convection	s
h_t	Heat exchange coefficient	W m^{-2} K^{-1}
Nu	Nusselt non-dimensional number	-
Re	Reynolds non-dimensional number	-
Pr	Prandlt non-dimensional number	-
d_p	Particle diameter	m
ρ_g	Volumetric weight of the gas	Kg/m^3
cp_g	Mass heat capacity of the gas	KJ Kg^{-1} K^{-1}
λ_g	Thermal conductivity of the bed	W m^{-1} K^{-1}
μ_g	Dynamic viscosity of the gas	Pa s
v_g	Gas speed	m s^{-1}
$t_{int\ diff}$	Characteristic time of internal mass diffusion	S
D_{eff}	Effective diffusion coefficient	m^2 s^{-1}
D	Diffusion coefficient	m^2 s^{-1}
ε	Porosity	-
τ	Tortuosity	-
T	Temperature	K
M_{H2O}	Molecular weight of water	0.018 kg mol^{-1}
M_{N2}	Molecular weight of nitrogen	0.028 kg mol^{-1}
M_{He}	Molecular weight of helium	0.002 kg mol^{-1}
$\sum v_{H2O}$	Atomic diffusion volume of water	12.7
$\sum v_{N2}$	Atomic diffusion volume of nitrogen	17.9
$\sum v_{He}$	Atomic diffusion volume of helium	2.88
P_g	Total pressure of gases	Pa
εa	Absolute error	-
εr	Relative error	%

Abbreviations list

AHC	Agglomerative Hierarchical Clustering
ASE	accelerated solvent extractor
ASTM	American Society for Testing and Materials
C^{I}	«cellulose I» fraction deduced from the «DMSO residue» fraction
C^{II}	«cellulose II» extracted fraction
CEN	European Committee for Standardization
Ch	Carbohydrate-derived chemical compound (in Py-GC/MS)
CH	«cellulose II»/«hemicelluloses 1» binary mixture
CHL	«cellulose II»/«hemicelluloses 1»/«lignin» ternary mixture
CL	«cellulose II»/«lignin» binary mixture
CTC	cellulose tricarbanilates
CV	calorific value
DMAC	dimethylacetamide
DMSO	dimethyl sulfoxide
DMSOr	«DMSO residue» fraction
DP	degrees of polymerization
DRI	differential refractometer
EEA	European Environment Agency
EI	electron ionization ion source
EIC	Extracted-Ion Chromatogram
FID	Flame Ionization Detection
FTIR	Fourier Transform Infrared Spectroscopy
G- or G	guaiacyl- lignin unit
GC	Gas Chromatography
Glu	glucan unit from cellulose and hemicelluloses or glucose sugar
GPC	gel permeation chromatography
H- or H	hydroxyphenyl- lignin unit
H_1	«hemicelluloses 1» extracted fraction
H_2	«hemicelluloses 2» extracted fraction
HHV	High Heating Value
HL	« hemicelluloses 1»/«lignin» binary mixture
HPLC	High Performance Liquid Chromatography
HV	heating value
IAE	International Agency of the Energy
ICP-AES	Inductively Coupled Plasma Atomic Emission Spectroscopy
L	«lignin» extracted fraction
LALS	Low-Angle Light Scattering
LCC	lignin–carbohydrate complexes
LHV	Low Heating Value

Lg	Lignin-derived chemical compound (in Py-GC/MS)
LS	Light Scattering
MC	Moisture content
MHS	Mark-Houwink-Sakurada
MMD	molar mass distribution
MS	Mass Spectrometry
MSW	municipal solid waste
PCA	Principal Component Analysis
Py-GC/MS	analytical pyrolysis coupled to a Gas Chromatograph and a Mass Spectrometer
q_{gross}	gross calorific value
q_{net}	Net calorific value
RALS	Right-Angle Light Scattering
rawb or rb	raw biomass
S- or S	syringyl- lignin unit
SEC	size-exclusion chromatography
SRC	short rotation coppices
TAPPI	Technical Association of the Pulp and Paper Industry
TDT	thermal decomposition temperature
TGA	thermobalance
TGA-GC/MS	thermobalance coupled to a Gas Chromatograph and a Mass Spectrometer
TIC	Total Ion Chromatogram
Toe	Ton of oil equivalent
UV	ultra-violet spectrophotometry
VSRC	very short rotation coppices
XRD	X-ray diffraction
Xyl	xylan unit from hemicelluloses or xylose sugar

INTRODUCTION

INTRODUCTION

Biomass resources have been used since the Antiquity by humans in order to satisfy their living requirements, including food, heating, clothing, construction and leisure. They were traditionally grown for human requirements, or directly cultivated for their transformation, as it is the case of energy production. At the same time, the interaction of humans with biomass resources has always generated residues. These residues have sometimes been neglected and other times recycled, at the origins probably intuitively, to contribute to the human's life quality. Regional climate, humans needs and historical antecedents strongly influence biomass availability in an area and explain the heterogeneity of its production, even in Europe [1,2].

The use of raw biomass or biomass waste usually requires the improvement of some of its properties, such as reducing moisture content, to improve storage and prevent degradation, or increasing the heating value, to improve the combustion yield. In this way, thermochemical conversion processes, and among them torrefaction, can play a crucial role in upgrading biomass properties and, in general, in the large scale valorization of underexploited biomass and biowaste resources [3]. This process is especially suitable for lignocellulosic biomasses with low moisture content, which includes coniferous and deciduous wood, agricultural by-products and herbaceous crops.

Lignocellulosic biomass is formed by a complex structure including cellulose, hemicelluloses and lignin [4,5]. The proportions and distribution of these macromolecular components in biomass physical structure is complex and depends on the type of species. Besides, interactions between cellulose, hemicelluloses and lignin confer a significant resistance to the structure [4]. As a consequence, it constitutes a strongly heterogeneous and complex resource whose behavior needs to be linked to its properties.

Torrefaction is a mild thermochemical treatment of biomass, typically occurring between 200 and 300 °C during a few tens of minutes, at atmospheric pressure and in default of oxygen [6,7]. The solid product obtained has properties close to coal in terms of heating value, carbon content, hydrophobicity, grindability as well as flowability, and is therefore suitable as fuel for combustion, co-combustion or gasification [8–10]. During torrefaction, gaseous products are released, including permanent gases (mainly CO and CO_2) and condensable species (composed by water, acids, phenols, etc.) [6]. The production of some of these volatile species can damage the torrefaction installation, as for example a high acid production. However, other species may also be valorized as source of high-added value "green" chemicals [11–13]. It is crucial to characterize the production of volatile species, as well as the solid transformation, in order to optimize the operating conditions and the control of the torrefaction process, as well as to design industrial torrefaction units.

There have been many torrefaction studies during the last ten years in literature. However, only a single or few biomasses were considered in each study [14–23]. Furthermore, those torrefaction studies frequently focused either on solid transformation or on volatile/gaseous species release, without considering systematically both aspects simultaneously [24–28]. While permanent gases were deeply analyzed [17], volatile species quantification was usually limited with the proposed set-ups, particularly for the chemical compounds released in minor amounts [6]. At the same time, torrefaction studies were generally based on commercial compounds to represent cellulose, hemicelluloses and lignin, due to the difficulties encountered to extract them from biomass structure [29].

The main objective of this work is to assess the impact of biomass properties, mainly represented by the macromolecular composition on cellulose, hemicelluloses and lignin, on biomass torrefaction issues. For this purpose, the torrefaction of 14 biomasses representative of the European diversity, characterized in depth, was analyzed in terms of solid mass loss and volatile species production at lab-scale. At the same time, cellulose, hemicellulose and lignin fractions were extracted from 5 of these biomasses, deeply characterized, and their behavior in torrefaction was studied. The final goal of this study was to create a mathematical model able to associate biomass macromolecular composition and its behavior in torrefaction.

In chapter I, the context of the study is described. First of all, the resource lignocellulosic biomass is presented in terms of definition, different types of species included, availability, structure and composition, as well as its main properties. Secondly, the thermochemical conversion process of torrefaction is introduced, particularly the main steps involved and the products obtained.

In chapter II, the state-of-the-art of biomass torrefaction is reported, considering results from previous studies on the analysis of torrefaction products, as well as on the description of the main physical and chemical phenomena involved in biomass transformation. The influence of temperature and duration in the process is also evaluated. Finally, a review of the torrefaction models is carried out, going from the first models proposed for cellulose pyrolysis to the current models describing biomass transformation through cellulose, hemicelluloses and lignin.

In chapter III, the materials selected for this work are presented and characterized. This includes 14 biomasses representative of the European diversity. An optimized extraction procedure of the macromolecular components of biomass is proposed and applied to 5 of the biomasses representatives of the main biomass families. These extracted macromolecular components are also presented and characterized. In a second part of the chapter, the lab-scale set-up conceived for this work is presented. It consists of a thermobalance (TGA) coupled to a gas chromatography and mass spectrometry analyzer (GC/MS). A storage system composed by 16

heated loops was introduced between TGA and GC/MS, so as to allow the sampling of the volatile species released at different torrefaction temperatures. As a result, a single torrefaction experiment allows to simultaneously follow the solid mass loss and the production profiles of 23 volatile species released during torrefaction.

In chapter IV, the results obtained from the TGA-GC/MS torrefaction experiments performed on raw biomasses and extracted macromolecular components are analyzed and discussed regarding their macromolecular composition and biomass family.

The first part of chapter V reports the principal component analysis (PCA) performed on the dataset of the 14 biomasses, composed by their characterization and behavior in torrefaction in TGA-GS/MS, regarding both solid mass loss and volatile species production. A double objective was defined for this PCA: firstly, studying the variability of biomass characterization and behavior during torrefaction inside each biomass family; secondly, linking biomass properties to the behavior during torrefaction. In the second part of the chapter, an improved approach of the torrefaction additive model is proposed, based on the extracted macromolecular components characterized and analyzed during torrefaction. The interactions between macromolecular components in biomasses are intended to be assessed through the difference in the behavior in torrefaction of the additive model and the raw resource.

-I-

CONTEXT OF THE STUDY

I. CONTEXT OF THE STUDY

In this chapter, the general context of this study is presented. First of all, the heterogeneity of lignocellulosic biomass justifies the importance of firstly establishing a definition and a classification of biomass. Then, the available potential of the resource is assessed as well as its main properties. In a second step, torrefaction is introduced, in terms of process description, achievements and main products obtained.

1. Lignocellulosic biomass

1.1. Definition

Biomass is the material resulting from living, or recently living biological organisms [30]. This large definition covers a range of organic materials recently produced from plants, and animals that feed on the plants, as well as by-products and waste from agricultural activities, food processing and domestic organic waste [31,32].

Lignocellulosic biomass is produced by green plants during photosynthesis. This process consumes water and carbon dioxide (CO_2) to produce carbohydrates storing energy for the plant in their bonds. The main advantage of lignocellulosic biomass is that it is a renewable resource, when managed in a sustainable way [33].

1.2. Classification

The most common biomass classification in the literature is based on biomass origin [32]:

- **Forestry biomass:** it consists in woody plants, characterized by slow growth and composed of tightly bound fibers. There are two main types of wood [34]:
  - **Hardwood:** wood originated from angiosperms (flowering plants), typically broadleaf, deciduous trees. Some examples are ash wood, birch, beech and oak.
  - **Softwood:** woods derived from gymnosperms (mostly conifers), generally needle-leaved evergreen trees. Some examples are pine, spruce, redwood and Douglas fir.

  Short (or very short) rotation coppices (SRC or VSRC) refer to woody fast-growing tree species. They produce high biomass yields in a short period of time, typically 3 to 4 years for VSRC or 8 to 10 years for SRC, and are usually destined to energy purposes [6,7]. Examples of SRC are willow, poplar and eucalyptus.

- **Agricultural biomass:** it includes cultures for food production and herbaceous plants and grasses. Examples of agricultural biomasses are cereal straw, fruit brunches and herbaceous energy cultures like miscanthus, switch grass or reed canary grass [35].
- **Aquatic plants:** algae are an important subject of research in this field, particularly the third-generation of biofuels derived from algae and micro algae [36].

Moisture is a major property to define biomass suitability for conversion process. This is

especially important in case of energy production, as part of the heat provided would be used in evaporating moisture. [37]. Biomasses can therefore be classified as:

- **Dry biomasses:** when their moisture is below around 60 % before harvesting, such as wood, herbaceous crops and cereal straw. These biomasses are more suitable for direct combustion or thermochemical conversion.
- **Wet biomasses:** biomasses with moisture above 60 %, such as algae, fruit residues or manures. They are more appropriate to be valorized through wet processes, such as anaerobic digestion or hydrothermal processes [32].

In terms of utilization, agricultural biomass was the first in being used for energy production, with the typical examples of sugarcane or beetroot converted into bioethanol (first generation biofuels). As a consequence, the competition with food production led to a rise in food prices, especially in emergent countries. At this point, a second generation of biofuels was developed by using lignocellulosic biomass from agricultural waste.

Finally, biomass waste can be classified according to their production and reuse aim (International Agency of the Energy, IAE) [31]:

- **Primary residues**, coming from the harvesting of food and fiber crops cultivated for their main products. Examples are wheat straw and tree branches from timber wood.
- **Secondary residues**, derived from food, fiber and material processing and as animal production wastes, such as corn cob or grape seed cake.
- **Tertiary residues**, after use of the main product. Some examples are demolition timber, sewage sludge, and municipal solid waste (MSW).

1.3. Available potential

In terms of biomass availability potential, four types of potential were defined for bioenergy production purposes and can be generally considered for biomass and biowaste demand for conversion [38]:

- **Theoretical potential:** it corresponds to the energy contained in raw, unprocessed biomass.
- **Technical potential:** it limits the previous potential by the current technological progress.
- **Economic potential:** it restricts technical potential with criteria of economic profitability.
- **Implementation potential:** it adds the consideration of the socio-political conditions.
- **Sustainable implementation potential:** it restraints one or several of the previous potentials with environmental, economic and social sustainability criteria.

Furthermore, it is crucial to evaluate biomass potential in function of the regional climate and historical conditions, which condition the biomass availability and explain the heterogeneity of biomass production [1,2].

The total biomass worldwide was estimated in 2008 to 1800 billion tons on the ground, 4 billion tons in the ocean and a comparative amount in soil [37]. On an energy basis, the total biomass on the ground (33000 EJ) corresponds to at least 80 times the global annual energy consumption.

Solid biomass appeared as the main bioenergy source for the EU-28 gross inland consumption in 2015, representing 70% (95.285 ktoe[1]) of the total consumption (Figure I.1) [40]. Solid biomass is mainly used in residential consumption. Wood pellets represented only 6,3% of the total biomass used for bioenergy in 2015, while wood chips were a more recurrent biofuel, used both for industrial and small scale applications. This ratio between pellets and wood chips will tend to be reversed in the next decade, due to pellets advantages such as energy densification and easier handling, storage and transporting due to their higher stability. The pellet production was ten times higher in 2016 compared to 2000, representing about 29 million tons in the world [41]. Secondly, liquid biofuel, mainly as biodiesel and biogas, accounts for about 23% of the total gross inland consumption of bioenergy. It is noticeable that most of the agricultural biomass use is dedicated to liquid biofuel production, while woody biomass is typically used as solid biofuel [40].

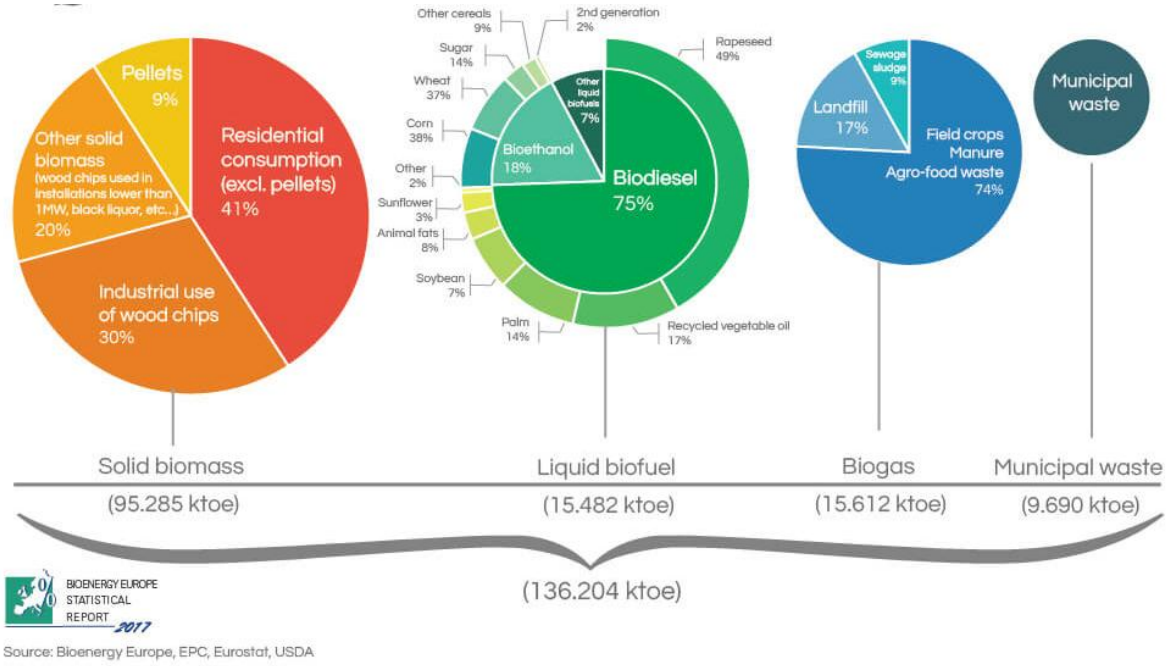


Figure I.1. Estimation of EU-28 gross inland energy consumption of biomass per use and feedstock in 2015 (in ktoe[1]) [40]

Finally, the part of bioenergy demand in Europe for biofuels is expected to present a considerable increase until 2020, according to National Renewable Energy Action Plans [42].

1.4. Structure

Lignocellulosic biomasses present in general the same basic cell wall architecture, formed by a

[1] Ton of oil equivalent (toe) is a conventional unit of measurement used for statistical-comparative purposes. It corresponds to the amount of energy released by burning one ton of crude oil [39].

cellulose microfibril network surrounded by a matrix of hemicellulose and small amounts of lignin. The microfibrils, highly straight due to their mostly crystalline nature, are organized in concentric lamellae, irregularly spaced but approximately parallel. Interactions are established between these three macromolecular components of the biomass, conferring significant resistance to the structure (Figure I.2) [4]. The cell wall structure, composition and properties of lignocellulosic biomass were largely studied in the literature [43].

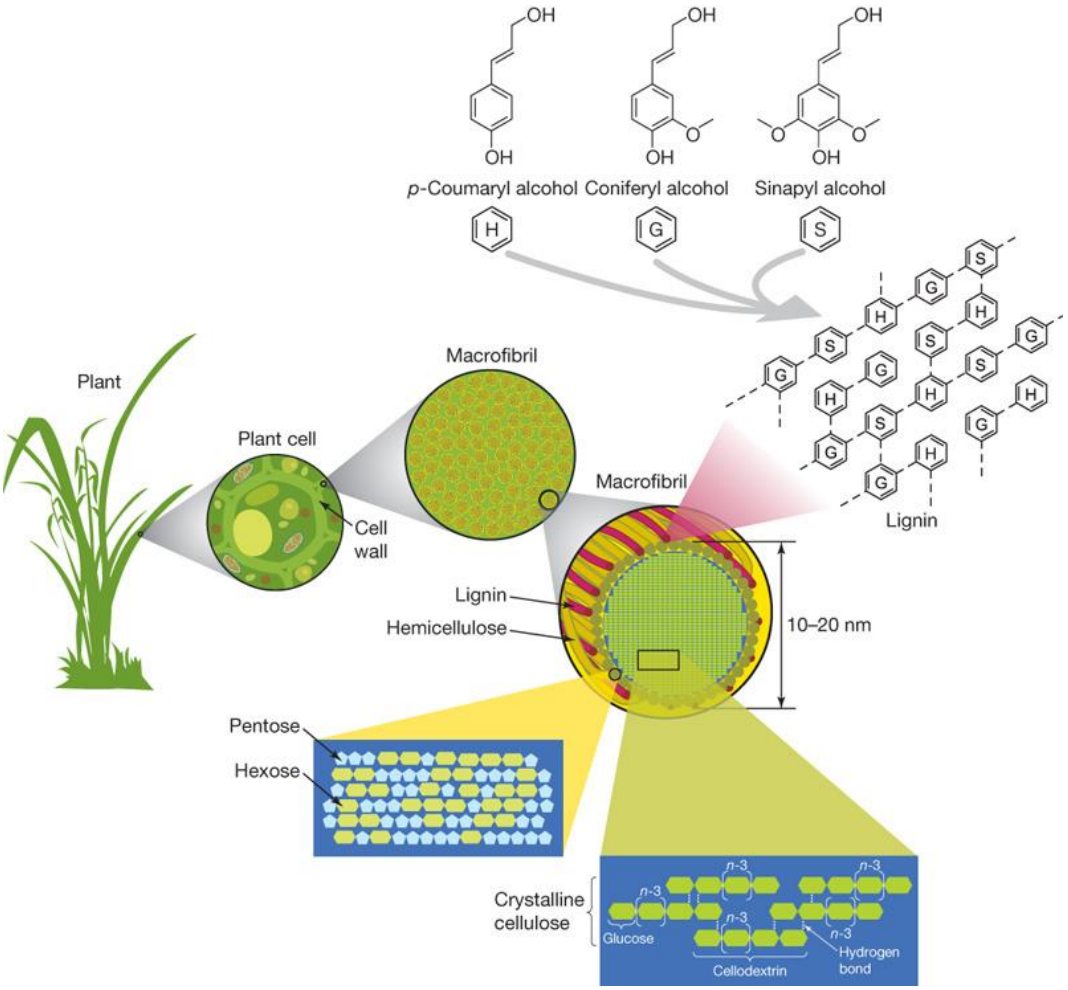


Figure I.2. Structure of lignocellulosic biomass, from the plant to the macromolecular scale [44]

Important differences exist between hardwood and softwood in cell structure complexity and cell types. Softwood presents a simpler structure with only two cell types mainly invariable. Hardwood are characterized by a higher degree of variability within a higher number of cell types, presenting also a characteristic type of cell (vessel element or pore), inexistent in softwood [45]. In both cases, tissues of woody biomasses also contain lignin in secondary cell walls [46]. Even if the cell structure of agricultural biomasses and herbaceous crops is close to that of hardwood, the main differences concern the macromolecular components forming the cell walls, how they are linked together, and the abundance and nature of pectins, proteins and phenolic compounds [23].

1.5. Composition

1.5.1. Elemental composition

Lignocellulosic biomass mainly consists of carbon (C), oxygen (O) and hydrogen (H), as it is composed of organic polymers. It is precisely the oxidation of carbon present in biomass which releases the energy contained in the biomass fuel, as covalent C-C bonds are stronger than C-O or C-H bonds [39].

Minor amounts of inorganic elements are also present in biomass, corresponding to ash in the macromolecular composition. These elements are alkali and earth-alkali metals, such as silicon (Si), aluminum (Al), iron (Fe), calcium (Ca), magnesium (Mg), sodium (Na), potassium (K), sulphur (S) and phosphorous (P). The presence of inorganics is enhanced in agricultural biomasses, biomass waste and treated biomass such as tertiary residues [47].

1.5.2. Macromolecular composition

Lignocellulosic biomass is principally formed of cellulose, hemicelluloses and lignin (Figure I.1). While cellulose and hemicelluloses are made up of polysaccharides, lignin is an oxygenated polymer based on phenylpropane units [5]. The proportions and distribution of these macromolecular components in biomass structure is complex and dependent on the biomass type (Table I.1). Minor amounts of proteins, minerals and other components are also in biomass composition [48]. Water is also present in biomass, either as free water or as bound water:

- **Free water:** it corresponds to liquid water within the cells. It corresponds to the extrinsic moisture, which is influenced by the prevailing weather conditions during harvesting.
- **Bound water:** it refers to moisture absorbed in the hydrogen-bonds of the hydroxyl groups between cell wall components. It is intrinsic moisture, which is independent of weather effects [32].

Table I.1. Macromolecular composition for several lignocellulosic biomasses [12,49]

Lignocellulosic biomass	**Cellulose**	**Hemicelluloses**	**Lignin**
		% wmf	
Hardwood stems	40–55	24–40	18–25
Softwood stems	45–50	25–35	25–35
Leaves	15–20	80–85	0
Grasses	25–40	35–50	10–30
Agricultural by-products	25-50	10-50	15-40
Nut shells	25–30	25–30	30–40
Corn cobs	45	35	15
Wheat straw	30	50	15

1.5.2.1. Cellulose

Cellulose is a major structural component of cell walls, which provides mechanical strength to lignocellulosic biomass. It is the most abundant organic compound in the world, followed by hemicelluloses [37]. It is present in biomass under the shape of microfibrils of between 2 and 20 nm diameter, while their length can reach several tens of microns [50]. Each cellulose microfibril consists in a semi-crystalline macromolecular structure formed by a long straight chain of glucose molecules linked by β-1,4 glycosidic bonds and alternatively rotated by 180° (Figure I.3) [51]. Cellobiose is the monomeric unit of the cellulose polymer, formed by two linked glucose molecules [48]. Other authors consider (1,4)-D-glucopyranose as the monomeric unit of cellulose, and in this case the generic molecular formula of cellulose is $(C_6H_{10}O_5)_n$. In terms of nomenclature, cellulose can also be considered as β-1,4 glucan chains, which are linked together through extensive hydrogen bonding, forming linear organized arrays of chains. The order in the glucan chains in the microfibrils is sometimes altered, leading to disordered areas along the length of microfibrils. These more likely-amorphous regions are suspected to be more propitious for the association of hemicelluloses with cellulose microfibrils [52].

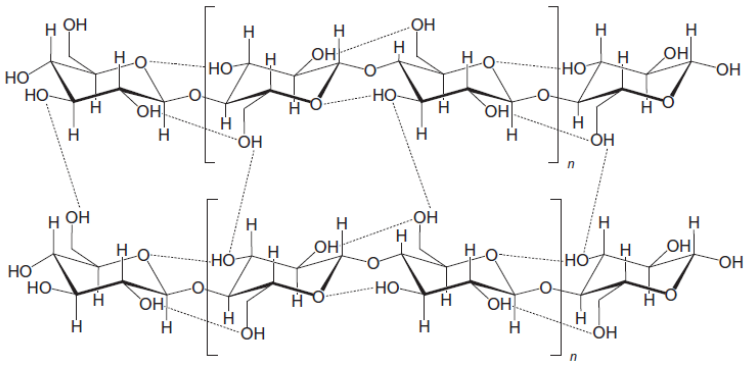


Figure I.3. Structure of two hydrogen-bonded cellulose chains formed by cellobiose units [51]

Cellulose main properties are the average molecular weight and the degree of polymerization, which determines the degree of fragmentation of the molecule and the length of the polymer chains, and crystallinity, which is related to the arrangement of glucan chains in cellulose structure. The degree of polymerization in number (DP*n*), related to the number of glucose units in cellulose chain, of native cellulose in biomass is higher than 10 000, for an average molecular weight up to 2 000 000 [32,53]. On the other hand, crystallinity of cellulose microfibrils makes them resistant to hydrolysis, as well as to acid and alkali attacks. Cellulose crystallinity is expressed by the crystallinity index (CrI). It represents the percentage of the crystalline part present in the total cellulose. It is determined by X-ray diffraction (XRD) and NMR spectroscopy [51].

1.5.2.2. Hemicelluloses

Hemicelluloses are heterogeneous biomass components whose function is to contribute to the

strength of cellulose microfibrils by linking them together and forming a cohesive network. More precisely, a fraction of hemicelluloses is oriented in the same way as microfibrils, associated with the cellulose in their surface. At the same time, other hemicelluloses are bridging links between microfibrils of cellulose, and also with lignin [4].

Chemically, hemicelluloses are heteropolysaccharides formed by several types of saccharides (Figure I.4). These sugar molecules can be composed of five carbon atoms, namely *pentoses* (arabinose, xylose), or by six carbon atoms, called *hexoses* (galactose, glucose and mannose). Hexuronic acids (glucuronic acid) can also be present in the structure, as well as residual acetyl groups connected to the chain (usually in xylans and arabinoxylans [52]). The structure of hemicelluloses is conditioned by the main sugar involved in the polymer construction, the frequency and the nature of the ramifications and the degree of polymerization [54].

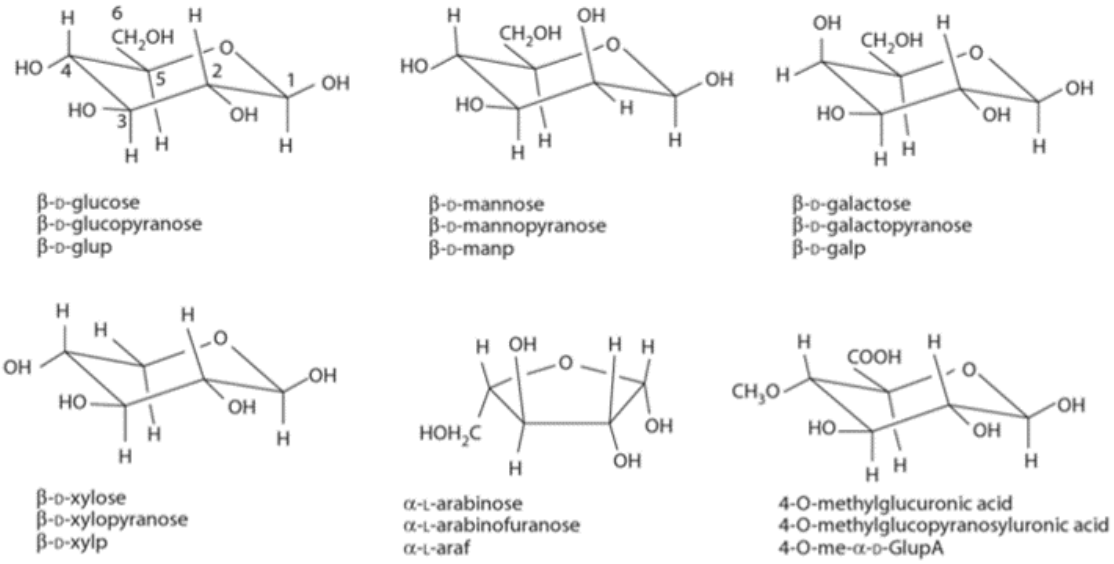


Figure I.4. Principal sugar components of hemicelluloses in biomass [34]

A classification of hemicelluloses was proposed considering four structurally different cell-wall polysaccharides present in biomass: xylans, mannans, β-glucans and their mixed linkages and xyloglucans [55]. Sugars, which are the building blocks of hemicellulose polymers, depend on biomass type. For example, while softwood hemicelluloses are composed mainly by mannans and glucomannans, hardwood presents xylan-based hemicelluloses. Herbaceous plants contain also glucuronoarabinoxylan and β-glucan in their hemicelluloses. Other sugars, like arabinogalactan, are present in low amounts in hemicelluloses of all types of biomass [46].

- **Xylans or D-xyloglycans:** xylan-type polysaccharides are the main hemicellulose components of secondary cell walls. They represent about 20–30% of the biomass of hardwoods and herbaceous plants and up to 50% for grasses and cereals [55]. These abundance is the recurrent reason presented in literature by authors using commercially available xylan as a model feedstock to represent hemicellulose in biomass modelling [56–59]. Structurally, xylans are heteropolymers with β-(1→4)-D-xylopyranose units linked by

β-glycosidic bonds, forming a central chain with short carbohydrate ramifications. Structurally, xylans can be classified in two types:

- *Homoxylans*, exclusively formed by non-ramified β-(1→4)-D-xylopyranose units.
- *Heteroxylans*, which includes glucuronoxylans and (arabino)glucuronoxylans in deciduous wood and (glucurono)arabino-xylans complex heteroxylans in cereal grains. The most abundant xylans are glucuronoxylans (Figure I.5).

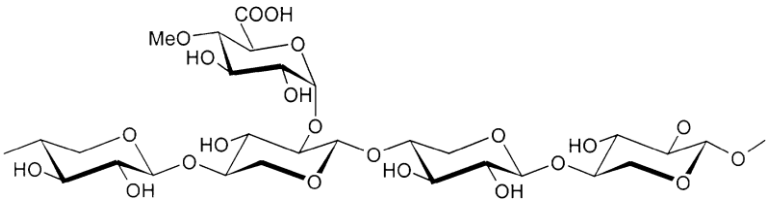


Figure I.5. Primary structure of 4-O-methyl-d-glucurono-d-xylan (MGX) [55]

- **Mannans or D-Mannoglycans**: these polysaccharides are the second most abundant hemicelluloses family. They are sub-divided into:
  - *Galactomannans*: the main linear chain is exclusively formed by β-(1→4)-linked D-mannopyranose units. An example is arabinogalactan [46] (Figure I.6).

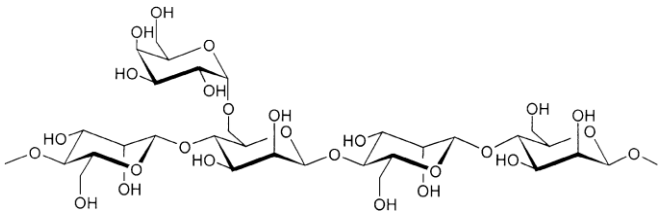


Figure 6. Primary structure of D-galacto-D-mannan [55]

  - *Glucomannans and galactoglucomannans*: the main chain of these polysaccharides presents both β-(1→4)-linked D-mannopyranose and β-(1→4)-linked D-glucopyranose units (Figure I.7). These hemicelluloses are typically present in coniferous wood.

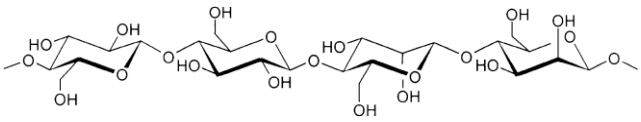


Figure I.7. Primary structure of D-gluco-D-mannan [34,55]

- **Other hemicelluloses:**
  - *Xylo-D-glucans*: xyloglucans are common for all higher plants and have been reported as forming the major hemicelluloses in many primary cell walls [52]. Xyloglucans are formed by a cellulosic linear chain of *β*-D-glucose units ramified by *β*-D-xylose units at position 6 (Figure I.8). Besides, these polysaccharides usually establish hydrogen bonds to the cellulose microfibrils and covalent bonds with other elements of the cell wall, such as pectin [55].

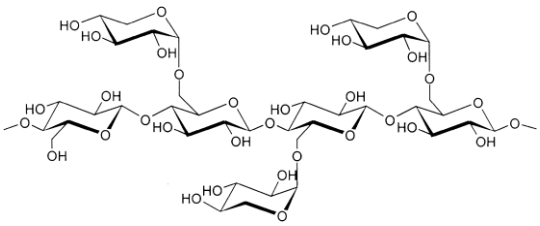


Figure I.8. Primary structure of D-xylo-D-glucan [55]

- *Mixed-linkage β-D-glucans*: they consist of an unbranched homopolymer formed by blocks of (1→4)-linkage sequences of D-glucopyranose units separated by single (1→3)-linkages, in a percentage of about 70% for (1→4)-linked and 30% for (1→3)-linked (Figure I.9). The presence of these mixed-linked glucans is well-known in grasses [54].

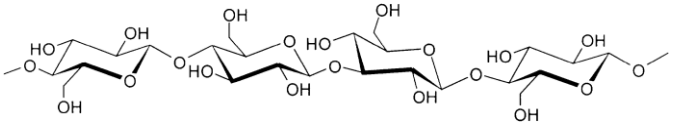


Figure I.9. Primary structure of mixed linkage (1→3, 1→4)-D-glucan (β-glucan) [55]

Hemicelluloses present a low degree of polymerization (DPn), between 80 and 200, for a generic molecular formula of $(C_5H_8O_4)_n$ or $(C_6H_{10}O_5)_n$, in function of their composition in pentoses or hexoses, respectively [37,60]. Concerning the organization of the structure in hemicelluloses, the substitution in the linear sugar chains by additional sugar side-chains results in the lack of crystallinity typical of a highly branched structure [52]. As a result, comparing to cellulose, hemicellulose chains are much smaller and disorganized, which makes it more vulnerable [48].

1.5.2.3. Lignin

Lignin is a polymer based on phenolic compounds which forms a protective layer for the plant walls by encasing the polysaccharides (cellulose and hemicellulose) of the cell walls [48]. At the same time, covalent bonds exist between hemicellulose and lignin, which results in a structured resistant microfibrillar sheath or cortex [4]. In this structure, lignin is rather located in middle lamella of woods than in secondary wall as cellulose and hemicellulose [61] (Figure I.1).

The basic structural unit of lignin is phenylpropane, which presents ether (C-O-C, about 70%) and carbon (C-C, about 30%) linkages in the lignin structure [61]. Lignins were reported to be derived from the copolymerization of three alcohols derived from phenylpropane (Figure I.10) [62]:

- **p-Coumarylic alcohol** or 4-(3-hydroxy-1-propenyl)phenol.
- **Coniferyl alcohol** or 4-(3-hydroxy-1-propenyl)-2-methoxyphenol.
- **Synapyl alcohol** or 4-(3-hydroxy-1-propenyl)-2,6-dimethoxyphenol.

Their ratio in the lignin polymer differs in function of the plants, wood tissues and cell wall layers [44]. As a result, lignin structural units are represented by H (phenyl or coumarylic), G

(guaiacyl or coniferyl) and S (synapyl).

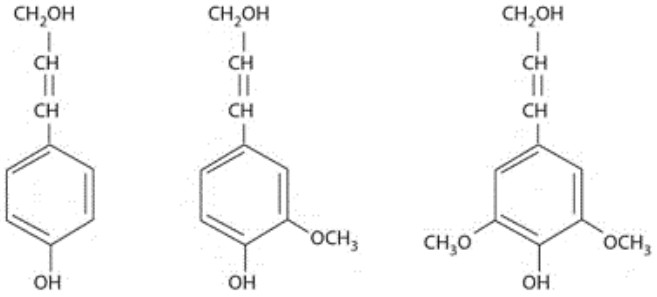


Figure I.10. Chemical structures of lignin precursors: p-coumaryl alcohol (left), coniferyl alcohol (center) and sinapyl alcohol (right) [34]

Lignin is a complex 3-dimensional amorphous structure not yet completely elucidated. This complexity refers mainly to the intermonomeric linkages formation. These links are supposed to be formed by random reactions of the phenoxy- radicals generated by enzymatic oxidation of the three phenylpropane monomers. Besides, the monomeric composition and the nature and proportions of the intermonomeric bonds depends on biochemical factors like plant species, their stage of development or their cytological origin [62]. It has been identified that lignin from softwood are formed by G units (90%) and some H units, mainly, while lignin constituting hardwood contains varying ratios of G and S units. Agricultural biomass and herbaceous crops present variable ratios of H, G and S units [63].

1.5.2.4. Extractives

Extractives are referred to an heterogeneous group of compounds that can be obtained from biomass through by dissolving them in organic solvents, e.g. benzene, acetone, and alcohol, or water [64,65]. The major components of lipophilic wood extractives, which are often called pitch, are triglycerides, fatty acids, resin acids, steryl esters and sterols. Wood also contains hydrophilic extractives such as lignans [66].

Some extractives, such as polyphenols and lignans, might present benefits for human health and antioxidant properties [67,68]. Wood extractives were studied in pulp and paper processes as they were identified as responsible for a decrease of the final quality of the product and for producing toxic process effluents [69,70].

1.5.2.5. Ash

Ash content consists in the inorganic elements present in raw biomass. Typical values of ash content per biomass family are shown in Table I.2. Agricultural biomass contains a more significant ash content than forestry resources, except for woody bark [39].

Table I.2. Ash content for several lignocellulosic biomasses [71]

Lignocellulosic biomass	**Ash content (wmf%)** as measured
Hardwood	0.5 – 3.0
Softwood	0.5 – 3.0
SRC	1.0 – 5.0
Grasses	3.0 – 10.0
Agricultural crops	5.0 – 15.0
Microalgae	8.5 – 10.5

The form under which these elements are present in biomass, as well as their linkages with macromolecular components, are not well-known at the moment. These elements remain mostly unaltered after the thermal treatment, being part of the solid product.

1.5.3. Interactions between macromolecular components

Some interactions between biomass macromolecular components have already been discussed above. This is the case of the hydrogen bonds between cellulose and hemicellulose and the intermonomeric linkages of lignin. These interactions contribute to maintain the shape and the strength in biomass structure. Nevertheless, the determination of these interactions is carried out by experimentations which isolate biomass components. As this extraction usually changes the structure of macromolecular components, interactions between them have not been completely decrypted yet [48].

Generally, lignocellulosic biomass consists in a polymer whose components present four main types of linkages of different chemical nature: ether, ester, carbon-to-carbon and hydrogen bonds [48]. These links can be classified in two categories, in function of the nature of the elements of the biomass polymer that they connect:

- **Intrapolymer linkages:** they provide links inside the cellulose, hemicellulose and lignin macromolecules present in biomass.
  - In the case of *cellulose*, the glucose units forming each chain are linked by a 1-4 β D-glycosidic bond. This bond can also be considered as an ether bond, since it consists of two carbon atoms with an oxygen in the middle [48]. Cellulose chains are then linked by hydrogen bonds between two hydroxyl groups of different polymer chains, which contributes to the straightness and the crystallinity of the structure [5], as it has been previously mentioned.
  - *Hemicellulose* structure is built also mainly by ether bonds, such as the glycosidic bonds. In contrast to cellulose, hydrogen bonds are absent in the molecule, but there are significant amount of carboxyl groups, present in carboxyl, ester or salt form [48].

- In *lignin*, the most abundant is ether-type bonds, representing around 70% of the total bonds between the monomer units, while the C-C linkages constitute the remaining 30%. The ether bond between the β-carbon and the 4-carbon, named the β-O-4' bond, is the most common bond in lignin and is also the most commonly broken during biomass processing (Figure I.11) [72].

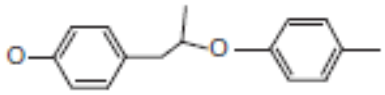


Figure I.11. β–O–4' bond (or β-aryl ether) from lignin [72]

- **Interpolymer linkages:** they connect macromolecular components together to form the complex structure of biomass.
  - *Cellulose* most important interpolymer links are hydrogen bonds. This linkage is not only established between cellulose chains, but also between cellulose and hemicellulose hydroxyl groups, with the same function of reinforcing the structure of the biomass fiber. In this case, this linkage is not expected to be as strong as the interlinkage, as hemicellulose lacks of primary alcohol functional group external to the pyranoside ring [48].
  - The main link of *hemicellulose* is through hydrogen bonds, mostly with cellulose and also with lignin. Sugar residues in hemicellulose chains are highly substituted with O-acetyl groups, uronic acid moieties and other saccharide units. They are covalently bonded to some parts of the lignin structure [73,74].
  - Concerning *lignin*, several types of covalent bonds have been identified between lignin and the other polysaccharides of wood, especially with hemicelluloses, but also with cellulose and pectin. Literature clearly indicates the existence of phenyl glycosidic bonds and ether-carbon bonds. Nevertheless, carbon-carbon (C-C) bonds and esters-carbon have also been suggested. These bonds are named as lignin–carbohydrate complexes (LCC, Figure I.12). They are still poorly known and very frequent in lignin, participating in the resistance to swelling and inflexibility of the polysaccharides [72]. There would also be hydrogen bonds between lignin and polysaccharides [48].

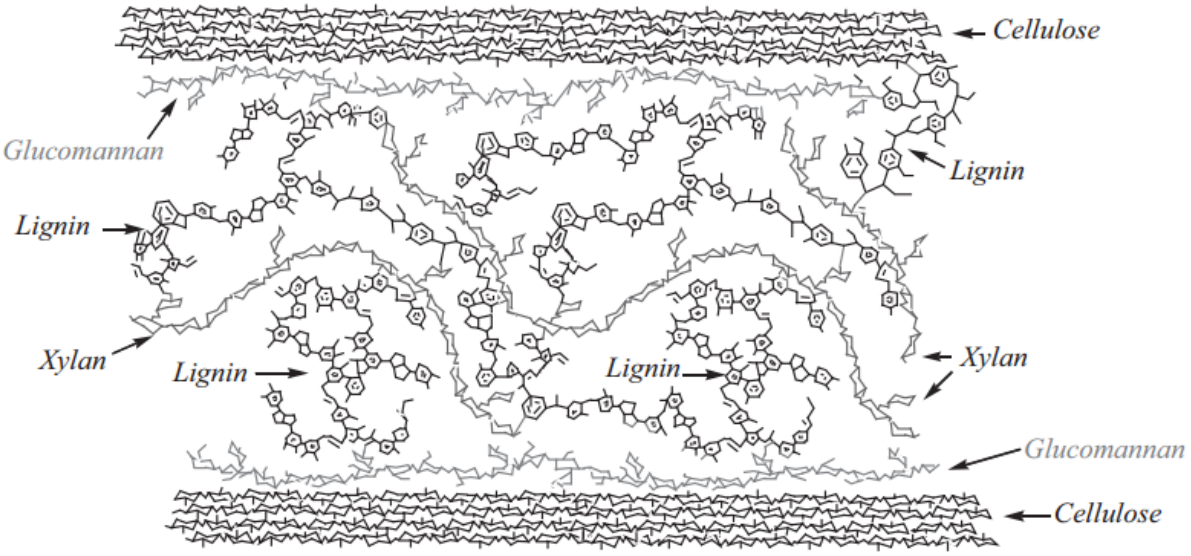


Figure I.12. Lignin-Carbohydrate complexes (LCC) form a network in biomass structure [72]

1.6. Biomass properties

1.6.1. Moisture

As explained in I.1.2, moisture is an important parameter which influences the choice of the most suitable treatment.

Moisture content (MC) of a biomass represents the mass of water in relation to the mass of the oven-dried biomass (Eq.1) [75]. The standard procedure considers a drying time of 24h at 105°C, or until constant weight of dried biomass (ASTM D4442-15) [76].

$$Moisture\ content\ (MC, oven-dry\ basis)\ \% = \left(\frac{W_{water}}{W_{oven-dry\ wood}}\right) * 100 \qquad \text{Eq. 1}$$

1.6.2. Density/volumetric weight

The volumetric weight or density (ρ) of wood is variable because both mass and volume depend on moisture content [45]. That is the reason why moisture content must also be precised for a given value of biomass density.

Density is considered as a physical parameter equivalent to volumetric weight. *Absolute density* or *skeletal density* is obtained when the volume measured excludes pores and void spaces. Density can be referred to a single particle (*particle density*) or to a bed of particles (bed density). *Biomass density* denotes the availabily of a type of biomass in a geographic area [77].

1.6.3. Thermal properties

The main thermal properties considered for biomass are heating value and heat capacity. Other parameters as thermal conductivity, thermal diffusivity and coefficient of thermal expansion are considered for wood, which was deeper studied than other biomasses in this sense [45].

Heating value (HV) or calorific value (CV) is the amount of energy released during complete combustion per unit of mass or volume. The standard for its measurement was defined for coal (ASTM D5865 – 13). Moisture content strongly influences this parameter, being part of the energy destined to moisture evaporation [39]. This allows to distinguish between:

- **Low Heating Value (LHV):** quantity of energy invested in heating biomass per mass unit, without considering moisture evaporation [39].
- **High Heating Value (HHV)**: including also energy needed to evaporate moisture during combustion as available energy [39,78].

  Elemental composition was shown to impact the HV. Boie proposed a correlation for estimating the HHV from biomass elemental composition ([79] cited by [80], Eq. 3). Concerning inorganics, a high ash content implies a decrease in biomass HV [9].

$$HHV\ \left[\frac{kJ}{kg}\right] = 351.70\,C + 1162.49\,H + 104.67\,S - 110.95\,O + 62.80\,N \qquad \text{Eq.3}$$

- **Heat capacity (c_p)** represents the amount of energy necessary to increase one unit of mass (Kg, in the SI) by one unit of temperature (K). In the case of wood, it has been demonstrated that the heat capacity is dependent on the temperature and moisture content, but is practically independent of density. A correlation has been proposed for estimating wood heat capacity in function of the temperature (Eq. 4) [81].

$$c_p = 5.340\,T - 299\ \ (J\,Kg^{-1}K^{-1}) \qquad \text{Eq. 4}$$

1.7. Biomass conversion

Biomass conversion to useful products, either for their direct use or for their further conversion, firstly requires a physical preparation. This might consist of an energy and mass densification through pelletizing, a reduction of the moisture content by drying or a diminution of the particle size through grinding and shredding.

Biomass can be valorized through chemical conversion processes, this is, by changing its chemical structure. The main routes for this are thermochemical conversion, principally based on temperature, and biological conversion, mainly due to microorganisms or biological transformations. Thermochemical conversion processes are strongly conditioned by biomass moisture content. As a result, dry biomasses are suitable for processes where temperature is the main agent in biomass conversion. In the case of biomasses with a high moisture content, pressure is also required to operate the transformation (Figure I.13).

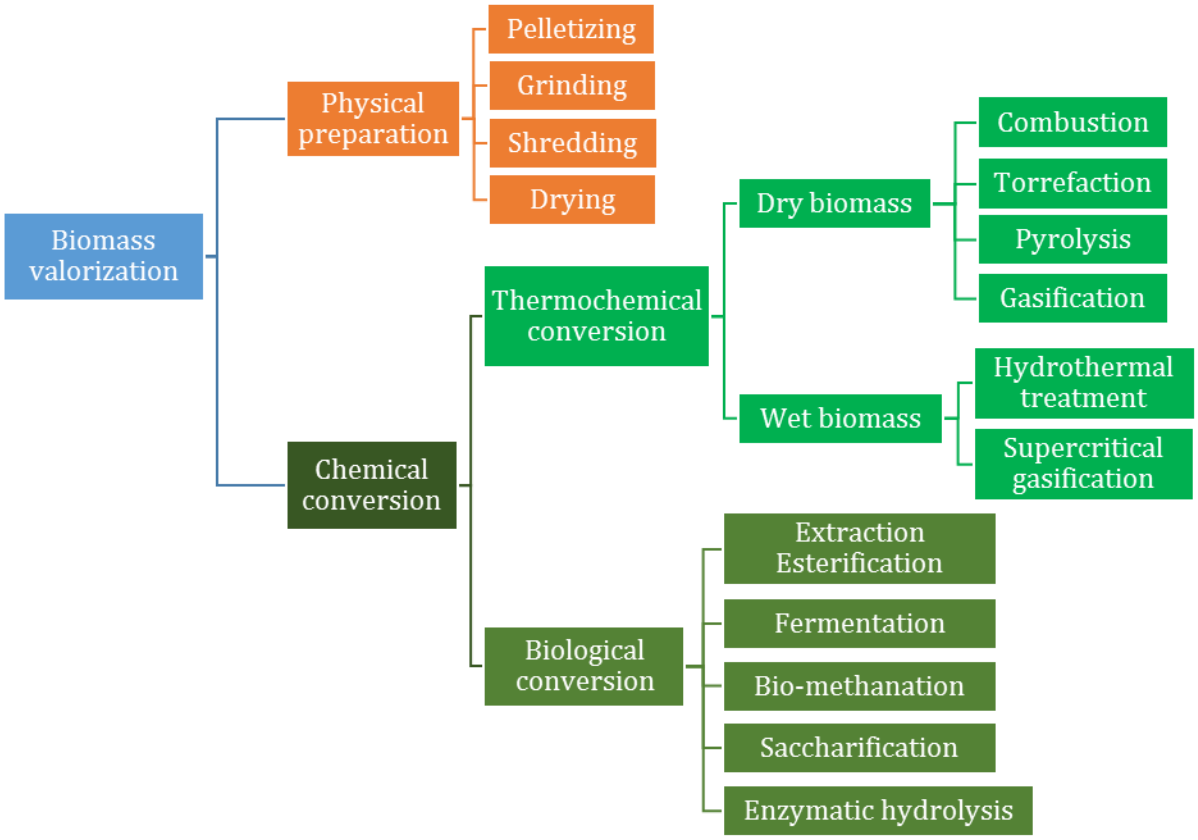


Figure I.13. Scheme of the main steps involved in biomass valorization

The MOBILE FLIP European H2020 project aims at developing and demonstrating mobile processes for the treatment of underexploited agro- and forest based biomass resources into products and intermediates. To do this, pelletizing, torrefaction, slow pyrolysis, hydrothermal carbonization and saccharification technologies were evaluated in terms of raw material flexibility, as the biomass resources are typically scattered and seasonal. The products vary depending on the process concept, being typically fuels as such or for co-combustion (pellets, torrefied solid and pellets, biocoals), biochars for soil remediation, biodegradable pesticides for agricultural or forestry use or chemicals for wood panel industry and sugars and hydrolysable cellulose as intermediate for the sugar platform [82].

In this context, biomass thermochemical conversion through torrefaction was selected as the subject of this study.

2. Torrefaction

2.1. Definition

Torrefaction is a mild thermal treatment that consists in the heating of biomass in an inert atmosphere, at atmospheric pressure, between 200 and 300 °C, from several tens of minutes to one hour [9]. Biomass torrefaction produces a solid with properties closer to coal, and releases some incondensable gases and volatile species, including water.

2.2. History

Torrefaction was historically used for coffee beans, nuts or seeds roasting in hot air. The most famous application of torrefaction is in coffee processing, which has been extensively developed in the 19th century. The aim of this process is to enhance coffee flavor through chemical reactions between the organic compounds present in green coffee grains. Torrefaction was also used in thermo-wood production for outdoor furniture and boats, through a process developed in Finland in the 1980s. Torrefaction for energy purposes was already studied in France in the 1930s [83]. However, the application for producing high calorific biofuels from wood and agricultural crops was rather developed since 2000. The interest in biomass torrefaction has greatly increased during the last decade, going from only few scientific papers with “biomass” and “torrefaction” as keywords from 2000 to 2010 to more than 200 papers in 2017 *(source: Scopus)* (Figure I.14).

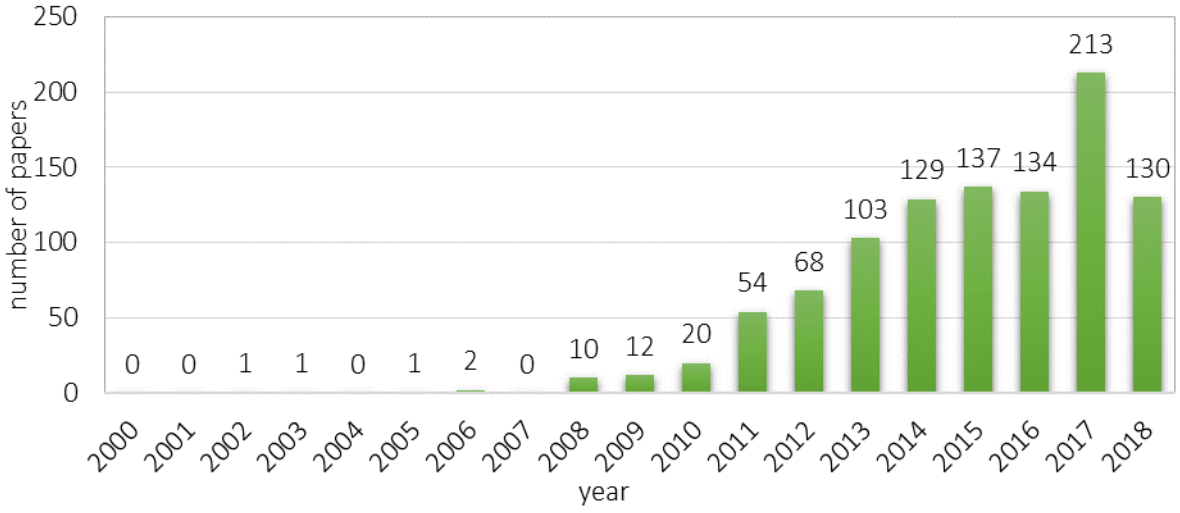


Figure I.14. Articles listed in Scopus with "torrefaction" and "biomass" included in "Article title, abstract, keywords" in the last two decades (research carried out the 2018/09/02)

2.3. Torrefaction products

Torrefaction products are a torrefied solid (about 70%), that can be named biocoal [78,84], and some gaseous species released (about 30%). The yield of production of torrefied solid decreases with temperature, as it is converted into volatile species, whose release is enhanced by increasing the torrefaction temperature [85]. Examples of mass and energy yields are detailed in

Table I.3. Solid mass loss in function of torrefaction operating conditions

Biomass	T (°C)	t (min)	Solid mass loss	Source
Bamboo	230	60	51.5	[86]
	260	60	59.0	
	300	60	62.0	
Willow	230	60	35.0	
	260	60	53.8	
	300	60	60.0	
Loblolly pine chips	270	2.5	16.4	[87]
	300	2.5	24.4	
	330	2.5	48.5	
Norway spruce	260	25	10.4	[88]
	310	25	41.1	
Leucaena	225	30	13.5	[89]
	250	30	27.0	
	275	30	45.7	
Reed canary grass	300	30	38.5	[21,27]
Wheat straw	300	30	44.9	
Willow	300	30	28.0	
Wheat straw	250	81.5	21.6	[16]
	300	81.5	58.0	
Empty fruit bunch	220	30	56.9	[27]
	250	30	63.0	
	300	30	75.8	

2.3.1. Torrefied solid

Torrefaction main purpose is to improve solid properties regarding raw biomass. It leads to heating and processing properties closer to those of coal. Torrefaction also improves uniformity in solid properties. In this sense, seasonal influences on physical and chemical properties are reduced after a torrefaction treatment of the raw materials [20].

The **mass or solid yield** represents the percentage of the initial mass of raw biomass transformed into torrefied solid product. It corresponds to solid mass loss (Eq. 6) [21], whose contrary is remaining solid mass [22]. As mass yield is based on the reactive part of the biomass, it is typically expressed on a dry ash free basis (daf) [78] or in weight moisture free basis (% wmf). This last notation was adopted in the current study.

$$Y_{mass}\,(\%) = \left(\frac{m_{product}}{m_{feed}}\right)_{daf} \times 100 \qquad \text{Eq. 6}$$

2.3.1.1. Hydrophobicity

The physical evolution of biomass structure allows to obtain a hydrophobic material, with an easier storage, independent of bacteriological attacks, and reduced transport costs. More precisely, hydroxyl groups and hydrogen bounds are mainly present in cellulose and hemicelluloses, which confer a relative hygroscopic character to the cell walls. Although lignin also presents some hydroxyl groups, it is a comparatively hydrophobic molecule, which limits the affinity of raw biomass with water [34]. Indeed, the diminution of the hydrophobicity of raw biomass caused by thermal pretreatments has its origins in the breakdown of these hydroxyl groups [90].

2.3.1.2. Energy densification

Torrefaction leads to an energy densification of the material, that is, an increase in the energy content of the material per mass unit. The energy density of the torrefied material generally can go up to 120% of the original material [91].

Energy densification is related to changes in biomass elemental composition [90,92]. Torrefaction implies the removal of oxygen from the final solid product. The high presence of oxygen in raw biomass is translated in a low carbon to oxygen (C/O) ratio. As oxygen is diminished, the heating value is augmented with torrefaction severity [88], which depends on biomass type [83], and smoke generation in combustion is diminished [83]. The improvement of thermal properties is also favored by the hydrophobic character of the torrefied biomass.

2.3.1.3. Flowability

Torrefied biomass was reported in the literature to have optimized rheological properties, that is, a better ability to flow, compared to raw biomass [5]. This is explained by the fact that biomass particles become more spherical during the torrefaction process [20,93].

2.3.1.4. Grindability

The tenacious and fibrous structure of raw biomass converts grinding in a high energy intensive process. Improving biomass grindability is translated into the increase in weight percentage of fine particles for an identical energy (or electricity) consumption during grinding [20].

According to [94], hemicellulose is the macromolecular component in biomass responsible of the grinding resistance. Torrefaction facilitates grinding, as it breaks hemicellulose links between biomass fibers, making its structure more friable [95]. Furthermore, hemicellulose is the most degraded biomass component in torrefaction, and its removal would be also the

responsible of the easier grindability of the torrefied biomass.

Torrefaction was reported to result in a reduction of 50 to 85% of the electricity consumption for size reduction when compared to that of fresh wood [78]. The energy required to pulverize the torrefied material would be reduced to a maximum of 10% of that needed for the raw biomass [46]. However, the improvement of grindability depends on the severity of torrefaction [20,96].

2.3.2. Gaseous species

Gaseous species released are classified into non-condensable species or permanent gases and condensable species. Permanent gases are mainly CO_2 and CO. Volatile species are mostly composed by fatty acids, phenols, acids, alcohols, furans and ketones [94]. Water is the most abundant condensable species released. It can be cooled, together with volatile species, usually between 0 and -80°C, and converted into liquid [97].

Generally, the main species present in the condensable fraction are acids, methanol, furfural, hydroxyacetone, and phenolic compounds [91]. Condensable species include water vapor, which is the most abundant. Its release during torrefaction leads to significant losses in O and H, which are responsible of the higher C/O and C/H ratios of the torrefied product [23].

The proportions between permanent and condensable gases produced in torrefaction are about a third and two thirds of the total released gases, respectively, depending on the operating conditions. According to [98], for a torrefaction at 250°C, permanent gases represent about 6-12% and condensable species, including water, correspond to 22-30% of the product composition in mass percentage of initial wet biomass.

Some of the gases released during torrefaction can be easily condensed into liquid by cooling traps with liquid nitrogen or ice [6,99] or by a condenser with a continuous cooling water flow [100]. That is the reason why some authors refers to a 'liquid product', called bio-oil in pyrolysis, independent of the 'gas product', instead of talking about permanent and condensable gases [101].

All gases produced in torrefaction at industrial scale are usually destined to combustion, without distinction between permanent gases and condensable species. Burning torrefaction supplies energy to compensate the heat duty in torrefaction and drying, if it is required. At the same time, this energy supply compensates the heat losses of the process. The interest on burning torrefaction gases requires a low water content and CO_2/CO ratio [78]. However, previous studies assessed the recovery of volatile species from the torrefaction gases as a source of high-added-value products that can contribute to the economical balance of the torrefaction process [12,13]. This recovery of the volatile species might also be interesting if a high production of chemical compounds harmful for the process is detected. At present, the valorization of the condensable species released in torrefaction remains at lab scale, particularly because of the

difficulties to separate the chemical compounds integrating the mixture of volatile species [11].

2.4. Torrefaction technologies

Biomass processing through torrefaction typically requires several steps (Figure I.15). A previous drying step of the raw material may be required, typically taking place at 105°C for 24h or until reaching a moisture content below 10 %. This operation can take place in a separate reactor (dryer). After that, a heating step until the torrefaction temperature (200-250°C) named post-drying is necessary. The solid material already suffers a little mass loss in this step, usually below 5%. Once the torrefaction temperature is reached, the core of the thermochemical conversion is carried out: the raw material is transformed by losing mass, which is released as a gaseous phase containing permanent gases, water and condensable species. Finally, a cooling stage is necessary to bring torrefied biomass to ambient conditions. During this last period no further mass loss takes place, but some evaporation of adsorbed reaction products may occur [78,102].

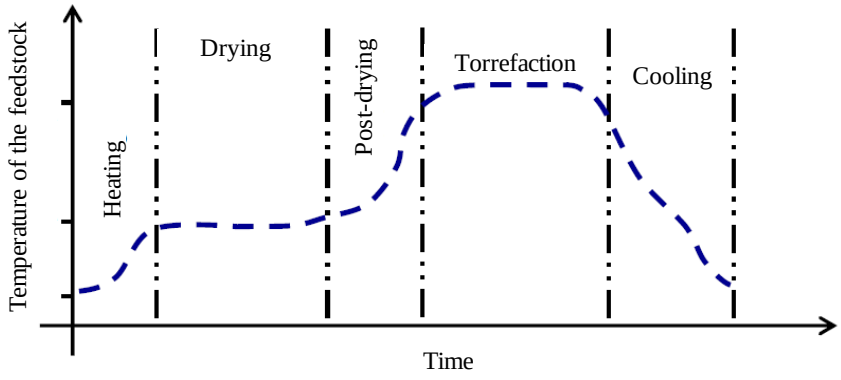
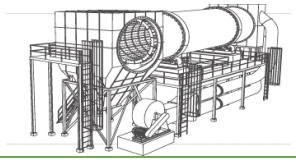
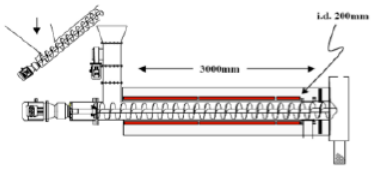
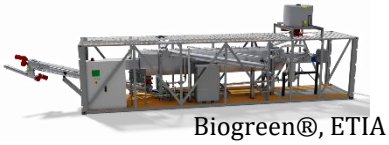
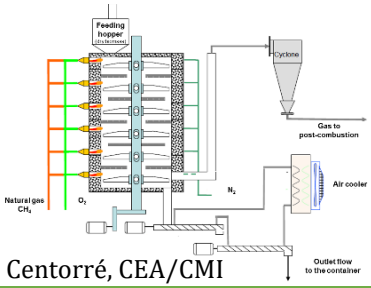
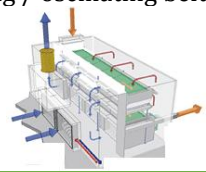
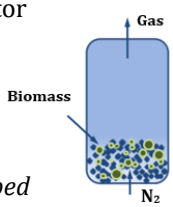
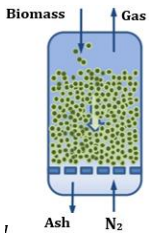


Figure I.15. Processing stages of torrefaction [84]

Most of the reactor technologies used in biomass torrefaction are derived from modifications of technologies originally developed for other applications. The main factors conditioning the suitable reactor technology for a feedstock are its characteristics, and principally particle size, which goes from sawdust to large particles. Otherwise, the feedstock needs to be adapted to a given torrefaction technology through size reduction or, inversely, removal of the fine particles or mass densification by pelletizing, for example. The moisture content is also a critical parameter of the feedstock, as part of the heating in the torrefaction reactor will be devoted to remove water. As a result, a previous drying, either in torrefaction reactor or in a separate dryer, may be required. Table I.4 summarizes the main technologies used in biomass torrefaction [103].

Table I.4. Main torrefaction technologies [103–106]

Technology	Advantages	Disadvantages	Companies
Rotating drum reactor 	✓ proven technology ✓ robust and low cost ✓ residence time control ✓ particle mixing ✓ heat exchange	× ↑ fine particles (attrition) × limited scalability (modular set-up) × mobile parts × not compact	Andritz (AT); CENER (SP); EarthCare Products; Teal Sales Inc (USA) Torr-Coal (NL)
Screw conveyor reactor (undirect heating) 	✓ proven technology ✓ residence time control ✓ versatile configuration (vertical or horizontal) ✓ relatively inexpensive ✓ uniform mixing	× low heat transfer × limited scalability × sensitive to biomass density and particle size	Agri-tech Producers (USA); Arigna Fuels (IR); BioEndev (SWE); Solvay Biomass Energy (USA)
Heated screw conveyor reactor  Biogreen®, ETIA	✓ proven technology ✓ residence time control ✓ good heat transfer ✓ easy to scale up ✓ mobile	× high electricity cost × sensitive to biomass density and particle size	ETIA (FR);
Multiple hearth furnace/ Herreshoff oven  Centorré, CEA/CMI	✓ proven technology ✓ residence time control ✓ uniform mixing ✓ gradual heating ✓ drying possible in upper layers ✓ easy scalability ✓ large range of particle sizes ✓ solid/gases measures per step	× mobile parts × biomass conveying (if non-uniform particles) × not compact × low heat transfer × limited capacity	CEA/CMI (FR/BE); Integro Earth Fuels (USA); Terra Green Energy (USA); Wyssmont (USA)
Vibrating / oscillating belt reactor 	✓ residence time control ✓ uniform mixing	× mobile parts	Cirad (FR)
Fluidized bed reactor  *bubbling fluidized bed*	✓ proven technology ✓ easy scalability ✓ uniform mixing ✓ intense contact solid/gas ✓ intense heat transfer ✓ compact reactor design	× sensitive to fines particles × separation of the fluidizing media × heterogeneity in the torrefied product dependent on T(bed)	Airex (CAN); Bioenergy Development & Production (CAN); Topell (NL)
Moving/fixed bed  *updraft fixed bed*	✓ proven technology ✓ few mobile parts ✓ ↓ reactor volume ✓ ↑ degree of filling of the reactor ✓ heat exchange homogeneous	× non-uniform mixing × risk of gas/heat channeling in the bed × risk of non-uniform product × particle size sensitive × ↑ fine particles (attrition) × limited scalability	Andritz/ECN (DK/NL); AREVA, LMK Energy (FR); Grupo Lantec (SP); New Earth Renewable Energy Fuels (USA); Torrec (FI)
Microwave reactor 	↑T thanks to microwaves (vibration of water molecules inside biomass)	× electricity consumption × energy efficiency × operational costs	Rotawave (UK)

3. Objective of the work

In this context, the objective of this work is to assess the impact of biomass properties on its conversion in torrefaction. This evaluation will be carried out both in terms of solid mass loss and of volatile species release, and versus the main operating conditions (temperature and time). To do this, biomass will be represented through its main macromolecular composition, namely cellulose, hemicelluloses and lignin.

After analyzing the state-of-the-art of biomass torrefaction, a detailed approach of the work based on this objective will be proposed.

-II-

STATE-OF-THE-ART OF BIOMASS TORREFACTION

II. STATE-OF-THE-ART OF BIOMASS TORREFACTION

In this chapter, the state-of-the-art of biomass torrefaction is firstly analyzed in terms of the torrefaction products studied in previous works. Secondly, chemical and physical phenomena occurring for biomass macromolecular components in their transformation through torrefaction are assessed, as well as the influence of the operating conditions in the process. Finally, the current development state of the biomass torrefaction models is assessed.

Pyrolysis studies considering mild conditions corresponding to torrefaction, namely between around 200 and 350°C, are also considered in this analysis. This is justified by the fact that many studies including torrefaction conditions are included in pyrolysis studies.

1. Torrefaction products

1.1. Torrefied solid

Torrefied solid is typically characterized in terms of the evolution of its elemental composition in carbon (C), hydrogen (H) and oxygen (O), which can be expressed as H/C and O/C ratios. Torrefaction transforms raw biomass, characterized by high H/C and O/C ratios, in a torrefied product with properties closer to those of coal, represented by low H/C and O/C ratios. Biomass properties are modified in function of the degree of severity of torrefaction, enhanced by temperature and residence time [84]. Atomic O/C and H/C ratios in raw biomass are about 0.4–0.8 and 1.2–2.0, respectively, while after biomass torrefaction they decrease to 0.1–0.7 and 0.7–1.6[9].

The change in the solid structure due to thermochemical conversion through torrefaction was studied in the literature through Nuclear Magnetic Resonance (NMR), analytical pyrolysis-GC/MS and FTIR characterizations [13,107–111]. These techniques were sometimes applied until temperatures higher than those for torrefaction. This allowed to show the complete transformation of biomass macromolecular components, which happens until pyrolysis temperatures around 800°C, depending on the authors [9]. In-situ characterization of the evolution of the solid structure through thermochemical is rare and was exclusively found for catalytic pyrolysis [112,113].

1.2. Gaseous products

The analytical techniques devoted to detect and quantify gaseous species in torrefaction are usually FTIR (Fourier Transform Infrared Spectroscopy), HPLC (High Performance Liquid Chromatography) and GC (Gas Chromatography), alone or combined with MS (Mass Spectrometry) or FID (Flame Ionization Detection) [21,98,99] (Table II.1). Permanent gases can be analyzed on-line by these techniques or collected in a gas bag for subsequent analysis [17]. On the other hand, condensable species are usually collected in cold traps and then analyzed off-line [6].

1.2.1. Permanent gases

Carbon dioxide (CO_2) and carbon monoxide (CO) are the main gas products released during torrefaction (Table II.1). They contribute to significant losses in oxygen, which leads to a higher C/O rate of the torrefied product [23]. An order of magnitude of the production of these permanent gases at typical torrefaction conditions (250°C, 30 min) is about 90-70% CO_2 and 10-30% CO [99].

Other permanent gases formed in smaller amounts are methane [21] and C2 hydrocarbons (ethane, ethylene) [23]. Some authors have also detected C3 hydrocarbons (propane, propene) [98], oxygen [91] or hydrogen (Table II.1) [94]. Traces of oxygen can also be detected.

The formation of CO_2 is believed to be a by-product of decarboxylation of acid groups in wood. CO may be due to a secondary 'water gas shift reaction', which forms CO by the reaction of CO_2 and steam with porous char at higher temperatures [91]. Another possibility of formation of CO is through other reactions catalyzed by transition metals present in biomass ash, which are also susceptible to catalyze water gas shift reaction, rather at gasification temperatures [99,114].

The production of CO is promoted by a high treatment temperature, while the CO_2 content in the gaseous mixture decreased [115]. This is represented by a decrease in the CO_2/CO ratio with the increasing treatment temperature. The amount of volatile species released also increases with the increasing torrefaction temperature [99].

1.2.2. Condensable products

Examples of condensable gases detected in several torrefaction experiments for different biomasses are listed in Table II.2.

The type and amount of volatiles released depend on the feedstock. In fact, torrefaction of deciduous wood is characterized by a more significant devolatilization and carbonization than torrefaction of coniferous wood [99]. At the same time, the volatile species produced also differ. Accordingly, acetic acid formation is enhanced by the presence of xylan (hardwood) in raw biomass, while glucomannan (softwood) leads to formic acid production. Prins explained this difference between willow and larch by the presence of acetoxy- and methoxy-groups attached to the xylose units of the deciduous wood, which form acetic acid and methanol under torrefaction conditions. Larch produce more formic acid due to its coniferous nature (Table II.2) [99].

Table II. 1. Non condensable gases detected in torrefaction experiments for several biomass types

Biomass	T (°C)	t (min)	Detection technique	CO_2	CO	CH_4	C_2H_4	H_2	Other	Source
Pine wood	300	120 min	GC off-line	X	X	-	-	-	-	[116]
Willow	250	5 – 15 – 30 min	Micro GC	M	X	T	-	T	-	[99]
Larch	250	5 – 15 – 30 min	Micro GC	M	X	T	-	T	-	
Straw	250	30 min	Micro GC	M	X	T	-	T	-	
Aspen	300	90 min	GCMS	X	X	X	-	X	-	[94]
Spruce	250	20 min	FTIR	M	X	X	X	X	-	[98]
Beech	250	20 min	FTIR	M	X	X	X	X	Propane, propene	
	285	20 min	FTIR	M	X	X	-	X	Propane, propene	
Beech	220	180 min	FTIR	M	X	-	-	-	-	[6]
	250	180 min	FTIR	M	X	-	-	-	-	
	280	180 min	FTIR	M	X	-	-	-	-	
	300	180 min	FTIR	M	X	-	-	-	-	
Leucaena	250	120 min	MS	X	X	-	-	-	-	[89]
Reed canary grass	290	45 min	FTIR	X	X	X	-	-	-	[21]
Pine	260	17.5 min	GC	X	X	-	-	-	-	[117]
Pine	250	60 min	GC	M	X	-	-	-	-	[23]
	280	60 min	GC	M	X	X	-	-	C2-hydrocarbons (ethane, ethene and acetylene)	
Lucern	250	60 min	GC	M	X	X	-	-	C2-hydrocarbons	
	280	60 min	GC	M	X	X	-	-	C2-hydrocarbons	
Bagasse	250	60 min	GC	M	X	-	-	-	C2-hydrocarbons	
	280	60 min	GC	M	X	X	-	-	C2-hydrocarbons	
Hemicelluloses (commercial)[a]	200-300	(10 °C/min)	FTIR	X	X	X	-	-	-	[46]

M: major (if identified); X: detected; T: traces.

[a] Commercial hemicelluloses: beta-glucan, arabino-galactan, arabinoxylan, galactomannan, glucomannan, xyloglucan, xylan.

Table II.2. Condensable gases detected in torrefaction experiments for several biomass types

Biomass	T (°C)	t (min)	Detection technique	Methanol	Ethanol	Phenol	Furfural	Hydroxy acetone	Acetic acid	Formic acid	Lactic acid	Levoglucosan	Formaldehyde	Acetaldehyde	Water	Other	Source
	230	50		X	-	-	X	X	M	X	X	-	-	-	M	-	[99]
	250	30		X	-	-	X	X	M	X	X	-	-	-	M	-	
Willow	270	15	Micro GC	X	-	-	X	X	M	X	X	-	-	-	M	-	
	290	10		X	-	-	X	X	M	X	X	-	-	-	M	-	
	300	10		X	-	-	X	X	M	X	X	-	-	-	M	-	
	230	50		X	-	-	X	X	X	M	X	-	-	-	M	-	
Larch	250	30	Micro GC	X	-	-	X	X	X	M	X	-	-	-	M	-	
	270	15		X	-	-	X	X	X	M	X	-	-	-	M	-	
	290	10		M	-	-	X	X	X	M	M	-	-	-	M	-	
Straw	250	30	Micro GC	X	-	-	X	X	M	X	X	-	-	-	X	-	
Aspen	300	90	GCMS	-		-	-	-	X	X	-	-	-	-	X	-	[94]
Spruce	250	20	FTIR/GCMS-FID	X	X	-	X	-	X	-	X	X	X	-	X	-	[98]
Beech	250	20	FTIR/GCMS-FID	X	X	-	X	-	X	-	X	X	X	X	X		
	285	20		X	X	-	X	-	X	X	X	X	X	X	X	Acetone	
	220	180		X	-	-	-	-	X	-	-	-	X	-	X	-	[6]
Beech	250	180	FTIR	X	-	-	X	-	X	X	-	-	X	-	X	-	
	280	180		X	-	-	X	-	X	X	-	-	X	-	X	-	
	300	180		X	-	-	X	-	X	X	-	-	X	-	X	-	
Leucaena	250	30	GCMS	-	-	-	-	-	X	-	-	-	-		X	Acetic anhydride	[89]
	275	30		-	-	-	X	-	X	-	-	-	-		X	3-Methylbutanol, Acetic anhydride	
Reed canary grass	290	45	FTIR	X	-	X	X	-	X	X	-	-	X	X	M	Phenol, acetone	[21]
Pine	260	17.5	GC	X	-		X	-	M	X	-	-	-	-	M	-	[117]
	220																[118]
Lauan	250	120	GCMS	[b]	[b]	X	[b]	[b]	[b]	[b]	[b]	[b]	[b]	[b]	[b]	Focused on phenols[b]	
	280																

M: major, X: detected. [a] Condensed gases analyzed in a GCMS which does not detect species with a molecular weight under 45. M: major, X: detected. [b] Experiment focused on aromatic compounds, other species usually present were not measured.

2. Influence of the operating conditions

2.1. Temperature and residence time

Temperature and residence time, also named holding time, are the most frequently studied parameters for biomass torrefaction in the literature. Their increase leads to a diminution in the solid yield, as the higher the temperature, the more oxygenated groups become unstable and are transformed into volatiles [119]. At the same time, aromaticity increases with increasing temperature due to the deoxygenation and dehydration reactions [120].

Torrefaction occurs between 200 and 300°C. At this temperature range, the three macromolecular components of the biomass are degraded at a different extent. While hemicellulose suffers a significant decomposition, cellulose and lignin are only slightly altered. This is explained by the fact that the degradation temperature ranges for the macromolecular components of the biomass does not overlap with the torrefaction temperatures range. Experimentally, Chen explained that torrefaction at 230°C and 260°C only impacted notably hemicelluloses, while if the temperature was increased to 290°C, cellulose also started to decompose [121]. Li proved by its experiments that a high temperature and long residence time resulted in a torrefied sample with low mass and energy yields [120].

On the other hand, the biomass type also influences the starting degradation temperature and its extent. Thus, Grønli demonstrated that softwood is more sensitive to temperature, as it started to degrade at lower temperatures than hardwood and their yield of char production are more important [122]. This can also be explained by the degradation temperatures of the macromolecular components, as softwood and hardwood differ in the proportions of their hemicellulose, cellulose and lignin, as well as in the internal structure [45].

In general, the impact of the torrefaction temperature is higher than the influence of the residence time [26].

2.2. Heating rate

The heating rate defines the type of torrefaction operation: static (isothermal) or dynamic (non-isothermal). Static torrefaction is characterized by a high heating rate from room temperature and then a holding time at isothermal conditions at the selected torrefaction temperature. As this operation mode is frequent for medium and high capacity units, it is also used in laboratory experiments [90,94]. On the other hand, dynamic torrefaction consists on applying a low heating rate until the selected temperature. This type of operation allows to study the evolution of the torrefaction with temperature [17,19,122,123]. Sometimes, a slow heating ramp and an isothermal stage are combined in torrefaction experiments [27,121]. It has been reported that heating rates until 50 K/min do not influence solid yield [18].

The selection of the heating rate and the operation mode affects significantly torrefaction

results. Heating rates between 1 and 100 K/min are considered as slow [116], while about 1000 K/min are considered as very fast [94]. A very slow heating will implicate that part of the weight loss occurs during the warm-up phase, which complicates the kinetic modelling of torrefaction. On the contrary, a very fast heating cannot ensure the kinetic control of the reaction because of the probable presence of heat transfer limitations. In torrefaction, the heating phase is quite short, as it goes from room temperature until about 200 to 250 °C, in function of the selected torrefaction temperature. That is the reason why it is commonly accepted that weight loss during the heating phase at low heating rates is not significant [99]. Nevertheless, other authors affirm that building models based on experiments at very fast heating rates permits to decouple transport and kinetic effects arising from temperature ramping [94].

The influence of the heating rate in torrefaction and pyrolysis experiments was studied in the literature. Williams observed that an increase in the heating rate from 5 to 80 K/min implied a transference of the maximum value of the weight loss curves to higher temperatures [116], presumably because of heat transfer limitations. Broström also confirmed this and justified the simultaneous use of experimental data from torrefaction experiments at different heating rates (here, h) in order to avoid possible compensation effects in the kinetic parameters. Several experiments also pointed out a slight increase of the volatile yield with the heating rate, while char yield and reactivity were also affected [17,19,124].

2.3. Atmosphere and pressure

Torrefaction is usually performed under an inert atmosphere. Nitrogen [18,100], helium [46,94] and argon [125] are the most common gases involved in torrefaction experiments. The influence of the selection of one of these gases in torrefaction was not found in the literature, but it was supposed to be negligible. The usual gas flow in torrefaction on thermobalance are between 25 et 100 mL/min [20,100,124]. For small lab-scale pilot devices, gas flows can oscillate between 0.5 and 5 L/h [27,97,125].

Torrefaction may also be carried out under oxidative conditions, by partially substituting the atmosphere by air or oxygen. In this case, two successive steps occur during biomass torrefaction: first ordinary torrefaction and then biomass oxidation [19,126], which is not observed in inert atmosphere. With oxidative torrefaction, an increase in oxygen concentration results in a lower degradation temperature and a higher decomposition rate [127,128]. At the same time, the solid yield decreases with an increase in reaction temperature or oxygen concentration [129–131]. It has also been demonstrated that the impact of torrefaction temperature prevails over the oxygen concentration [26].

Carbon dioxide has also been proposed in the literature as a suitable atmosphere for biomass torrefaction. The interest of this gas is its important percentage in the composition of the permanent gases released during torrefaction, which are susceptible to be recirculated to the

torrefaction process for its heating, which may result in lower operation costs [132]. Lu demonstrated that, at a given torrefaction temperature, using air and carbon dioxide as the carrier gas leads to a more significant diminution of the volatile matter present on the char produced, while its fixed carbon content is higher. These results suggest that the influence of the temperature in torrefaction results is more important than that of the carrier gas [100], which is not a common point of accord between torrefaction studies in the literature.

The influence of the addition of pressurized water to the biomass torrefaction atmosphere has derived into a sensibly different operation, named wet torrefaction. The char obtained in this type of torrefaction has been reported to be more hydrophobic and to present a higher energy density for the same mass yield. As wet torrefaction is carried out under high pressure and in presence of water vapor, the transformations in biomass components occur at lower temperature (180 to 260°C). Yan's experiments showed that hemicelluloses reactivity in water is higher, being completely converted at 260°C. In these conditions, both cellulose and lignin reacted to some extent [90]. On the other hand, the influence of the addition of water vapor to torrefaction at atmospheric pressure, as a certain relative moisture content, appears not to have been treated in the literature for the moment.

As torrefaction is typically carried out at atmospheric pressure, the influence of this parameter neither seems to have been analyzed in the literature for dry torrefaction yet. In the case of pyrolysis, the properties of the produced char, specially its reactivity, have been reported to be dependent of the pressure [19].

3. Phenomenology in biomass torrefaction

3.1. Physical phenomena

Physical phenomena involved in biomass torrefaction are heat and mass transfers. Heat transfer phenomena can be classified as:

- **External heat transfer phenomena:** they occur between the environment and the entity of study (bed or particle), thanks to:
  - *External convection*, through an external fluid at higher temperature, typically a gas.
  - *External radiation*, though an external source at higher temperature.

  External convection is usually the dominant external heat transfer phenomenon, while radiation predominates at higher temperatures, typically from 600 to 800 °C [133].
- **Internal heat transfer phenomena:** they are intrinsic to the entity of study (bed or particle):
  - *Internal conduction*, due to the gradient of temperatures from the border of the entity of study, externally heated, and the entity of study. Conduction happens between

particles in the bed or between areas at different temperature in the particle.

Internal conduction is the fastest heat transfer phenomenon both inside the bed and the particle, so internal radiation is supposed to be negligible (Figures II.1 and II.2) [18].

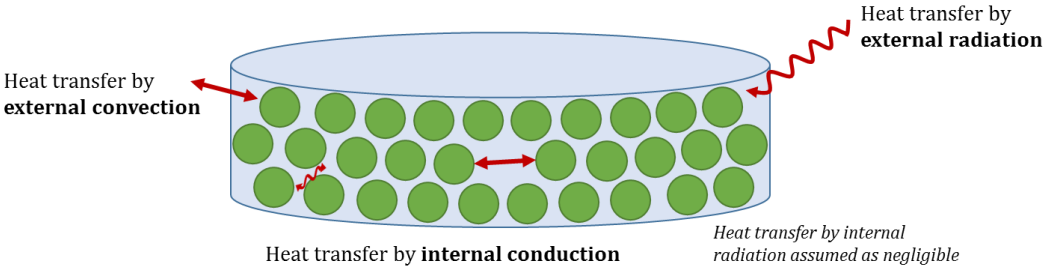


Figure II.1. Scheme of physical phenomena occurring in a bed of particles in biomass torrefaction

Both at bed and at particle scale, mass transfer of the gaseous products released in torrefaction happens by diffusion. However, this physical phenomenon can be considered as instantaneous in the bed of particles, and it can be neglected for the kinetic modelling. At particle-scale, it usually happens faster than thermal phenomena (Figure II.2) [18].

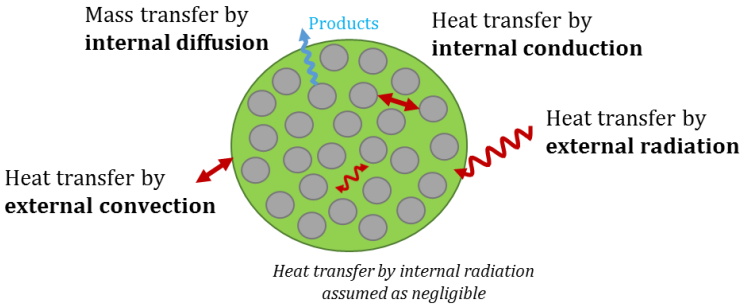


Figure II.2. Scheme of physical phenomena occurring in a particle in biomass torrefaction

3.2. Chemical phenomena

Chemical phenomena involved in biomass torrefaction are related to the degradation of the macromolecular components of biomass. Their proportion and distribution in the raw material are the critical properties determining the extent of biomass transformation through torrefaction.

Experimental studies have already demonstrated that the behavior in torrefaction of the three macromolecular components of biomass is significantly different [134,20,121,7]. In fact, they present different ranges of the thermal decomposition temperature (TDT), which corresponds to the interval of temperatures in the thermal treatment inducing the major percentage of their degradation.

- **Cellulose:** its high-organized crystalline structure makes its TDT range a bit higher than torrefaction temperatures, starting at 315 [9] to 325°C [116]. However, some authors have observed a beginning of its degradation at 275°C [135]. Cellulose is transformed until about 350°C [135], 375°C [22] or 400°C [9], depending on the studies. The major

decomposition happens between 330 and 370°C [29]. Its degradation in torrefaction is thus only limited.

- **Hemicelluloses:** this component is the first to degrade from temperatures about 225 [22] to 250°C [116], until temperatures about 325 to 350°C, according to the authors. As torrefaction typical temperatures are in this range (200-300°C), hemicelluloses are the most degraded component from biomass under these conditions.
- **Lignin:** it presents a progressive degradation during torrefaction. Its TDT range starts at about 200°C [116,135] to 250°C [99] until high pyrolysis temperatures about 500°C [22], 600°C [17], 720°C [116] or even 900°C, in function of the authors [9]. It is only partially degraded in the temperature range of torrefaction.
- **Extractives:** their influence on biomass thermochemical conversion has been very rarely studied in the literature [136,137]. Furthermore, most extractive species present lower volatilization temperatures and are supposed to be released at lower temperatures than torrefaction ones.
- **Ash:** some previous studies assessed the role of inorganic elements in thermochemical conversion. Even if this influence was clearly identified at gasification temperatures [71,138], their impact on biomass torrefaction still needs to be clarified. Some authors have signaled the influence of the presence of certain metals, like potassium (K), silicon (Si) and phosphorous (P), in the kinetics of biomass torrefaction [27,71,85]. These studies pointed out a catalytic effect of potassium on mass loss during torrefaction [139–141]. However the experiments carried out were based either on a direct addition or an impregnation with commercial compounds or a doping of a modified biomass structure. A study on the impact of this representation of inorganics in biomass structure would explain these results.

The main responsible of the solid transformation in torrefaction are hemicelluloses, which are the most degraded macromolecular component at torrefaction temperatures.

The behavior of the macromolecular components of biomass in torrefaction has been usually characterized through commercial compounds. The reason for such approach is often adopted due to the difficulties to extract these components directly from the biomass due to its complex structural matrix.

- **Cellulose** is typically extracted from biomass, after completely removing lignin by a chlorite treatment, by an acid hydrolysis. This treatment breaks the links with hemicellulose sugars and amorphous cellulose, which may affect cellulose reactivity. A weak acid treatment may allow to obtain a high crystalline structure, by removing only the amorphous part of cellulose. However, a strong acid treatment would lead to a more

degraded structure with a considerable decrease of the polymerization degree. The advantage of this treatment is that it preserves the crystalline cellulose allomorph I structure from native cellulose.

An alternative treatment proposed consists in the alkaline solubilization of residual hemicelluloses. This treatment allows to preserve amorphous zones of cellulose, as well as a higher polymerization degree of the cellulose chains. In counterparty, due to the high concentration of alkali, the treatment changes the cellulose crystalline structure to a type II due to mercerization.

- The main **hemicelluloses** fraction is typically obtained by DMSO (dimethyl sulfoxide) extraction (also after removing lignin by chlorite). This fraction does not contain all hemicelluloses in biomass. Therefore, a secondary fraction can be isolated from the residue after DMSO extraction though a strong alkaline treatment which separates cellulose and residual hemicelluloses. However, the hemicellulose structure is slightly modified, principally in terms of its acetyl group content, removed by the treatment.
- **Lignin** can be extracted from biomass through the dioxane procedure, the milled wood lignin and the Klason lignin. Milled wood lignin involves very long ball milling followed by purification steps and finally a dioxane extraction. This method leads to low yields of production, being the purity only moderate. The Klason procedure was shown to be suitable to quantify lignin in biomass, but not to extract it, as the strong acid treatment applied influences the condensation degree of the lignin structure. Recently, the enzymatic mild acidolysis for lignin obtention (EMAL) was proposed [142]. Even if this technique produces a lignin of excellent purity, the yields of production remain low. Lignin extraction from raw biomass through dioxane allows to obtain a compromise between a good purity and an acceptable yield [62]. This method was chosen in this study.

Two different types of mechanisms were identified in the thermal conversion of biomass constituents, from low temperature to pyrolysis conditions:

- **Primary mechanisms:** they refer to the transformations happening in the solid matrix, principally consisting in the degradation of biomass macromolecular components through chemical bond scission. In function of the nature of the bonds broken, three pathways were described [119]:
  - *Char formation*: it consists in the conversion of raw biomass in a solid residue with a higher reticulation degree and thermal stability. This transformation happens thanks to intra- and intermolecular rearrangement reactions, typically forming aromatic rings which associate together into a polycyclic structure. Water and permanent gases are released in this process.
  - *Depolymerization*: it implies bond breaking between the monomeric units composing

biomass constituents, followed by a stabilization of the two smaller chains formed. The polymerization degree of the macromolecular component is lowered. This process continues until the chains formed are volatile molecules. As a result, the molecules usually formed resemble to the monomeric unit of the macromolecular component from which they are derived. This process is enhanced by high temperatures and heating rates.

- *Fragmentation*: it consists in the scission of covalent bonds in the macromolecular component that releases low molecular weight species, such as permanent gases and condensable species. Due to the high energy contained in covalent bonds, this process is favored at higher temperatures and is only rarely observed in torrefaction.

- **Secondary mechanisms:** they describe reactions of stabilization of the volatile species released [119]. This includes:
  - *Cracking*: chemical bonds in volatile species are broken to stabilize them into lower molecular weight species. The resulting molecules are similar to those from the fragmentation mechanism, which make differentiation of these two pathways difficult.
  - *Recombination or recondensation*: it implies the formation of chemical bonds between volatile compounds to stabilize them, which can affect their volatility. This mechanism requires pyrolysis temperatures.

In the next section, the chemical phenomena involved in the transformation of cellulose, hemicellulose and lignin in torrefaction are discussed (synthesis on Table II.3).

3.2.1. Cellulose

Cellulose degradation was deeply studied in the literature, frequently under pyrolysis temperatures due to its TDT range [143–149,107,150–155,108]. Specific studies were carried out about macromolecular components behavior in torrefaction, including cellulose [7,56,121,156]. However, these studies were usually carried out by considering commercial microcrystalline cellulose as model compound, which may differ from the native cellulose in biomass in terms of average molecular weight and polymerization degree. These parameters are strongly dependent on the severity of the extraction procedure used for isolating cellulose. Acid hydrolysis is generally used for the extraction of the most common commercial microcrystalline celluloses in the market. It mainly consists in a strong acid attack, which has shown to notably impact the reactivity and crystallinity of cellulose. Even if the cellulose extracted by this method keeps the type I structure as native cellulose in biomass, its behavior was strongly modified [53].

The main steps in the transformation of cellulose through thermal conversion are the transformation of the raw cellulose into an active cellulose, also named anhydrocellulose, and the depolymerization.

The formation of an intermediate was identified as the first step in cellulose thermal conversion, called active cellulose or anhydrocellulose, in function of the mechanism leading to its production. Some authors suggested that this intermediate was formed through a partial depolymerization of cellulose, forming levoglucosan (Figure II.3, A), then further decomposed into char and volatiles. However, there are still many points of disaccord about the properties of this intermediate and the concrete mechanism of its formation [157]. Other authors proposed also a dehydration reaction to achieve the intermediate under the form of anhydrocellulose, releasing water, CO and CO_2 in its formation [145,158,159]. A review of this topic summarized the formation of the cellulose intermediate by both concurrent reactions, the heating rate being the determining factor for the dominance of one or other mechanism [119].

Dehydration reactions were already detected at low torrefaction temperatures, firstly producing water (from 200°C) and then releasing CO, CO_2 and small organic compounds (rather from 280°C) [160]. Water elimination can be intermolecular from the beginning of torrefaction, through hydrogen bonds between two cellulose chains. This mechanism increases the reticulation degree of the cellulose polymer through the formation of supplementary covalent bonds. A second dehydration mechanism, from later intermediate torrefaction temperatures, is intramolecular, from the glucopyranose unit. This pathway leads to the formation of carbon-carbon double bonds (C=C) and aromatic rings in the solid residue [159].

Cellulose transformation through depolymerization reactions may start before 300 °C. This mechanism, also named transglycosylation, consists in the scission of the β-1,4 glycosidic linkage between glucopyranose units, which leads to the formation of levoglucosan. Water released in simultaneous dehydration reactions was identified to take part in this transformation [159].

The highest cellulose decomposition was signaled to happen beyond 300°C, as the reactivity of the glucosidic bond between cellulose monomers rises significantly. Levoglucosan is still formed, also under the dehydrated form of levoglucosenone, together with a high proportion of anhydro-oligosaccharides and anhydro-saccharides. Levoglucosan can suffer a secondary reaction of contraction of the pyran ring and appear in a furan form, more stable. This transformation happens also in the char residue (Figure II.3, B) [154]. This transformation implies the elimination of some oxygenated groups and the formation of C=C bonds leading to furan rings in the char. In this degradation phase, some furan-type volatile species are also detected (5-hydroxymethylfurfural (5-HMF), 5-methylfurfural, furfural and furfury alcohol, Figure II.3, C). They can be formed through similar mechanisms of scission of relatively weak linkages, either by direct ring-opening and rearrangement reactions from the depolymerization from cellulose monomers or by secondary reactions of levoglucosan. Furfural, also detected in significant amounts, was proposed to be formed through the dehydroxymethylation of the side chain of the furan ring of the 5-HMF. Other proposed mechanism was from secondary reactions of 5-HMF, leading to rearrangement reactions to form aryl compounds, such as phenol [152]. Finally,

depolymerization reactions also lead to unstable fragments with carbonyl and carboxyl functions, which suffer dehydration and fragmentation stabilization reactions. Water, CO, CO_2 and low molecular weight organic compounds (hydroxyacetaldehyde, acetaldehyde, hydroxyacetone) are released as a result of these reactions [161]. However, other works pointed out hydroxyacetone as mainly produced from the direct conversion of cellulose molecules and partly from the secondary decomposition of levoglucosan [152].

At higher temperatures, rather in the pyrolysis temperature range, the cellulose char continues to be transformed into a more aromatic structure (charring process). This transformation continues until 800 °C, releasing methane (CH_4), CO and H_2 [152].

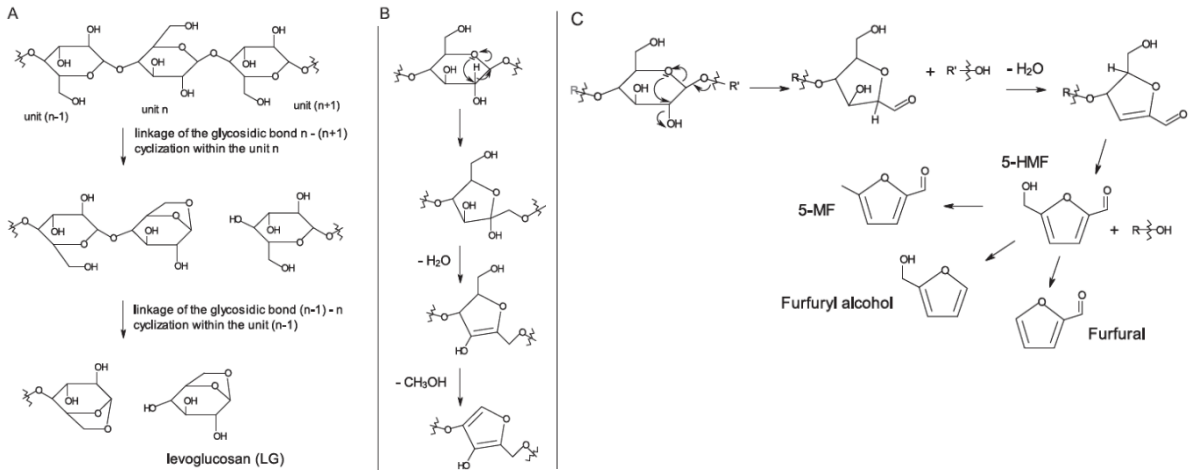


Figure II.3. Mechanisms proposed for the cellulose conversion into levoglucosan (A), cyclization of the glucopyranose monomer into a furan ring (B) and formation of furan volatile compounds (C) [119]

3.2.2. Hemicelluloses

The major part of the degradation of hemicelluloses in thermochemical conversion was reported to happen in the torrefaction temperature range, for temperatures going until 350°C. Its conversion is strongly affected by the sugar composition [46]. Indeed, xylan-based hemicelluloses, such as those from deciduous wood, would be more reactive and more easily degradable than mannan-based hemicelluloses, principally corresponding to those from coniferous wood [22].

As for cellulose, hemicelluloses behavior in torrefaction was traditionally characterized through commercial compounds, namely xylan and, in some cases, also by glucomannan [6,162]. The heterogeneity in the structural units of hemicellulose and their position between cellulose microfibrils in biomass, linked to them, make their extraction from biomass difficult.

The mechanism of hemicelluloses degradation starts by a dehydration and a rupture of the less stable linkages, followed by a depolymerization of the main chain, composed by xylopyranose units in the case of xylan and mannopyranose units in the case of mannan. At temperatures higher than the torrefaction ones (> 350°C), the rearrangement of the residue might occur

during the charring process.

The release of water is enhanced from 200°C. At this temperature, methanol and formic acid start to be released, as a consequence of the breaking of weak linkages between small substituents and the main polymer chains. Methanol is produced from the rupture of the methoxy- group of the 4-O-methyl-α-D-glucuronic acid [99], while formic acid derives from the scission of the carboxylic group from the hexuronic acids. A similar mechanism to that of formic acid was proposed for the production of propionic acid [163]. When temperature increases, the elimination of the O-acetyl groups linked to the main xylan chain is enhanced and leads to the main production of acetic acid [57,164]. A secondary pathway was described, consisting of a production by the 4-O-methylglucuronic acid after the elimination of the carbonyl and O-methyl groups [163].

Depolymerization reactions were reported to start from 220°C, with the detection of furfural from this temperature. These reactions principally lead to furan production, as these compounds are directly derived from hexose and pentose building blocks from hemicelluloses. At low to intermediate torrefaction temperatures, depolymerization of terminal and lateral elements of the xylan chains would occur. This mechanisms is strongly enhanced by rising temperature, as glycosidic linkages become unstable and the scission of intermediate units of the hemicellulose chains also happens [119]. Hexose-based sugars, such as glucomannan, also lead to a high production of furan compounds, as the pyran rings can suffer a rearrangement to more stable xylan rings [162]. Hemicellulose depolymerization produces unstable intermediaries with new chemical functions. These fractions suffer dehydration, fragmentation and secondary reaction, which results in the production of small compounds such as linear ketones (principally hydroxyacetone), cyclopentenones and acetic acid [46,99,162,165–168].

At temperatures higher than 300°C, the formation of methylphenols and other phenolic compounds with small substituents was reported [29,165]. This process is a consequence of the charring of the solid residue, whose aromaticity increases with temperature.

Shen proposed a mechanism of degradation of xylan-based hemicelluloses (Figure II.4A and B). This mechanism occurs under torrefaction conditions, with the exception of the pathways leading to the formation of CO and methane, which would happen at pyrolysis temperatures. It presents the formation of the main volatile species derived from hemicelluloses in torrefaction.

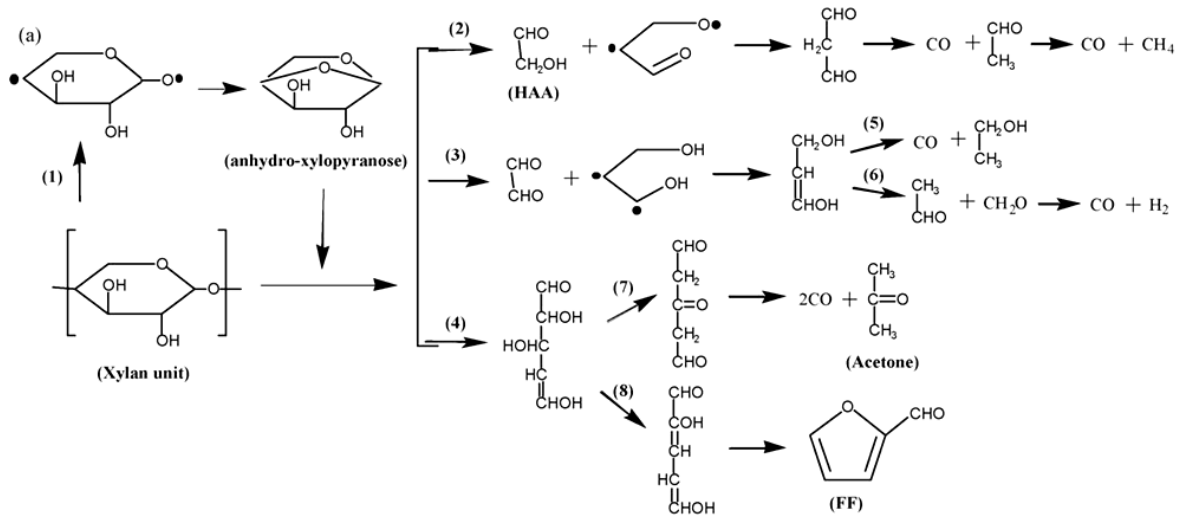


Figure II.4A. Mechanisms proposed for the conversion of the xylan-based hemicelluloses represented by the main xylan chain [163]

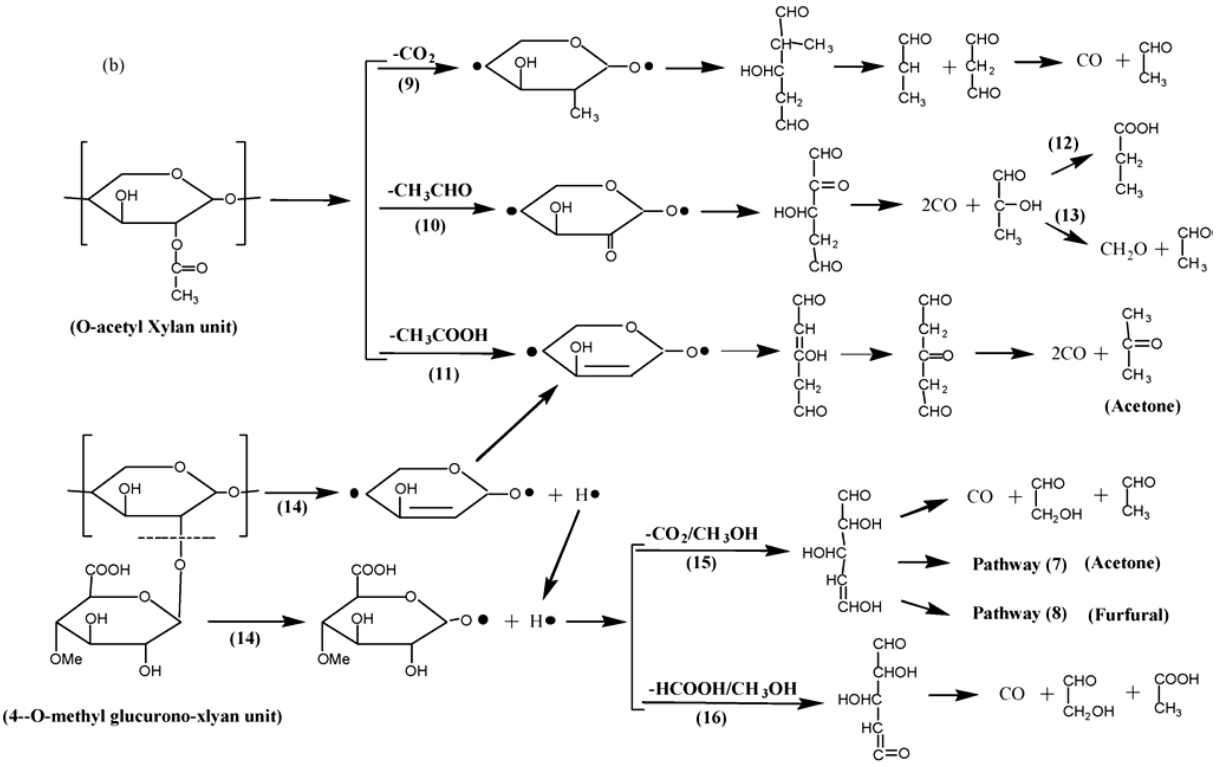


Figure II.4B. Mechanisms proposed for the conversion of the xylan-based hemicelluloses represented by the O-acetyl xylan unit (b) and the 4-O-methylglucuronic acid unit (c) [163]

3.2.3. Lignin

Lignin is only partially degraded under the torrefaction temperature, even if its degradation smoothly starts from low to intermediate torrefaction temperatures.

Lignin degradation was deeply studied under pyrolysis conditions and by Py-GC/MS experiments, which allowed to elucidate its complete degradation pathway [169–173]. According to these studies, a separation with the increasing pyrolysis temperature was observed for lignin units in function of the length and the chemical nature of the substituents of the

phenolic rings. Higher dissociation energy is needed for the degradation of carbon-carbon than carbon-oxygen bonds among lignin units [174]. As a result, G- and S- phenolic derivatives containing C=C and C=O structures in side chain were reported to be formed in a primary pyrolysis stage in the temperature range of 200-400 °C, in which β-ether bond is degraded. Then, the formation of the G- and S-type derivatives with a double bond in the side-chain, namely 4-vinylguaiacol and 4-vinylsyringol, tended to occur at lower pyrolysis temperatures compared to the formation of the saturated 2-C-side-chain derivatives, namely 4-ethylguaiacol and ethylsyringol. The short side-chain derivatives (1-C) such as 4-methylguaiacol and 4-methylsyringol would be derived from secondary pyrolysis cracking reactions of the side-chain C–C bonds. This scission increases the monomer yields and implies the transition of the products from unsaturated to saturated alkyls side chains [174]. Finally, at higher pyrolysis temperatures, the basic lignin structures were released, namely guaiacol and syringol. They correspond to the basic-non-substituted-structure of lignin, which explains their more difficult removal from biomass structure. They could come from secondary pyrolysis reactions involving the rupture of ramifications between aromatic rings [47]. However, these products can also be formed from the condensed lignin substructures similar as methyl derivatives [175,176]. Some authors have pointed out that this moment corresponds to the highest decomposition rate of lignin and the maximum production of phenols [177,178].

Under torrefaction conditions, dehydration reactions through the hydroxyl substituents of the phenolic rings occur from low temperatures. When the hydroxyl group is linked to the C-γ of the phenylpropane unit, the scission between this carbon and the contiguous one leads to the formation of formaldehyde. The degradation of the β-O-4 bonds, the most common one in lignin structure, happens from intermediate torrefaction temperatures. It is related to the release of substituted phenolic compounds close to the original structure of lignin [29,179]. This includes phenolic compounds with oxygenated substituents, such as eugenol, isoeugenol and vanillin, as well as with saturated side-chains, such as 2-methoxy-4-vinylphenol. However, according to the previous studies from the literature, the production in torrefaction of phenolic compounds with small side-chains, such as phenol and guaiacol, seems rare and these compounds might be derived from hemicelluloses. The scission of the β-O-4 bonds, as well as of small side-chains of the phenolic groups, can lead to the release of functional groups, such as hydroxyl groups present in the α-carbon of the propyl side chain [175]. These groups lead to the production of small molecules, such as hydroxyacetone and acetic acid, but in a minor extent than hemicelluloses [29].

Table II.3. Origin and proposed mechanism of formation of volatile species in biomass torrefaction

Chemical compound	Literature cell	hem	lign	Mechanism	Torref T	Source
Acids		**X**		Dehydration, fragmentation and secondary reactions of unstable intermediaries from depolymerization	~ to ↑ T	[46,99,165–168]
	X				↑ T	[161]
			X	Scission of β-O-4 bonds or of small side chains of the phenylpropane units		[175]
acetic acid		**X**		- elimination of O-acetyl groups linked to the main xylan chain	~ to ↑ T	[57,164]
		X		- 4-O-methylglucuronic acid after elimination of C=O, O-CH_3 (secondary pathway)		[163]
formic, propionic acid		**X**		Scission of the carboxylic group from the hexuronic acids		[163]
Furans	**X**			Scission of relatively weak linkages by: a)direct ring-opening and rearrangement during depolymerization; b) secondary reactions of levoglucosan		[152]
		X		Depolymerization reactions:	> 220°C	[119]
				- of terminal and lateral elements of xylan chains	↓ to ↑ T	
				- of glycosidic linkages between intermediate hemicellulose sugar units	~ to ↑ T	
				- of pyran rings (hexoses), through rearrangement in more stable xylan (pentose) rings	~ to ↑ T	[162]
furfural	**X**	**X**		a) dehydroxymethylation of the side chain of the furan ring of 5-HMF; b)rearrangement reactions of 5-HMF		[152]
Phenols			**X**	Degradation of the β-O-4 bonds, the most common in lignin structure, releasing substituted phenolic compounds close to the original structure of lignin	~ to ↑ T	[29,179]
	X			rearrangement reactions of 5-HMF and furfural to form aryl compounds		[152]
		X		Charring of solid residue (methylphenols and phenolic compounds with small substituents)	> 300°C	[29,165]
phenol, guaiacol, syringol			**X**	Degradation of the β-O-4 bonds	↑ T	[29,179]
2-methoxy-4-vinylphenol			**X**			
eugenol			**X**	Degradation of the β-O-4 bonds	~ to ↑ T	[29,179]
vanillin			**X**			
Linear ketones	X			Dehydration, fragmentation and secondary reactions of unstable intermediaries from depolymerization	> 280°C	[160]
		X			~ to ↑ T	
hydroxyacetone	X			Secondary decomposition of levoglucosan		[152]
		X		Dehydration, fragmentation and secondary reactions of unstable intermediaries from depolymerization		
			X	From hydroxyl groups from the C- α of the side chain of the phenylpropane unit		[175]
Cyclic ketones		**X**		Dehydration, fragmentation and secondary reactions of unstable intermediaries from depolymerization	~ to ↑ T	[46,99,165–168]
methanol		**X**		Rupture of methoxy- group of 4-O-methyl-α-D-glucuronic acid		[99]
formaldehyde			**X**	scission of C-γ of phenylpropane unit with OH and the contiguous C (dehydration)	↓ to ↑ T	[29,179]
levoglucosan	**X**			scission of the β-1,4 glycosidic linkage between glucopyranose monomeric units (transglycosylation)	≥ 300	[159]

X: proposed origin in the literature; **X:** main mechanism

3.3. Characteristic time analysis

The characteristic time of a phenomenon is defined as the theoretical time needed for the process to occur entirely when the process is only controlled by the involved phenomenon [180]. In order to compare characteristic times of phenomena, several dimensionless numbers were defined. They compare chemical reaction to external convection (Dämkholer number, Da) [181] or to internal conduction (pyrolysis number, Py) [182].

Two scales must be considered in the characteristic time analysis: bed- and particle-scale [114,180]. Bed-scale analysis refers to the characteristic time analysis in the bed of particles of a given device or experiment, while particle-scale analysis focuses this analysis on a single isolated particle inside the bed. In both cases, thermal and chemical phenomena occurring during torrefaction, either in the bed of particles or around and inside the single particle, are studied. These phenomena will be described in the next sections.

A characteristic time study of the regime of transformation in pyrolysis experiments has already been presented [183]. In this study, the influence of the particle size and the temperature in the regime that governs this process has been presented as a regime map at particle-scale. Nevertheless, characteristic time analysis for torrefaction has only been briefly discussed by two authors in the literature [22,114], concluding that chemical regime is generally attained under torrefaction conditions. This chemical regime was directly assumed with no justification by other authors in their torrefaction experiments [94]. Furthermore, due to the lower torrefaction temperatures compared to those from pyrolysis and gasification, bed-scale characteristic time analysis in torrefaction devices was often neglected.

4. Modelling of biomass torrefaction

Some authors considered torrefaction as a mild pyrolysis process, as its temperature range corresponds to the lower pyrolysis temperatures [124,125,184]. The results presented in the literature following this approach are also considered for biomass torrefaction.

The most common modelling schemes proposed for pyrolysis, both for biomass and for its macromolecular components, consist of one or several consecutive or parallel reactions. The evolution of the proposed models is traced in Tables II.4 and II.5.

Cellulose pyrolysis was the most common modelled compound since the beginning of pyrolysis modelling, with a first review on the topic carried out by Shafizadeh in 1982 [185]. Initial cellulose models were based on the formation of active cellulose as the first step in cellulose pyrolysis. These schemes were strongly analyzed, discussed, partially modified and completed until nowadays (Table II.4). However, one of the most controversial points is the nature of active cellulose [157], which is still unknown [186]. It was recently associated with the formation of reducing end groups in the cellulose macromolecule, which are supposed to activate crystalline

cellulose [187].

Biomass pyrolysis models started to be developed by Shafizadeh and Chin, who proposed a global scheme of three competitive reactions in parallel leading to the formation of gas, liquids (tar) and char [188] (Table II.4). A modification of this model was proposed by Koufopanos [189], who added intermediate common mechanism for the formation of gases and condensable species.

Pyrolysis models are developed by the fitting technique with experimental data, which typically supposes a first reaction rate for a sequence of simultaneous and/or consecutive reactions of known or representative stoichiometry. To do this, the 2-succesive-step model developed by Di Blasi and Lanzetta [58] is one of the most used kinetic schemes nowadays (Table II.4). It considers the competition between the formation of volatiles and solid products shown at each step. Initially developed for hardwood hemicelluloses based on xylan, it was then applied to numerous models describing biomass pyrolysis through its macromolecular components [22,7,162,122,19]. One example of application was carried out by Prins, who estimated the kinetics of wood torrefaction [22,99]. Volatile species composition for each reaction of the Di Blasi scheme was calculated by Bates and Ghoniem for willow[17], based on the kinetics and analysis of products from Prins. Nocquet proposed a kinetic model for beech based on the behavior of commercial cellulose, xylan and lignin, by adding the influence of the acetyl groups content [7].

A new generation of pyrolysis models started with the model proposed by Ranzi [190] (Table II.5). This model is based on a lumped chemical mechanism based on cellulose, hemicelluloses and three phenolic model compounds for lignin. This kind of models consists of regrouping or “lumping” organic compounds with similar chemical formula, so as to treat them as a single representative species. The Ranzi model reaffirmed the importance of considering the behavior of biomass macromolecular components to predict the global behavior of biomass in torrefaction. This approach facilitated the application of the model to a large panel of biomasses. This model was proved to correctly predict solid mass loss evolution in TGA and fast pyrolysis experiments [186]. The prediction of gaseous product yields was strongly improved by the Ranzi model, which includes the main permanent gases, hydroxymethylfurfural, some phenolic compounds, alcohols and ketones. However, this model shows its limitations principally by considering xylan as representative of hemicelluloses and not considering neither inorganic elements in biomass, which might play a role in pyrolysis conditions, nor interactions between macromolecular components. Furthermore, secondary charring reactions are not described. The Ranzi model was further developed and modified by several authors [98,191–194].

Anca-Couce proposed a modified Ranzi Model (the RAC model), in which these reactions are described and the influence of the inorganic elements is partially taken into account [98,186,193].

However, a higher level of detail is still required to describe how macromolecular components are transformed though torrefaction and, by extension, pyrolysis. The work carried out by Dussan essentially contributed to this . Based on the Ranzi model, together with existing data on biomass pyrolysis and torrefaction, and considering a higher level of detail in biomass characterization, she proposed a more detailed mechanism of transformation of hemicelluloses and lignin through torrefaction. In the first case, five model compounds were selected to reproduce the main sugar units of hemicelluloses from woody, herbaceous and agricultural biomasses (xylan with acetyl and 4-methyl-D-glucuronic acid groups, arabinoxylan, xyloglucan, glucomannan and β-glucan). Mechanisms associated to pentose and hexose-based sugars are described, which overcomes the limitation of exclusively using xylan in previous models (Figure II.5, compounds highlighted in blue were added in comparison to the Ranzi model) [195].

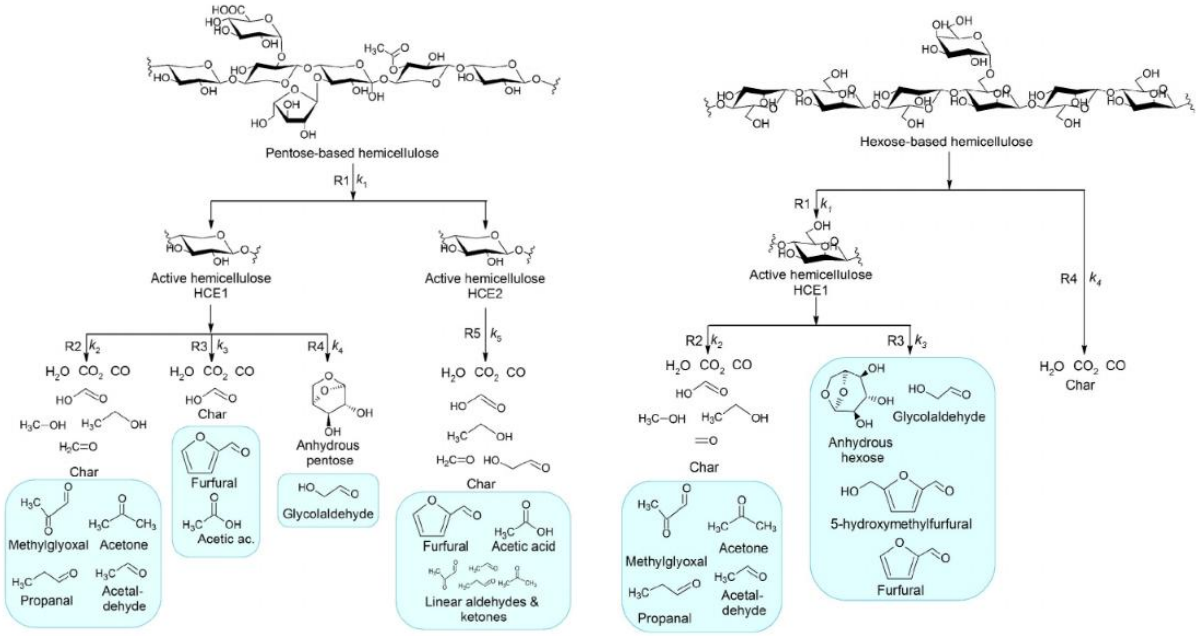


Figure II.5. Reaction mechanism scheme of the pyrolytic conversion of pentose (left) and hexose (right)-based hemicellulose model compounds [195]

Dussan also proposed a detailed model for the conversion of lignin in torrefaction [196]. It relies on the definition of dimeric pseudo-components containing phenolic functionalities. These dimers consist of two base units of lignin, namely, p-hydroxyphenyl, guaiacyl and syringyl groups, linked through β–O–4' aryl ether bonds. The composition of lignin from woody, herbaceous and agricultural biomasses on its base units was considered from measurements in real biomass and native lignin through wet derivatization (methoxyl group content) and non-destructive spectroscopic techniques (NMR). Data from pyrolysis experiments on lignin in the literature was also considered to test the model. The proposed model accurately describes the effects of heating rate and temperature on the product distribution from lignin pyrolysis. It also achieves a better prediction of the monoaromatic content of the condensable products. However, more detailed data about lignin conversion through pyrolysis and torrefaction, as well as about cellulose and hemicelluloses, would be required to continue refining these models.

Table II.4. Synthesis of the evolution of the pyrolysis models applicable to torrefaction

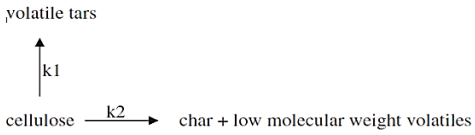
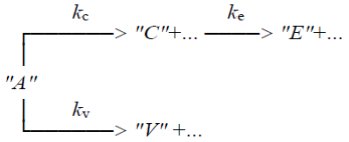
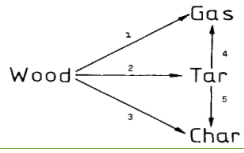
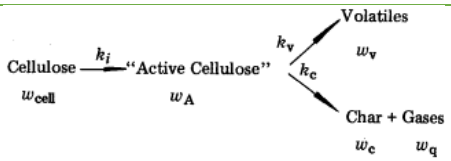
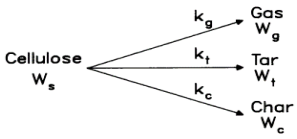
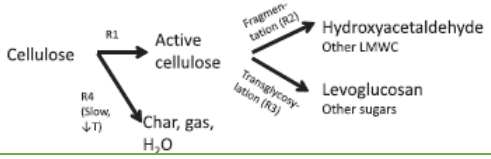
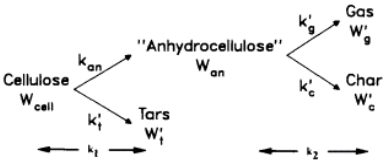
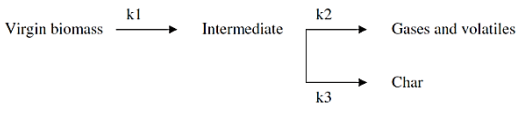
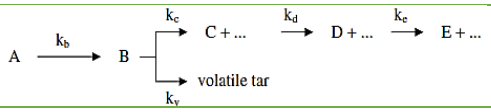
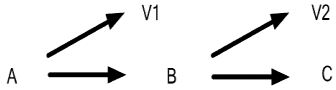
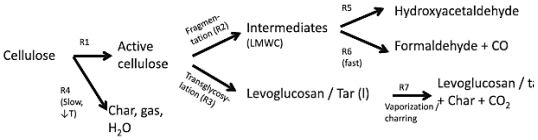
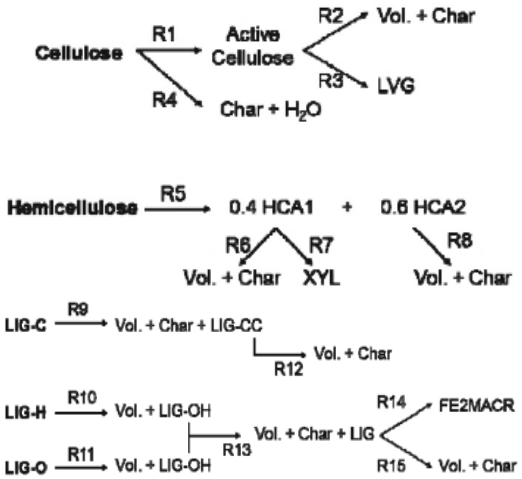
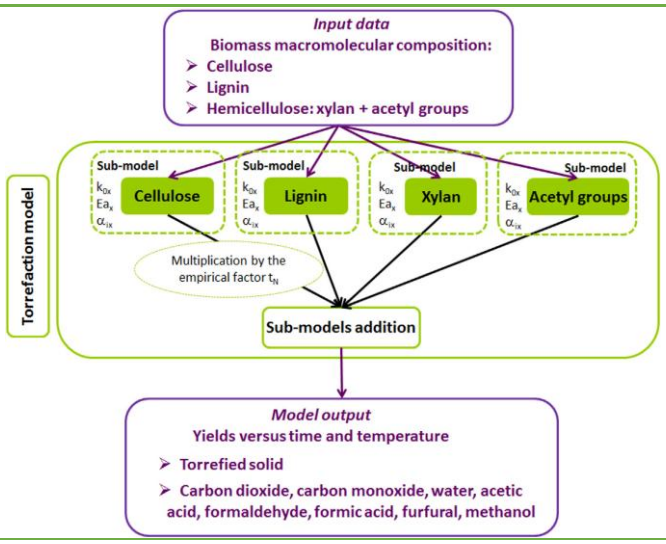
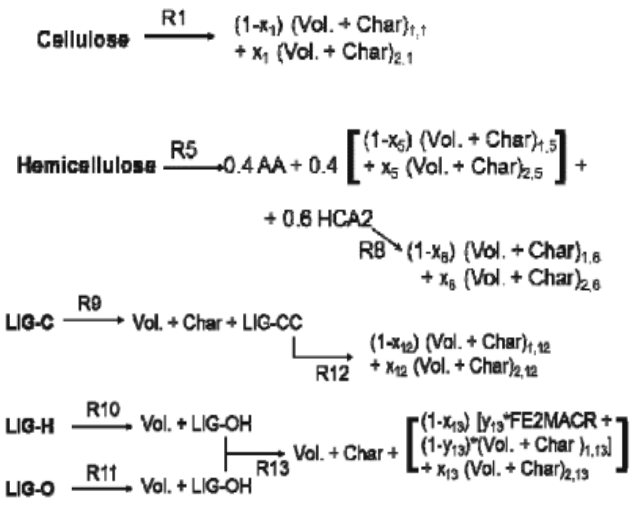
Name	Year	Scheme	Process	T (°C)	Ref.	Used in
Kilzer, Broido	1969 - 1975		Cellulose low temperature pyrolysis	370	[146, 197]	
Arseneau	1971		Thermal decomposition of cellulose	200 - 270	[145]	[198]
Shafizadeh, Chin	1977		Wood torrefaction/ mild pyrolysis	300-400	[199]	[188]
Broido-Shafizadeh and Bradbury	1979		Cellulose torrefaction/ mild pyrolysis	250-340	[147]	
Thurner and Mann (1981), then Kilzer-Broido (1988)	1981 - 1988		Cellulose torrefaction	300-400	[200]	[99,22, 58,201, 202,96, 16]
Piskorz	1988		Cellulose pyrolysis	300-800	[158]	
Modified Kilzer-Broido Model by Agrawal	1988		Cellulose torrefaction	250 - 360	[148, 149]	
Koufopanos	1989		Biomass pyrolysis	100 - 440	[189]	
Broido-Shafizadeh (revVárhegyi)	1994		Cellulose pyrolysis	220 - 370	[198]	[96,125]
Di Blasi-Lanzetta	1997		Pyrolysis (developed for hemicelluloses)	200 - 340	[58]	[134,7, 96,80]
Banyasz	2001		Cellulose pyrolysis	400 - 800	[203]	
Klinger	2013	$Biomass \xrightarrow{k_{1,i}} R_1 + \sum \alpha_{1,i} P_{1,i}$ $R_{j-1} \xrightarrow{k_{j,i}} R_j + \sum \alpha_{j,i} P_{j,i}$	Unified model torrefaction/ pyrolysis	260 - 425	[94,204]	

Table II.5. Synthesis of the evolution of the detailed pyrolysis models applicable to torrefaction

Name	Year	Scheme	Process	T (°C)	Ref.
Ranzi	2008 – 2015		Pyrolysis	150 - 450	[125–127, 129]
Nocquet	2014		Torrefaction	200 – 300	[7]
Anca-Couce	2016	 ** Adapted from pyrolysis model proposed by Ranzi (2008)*	Torrefaction	150 - 450	[193]
Dussan	2017	Detailed model for hexose-based and pentose-based sugars in hemicelluloses pyrolysis *(details in* [195]*)*	Pyrolysis	150 - 450	[195]
Dussan	2018	Detailed model for lignin pyrolysis based on β–O–4' linked dimers of lignin base units *(details in* [196]*)*	Pyrolysis	150 - 450	[196]

5. Conclusion and approach

Biomass structure was deeply described in the literature. However, some elements still need to be clarified, such as the lignin structure and the interactions between macromolecular components.

Previous torrefaction studies typically considered isothermal conditions. Including non-isothermal and isothermal conditions in the same experiment is not frequent. Furthermore, chemical regime is not always checked and often directly assumed, which is controversial, especially at bed-scale.

Many studies described the nature and the proportions of water and permanent gases, principally CO and CO_2. When dealing with the condensable fraction of the torrefaction emissions, the studies are less frequent and are usually focused on a reduced number of species. Furthermore, the influence of torrefaction temperature on the volatile species production is seldom described.

Models exclusively developed for torrefaction were not proposed, as pyrolysis models were considered valid in this case. The most recurrent approach to represent biomass behavior in torrefaction is through the individual behavior of cellulose, hemicelluloses and lignin, typically considered as additive and weighted by the macromolecular composition of the raw material. The influence of ash under torrefaction conditions was not completely elucidated. Extractives are supposed to be removed from biomass at lower temperatures than those required for torrefaction.

Torrefaction models were usually developed by considering commercial compounds to represent biomass macromolecular components. This choice is mainly justified by the challenge of extracting representative cellulose, hemicelluloses and lignin from biomass. This representation through commercial compounds does not allow to distinguish between different biomasses, which was shown to be crucial for the biomass behavior in torrefaction. Last studies proposed a more detailed definition of cellulose, hemicelluloses and lignin composition and structure, leading to a better representation of solid mass loss and gases release in biomass torrefaction.

As a consequence of this state-of-the-art, the selected approach for this work proposes to:

- Consider a larger biomass database than in previous studies, so as to improve the representativeness of resource heterogeneity.
- Select operating conditions for biomass torrefaction ensuring the chemical regime.
- Propose an optimized extraction procedure to obtain extracted cellulose, hemicelluloses and lignin from different biomasses.
- Simultaneously study solid mass loss and volatile species release in biomass torrefaction at lab-scale in function of time and temperature.

- Assess the influence of interactions between cellulose, hemicelluloses and lignin in biomass torrefaction in function of the biomass type.
- Improve the additive model based on the macromolecular composition of biomass by substituting commercial compounds by extracted cellulose, hemicelluloses and lignin.

-III-

MATERIALS AND METHODS

III. MATERIALS AND METHODS

In this section, raw biomasses are presented and characterized, among which a reduced number is selected as reference biomasses. Secondly, the optimized extraction procedure to obtain macromolecular components from the reference biomasses is presented and the extracted fractions are characterized. Thirdly, the experimental set-up selected for biomass torrefaction experiments, composed of a TGA-GC/MS coupled through a heated storage loop system, is introduced. In parallel, the experimental procedure for the torrefaction experiments and the methodology of the data treatment are applied to the results obtained.

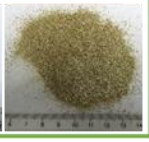
1. Raw materials

1.1. Raw biomasses

14 biomass samples were selected in order to represent European diversity, while taking into account potential availability for energy recovery (Table III.1). They were classified according to the following families:

- Coniferous wood: pine, pine forest residues and Scot pine bark.
- Deciduous wood: ash wood, beech, poplar and willow.
- Herbaceous crops: miscanthus and reed canary grass.
- Agricultural by-products: corn cob, grape seed cake, sunflower seed shells and wheat straw (2 types).

Table III.1. Biomass samples (raw and after preparation, < 500µm)

	Deciduous wood				**Coniferous wood**		
	Ash-wood	Beech	Poplar	Willow	Pine	Pine forest residues	Scot pine bark
Raw							
< 500 µm							
	Herbaceous crops		**Agricultural by-products**				
	Miscanthus	Reed canary grass	Corn cob	Grape seed cake	Sunflower shells	Wheat straw (French)	Wheat straw (Swedish)
Raw							
< 500 µm							

Pine forest residues, Scot pine bark, reed canary grass and one sample of wheat straw were harvested in Sweden. The other samples were harvested in the South of France. Biomass sample preparation is described in Table III.2.

Table III.2. Biomass preparation steps

Operation	**drying**	**shredding**	**grinding**	**sampling**
Device/procedure	blowing heated air (40-60°C) through a perforated floor	Lindner Micromat 2000 (Linder-Recylingtech GmbH, Spittal, Austria)	Universal cutting mill Fritsch Pulverisette 19 (Fritsch GmbH, Idar-Oberstein, Germany)	standard XP CENT/TS 14780
Condition/objective	until about 5% moisture content	with a 15 mm screen size	below 500 µm	sample homogeneity and representativeness
Biomass				
Deciduous wood				
Ash-wood	X	X	X	X
Beech	X	X	X	X
Poplar	X	X	X	X
Willow	X	X	X	X
Coniferous wood				
Pine	X	X	X	X
Pine forest residues	X	X	X	X
Scot pine bark	X	X	X	X
Herbaceous crops				
Miscanthus		X	X	X
Reed canary grass		X	X	X
Agricultural by-products				
Corn cob		X	X	X
Grape seed cake			X	X
Sunflower shells			X	X
Wheat straw (French)		X	X	X
Wheat straw (Swedish)		X	X	X

Six complementary biomasses, usually involved in forest fires in the South of Europe, were also studied in terms of macromolecular composition and behavior in torrefaction (see Annex I).

Biomass properties were measured according to European standards on solid biofuels when existing and internal methods based on best practices otherwise (Tables 3 and 4, see details in Annex II). Mass balance is shown as measured (in wmf, weight-moisture-free basis). Neutral sugars were normalized in the determination of the polysaccharide sugar composition, by separating the functional groups (acetyl groups, also named acetates), because of their different quantification method.

Table III.3. Macromolecular composition measured for the raw dried biomasses

	Cellulose	Hemicell	Lignin	Extractives	Ash	*Mass balance*
Standards	*TAPPI T249 cm-85*		*TAPPI T222 om-83*	*Internal method*	*XP CEN/TS 14775*	-
Biomass	**% wmf***					
Deciduous wood						
Ash-wood	36.6	20.8	26.3	10.0	2.8	*96.5*
Beech	41.3	25.3	26.5	1.9	0.8	*95.7*
Poplar	42.7	21.8	26.9	4.4	2.8	*98.5*
Willow	44.3	22.6	25.1	8.0	2.3	*102.3*
Coniferous wood						
Pine	38.5	27.3	27.5	8.4	1.3	*103.0*
Pine forest residues	22.3	27.9	27.5	18.9	2.2	*98.8*
Scot pine bark	21.9	18.3	40.7	15.2	2.8	*98.9*
Herbaceous crops						
Miscanthus	45.3	22.6	20.2	8.6	2.8	*99.5*
Reed canary grass	39.5	25.7	24.7	6.4	6.6	*102.8*
Agricultural by-products						
Corn cob	38.4	34.8	15.9	6.9	1.9	*97.7*
Grape seed cake	7.8	21.9	62.8	7.6	4.2	*104.2*
Sunflower shells	37.0	26.4	25.9	10.7	3.2	*103.2*
Wheat straw (French)	37.5	23.8	20.5	15.7	8.3	*105.9*
Wheat straw (Swedish)	38.1	24.7	22.4	7.8	9.3	*102.3*

** % wmf = weight-moisture-free*

Biomass properties (Table III.3) were found to be in agreement with literature [205–207]. Woody biomasses, in particular softwood bark, tended to have higher contents in lignin than agricultural biomasses. Woody biomasses were also characterized by lower ash contents. Extractives content appeared to be higher in coniferous wood and in some agricultural biomasses, namely sunflower seed shells and wheat straw. This result may be considered with caution as different methods are commonly used for woody and agricultural biomasses, and here the method used was the same as for wood. The combination of methods suitable for woody and agricultural biomasses in the determination of biomass macromolecular composition might contribute to explain mass balances in Table III.3, not strictly equal to 100% in every case. Hemicelluloses were found in variable amounts among samples. Interestingly, the highest amount was found in corn cob and the lowest amount in grape seed cake, despite the fact that these biomasses are both from agricultural type. In general, woody biomasses have shown values of macromolecular composition and of ratios between the macromolecular elements that are closer than in the case of agricultural biomasses, whose macromolecular characterization is more heterogeneous.

Macromolecular composition of herbaceous crops was intermediate to that of woods and agricultural biomasses. Willow presented a characterization close to that of herbaceous

biomasses. Indeed, it can be either considered as a deciduous wood, which is the case of this study, or as a short rotation coppice (SRC). This classification is due to its particular growing procedure, being usually harvested at an early age, which leads to a higher ash content and a lower lignin content [21,208]. Finally, it is noteworthy that the two wheat straws from different origins had very close ash and lignin amounts but significantly different amounts in cellulose, hemicellulose and extractives.

Table III.4. Neutral monosugar distribution and functional groups measured for the raw biomasses

	Neutral sugar balance (normalized)					Functional groups
	Glucose	Xylose	Mannose	Galactose	Arabinose	Acetyl groups
Standards	*ASTM E1758*					*Internal method*
Biomass	**%***					**% wmf****
Deciduous wood						
Ash-wood	69.2	24.9	2.0	1.1	2.7	3.6
Beech	63.9	29.1	3.0	2.0	2.0	8.3
Poplar	68.9	22.7	4.3	2.0	2.2	5.9
Willow	69.1	21.8	2.8	3.0	3.4	4.9
Coniferous wood						
Pine	70.6	8.2	16.9	2.8	1.6	1.7
Pine forest residues	58.8	10.7	14.4	8.7	7.5	2.7
Scot pine bark	64.3	7.9	9.9	7.1	10.9	1.6
Herbaceous crops						
Miscanthus	69.9	26.1	0.5	0.7	2.9	2.6
Reed canary grass	61.0	29.9	0.4	3.1	5.6	5.0
Agricultural by-products						
Corn cob	52.4	39.4	0.0	2.5	5.7	5.0
Grape seed cake	33.6	48.2	7.4	5.2	5.6	3.1
Sunflower shells	59.5	30.7	1.0	2.2	6.6	7.5
Wheat straw (French)	63.7	29.7	0.8	1.6	4.2	1.7
Wheat straw (Swedish)	61.0	32.5	0.3	1.6	4.6	3.7

**% of total monosugars; ** % wmf = weight-moisture-free (not normalized)*

Sugar composition of cellulose and hemicelluloses was found in agreement with the literature [46,54,60] (Table III.4). Hemicelluloses are mainly composed of xylose for all biomass types except for resinous wood, in which glucomannan predominates. Arabinose and galactose are present in lower amounts, variable depending on the biomass.

Mass elemental compositions were determined according to the standards (see details in Annex II) and reported in Table III.5a. Atomic decomposition was calculated from the measured values of mass elemental composition and indicated in Table III.5b. Oxygen content was calculated by difference, considering ash. Sulfur and chlorine content were also measured.

Table III.5a. Mass elemental composition measured for the different biomass samples

	C	H	O	N	ash
Standards	*XP CEN/ TS15104*	*XPCEN/ TS15105*	by difference	*XPCEN/ TS15107*	XP CEN/ TS 14775
Biomass			**% wmf***		
Deciduous wood					
Ash-wood	49.2	5.9	41.8	0.3	2.8
Beech	49.1	6.0	43.9	0.2	0.8
Poplar	49.0	5.9	42.1	0.2	2.8
Willow	48.6	5.9	42.8	0.5	2.3
Coniferous wood					
Pine	51.3	6.2	40.9	0.3	1.3
Pine forest residues	51.2	6.0	40.1	0.7	2.2
Scot pine bark	52.5	5.7	38.6	0.4	2.8
Herbaceous crops					
Miscanthus	48.3	6.0	42.6	0.3	2.8
Reed canary grass	47.4	5.9	39.4	0.7	6.6
Agricultural by-products					
Corn cob	47.4	6.1	44.3	0.4	1.9
Grape seed cake	50.6	5.8	37.0	2.5	4.2
Sunflower shells	51.5	6.3	38.3	0.8	3.2
Wheat straw (French)	45.2	5.7	40.0	0.8	8.3
Wheat straw (Swedish)	44.6	5.6	40.0	0.5	9.3

** % wmf = weight-moisture-free*

Table III.5b. Atomic decomposition for the raw biomasses

	C	H	O	N
Biomass			**atomic decomposition**	
Deciduous wood				
Ash-wood	**1**	1.439	0.637	0.0052
Beech	**1**	1.466	0.671	0.0035
Poplar	**1**	1.445	0.644	0.0035
Willow	**1**	1.457	0.660	0.0088
Coniferous wood				
Pine	**1**	1.450	0.598	0.0050
Pine forest residues	**1**	1.406	0.587	0.0117
Scot pine bark	**1**	1.303	0.551	0.0065
Herbaceous crops				
Miscanthus	**1**	1.491	0.661	0.0053
Reed canary grass	**1**	1.494	0.623	0.0127
Agricultural by-products				
Corn cob	**1**	1.544	0.701	0.0072
Grape seed cake	**1**	1.375	0.548	0.0423
Sunflower shells	**1**	1.468	0.558	0.0133
Wheat straw (French)	**1**	1.513	0.664	0.0152
Wheat straw (Swedish)	**1**	1.507	0.673	0.0096

A homogeneity in the elemental composition was observed for the biomasses studied. The molar proportions of the main biomass components, namely carbon (C), hydrogen (H) and oxygen (O) content were around 1:1.5:0.5, respectively. Nitrogen content was found in minor amounts for all biomasses, slightly higher for agricultural by-products due to their higher protein content. These results show that elemental composition does not seem to be suitable to represent biomass variability and, consequently, the incidence of this variability on biomass behavior in torrefaction.

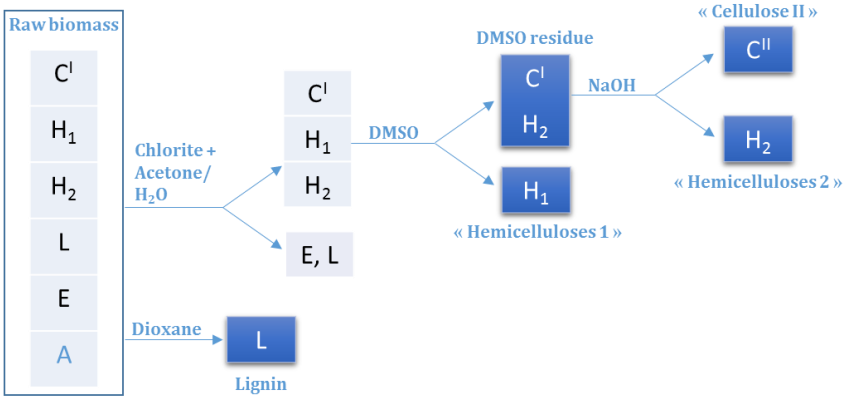
After the analysis of the raw biomasses, 5 of them were considered as "reference biomasses", representative of their respective family: ash-wood, beech, pine, miscanthus, and wheat straw.

1.2. Extracted macromolecular components from reference biomass

In this section, cellulose-, hemicellulose- and lignin-based fractions were extracted from the five reference biomasses. The objective was to improve the representativeness of biomass macromolecular components, typically carried out through commercial compounds. A special attention was paid to the extraction procedure.

1.2.1. Extraction procedure

Biomass macromolecular components were extracted according to a sequence of in-house developed methods (Figure III.1), selected to overcome difficulties reported in the literature to separate cellulose, hemicelluloses and lignin (see section II.3.2).



Macromolecular component	Abbreviation
Cellulose	C^I and C^{II}
Hemicelluloses	H_1
	H_2
Lignin	L
Extractives	E
Ash	A

Figure III.1. Procedure of extraction of the macromolecular components of biomass (dark blue boxes represent available fractions for characterization and torrefaction, including raw biomass)

Lignin was extracted from biomass with dioxane in an acid medium [209]. The solubilized lignin was precipitated by evaporating half of the volume of the solution under low pressure. Then water was added and the previous steps were repeated until dioxane was completely eliminated.

As the lignin extraction is performed in acidic medium, the polysaccharides (hemicelluloses and cellulose) could be partially hydrolyzed. Therefore, a new sample was used to isolate these fractions. To obtain them, extractives and traces of lignin were firstly removed. Extractives were

removed by a water/acetone treatment. Then, a treatment with sodium chlorite under acetate/ac acid buffer (pH=4.6) at 70°C until no residual lignin could be detected. Extraction time varied between one and two weeks depending on the lignin content and raw materials. After this step, the remaining part of the biomass consisted of cellulose and hemicelluloses. To separate these two components, a DMSO (dimethyl sulfoxyde) treatment (4 h under reflux) and an alkaline hydrolysis (NaOH 2.5 M, 60°C, 30 minutes) were performed successively.

A main fraction of hemicellulose, called « hemicelluloses 1 », was obtained from the liquid fraction derived from the DMSO extraction, which was dialyzed with membranes. A complementary fraction, called « hemicelluloses 2 », still present in the residual fraction after DMSO treatment, was recovered and separated from cellulose through the alkaline hydrolysis residue. After filtration, the liquid phase was neutralized with H_2SO_4, dialyzed with membranes and lyophilized.

The solid fraction obtained after strong alkaline treatment aimed to obtain an acceptably pure cellulose, which was verified by its glucan content, close to 100 %. However, the operating conditions of this hydrolysis are suspected to induce mercerization (conversion of native cellulose structure type I into a different allomorph, the so-called cellulose II), even if the sugar composition is preserved. For this reason, the solid fraction obtained after DMSO extraction, called « DMSO residue » was also fully characterized.

X-Ray diffraction (XRD) characterizations of the « cellulose II » and « DMSO residue » extracted fractions were then carried out to investigate possible changes in cellulose structure (Figure III.2). To do this, an XPERT-PRO MPD Diffractometer system was used, with the measuring program from PANalytical. The selected anode material was copper, with a selected wavelength Kα (Cu) = 1.5419 Å. The reflexion method was Bragg Brentano type.

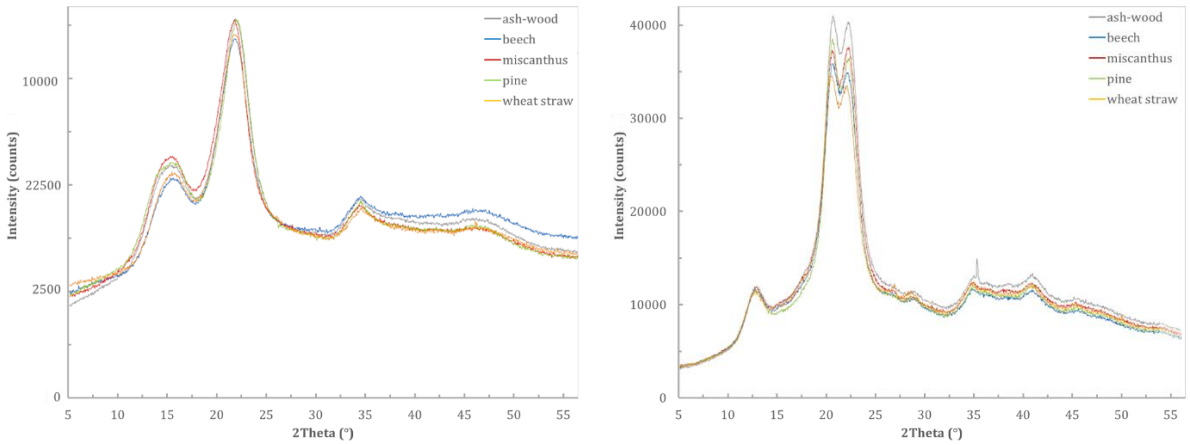


Figure III.2. XRD characterization of « DMSO residue » (left) « cellulose II » (right) fractions from the 5 reference biomasses

The results confirmed the mercerization of the cellulose crystalline structure, from a cellulose crystalline structure type I (Figure III.2, left) for the « DMSO residue » to a cellulose crystalline structure type II (Figure III.2, right) for the « cellulose II » fractions.

The mercerization in alkaline medium is due to Na^+ ions going into the cellulose structure and separating glucan chains. Then, these chains recrystallize in an anti-parallel structure with higher stability, named « cellulose II» [210]. This structure differs from the native cellulose in biomass, called « cellulose I » and formed by parallel glucan chains. In the extraction procedure, « cellulose I » is preserved in all steps until the « DMSO residue », and before hydrolysis. This is the reason why the « DMSO residue » fraction was also analyzed in terms of characterization and behavior in torrefaction.

An extraction of the cellulose fraction through an acid treatment, as typically done for commercial microcrystalline cellulose, would avoid this reorganization and preserve the cellulose crystalline structure type I. However, several drawbacks are associated to this acidic extraction, such as important changes in the cellulose reactivity and crystallinity, which are supposed to affect cellulose transformation through torrefaction in a higher extent [211]. As a result, the alkaline extraction allows to obtain more preserved cellulose fractions, which intend to be more representative of native cellulose in biomass, with the exception of the crystalline structure type. In this work, the influence of this structure in cellulose conversion in torrefaction can be assessed thanks to the comparison of the « DMSO residue » and the « cellulose II » fraction in torrefaction.

« Hemicelluloses 1 » and « Hemicelluloses 2 » fractions were lyophilized for removing water without heating, so as to facilitate their handling in torrefaction experiments. « Cellulose II» fractions were directly air-dried. A part of the « DMSO residue » fraction was dried at 105°C for 24 hours, as its nature allowed to directly use it in torrefaction experiments. A second part was lyophilized for the XDR crystallinity tests. In all cases, lyophillization did not exhibit any effect on extracted fractions behavior or composition. Lyophilized polysaccharide derived fractions are under the shape of a cotton-like material, which was directly characterized and torrefied. A grinding operation of this material would cause important mass loss of the fractions, which are only available in low amounts due to the constraints of the extraction procedure. However, the repeatability of the experiments confirmed the representativeness of directly analyzing this material. The « lignin » fraction was dried at room temperature (several days) and manually ground.

1.2.2. Cellulose

1.2.2.1. « Cellulose II » fraction

« Cellulose II » fractions are presented under a cotton-like form, due to the fibrous nature of the fraction (Figure III.3).

« cellulose II » fraction



Figure III.3. Samples of « cellulose II » fractions from the five reference biomasses

The sugar distribution of the « cellulose II » fractions proves the high purity of the extracted cellulose, principally constituted of glucose and only minor amounts of mannose for ash-wood and pine celluloses (Table III.6). Commercial microcrystalline cellulose Avicel presents a lower purity compared to « cellulose II » fractions.

Table III.6. Monomer sugars distribution of « cellulose II » fraction and of the commercial microcrystalline cellulose

	Monomer sugars (normalized)				
	Glucose	**Xylose**	**Mannose**	**Galactose**	**Arabinose**
Biomass			**%**		
Ash-wood	98.2	0.0	1.8	0.0	0.0
Beech	100.0	0.0	0.0	0.0	0.0
Miscanthus	100.0	0.0	0.0	0.0	0.0
Pine	99.1	0.0	0.9	0.0	0.0
Wheat straw	100.0	0.0	0.0	0.0	0.0
Commercial microcrystalline cellulose Avicel	96.1	2.4	1.5	0.0	0.0

% of the total monosugars

« Cellulose II » extracted fractions and commercial microcrystalline cellulose Avicel were deeply characterized in terms of molar mass distribution, average molar mass and polymerization degree through size-exclusion chromatography (SEC, see Annex III). The results of this study show a higher polymerization degree and average molar mass for the « cellulose II » fractions compared to commercial microcrystalline cellulose Avicel. The molar mass distribution was shown to be narrower for the extracted fractions. As a result, the « cellulose II » fractions seem closer to native cellulose in biomass.

1.2.2.2. « DMSO residue » fraction

« DMSO residue » fractions were considered as they are mainly constituted of cellulose in the allomorphic form of native cellulose in biomass, namely cellulose I. This was proved by their main composition in glucose (Table III.7). The fibrous shape of this fraction (Figure III.4) is similar to that of the « cellulose II » samples (Figure III.3). However, hemicellulose-based sugars and acetyl groups were found in non-negligible amounts. The proportion of cellulose and hemicelluloses in the « DMSO residue » fractions seems close for all the extracted fractions, due to the similar glucose to xylose ratios, which are the major sugars of cellulose and

hemicelluloses, respectively. A higher amount of xylose than mannose is observed for all biomasses except for wheat straw. In the case of pine, this fraction only contains xylose. However, the composition of this fraction in cellulose and residual hemicelluloses will be estimated in the Modelling section (see V.2 section).

« DMSO residue » fraction



Figure III.4. Samples of the « DMSO residue » fraction from the five reference biomasses

Table III.7. Monomer sugars distribution (including acetates) of « DMSO residue » fraction

	Monomer sugars (normalized)					
	Glucose	Xylose	Mannose	Galactose	Arabinose	Acetyl groups
Biomass	%					
Ash-wood	77.3	14.9	1.8	0.0	0.8	5.2
Beech	78.3	16.2	0.0	0.0	0.4	5.0
Miscanthus	76.6	11.9	5.9	0.2	0.3	5.2
Pine	78.7	16.2	0.0	0.0	1.2	4.0
Wheat straw	78.5	5.4	11.5	0.2	0.5	3.8

% of the total monosugars (including acetates)

1.2.3. Hemicelluloses

1.2.3.1. « Hemicelluloses 1 » fraction

The « hemicelluloses 1 » fraction is presented under a cotton-like form (Figure III.5), due to the lyophilization treatment, which leads to a less dense than « cellulose II » fraction (Figure III.3).

« hemicelluloses 1 » fraction



Figure III.5. Samples of the « hemicelluloses 1 » fraction from the five reference biomasses

The characterization of the « hemicelluloses 1 » fractions in terms of monomer sugars corresponds to a typical sugar composition of hemicellulose from biomass (Table III.8). The major quantified sugar compound is xylose for all fractions except for pine « hemicelluloses 1 », whose major sugar monomer is mannose, as expected. Considerable amounts of acetyl groups were also measured for all fractions, corresponding to substituents of hemicellulose chains. This might indicate the low severity of the extraction treatment to obtain this fraction.

Table III.8. Monomer sugars distribution (including acetates) of « hemicelluloses 1 » fraction

	Monomer sugars (normalized)					
	Glucose	Xylose	Mannose	Galactose	Arabinose	Acetyl groups
Biomass	%					
Ash-wood	5.5	72.4	0.0	0.3	0.6	21.2
Beech	0.2	75.9	0.0	0.4	0.6	22.9
Miscanthus	12.5	64.4	0.0	0.7	5.9	16.5
Pine	14.8	18.4	49.2	4.1	3.0	10.5
Wheat straw	32.3	52.0	0.0	1.6	4.9	9.1

% of the total monosugars (including acetates)

1.2.2.3. « Hemicelluloses 2 » fraction

« Hemicelluloses 2 » fractions were lyophilized and recuperated in a more compact and denser form than « hemicelluloses 1 » fractions, equivalent for the five reference biomasses (Figure III.6). This might be derived from their direct separation from cellulose in « DMSO residue ».



Figure III.6. Samples of « hemicelluloses 2 » fraction from wheat straw

« Hemicelluloses 2 » fraction (Table III.9) presents a different sugar composition from that of the « hemicelluloses 1 » fraction (Table III.8). Glucose is mostly present in « hemicelluloses 1 » fraction for pine and wheat straw hemicelluloses, while it is the contrary case for beech and ash-wood. Xylose composition is close for the two hemicelluloses fractions, except for those from pine, containing xylose principally in « hemicelluloses 2 ». Important differences were also observed in mannose content between hemicellulose fractions. While mannose from pine is entirely extracted in « hemicelluloses 1 » fraction (0% mannose content in « hemicelluloses 2 », Table III.9), those from wheat straw and miscanthus hemicelluloses are completely included in fraction « hemicelluloses 2 » (0% mannose content in « hemicelluloses 1 », Table III.8). Interestingly, mannose from ash-wood is exclusively found in the pine « cellulose » fraction. These differences might indicate different stability of the sugars including mannose in function of the biomass type. In the case of pine, most of the galactose is found in « hemicelluloses 1 » fraction, together with mannose, as they are associated in galactomannan and galactoglucomannan sugars in softwood. Acetyls are mostly present in « hemicelluloses 1 » fraction, as the alkaline treatment to obtain the second fractions destroys the acetate functional group in hemicelluloses. These differences in composition lead to think about that these « hemicelluloses » fractions are independent.

Table III.9. Monomer sugars distribution (including acetates) of « hemicelluloses 2 » fraction

	Monomer sugars (normalized)					
	Glucose	Xylose	Mannose	Galactose	Arabinose	Acetyl groups
Biomass	%					
Ash-wood	16.7	75.8	0.0	0.8	5.8	0.9
Beech	12.3	79.9	0.0	0.8	6.2	0.8
Miscanthus	9.8	86.4	2.0	0.6	0.6	0.7
Pine	6.2	80.2	7.5	0.7	4.2	1.2
Wheat straw	9.9	46.6	33.3	3.1	6.4	0.8

% of the total monosugars (including acetates)

1.2.4. Lignin

Lignin fractions were present under the form of a fine powder, whose color is varying in function of the biomass (Figure III.7).

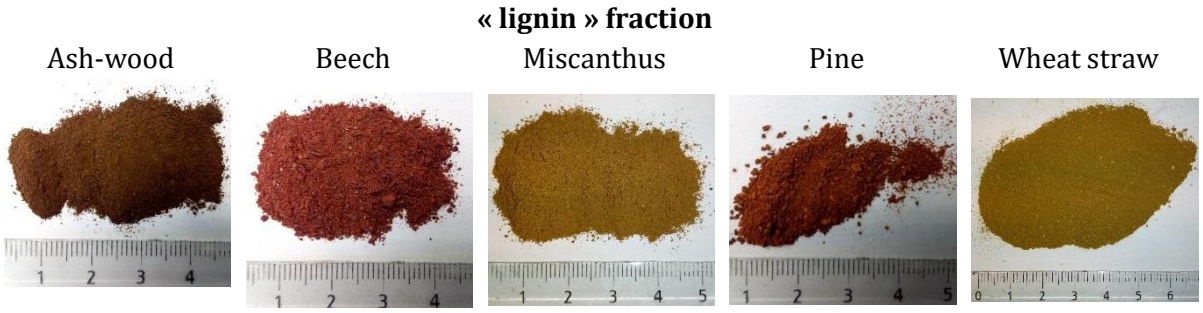


Figure III.7. Samples of the « lignin » fraction from the five reference biomasses

Sugar characterization is not possible for lignin, due to its nature as a phenyl-propane-based polymer. As a result, carbohydrates are under the detection limit and thus assumed as negligible.

The composition of lignin can be assessed in terms of hydroxyphenyl- (H-), guaiacyl- (G-) and syringyl- (S-) units. However, this measurement is difficult to obtain and requires NMR characterizations, which could not be carried out in this work. For further discussion, the composition of lignin described in the literature will be utilized. The differences in the kinetic behavior of «lignin» fractions can be explained based on the structural differences between lignin in biomass. Dividing wood into two categories, hardwood (deciduous wood, angiosperm) and softwood (coniferous wood, gymnosperm), it has been identified that lignin from softwood is principally formed by G units (90%) and some H units. On the other hand, lignin constituting hardwood contains varying ratios of G and S units. Finally, lignin from herbaceous biomasses would be formed by the three types of units [63].

1.3. Mixtures of extracted macromolecular components from reference biomasses

Torrefaction experiments were carried out to check the existence of interactions between constituents based on ternary and binary mixtures of the 3 main extracted biomass components from the 5 biomasses, namely « cellulose II », « hemicellulose 1 » and « lignin » fractions.

The proportions of the fractions in the ternary mixture for each biomass correspond to the proportions of cellulose, hemicellulose and lignin in the raw material, respectively (Table III.10). This supposes that the biomass macromolecular composition only contains these three components (ash is considered inert and extractives to be removed at temperatures below 200°C, as discussed in II.3.2 section). The limitation of these ternary mixtures to reproduce biomass behavior in torrefaction is due to the fact that interactions between macromolecular components, broken during the extraction of the fractions, cannot be reproduced.

Table III.10. Proportions of the extracted fractions in the ternary mixture

Biomass	Nomenclature of the mixture	« Cellulose II »	« Hemicelluloses 1 »	« Lignin »
Ash-wood	CHL	0.41	0.29	0.30
Beech	CHL	0.45	0.28	0.27
Miscanthus	CHL	0.52	0.26	0.23
Pine	CHL	0.44	0.29	0.27
Wheat straw (French)	CHL	0.45	0.25	0.30

In the case of the binary mixtures for beech, the proportions in the mixture were calculated by assuming that the biomass composition was reduced to two macromolecular components (Table III.11). These mixtures, already suggested in previous studies [18], do not intend to represent the whole raw material, but to give insights about the interactions between macromolecular components in torrefaction.

Table III.11. Proportions of the extracted fractions in the binary mixture

Biomass	Nomenclature of the mixture	« Cellulose »	« Hemicelluloses 1 »	« Lignin »
Beech	CH	0.62	0.38	-
Beech	CL	0.61	-	0.39
Beech	HL	-	0.51	0.49

Fractions were mixed thanks to a hand mortar and pestle. The physical form of the fractions was « cotton-type » for «cellulose» and «hemicelluloses 1», while lignin samples were in the form of fine powders. Significant mass losses occurred when handling mixtures including «lignin» fraction (Figure III.8). Despite this difficulty and even if the result of the manual mixture was not

visually homogeneous due to the nature of the fractions, the repeatability of the experiments was similar to that of raw biomasses.

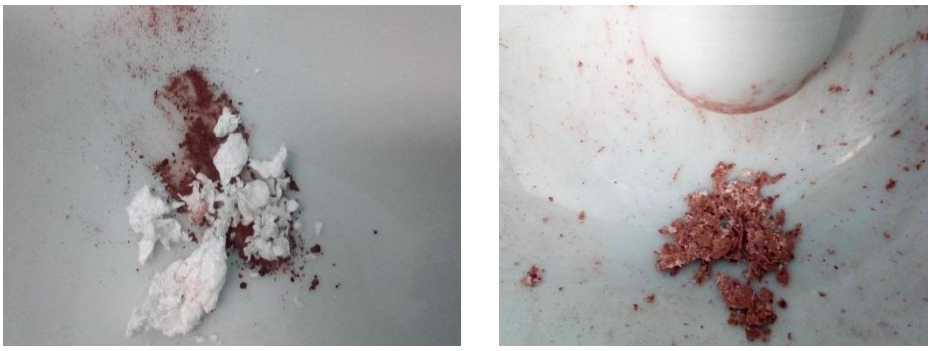


Figure III.8. Preparation of beech ternary mixture before (left) and after (right) physical mixing

1.4. Commercial compounds

Commercial xylan from beech was used for preliminary tests, in the form of powder below 200 µm and produced by the company Aldrich (product code X4252, CAS number 9014-63-5). Preliminary experiments were carried out to fix the operating conditions (sample mass, heating rate) that ensure the chemical regime (see section III.3.1).

Commercial microcrystalline cellulose Avicel PH-101 (~50µm particle size, produced by Aldrich, CAS number 9004-34-6) was also studied. The objective was to compare its performances during torrefaction with those of the corresponding extracted macromolecular components of the selected biomasses.

2. Experimental set-up

An original experimental set-up was conceived to be able to simultaneously determine kinetics of condensable species formation and of solid mass loss through one single torrefaction experiment. The set-up (Figure III.9) was composed of a thermogravimetric analyzer (TGA) coupled with a gas chromatography mass spectrometer device (GC/MS). The introduction of a 16-loop-heated storage system between TGA and GC/MS allowed to sample volatile species released at different torrefaction temperatures. Volatile samples were stored in gas phase until their analysis in GC/MS, which overcomes the difference in terms of duration between the torrefaction experiment and each GC/MS analysis. The main limitation of this device is the impossibility of measuring water and permanent gases, as well as the total volatile species produced. Indeed, solid mass loss and volatiles species production profiles can be followed in function of torrefaction time and temperature. However, mass balance of the torrefaction products cannot be established.

2.1. Study of solid mass loss in thermobalance

Torrefaction experiments were performed in a thermogravimetric analyzer (TGA, 92-16.18 SETARAM TGA 92, Figure III.9).

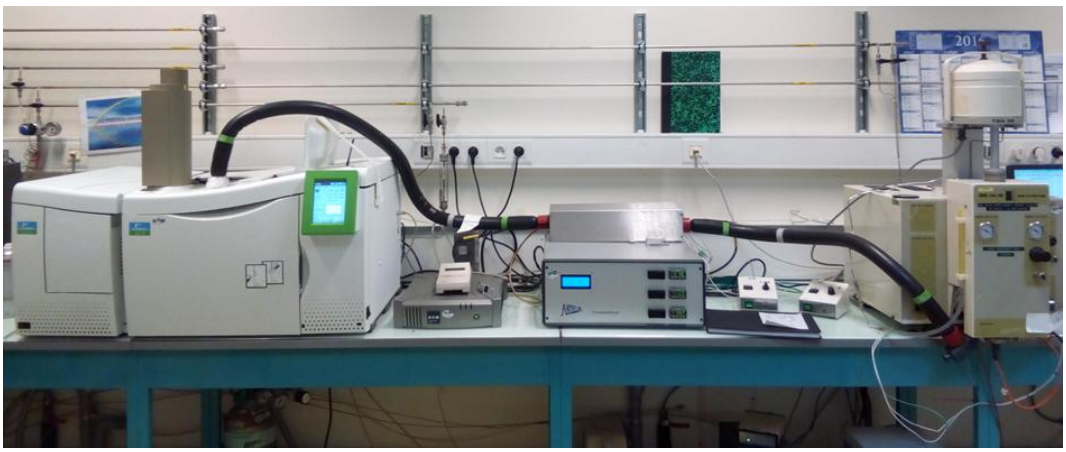


Figure III.9. Lab-scale coupling between TGA and GC/MS through a heated storage loop system

About 100 mg of sample (raw biomass, extracted fractions and their mixtures and commercial compounds) were loaded in a three-plate crucible of 10 mm in diameter, corresponding to a maximum bed thickness of 2 mm of biomass per plate, and suspended in the TGA oven (Figure III.10). The exception was for the « hemicelluloses 1 » fractions, whose low density only allowed to introduce 50 mg of sample, and for the « hemicelluloses 2 » samples, which were limited to 25 mg because of the lack of material. The position of the three-plate crucible in the TGA oven was checked to guarantee that the three biomass layers were positioned in the isothermal zone of the reactor [212]. The maximum bed thickness in each plate of the crucible was determined through characteristic time calculations (see Annex IV).

Samples were torrefied under a 50 mL/min helium (He) flow in the thermobalance. First, the sample was heated from 200 to 300 °C at a heating rate of 3 °C/min, and then kept at 300°C for 30 min. Helium was chosen as carrier gas because of the further GC/MS analysis of the torrefaction gases. Tests performed with N_2 were shown to give the same results in terms of mass loss kinetics. 200°C was considered the reference temperature for the comparison of the TGA data, as at this temperature the moisture content can be considered as negligible and reactions associated to torrefaction have not started yet [18].

Preliminary experiments have confirmed that the selected crucible configuration and experimental conditions ensure chemical regime [213]. This regime was reached for all samples thanks to the temperature rise conditions (see section III.3.1 and Annex IV), allowing the representativeness of the results.

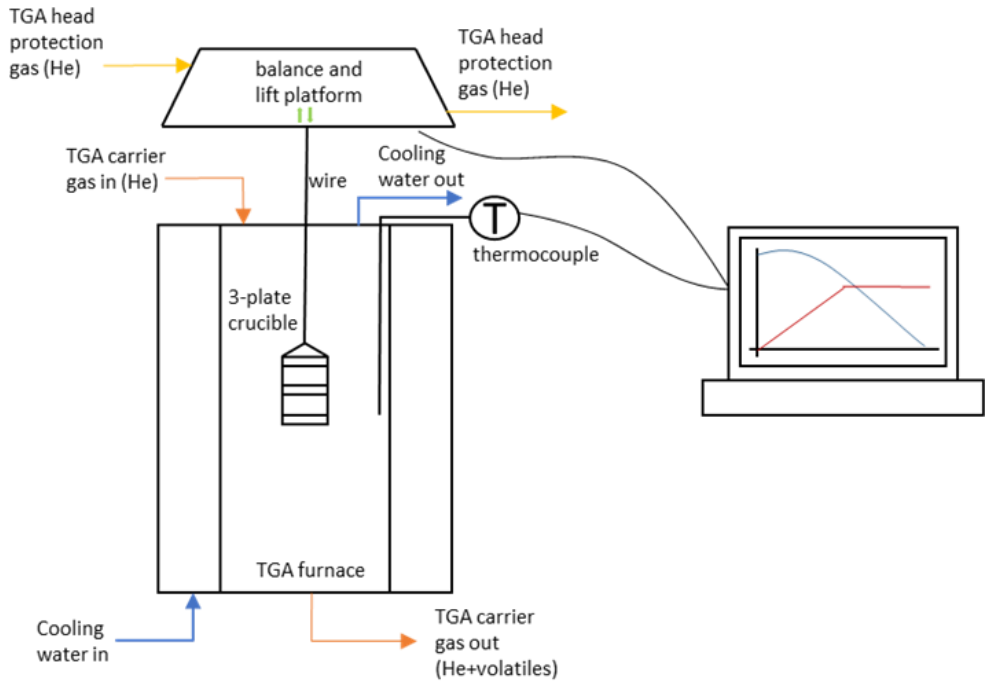


Figure III.10. Scheme of the thermobalance with the three-plate crucible

2.2. Study of the volatile species release in GC/MS

The chemical composition of each stored volatile fraction was analyzed in GC/MS (Perkin-Elmer Clarus 580/Clarus SQ8S). The GC device consisted of a capillary column Perkin-Elmer Elite-1701 (composition: 14% cyanopropylphenil-85% dimethyl polysiloxane). This non-polar stationary phase is suitable for a large spectrum of chemical species, which justifies its selection for the complex torrefaction gaseous mixture, even if it is not the most suitable for acids and alcohols. The dimensions of the capillary column were 60 m length, 0.25 mm of internal diameter and 0.25 µm of film thickness. The injection in the column was direct from the heated storage loop system, by a 1mL/min helium carrier flow that swept the loop and pushed its content in the GC column (split-less injection). This helium flow was supposed to establish a laminar regime inside the GC column. The characteristics of GC temperature profile are indicated in Figure III.11 [212].

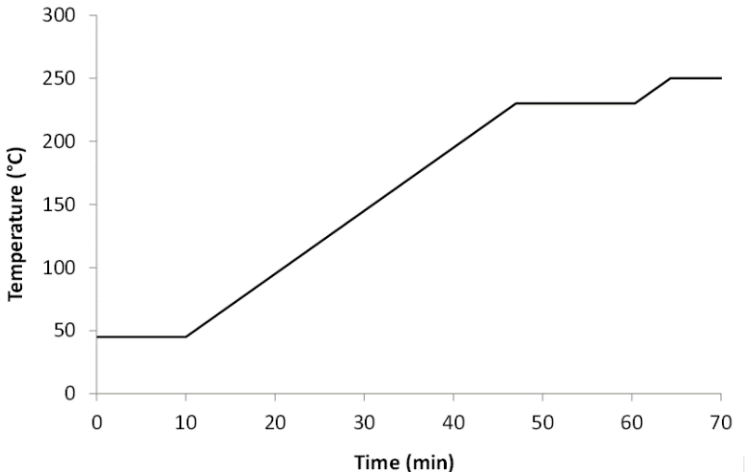


Figure III.11. Temperature profile in the GC column during analysis

Concerning the MS apparatus, it consisted of an Electron Ionization (EI) ion source. The range of m/z considered is 28 to 300, in order to avoid the peak of air (oxygen, nitrogen). Chemical species were identified from the chromatogram by using the NIST library.

2.3. Coupling TGA-GC/MS by a heated storage loop system

For each experiment, volatiles released during torrefaction were sampled every 10°C, between 200 and 300°C, at 3°C/min, thanks to a heated storage loop system (Chromatostock, Antelia). A difference exists in the experimental times for the production of volatile species in torrefaction (about 60 min) and the analysis of each gaseous fraction in GC/MS (70 min). The direct coupling of these two devices will only allow two GC/MS analysis per torrefaction experiment in the thermobalance. To overcome this limitation, volatile species are sampled at different degrees of progression of torrefaction and stored in the heated loop system, waiting for the further GC/MS analysis.

Gaseous samples are stored at 200°C. This temperature allows to maintain volatile species in gaseous phase. It has been proved that the composition of the stored volatile phase remains unchanged during the storage, until a maximum of 24 hours [212].

The heated storage loop system was controlled from the computer by indicating the sampling time for each loop. As a result, gases released during torrefaction in the thermobalance circulate through a loop until the sampling time is over. At this point, the three-port-valve of the system switched to the next loop, keeping the last fraction of torrefaction gases stored in the previous loop (0.5 mL, which corresponds to the volume of the loop). As a result, a maximum of 16 gaseous samples can be stored to further analysis. Two valves allow the control of the loop system of the Chromatostock (Figure III.12). They can adopt two positions:

- In position V1, the loop receives the gaseous sample released in torrefaction in the TGA.
- In position V2, the loop releases the gaseous sample to be swept to the GC/MS by the carrier gas (helium, 1 mL/min), for further analysis.

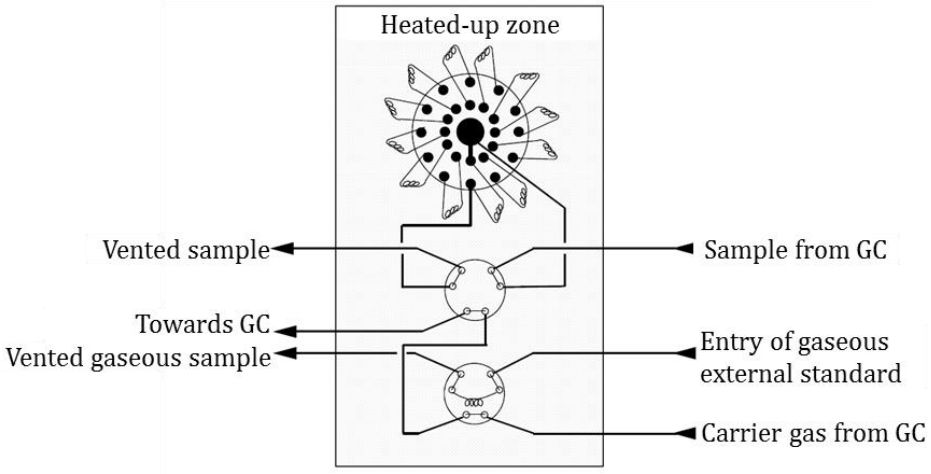


Figure III.12. Chromatostock loops storage scheme

Eleven of the sixteen available loops were used, while five loops 1, 3, 7, 11 and 14 were discarded because of leaking (Table III.12, NC: not considered, see Annex V). For the further GC/MS analysis of each gaseous sample, eleven points will describe the production of each volatile species during torrefaction.

Table III.12. Sampling temperatures for each loop from the heated storage loops system

loops	*1*	**2**	*3*	**4**	**5**	**6**	*7*	**8**	**9**	**10**	*11*	**12**	**13**	*14*	**15**	**16**
T (°C)	*NC*	200	*NC*	210	220	230	*NC*	240	250	260	*NC*	270	280	*NC*	290	300

3. Definition of the experimental conditions

The objective of this section is to display the way the experimental conditions were theoretically defined for ensuring the chemical regime, in order to build a model of biomass torrefaction governed by chemical transformations and independent of heat transfer. The resulting mass of the sample and the heating rate were checked with preliminary experiments using commercial xylan from beech. This feedstock was chosen for being reported in literature as a good representative of the hemicelluloses. Its decomposition can be completely observed in the range of temperatures of torrefaction [116].

3.1. Characteristic time calculations

A characteristic time analysis was applied to torrefaction, based on dimensional analysis (non-dimensional numbers) and on the similarities with the previous studies concerning pyrolysis and gasification. In torrefaction, characteristic time for chemical transformation corresponds to the torrefaction time. In a first approach, the kinetic law proposed by Prins for willow under torrefaction conditions and a nitrogen atmosphere [22,99] was considered as applicable for this case. Concerning heat transfer, characteristic times are defined as typically, according to heat transfer laws in each case [114,133]. Detailed calculations of characteristic times in torrefaction are included in Annex IV, while the regime maps at bed and particle scale are presented in the next sections.

3.1.1. Torrefaction regimes with temperature and particle size

The influence of the particle size and the temperature in the thermal or chemical regime in torrefaction was studied (Figure III.13). Internal conduction was considered for the comparison with torrefaction, being their ratio represented by the Py number. The limits for the regimes are determined by a ratio of 10 between torrefaction and internal conduction times.

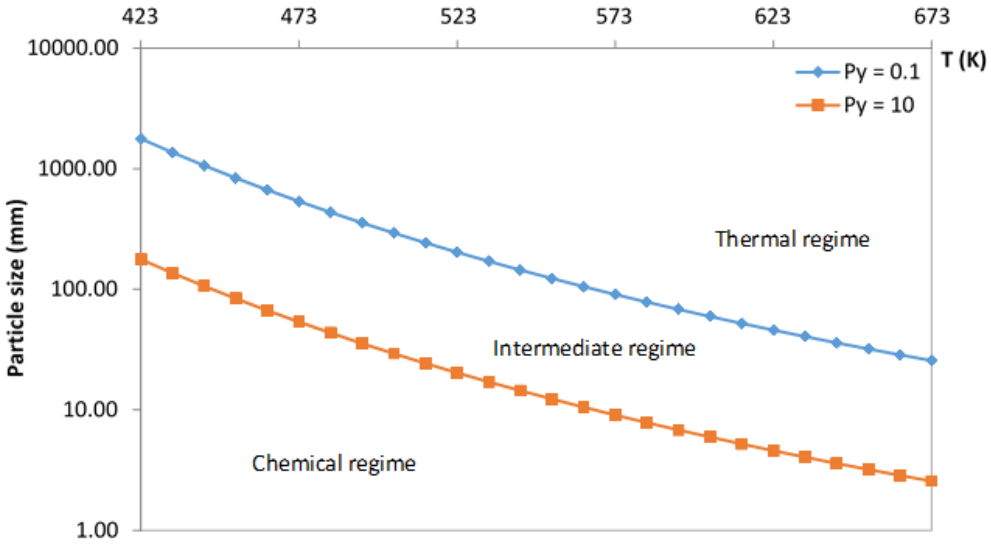


Figure III.13. Torrefaction regime versus temperature and particle size for TGA-GC/MS

The points in the area above the Py = 0.1 curve correspond to the thermal regime, while those under the Py = 10 curve correspond to the chemical regime. Between these two curves, an intermediate regime is established. In the range of temperatures for torrefaction (473 – 573 K), the chemical regime governs the process for particles with a diameter below 10 and 55 mm in function of the torrefaction temperature.

These curves were plotted for an extended range of temperatures in order to show that the limit of the particle diameter in pyrolysis is much lower, as it was presented previously in the literature [114]. The comparison of these results with pyrolysis must be considered relatively carefully, as the kinetic law is different and only the order of magnitude can be considered as a reliable value. The regime map allows to quickly predict the regime for the TGA-GC/MS experiments, for identical operating conditions except the particle diameter.

3.1.2. Torrefaction regimes with temperature and bed thickness

The influence of the bed thickness and the temperature on the thermal or chemical regime in torrefaction was also studied (Figure III.14). As in the previous case, the ratio between torrefaction time and internal convection was also used (Py number) and the regions were delimited.

The regime map showed a limit of bed thickness for ensuring the chemical regime in torrefaction experiments between 25 mm and 4 mm, at the defined operating conditions in TGA-GC/MS. This last value is considered as being the most restraint value and indicates the maximum tolerated bed thickness, which was respected in all torrefaction experiments.

As at particle-scale, this graphic allows to quickly predict the regime of the experiments, if all the operating conditions remain unchanged and only the bed thickness is modified.

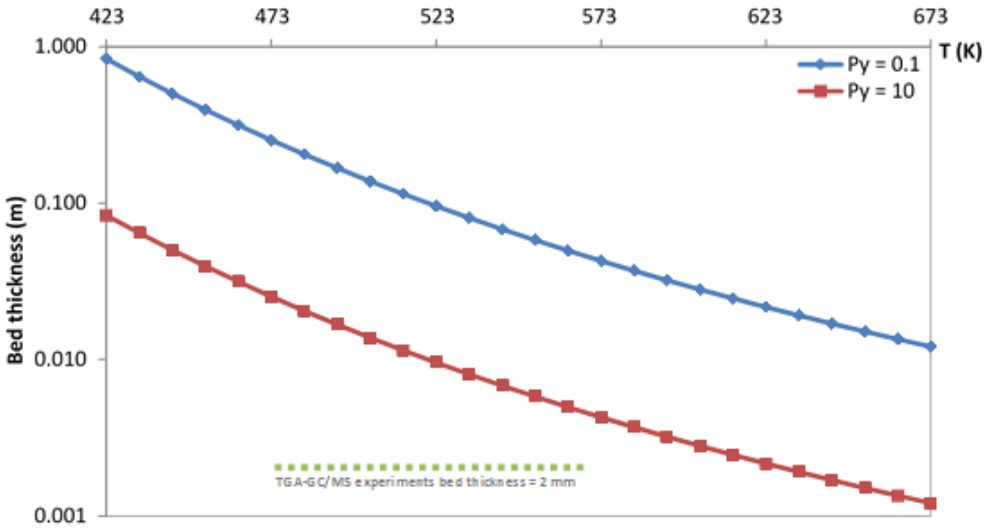


Figure III.14. Torrefaction regime versus temperature and bed thickness for TGA-GC/MS (extended T range)

3.2. Preliminary experiments with commercial xylan from beech

The evolution of solid mass in torrefaction experiments was studied for commercial xylan from beech in TGA. In order to establish the operating conditions ensuring the chemical regime, the parameters of study were the heating rate in the TGA oven and the sample mass involved in torrefaction.

Several experiments were carried out with the same sample mass (150 mg) of commercial xylan from beech and at different heating rates (1, 3 and 5°C/min, Figure III.15). According to characteristic time calculations, 5 °C/min is near to the limit of the chemical regime. 3°C/min was preferred as the heating rate for experiments, so as to keep a reasonable time of experiment by guaranteeing suitable operating conditions for the chemical regime.

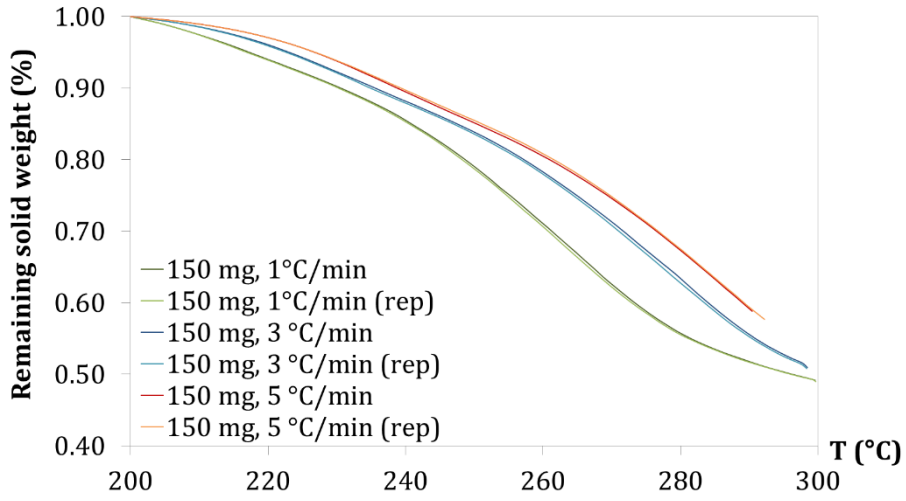


Figure III.15. Evolution of solid weight versus temperature for different heating rates and the same sample mass (150 mg) of commercial xylan from beech in TGA torrefaction experiments

On the other hand, thermogravimetric experiments usually consider a sample mass around 5 mg in a simple-plate crucible [124,214]. In the case of the TGA-GC/MS set-up, a considerably higher mass is required to produce volatiles in a detectable amount by the GC/MS detector. As a result, sample mass was set to between 50 and 150 mg in preliminary experiments with commercial xylan, at a fixed heating rate of 3 °C/min. The bed thickness per plate of the three-plate-crucible represented a maximum of 2 mm for the highest mass (150 mg) which ensures chemical regime and is in agreement with the experimental results (Figure III.16).

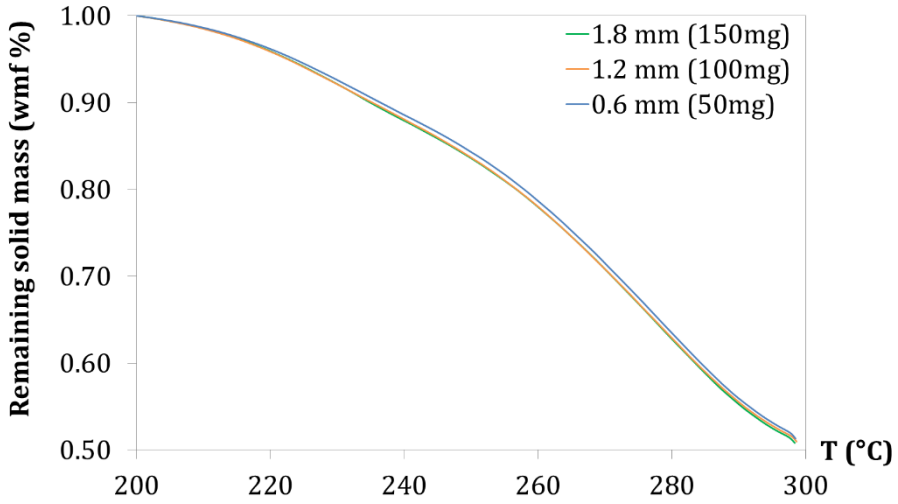


Figure III.16. Evolution of solid weight versus temperature for different sample mass of commercial xylan from beech in TGA torrefaction experiments at 3°C/min

Concerning the volatile production (Figure III.17), dependent on the mass sample, the intermediate mass of 100 mg was selected as a good compromise between minimizing the sample mass (and the bed thickness) and producing a detectable amount of the maximum number of volatile species. The exception, as explained earlier, was for hemicellulose fractions, namely 50 mg for « hemicelluloses 1 » and 25 mg for « hemicelluloses 2 ».

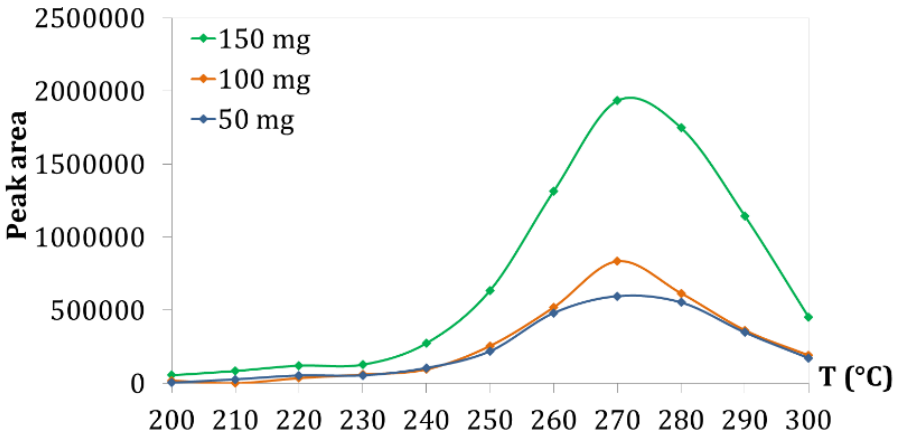


Figure III.17. Furfural production in TGA torrefaction experiments of commercial xylan from beech in function of the mass sample, 3°C/min heating rate

4. Data treatment

This section explains how experimental data about solid transformation (TGA) and volatile species release (GC/MS) were treated.

4.1. Solid transformation (TGA)

Experimental data extracted from the thermobalance (TGA) consist of one experimental point (temperature, time, mass) every 10 s, in order to optimize the volume of data treated.

The experimental data from the thermobalance was used to calculate two parameters concerning solid transformation in torrefaction: the remaining solid mass and the solid degradation rate.

- **% of remaining solid mass (% wmf):** remaining mass of the solid sample at one point of the transformation (m_i, at t_i) regarding the initial mass of the solid sample (m_0, at t_0). It represents the inverse part of the solid mass loss.

$$\%\ remaining\ solid\ mass\ (wmf) = \frac{m_i}{m_0} \times 100 \qquad \text{Eq. 2}$$

$$\%\ solid\ mass\ loss = 1 - \%\ remaining\ solid\ mass \qquad \text{Eq. 3}$$

- **Solid degradation rate (absolute, g/min, or relative, %wmf/min):** variation of mass of solid sample between two measurements as a function of time. It represents the kinetic rate of degradation of the solid sample, mathematically equivalent to the derived curve of the solid mass (m) or the remaining solid mass (%wmf) in absolute value.

$$\%\ Absolute\ solid\ degradation\ rate\ \left(\frac{g}{min}\right) = \frac{m_{i-1} - m_{i+1}}{t_{i-1} - t_{i+1}} \times 100 \qquad \text{Eq. 4}$$

$$\%\ Relative\ solid\ degradation\ rate\ \left(\frac{\%\ wmf}{min}\right) = \frac{\%wmf_{\ i-1} - \%wmf_{\ i+1}}{\%wmf_{\ 0}} \times \frac{1}{t_{i-1} - t_{i+1}} \times 100 \qquad \text{Eq. 5}$$

Excellent repeatability was found for the solid degradation in experiments, with relative difference lower than 1% (see Annex VI).

Both remaining solid mass and solid degradation rates were plotted as a function of time, including the representation of the thermal program of the torrefaction. In the case of the degradation rates, the represented values correspond to the mobile average of the calculated degradation rates (with 11 points), in order to obtain smoothed degradation rate profiles, independent of the small fluctuations of the measurements in the thermobalance.

Mass was normalized considering the beginning of torrefaction at 200°C. At this temperature, the remaining free water was removed, so that the moisture of the sample was considered as negligible. The transformation of the solid was shown to be negligible between the initial temperature of the experimentation (70°C) and the reference temperature for the normalization

(200°C) compared to the degradation in torrefaction (200 to 300°C, Table III.13). Ash was assumed to be inert in the torrefaction temperature range (200-300°C), while extractives were considered to be removed before the beginning of torrefaction (see section II.3.2).

Table III.13. Solid mass at different times of the torrefaction experiment in TGA (initial 70°C, reference at 200°C and final 300°C/30min)

	solid mass (mg)			% solid mass loss (%)	
Experiment	Initial, $t_{70°C}$	Ref, $t_{200°C}$	Final, $t_{300°C/30min}$	$\frac{m(t_0) - m(t_{200°C})}{m(t_0)}$	$\frac{m(t_{200°C}) - m(t_{300°C,30min})}{m(t_{200°C})}$
Corn cob cake	98.7	98.5	40.1	2.4%	58.3%
Grape seed cake	100.8	99.7	64.7	3.1%	33.8%
Pine forest residues	99.7	99.3	52.9	3.3%	45.2%
Poplar	102.8	102.3	47.2	1.1%	53.5%
Reed canary grass	95.3	95.0	50.8	1.3%	46.1%
Scot pine bark	96.4	96.0	56.1	2.9%	40.1%
Sunflower seed shells	98.8	98.3	43.4	3.2%	.54.6%
Wheat straw (Swedish)	97.5	97.2	43.8	1.5%	54.4%
Willow	98.5	97.9	52.5	2.1%	45.6%

4.2. Volatile species release (GC/MS)

4.2.1. Identification

Each gaseous sample generates one chromatogram (as in the example, Figure III.18). Each peak in the chromatogram corresponds to a chemical compound, whose position is defined by the retention time.

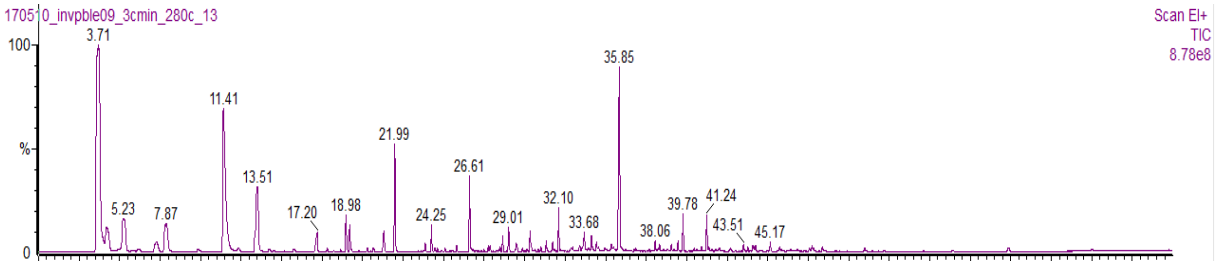


Figure III.18. Example of chromatogram for wheat straw at a torrefaction temperature of 280°C

The chemical compound corresponding to each peak can be identified by the integration of the mass spectrum included in the peak and by comparison with the database of the NIST library. The comparison of an experimental mass spectrum with the NIST database is represented by the Match and RMatch parameters. A correct correspondence between the experimental mass spectra and the one in the library for a given compound is represented by high values of Match/RMatch, between 850 and 1000.

Only part of the peaks in the chromatogram can be attributed to a chemical compound according to the database of the NIST library. This can be explained because some peaks are co-eluted in the GC column, as well as because not all the chemical compounds are included in this library. On the other hand, it is also possible to detect additional chemical compounds by comparing their mass spectra with the literature [215–218].

In order to better define peaks and to avoid overlapping, it is possible to work only with the most characteristic mass and charge peaks of the spectra corresponding to a chemical compound, this is, its characteristic m/z. For two co-eluted peaks, the extraction of the characteristic m/z of each peak allows, in most of the cases, the separation of both peaks. As the chromatograms present peaks from diverse chemical origins and they are usually not well-separated, it was decided to work with the characteristic m/z for each chemical compound. This implies the consideration of the Extracted-Ion Chromatogram (EIC) instead of the Total Ion Chromatogram (TIC) for each peak. The selected m/z for each chemical compound is one of the major m/z in the mass spectra of a peak which is different from the major m/z of other near peaks in the spectra.

The volatile species identified during the different experiments are listed in Table III.14, together with the considered characteristic m/z for each chemical compound. They mainly include acids, furans, alcohols, phenols and ketones, in agreement with the literature [6,11,12,14,46,99,154].

Table III.14. Identified and quantified chemical compounds released in biomass torrefaction experiments in TGA-GC/MS, with their characteristic m/z

Chemical compound	m/z	Identified	Quanified	Chemical compound	m/z	Identified	Quantified
Acids				**Phenols**			
formic acid	45	X	X	phenol	94	X	X
acetic acid	43	X	X	phenol, 2-methoxy (guaiacol)	109	X	X
propionic acid	74	X	X	phenol, 2,6-dimethoxy- (syringol)	154	X	X
2-propenoic acid	72	X		2-methoxy-4-vinylphenol	150	X	X
larixic acid (maltol)	126	X		cathecol	110	X	X
2-butenoic acid	86	X		isoeugenol (cis+trans)	164	X	X
3-Furancarboxylic acid	112	X		eugenol	164	X	X
Furans				vanillin	151	X	X
furan	68	X	X	phenol, 2-methoxy-4-methyl- (creosol)	95	X	
3-furaldehyde	95	X	X	phenol,4-ethyl-2-methoxy	137	X	
furfural	96	X	X	P-propylguaiacol	137	X	
2-furanmethanol	98	X	X	**Linear ketones**			
acetylfuran	95	X	X	2,3-butanedione	86	X	
2(5H)-furanone	55	X	X	3-pentanone	57	X	
furan, 2-methyl-	82	X		2,3-pentanedione	43	X	X
2-furancarboxylic acid, methyl ester	95	X		hydroxyacetone	43	X	X
2-furancarboxaldehyde, 5-methyl-	110	X		1-hydroxy, 2-butanone	57	X	
2,5-furandione, 3-methyl-	68	X		2-propanone,1-(acetyloxy)-	43	X	X
ethanone, 1-(3-hydroxy-2-furanyl)- (Isomaltol)	111	X		2-butanone	43	X	
Alcohols				2-butanone, 1-(acetyloxy)-	57	X	
methanol	31	X	X	**Cyclic ketones**			
Aldehydes				4-cyclopentene-1,3-dione	96	X	X
formaldehyde	30			1,2-cyclopentanedione	98	X	
acetylformaldehyde	72	X	X	2-cyclopenten-1-one, 2-hydroxy-3-methyl-	112	X	
Other compounds							
benzaldehyde, 4-hydroxy-3,5-dimethoxy-	182	X		2-hydroxy-gamma-butyrolactone	57	X	
levoglucosenone	98	X		1,4;3,6-dianhydro-(a)-d-glucopyranose	69	X	
4H-pyran-4-one	96	X		acetic acid, hydroxy-, methyl- ester	31	X	

4.2.2. Semi-quantification

For each gas sample, peak area information was extracted by integrating each peak corresponding to an identified chemical compound. This operation was repeated with the 11 chromatograms by a semi-quantification method programmed in the GC/MS software. The parameters of this method are, for each chemical compound:

- the retention time (to indicate its position in the chromatogram), with a margin of +/- 0.2min,
- the characteristic m/z to be extracted from the peak before peak integration (to avoid co-elution and overlapping peaks) and
- the mass spectrum of the chemical compound (to compare with the average mass spectra of the peak in the chromatogram and check that the peak is correctly identified).

The integration of peak area information for all chemical compounds at the 11 torrefaction temperatures allows to describe the profile of formation of each volatile during the non-isothermal torrefaction. The minimum peak area considered as significant corresponds to 3 times the background of the analytical instrument (GC/MS).

4.2.2. Quantification

4.2.2.1. Calibration of volatile species in GC/MS

The area of each peak in the chromatogram is proportional to the concentration of the corresponding chemical compound. The relationship between peak area and the concentration of the species in the gas mixture can be established by calibrating each detected chemical compound in the GC/MS with an analytical standard.

23 of the 51 volatile species identified in TGA-GC/MS torrefaction experiments were calibrated (Table III.14). The choice of these species was based on the following criteria:

- Volatile species detected in significant amount (> 50 000 peak area units for at least 2 points of temperature for a given volatile).
- Availability of commercial standard.
- Representativeness of a chemical family of volatiles.

The detail of the calibration curves is indicated in Annex VII.

4.2.2.2. Volatile species production

Initially, the profiles of production of volatile species were expressed in peak areas, proportional to the mass of the volatile species released at a given time, in function of temperature. For a quantitative comparison, the profiles of formation of volatile species were converted into a mass ratio between the mass of volatile species instantaneously produced compared to the corresponding mass of biomass converted, at a given time, in function of temperature.

For a given volatile species, the volatile production curve (peak area = f(T)) was converted into a

mass of volatile released with the corresponding calibration curve:

$$peak\ area\ calibration\ curve\ \ peak\ area = f(mass) \rightarrow mass\left(volatile\ species\ A\ production\right)\ [\square g] \qquad \text{Eq. 6}$$

Secondly, the mass of volatile species A was normalized to 100 mg of initial biomass by division by the initial mass of biomass in the experiment.

$$mass\left(volatile\ species\ A,\ normalised\right) = mass\left(volatile\ species\ A\right)\frac{100\ mg}{m0\ (biomass\ ,experiment\ )\ mg}\ [\square g] \qquad \text{Eq. 7}$$

This mass production for a given volatile species was referred to the amount of volatile species stored in the corresponding heated storage loop (0.5 mL volume), filled with the volatile species continuously produced in torrefaction and carried by an helium flow of 50 mL/min. The storage loop was continuously swept with the flow of volatiles and helium, until the system valves switched and the last 0.5mL fraction of gases kept stored for GC/MS analysis. When all the storage loops were filled, the integral gaseous fraction in each loop was analyzed in GC/MS. The peak area, transformed into mass with the calibration rate, corresponded thus to a sampling time of 0.01min of the torrefaction gases. This implies that the volatile production determined can be expressed as a production rate:

$$\frac{mass\ (volatile\ species\ A)}{0.01(sampling\ time)} = production\ rate\left(volatile\ species\ A\right)\ \ [\square g/min] \qquad \text{Eq. 8}$$

On the other hand, a relationship can be established by the production rate of a given volatile species and the degradation rate of biomass in torrefaction:

$$\frac{production\ \ rate\ (volatile\ \ species\ \ A)}{degradation\ \ \ rate\ (biomass\ )} = \frac{\square g/min\ (volatile\ \ species\ \ A\ produced\ )}{\square g/min\ (biomass\ \ transformed\ )} \qquad \text{Eq. 9}$$

As a result, the production of each volatile species is compared for different biomasses without influence of their nature or degradation profile. As the production of volatile species is expressed in a mass basis, the profiles of production corresponding to different chemical species can be also compared. The representation of the production profiles of the volatiles species in function of time and temperature in the graphics is assisted by the “B-spline” representation of the OriginLab 9.1 software. The objective of this tool is to approximately trace continuous production profiles thanks to the individual points measured for each torrefaction temperature. This tool helps to smooth local pronounced variability of the production that is frequently derived from the error in the measurement. Furthermore, temperature points for which a given volatile species was not detected or under the detection limit were not taken into account in the production profiles.

4.3. Uncertainty estimation

The repeatability of torrefaction experiments was checked by carrying out each experiment twice in TGA-GC/MS for a given biomass. The standard deviation in mass loss calculations was below 0.5 %. The relative uncertainty on volatile species yield was typically between 10 and 25 %. This is considered to be satisfactory by taking into account the uncertainties due to sampling and to the small amounts to be detected. More details about the calculations of these uncertainties in measurements are included in Annex VI.

4.4. Principal Component Analysis

The comparison of the biomass characterization, solid mass loss and volatile species production profiles in torrefaction were firstly carried out visually (see section IV), and secondly by applying Multivariate Data Analysis (MVDA), in particular Principal Component Analysis (PCA, see section V.1).

In the case of the 23 volatile species released that could be quantified for the 14 biomasses studied, and this for 11 points of temperature, it happens that the number of observations (biomass samples) is lower than the number of variables (volatile species). In the case of biomass characterization and solid mass loss, the number of observations and variables remains comparable. It has been reported that classical statistical methods present limitations in data analysis when having a reduced number of observations for a higher number of variables [219,220]. That is the reason why MVDA, and particularly PCA, was selected as a statistical tool for data analysis. Before carrying out PCA, variables were centered and reduced to a standard normal distribution so that all variables have the same influence.

MVDA is a statistical tool enabling to identify groups of variables behaving similarly in a complex dataset, as well as major trends and potential outliers. PCA allows to reduce a large set of variables to a small set that still contains most of the information of the large set [219]. More precisely, PCA detects linear dependencies between variables and substitutes groups of correlated variables with new, uncorrelated variables named principal components (PCs) [221].

To do this, PCA transforms the original system of axis in a new dimensional space where the first axis (PC1) contains the highest variance, the second one (PC2, orthogonal to PC1), contains the second highest variance, and so forth (Figure III.19). The maximum number of dimensions of this new space corresponds to the number of variables and captures the full variance of the dataset [221]. However, the number of variability sources is reduced compared to the original dataset by selecting a reduced number of new PC axis that represents a satisfactory percentage of the dataset variability.

As a result, the observations of the measured variables are changed into new values, named scores, obtained by projecting the variation in the new PCA axis. This result is visualized in the score plot, which represents the relationship between the sample points based on their

maximum variation. The proximity of the samples in the score plot indicates their similarity. A sample's position in the score plot is determined by the contributions of the variables to the PCs, given by the loading values or loadings. These values represent the partial contribution of each variable, which is calculated by the cosine of the angle between the variable in the original dimensional space and the tilt in the new PCA plane. The loadings are visualized in a loading plot, in which each variable is represented by a data point. The variables are represented in this plot according to their weights for the first and second principal components (PC1 and PC2). Variables are better represented whether they are closer to the circle in the loading plot. On the contrary variables located close to the origin have low weight for the represented principal components.

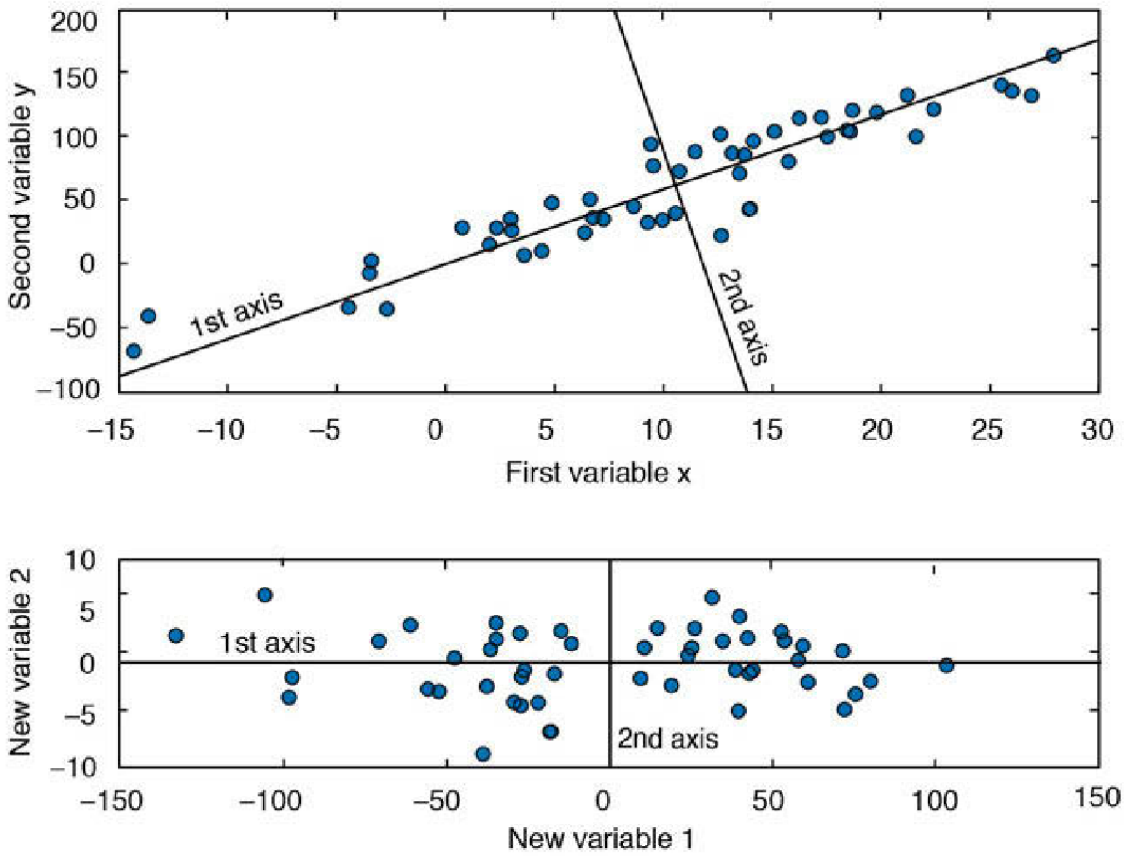


Figure III.19. Raw data (top) and resulting Principal Component Analysis (PCA, bottom) for a bivariate set of data [221]

Observations in PCA score plot and in the corresponding loading plot are related: observations grouped in one given region of the score plot are associated with relatively higher values for variables clustered in the equivalent region of the loading plot. On the contrary, these observations are anticorrelated to the variables situated in the opposite part of the loading plot.

5. Conclusion

The main conclusions derived from this chapter are the following ones:

- The selection of 14 biomasses representative of the European diversity constitutes a more consequent database than in previous studies, both in terms of biomass characterization and of its behavior in torrefaction.
- The optimization of the extracted procedure of the macromolecular components allowed to directly obtain cellulose, hemicellulose and lignin fractions from 5 biomasses representative of the main biomass families (deciduous wood—2 samples—, coniferous wood, herbaceous crops and agricultural by-products). This ensures:
    - A higher representativeness of the native macromolecular components in biomass than by using commercial compounds.
    - The possibility to assess the different properties of cellulose, hemicelluloses and lignin in function of the biomass family, as well as their incidence on biomass behavior in torrefaction.
- The use of a TGA coupled to a GC/MS analyzer through a heated storage loop system allowed the simultaneous analysis of solid mass and of volatile species production in function of torrefaction time and temperature through one single experiment.
- By guaranteeing the chemical regime in the torrefaction experiments, both at bed and particle scales, the obtained results can be used for further modelling.

-IV-
RESULTS
AND DISCUSSION

IV. RESULTS AND DISCUSSION

In this section, the results obtained in torrefaction experiments in TGA-GC/MS are presented. This includes, in the first part, the 14 raw biomasses, and in the second part, the extracted fractions from the reference biomasses. The results are analyzed in terms of solid mass loss and degradation rates, as well as in terms of production profiles of the 23 volatile species that were quantified in torrefaction experiments. The obtained results are discussed in relation to the biomass macromolecular composition and biomass family.

1. Raw biomasses

1.1. Raw biomasses

The named biomass database is composed of the following biomasses:

- Coniferous wood: pine, pine forest residues and Scot pine bark.
- Deciduous wood: ash-wood, beech, poplar and willow.
- Herbaceous crops: miscanthus and reed canary grass.
- Agricultural by-products: corn cob, grape seed cake, sunflower seed shells and wheat straw (2 types).

Samples of these raw biomasses underwent a non-isothermal torrefaction between 200 and 300°C, at 3°C/min, followed by an isothermal torrefaction at 300°C for 30 minutes (Figure IV.1). In the following section, they are characterized in terms of solid kinetics and volatile species release. Performing torrefaction at this temperature range in chemical regime helps the identification of the influence of each macromolecular component in biomass torrefaction. Indeed, at higher torrefaction temperatures (300 to 350°C), the decomposition of cellulose, hemicellulose and lignin is simultaneous, which complicates the separation of the phenomena involved [6,20,22,121].

The suitability of the biomass database to represent biomass diversity is assessed through 6 complementary biomasses analyzed in torrefaction in TGA-GC/MS (see details in Annex I).

1.1.1. Solid mass loss kinetics during torrefaction

Solid mass loss was calculated versus temperature and time (Figure IV.1). The corresponding degradation rates curves were also plotted (Figure IV.2). Reference biomasses are indicated in dotted lines.

Previous studies have considered a single biomass per family for the study of solid kinetics in torrefaction [12,22,23,28]. To check this hypothesis, one biomass was selected per biomass family except for deciduous wood. The selected biomasses were ash-wood and beech for deciduous wood, pine for coniferous wood, one wheat straw for agricultural coproducts and miscanthus for herbaceous crops (represented by dotted lines in Figures IV.1 and IV.2).

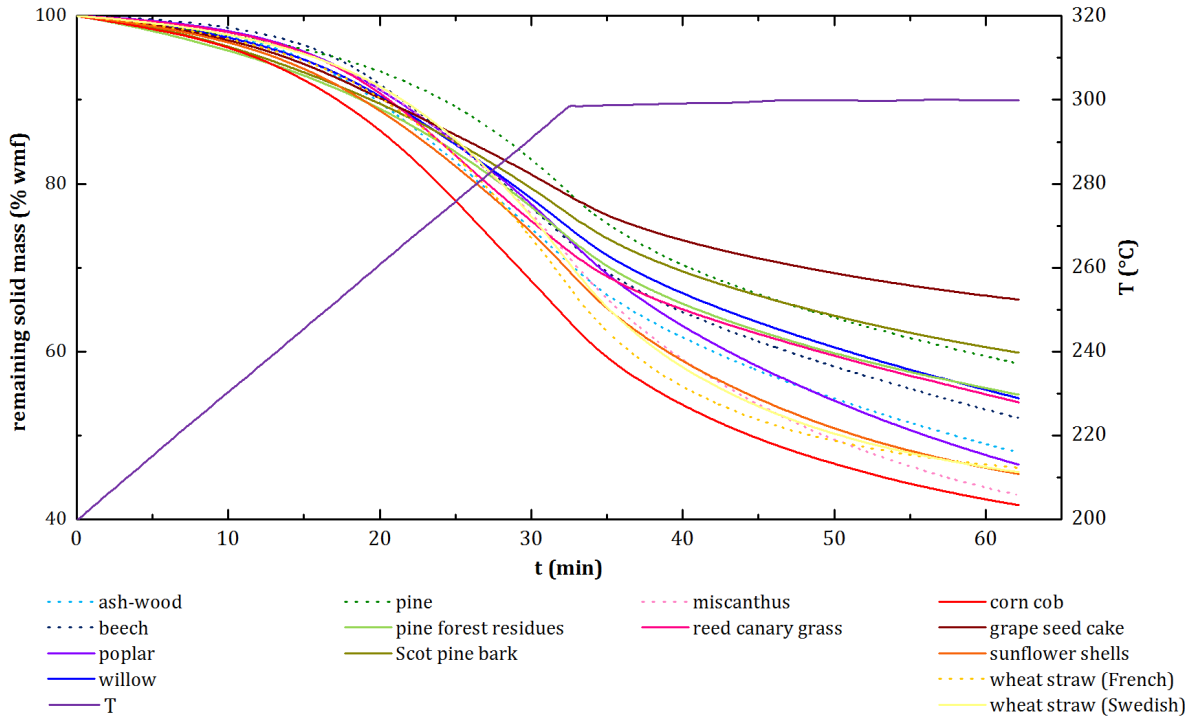


Figure IV.1. Remaining solid mass versus temperature and time obtained for the different raw biomasses in torrefaction in TGA-GC/MS

The final remaining solid mass varied according to the 14 biomasses between 20 and 36 % at the end of the non-isothermal stage and between 33 and 58 % after the isothermal stage (Figure IV.1). There is therefore about a factor 2 between mass losses according to biomasses, which means, in a process viewpoint, that torrefaction conditions in industrial units should be tuned depending on biomass type.

The highest mass loss was obtained for corn cob (58.3 %), closely followed by miscanthus (57.1 %) and sunflower seed shells (54.6 %), while the lowest mass loss was found for grape seed cake (33.8 %). Such result shows the large diversity of the agricultural byproducts and the impossibility to describe them through one single representative type. It is noteworthy that among the agricultural biomasses, the two wheat straws had very similar final mass loss of 53.9 and 54.4 % respectively, which would tend to suggest that torrefaction behavior might be associated to each species. Eventually, woody biomasses were found to be in the middle of the mass loss range, with about 5 % of difference among the different samples considered (53.5 to 47.9 %). It is interesting to note that, among these woody samples, all coniferous samples showed lower mass loss than the deciduous samples. This result tends to be in agreement with previous results from literature, which mention coniferous wood as less reactive under torrefaction conditions [22].

Two main degradation rate profiles could be identified in the non-isothermal part of the curves (Figure IV.2). The first profile corresponds to a progressive acceleration of the degradation

during the heating period. This is the case of wheat straws, miscanthus, pine, Scot pine bark and pine forest residues. The second typical biomass degradation pattern corresponds to an initial acceleration of the solid degradation until 250-270°C, followed by a slower solid degradation until 300°C. This behavior could be observed for grape seed cake, sunflower seed shells and deciduous woods. Finally, two extreme cases of this second behavior are observed, for reed canary grass and for corn cob. For reed canary grass, the solid degradation increases until 275°C, and then the degradation rate slightly decreases. For corn cob, the acceleration of the degradation rate occurs before 280°C and then stabilizes until 300°C. The deceleration of the solid degradation in the isothermal torrefaction (300°C, 30 min, Figure IV.1 and Figure IV.2) is more accentuated for wheat straws, followed by miscanthus, sunflower seed shells and corn cob. Finally, grape seed cake, hardwood and softwood deceleration is more attenuated. It is also interesting to highlight that, for an equivalent final mass loss, the degradation profile can be different. This is the case of corn cob and miscanthus.

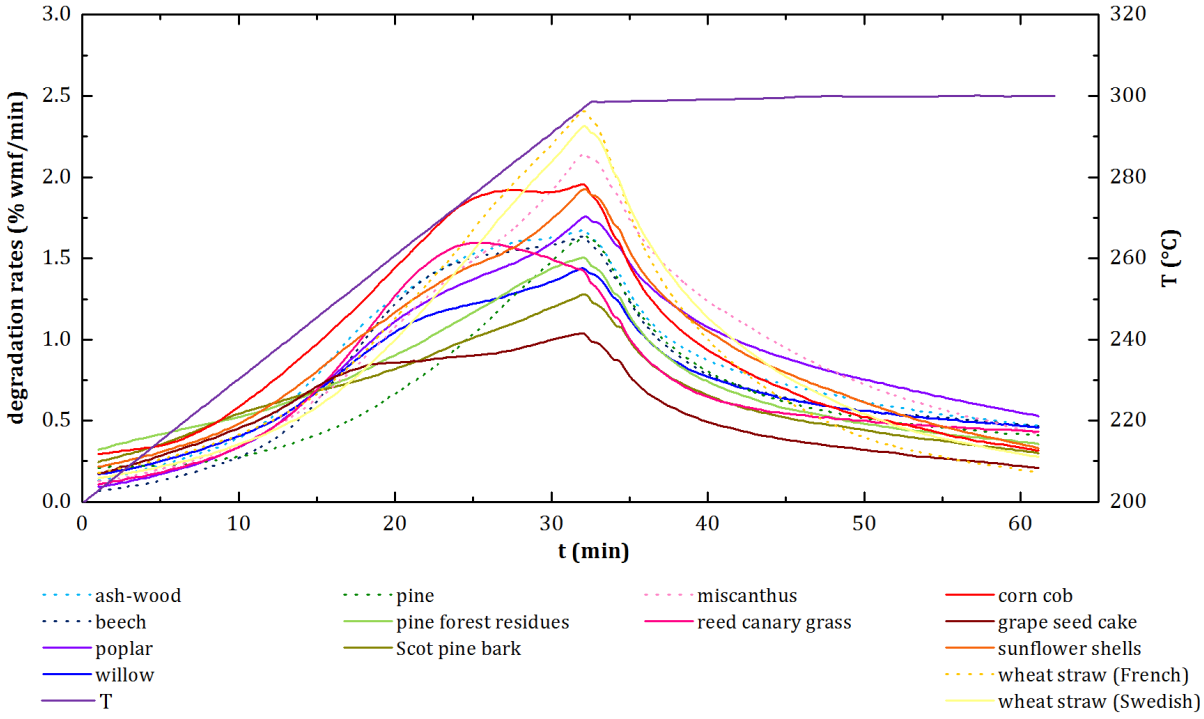


Figure IV.2. Degradation rates versus temperature and time obtained for the different raw biomasses in torrefaction in TGA-GC/MS

By analyzing biomass non-isothermal torrefaction per family (Figure IV.2), the three selected deciduous woods (beech, poplar and ash-wood) present a very similar solid degradation profile, also close to that of willow. This could be explained by their similar macromolecular composition. However, this criterion does not seem to be sufficient to describe biomass transformation in torrefaction. Herbaceous biomasses (reed canary grass and miscanthus) present a similar cellulose, hemicellulose and lignin content to that of deciduous wood, but their

degradation pattern in torrefaction is different. A more detailed characterization of biomass macromolecular composition could help to explain this difference. For example, in the case of lignin, softwood lignin consists of G- (guaiacyl-) units, while hardwood lignin is known to consist of G- and S- (syringyl-) units [63]; lignin from herbaceous plants also contains H- (phenyl-) units [222]. The three coniferous wood samples also seemed to have similar behaviors, different to that of deciduous wood, in relation with their specific cellulose, hemicellulose and lignin composition. On the contrary, agricultural byproducts had different degradation profiles, which could be related to their differences in macromolecular composition and should be therefore seen as a very heterogeneous group.

In the isothermal torrefaction stage at 300°C, some agricultural biomasses such as wheat straws, sunflower seed shells and miscanthus show a more marked decrease of the degradation rate, compared to that of wood, which tends to stabilize.

By analyzing in depth degradation rate profiles (Figure IV.2), grape seed cake degradation profile seems to be particularly marked by the degradation pattern of lignin. The relative stabilization of its degradation rate between 250°C and 300°C could be explained by its high lignin content (62.7 %) and its very low cellulose content (7.8 %), which is in agreement with previous studies [22]. On the contrary, this stabilization of the degradation rate does not happen for Scot pine bark: despite its high lignin content (40.7 %), a high cellulose content (24.0 %) might compensate the loss mass at high torrefaction temperatures (270 to 280°C). Scot pine bark degradation rate profile is closer to that of coniferous wood, more sharpened at intermediate and high torrefaction temperatures (250 to 300°C). This difference could be explained by the higher cellulose content of pine compared to those of pine forest residues and of Scot pine bark, as cellulose decomposition occurs around 300°C. On the other hand, the enhanced acceleration of corn cob degradation at low temperatures (215 to 275 °C) could be explained by a higher polysaccharide content (40.5 % for cellulose and 37.7 % for hemicellulose). No evidence was found to explain the stabilization of the corn cob degradation rate at higher torrefaction temperatures. The higher weight loss of deciduous wood compared to that of coniferous could be explained by their different hemicellulose composition: xylan-based hemicelluloses from hardwood would be more reactive than softwood hemicelluloses, mainly composed of mannose-based sugars (Table III.4) [46,99].

The quality of the remaining solid product after torrefaction was evaluated in terms of elemental composition in C, H and O (Figure IV.3). The results show an increase of the carbon content from 17.5 to 48.4% for beech and French wheat straw, respectively. The composition in O decreased consequently from 19.0 to 46.5%, respectively for pine and French wheat straw. The composition in H remains low and was only slightly affected after torrefaction.

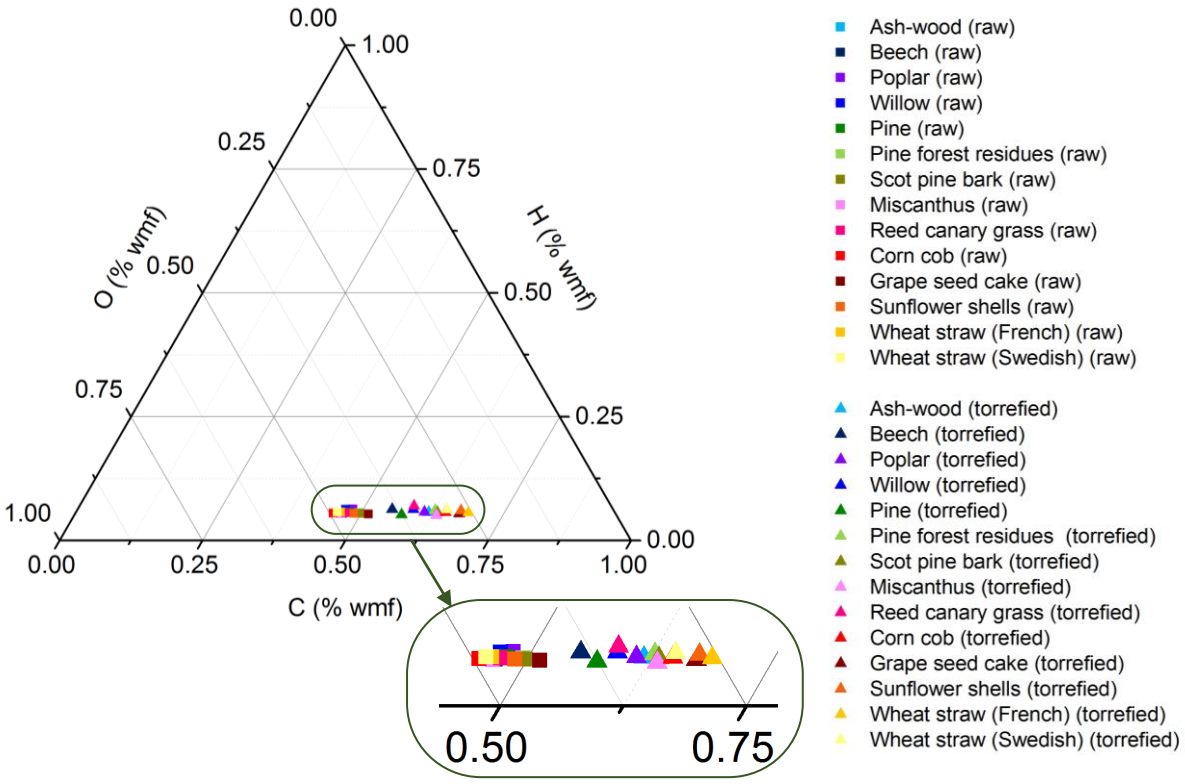


Figure IV.3. Ternary diagram of CHO elemental composition of raw and torrefied biomass in TGA-GC/MS

These results suggest that torrefaction behavior strongly depends on biomass type and its macromolecular composition. As a first approach, two categories of solid degradation profiles may be considered to describe non-isothermal torrefaction. These categories would correspond to agricultural biomasses/coniferous wood/herbaceous crops behavior on the one hand, and to deciduous wood behavior on the other hand. In the subsequent isothermal torrefaction step, all biomasses show a more or less marked gradual deceleration in their degradation profile

1.1.2. Volatile species release

The total production of quantified volatile species released per g of biomass transformed at the end of the non-isothermal torrefaction was calculated and plotted on Figure IV.4. The total production of quantified volatile species was found to lie between 0.01 and 0.03 g (volatile species produced)/g (biomass transformed). As mentioned in chapter I, about 15 % of the mass loss in torrefaction is said to be found as permanent gases, 30 to 50 % as water, and the rest as dry condensable species [6]. As the mass loss is of about 0.2 to 0.4 g/g (initial biomass) for the non-isothermal step of the torrefaction, the quantified part of the volatile species would represent between 10 and 33% of the total dry condensable species produced in torrefaction. This result seems satisfactory compared to the state-of-the art in the field. It can be explained by the limits of the technique, especially the complexity of the chromatograms which implies a challenging identification of some volatile species because of peaks overlapping. Furthermore, about thirty other minor chemical species have been identified but could not be quantified (see Table III.14).

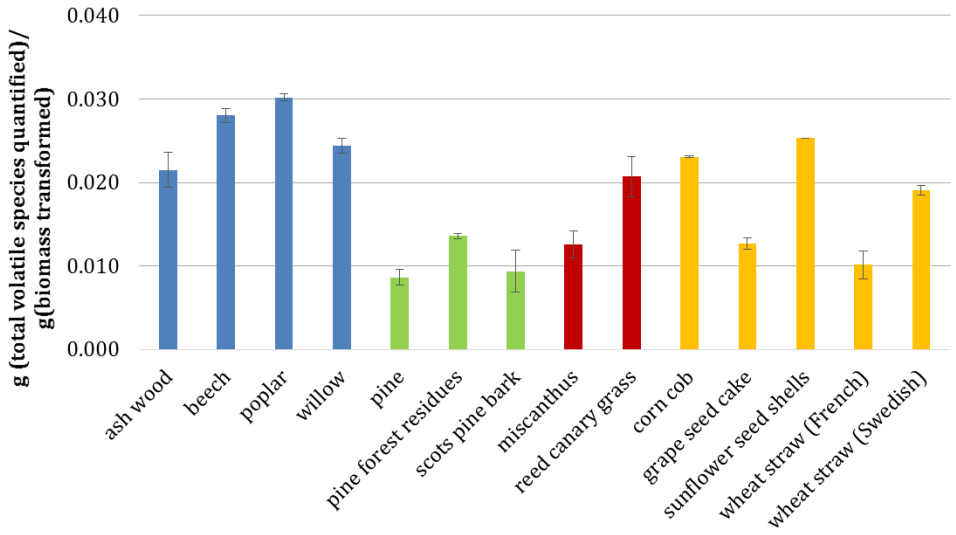


Figure IV.4. Total production of quantified volatile species released per mass of biomass transformed after a non-isothermal torrefaction (200-300°C, 3°C/min)

The total production of volatile species seems similar for biomasses from a same family in the case of deciduous and coniferous woods, whereas a larger range could be observed for agricultural coproducts and herbaceous crops. This can be explained by the heterogeneity of agricultural biomass in terms of its macromolecular composition, as mentioned previously. The total production of volatile species was found different for the two wheat straws, although their composition and behavior were similar regarding solid mass loss.

To analyze their distribution, the quantified volatile species were gathered per chemical family for each biomass (Figure IV.5).

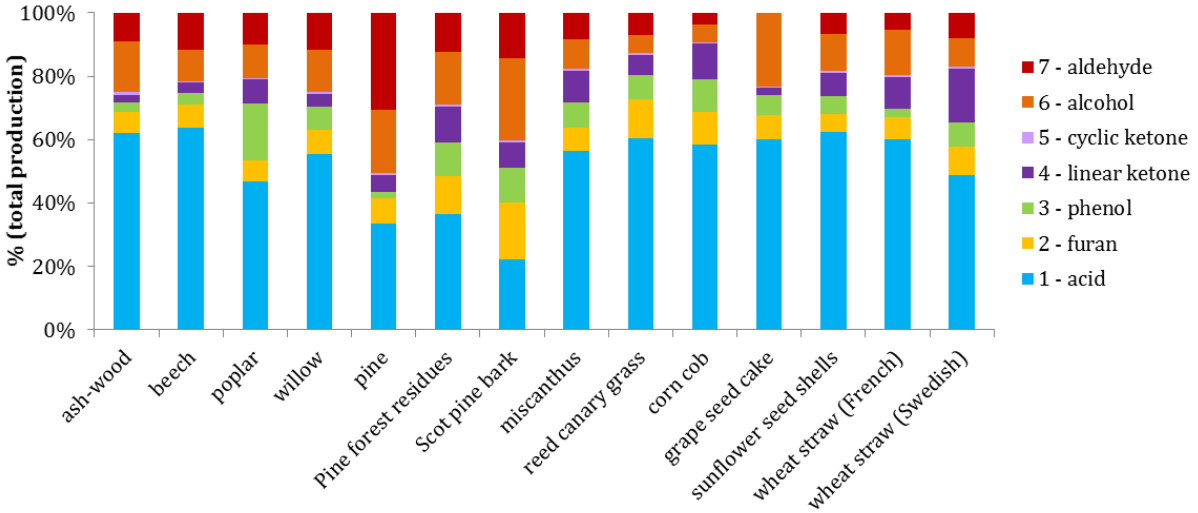


Figure IV.5. Distribution of the total production of volatile species per chemical family obtained in torrefaction of raw biomasses in TGA-GC/MS

Inside one biomass family, the distribution of the volatile species was found quite similar. Acids

were the main chemical compounds (mainly acetic acid), followed by alcohols (methanol) and aldehydes (formaldehyde), except for pine bark, for which acids were produced in comparable amounts to the other chemical compounds. The proportion of alcohols and aldehydes in the total volatile species production was higher for coniferous woods, including bark, in detriment of acid production. Furans, ketones and phenols were also produced for all biomasses in variable proportions. This behavior is in agreement with the similarities in the macromolecular composition of the biomasses per biological family (see Tables III.3 and III.4) and is supported by previous studies (see Table II.2).

The evolution of the production profiles of the quantified volatile species was studied versus time and temperature for the 14 biomasses (Figures IV.6 to IV.12).

Several chemical compounds showed similar production profiles for biomasses of the same family. This is the case for the deciduous woods, especially for ash-wood and willow, and, to a minor extent, for poplar and beech. Coniferous woods also tended to have similar patterns of volatile species formation. As stated in the section about solid mass loss, agricultural biomasses constitute a heterogeneous group in terms of macromolecular composition (see section III.1.1) and, consequently, of torrefaction behavior. However, it is noteworthy that almost identical volatile release profiles could be observed for the two wheat straws (Figures IV.6 to IV.12). As a first approach, volatile species release in torrefaction seems therefore to be characteristic of each biomass species. This behavior in torrefaction may be conditioned by the elemental and macromolecular and composition of the plant, as well as by the arrangement of its macromolecular components by intra- and inter- linkages in the structure [48,72].

The results suggest that the maximum temperature of formation mainly differs according to the chemical compound, and only to a lower extent according to the biomass type, which might be related to the mechanisms of formation of the volatile species in torrefaction.

The production peak of acetic acid, which was the main volatile species detected, generally occurs at temperatures lower than 300°C (Figure IV.6, left). In the case of coniferous wood, the production profile is less marked, with a maximum at lower temperatures. According to the literature, acetic acid formation is enhanced by the presence of xylan, while glucomannan, less reactive, leads to formic acid production (Table II.3). As a result, the lower temperature maximum for coniferous wood could be derived from their lower xylose content, which reacts at lower temperatures than mannose, typically present in coniferous wood (see section II.3.2).

The production of methanol, which is also expected to be mainly produced by hemicelluloses (Table II.3), is maximal at low temperatures (Figure IV.6, right). This different profile compared to that of acetic acid could be derived from a second source of release of methanol, which could correspond to the scission of the methoxy- groups attached to phenolic units from lignin.

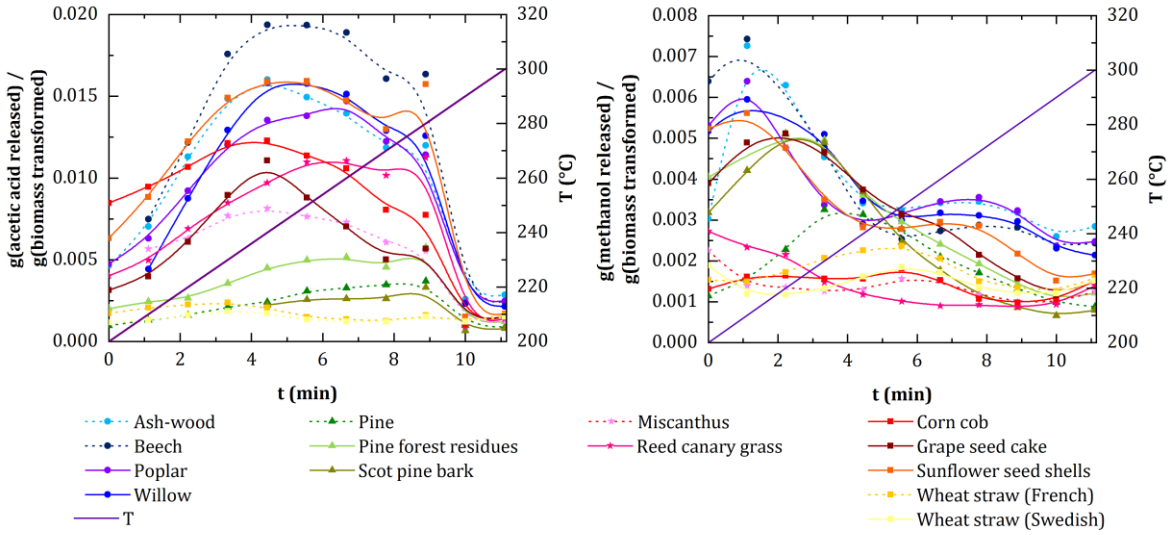


Figure IV.6. Production profile of acetic acid (left) and methanol (right) versus temperature and time obtained for raw biomasses in torrefaction in TGA-GC/MS

Different production profiles were determined for formic acid and propionic acid. For formic acid, an irregular production was measured in function of temperature. This is probably due to the experimental difficulties to quantify this compound in a complex volatile mixture (Figure IV.7, left). The production of propionic acid appeared to be enhanced with the torrefaction temperature (Figure IV.7, right). Corn cob and wheat straws showed a higher production of this compound, which has been reported in the literature to partially derive from extractives conversion and from hexuronic acids in hemicelluloses (Table II.3).

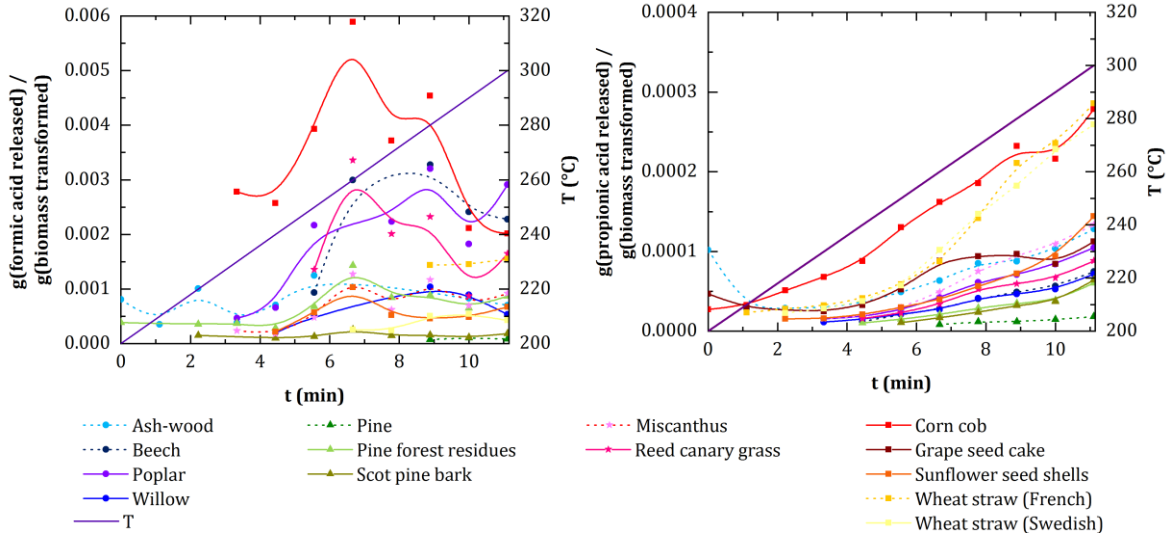


Figure IV.7. Production profile of formic acid (left) and propionic acid (right) versus temperature and time obtained for raw biomasses in torrefaction in TGA-GC/MS

The production of furfural is maximal at temperatures below 300°C (Figure IV.8, left). This result is in agreement with previous studies, reporting that furfural was mainly produced at low temperature, derived from cellulose and hemicellulose decomposition (Table II.3). Other furans

(represented by 3-furaldehyde) were mostly released at higher torrefaction temperatures, more related to the degradation of cellulose (Figure IV.8, right).

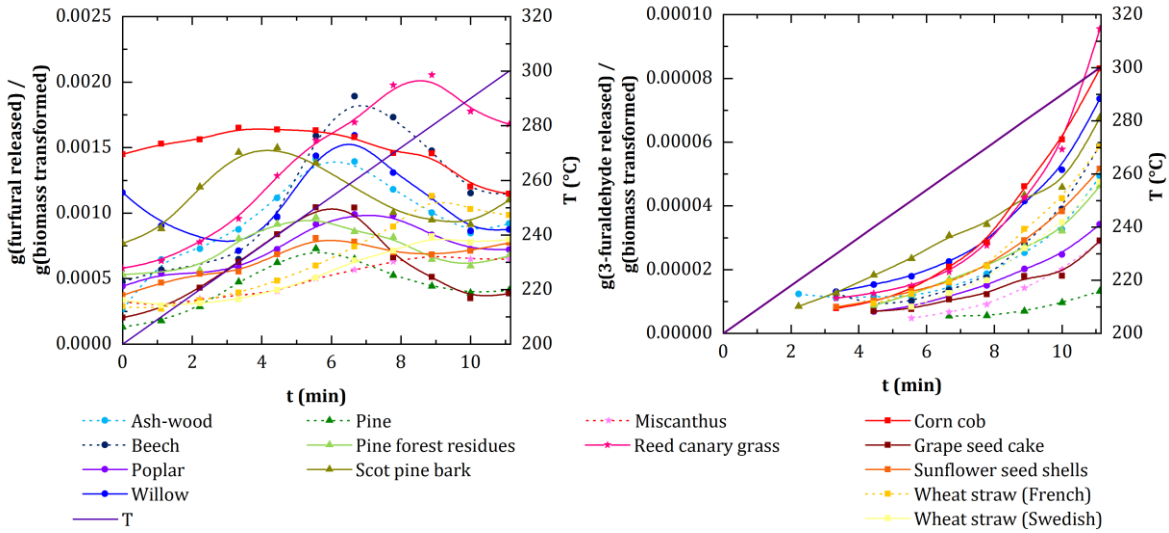


Figure IV.8. Production profile of furfural (left) and 3-furaldehyde (right) versus temperature and time obtained for raw biomasses in torrefaction in TGA-GC/MS

Phenolic compounds are known to be derived from lignin, which is only partially and progressively degraded under torrefaction conditions. Syringol is not produced by coniferous wood, which is in agreement with the lack of syringyl- units in lignin of this kind of essence [172]. The production of phenolic compounds representing the lignin-base units, namely phenol, guaiacol and syringol, is enhanced by the torrefaction temperature increase (Figure IV.9). This acceleration of the production starts at slightly earlier temperatures for syringol, followed by guaiacol and phenol.

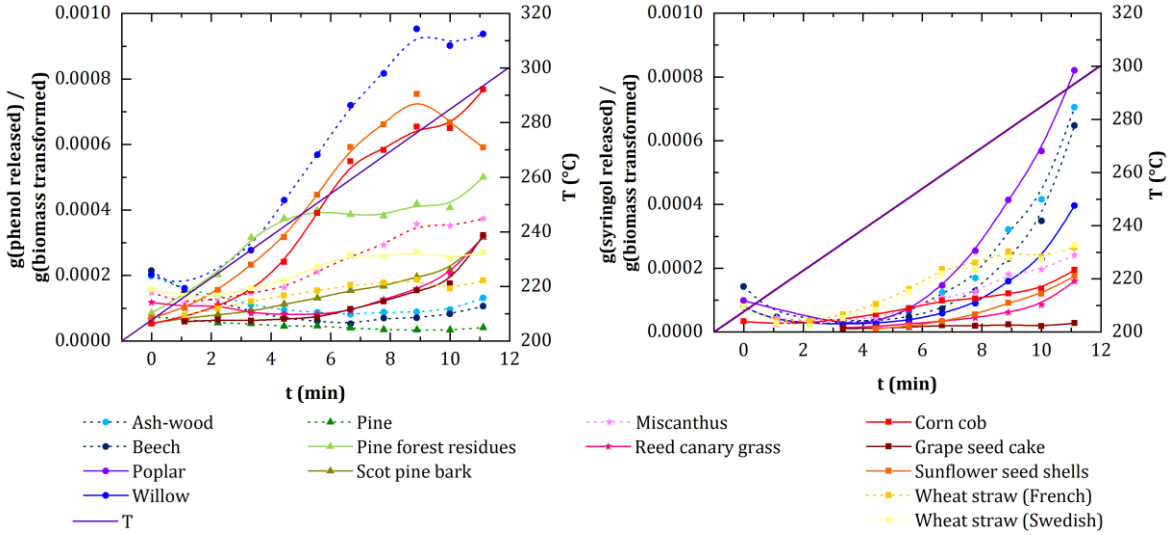


Figure IV.9. Production profile of phenol (left) and syringol (right) versus temperature and time obtained for raw biomasses in torrefaction in TGA-GC/MS

No other syringyl-derived compounds were detected in torrefaction apart from syringol. On the other hand, guaiacyl-derived compounds were detected for all biomasses (Figure IV.10). Eugenol and isoeugenol (cis/trans) are mostly produced at high torrefaction temperatures and for woody biomasses. Other guaiacyl-phenolic compounds, such as eugenol and vanillin, are largely present at low torrefaction temperatures (200-210°C), which may be at least partially due to the degradation of extractives present in biomass. In general, the production profiles of the volatile species derived from the same lignin unit are similar (phenyl-, guaiacyl-, syringyl-), respectively, particularly for woods. Furthermore, the production of the substituted phenolic compound, such as vanillin (Figure IV.10), tends to start its release in torrefaction at lower torrefaction temperatures than the lignin-base phenolic compounds, guaiacol in this case (Figure IV.9). These results are in agreement with the analytical fractionated Py-GC/MS tests carried out on 8 of these biomasses between 250 and 500°C (Annex VIII).

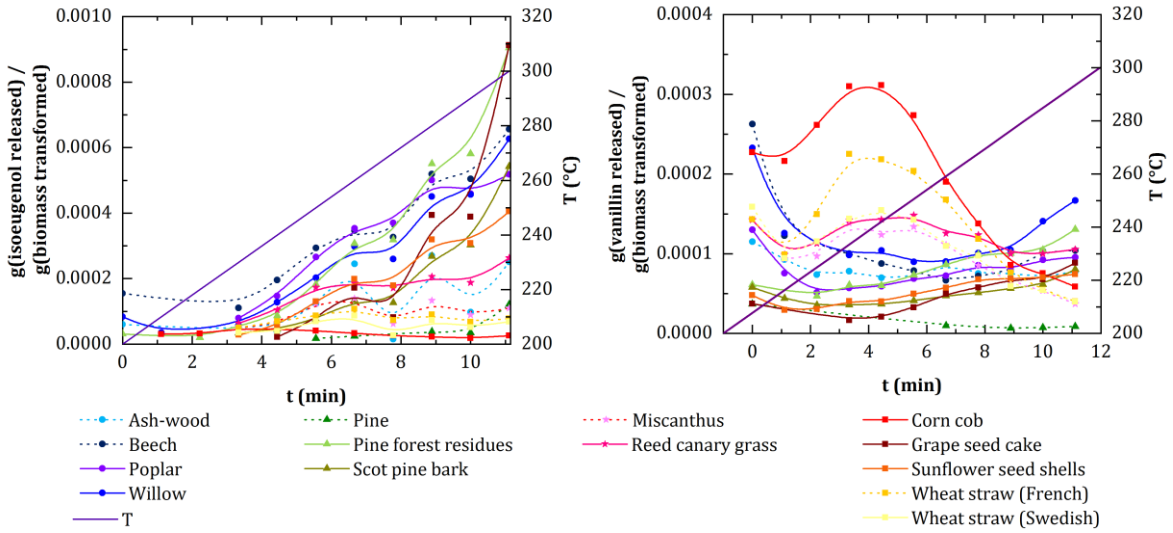


Figure IV.10. Production profile of isoeugenol (left) and vanillin (right) versus temperature and time obtained for raw biomasses in torrefaction in TGA-GC/MS

Formaldehyde is rather produced by wood at higher torrefaction temperatures. However, it was not detected for grape seed cake, which is the biomass with the highest lignin content. This could be due to a difference in the structure of the lignin from this agricultural biomass, supposed to be composed of H-, G- and S- units, while lignin from coniferous wood is mostly composed of G-units. Its production profile generally tends to be independent of the torrefaction temperature, except for woody biomasses (Figure IV.11).

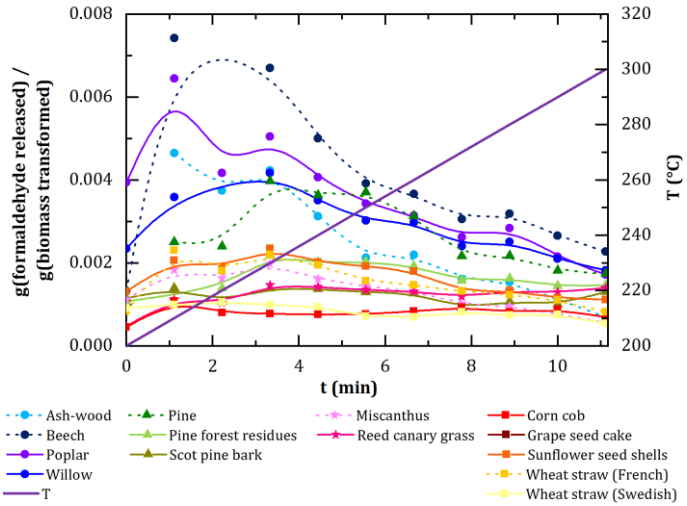


Figure IV.11. Production profile of formaldehyde versus temperature and time obtained for raw biomasses in torrefaction in TGA-GC/MS

Similarities were found between corn cob and the two wheat straws for guaiacol, acetylfuran and vanillin (Figure IV.10). On the other hand, grape seed cake and sunflower seed shells exhibited very different volatile species release profiles compared to the other biomasses. In the case of grape seed cake, this may be attributed to its exceptionally high content in lignin. The composition of sunflower seed shells is similar to the other biomasses, except for ash content, whose influence in torrefaction is not clearly determined [12]. A detailed study of the structure of grape seed cake and sunflower seed shells, which seem to be particularly different in the family of agricultural biomasses, could help to explain these differences. It is interesting to note that herbaceous biomasses generally remain close to agricultural byproducts, certainly due to their similar biological structure and, in some cases, macromolecular composition (example for 2-propanone, 1-(acetyloxy)-, Figure IV.12). This observation is in agreement with the results of the Principal Component Analysis (see V.1 section).

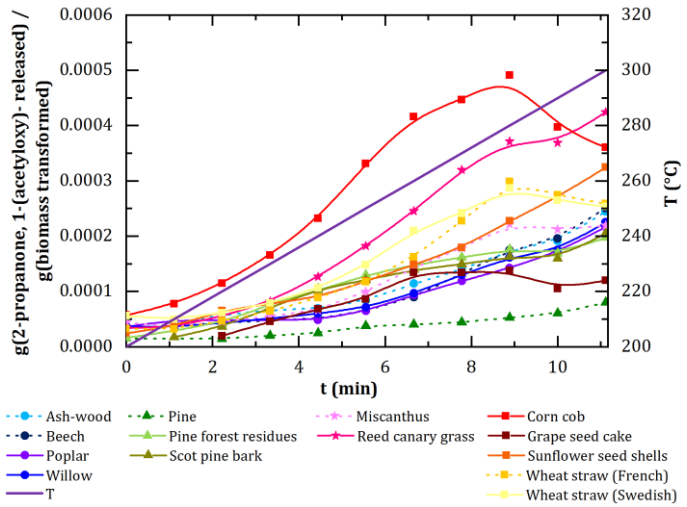


Figure IV.12 Production profile of 2-propanone, 1-(acetyloxy)- versus temperature and time obtained for raw biomasses in torrefaction in TGA-GC/MS

Finally, as a first approach, a representative of each main wood family, namely deciduous and resinous, seems to be sufficient to describe the formation of volatiles. For agricultural biomasses, one representative may be sufficient for herbaceous biomasses but would not be sufficient for agricultural by-products since this group is too heterogeneous [223].

For deeper analysis of the impact of biomass characteristics in torrefaction and further modelling, 5 biomasses were selected. This limited number is due to experimental constraints. As a result, one biomass of each biomass family was selected. A deciduous wood was added, so as to check the similarities in the behavior in torrefaction inside this family. Wheat straw was selected as representative of agricultural by-products due to its frequent use. However, an additional agricultural biomass was not selected because of the high heterogeneity of the family. As a result, the selected biomasses for extracting their macromolecular components and study their behavior in torrefaction are:

- Coniferous wood: pine.
- Deciduous wood: ash-wood and beech.
- Herbaceous crops: miscanthus.
- Agricultural by-products: wheat straw (French, directly called wheat straw below).

2. Extracted macromolecular components from the reference biomasses

Five extracted fractions were obtained through the extraction procedure described in III.1.3 and applied to the five selected biomasses: ash-wood, beech, miscanthus, pine and wheat straw:

- Cellulose: composed of two fractions: «cellulose II» (main fraction) and «DMSO residue» (complementary fraction– cellulose I).
- Hemicelluloses: composed of two fractions, «hemicelluloses 1» (main fraction) and «hemicelluloses 2» (complementary fraction).
- Lignin: exclusively present in the «lignin» fraction.

2.1. Cellulose

The extraction procedure leads to two fractions containing extracted cellulose:

- Cellulose is mainly present in the fraction named «cellulose II».
- An equivalent amount of cellulose is present in the «DMSO residue», which preserves the allomorphic cellulose I structure from native biomass, together with residual hemicelluloses.

2.1.1. «Cellulose II» fraction

2.1.1.1. Solid transformation

Solid mass loss was calculated versus temperature and time for the «cellulose II» fraction from 5 biomasses (ash-wood, beech, miscanthus, pine, wheat straw, Figure IV.13). The commercial microcrystalline cellulose Avicel (cellulose I) was also considered for comparison.

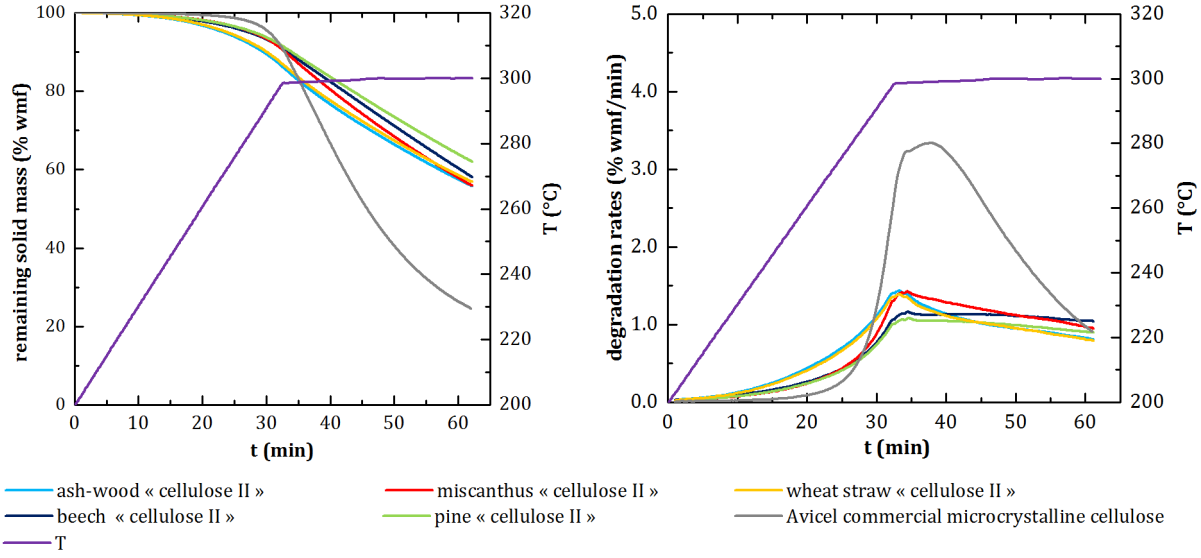


Figure IV.13. Remaining solid mass (left) and degradation rates (right) versus time and temperature obtained in torrefaction for «cellulose II» fractions from 5 biomasses and for commercial microcrystalline cellulose Avicel in TGA-GC/MS

The degradation profile was generally similar for all «cellulose II» fractions whatever the biomass, with a slightly higher acceleration of the degradation for miscanthus (Figure IV.13). The final remaining solid mass at the end of the non-isothermal torrefaction was in the same order of magnitude for all samples, varying from 92.2 to 86.6 %wmf, while it is of 91.7 %wmf for commercial microcrystalline cellulose. Concerning the subsequent isothermal torrefaction step (300°C, 30 min), the final remaining solid mass for «cellulose II» fractions was between 66.0 and 55.8 %wmf, while the commercial cellulose suffered an intense degradation until a final remaining solid mass of 24.6 %wmf (Figure IV.13, left). These results are in agreement with the literature, as previous studies indicate that cellulose degradation rather starts at 300 to 350°C [116,135], so it is only slightly degraded below 300°C (see section II.3.2.1).

Degradation rates curves (Figure IV.13, right) showed similar profiles for the five «cellulose II» fractions, very close to the behavior of ash-wood and wheat straw «cellulose II» fractions on the one hand, and those of beech and pine «cellulose II» on the other hand. The acceleration in the degradation of these fractions appeared to be progressive from early torrefaction temperatures in the non-isothermal step (230°C), while the degradation of the commercial microcrystalline cellulose only started in a notable way at 280°C. On the contrary, the microcrystalline cellulose was highly degraded during the isothermal torrefaction step (300°C, 30 min), firstly at a high

degradation rate (around 3.3%) that then decreased in function of time. The degradation rate of «cellulose II» fractions in the isothermal step started around 1.0 % wmf/min for pine and 1.4% for ash-wood «cellulose II». It was stable for pine and beech fractions, slightly decreasing for miscanthus fraction and more decelerated with time for wheat straw and ash-wood fractions. The final degradation rate was in the same order of magnitude for the 6 samples (around 1.0%).

By analyzing these results, a first observation appears regarding commercial cellulose Avicel. The decomposition profile of microcrystalline cellulose Avicel in TGA torrefaction is noticeably different from that of the five extracted celluloses. The main reasons for this different behavior are related to the properties of these samples, namely:

- **Sugar composition** (see Table III.6): the commercial microcrystalline cellulose presents a higher proportion of hemicellulose sugars than the «cellulose II» fractions, which indicates its low purity. This hemicellulose sugar content in Avicel (3.9 % of the total monosugars) might contribute to its degradation below 300°C (around 8.3 % wmf of the mass loss).
- **Polymerization degree** (Dp, see Annex II, Table A.III.1): this parameter is about 4 times higher for extracted «cellulose II» fraction compared to commercial microcrystalline cellulose. It has been observed that a lower polymerization degree implies a lower starting temperature of cellulose degradation (Annex IX). However, an order of magnitude of 20 is needed in Dp to observe a remarkable difference in the degradation. The higher polymerization degree of the «cellulose II» fractions compared to that of Avicel indicated that they are less fragmented, so more representative of native cellulose. However, in both cases, the polymerization degree remains much lower than in native cellulose, which still may impact the real starting temperature of cellulose degradation in torrefaction.
- **Average molar mass** (see Annex II, Figure A.III.1): equivalent observations to those discussed for the Dp were obtained for this parameter. Furthermore, the narrower molar mass distribution of the «cellulose II» fractions compared to that of Avicel might be responsible of the progressive degradation of the fractions, as cellulose chains are more homogeneous in chain length and thus might behave similarly.
- **Allomorphic structure** (see III.1.2.1, Figure III.2): the cellulose II structure of extracted «cellulose II» fractions is suspected to be more reactive than the cellulose I structure of the commercial microcrystalline cellulose. This might contribute to the degradation of the «cellulose II» fractions at lower temperatures than for Avicel.
- **Presence of amorphous areas**: although the crystallinity index could not be measured, the alkaline treatment to obtain «cellulose II» is known to preserve amorphous areas in cellulose. On the contrary, the acid hydrolysis to obtain commercial microcrystalline cellulose only preserves crystalline cellulose chains (see section II.3.2). The amorphous

regions might be less stable and suffer an earlier degradation through torrefaction, which might also contribute to explain the degradation of the «cellulose II» fractions from lower temperatures than for commercial microcrystalline cellulose.

These results suggest that the presence of amorphous areas in «cellulose II» fractions might have a more significant impact on cellulose degradation than differences in the polymerization degree between these fractions and the commercial cellulose. However, the considerably higher polymerization degree of native cellulose in biomass compared to those of these samples is suggested to strongly impact the starting temperature of cellulose degradation, by switching it to higher temperatures than those observed (below 300°C). This suggests that the observed remaining solid mass profiles are correct (Figure IV.13) but might be switched shifted to higher temperatures for native cellulose in biomass. However, in a first approach, representing cellulose through «cellulose II» fractions instead of commercial microcrystalline cellulose seems more suitable.

The quality of the solid product after torrefaction was assessed through the evolution of the elemental composition in C, H and O (Figure IV.14). It is noteworthy that the similar elemental composition of the «cellulose II» fractions leads to small differences in the elemental composition of the corresponding torrefied fractions. The increase in carbon content in the torrefied «cellulose II» is between 22.3 and 29.2%, while their oxygen content is reduced between 15.3 and 22.2%. As a result, the change in the elemental composition of the solid through torrefaction remains limited for the «cellulose II» fractions compared to that of raw biomass. This change is related to the solid mass loss suffered by «cellulose II» fractions through torrefaction.

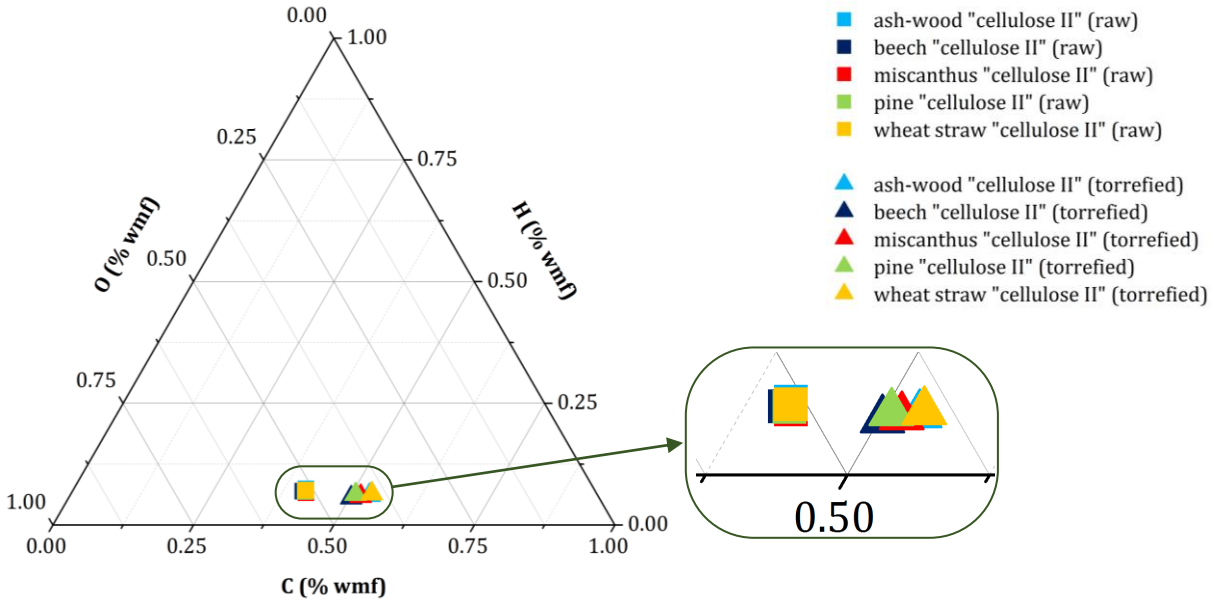


Figure IV.14. Ternary diagram of CHO elemental composition of raw and torrefied «cellulose II» in TGA-GC/MS

To sum up, the behavior of the five «cellulose II» was shown to be similar. In terms of representing the cellulose degradation through torrefaction, it seems preferable to consider one «cellulose II» fraction rather than the commercial microcrystalline cellulose. This hypothesis needs to be confirmed by the analysis of the influence of cellulose configuration (type I, as native in biomass, estimated from the «DMSO residue» fractions, or type II, in «cellulose II») in cellulose degradation in torrefaction, which will be developed later (see section V.2.3).

2.1.1.2. Volatile species release

The total mass of quantified volatile species was estimated for «cellulose II» fractions by adding the production of the individual volatile species. This represents from 0.01 mg of total quantified volatile species for commercial cellulose to 0.1 mg for ash-wood «cellulose II». This amount of volatile species is released by 81.5 to 134 mg of the corresponding «cellulose II» fraction, respectively, by normalizing the torrefaction experiments to 1 g of initial raw material. The quantified volatile species production, even if low, was representative of cellulose degradation due to its chemical composition, which will be discussed later. Furthermore, the limited degradation of cellulose in torrefaction below 300°C leads to a low release of volatile species. The difference between commercial microcrystalline cellulose and extracted fractions is again clear.

Secondly, by grouping the quantified volatile compounds per chemical family (Figure IV.15), it is noticeable that the main products in cellulose II torrefaction are acetic acid and furans, followed by ketones and methanol (alcohol). Phenols are detected in trace amounts, which could come from impurities derived from the extraction procedure, and are considered as negligible. Formaldehyde (aldehydes) is not produced, which is consistent with the fact that it would mainly be released in lignin decomposition (see Table II.3). Anhydro-oligosaccharides and anhydro-saccharides have been reported as produced in cellulose torrefaction at low temperatures. However, with the exception of levoglucosenone, they could not be detected here.

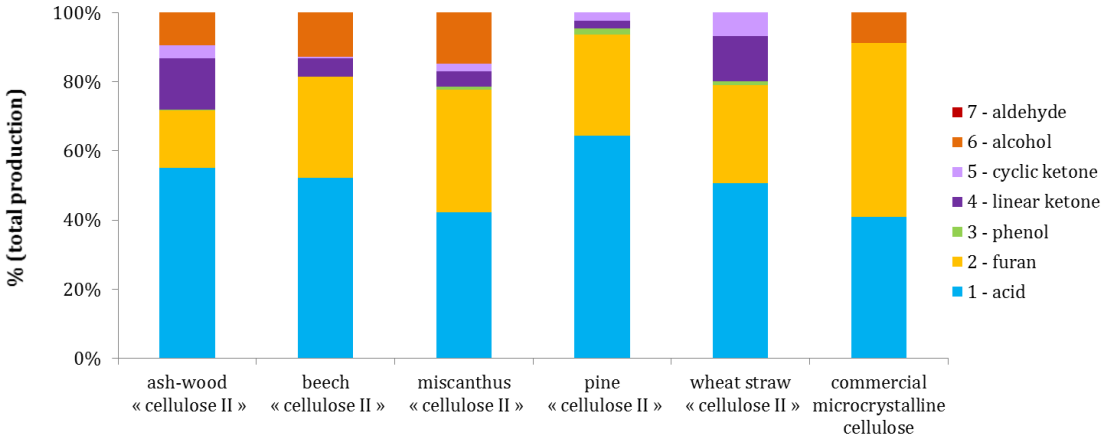


Figure IV.15. Distribution of the total production of volatile species per chemical family obtained during torrefaction of «cellulose II» extracted fractions from 5 biomasses and the commercial microcrystalline cellulose Avicel in TGA-GC/MS

By integrating the total production of each volatile species, the volatile species quantified were acetic acid (42.2 to 64.3 % of the quantified total volatile species production, in function of the «cellulose II» fraction), methanol (0.0 to 14.8 %), furfural (9.4 to 32.0 %) and hydroxyacetone (1.0 to 14.3 %). Significant amounts were also detected for 4-cyclopentene-1,3-dione (0.3 to 6.8 %) and 2(5H)-furanone (1.3 to 7.0 %). In the torrefaction of the commercial microcrystalline cellulose, only few species were detected at high torrefaction temperatures. The yields of these volatile species were much lower, and only acetic acid (40.7 %), furfural (37.7 %), furan (12.9 %) and methanol (8.7 %) were quantified. As a result, commercial cellulose will not be considered in the analysis of the profiles of formation of volatile species (Figures IV.16 to IV.19). Levoglucosenone was one of the main volatile species detected in the torrefaction of cellulose, but it could not be quantified.

Acetic acid was the main quantified compound released in the torrefaction of «cellulose II» fractions. Its profile of formation was shown to be constant during the experiments (Figure IV.16), even if cellulose degradation is enhanced at high torrefaction temperatures (Figure IV.13). This could indicate it as independent of the torrefaction progress or the operating conditions in the degradation of «cellulose II» in torrefaction. Even if it was the major compound measured, its production in function of the temperature, below 0.001 g (acetic acid released)/g(«cellulose II» transformed), remains much lower than that of hemicelluloses, the main source of acetic acid in biomass. Acetic acid might originate from dehydration, fragmentation and secondary reactions of unstable intermediaries from cellulose depolymerization (see Table II.3).

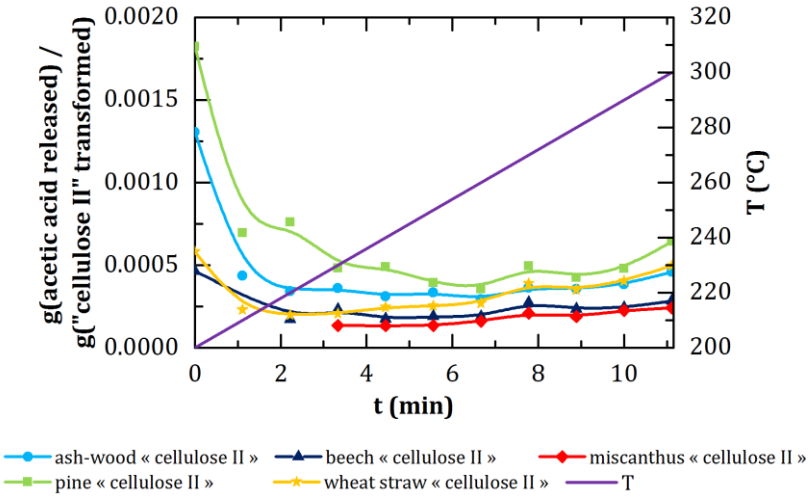


Figure IV.16. Production profile of acetic acid versus temperature and time for «cellulose II» fractions in torrefaction in TGA-GC/MS

The origin of furans in the thermal decomposition of cellulose was pointed out as depolymerization reactions taking place at temperatures higher than 300°C. More precisely, a contraction of the pyran ring of levoglucosan through the elimination of oxygenated groups and

the formation of double bonds C=C could end in a furan ring in cellulose char. Then, weak bonds might break and liberate furan compounds such as 5-hydroxymethylfurfural (5-HMF), 5-methylfurfural (5-MF), furfural and furfuryl alcohol (see Table II.3). These compounds, except furfural, were not detected in this case. Shen pointed out that furfural is produced from the secondary reaction of 5-HMF, derived from levoglucosan [224], simultaneously with the release of formaldehyde through the dehydroxymethylation reaction of the side chain of the furan ring [152]. In the torrefaction experiments of this study, furfural was measured from low temperatures, around 230°C, for all «cellulose II» fractions (Figure IV.17, left). This could be explained by the fact that the crystallinity degree was lower to that of the commercial microcrystalline cellulose, which was the typical model used for representing cellulose in thermochemical conversion. In the literature, an increase in the furan yield has been reported in the pyrolysis of celluloses with a lowered crystallinity [225,226]. This can also explain the higher furan yield detected for other compounds of this chemical family different from furfural, such as furan, acetylfuran or 2(5H)-furanone (Figure IV.17, right). These compounds started to be released at temperatures between 260 and 280°C in the torrefaction of «cellulose II» fractions. While no trend can be deduced in furan release, acetylfuran and 2(5H)-furanone show ascendant profiles of formation, with a local minimum at 290°C measured for the release of 2(5H)-furanone from all «cellulose II» fractions. Their mechanism of formation might be close to that of other furan products, as described previously.

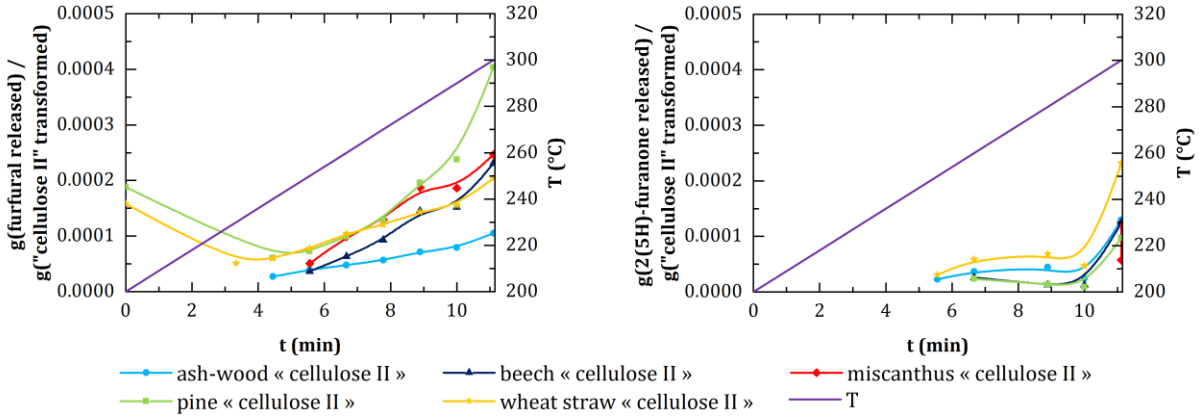


Figure IV.17. Production profile of furfural (left) and 2(5H)-furanone (right) versus temperature and time for «cellulose II» fractions in torrefaction in TGA-GC/MS

Small compounds, such as hydroxyacetone, have been detected in the literature after depolymerization, in secondary reactions of fragmentation and dehydration, taking place at temperatures below 300°C (see Table II.3). Hydroxyacetone would be mainly produced from the direct conversion of cellulose molecules and partly from the secondary decomposition of levoglucosan [152]. In this study, hydroxyacetone production started from 250 to 260°C for ash-wood and wheat straw «cellulose», followed by an increasing production until 300°C, while it is only detected at this temperature for the other fractions (Figure IV.18, left). This earlier

production could be derived from the more fragmented and amorphous structure of the «cellulose II» fractions, rather closer to cellulose in biomass compared to the commercial microcrystalline cellulose, which was traditionally used to describe cellulose degradation in torrefaction. The decomposition of hydroxyacetone in cellulose thermal conversion was pointed out to lead to formaldehyde and acetaldehyde [57]. However, none of these compounds was detected in this case, so this transformation might happen at higher temperatures. A second linear ketone, 2-propanone,1-(acetyloxy)-, was also detected from 280°C for all «cellulose II» fractions, with a total volatile production per fraction below 1.0 % of the total quantified volatile species for a given fraction. Its production is characterized by a growing profile, whose shape is equivalent for all «cellulose II» fractions (Figure IV.18, right).

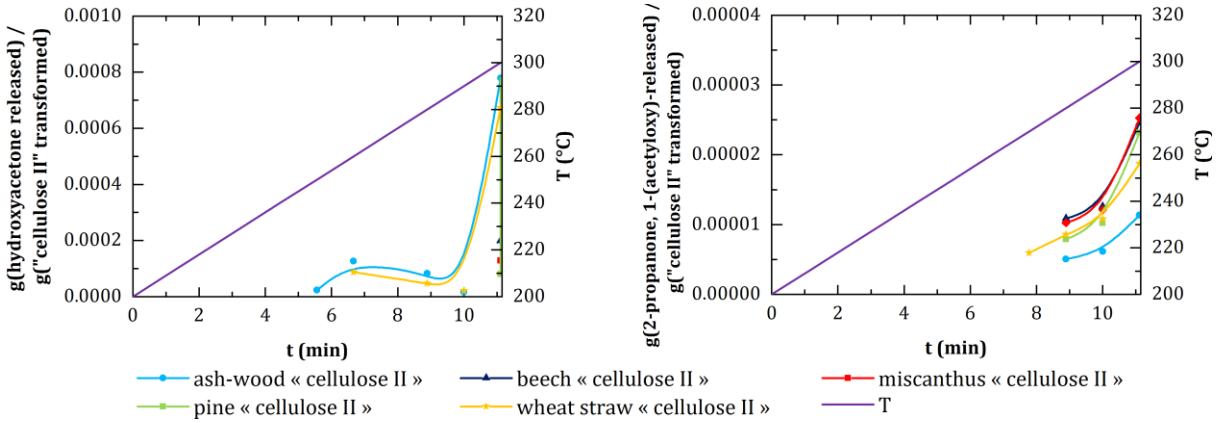


Figure IV.18. Production profile of hydroxyacetone (left) and 2-propanone, 1-(acetyloxy)- (right) versus temperature and time for «cellulose II» fractions in torrefaction in TGA-GC/MS

Methanol and 4-cyclopentene-1,3-dione were detected in low amounts, in all cases lower than 0.001 g(volatile species released) / g(«cellulose II» transformed) (Figure IV.19). In both cases, these products are not typical products from cellulose decomposition. While cyclic ketones are typically produced in hemicellulose depolymerization [162,163,227], only rare studies have also detected cyclopentenes in high temperature pyrolysis of cellulose [228] (see Table II.3). However, the mechanism for its formation could not be elucidated. Methanol was reported to be principally released in the scission of the methoxy groups attached to phenolic units from lignin, as well as in the fragmentation of the methoxy group of the 4-O-methyl-α-D glucuronic acid from hemicelluloses. Some authors suggested that methanol could derive from cellulose through secondary decomposition of anhydrosugars, especially from levoglucosan, but rather at high temperatures and long residence time [152]. However, the low production suggests that, as in the case of the cyclopentenedione, this mechanism is not preponderant in cellulose decomposition.

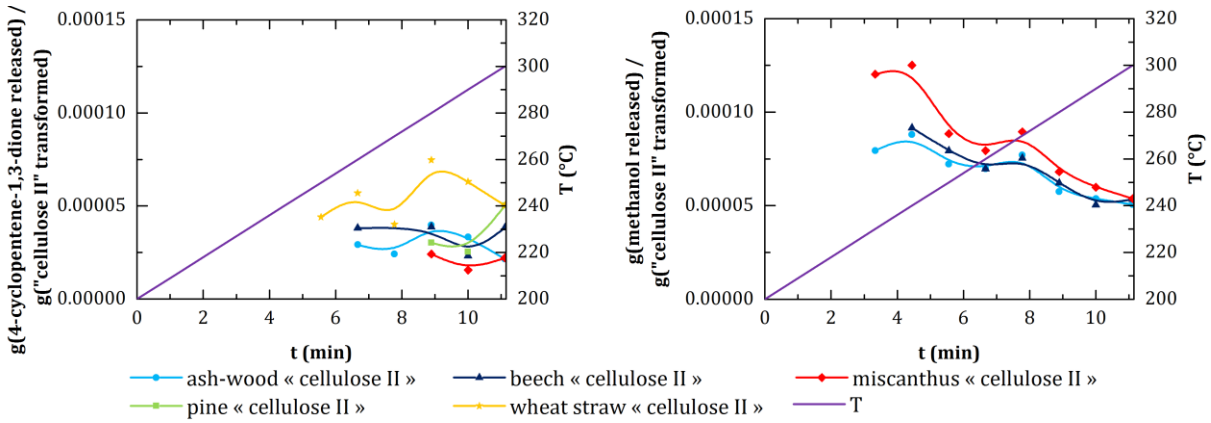


Figure IV.19. Production profile of 4-cyclopentene-1,3-dione (left) and methanol (right) versus temperature and time for «cellulose II» fractions in torrefaction in TGA-GC/MS

To summarize, the low degradation of cellulose II during the non-isothermal torrefaction step leads to a low release of chemical species. The main compounds derived from cellulose II are furans, especially furfural, and linear ketones. Acetic acid was also detected in a significant amount, but its mechanism of formation could not be clearly elucidated. Other compounds, such as methanol and 4-cyclopentene-1,3-dione were detected, even if they are supposed to be mainly produced by other biomass fractions.

2.1.2. «DMSO residue» fraction

A complementary fraction, named «DMSO residue», was also analyzed in torrefaction. It consists in the cellulose fraction with preserved cellulose I allomorphic structure and contains residual hemicelluloses.

2.1.2.1. Solid transformation

The final remaining solid mass observed for the «DMSO residue» fractions at the end of the torrefaction experiment is between 42.1 %wmf for ash-wood «DMSO residue» and 64.1 %wmf for the corresponding pine fraction (Figure IV.20, left). Beech, miscanthus and wheat straw residues exhibit intermediate values. Degradation rates are soft and below 1.9 %wmf/min for all «DMSO residue» fractions (Figure IV.20, right). This fraction exhibits a higher degradation through torrefaction compared to that of «cellulose II», presumably because of the presence of hemicellulose. Degradation profiles are similar to those of the equivalent «cellulose II» fractions, with a sensibly higher maximum in the degradation rate at 300°C.

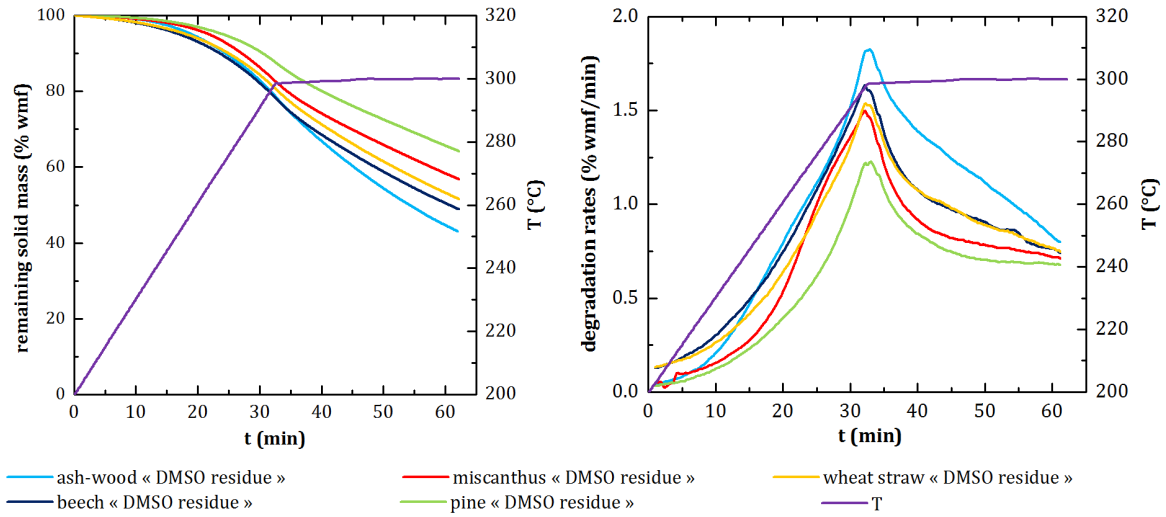


Figure IV.20. Remaining solid mass (left) and degradation rates (right) versus time and temperature obtained in torrefaction for «DMSO residue» fractions from 5 biomasses in torrefaction in TGA-GC/MS

Considering the non-isothermal torrefaction step, the kinetic pattern of the 5 «DMSO fractions» seems similar regarding the remaining solid mass curves (Figure IV.20, left). However, three main profiles of transformation can be distinguished by the corresponding degradation rate curves (Figure IV.20, right). The first type of kinetic behavior was detected for the ash-wood «DMSO residue». Its degradation rate profile is characterized by a global and soft acceleration of the mass loss discretely interrupted by a short deceleration phase between around 240 to 275 °C. This kind of profile is also observed for beech, whose deceleration phase is shorter, from around 265 to 275°C, and even more discreet. The second kinetic profile was distinguished for miscanthus «DMSO residue». Its behavior is close to that of deciduous wood, with a sharper distinction between the acceleration and the deceleration steps and without the last acceleration step before 300°C. Finally, pine «DMSO residue» presents a different solid kinetic behavior, which consists in an acceleration of the mass loss until the end of the non-isothermal torrefaction. The degradation profile of wheat straw «DMSO residue» was not included in any group, as it seems to present a minor change in the mass loss acceleration around 283 °C whose nature is not clear. A second derivative of the remaining solid mass curve versus time, which would represent the acceleration of the mass loss, would be required to distinguish it.

The kinetic profiles of solid degradation in the following isothermal step can be similarly grouped, with the exception of the closer behavior of beech «DMSO residue» to that of wheat straw rather than to that of ash-wood. It is noteworthy that the final degradation rate after 30 minutes at 300°C is relatively close for all biomasses (around 0.7 to 0.8 %wmf/min), while their degradation rate values at the beginning of this step were moderately different (1.2 to 1.7 %wmf/min). The mass loss deceleration of the ash-wood «DMSO residue» is approximately constant, which is not the case for the other fractions.

The evolution of the elemental composition of the solid through torrefaction (Figure IV.21) show that the increase in carbon content is related to the mass loss and independent of biomass type.

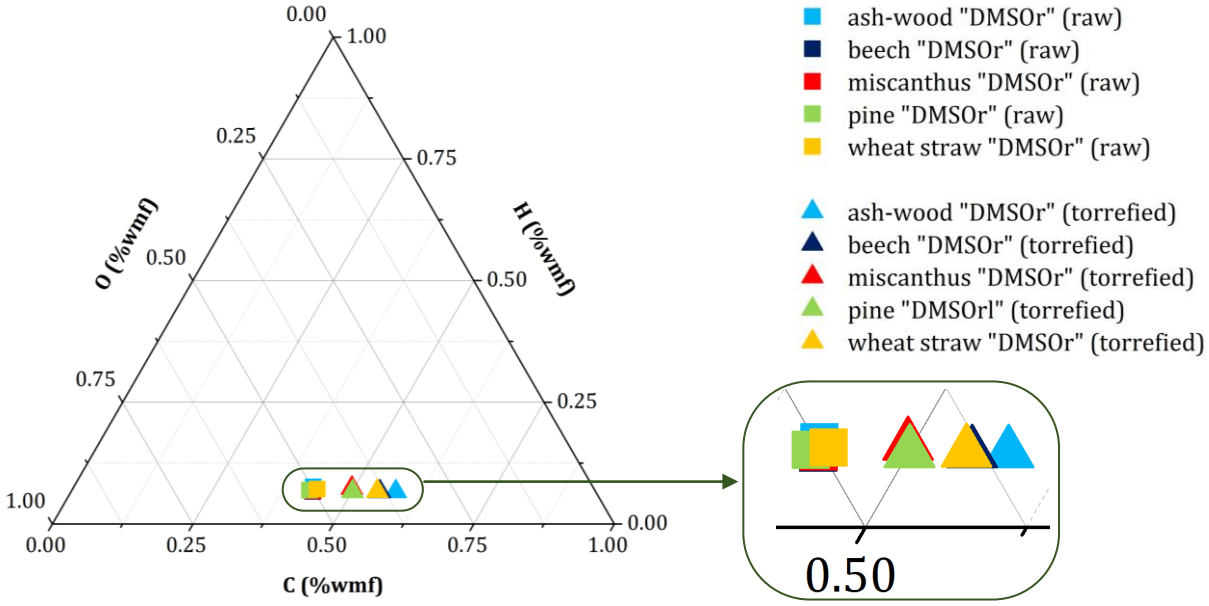


Figure IV.21. Ternary diagram of CHO elemental composition of raw and torrefied «DMSO residue» fractions in TGA-GC/MS

Both the remaining solid mass and the degradation rates profiles of the «DMSO residue» remain close to those of the «cellulose II» fraction. However, the presence of hemicelluloses in this fraction leads to a more enhanced degradation. The crystalline structure of the «cellulose II» fractions can also play a role in this behavior. A sugar mass balance on the polysaccharide based extracted fractions was carried out in order to extract the «cellulose I» fraction from the «DMSO residue» behavior and to determine the influence of the cellulose crystalline structure in biomass torrefaction (see section V.2).

2.1.2.2. Volatile species release

The total mass of quantified volatile species estimated represents between 0.3 to 0.8 mg of total quantified volatile species in function of the «DMSO residue» fraction, for a converted solid mass between 120 to 209 mg of 1 g of initial raw material. This result remains comparable to that of «cellulose II» fractions, which were degraded in a minor extent and, proportionally, a lower amount of volatile species was quantified.

More precisely, an analysis was carried out of the total production of the volatile species from the same chemical family released in the non-isothermal torrefaction (Figure IV.22). Acids are the chemical compounds released in a major proportion (57.0 to 62.5 %), followed by furans, ketones and alcohols (methanol). Aldehydes (formaldehyde) and phenols are detected in trace amounts. This composition is relatively close to that obtained for the «cellulose II» fractions, with a higher proportion of acetic acid in this case due to the presence of hemicelluloses.

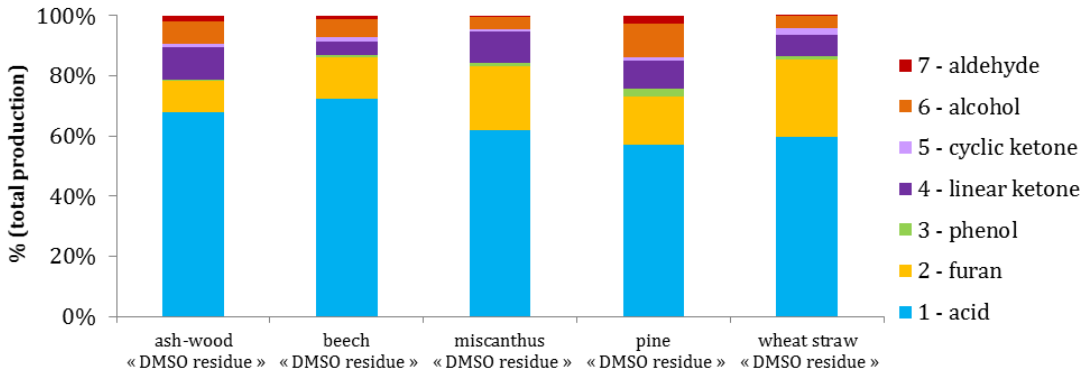


Figure IV.22. Distribution of the total production of volatile species per chemical family obtained during torrefaction of «DMSO residue» extracted fractions from 5 biomasses in TGA-GC/MS

In a second step, the production of the quantified species versus time and temperature were analyzed (Figures IV.23 to IV.26) and compared to those from the «cellulose II» fractions (Figures IV.16 to IV.19). More chemical species are detected in this case compared to «cellulose II». This can be explained by the fact that the «DMSO residue» fractions contain hemicelluloses.

Acetic acid was again the main quantified compound released in the torrefaction of «DMSO residue» fractions. Its average production remains close to that from the «cellulose II» fractions but it exhibits a production profile with a maximum at intermediate torrefaction temperatures for all biomasses. This maximum occurs at higher temperatures for the pine fraction (Figure IV.23). The macromolecular composition of the «DMSO residue» fractions includes sugar derived from hemicelluloses, namely mannose for the ash-wood, miscanthus and wheat straw fractions, as well as a non-negligible proportion of xylose for all the fractions. As a result, the production profile of acetic acid reflects the presence of hemicelluloses in the fraction, which enhances the production of this compound.

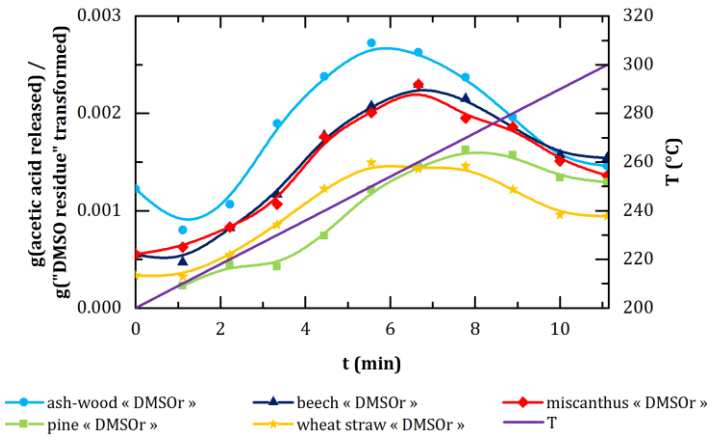


Figure IV.23. Production profile of acetic acid versus temperature and time for «DMSO residue» fractions in torrefaction in TGA-GC/MS

Furans were detected from intermediate torrefaction temperatures, even lower in the case of furfural, compared to the release of the «cellulose II» fractions. The production profiles were

shown to smoothly increase with torrefaction temperature. The local minima on the production profiles remain in the uncertainty of the measurement so they are not considered (Figure IV.24). Furans were reported to be extensively released in cellulose thermal decomposition at temperatures higher than 300°C. However, they can also be produced through the ring-opening and rearrangement reactions of the xylan unit, this mechanism being reported in the literature to happen from low torrefaction temperatures (see Table II.3). Consequently, the presence of hemicelluloses on the «DMSO residue» fractions induces an earlier production of furans.

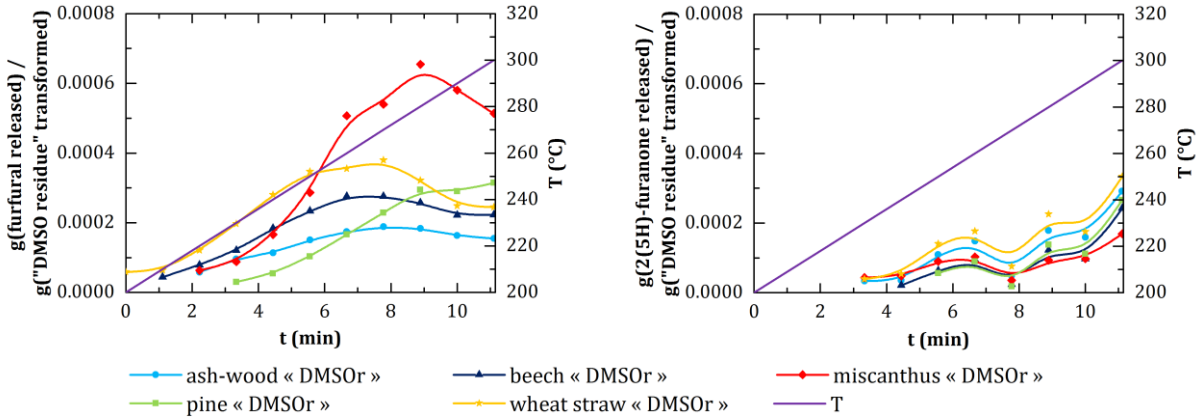


Figure IV.24. Production profile of furfural (left) and 2(5H)-furanone (right) versus temperature and time for «DMSO residue» fractions in torrefaction in TGA-GC/MS

Linear ketones are also detected from lower torrefaction temperatures than in the case of the «cellulose II» fractions. The production profiles remain in the same order of magnitude but again smoothly increase with the increasing torrefaction temperature (Figure IV.25). The hemicelluloses content of the «DMSO residue» fractions is probably at the origin of this behavior.

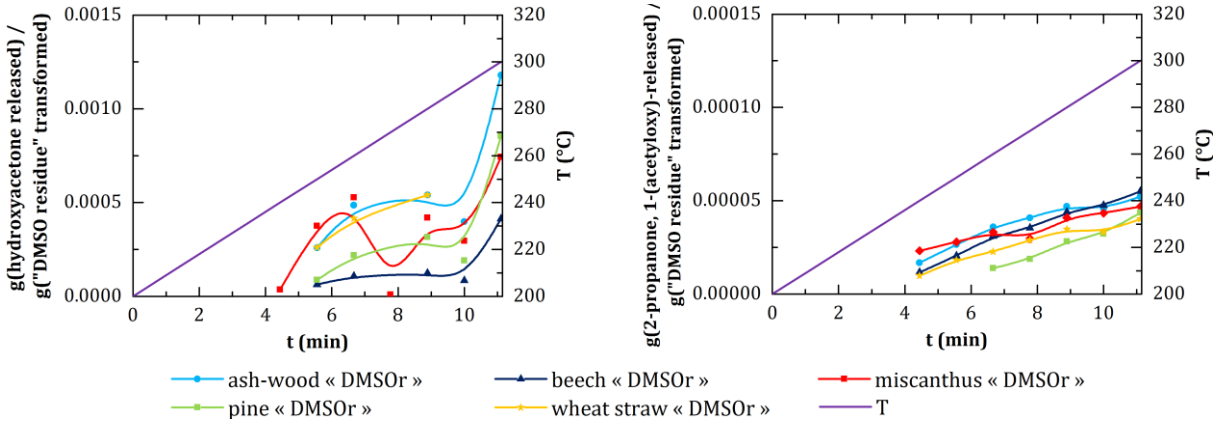


Figure IV.25. Production profile of hydroxyacetone (left) and 2-propanone, 1-(acetyloxy)- (right) versus temperature and time for « DMSO residue » fractions in torrefaction in TGA-GC/MS

Finally, similarities were also found for methanol and 4-cyclopentene-1,3-dione. Methanol exhibits a production profile which starts from lower torrefaction temperatures than in the case of the «cellulose II» fractions, and then tends to decrease at higher temperatures (Figure IV.26, left). However, the methanol production of the «DMSO residue» fractions is higher, presumably

because of the methanol production from hemicelluloses. In the case of the 4-cyclopentene-1,3-dione, production profiles are equivalent as the production remains very low, starting at lower torrefaction temperatures than in the case of the «cellulose II» fractions (Figure IV.26, right).

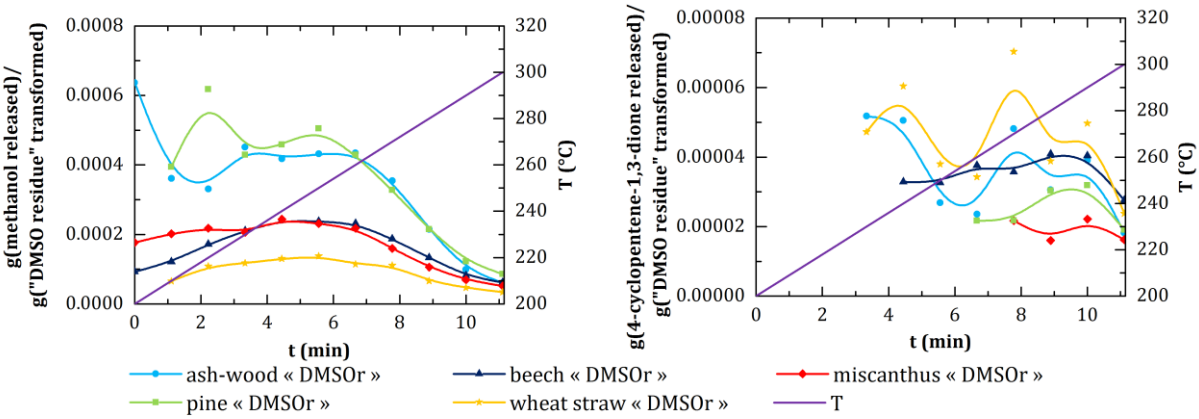


Figure IV.26. Production profile of 4-cyclopentene-1,3-dione (left) and methanol (right) versus temperature and time obtained for « DMSO residue » fractions in torrefaction in TGA-GC/MS

As a synthesis of the results obtained from the «DMSO residue» fractions, it can be highlighted that the presence of hemicelluloses in the fraction leads to a start of solid degradation at lower temperatures and to a higher degree of degradation at the end of the experiment.

2.2. Hemicelluloses

Hemicelluloses are principally recovered in the fraction called «hemicelluloses 1», obtained through DMSO extraction, according to the defined extraction procedure (III.1.2 section). However, a complementary hemicellulose fraction is recovered in the residue after DMSO, called «hemicelluloses 2».

2.2.1. «Hemicelluloses 1» fraction

2.2.1.1. Solid transformation

The final remaining mass loss after the non-isothermal step was around 32.0 to 36.7 %wmf, relatively close for fractions extracted from all biomasses, except for wheat straw (52.1 %wmf). After the isothermal step, final remaining solid mass is between 38.3 %wmf for wheat straw «hemicelluloses 1» and 23.7 %wmf for the miscanthus fraction (Figure IV.27, left). This values are in agreement with previous studies in the literature that pointed out hemicelluloses as the biomass macromolecular component which suffers the more severe degradation through torrefaction [6,7,121,227]. Degradation rate values are very diverse and depend on the transformation progress, going from 0.2 %wmf/min in the first seconds of the transformation to 0.07 %wmf/min at the end, as well as intermediate degradation rates between 2.0 %wmf/min for wheat straw «hemicelluloses 1» to 4.7 %wmf/min for the corresponding miscanthus extracted fraction (Figure IV.27, right).

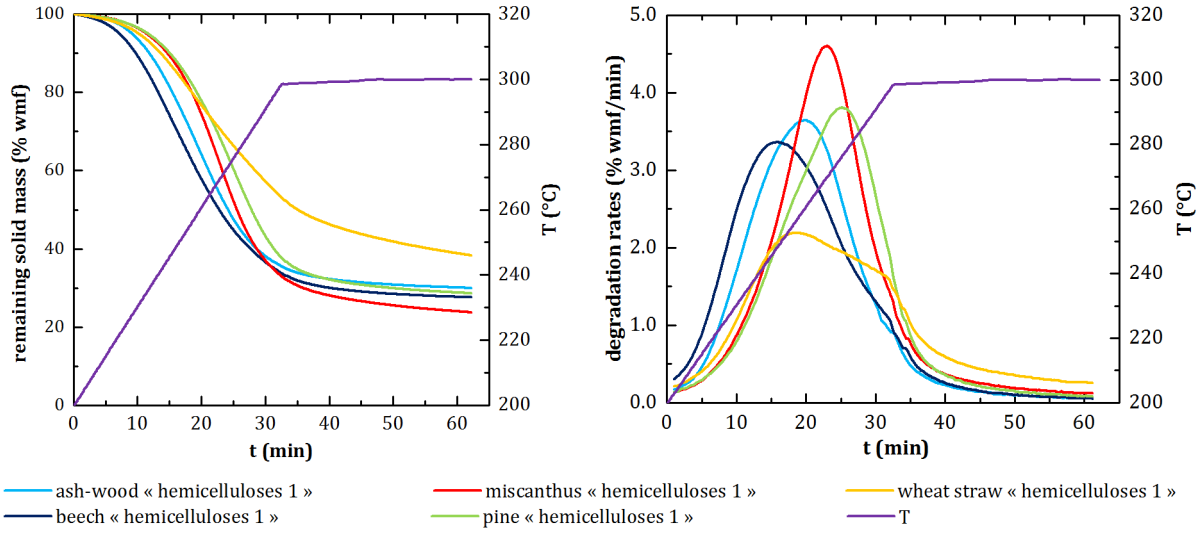


Figure IV.27. Remaining solid mass (left) and degradation rates (right) versus time and temperature obtained in torrefaction for «hemicelluloses 1» from 5 biomasses in TGA-GC/MS

The profiles of solid degradation were shown to be similar for the five «hemicelluloses 1» fractions considered, except for that of wheat straw (Figure IV.27, right). It is noteworthy that the maximum in the degradation rate is not reached at the end of the non-isothermal torrefaction step, as for other extracted fractions, but around the middle of this step. Then, there is a general deceleration of the mass loss, surprisingly without a major change in the degradation pattern between the non-isothermal and the isothermal steps, except for the wheat straw fraction. Only several minutes after the beginning of the isothermal step, ash-wood, beech and pine «hemicelluloses 1» tend to stabilize their solid mass loss, while this stabilization is less remarkable for the corresponding fractions from miscanthus and wheat straw (Figure IV.27, left).

Resemblances in solid kinetics in the non-isothermal torrefaction stage can be identified for classifying the considered fractions into three groups. First of all, deciduous wood (ash-wood and beech) present a regular acceleration of the solid mass loss, about 2.5 min after the beginning of the transformation. This acceleration seems to start a little later for ash-wood «hemicelluloses 1» fraction, compared to that from beech. The maximum degradation rate is achieved at 245 °C for beech and at 260°C for ash-wood fractions. These similarities could be explained by their similar composition in xylose (around 75% wmf) and acetyl groups (around 22% wmf).

The kinetic behavior pattern of miscanthus «hemicelluloses 1» is very close to that of the previous fractions, having a more retarded starting in the acceleration of the solid mass loss and showing a more sharpen slope until the highest degradation rates, which are reached around 270 °C. The main difference in its sugar composition is the higher glucose content (12.5 %wmf), in detriment to a reduction in the xylose (64.4 %wmf) and acetyl groups (16.5 %) content.

The degradation rate profile of pine «hemicelluloses 1» is intermediate to those of the respective miscanthus and deciduous wood fractions. The maximum in the degradation rate, in the same order of magnitude of those of deciduous wood fractions, is attained at 278 °C. A very slight deceleration can be appreciated around 250°C with a small change in the curvature shape of the degradation rate, without a significant impact in the global trend of this parameter. The sugar composition of «hemicelluloses 1» fraction from pine is mainly mannose (49.2 %wmf), followed by lower amounts of xylose (18.4 % wmf) and glucose (14.8 %wmf). Mannose-based sugars have been reported in the literature as less reactive than xylose-based ones (see section II.3.2), which can explain that the maximum in the degradation of «hemicelluloses 1» from pine is reached later.

Finally, wheat straw «hemicelluloses 1» exhibits a typical kinetic behavior until 250°C, close to that of the other corresponding fractions but with a slower acceleration. However, the mass loss of this fraction is decelerated from this temperature until the end of the non-isothermal torrefaction, by losing around 0.7 %wmf/min in this period. The particular behavior of this fraction was checked as reproducible and could be due to its high glucose content compared to the xylose content. This indicates that a high glucose content might mitigate the degradation of a given hemicellulose fraction.

The elemental composition of the solid was characterized after and before torrefaction for the extracted «hemicelluloses 1» fractions (Figure IV.28). Firstly, it can be observed that the extent in the evolution of the elemental composition is highly dependent on the hemicellulose fractions, this transformation being very limited for wheat straw and more pronounced for the woody samples. The enrichment of the carbon content in the solid goes from 10.5 to 50.1%, in detriment to a decrease in the oxygen content from 6.2 to 42.4% and sensible changes in the hydrogen content. It is noteworthy that the wheat straw sample suffers a more pronounced decrease of its hydrogen content compared to its oxygen content, in proportion (28.7 and 6.2%, respectively). In this case, solid mass loss is not directly correlated to changes in elemental composition. These results confirm the influence of the sugar composition on hemicelluloses conversion through torrefaction.

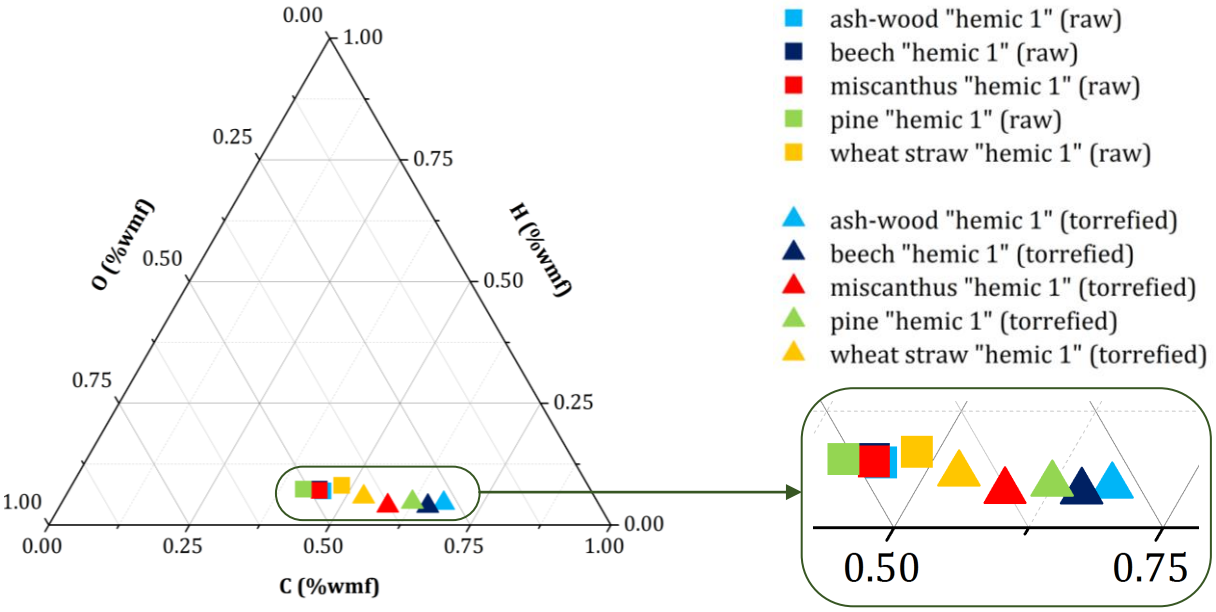


Figure IV.28. Ternary diagram of CHO elemental composition of raw and torrefied «hemicelluloses 1» fractions in TGA-GC/MS

2.2.1.2. Volatile species release

The total production of volatile species that could be quantified was estimated to be between 2.0 and 6.8 mg of volatile species for wheat straw and beech «hemicelluloses 1» fractions, respectively. These values are related to 466.0 to 667.5 mg of «hemicelluloses 1» transformed, respectively. This result, which represents about 1 % of the biomass conversion, can be explained by the fact that hemicelluloses release anhydrosugars in their thermal decomposition, which could not be detected with our system. Furthermore, one of the main peaks in the chromatogram, which was suspected to correspond to a sugar-derived molecule, could not be identified neither by the MS library nor by comparison with the literature [217,218]. This is a typical problem for torrefaction and analytical pyrolysis that has already been described in the literature [46].

By considering the total production of the volatile species released per chemical family, acids appear as the main compounds derived from the torrefaction of «hemicelluloses 1», followed by furans and methanol (Figure IV.29). Minor amounts of formaldehyde are also detected, which are comparable to furans percentage in the case of pine «hemicelluloses 1». This could correspond to traces of other macromolecular components in the fraction, derived from the extraction procedure.

The major volatile species detected is acetic acid, with a production constituting from 58.4 % of the total volatile species quantified for wheat straw «hemicelluloses 1» to 86.7 % for the ash-wood fraction. Furfural is the second main detected compound, between 4.8 % for the ash-wood fraction and 26.1 % for the wheat straw one. Thirdly, methanol (3.8 to 10.8 %) was quantified. Significant amounts of formaldehyde were detected for the pine fraction (9.9 %) and the wheat

straw (7.8 %) fractions, being minor for the other fractions. Formic acid was also detected for ash-wood (2.0 %) and pine (3.6 %) «hemicelluloses 1». Ketones and other furans were detected in minor amounts (< 1.5 %).

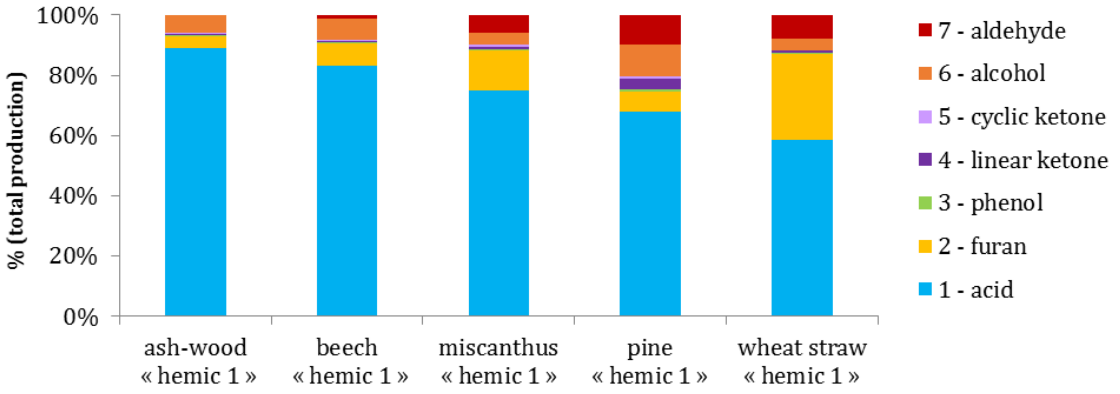


Figure IV.29. Distribution of the total production of volatile species per chemical family obtained during torrefaction of «hemicelluloses 1» extracted fractions from 5 biomasses in TGA-GC/MS

After this analysis, the profile of formation of each quantified volatile species versus time and temperature was considered (Figures IV.30 to IV.34).

As in the case of the «cellulose II» fraction, acetic acid was the major quantified compound released in the torrefaction of «hemicelluloses 1» fractions for all biomasses. However, in this case, its production is more than 10 times higher, and the production profiles are ascendant with the increasing torrefaction temperature (Figure IV.30). The production of acetic acid is related to the fragmentation of acetoxy- (or acetyl) groups attached to the xylose units in deciduous wood [99]. This reaction was described as essentially occurring at the beginning of xylan conversion [29], which is in accord with the production detected from low torrefaction temperatures. It can also be formed by the ring-scission between xylose and the uronic acid residues [163,165] (see Table II.3). The highest acetyl content was found for beech «hemicelluloses 1» (22.9 %), followed by ash-wood «hemicelluloses 1» (21.2 %), which were the highest two profiles of production (Figure IV.39). On the other hand, glucomannan-based «hemicelluloses 1», as it is the case for the pine fraction (49.2 %) rather produce formic acid [46]. Hemicelluloses containing glucomannan were reported in the literature as less reactive than hemicelluloses based on xylan, which is in accord with the much lower production of formic acid compared to that of acetic acid. However, the maximum of formic acid production, detected around 260°C, contrasts with this hypothesis, as acetic acid profiles do not reach a maximum in the torrefaction experiments. This might be explained by the fact that reproducibility of formic acid quantification was shown to be less accurate than for other compounds.

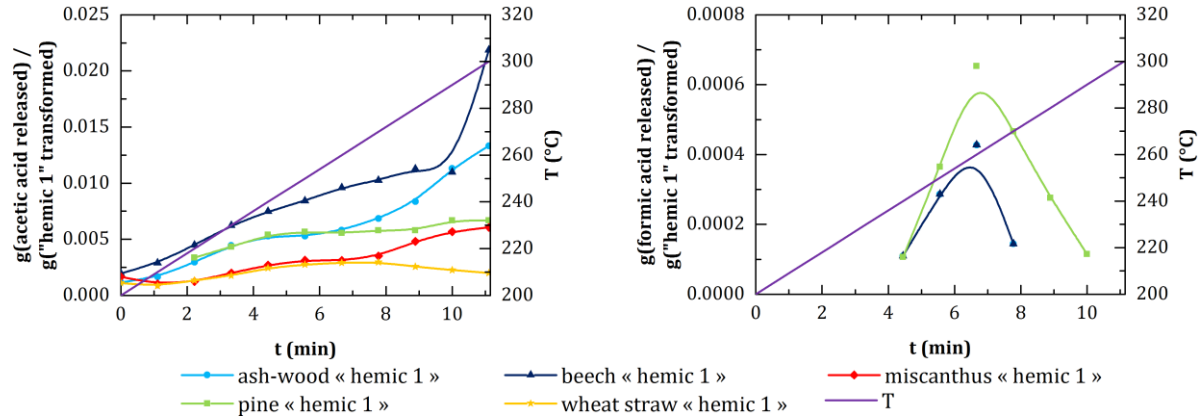


Figure IV.30. Production profile of acetic acid (left) and formic acid (right) versus temperature and time for «hemicelluloses 1» fractions in torrefaction in TGA-GC/MS

Furfural was detected from low torrefaction temperatures, exhibiting ascendant profiles with the increasing torrefaction temperature (Figure IV.31, left). Local minima were found for beech (230°C), pine and wheat straw «hemicelluloses 1», while the other profiles were rather ascendant. The release of furfural is attributed to the ring-open and rearrangement reactions of the xylan unit, being several mechanisms proposed to explain in detail its formation [163] (see Table II.3). Its production has been reported in the literature from low torrefaction temperatures [163], which in agreement with the production profiles obtained. However, no evidence was found to explain the local minima for three of the profiles. In general, furan production is related to depolymerization reactions occurring by cleavage of glycosidic linkages between hemicellulose sugar units, typically from around 240°C for xylan-based hemicelluloses (5 C-atoms). Glucomannan-based hemicelluloses, as it is the case for pine, also lead to furan production [162]. This is because pyran rings derived from glucomannan (6 C-atoms) tend to change into more stable furan rings (5 C-atoms) [29]. However, the decomposition of these hemicelluloses would rather start from around 270°C [29,99]. The production profile of other furans follows the example of 2(5H)-furanone (Figure IV.31, right): an increasing profile with increasing temperature, detected from intermediate torrefaction temperatures. In some cases, furan production from pine was detected one or two temperature points later (~ 10 to 20 °C) than for other biomasses (furan, 3-furaldehyde, acetylfuran). Two local minima at 270 and 290°C were observed for 2(5H)-furanone, which indicates two different mechanisms of formation. However, no evidence was found to go into detail about them and they are in the order of magnitude of the incertitude of the measurement.

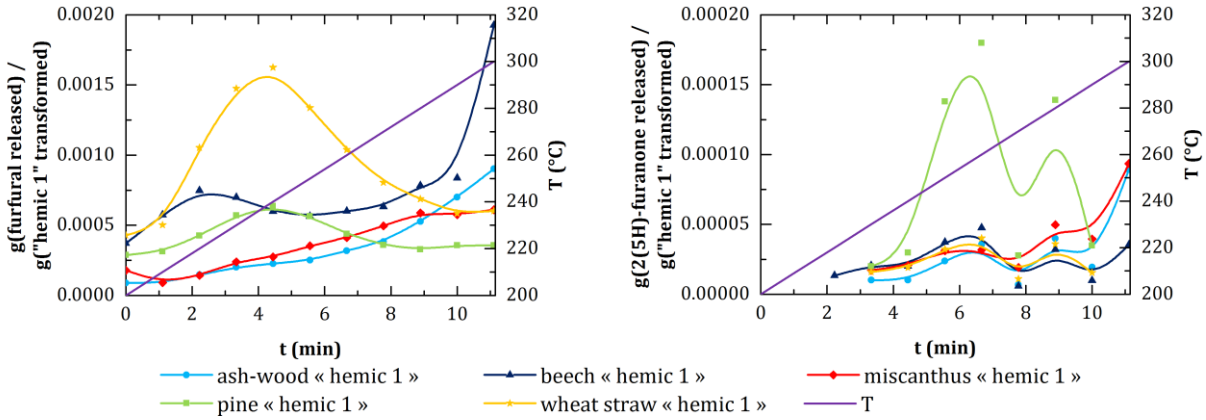


Figure IV.31. Production profile of furfural (left) and 2(5H)-furanone (right) versus temperature and time for «hemicelluloses 1» fractions in torrefaction in TGA-GC/MS

Linear ketones such as hydroxyacetone and 2-propanone, 1-(acetyloxy)- were detected in hemicelluloses decomposition. Their profile of production was shown to be mainly increasing with the increasing torrefaction temperature for woods, slightly moderate for miscanthus and rather constant for wheat straw «hemicelluloses 1» (Figure IV.32). As in the case of 2(5H)-furanone, the production profile of hydroxyacetone show local minima at 270 and 290 °C, in this case in the order of magnitude of the incertitude of the quantification. Ketones and other small compounds may come from the rapid depolymerization of hemicelluloses, directly or through unstable intermediates which go through dehydration, fragmentation and secondary reactions. Cyclic ketones can be also formed through this pathway, derived from pyran or furan rings [29].

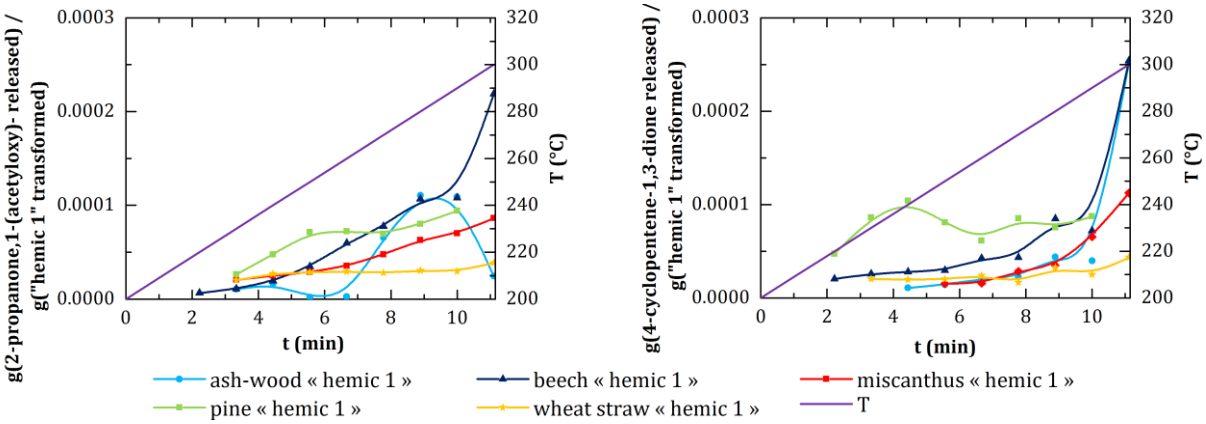


Figure IV.32. Production profile of 2-propanone, 1-(acetyloxy)- (left) and 4-cyclopentene, 1,3-dione (right) versus temperature and time for «hemicelluloses 1» fractions in torrefaction in TGA-GC/MS

The production of methanol was shown to be independent of the temperature, except for pine «hemicelluloses 1» (Figure IV.33). A local maximum can be appreciated at intermediate torrefaction temperatures, particularly for deciduous wood for «hemicelluloses 1» fractions. This compound is attributed to the scission of the methoxy- group on C4 position of 4-O-methyl-α-D-glucuronic acid [163], which is a ramification of the xylan chain in hemicellulose structure

[54]. Some studies reported that the yield of methanol slightly changes at higher temperatures, as no competitive reaction consume the methoxy groups [163]. This mechanism may occur at temperatures higher than 300°C, and it was not observed in this study. No evidence was found to explain the linear decrease in methanol production for pine «hemicelluloses 1». However, the particular structure of pine hemicelluloses, mainly based on glucomannan units instead of being based on xylan units, might be at the origin of this difference.

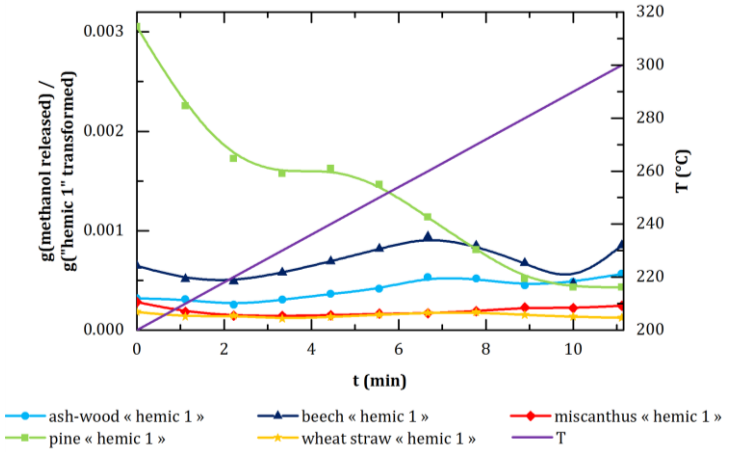


Figure IV.33. Production profile of methanol versus temperature and time obtained for «hemicelluloses 1» fractions in torrefaction in TGA-GC/MS

Other minor compounds detected in hemicelluloses torrefaction were formaldehyde (except for ash-wood «hemicelluloses 1») and propionic acid (Figure IV.34), in both cases below 0.001 g (volatile species released) / g («hemicelluloses 1» transformed). Formaldehyde release, significant for pine and wheat straw «hemicelluloses 1» fractions, presents a production profile independent of the torrefaction temperature and rather constant (Figure IV.34, left). This compound is principally released in lignin decomposition, and partially from cellulose, due to the hydroxymethyl groups (CH_2OH) only present in these constituents [6]. As a result, its formation from hemicellulose may derive from traces of lignin in the structure or from fragmentation reactions after depolymerization, as in the case of linear ketones and other small molecules. In the case of propionic acid, the profiles of production were found to be increasing with increasing torrefaction temperature for all «hemicelluloses 1» fractions (Figure IV.34, right). A mechanism of production of the propionic acid from the xylan unit with an 0-acetyl substituent was proposed by Shen, who also indicated a competition of this mechanism with a pathway of production of acetic acid [163]. This competition might slightly be appreciated in this case through the increase of acetic acid production at high torrefaction temperatures for miscanthus «hemicelluloses 1» while the propionic acid production diminishes. However, the observation is not conclusive as it is not observed for the other fractions.

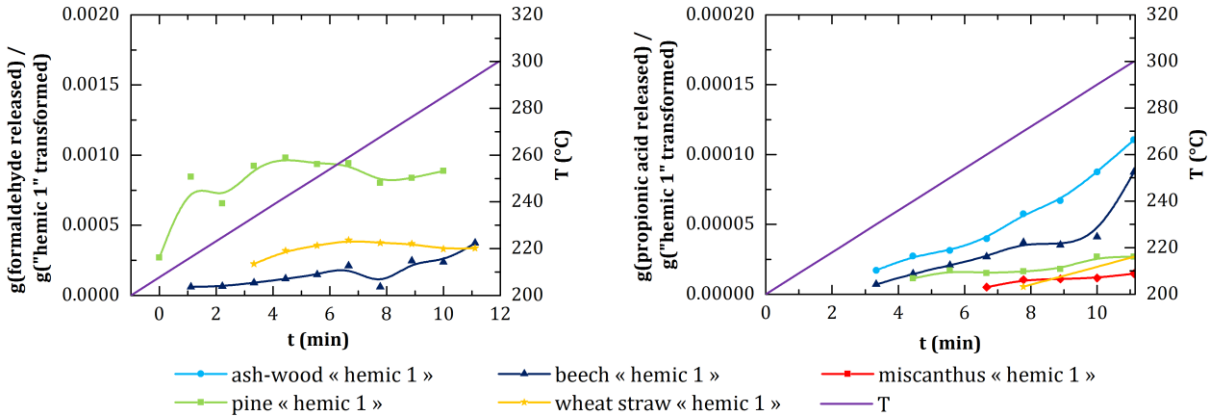


Figure IV.34. Production profile of formaldehyde (left) and propionic acid (right) versus temperature and time obtained for «hemicelluloses 1» fractions in torrefaction in TGA-GC/MS

Finally, traces of basic phenolic compounds such as guaiacol and syringol were detected for woody biomasses, while traces of phenol were detected for all «hemicelluloses 1» fraction, in all cases below 0.0001 g(volatile species released) / g(«hemicelluloses 1» trasformed) but with reproducible measurements. In the literature, the only phenolic compound identified in hemicelluloses pyrolysis was 2-methoxy-4-vinylphenol, not detected in our case and pointed out as derived from the lignin-like compound ferulic acid, combined to arabinoxylan in some plants [46]. The traces of these phenolic compounds could come from impurities derived from the extraction procedure that might be rests of the lignin-carbohydrate complexes (LCC) cross-linking hemicelluloses and lignin [72].

To sum up, hemicelluloses are the most degraded macromolecular component from biomass in the torrefaction temperatures interval. As a result, a high release of volatile species occurs, from which only a small fraction could be quantified. However, the composition of the quantified fraction is considered as representative, as it is in accord with the major detected compounds from hemicelluloses decomposition in the literature. The study of the production profiles of the volatile species released could contribute to explain the formation pathway of the detected species.

2.2.2. «Hemicelluloses 2» fraction

The «DMSO residue» fraction contains a residual part of hemicelluloses, as they could not be completely separated from the DMSO extraction. The objective of this section is, first, to compare the macromolecular composition and behavior in torrefaction of the «hemicelluloses 1» and «hemicelluloses 2» fractions, and secondly, to evaluate the suitability of completing the representation of hemicelluloses with the complementary fraction «hemicelluloses 2».

2.2.2.1. Solid transformation

The final remaining mass loss, after the non-isothermal step, was close for all the fractions considered, between 24.9 %wmf for miscanthus «hemicelluloses 2» and 33.3 %wmf for the corresponding wheat straw extracted fraction (Figure IV.35, left). Degradation rates are in the order of magnitude of those for the corresponding «hemicelluloses 1» fractions, rising up to around 3.1 %wmf/min for the ash-wood and pine fractions until to 4.7 %wmf/min for the miscanthus fraction, and decreasing until values below 0.1 %wmf/min at the end of the isothermal step (Figure IV.35, right).

For both «hemicelluloses» fractions, 1 (Figure IV.27) and 2 (Figure IV.35), a similar behavior was found in all cases, except for the wheat straw, for which «hemicelluloses 2» fractions are degraded faster with minor differences in the temperature of the maximum degradation rates. These differences can be explained by the differences in the sugar composition of both fractions.

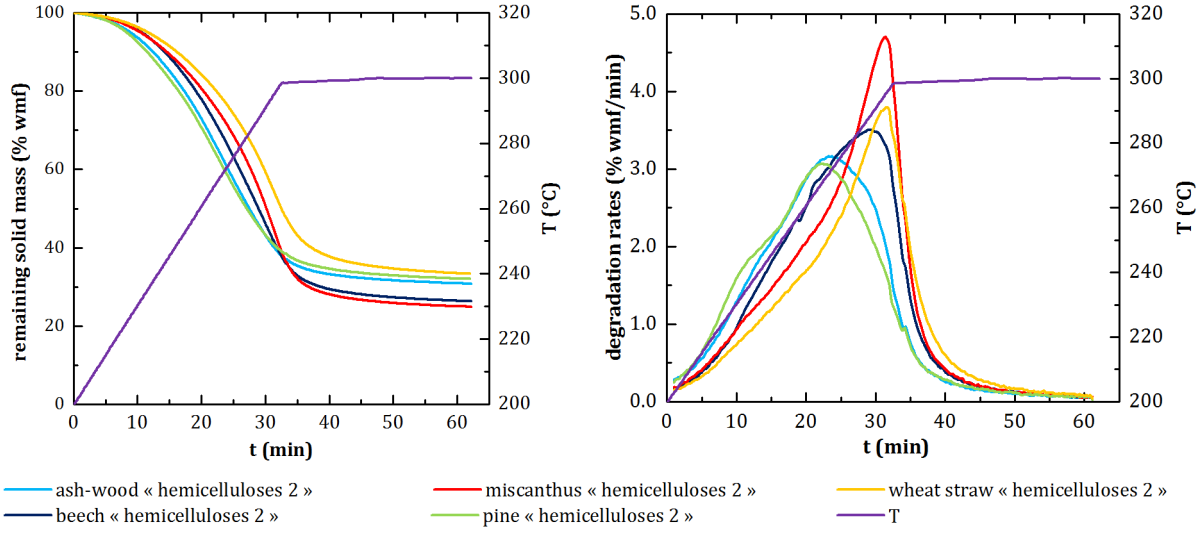


Figure IV.35. Remaining solid mass (left) and degradation rates (right) versus time and temperature obtained in torrefaction for «hemicelluloses 2» from 5 biomasses in TGA-GC/MS

The most significant change in solid mass loss profile occurs at the beginning of the 300°C isothermal torrefaction for ash-wood and pine «hemicelluloses 2», while it takes place some minutes later for miscanthus, beech and wheat straw fractions (Figure IV.35, left). Degradation rate profiles show significant changes in solid kinetic behavior during the non-isothermal stage in all cases. The maximum in the degradation rate profiles is reached around 275 °C for pine and ash-wood «hemicelluloses 2» and around 295°C for the equivalent wheat straw and miscanthus fractions (Figure IV.35, right), which represents higher temperatures than in the case of the degradation rate profiles of «hemicelluloses 1» fractions.

«Hemicelluloses 2» fractions can be classified into three groups according to their kinetic solid behavior: the first one concerns ash-wood and pine, the second one beech and miscanthus

fractions, while the wheat straw fraction behaves slightly differently. This behavior is not coherent with the very close sugar composition of ash-wood and beech fractions on the one hand and pine and miscanthus fraction on the other hand. This could indicate that such a small difference in the ratio glucose/xylose as it is the case for these fractions does not impact the hemicellulose transformation. However, wheat straw «hemicelluloses 2» fraction composition is closer to those of pine and miscanthus fractions but with a higher component of mannose in detriment of the xylose composition. This high mannose content was shown to have an impact in hemicelluloses degradation, as its transformation is much slower.

Going more into the detail of the curves, ash-wood, beech and pine fractions present a global acceleration trend in the solid mass loss, which is briefly interrupted by a deceleration at around 240°C, especially remarkable for the pine fraction. After that, woody fractions reach the maximum of the degradation rate, notably before the end of the non-isothermal torrefaction. The degradation trend for wheat straw and miscanthus «hemicelluloses 2» consists of an acceleration of the mass loss until the maximum, attained slightly before the end of the non-isothermal torrefaction. In both cases, the maximum of the degradation rate is followed by a deceleration of the solid mass loss which tends to stabilize in the isothermal stage. This stabilization of the mass loss seems to be faster for «hemicelluloses 2» from all fractions except that of wheat straw. This slower degradation of the wheat straw «hemicelluloses 2» seems to be due to its high mannose content.

In this case, it was not possible to carry out the analysis about the evolution of the elemental composition of the solid before and after torrefaction due to the lack of material.

2.2.2.2. Volatile species release

The total production of volatile species for each «hemicelluloses 2» fraction that could be quantified was estimated to be between 4.0 and 8.0 mg for wheat straw and pine «hemicelluloses 2» fractions, respectively. These values are related to 487.0 to 604.0 mg of «hemicelluloses 2» transformed, respectively. As in the case of the «hemicelluloses 1» fractions, this result represents about 1 % of the biomass conversion. The low value can also be explained by the impossibility of quantifying anhydrosugars thermal decomposition with our system. However, as it was discussed for «hemicelluloses 1», the profiles of solid degradation and of volatile species production were shown to be in accord with the literature, so they were shown to be representative from hemicelluloses behavior in torrefaction.

In the case of «hemicelluloses 2», the composition of the volatile species is not the typical one for hemicelluloses in torrefaction (Figure IV.36). The results show a lower proportion of acids in the volatile species compared to that from the «hemicelluloses 1» fractions, which is derived from the removal of the acetyl groups from hemicelluloses due to the alkaline treatment. This is consequently translated into an increase of the proportion of methanol and formaldehyde, and,

in a minor extent, of furans and ketones. Some species typically involved in the thermal degradation of hemicelluloses were detected in significant amounts. As a result, this fraction can be considered as not representative of the behavior of hemicelluloses in torrefaction in terms of volatile species release, but it can complement the «hemicelluloses 1» fraction to reconstruct the behavior of the «total hemicelluloses» in torrefaction (see section V.2.3).

By considering the individual volatile species released, the major volatile species vary in function of the biomass type between methanol, formaldehyde, furfural and acetic acid (percentages of the total production between 11.3 and 33.3% per compound). Significant proportions of hydroxyacetone and 2(5H)-furanone were also quantified in the volatile species, particularly from the «hemicelluloses 2» fractions from ash-wood, beech and pine. In particular, the proportion of hydroxyacetone in the volatile species mixtures is higher than that quantified for the «hemicelluloses 1» fractions.

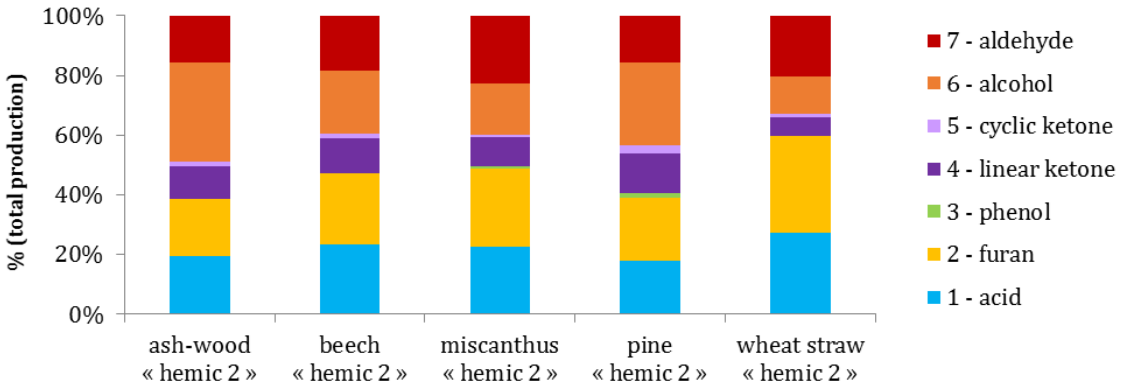


Figure IV.36. Distribution of the total production of volatile species per chemical family obtained during torrefaction of «hemicelluloses 2» extracted fractions from 5 biomasses in TGA-GC/MS

The production profiles of the volatile species released were also studied, as in previous sections, versus time and temperature and in function of the biomass type (Figures IV.37 to IV.41). More volatile species are detected in trace amounts for «hemicelluloses 2». However, important species in the thermal degradation of hemicelluloses are quantified in significant amounts, such as hydroxyacetone and methanol.

Acetic acid was one of the major compounds detected despite the removal of most of the acetyl by the alkaline treatment to obtain this fraction. This removal is confirmed by the acetyl composition of «hemicelluloses 2» fractions compared to those of «hemicelluloses 1» (from 1.0 % to 3.1-22.9 %, respectively). This implies that the production profile of acetic acid is not representative of the main source of acetic acid release from hemicelluloses, which corresponds to the scission of the acetyl groups from xylose units. However, this profile might represent the release of acetic acid from hemicelluloses by other mechanisms, together with the formation from the residual acetic groups. The rather constant production in function of the torrefaction

temperature (Figure IV.37) might correspond to small molecule release during the scission of the sugars involved in hemicelluloses chains, such as ring-scission between xylose and uronic acid residues [163,165].

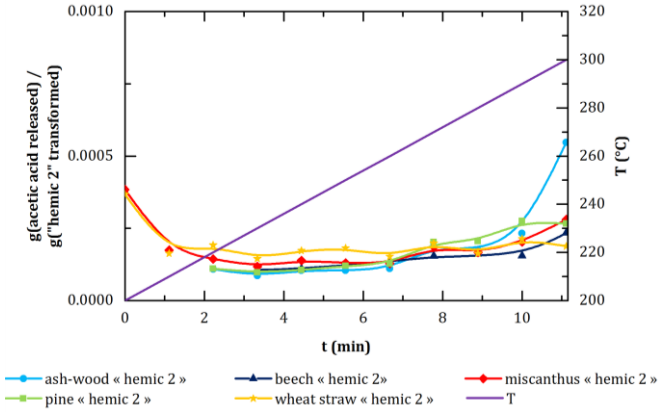


Figure IV.37. Production profile of acetic acid versus temperature and time obtained for «hemicelluloses 2» fractions in torrefaction in TGA-GC/MS

Furfural was also detected among the major volatile species released in the torrefaction of «hemicelluloses 2» fractions. However, as in the case of acetic acid, the production profile is rather constant with torrefaction temperature (Figure IV.38, left), which does not correspond to that of «hemicelluloses 1» fractions. Similar mechanisms as in the case of «hemicelluloses 1» are supposed to be at the origin of this compound. The constant production with torrefaction temperature might represent rearrangements in xylan structures that happen from low temperatures [163]. As in the case of the fraction 1 of hemicelluloses, higher production rates of furans were detected for glucomannan based-hemicelluloses, namely pine and wheat straw «hemicelluloses 2» (7.5 and 33.3 % of mannose, respectively, in their composition). An equivalent case was found for 2(5H)-furanone (Figure IV.38, right).

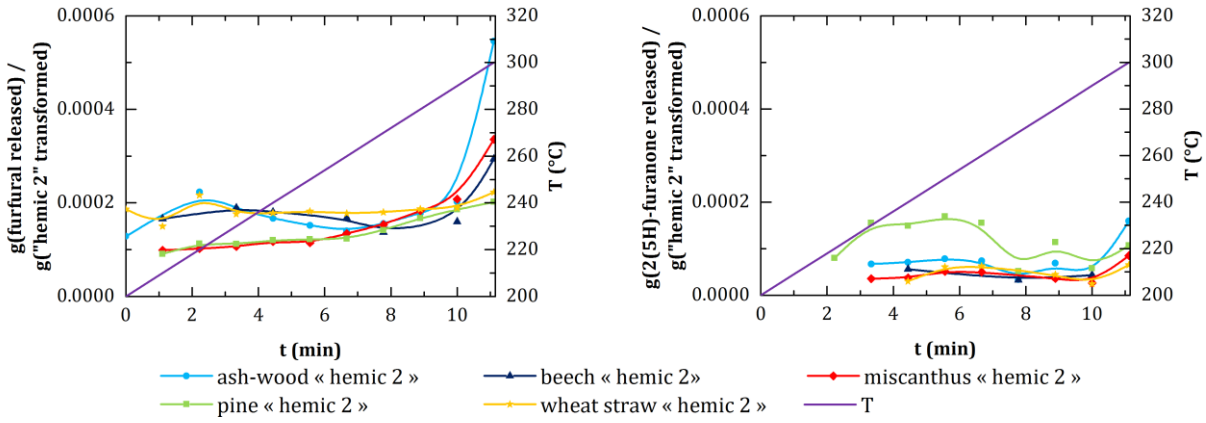


Figure IV.38. Production profile of furfural (left) and 2(5H)-furanone (right) versus temperature and time obtained for «hemicelluloses 2» fractions in torrefaction in TGA-GC/MS

Linear ketones, namely hydroxyacetone and 2-propanone,1-(acetyloxy)- were detected in higher

amounts than for the corresponding «hemicelluloses 1» fractions. On the contrary, the production of 4-cyclopentene-1,3-dione is higher for this last fraction. The production profile of hydroxyacetone shows two marked local minima at 270 and 290°C for all the «hemicelluloses 2» fractions (Figure IV.39, left). On the other hand, 2-propanone,1-(acetyloxy)- production increases with the increasing torrefaction temperature without significant differences among the hemicelluloses fractions (Figure IV.39, right). The quantified production profiles of linear and cyclic ketones are equivalent for both hemicelluloses fractions.

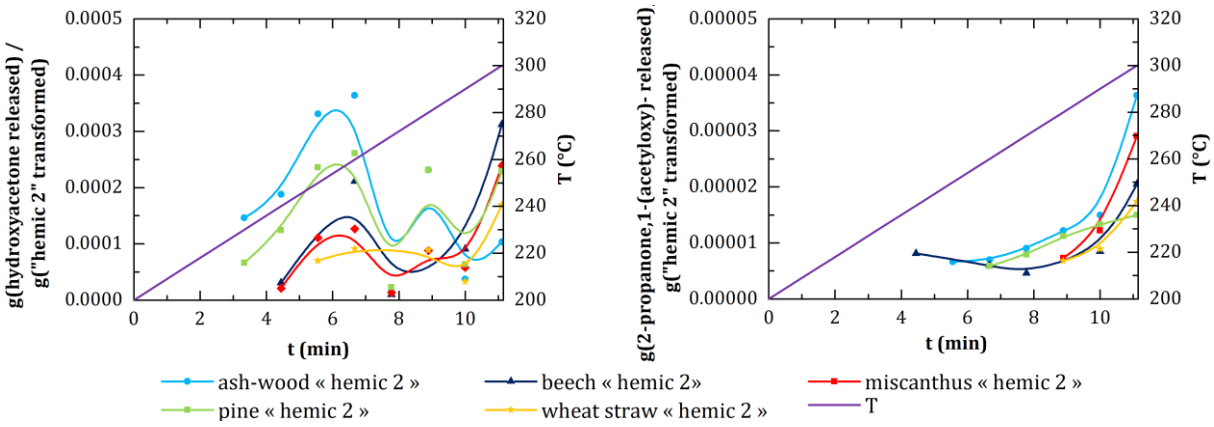


Figure IV.39. Production profile of hydroxyacetone (left) and 2-propanone, 1-(acetyloxy-)- (right) versus temperature and time for «hemicelluloses 2» fractions in torrefaction in TGA-GC/MS

Methanol production was enhanced at lower torrefaction temperatures (Figure IV.40), which is in contrast with the rather constant production measured for «hemicelluloses 1» (Figure IV.33). It is important to note that in this case, methanol production is about 10 times lower than in the «hemicelluloses 1» case, so the first methanol production profiles will be considered as more representative for hemicelluloses behavior in torrefaction.

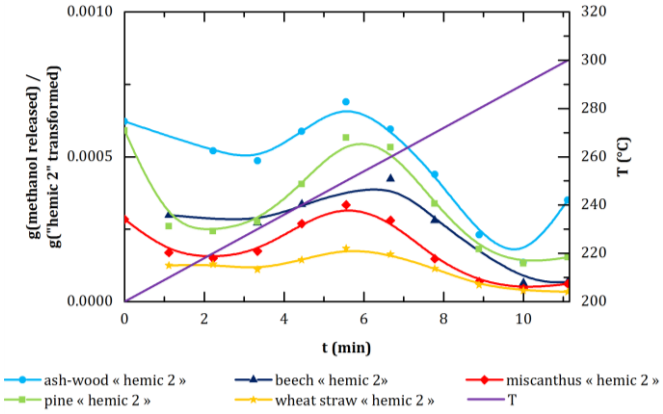


Figure IV.40. Production profile of methanol versus temperature and time obtained for «hemicelluloses 2» fractions in torrefaction in TGA-GC/MS

The production of formaldehyde remains in the same order of magnitude of that of the «hemicelluloses 1» fractions. At the same time, the shapes of the production profiles are also

rather constant with the torrefaction temperature (Figure IV.41), so comparable between both hemicelluloses fractions (Figure IV.34, left). The exception is for the first two points at the lower torrefaction temperatures. However, this difference cannot be considered as significant to describe a pattern of formation of this species.

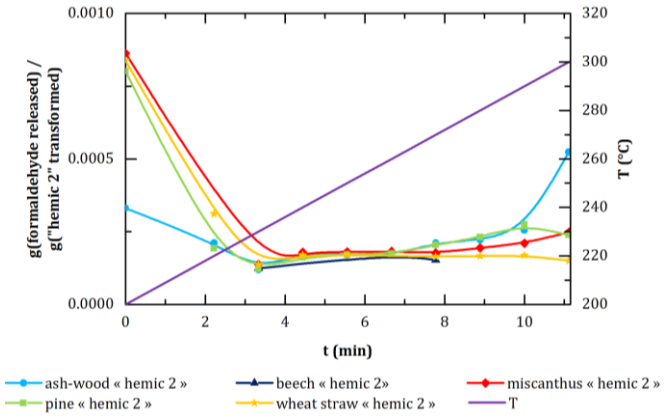


Figure IV.41. Production profile of formaldehyde versus temperature and time obtained for «hemicelluloses 2» fractions in torrefaction in TGA-GC/MS

To sum up, the production profiles of the volatile species released in the torrefaction of the «hemicelluloses 2» fractions are equivalent to those from the «hemicelluloses 1» fractions when the production is in the same order of magnitude for both hemicelluloses fractions. In some cases, a lower production was measured, together with production profiles independent from the torrefaction temperature. Even if these profiles can contribute to explain mechanisms leading to the formation of the volatile species, the production profiles obtained for the «hemicelluloses 1» fractions are considered as more representative, except in the case of hydroxyacetone. For this compound, the shape of the production profile was close for both cellulose fractions but the quantified production was higher in the case of the «hemicelluloses 2» fractions.

2.3. Lignin

Lignin was extracted in a single fraction from biomass, called «lignin» fraction.

2.3.1. Solid transformation

The final remaining solid mass observed for the «lignin» fractions at the end of the torrefaction experiment goes from 65.1 %wmf for pine «lignin» to around 70.0 %wmf for ash-wood and beech (Figure IV.42, left). Degradation rates are low for all «lignin» fractions, below 1.1 %wmf/min (Figure IV.42, right).

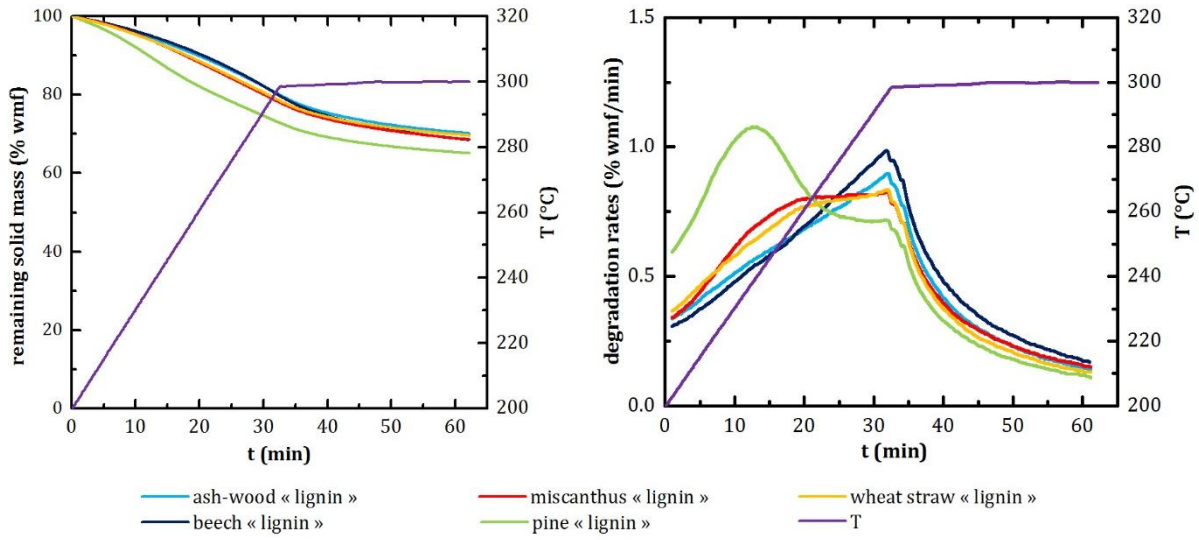


Figure IV.42. Remaining solid mass (left) and degradation rates (right) versus time and temperature obtained in torrefaction for «lignin» fractions from 5 biomasses in TGA-GC/MS

Three solid kinetic behaviors can be distinguished between the «lignin» fractions analyzed in the non-isothermal torrefaction step (0 to 33.3 min, Figure IV.42, left): one behavior pattern corresponds to «lignin» from deciduous wood (ash-wood and beech), the second one to that from agricultural by-products and herbaceous crops (wheat straw and miscanthus) and the last one to that of coniferous wood (pine). These patterns are confirmed by the derived curve of the remaining solid mass, representing the degradation rates (Figure IV.42, right). More precisely, in the non-isothermal torrefaction, ash-wood and beech «lignin» present a rather constant acceleration of the degradation rate, until 300°C, with a slight change in the tendency around 250°C. This change is more marked for wheat straw and miscanthus «lignin» which increase their degradation rate from the beginning of the torrefaction and then tend to stabilize it from around 250°C. Finally, the degradation rate of pine «lignin» increases until around 235°C, then decreases and finally tends to stabilize from 275°C. In the isothermal torrefaction step, the degradation rate of all biomasses progressively decreases with a similar pattern for all the «lignin» fractions.

Lignin was reported to be only partially degraded in the temperature range of torrefaction (see II.3.2.3), which is in accord with the low mass loss measured for the «lignin» fractions after torrefaction. This progressive degradation is also in accord with the soft profile of the remaining solid mass curves versus time and temperature and with the low degradation rates observed.

Considering differences in lignin structure in function of the biomass type together with the experimental results, G-type lignin would seem to be more easily degraded than H-type lignin and finally than S-type lignin. However, these differences in the degradation patterns could be also due to cleavage of internal bonds in lignin units. The profiles of formation of phenolic

volatile species of H- G- and S- types, derived from lignin can help to explain these differences in mass loss between «lignin» fractions.

The evolution of the elemental composition of the «lignin» fractions due to torrefaction is represented in Figure IV.43. All «lignin» fractions present a similar elemental composition, except pine «lignin», which is richer in carbon. The enrichment in the carbon content of «lignin» fractions is between 19.2 and 27.3%, comparable to that of the «cellulose II» fraction. This is associated with a diminution in oxygen from 29.6 to 59.1%. This diminution might be explained by a high production of permanent gases (not measured) and/or by the high oxygen content of the phenolic compounds released.

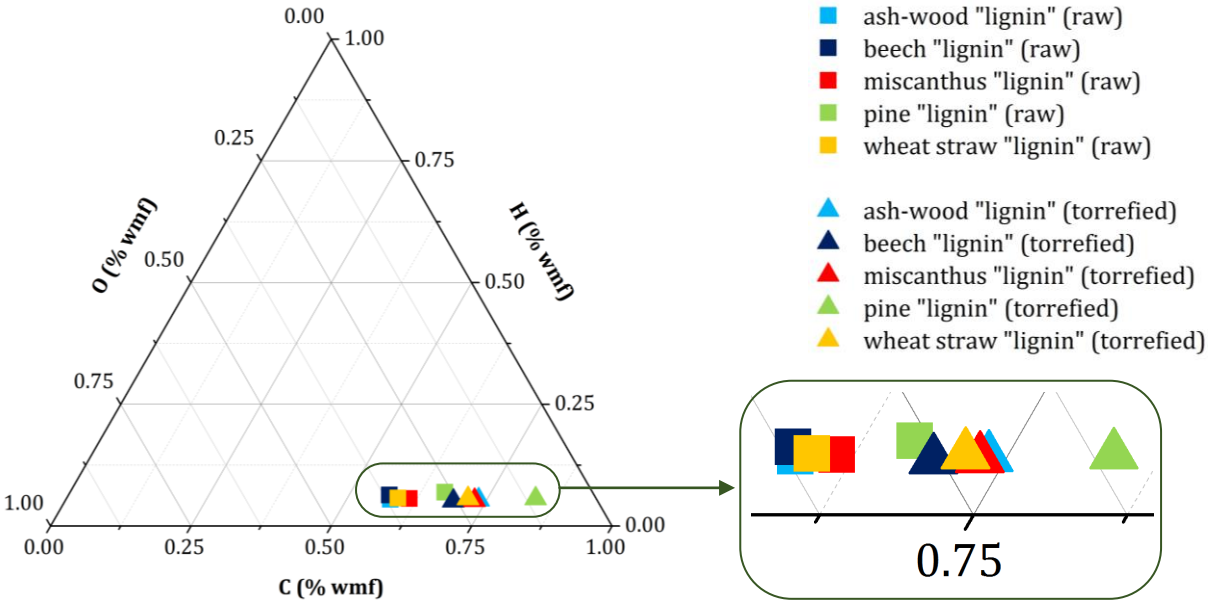


Figure IV.43. Ternary diagram of CHO elemental composition of raw and torrefied «lignin» in TGA-GC/MS

2.3.2. Volatile species release

First of all, the total production of each quantified volatile species was calculated by the integration of the corresponding release curve of the volatile species versus time in the non-isothermal torrefaction interval. The total production of quantified volatile species was then estimated by adding the production of the individual compounds. This total quantified volatile species production was between 1.0 mg (total volatile species released) for beech «lignin» to 4.1 mg for miscanthus «lignin», which is related to 192.6 mg and 270.1 mg of «lignin» transformed, respectively. In the case of pine, these values were 1.3 mg of total volatile species quantified for 270.1 mg of «lignin» transformed. The fact that a lower mass of volatile species was quantified for pine «lignin», which is the «lignin» fraction with the higher mass loss, responds to the fact that not all volatile species could be neither identified nor quantified. Even if the main species could be measured, as discussed later, a high variety of minor phenolic compounds are released in lignin decomposition, which explains this difference. For example, many guaiacyl derivatives

could be measured, while the corresponding syringyl derivatives were not detected. This could be due to the limitations of the GC/MS column selected, or due to their lack of production under these operating conditions.

In a second step, the total production of the volatile species was grouped by chemical family of the released compounds (Figure IV.44). Phenols appear as the major released compounds, followed by formaldehyde. Both are reported in the literature to be typical compounds released in lignin degradation [229]. Methanol and acetic acid are also significantly released, while furans and ketones are formed in a minor extent. This observation is in agreement with previous studies that have pointed out ketones and furans as principally derived from polysaccharides.

By considering individually the volatile species released, the major volatile species detected are formaldehyde (from 20.5 to 51.4 % of the total volatile species quantified), 2-methoxy-4-vinylphenol (4.5 to 22.6 %), methanol (10.0 to 16.9 %, excepted for beech «lignin», 27.2 %), isoeugenol (6.5 to 14.0 %) and acetic acid (4.2 to 16.0 %). Minor amounts of other compounds, mainly phenolic, are produced, such as vanillin (3.1 to 7.1 %), syringol, guaiacol, phenol, eugenol (< 2.5 % for each compound), but also furfural (1.3 to 11.0 %).

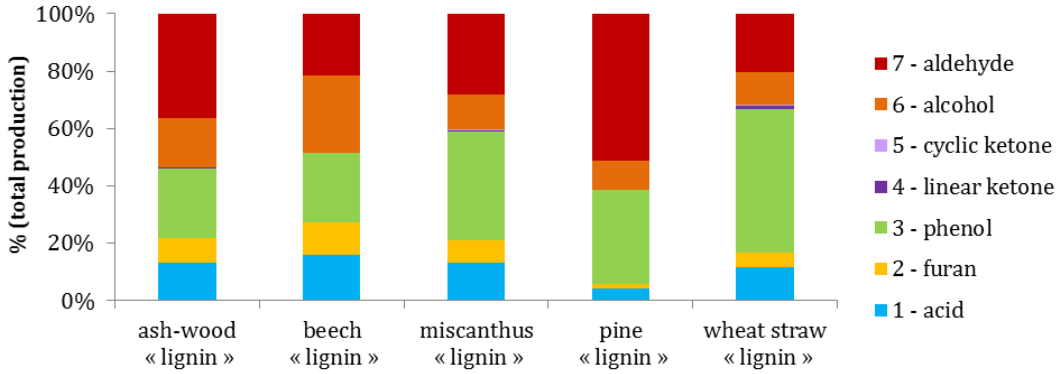


Figure IV.44. Distribution of the total production of volatile species per chemical family obtained during torrefaction of «lignin» extracted fractions from 5 biomasses in TGA-GC/MS

Secondly, the production profiles of the volatile species were studied (Figures IV.45 to IV.50).

The profile of release of formaldehyde was shown to be rather uniform during the non-isothermal torrefaction (Figure IV.45), around 0.002 to 0.006 g (formaldehyde released) / g («lignin» transformed). This compound has been reported in the literature to be released from low temperatures, even from 180°C, as a result of the fragmentation between the carbons Cβ and Cγ in the propyl chain in lignin structure, when the hydroxyl group is linked to the Cγ. This scission would liberate a terminal hydroxymethylene group (–CH_2OH), which implies the formation of formaldehyde [229,230].

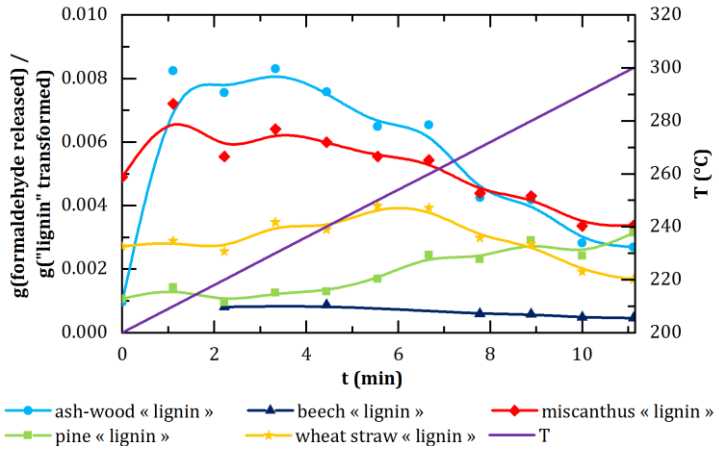


Figure IV.45. Production profile of formaldehyde versus temperature and time obtained for «lignin» fractions in torrefaction in TGA-GC/MS

Phenols are the main volatile species released in lignin decomposition due to the phenyl propane-based structure of lignin [62,63,231,232]. The formation of phenols has been explained in the literature as derived from the dehydration of the hydroxyl- groups in the alkyl side chain of the lignin basic units, followed by the cleavage of ether bonds between these units [177]. At lower temperatures, the α-O-4 (200°C) and the β-O-4 linkages within monomer units in lignin can start to break and liberate phenolic compounds whose structure is close to that of the substituted lignin monomers [29,172]. That is the reason why phenolic compounds with an aliphatic substituent are typically released from early torrefaction temperatures. This behavior was also observed in analytical fractionated Py-GC/MS experiments (Annex VIII). Going into detail in the detected compounds, 2-methoxy-4-vinylphenol, eugenol, and isoeugenol show increasing profiles with increasing torrefaction temperature, with the exception of two local minima at 270°C and 290°C in the three cases (Figure IV.46). No explanation was found to justify this minimum. The production rate of 2-methoxy-4-vinylphenol goes up to 0.007 to 0.008 g(compound released)/g(«lignin» transformed) for wheat straw and miscanthus «lignin», while its value is lowered to around 0.002 g/g for coniferous and deciduous “lignin” fractions. In the case of isoeugenol, the maximum production rate reached is between 0.004 and 0.002 g(isoeugenol released)/g («lignin» transformed), while the production of eugenol is about 10 times lower. On the other hand, vanillin shows a constant profile of formation with the torrefaction temperature, where the production rate is between 0.6 and 0.2 mg(vanillin released)/g(«lignin» transformed) (Figure IV.46, right). Finally, cathecol was detected in traces, below 0.1 mg(cathecol released)/g(«lignin» transformed) at temperatures higher than 260°C.

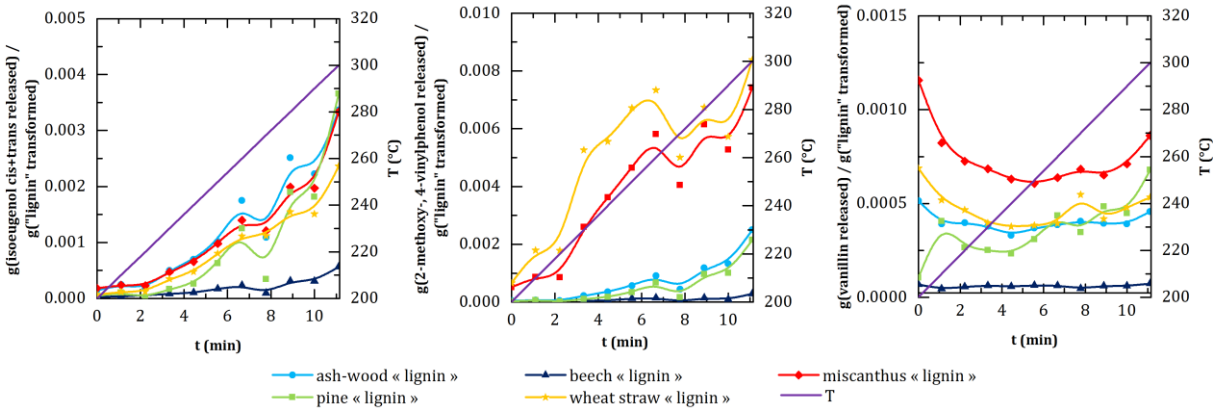


Figure IV.46. Production profiles of 2-methoxy-4-vinylphenol (left), isoeugenol (center) and vanillin (right) versus temperature and time for «lignin» fractions in torrefaction in TGA-GC/MS

At higher temperatures, most of the remaining C-C bonds within and between the alkyl chains become unstable and break, releasing phenolic compounds with a small substituent (methyl-type, for example) or without lateral chain, such as phenol guaiacol and syringol (Figure IV.47). In the literature, these phenomena have been reported to take place from 300°C, through the cleavage of condensed linkages of lignin such a β-1 and β-5, which has been reported to form high yield of guaiacol and 4-methylguaiacol, respectively, but would occur at pyrolysis temperatures higher than 400 to 450°C. A third mechanism of formation was described, from the condensed lignin substructures similar to methyl derivatives [175,176] (see Table II.3). However, these phenolic compounds were detected at temperatures below 300°C, which might indicate that their mechanism of formation would be possible from lower temperatures for the «lignin» fractions. The production of phenol, guaiacol and syringol was shown to increase with the increasing torrefaction temperatures following a likely-exponential profile of formation (Figure IV.47). The maximum of their formation rate is attained at 300°C and it is around 0.001 g(volatile species released)/g(«lignin» transformed) for syringol, and slightly lower for phenol and guaiacol.

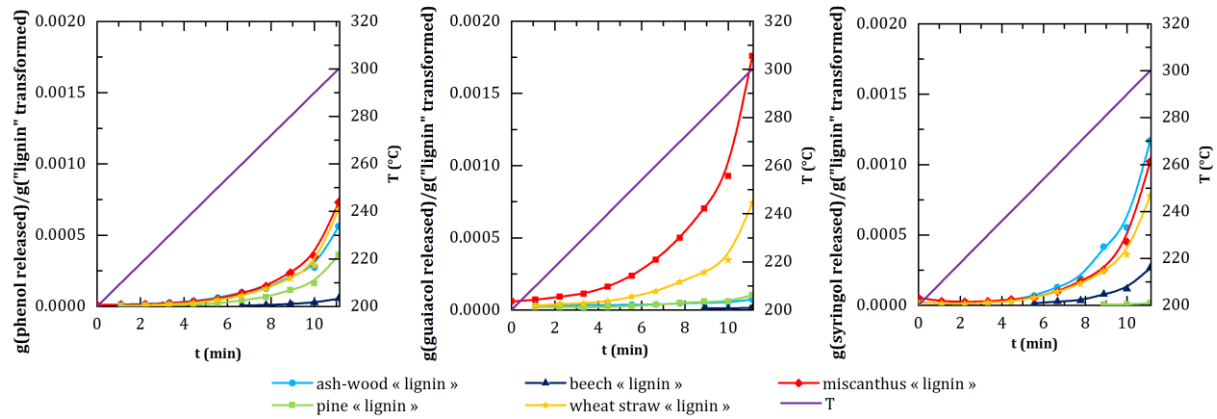


Figure IV.47. Production profiles of phenol (left), guaiacol (center) and syringol (right) versus temperature and time for «lignin» fractions in torrefaction in TGA-GC/MS

In the case of methanol, its formation starts at early torrefaction temperatures and then its production rises with increasing torrefaction temperature (Figure IV.48). This compound, together with methane, has been reported to be mainly produced in the fragmentation of methoxy- groups linked to aromatic rings from lignin, at temperatures higher than 400 °C [229]. This scission seems to occur earlier in our case and will be analyzed together with the formation of other small compounds such as acetic acid.

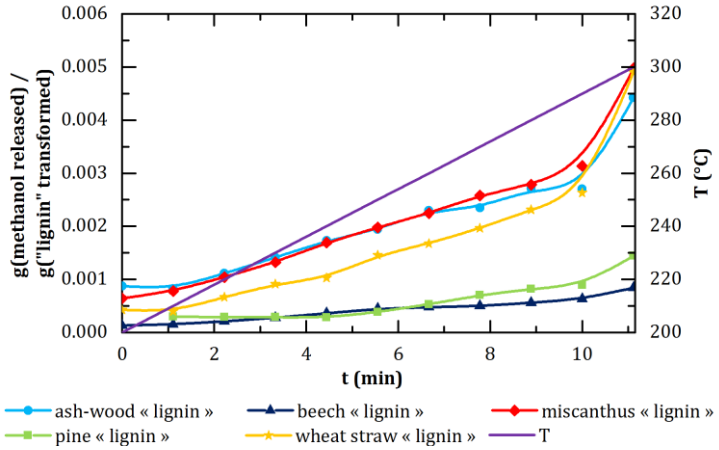


Figure IV.48. Production profiles of methanol versus temperature and time for «lignin» fractions in torrefaction in TGA-GC/MS

Smaller amounts than those released by hemicelluloses are detected for acetic acid. It can be produced from the scission of the alkyl chains from phenyl units in lignin, together with other small chemical compounds usually up to 3 carbons. Acetic acid was detected from early torrefaction temperatures around 200°C instead of from 300°C as it was pointed out in the literature. As its mechanism of formation seems linked to that of phenolic compounds without alkyl chain, this observation remains coherent with the hypothesis that this mechanism might happen since early torrefaction conditions in our experiments. The profile of formation of acetic acid is constant with torrefaction temperature, as in the case of formaldehyde but between 0.003 and <0.001 g(acetic acid released)/g(«lignin» transformed) (Figure IV.49). This contrasts with the increasing profiles of formation of the small phenolic compounds with increasing torrefaction temperature. This might indicate that C-C bonds liberating alkyl lateral chains from the phenolic compounds might break independently to the fact that these phenolic compounds are still linked to the «lignin» fraction through the α-O-4 and the β-O-4 bounds. It would also be the case for the release of methanol from lateral methoxy- groups of phenyl units. This hypothesis would suppose the similar stability of this kind of linkages in the «lignin» fractions, which are “milled wood lignin” type. However, no evidence was found in the literature to firmly support this hypothesis.

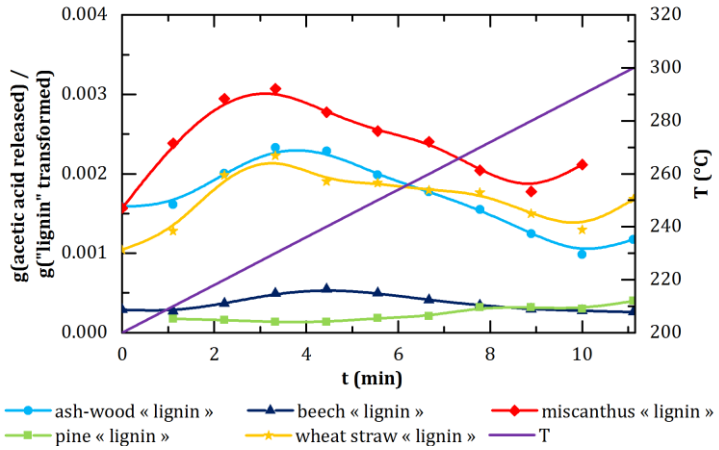


Figure IV.49. Production profiles of acetic acid versus temperature and time obtained for «lignin» fractions in torrefaction in TGA-GC/MS

Furfural was detected at production rates below 0.003 g(furfural released)/g(«lignin» transformed), while other furan compounds were also detected in minor amounts, <0.001 g/g. The profile of formation of furan was shown to be decreasing with increasing torrefaction temperature (Figure IV.50); for other furans, it is mainly constant and independent of the temperature, except for furan, which is increasing.

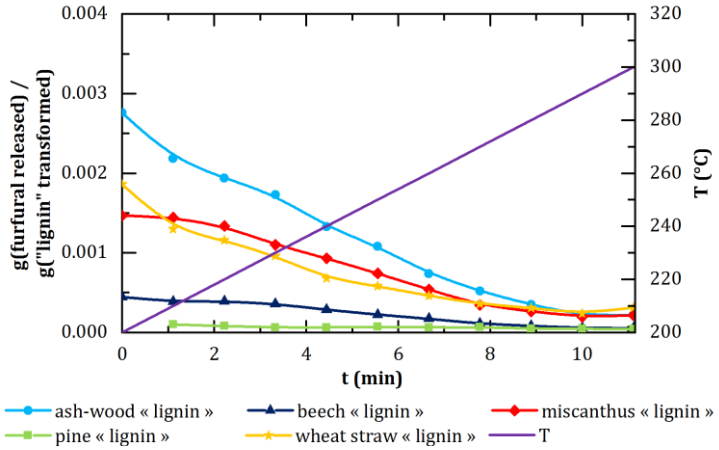


Figure IV.50. Production profiles of furfural versus temperature and time obtained for «lignin» fractions in torrefaction in TGA-GC/MS

To summarize, lignin is progressively degraded from 200°C, but this degradation is quite limited in the torrefaction temperatures range. The volatile species release of lignin in torrefaction is characterized by presenting a large variety of phenolic compounds, formaldehyde, methanol and acetic acid. Substituted-phenolic compounds (i.e. isoeugenol) were reported to be released slightly earlier than main lignin units (i.e. guaiacol), which is in accord with previous results obtained in Py-GC/MS at higher temperatures. The production profiles of the chemical species released were analyzed so as to assess the origin of these volatile species from lignin structure.

2.4. Mixtures of extracted macromolecular components from the reference biomasses

2.4.1. Ternary mixtures

Ternary mixtures of the extracted fractions «cellulose», «hemicelluloses 1» and «lignin» were carried out for the 5 reference biomasses. The extracted fractions were physically mixed in the proportions that cellulose, hemicelluloses and lignin are in raw biomass. The objective of this section is to study the behavior of the extracted fractions together in torrefaction and to determine if there are interactions in solid phase between them.

2.4.1.1. Solid transformation

Solid mass loss was calculated versus temperature and time for the 5 ternary mixtures of extracted «cellulose», «hemicelluloses 1» and «lignin» from the 5 selected biomasses (ash-wood, beech, miscanthus, pine, wheat straw). The experiments consisted of a non-isothermal torrefaction between 200 and 300°C, at 3°C/min, followed by an isothermal torrefaction at 300°C for 30 minutes (Figure IV.51).

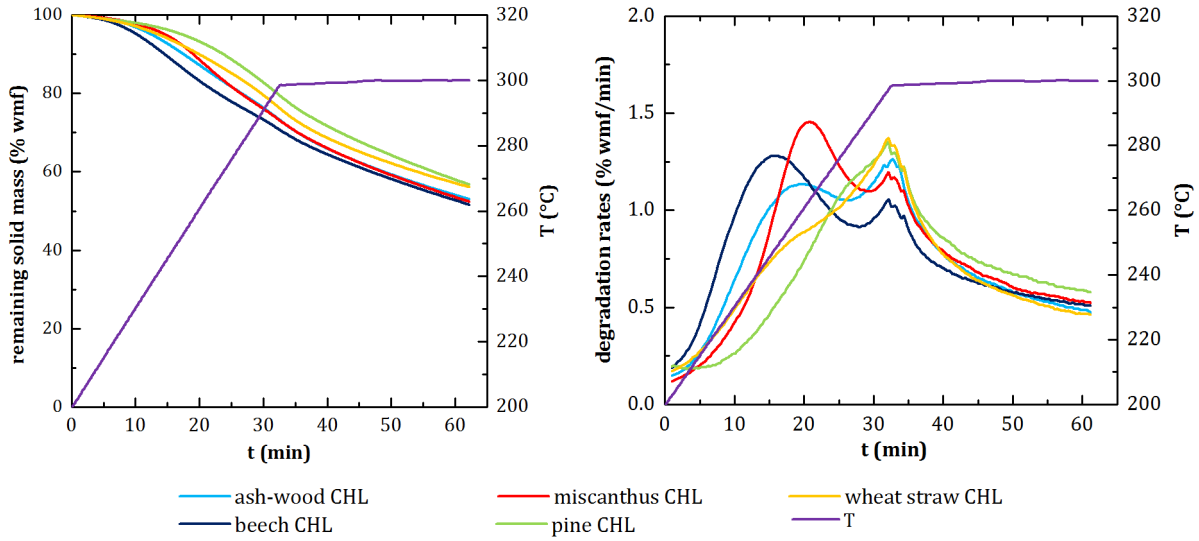


Figure IV.51. Remaining solid mass (left) and degradation rates (right) versus time and temperature obtained for ternary mixtures in torrefaction in TGA-GC/MS

The final remaining solid mass of the ternary mixtures is between 51.6 %wmf for beech and 56.7%wmf for pine mixture (Figure IV.51, left). Interesting information can be extracted from the shape of the degradation rates profiles (Figure IV.51, right). They present an initial maximum between 245 and 260°C, especially marked for ash-wood, beech and miscanthus mixtures. For the wheat straw mixture, this maximum appears as a change in the behavior pattern, which corresponds to an inversion of the convexity of the degradation rates curve. For the pine mixture, the maximum is more discrete and happens at temperatures closer to 300°C. This first maximum is followed by a second relative maximum around 300°C, in this case for all

mixtures, which is interrupted by the progressive decrease of the degradation rates in the isothermal step.

By comparing the behavior of the ternary mixtures (Figure IV.51) to that of the raw biomass (Figures IV.1 and IV.2), important differences stand out, either in the non-isothermal or in the isothermal torrefaction steps, in function of the biomass type. This result suggests that interactions between macromolecular components play a crucial role to determine the pattern of degradation of a given biomass in torrefaction. The physical mixture of the extracted fractions in the proportions as they are present in biomass was shown not to allow the reproduction of these interactions. A deeper comparison of these results with the additive torrefaction model derived from the fractions involved in the ternary mixtures, as well as to raw biomass, will be carried out in chapter V.

2.4.1.2. Volatile species release

The detected chemical compounds for the ternary mixtures are in agreement with those identified and quantified for the raw biomasses. However, more species are detected in traces in this case.

The total volatile species production was estimated to be between 0.2 and 0.9 mg of volatile species released for a transformed solid mass between 202 and 283 mg, respectively for pine and beech ternary mixtures. The estimated production for the equivalent raw biomasses was between 1.8 and 8.0 mg of volatile species released for a transformed solid mass between 206 and 320 mg. However, in the case of the raw materials, the highest quantified mass of volatile species corresponded to beech, while the highest mass loss was found for wheat straw. In the case of the ternary mixtures, the highest quantified mass of volatile species coincided with the highest mass loss, for beech in both cases. This difference in the order of magnitude of the total volatile species production can be due to the fact that the ternary mixtures are composed by the physical mixture of the three extracted fractions «cellulose», «hemicelluloses 1» and «lignin» from each biomass. Bonds between biomass macromolecular components cannot be reconstructed by physically mixing the fractions. Indeed, small molecules are known to be typically released in reactions of scission of cellulose, hemicelluloses and lignin from the biomass matrix. On the other hand, it is important to note that the experimental procedure to physically mix the fractions involved in the mixtures implies a high loss of the lignin fraction, due to its different nature compared to cellulose and hemicelluloses fractions (powder in the case of lignin, cotton-like agglomerates for the other fractions). This can explain the strong diminution of the phenolic compounds proportion in the volatile species in the ternary mixtures.

The total production of each individual chemical species was added to other species from the same chemical family, so as to study the proportion of each type of chemical compounds in the

mixture of volatile species, from all torrefaction temperatures (Figure IV.52). Acids were revealed as the volatile species detected in the major proportions for all volatile species, especially due to the high production of acetic acid (from 47.1 to 73.5% of the total quantified production per biomass). However, in the case of pine and wheat straw, the proportion of acetic acid remains comparable to that of furans (47.1 to 35.7%, respectively). The high production of furans is mainly attributed to furfural (from 6.6 to 30.9%). By comparing this volatile species distribution per chemical families (Figure IV.52) to those from the raw biomasses (Figure IV.5), it is noteworthy that the proportions of the small molecules, such as ketones, methanol and formaldehyde were drastically diminished. This diminution is in agreement with previous observations.

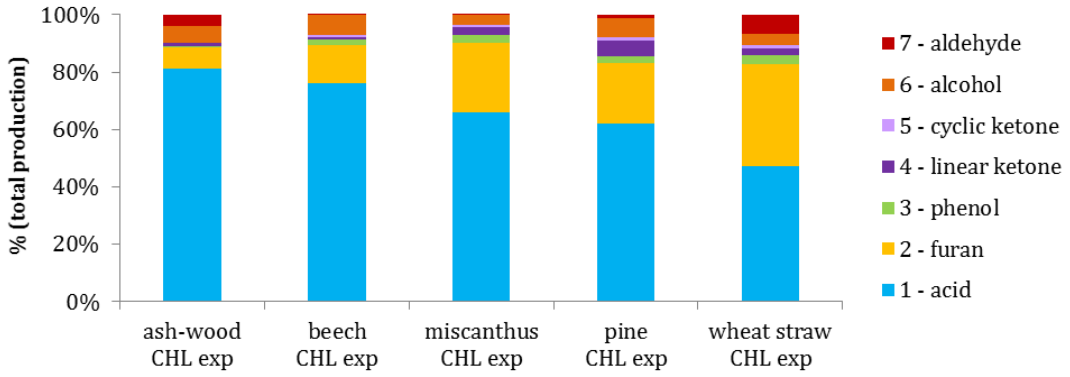


Figure IV.52. Distribution of the total production of volatile species per chemical family obtained during torrefaction of ternary mixtures (CHL) in TGA-GC/MS

Secondly, the production profiles of the quantified volatile species in the torrefaction of the ternary mixtures were studied (Figures IV.53 to IV.56).

The production profiles of the major detected compound, acetic acid, present an equivalent tendency to that of the corresponding profiles of the raw biomasses. An exception is the temperature of the maximum of the production detected for ash-wood and beech samples. This maximum is reached at lower temperatures in the case of the ternary mixtures (Figure IV.53), which could correspond with the fact that the macromolecular components are isolated in the ternary mixture. As a result, their conversion seems more feasible, so possible at lower temperatures, particularly because of the absence of inter-molecular bonding. On the other hand, the order of magnitude of the production is about 4 to 10 times lower. This diminution might also be explained by the isolation of the extracted fractions, as inter-molecular linkages between cellulose, hemicelluloses and lignin in raw biomass contribute to the release of this compound.

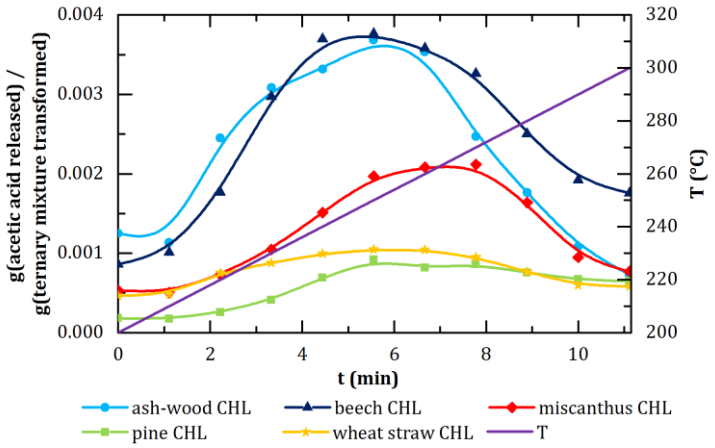


Figure IV.53. Production profile of acetic acid versus temperature and time obtained during torrefaction of the ternary mixtures in TGA-GC/MS

Formic and propionic acid were detected in lower amounts for the ternary mixtures than for the raw biomasses, which is in agreement with the previous observation. Formic acid was reported to be formed from the breaking of carboxylic acid function of the hexuronic acids in hemicelluloses [163]. These results might suggest that a lower number of carboxylic fractions in hemicelluloses would be available for this production route. A diminution in the propionic acid production could also be derived from the lack of extractives in the ternary mixtures. Furthermore, they could only be measured at few temperature points. As a result, they are not discussed in this section.

Furans were also detected in significant amounts, in all cases lower than those from the raw biomasses. It is noteworthy that the production profiles of furans globally remain with the same tendencies as those of the raw biomasses, with the exception of furfural (Figure IV.54). The disparity of the production profiles of furfural is conserved. However, the trends in the production profiles are different for the ternary mixtures and their corresponding raw biomasses. For example, the production profiles of furfural for the ternary mixture from wheat straw happens at low torrefaction temperatures, while the corresponding profile for the raw biomass is rather increasing with torrefaction temperature. The production of furfural by the ternary mixtures from beech and ash-wood is decreasing with torrefaction temperature, while the equivalent raw biomasses exhibit an increasing production with increasing torrefaction temperature, with a maximum around 260°C.

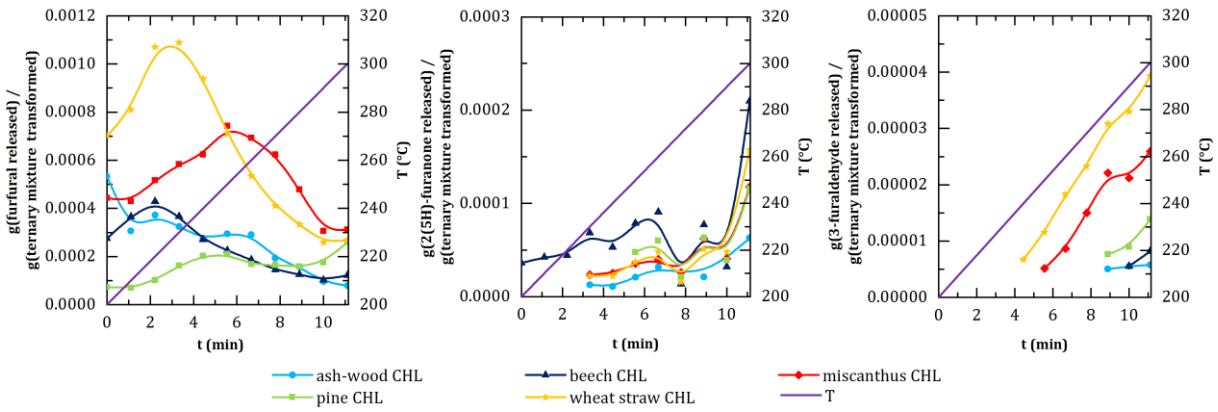


Figure IV.54. Production profiles of furfural (left), 2(5H)-furanone (center) and 3-furaldehyde (right) versus temperature and time obtained during torrefaction of the ternary in TGA-GC/MS

Formaldehyde and methanol were detected in significant amounts which remain lower than those released by the raw materials. The production profiles were shown to be similar to those of the equivalent raw biomasses, exhibiting a tendency independent of the torrefaction temperature (Figure IV.55).

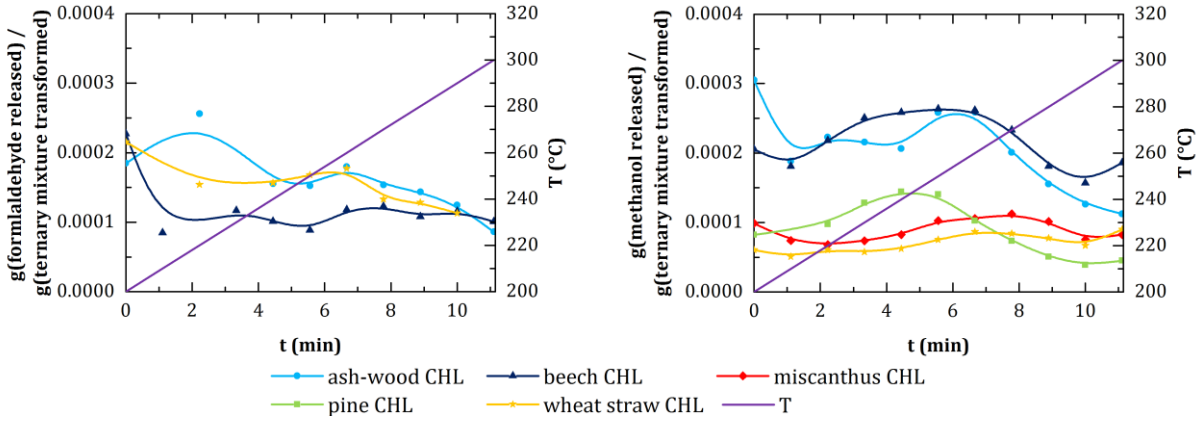


Figure IV.55. Production profiles of formaldehyde (left) and methanol (right) versus temperature and time obtained during torrefaction of the ternary mixtures in TGA-GC/MS

Linear ketones were detected in traces for the ternary mixtures, with the exception of hydroxyacetone. Only few points were detected for the cyclic ketone 4-cyclopentene-1,3-dione, between 260 and 300°C. The production profiles can be noticed as similar to those from the equivalent raw biomasses in a lowered order of magnitude (Figure IV.56). Similar reasons as those previously mentioned can be at the origin of this observation.

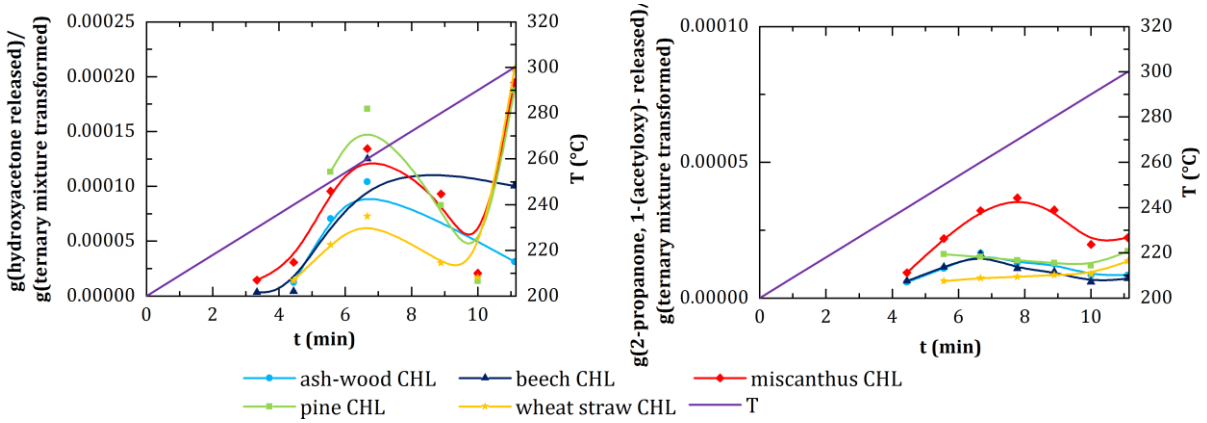


Figure IV.56. Production profiles of hydroxyacetone (left) and 2-propanone,1-(acetyloxy)- (right) versus temperature and time obtained during torrefaction of the ternary mixtures in TGA-GC/MS

All phenolic compounds identified for the raw biomasses were found in trace amounts in the ternary mixtures. This lowered production is derived from the lignin losses in the physical mixture of the extracted fractions. At the same time, these compounds were only detected at intermediate to high torrefaction temperatures, for few points, which complicates an accurate representation of the production profiles.

Finally, the analysis of the volatile species released by the ternary mixtures and the comparison to the equivalent data from the raw materials suggest that:

- The production profiles obtained in the torrefaction of the ternary mixtures for the lignin-derived compounds, such as phenols and formaldehyde, is not representative of the real release from lignin in biomass. This result is explained by experimental difficulties in the mixture of the three extracted fractions which lead to an important loss of lignin.

- Non-negligible amounts of small molecules, such as acetic acid, methanol and ketones, are released in fragmentation and rearrangement mechanisms between biomass macromolecular components. The absence of bonding between the extracted fractions in their physical mixture leads to a minor production of these species.

- Interactions in gas phase of the released volatile species cannot be highlighted by this method, due to the difference in the order of magnitude of the production profiles between the ternary mixtures and the corresponding raw biomasses.

2.4.2. Binary mixtures for beech

Beech and its extracted «cellulose», «hemicelluloses 1» and «lignin» fractions were selected for testing binary mixtures of the extracted fractions. These mixtures were called CH («cellulose II» «hemicelluloses 1»), CL («cellulose II» + «lignin») and HL («hemicelluloses 1» + «lignin»). The objective of this section is to compare the behavior of the main extracted fractions by pairs and

to determine whether there are interactions between them during torrefaction.

2.4.2.1. Solid transformation

The behavior of the binary mixtures of beech extracted fractions was compared in torrefaction with the classical operating conditions program, as in previous sections (Figure IV.57). The kinetic profiles obtained for the beech ternary mixture and for the raw biomass were also added to this graph for comparison.

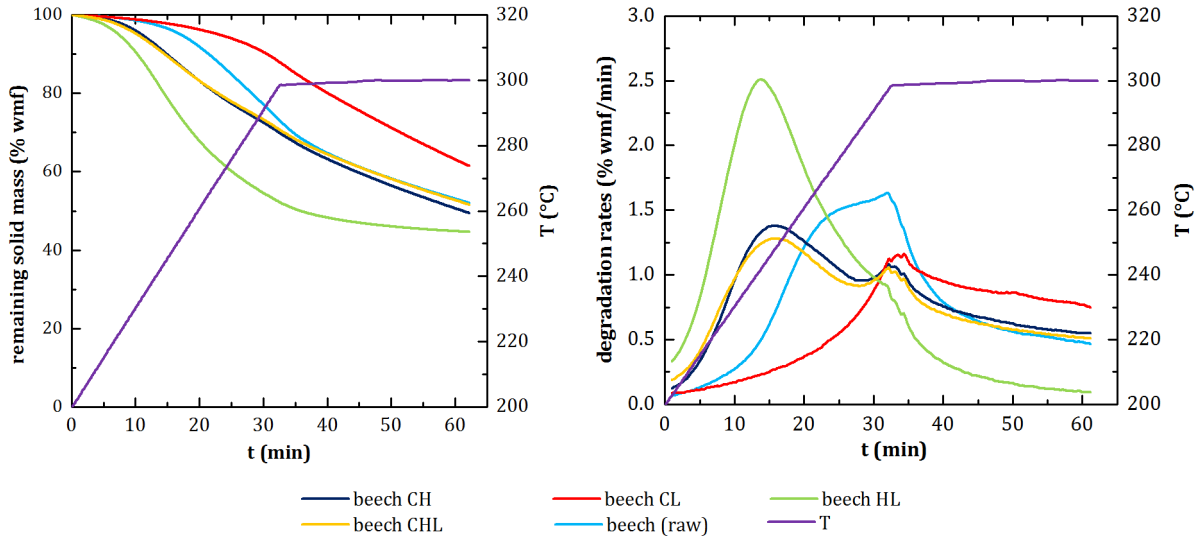


Figure IV.57. Remaining solid mass (left) and degradation rates (right) versus time and temperature obtained in torrefaction for beech (raw), binary and ternary mixtures in TGA-GC/MS

The degradation of the binary fractions in the non-isothermal torrefaction was shown to be different from that of the ternary mixture, which was logically closely coincident with that of the raw biomass (Figure IV.57). This behavior may suggest that, in the case of beech, all biomass macromolecular components influence biomass transformation through torrefaction. The fastest and more accentuated degradation profile was found for the HL binary mixture in the non-isothermal step, while the slowest degradation corresponded to the CL mixture. This observation is in accord with the temperature intervals proposed in the literature for the degradation of the biomass macromolecular components. According to this, hemicelluloses are mostly degraded in the typical torrefaction temperature range (200 to 300°C), while lignin only starts to be progressively degraded under these conditions and cellulose is only little degraded from temperatures close to 300°C (see section II.3.2).

In the isothermal step, the CH binary mixture exhibits an equivalent behavior to that of raw biomass and of ternary mixture (Figure IV.57). This observation is in accord with the fact that the degradation of cellulose mostly happens at temperatures close and up to 300°C. The shape of the degradation profile of the CL binary mixture is close to that of the previous fractions, which

supports this hypothesis. Oppositely, the profile of HL fraction suffers a deceleration from temperatures below 300°C, which continues in the isothermal step and tends to stabilize at lower degradation rates, close to zero. Even if the composition of the binary mixture is equivalent for the two fractions involved, the behavior of the HL mixture is closer to that of the «hemicelluloses 1» fraction. This observation suggests a low influence of lignin in the degradation patterns at these temperatures, which can be also deduced from the kinetic profile of the CL mixture. However, this affirmation needs to be carefully taken into account, as the selected operating conditions to achieve the isothermal step, even if the chemical regime is ensured, could have influenced biomass structure during its transformation. At the same time, the differences in the nature of the extracted fractions that are physically mixed inevitably results in lignin loses, that is, in a diminution of the lignin content in binary and ternary mixtures.

The CH mixture can be also compared to the corresponding «DMSO residue» fraction from beech. Both the mixture and the fraction are composed by cellulose and hemicelluloses, but the proportions and the nature of the macromolecular components are different. However, the comparison of these two fractions can allow to estimate the influence of the nature, the proportions and the interactions between cellulose and hemicelluloses in torrefaction. In the case of the CH mixture, hemicelluloses correspond to the «hemicelluloses 1» fraction in the proportion that hemicelluloses are in the raw biomass. The «DMSO residue» includes the «hemicelluloses 2» fraction, with a different sugar composition than that of the «hemicelluloses 1», and which is chemically bonded to the «cellulose II» fraction. Furthermore, cellulose in CH mixture is type II, while «DMSO residue» cellulose is type I, as in native biomass. By comparing the CH mixture and the «DMSO residue» for beech, is it remarkable that in the first case the profile is closer to that of hemicelluloses degradation, due to the higher proportion of this macromolecular component in the mixture. Oppositely, in the case of the beech «DMSO residue», the shape of the degradation is closer to that of the «cellulose II» fraction.

To sum up, it has been confirmed that hemicelluloses are the macromolecular component principally influencing biomass solid degradation through torrefaction. Lignin is supposed to have only a minor influence in the degradation, while cellulose starts to impact biomass transformation from high torrefaction temperatures. These results did not suggest that there would be interactions in solid phase between macromolecular components represented by the extracted fractions, neither in binary nor in ternary mixtures. There is not a clear accord in the literature about the interactions in solid phase determined by the co-torrefaction of cellulose, hemicelluloses and lignin. On the one hand, Chen and Kuo affirmed that no interaction existed in this case for a ternary mixture (1:1:1 ratio), so that biomass can be considered as an additive sum of the behavior of its macromolecular constituents [121]. However, Nocquet's experiments showed interactions between cellulose and lignin with hemicelluloses in torrefaction at 280 to

300°C [18], for macromolecular components mixed in the proportions of raw biomass, which differs from the conclusions of the present study. Both experiments were carried out with commercial microcrystalline cellulose and hemicellulose sugars, while in the present study this approach was intended to be improved through extracted macromolecular components.

2.4.2.2. Volatile species release

The volatile species detected in the torrefaction of the binary mixtures are listed in Table IV.1. They were detailed for each binary mixture, as their different composition strongly influences the volatile species released in torrefaction.

Table IV.1. Quantified volatile species in the torrefaction of the binary mixtures containing «cellulose», «hemicelluloses 1» and «lignin»

BINARY MIXTURE	formic acid	acetic acid	propionic acid	furan	3-furaldehyde	furfural	2-furanmethanol	acetylfuran	2(5H)-furanone	phenol	phenol, 2-methoxy (guaiacol)	2-methoxy-4-vinylphenol	eugenol	cathecol	phenol, 2,6-dimethoxy- (syringol)	isoeugenol (cis+trans)	vanillin	2,3-pentanedione	hydroxyacetone	2-propanone,1-(acetyloxy)-	4-cyclopentene-1,3-dione	methanol	formaldehyde
CH	X	X	Tr	Tr	Tr	X	Tr	Tr	X	Tr	nd	nd	nd	nd	nd	nd	nd	Tr	X	X	X	X	X
CL	nd	X	nd	Tr	Tr	X	Tr	Tr	X	nd	Tr	Tr	nd	nd	Tr	X	Tr	nd	X	Tr	Tr	X	X
HL	X	X	Tr	Tr	Tr	X	Tr	Tr	X	Tr	X	X	Tr	nd	X	X	X	Tr	X	X	X	X	X

** Traces (≤ 0.0001g/g for all the quantified points of the profile of formation for a sample)*

In total, 0.1, 1.6 and 2.5 mg of volatile species were quantified for the CL, CH and HL binary mixtures, respectively, which corresponds to a transformed solid mass of 118, 299, 476 mg of mixture in each case. The disparities in the mass loss, which were discussed in the previous section, are in accord with the differences in the total quantified mass of volatile species. Mixtures containing cellulose (CH, CL) lead to a minor production of volatile species in the torrefaction temperature range, particularly when the mixture also includes lignin (CL). On the contrary, mixtures including hemicelluloses produce a higher amount of volatile species.

By classifying the total volatile species production per chemical families (Figure IV.58), strong similarities can be found for beech CH, HL and CHL mixtures. The proportions of volatile species of the same chemical nature in these cases is close to that of hemicelluloses, particularly for the high acid production, corresponding to acetic acid, and the important amounts of furans and methanol, together with minor amounts of ketones. The HL mixture includes very small

proportions of phenols and formaldehyde, derived from a limited transformation of lignin in the torrefaction temperature range. In the case of the CL mixture, the proportions of these two chemical families are higher, presumably because of the limited transformation of cellulose compared to that of hemicelluloses. It is noteworthy that the combination of the CL and either the CH or HL binary mixtures might lead to a composition of the total volatile species production closer to that of the raw material, rather than the obtained composition for the ternary mixture. This result might suggest that interactions between macromolecular compounds in biomass, which cannot be reproduced by the physical mixtures, might lead to a non-negligible volatile production, particularly of small chemical compounds, which impacts the proportions of the total volatile species released by biomass in torrefaction.

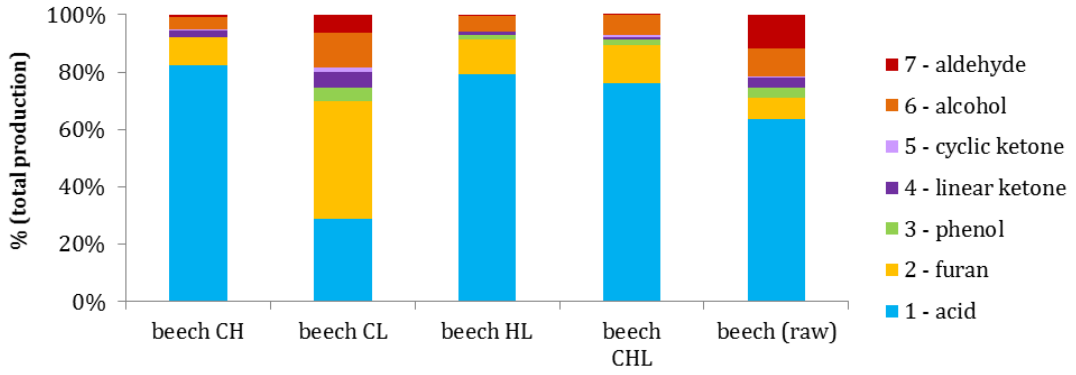


Figure IV.58. Distribution of the total production of volatile species per chemical family obtained during torrefaction of beech (raw), binary (CH/CL/HL) and ternary (CHL) mixtures in TGA-GC/MS

Secondly, the production profiles of the quantified volatile species in the torrefaction of the binary mixtures were studied (Figures IV.59 to IV.63).

Acetic acid was the major detected volatile species. Its production by the binary mixtures remains in the same order of magnitude for CH and HL binary mixtures, but it is doubled compared to the production by the ternary mixtures. The production profiles are similar in both cases, showing a maximum in the acetic acid production at intermediate torrefaction temperatures, as it was the case for the CHL mixture (Figure IV.59), but at lower temperatures than for the individual extracted fractions and the raw biomass. This difference might be due to the isolation of the macromolecular components in the physical mixtures, which makes them more accessible and more easily degradable. On the other hand, the production is much lower in the case of the CL mixture. This result certifies that the major production of acetic acid is derived from hemicelluloses, while celluloses and lignin only marginally contribute to this production.

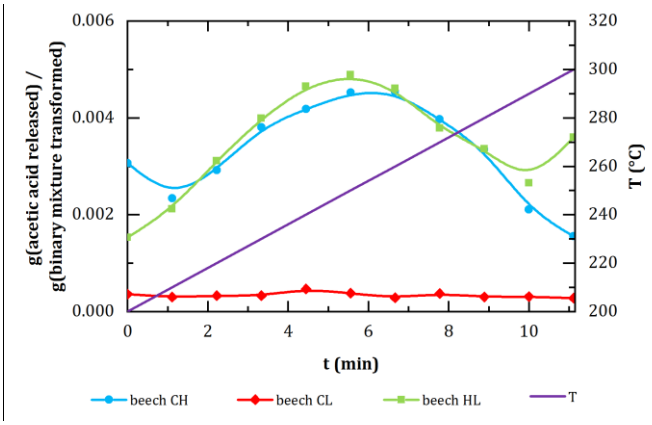


Figure IV.59. Production profile of acetic acid versus temperature and time obtained in torrefaction of binary mixtures in TGA-GC/MS

Formic and propionic acid were also detected in low amounts, slightly higher than for the ternary mixtures, and only at certain torrefaction temperatures, particularly in the case of formic acid. Consequently, they are not discussed in this section.

The production of furans is close for all binary mixtures, being in most of the cases slightly higher for the HL mixture, followed by the production of the CH and the CL mixtures, which produce lower amounts of volatile compounds. The production profiles exhibit equivalent tendencies to those of the ternary mixtures, the chemical compounds in this family presenting different release patterns in function of the torrefaction temperature (Figure IV.60). In the case of furfural, the production profiles are little dependent on the torrefaction temperature, except for the HL mixture. In this case, a minimum at low torrefaction temperatures appears, as it was found for the wheat straw ternary mixture, followed by a severe decreasing production with the increasing torrefaction temperature. This might correspond to a higher release of furfural at the beginning of hemicelluloses degradation, as lignin does not affect this behavior in a noticeable extent. Other furans show a production enhanced by the torrefaction temperature, with equivalent amounts of production for the three binary mixtures.

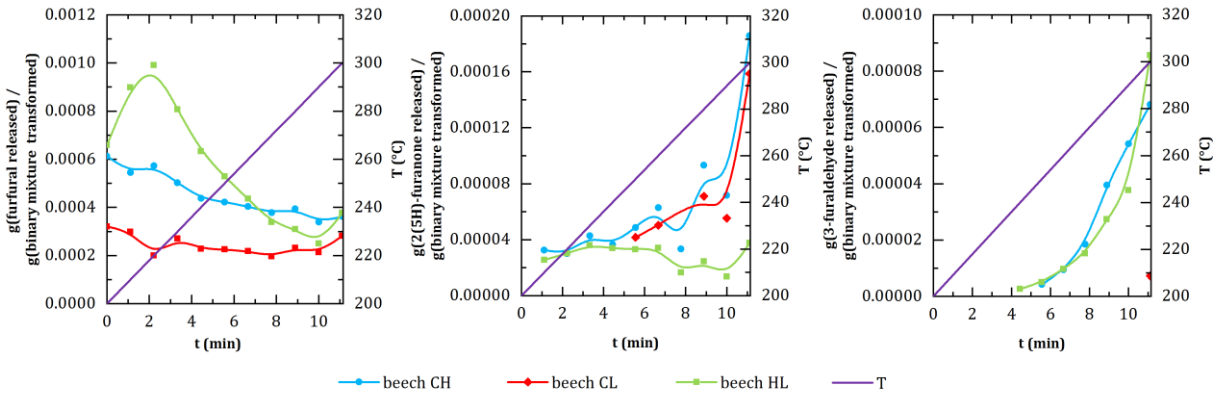


Figure IV.60. Production profiles of furfural (left), 2(5H)-furanone (center) and 3-furaldehyde (right) versus temperature and time obtained in torrefaction of binary mixtures in TGA-GC/MS

Phenolic compounds are detected in low amounts and this only for the lignin-based mixtures, with the exception of phenol, which was found in equivalent amounts for the HL and CH fractions (Figure IV.61). This observation might indicate the production of phenol by hemicelluloses, which is accord with previous observations on the hemicellulose fractions. This production might presumably be due to impurities from the extraction procedure, which might correspond to rests of the cross-links between hemicelluloses and lignin (LCC, lignin-carbohydrate complexes) [72]. Another production pathway could be derived from hemicellulose sugar rings rearranged in aromatic rings, but this mechanism mostly occurs at pyrolysis temperatures. In terms of production profiles, phenolic compounds generally exhibit an enhanced production with torrefaction temperature, as it was found for « lignin » fractions and raw biomasses.

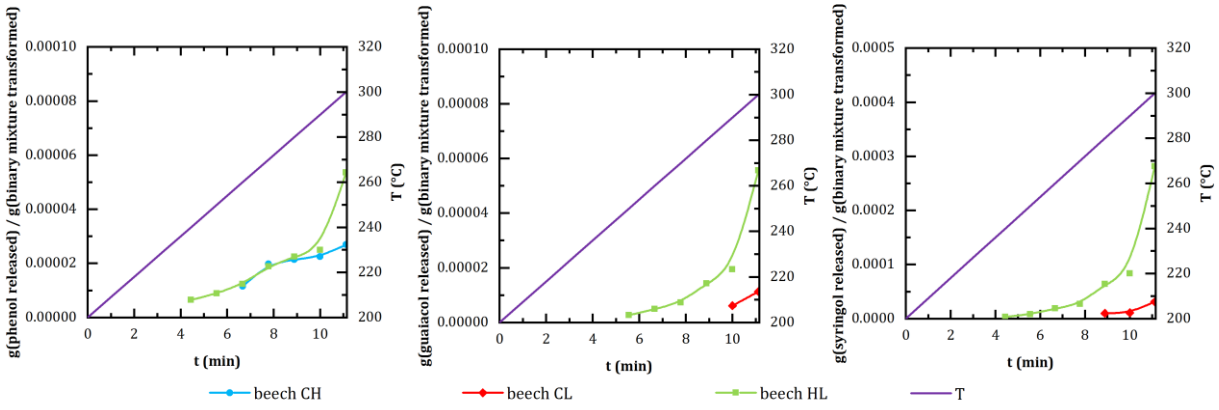


Figure IV.61. Production profiles of phenol (left), guaiacol (center) and syringol (right) versus temperature and time obtained in torrefaction of binary mixtures in TGA-GC/MS

The production of formaldehyde and methanol by the binary mixtures remains in the same order of magnitude than that of the ternary fractions. In the case of formaldehyde, this production is higher for the cellulose-lignin-based mixture, CL, with a production slowed down by the increase in torrefaction temperature. On the contrary, the production of this compound by the cellulose-hemicellulose-based fraction, CH, is slowly increasing with temperature (Figure IV.62). This different behavior might indicate the two different mechanisms of release of formaldeyde, principally by lignin from the beginning of the degradation, and with a boosted influence of the production by cellulose with increasing temperature. In the case of methanol, the results indicate that this compound is released by the three biomass macromolecular components by pathways that seem little dependent on torrefaction temperature.

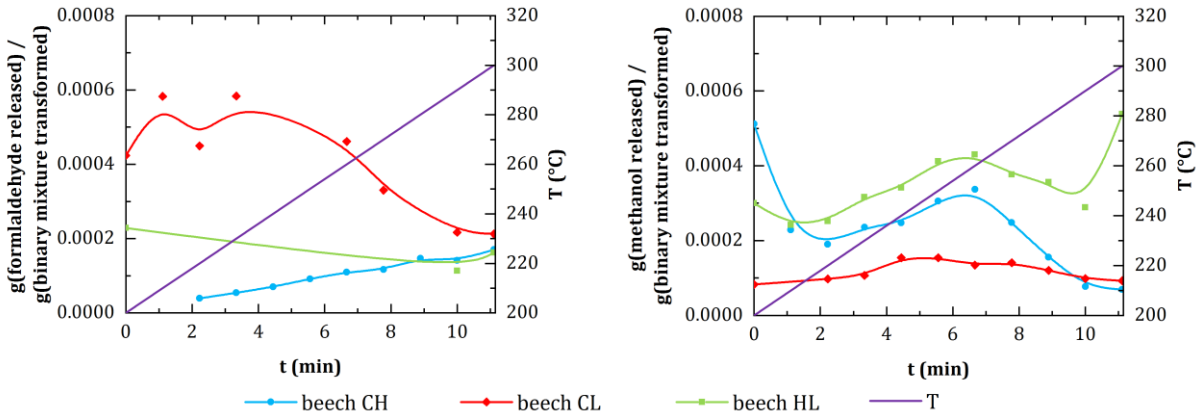


Figure IV.62. Production profiles of formaldehyde (left) and methanol (right) versus temperature and time obtained in torrefaction of binary mixtures in TGA-GC/MS

Significant amounts of linear and cyclic ketones were quantified for the hemicellulose-based mixtures (HL and CH), as well as of hydroxyacetone for the three binary mixtures. This behavior is in agreement with the origin of ketones in biomass degradation through torrefaction, which is principally from hemicelluloses and, in a minor extent, from cellulose (Table II.3). As observed for the ternary mixtures, the shape of the production profiles are close to those from the raw materials, with maxima of production manifested before 300°C and/or occurring at lower temperatures, as it is the case of 2-propanone,1-(acetyloxy)- (Figure IV.63).

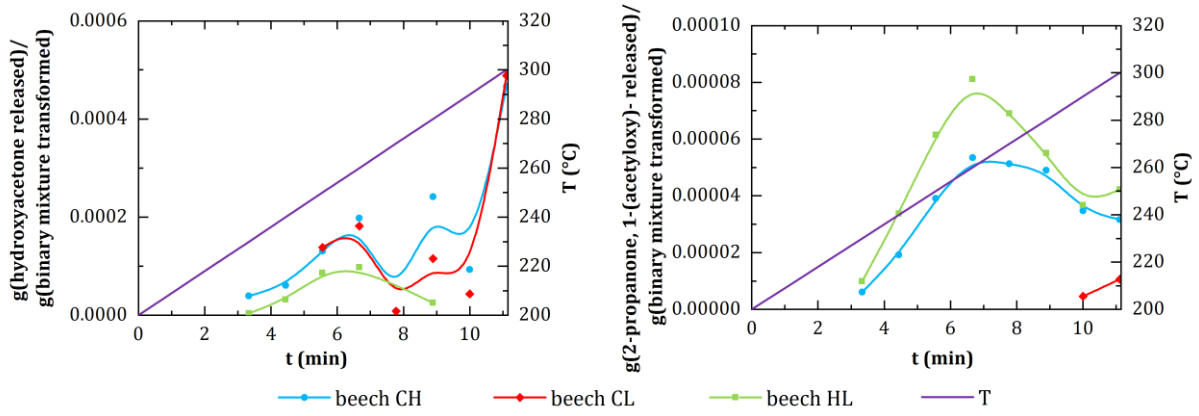


Figure IV.63. Production profiles of hydroxyacetone (left) and 2-propanone,1-(acetyloxy)- (right) versus temperature and time obtained in torrefaction of binary mixtures in TGA-GC/MS

To sum up, the study of the production profiles of the volatile species released by the binary mixtures of «cellulose», «hemicelluloses 1» and «lignin» fractions contributed to the elucidation of the pathways of formation of the volatile species released in biomass torrefaction, especially when two parallel mechanisms are susceptible to be involved in this formation. In general, the maximum in the production of a given volatile species is detected at lower temperatures than for the raw materials, due to the accessibility and the lack of intra-molecular bonding of the macromolecular components in the mixtures. However, it remains challenging to determine

interactions in solid phase of the macromolecular components composing the fractions through the binary mixtures, even if the degree of freedom of the variability is reduced compared to the ternary mixtures. This is mainly due to the impossibility to reproduce these interactions as they are in the raw material once the macromolecular components were physically separated from the biomass matrix. Undeniably, these interactions are responsible of an important part of the release of the volatile species in biomass torrefaction.

3. Synthesis of the results

In this section, the experimental results obtained are synthetized and compared with previous works in biomass torrefaction in the literature. The objective of this section is to establish the principles on which the torrefaction model will be constructed.

3.1. Solid kinetics

A panel of 14 biomasses, including deciduous and coniferous wood, agricultural by-products and herbaceous crops, was proposed to represent biomass diversity. The biomasses in the database were deeply characterized in terms of macromolecular and sugar composition, as well as in terms of solid kinetics and profiles of formation of 23 volatile species released in torrefaction. The number of biomasses studied is higher than in other previous torrefaction studies.

The suitability of the proposed biomass database for characterizing biomass behavior in torrefaction was checked with six complementary biomasses (Annex I). Their particularity is that they are typically involved in forest fires in the South of Europe. This study allowed to make correspondences between these biomasses and biomasses in the database and to check that their behavior in torrefaction can be predicted by the corresponding representative biomass family in the database.

Secondly, five biomasses from the database were selected in order to deeply characterize their behavior in torrefaction through their extracted macromolecular components, namely cellulose, hemicelluloses and lignin. An extraction procedure was proposed and the extracted fractions were reconstructed in function of the fractions obtained in each extraction step. As a result, the total hemicelluloses fraction was reconstructed from the two hemicellulose extracted fractions («hemicelluloses 1» and «hemicelluloses 2»). On the other hand, cellulose was extracted in a single fraction but a careful analysis was required as the extraction procedure changed the polymorphic structure of cellulose chains in the fraction. Indeed, «cellulose I», reconstructed from a complementary fraction representing native cellulose structure in biomass, and «cellulose II» fractions were compared in torrefaction.

The «cellulose II» fraction exhibited a similar behavior for the 5 fractions extracted from 5 different biomasses. This could be derived from the fact that cellulose is only slightly degraded

under 300°C. As a result, a single extracted cellulose fraction could be considered to represent cellulose behavior in torrefaction. On the contrary, the behavior of commercial microcrystalline cellulose (Avicel) was shown as very different from that of the average of the «cellulose II» fraction. The deep characterization of the «cellulose II» fraction compared to the commercial microcrystalline cellulose properties showed that the extracted fractions present a degree of polymerization (DP) and an average molecular mass higher and consequently closer to those of native cellulose in biomass, compared to the commercial cellulose. These differences can be interpreted as that the proposed extraction procedure allows to obtain a more representative cellulose fraction. An impact in the starting temperature for cellulose degradation in torrefaction was observed for pure cellulose when DP changes at around a factor of 20 or higher (Annex VIII). This observation might be valid when comparing extracted cellulose and native cellulose in biomass. The starting degradation temperature of the second might be higher than that of the extracted fractions, resulting in a shift of the observed degradation profile of cellulose to slight higher temperatures. Oppositely, the extracted «cellulose II» fractions present a different crystalline structure form that of the native cellulose in biomass, as checked with the «DMSO residue» fractions. The impact of this difference in the structure arrangement of the cellulose chains in the degradation of cellulose in torrefaction cannot be directly determined by these results. However, the close behavior of the «DMSO residue» to that of the «cellulose II» fractions may suggest a minor impact at the torrefaction temperatures. This hypothesis will be studied by estimating the behavior of «cellulose I» from the «DMSO residue» fractions, through a sugar mass balance on the composition of the extracted fractions (section V.2.3).

Hemicelluloses are the most degraded biomass macromolecular component in the temperature range of torrefaction. This behavior was reflected in the high degradation rates and final remaining solid mass values obtained for all hemicelluloses fractions. The behavior of each hemicellulose fraction was shown to be conditioned by its sugar composition, especially if mannan is present in an important percentage compared to xylan, as the degradation of the first one happens at slightly higher temperatures than that of the latter. This suggests that a single hemicelluloses fraction is not sufficient to reproduce hemicelluloses behavior in torrefaction. Furthermore, both extracted fractions of hemicelluloses should be considered for each biomass to take into account the total sugar composition of the real hemicellulose in biomass. Consequently, the solid kinetics of the total «hemicelluloses» fraction will be reconstructed by the weighted behaviors of «hemicelluloses 1» and «hemicelluloses 2» for each biomass (section V.2.3).

Lignin degradation occurs from the beginning of torrefaction and is only partial in the torrefaction temperature range. The experimental results showed that lignin degradation is very dependent on its composition in H (phenyl-), G (guaiacyl-) and S (syringyl-) units, the most important difference in their behavior being for pine lignin (mostly guaiacyl lignin type).

Therefore, three extracted lignin fractions would be enough to represent the lignin degradation pattern in biomass torrefaction, namely pine lignin (principally G units), a deciduous wood lignin (G and S units) and an agricultural lignin (G, S, H units).

Regarding the elemental composition of the solid through torrefaction, expressed by the major composition in carbon, oxygen and hydrogen, the results show a notable change for the raw biomasses and the extracted hemicelluloses. This evolution is mainly reflected by the increase of the carbon content and the decrease of the oxygen content, while the hydrogen content slightly changes and remains low in all cases. Lignin and cellulose present only moderate changes in their composition, due to their limited degradation at torrefaction temperatures. These results are in agreement with previous works and allow to define the evolution of the macromolecular formula of the raw materials, as well as of their extracted macromolecular components, in torrefaction.

The behavior of the ternary mixtures of «cellulose II», «hemicelluloses 1» and «lignin» was compared in torrefaction to that of the corresponding raw biomasses. Important differences were revealed, either in the non-isothermal or in the isothermal torrefaction steps, in function of the biomass type. These differences might correspond to interactions between macromolecular components, which were shown to play a crucial role in biomass degradation through torrefaction, influence which is subject of controversy in the literature. The physical mixture of the extracted fractions in the proportions as they are present in biomass was shown not to allow to reproduce these interactions.

The study of the binary mixtures of «cellulose II», «hemicelluloses 1» and «lignin» confirms that hemicellulose is the most degraded macromolecular component during torrefaction. Lignin and cellulose are only partially degraded in the torrefaction temperature range, which might indicate that a good knowledge of hemicellulose degradation, influenced by its sugar composition, would be a good approach for predicting the final solid mass and the degradation profile of biomass in torrefaction. However, as in the previous case, the binary mixtures did not to allow to reproduce interactions between macromolecular components in biomass.

3.2. Volatile species release

Representing the production profiles of the volatile species released in torrefaction in function of the temperature, in chemical regime conditions, contributes to a better understanding of the mechanisms involved in the decomposition of cellulose, hemicelluloses and lignin. To synthetize the obtained results, the quantified volatile species in the torrefaction of the raw biomasses and the extracted fractions were indicated in Table IV.2. These results were qualitatively compared to those in the literature about biomass torrefaction. A higher amount of volatile species was detected and quantified for the raw biomasses. This number of species was reduced for the

extracted fractions, in function of their nature.

Some volatile species were released at lower temperatures than those indicated in the literature. This could be derived from the fact that experiments on biomass macromolecular components in the literature are typically carried out with commercial compounds. Furthermore, in the case of hemicelluloses, they are usually schematized by the behavior of commercial xylan, while it has been shown that other hemicellulose sugars, particularly mannose, play a non-negligible role in hemicelluloses degradation. The extracted procedure designed to obtain the fractions utilized in this work intends to produce macromolecular components that would be closer to those in the raw biomass compared to the equivalent commercial ones.

However, the limitations of the experimental set-up generally lead to a low quantification of the volatile species released. The representativeness of the results obtained was then ensured by deeply contrasting these results with previous studies concerning the degradation mechanisms proposed for biomass torrefaction. In general, a very good agreement was found between these results and those reported in the literature, with the exception of minor compounds not included in other studies.

The production of volatile species detected for the «cellulose II» fractions was higher than that of the commercial microcrystalline cellulose Avicel in the non-isothermal torrefaction step, due to the higher degradation of these fractions. Furthermore, the release of the volatile species started at intermediate to high torrefaction temperatures, below 300°C, while in the literature cellulose is reported to be degraded at higher temperatures. This could be derived from the fact that extracted celluloses present a higher degree of polymerization and molecular mass compared to those from the commercial microcrystalline cellulose and rather comparable to those of the native cellulose in biomass. The release of the volatile species from the «cellulose II» fractions was compared to those from the «DMSO residue» fractions, which are impacted by the presence of hemicelluloses and by the crystalline structure type for cellulose. The results might suggest that the crystalline structure type II for the «cellulose II» fractions, more stable than the crystalline structure type I in native cellulose and in the cellulose contained in the «DMSO residue» might not impact the production profiles of volatile species. However, this hypothesis could not been proved with the current results.

Hemicelluloses lead to the highest variety and production of volatile species in torrefaction, which is related to their high degradation in the torrefaction temperature range, more important than for cellulose and lignin. Volatile species from hemicelluloses are released from low torrefaction temperatures, which is in agreement with the early degradation of this macromolecular component in torrefaction. Furthermore, the volatile species released are strongly dependent on the sugar composition of hemicelluloses, as well as on the presence of acetyl groups, which lead to a high production of acetic acid. This chemical compound was

largely the major volatile species produced, followed by furfural and methanol. Formaldehyde was also detected in significant amounts for some biomasses, which suggests its production by hemicelluloses, and was not reported before in the literature. These results, together with the release of small molecules, such as linear ketones, can help to explain the degradation mechanisms involved in hemicelluloses conversion through torrefaction.

Lignin was only slightly degraded in the torrefaction temperature range, which leads to a low production of volatile species. The major detected compounds were formaldehyde and phenols, due to the phenolic nature of this fraction. Other minor compounds released are methanol, acetic acid and furans. The production profiles of volatile species obtained are in accord with previous studies in the literature and keep a certain parallelism with analytical fractionated fast Py-GC/MS studies on biomass. In the case of phenols, higher production temperatures were found for non-substituted phenols, such as guaiacol and syringol, compared to isoeugenol and vanillin, for example, which is in agreement with results in Py-GC/MS. Both studies contribute to explain the mechanisms involved in lignin thermochemical conversion and give hints on the strength of chemical bonds in lignin structure. A deeper characterization of lignin composition in phenyl- (H), guaiacyl- (G) and syringyl- (S) units will be very useful to correlate with the results obtained and the mechanisms proposed in the literature.

A lower production of volatile species was found for the ternary mixtures of «cellulose II», «hemicelluloses 1» and «lignin» extracted fractions, compared to that of the equivalent chemical compounds from the raw biomasses. This result indicates that the intra-molecular bonding between the macromolecular components in biomass, which are broken to separate the extracted fractions, leads to a non-negligible release of volatile species, particularly in the case of small volatile species (acetic acid, methanol). At the same time, important losses of lignin were registered in the preparation of the mixtures, which impacted the release of phenolic compounds and formaldehyde. Finally, interactions in gas phase of the released volatile species cannot be highlighted by this method, due to the difference in the order of magnitude of the production profiles between the ternary mixtures and the corresponding raw biomasses.

The torrefaction of binary mixtures of «cellulose II», «hemicelluloses 1» and «lignin» extracted fractions contributes to elucidate the mechanisms of release of the volatile species, especially when several pathways of formation occur in parallel (i.e. acetic acid, formaldehyde). Nevertheless, similar experimental problems as those reported for the ternary mixtures were found in lignin-based mixtures. As a result, interactions, neither in solid phase for the macromolecular components nor in gas phase between the volatile species released, could be highlighted by this method.

As a consequence of these results, it seems challenging at this state of the study to model the release of volatile species in biomass torrefaction through the extracted macromolecular

components. This is principally due to the lack of information about the volatile species release from the intra-molecular bonds between cellulose, hemicelluloses and lignin in biomass. Furthermore, biomass diversity strongly impacts the formation of volatile species though torrefaction, even for biomasses biologically close. This variability could be assessed for the solid transformation through torrefaction but still remains incomplete for the volatile species release. The information needed for the modelling of the volatile species release through the production profiles needs to be completed by a deep study on the behavior of interactions between macromolecular components. As a result, in the next section, this study will focus on:

- applying Principal Component Analysis (PCA) as an analysis tool able to assess biomass diversity in terms of characterization and behavior in torrefaction;
- modelling solid transformation through torrefaction by the approach of the extracted macromolecular components.

In all cases, the proposed database of 14 biomasses constitutes a strong base of comparison to assess the behavior in torrefaction of a new biomass. This is proposed to be carried out by comparing the composition of the new biomass to that of the biomasses in the database. The behavior of the closest biomass in the database might be a good starting point in the prediction of the behavior of the new biomass in torrefaction, both in terms of solid kinetics and in the production profiles of the volatile species released.

Table IV.2. Quantified volatile species in the torrefaction of extracted cellulose, hemicelluloses and lignin fractions, and of the 14 raw biomasses

	Extracted fractions					Raw biomass	Literature		
	«cellulose II»	«DMSO r»	«hemic 1»	«hemic 2»	«lignin»		cellulose	hemic	lignin
Acids							**X**	**X**	
acetic acid	X	X	X	X	X	X		X	
formic acid		X	X	X		X		X	
propionic acid		*	*	*	X	X			
Furans							**X**	**X**	
furan	*	x	X	*	*	X			
3-furaldehyde		*	X	X	*	*			
furfural	X	X	X	X	X	X	X	X	
2-furanmethanol		X	*	*	X	X	X		
acetylfuran	*	*	*		*	*			
2(5H)-furanone	X	X	X	X	*				
Phenols									**X**
phenol	*	*	*	*	X	X			
phenol, 2-methoxy (guaiacol)	*	*	*	*	X	X			
2-methoxy-4-vinylphenol					X	X			
eugenol					X	X			X
cathecol					X	X			
phenol, 2,6-dimethoxy-(syringol)			*		X	X			X
isoeugenol (cis+trans)			*		X	X			X
vanillin			*		X	X			
Linear ketones							**X**	**X**	
2,3-pentanedione	*	*	X	*	*	X			
hydroxyacetone	X	x	X	X	*	X	X	X	
2-propanone,1-(acetyloxy)-	X	*	X	*	*	X			
Cyclic ketones								**X**	
4-cyclopentene-1,3-dione	X	*	X	*	*	X		X	
Alcohols									
methanol	X	X	X	X	X	X		X	
Aldehydes									
formaldehyde		X	X	X	X	X			X

** Traces (≤ 0.0001g/g) for at all the quantified points of the production profile for a sample*

-V-

MODELLING

V. MODELLING

In this section, biomass characterization (in III.1.1) as well as its behavior in torrefaction (in IV.1) are quantitatively analyzed through Principal Component Analysis (PCA). The objective of this analysis is to identify which of biomass characteristics are influencing torrefaction results.

Secondly, the torrefaction model is built based on the experimental data obtained from the extracted macromolecular components (see IV.2) and based on the key parameters determined through the PCA.

1. Principal Component Analysis

Principal component analysis was the selected tool to study the impact of biomass diversity in terms of macromolecular and elemental characterization, as well as of biomass family, on biomass performances in torrefaction.

PCA was carried out with XLStats for Microsoft® Office® 2017 with different datasets and at different levels, including macromolecular and elemental characterization of biomasses, solid transformation in torrefaction and volatile species release in torrefaction, in these latter cases in function of the operating conditions.

1.1. Key parameters in biomass characterization

The macromolecular and the elemental characterization of the 14 biomasses, as listed on Table V.1 (III.1.1 section), were assessed by a PCA. The objective is to determine, from these properties, the key parameters required for characterizing biomass diversity. At the same time, properties of biomasses from the same biological family can be compared.

1.1.1. PCA on macromolecular and elemental composition

The selection of 4 groups of variables was necessary to achieve an acceptable representation of the high data variability (85.7%). The factor loadings of the variables obtained from the PCA were analyzed (Table V.1). Values in bold indicate components in each group (F1 to F4). The highest factor loading per group was highlighted.

PCA results indicate that the composition in cellulose, hemicelluloses, extractives and ash content (in the same group as lignin) are independent. If we select three principal components (F1, F2, F3), the results show that cellulose, hemicellulose and lignin content are necessary to describe biomass, as this choice represents a high percentage of the data variability (72.5 %). On the contrary, the parameters defining the elemental composition (C, H, O, N) are correlated, which indicates that these components cannot independently describe biomass composition. As a result, the elemental composition would not be sufficient to represent biomass heterogeneity, as it has been proposed in some models in the literature [80]. However, the high variability in

the data suggests separating elemental and macromolecular composition in further PCA evaluations, as their source of variability is different.

Concerning hemicelluloses composition in sugars, xylose seems correlated with cellulose. Mannose and galactose are anticorrelated to cellulose and correlated to lignin. Arabinose, which is independent from the three other sugars, is correlated with hemicelluloses content. This could be explained by the fact that mannose and galactose are especially present in softwood, which is usually characterized by a high lignin content. Xylose, related to celluloses, is the main sugar in hardwood hemicelluloses, cellulose and hemicellulose contents in this biomass type being usually higher than the lignin content. As a result, hemicelluloses sugar composition might be sufficiently described through its main sugar composition, typically in xylose or mannose.

Table V.1. Factor loadings of the PCA on macromolecular and elemental composition of 14 biomasses

	F1	F2	F3	F4
Variability (%)	34.3	21.8	16.3	13.2
Cellulose	**-0,853**	0,379	-0,062	0,109
Hemicelluloses	-0,276	0,397	**0,661**	-0,369
Lignin	**0,766**	-0,432	-0,292	-0,347
Extractives	0,513	-0,054	0,372	**0,653**
Ash	-0,263	**-0,788**	0,270	0,291
Xylose	**-0,770**	-0,198	0,304	-0,503
Mannose	**0,632**	0,545	-0,175	0,234
Galactose	**0,653**	0,310	0,554	0,162
Arabinose	0,182	-0,008	**0,911**	0,012
Carbon (C)	**0,784**	0,475	-0,166	-0,194
Hydrogen (H)	-0,064	**0,789**	-0,044	-0,405
Oxygen (O)	**-0,645**	0,169	-0,304	0,474
Nitrogen (N)	0,504	**-0,646**	-0,037	-0,424

This PCA did not allow the distinction of biomass groups in function of the macromolecular composition, which is in agreement with previous comments on biomass characterization (III.1.1 section). The main reasons are the heterogeneity of the resource and the low population studied (14 biomasses). In order to identify biomasses with a similar behavior, the Agglomerative Hierarchical Clustering (AHC) method was applied to the factor scores of the observations of the previous PCA (Figure V.1).

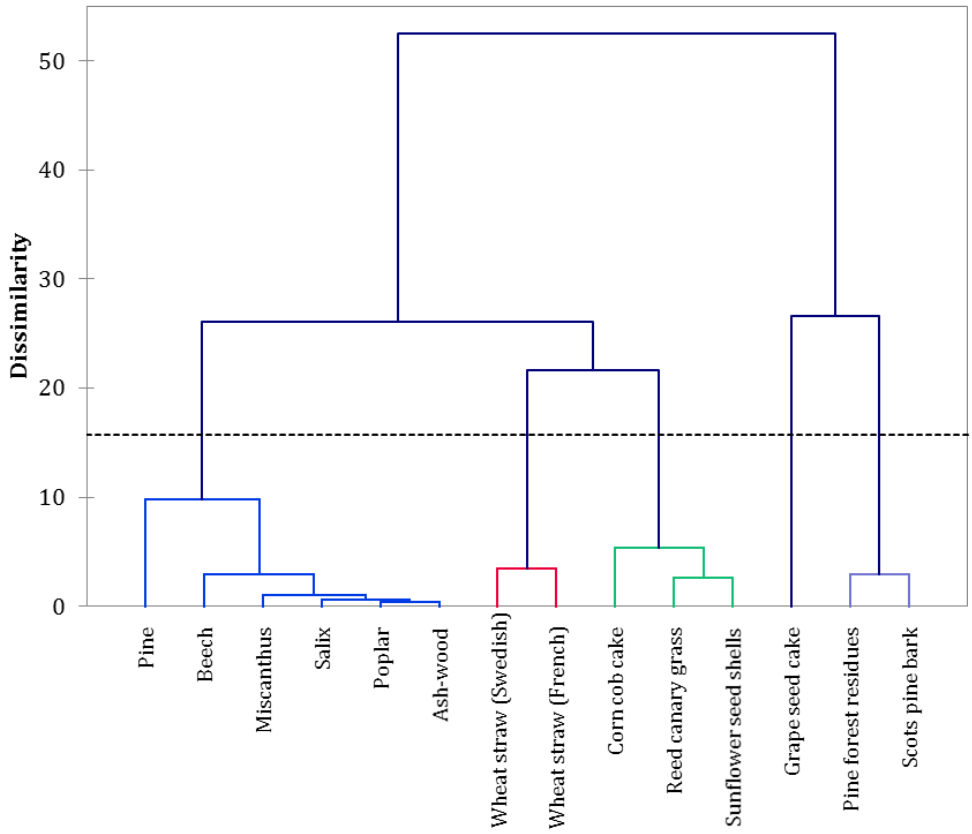


Figure V.1. AHC dendrogram of the factor scores of the observations from PCA (Table V.1).

Regarding the observed data, a hierarchy of 4 clusters represents the variability of the biomasses in terms of macromolecular composition. Miscanthus, pine, beech, willow (salix), poplar and ash-wood are grouped, although they belong to different families of biomasses (herbaceous crops, coniferous wood and deciduous wood). Woody biomasses are closer in cellulose, hemicelluloses and lignin composition. The main difference between deciduous and coniferous wood is the lignin content. Pine forest residues and Scot pine bark were classified together, close to grape seed cake probably because of their high lignin content. Agricultural biomasses are grouped by pairs, being together both wheat straws on the one side and corn cob cake, reed canary grass and sunflower seed shells on the other side. Herbaceous biomasses (reed canary grass and miscanthus) are not grouped together, neither all agricultural biomasses, because of the heterogeneity of their characterization in both cases.

This overall analysis on the 14 biomasses from the database shows that the diversity in biomass composition can be described through its cellulose, hemicellulose and lignin content. Similarities were found between biomasses belonging to the same family, particularly in the case of wood. Herbaceous crops and agricultural by-products present a more heterogeneous characterization.

1.1.2. PCA on biomass elemental composition

A second PCA was carried out on the main elemental composition (C, H, O, N) of the 14 biomasses of the database. In this case, the macromolecular composition was considered as supplementary variables, i.e. as variables that are not used for PCA definition. The result of this analysis leads to reduce to 2 Principal Components considered, representing 80.4 % of the variability of the raw data (Figure V.2, variability represented indicated for each Principal Component, F1 and F2).

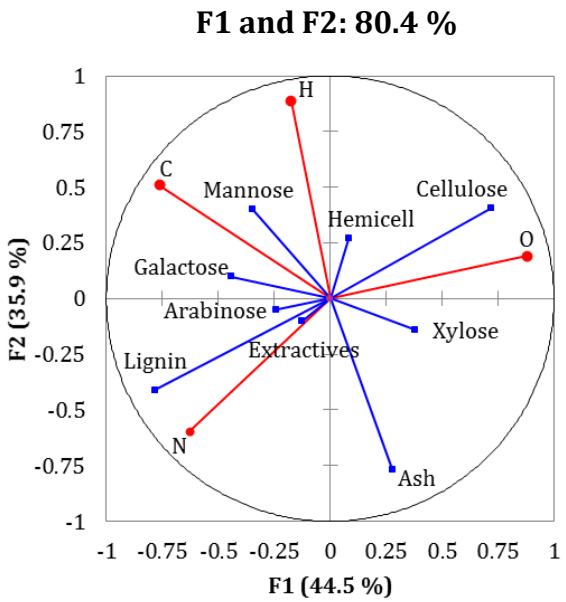


Figure V.2. Variables chart of the PCA on the elemental composition of 14 biomasses

This PCA shows a clear anticorrelation between the oxygen (O) and nitrogen (N) composition. At the same time, there is no correlation between oxygen and hydrogen (H) or carbon (C) composition. The high variability represented by 2 principal components suggests that these parameters are not independent, so not suitable for describing biomass diversity. This result is in agreement with observations about elemental composition (III.1.1).

Macromolecular composition was added as supplementary variable in the 2-dimension chart constructed through elemental composition data (Figure V.2). Elemental composition is close to the circle, so well-represented, while macromolecular composition is only well-represented in terms of cellulose, lignin and ash content. Extractives and hemicellulose content are not well-represented, but only one of them is independent regarding cellulose, hemicelluloses and lignin, adding a small part of the representation of data variability, as stated in section V.1.1.1 section. A correlation between cellulose and lignin can be confirmed, as well as the lack of correlation between cellulose, lignin and ash. However, this representation does not improve the representation of hemicelluloses and sugar composition.

In order to identify biomasses with a similar behavior, AHC methods were applied to the factor scores of the observations from the PCA results (Figure V.3).

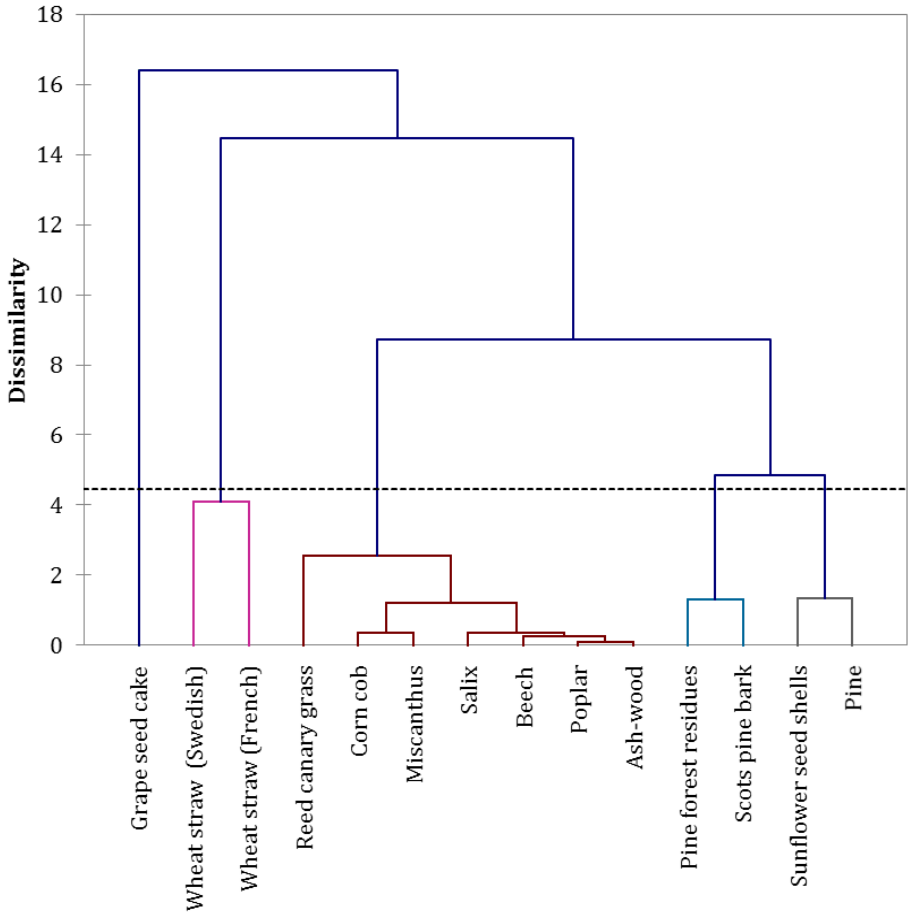


Figure V.3. AHC dendrogram of the factor scores of the observations from PCA (Figure V.2).

Regarding the observed data, a hierarchy of 4 clusters represents biomass variability in terms of main elemental composition. Grape seed cake is pointed out as a biomass with a particular characterization, not only in terms of macromolecular composition (Figure V.1), but also in terms of elemental composition (Figure V.3). The two wheat straws are close again. A third group would include coniferous wood (pine, pine forest residues and Scot pine bark) and sunflower seed shells. Finally, the last group includes 2 sub-groups: the deciduous wood group (salix (willow), beech, poplar and ash wood) and a mixed group of herbaceous crops (reed canary grass, miscanthus) and agricultural biomasses (corn cob). These results highlight similarities between coniferous and deciduous wood. They also suggest the intermediate position of herbaceous crops between deciduous wood and agricultural biomasses. The heterogeneity of the agricultural biomasses group appears again. In order to reduce biomass heterogeneity and avoid almost-duplicate data, a new analysis will be carried without grape seed cake and one of the wheat straws (Swedish).

As a result, PCA on elemental composition allows to conclude that this characterization is not the most suitable to represent biomass diversity, as similar values of the main parameters are found for all samples. However, a cluster of similar properties is again observed for deciduous and coniferous wood, which is not the case for agricultural biomasses.

1.1.3. PCA on macromolecular and elemental composition for 12 selected biomasses

A PCA analysis was carried out by considering only 12 biomasses out of 14, excluding grape seed cake and Swedish wheat straw from the data base. The macromolecular composition of the biomasses (cellulose, hemicelluloses, lignin, extractives and ash content) was selected as the main variables for the analysis, while the elemental composition (C, H, O, N) was relegated to supplementary variables (Figure V.4). The sugar composition of the hemicelluloses was not included.

Three principal components were selected, which improves the representation of the variability (94.0 %) compared to the PCA with all biomasses (V.1.1.1 section). The 3-dimensional representation was converted into 2-dimensions graphics by pairs of principal components, both for the variables charts (Figure V.4) and the observations charts (Figure V.5). The size of the points in the observations charts is proportional to the squared cosines of the observations (well-representativeness of the points). Biomasses from the same family are represented by the same color.

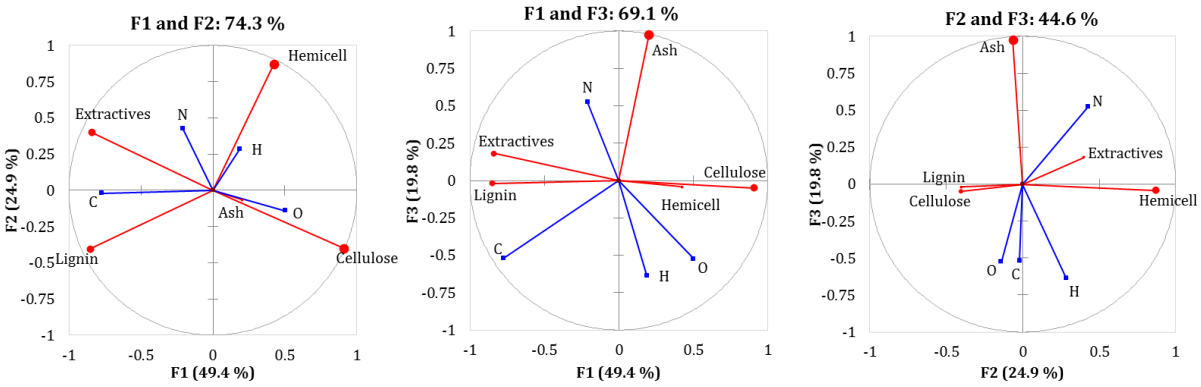
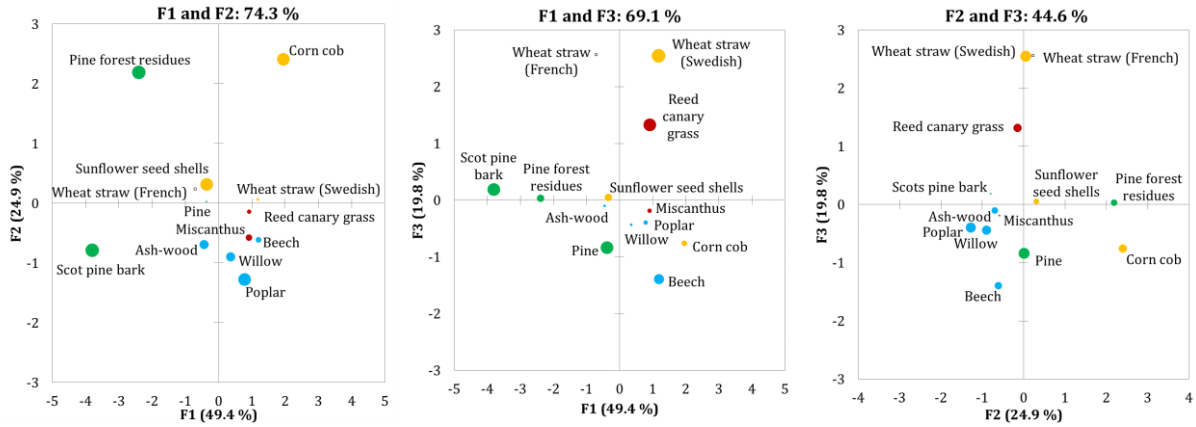


Figure V.4. Variables charts of the PCA on macromolecular composition of 12 biomasses



● deciduous wood ● coniferous wood ● herbaceous crops ● agricultural biomasses

Figure V.5. Observations charts of the PCA on macromolecular composition of 12 biomasses

Hemicelluloses representation is improved (very close to the circle in F1-F2 variable chart). Ash

content appears as closely correlated with the F3 axis. The variability in ash content of biomass might be described by this axis. Consequently, biomasses with the highest ash content, namely wheat straws and reed canary grass, present the highest values of the F3 component. On the contrary, biomasses with a low ash content are on the negative part of the F3 axis. On the other hand, hemicelluloses content is correlated to the F2 axis, which leads to high values of this principal component for biomasses with the highest hemicellulose content, namely corn cob and pine forest residues. In the case of the F1 axis, the correlation with cellulose content and the anti-correlation to lignin content are less well-defined. Biomasses with a high lignin content tend to be oriented to the negative part of the F1 axis; this is the case of Scot pine bark and pine forest residues; on the contrary, biomasses mostly based on cellulose are in the positive part of the F1 axis, namely miscanthus, poplar, beech or willow.

To sum up, biomass variability in terms of macromolecular composition could be represented by three independent principal components, which are cellulose (anticorrelated to lignin), hemicelluloses and ash content for the 12 selected biomasses in this PCA analysis. The representation of the variability was improved by removing outliers and duplicate biomasses.

These results demonstrate a high variability of biomass characterization, particularly in terms of macromolecular composition, which justifies the heterogeneity of the resource. It was shown that macromolecular composition is a suitable tool to define variability in biomass characterization, while the elemental composition showed its limitations. Biomass macromolecular composition can be represented by the cellulose, hemicelluloses and lignin content. Extractives and ash could be neglected by accepting a lower representation of the data variability. Concerning biomass samples, it stands out that biomasses from the same family can present strong differences in their composition. This was particularly remarkable for agricultural biomasses, while woody biomasses tend to show a closer composition.

1.2. Solid transformation

In a second step, the biomass behavior in terms of solid transformation during torrefaction was analyzed by PCA (data from IV.1.1 section). The objective of this analysis is to determine whether similarities exist in biomasses conversion through torrefaction, as a function of the temperature and of the duration of the treatment. Secondly, the influence of the composition in cellulose, hemicelluloses and lignin of the raw material in the solid transformation is assessed.

1.2.1. PCA of the solid transformation during the non-isothermal torrefaction step

A first PCA was carried out for the remaining solid mass of the 14 biomasses during the non-isothermal step of the torrefaction in TGA-GC/MS. Remaining solid mass points were considered every 10 °C, which corresponds to 3.3 minutes. Biomass macromolecular composition (Figure

V.6, left) and the ratios between macromolecular components (Figure V.6, right) were added to the PCA as supplementary variables. 2 principal components were selected, corresponding to 97.1% of the variability of the data.

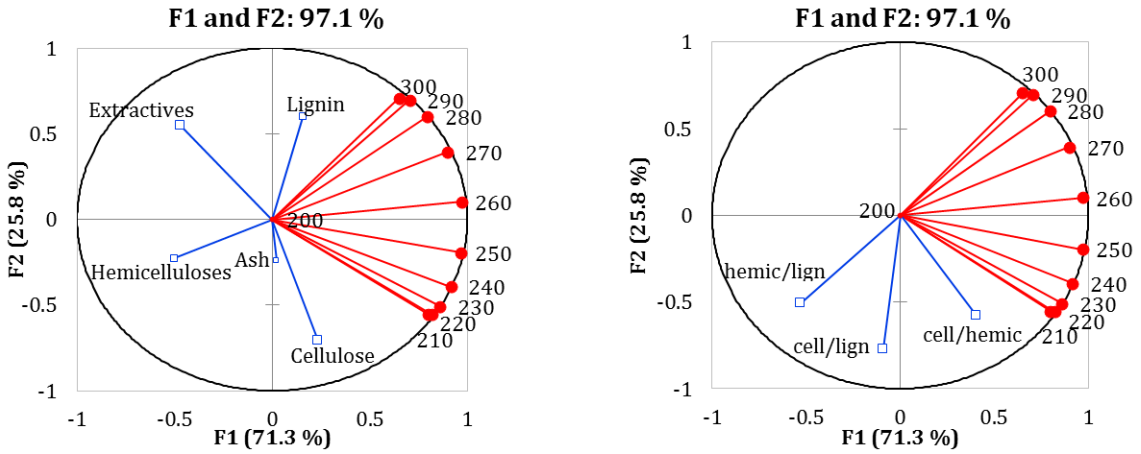


Figure V.6. Variables chart of the PCA on remaining solid mass versus temperature (variables) for non-isothermal torrefaction of 14 biomasses (macromolecular composition: supp. variables)

200°C coincides with the center of the variables chart, as it is the reference for mass loss (100% for all biomasses). All variables, except 200°C, are close to the limit of the circle, so well-represented. The results show a correlation between low torrefaction temperatures (210 to 240°C) on the one side and high torrefaction temperatures (280 to 300°C) on the other side, both groups being non-correlated. Torrefaction temperatures from 250 to 270°C present an intermediate behavior. The observation of two groups of temperatures is coherent with experimental results of solid mass loss in non-isothermal torrefaction, since a change in the kinetics curve is observed at an intermediate torrefaction temperature for most of the biomasses. However, the temperature of this trend change is different according to the biomass type, which explains the lack of clear distinction between these two groups.

The macromolecular composition is only acceptably represented as supplementary variables for cellulose and extractives (Figure V.6, left). The representation of the supplementary variables is improved with the ratios between macromolecular components, which appear to be acceptably represented in the variables chart (Figure V.6, right). The ratio hemicelluloses/lignin is anticorrelated with high torrefaction temperatures, while the ratio cellulose/hemicelluloses seems correlated with the low torrefaction temperatures. The ratio cellulose/lignin is anticorrelated with the F2 axis, so it can contribute to explain the behavior in the F2 direction for the observations chart. In this sense, a diminution in the cellulose/lignin ratio might explain the increase in the dispersion of the temperatures in the F2 axis direction: cellulose is mostly degraded at higher torrefaction temperatures (from 280-300°C), while lignin degradation in torrefaction is less pronounced and starts at intermediate temperatures (260-270°C). On the other hand, most of the degradation of hemicelluloses happens in the torrefaction temperature

range (240 to 300°C), starting at low and intermediate temperatures, which explains the anticorrelation of the hemicelluloses/lignin ratio with the high torrefaction temperatures. The correlation of the ratio cellulose/hemicelluloses with the low torrefaction temperatures is explained by the high torrefaction temperature needed for cellulose degradation, which contrasts with the low torrefaction temperature required for hemicelluloses transformation.

The observations chart (Figure V.7) includes well-represented observation points, as their size is proportional to the square cosine of the observations. There is an opposite behavior for corn cob and grape seed cake, explained by their opposite hemicellulose/lignin ratios. Coniferous biomasses can be grouped together and are correlated to the F2 axis, which corresponds to their high lignin content, despite the dissimilarities in the cellulose/lignin ratio. Their biological structure and the composition of their lignin are similar, mostly formed by guaiacyl- groups, which justifies their similar behavior in terms of solid transformation. Grape seed cake can be also grouped with coniferous biomasses due to its high lignin content. Biomass samples from herbaceous crops (red) and deciduous wood (blue) families are close, respectively. Agricultural biomasses are not grouped together, which responds to the heterogeneity in their composition.

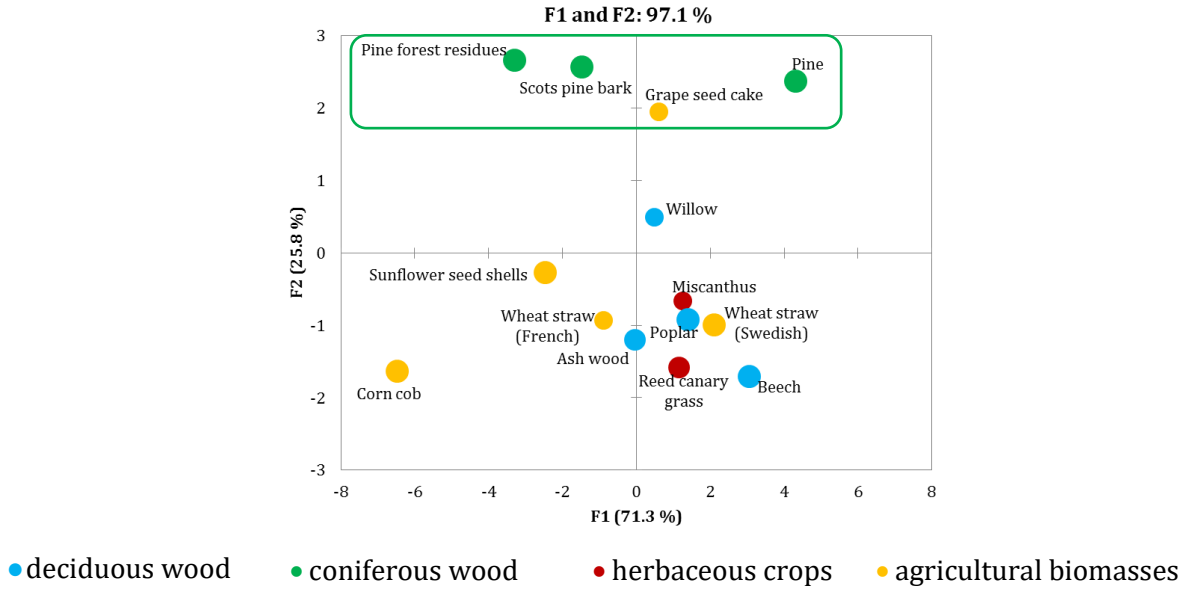


Figure V.7. Observations chart of the PCA on the remaining solid mass versus temperature (variables) for the non-isothermal torrefaction of the 14 biomasses (Figure V.6)

These results highlight a strong impact of the ratio between cellulose, hemicelluloses and lignin of a biomass on the mechanisms involved in solid transformation through torrefaction. Differences between biomass families were less marked than in previous PCA, except for coniferous wood.

1.2.2. PCA of the solid transformation during the isothermal torrefaction step

A PCA was carried out on the remaining solid mass of the 14 biomasses obtained during the isothermal step of torrefaction. Remaining solid mass points were considered every 3.75

minutes, as this parameter did not impact the PCA result. As in the previous case, macromolecular composition (Figure V.8, left) and ratios between cellulose, hemicellulose and lignin (Figure V.8, right) were added to PCA as supplementary variables. An accurate representation of the variability of the data is achieved with two principal components (99.7%).

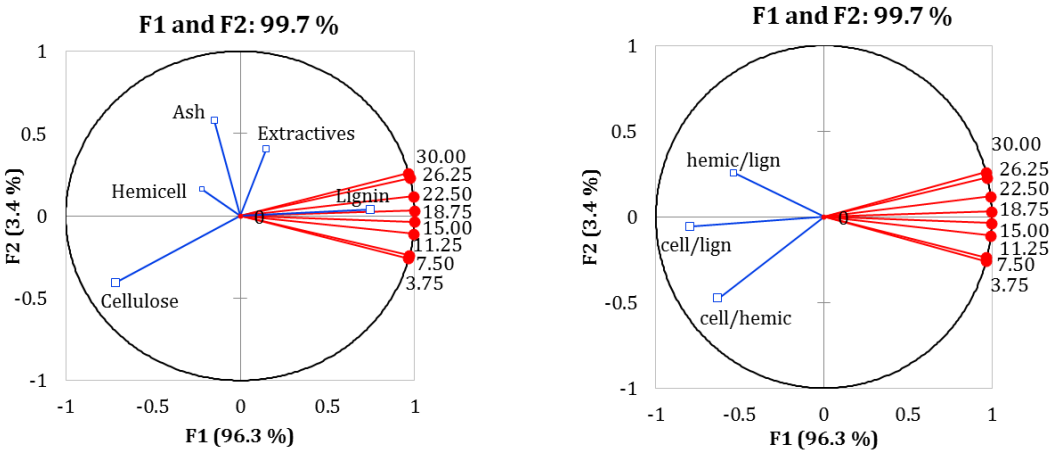


Figure V.8. Variables chart of the PCA on the remaining solid mass versus the duration of the isothermal step (variables: time, minutes) for the torrefaction of the 14 biomasses

While the time points in the variables chart are well-represented, only lignin and cellulose content can be considered as representative supplementary variables. Hemicellulose is not well-represented, probably because the main part of its degradation happens below 300°C. The time points are distributed in a similar way to the previous case (V.1.2.1 section). However, most of the variability is coincident to the F1 direction and only a minor part of it is represented by the F2 direction. The F1 axis seems correlated with the lignin content and high time values seem anticorrelated with the cellulose/lignin content. As a result, a high cellulose content in biomass implies a lower impact on the step duration for an isothermal torrefaction at 300°C. This can be explained by the fact that cellulose starts its thermal degradation at temperatures close to 300°C, the transformation being enhanced by time and increasing temperature, until around 400°C. The experimental behavior observed for the « cellulose II » fractions consists of an increase in the cellulose degradation rate until 300°C, followed by a deceleration during the isothermal step. In the case of the commercial microcrystalline cellulose Avicel, its degradation was enhanced in the isothermal step, at 300°C. This result supports the hypothesis that the extracted fractions contribute to a more suitable representation of cellulose behavior in torrefaction, compared to the commercial cellulose.

The observations chart derived from this PCA shows a distribution of the biomasses in the F1 axis in function of their increasing lignin content: the highest content for grape seed cake, followed by the coniferous wood and reed canary grass, deciduous wood and agricultural biomasses (Figure V.9). As a result, two groups can be distinguished: coniferous wood, close to grape seed cake, on the one hand, and deciduous wood, close to reed canary grass, on the other

hand. Agricultural biomasses and herbaceous crops (miscanthus and reed canary grass) are heterogeneous groups in terms of diverse behavior again in this case.

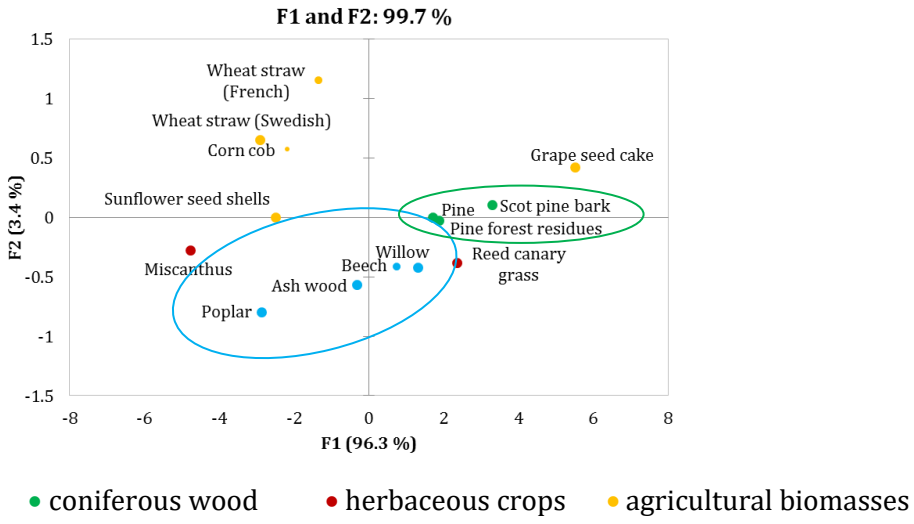


Figure V.9. Observations chart of the PCA on the remaining solid mass versus the duration of the isothermal step (variables: time, minutes) for the torrefaction of the 14 biomasses (Figure V.8)

This PCA points out the influence of the ratio cellulose/lignin of biomass composition on its solid transformation in the isothermal torrefaction step at 300 °C, while hemicelluloses might be already transformed at this point. Woody biomasses exhibit similar solid transformation patterns, while agricultural biomass and herbaceous crop behavior remain heterogeneous.

These results reinforce the theory that macromolecular composition has a critical impact on biomass behavior, and particularly on solid transformation through torrefaction.

1.3. Volatile species production

PCA was also carried out on the volatile species released in torrefaction. Three variables were identified in this case, which corresponds to the volatile species, the biomass samples and the torrefaction temperature. These factors were separated in two groups to facilitate PCA analysis. Firstly, the influence of temperature in the volatile species production in torrefaction is assessed for a selected biomass (beech, V.1.3.1 section). In the second case, the total volatile species production for the 14 biomasses is analyzed, without the influence of temperature (V.1.3.2 section).

1.3.1. PCA on beech data

In a first step, the influence of temperature on the production of volatile species in torrefaction is tested. A single biomass is considered, in order to discard the influence of the macromolecular composition on the volatile species production. To do this, beech was selected as a representative biomass. Two objectives were defined for this section:

- Determine the influence of the temperature in the volatile species production.
- Group volatile species in function of their similar production.

Data for this PCA corresponds to the instantaneous production quantified for each volatile species (observation) at each temperature point (variable), considered every 10 °C or 3.3 minutes.

A first PCA was carried out on the data from the production of the 23 quantified volatile species in function of the temperature for beech (Figure V.10). 2 principal components represent 98.9% of the variability. Volatile species from the same chemical family are represented by the same color in the observations chart, except the so-called « other compounds » that were not clearly separated (Figure V.10, right).

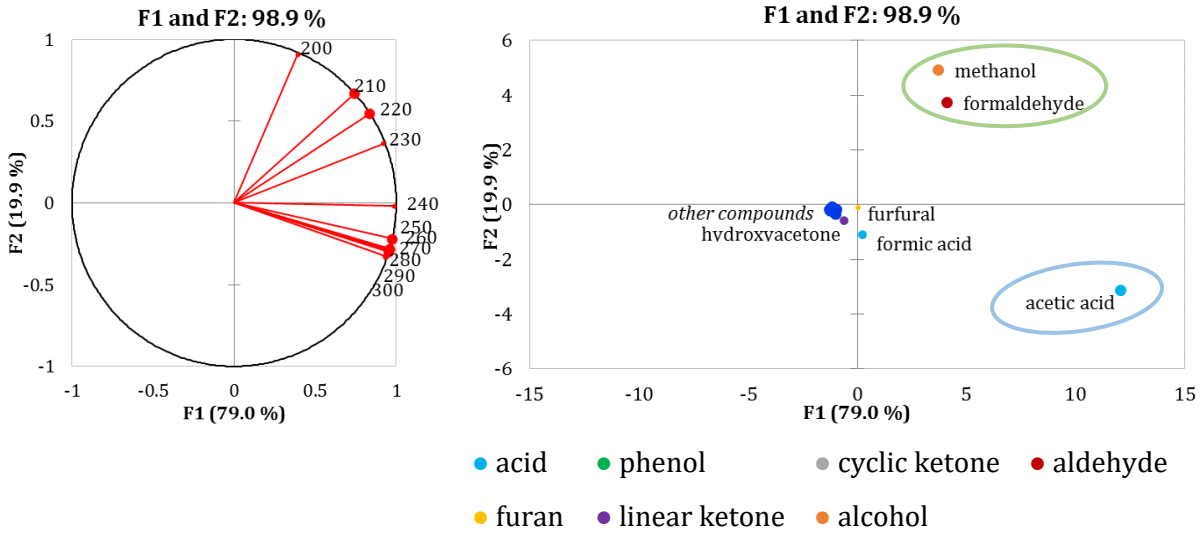


Figure V.10. Variables chart (left) and observations chart (right) of the PCA on the production of volatile species versus temperature (variable) for non-isothermal torrefaction of 14 biomasses

The variables chart shows two distinct groups of behavior, corresponding to the temperatures below and above 240°C (Figure V.10, left). This might be correlated to the degradation of hemicellulose, starting from 200°C, and the later degradation of cellulose, rather beginning at intermediate to higher torrefaction temperatures. All the volatile species are well-represented in the observations chart, except formic acid, furfural and hydroxyacetone. Three groups of observations can be distinguished, which correspond to acetic acid, methanol-formaldehyde and the rest of the volatile species. The separated volatile species are coincident to the major compounds released, and their position in the observations chart is in agreement with the different production profiles observed (IV.1.2). Indeed, methanol and formaldehyde might be present below 240°C, presumably corresponding to hemicelluloses and lignin decomposition, respectively. Acetic acid production, even if it follows hemicelluloses degradation, would be enhanced at intermediate to higher torrefaction temperatures. In both cases, observations are in agreement with the observed production profiles (see IV.1.2 section).

However, the high production of these species does not allow to distinguish any trend in the production of other minor species. To distinguish them, a second PCA was carried out on the same data excluding the main compounds, i.e. methanol, formaldehyde, acetic acid, formic acid and furfural (Figure V.11).

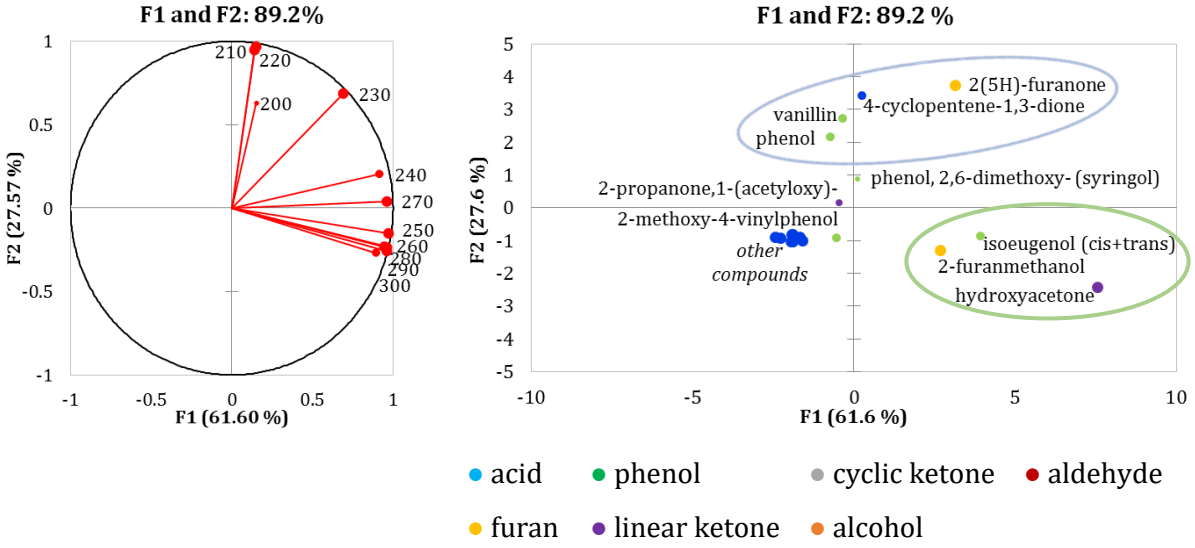


Figure V.11. Variables chart (left) and observations chart (right) of the PCA analysis (observations: 18 chemical compounds quantified in beech torrefaction, variables: temperature)

In this case, the variables chart shows differences between low and intermediate to high torrefaction temperatures (Figure V.11, left). However, the transition (240 to 270°C) is less marked than in the first PCA (Figure V.10, left). All observations are well-represented by two principal components (89.2% of the variability), except syringol, 2-methoxy-4-vinylphenol and 2-propanone,1-(acetyloxy)-. Principally, 3 groups of volatile species behavior can be distinguished: the first group, including 2(5H) furanone, vanillin, phenol and 4 cyclopentene 1,3 dione; the second group with isoeugenol, 2-furanmethanol and hydroxyacetone; and the third group with the other volatile components. It can be noticed that these groups do not correspond to chemical families of volatile species. For the first group, the production of the volatile species was shown to be generally independent of the torrefaction temperature. The exception is for 2(5H)-furanone, slightly separated from the other three compounds in the group, as its production softly rises from 270 to 300°C (see IV.1.2 section). In the case of vanillin, a higher production was detected at 200°C compared to intermediate temperatures, and this in general for deciduous wood, which might indicate a correlation of vanillin to the low torrefaction temperatures. The production of the second group, composed by isoeugenol, 2-furanmethanol and hydroxyacetone, seems correlated to high torrefaction temperatures. This behavior is in agreement with the production profiles, which are characterized by local minima at 270 and 290°C, with a production which is particularly enhanced close to 300°C (see IV.1.2 section). The species included in the third group mainly present an increasing production with increasing

torrefaction temperature (propionic acid, guaiacol, acetylfuran, 3-furaldehyde, furan, 2-methoxy-4-vinylphenol, eugenol, cathecol and 2,3-pentanedione). As a result, the production profiles of the volatile species seem to be more impacted by the progression in the degradation of biomass macromolecular components, which happens simultaneously, rather than by the chemical family of the volatile species.

These results lead to conclude that:

- The production of volatile species in beech torrefaction shows a different behavior before and after 240 °C, which might correspond to the degradation of hemicellulose and cellulose in function of the torrefaction temperature.
- Volatile species from the same chemical family tend to exhibit different behaviors in terms of production profiles in function of the temperature. The mechanisms involved in biomass macromolecular composition might be at the origin of these differences, rather than the chemical family.

1.3.2. PCA on raw biomasses

In a second step, the influence of the biomass type in the production of volatile species in torrefaction was tested. To do this, the integration of the area below the production curve of each volatile species per biomass was considered, which represents the total production per volatile species. The objectives of this analysis are the following ones:

- Determine the influence of the biomass macromolecular composition on the volatile species production in torrefaction.
- Group biomasses in function of their similarity of volatile species production.

First of all, all biomasses were analyzed (a). Secondly, biomasses were analyzed per family (b-d).

a) All biomasses

A first PCA was carried out on the volatile species production of the 14 biomasses of the database (Figure V.12). As the high variability of the data made it extremely complicated to perform a PCA on all the volatile species, only the 11 major volatile species separated in the previous analysis with beech (V.1.3.1 section) were considered. An attempt of classification of the biomasses (observations) in families of similar volatile species production (variables) is carried out.

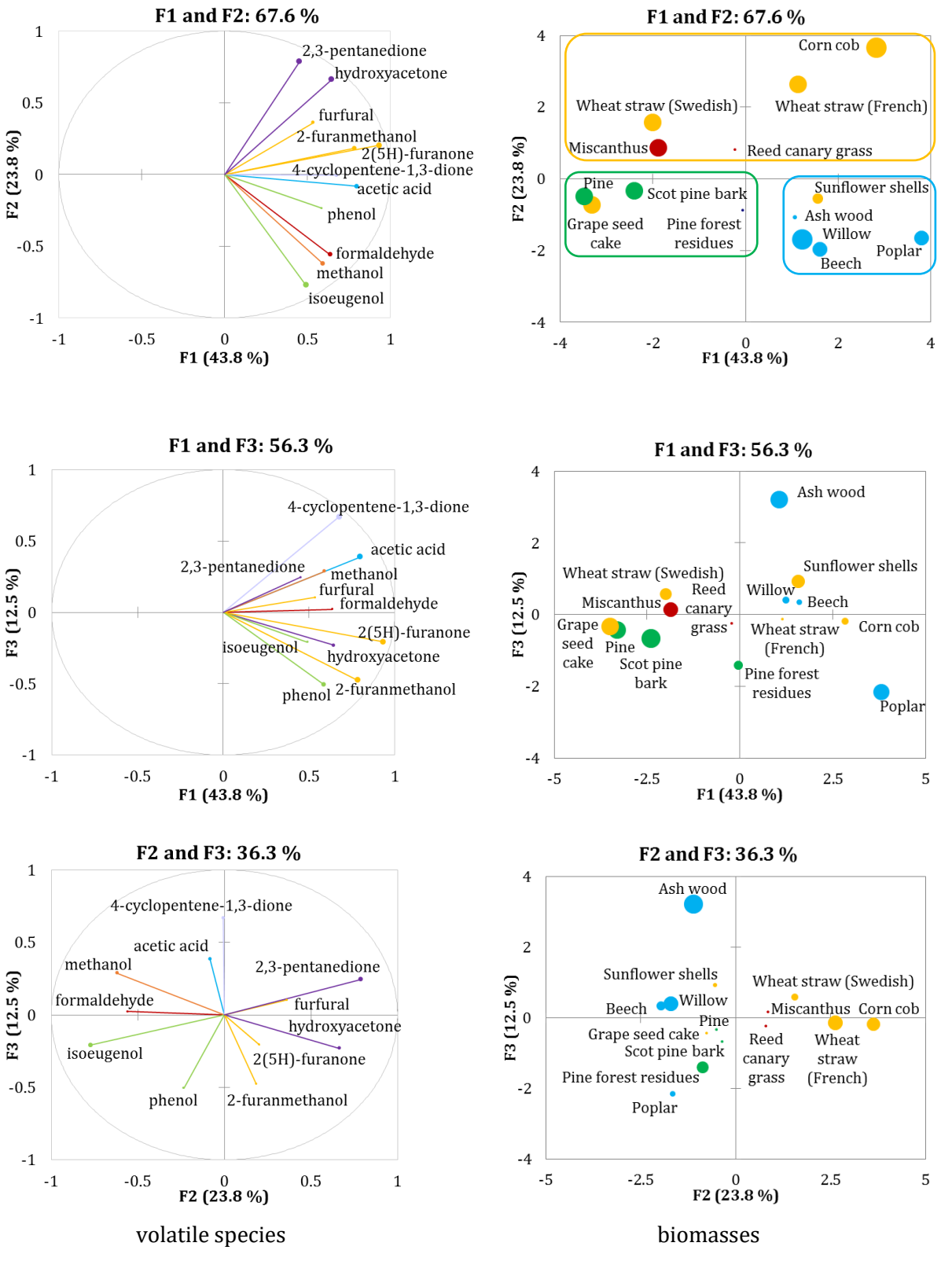


Figure V.12. Variables charts (left) and observations charts (right) of the PCA on the total major volatile species production in torrefaction for 14 biomasses

80.1% of the variability was represented by selecting three principal components. Three main groups of biomasses were identified, which are indicated in Figure V.12 (left, right). The first group corresponds to deciduous wood, in blue, and the second one, to coniferous wood, in green. Agricultural biomasses present a higher variability in terms of volatile species production and are not all grouped together in the yellow group. The behavior of grape seed cake is close to that of coniferous wood, presumably because of its high lignin content, which leads to a low volatile species release.

Volatile species behavior was shown to be diverse, with similarities between species from the same chemical nature (Figure V.12, left). However, volatile species are not perfectly-represented in this PCA, so these considerations must been taken into account carefully.

This analysis highlights the similitudes in volatile species release for deciduous and coniferous wood, while agricultural biomasses behavior is more heterogeneous. In all cases, volatile species release seems to be governed by biomass macromolecular composition. Similitudes might exist in the production of volatile species from the same chemical family, at least for major compounds.

In order to improve the representation of the total volatile species, as well as to consider all the volatile species quantified, a new PCA was carried out on the total production of the individual volatile species per biomass family (sections b to d). As biomass macromolecular composition is known to be the most influent factor on the nature of the volatile species released, it was included as supplementary variables in the analysis.

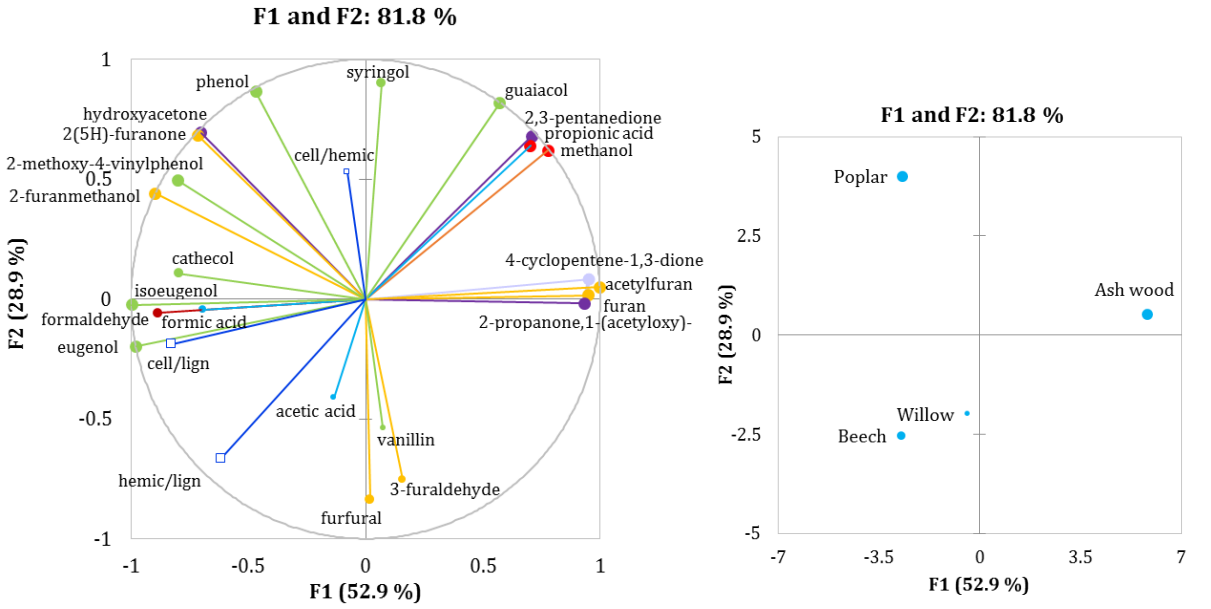
b) Deciduous wood (ash wood, beech, poplar, willow)

A PCA was carried out on the total volatile species production for the all quantified volatile species (23 chemical compounds) released in the torrefaction of deciduous wood. The variability of the data was represented by 2 Principal Components (81.8%), which is higher than in Figure V.12.

A good representation of the observations was achieved (Figure V.13, right), except for willow. The observations chart reveals a different volatile species release for the 4 deciduous woods. In the variables chart, volatile species from the same chemical family tend to be close, by forming several clusters per chemical family (Figure V.13, left).

The production of 4-cyclopentene-1,3-dione, acetylfuran, furan and 2-propanone, 1-(acetyloxy)- is shown to be enhanced for ash-wood (Figure V.13, left). On the contrary, its production of cathecol, isoeugenol, formaldehyde, formic acid and eugenol would be less important. In both cases the observations are in agreement with the experimental results. Ash-wood is strongly correlated to the F1 axis, which is anticorrelated to the cellulose/lignin ratio. This might indicate that a decrease in the lignin content leads to a higher production of the phenolic compounds

mentioned, while a decrease in the cellulose content leads to furans and ketones release, which is in agreement with previous studies in the literature. On the other hand, beech behavior would be principally controlled by the composition ratio between hemicelluloses and lignin. This ratio is anti-correlated to the production of methanol and 2,-pentanedione, which are known to be released from hemicelluloses. Interestingly lignin-base phenolic compounds, namely syringol and guaiacol, tend to be anti-correlated to a decrease in the lignin content. Finally, the poplar production of phenol, hydroxyacetone, 2(H)-furanone, 2-methoxy-4-vinylphenol and 2-furanmethanol is pointed out to be higher than for the other deciduous woods.



volatile species

- acid
- cyclic ketone
- furan
- alcohol
- phenol
- aldehyde
- linear ketone

biomasses

- deciduous wood
- herbaceous crops
- coniferous wood
- agricultural biomasses

Figure V.13. Variables chart (left) and observations chart (right) of the PCA on the total volatile species production in torrefaction for the deciduous biomasses

c) Coniferous wood (Pine, pine forest residues, scot pine bark) and grape seed cake

A second PCA was carried out on the volatile species released in the torrefaction of coniferous wood. Grape seed cake was added to this group due to its high lignin content. In this case, cellulose, hemicellulose and lignin content were directly represented as supplementary variables. 83.2% of the variability of the data was represented by 2 principal components. The observations are well-represented (Figure V.14, right), except for Scot pine bark.

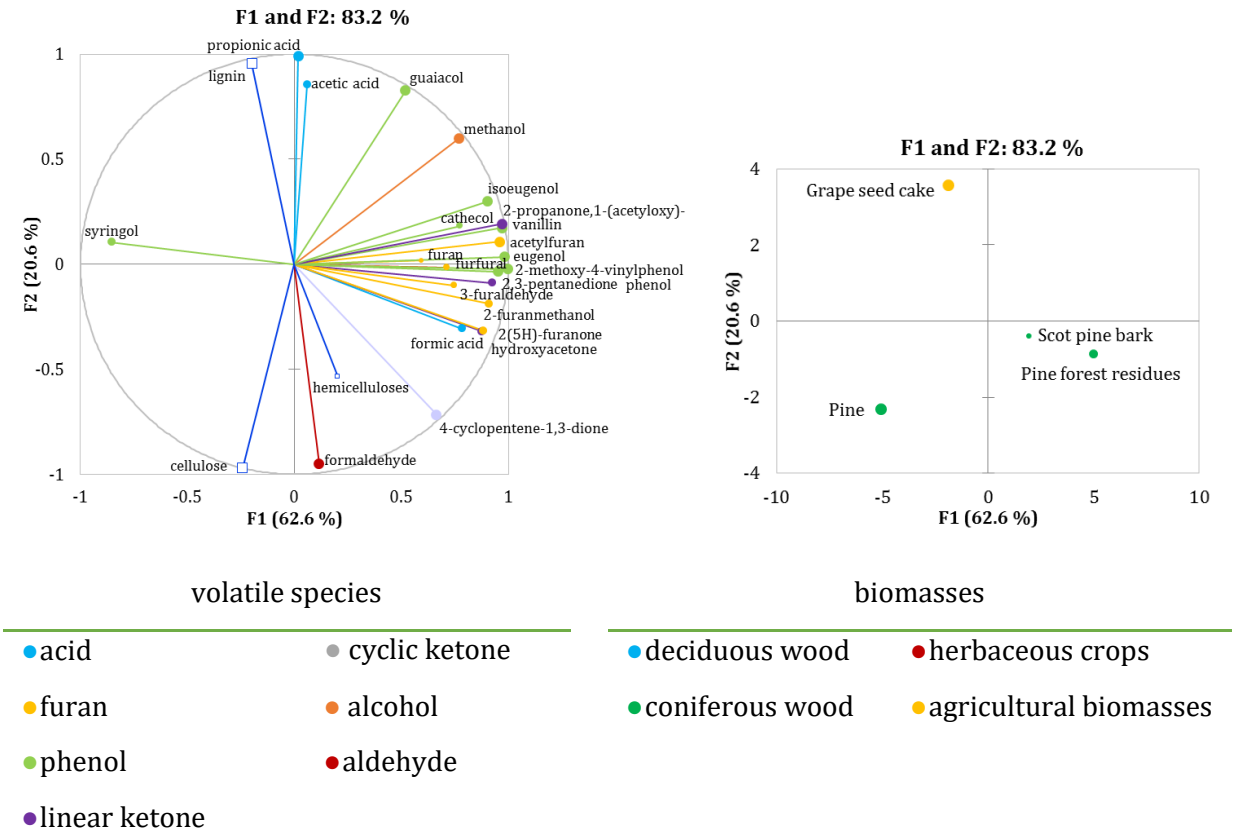


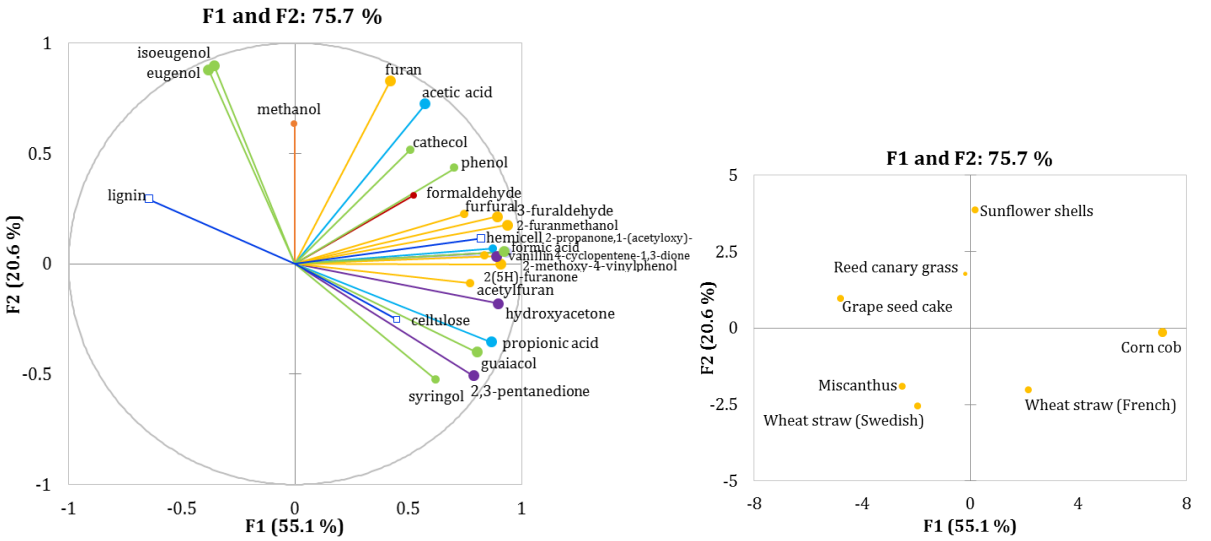
Figure V.14. Variables chart (left) and observations chart (right) of the PCA on the total volatile species production in torrefaction for the coniferous biomasses and grape seed cake

The observations chart shows different volatile species release for pine, pine forest residues and grape seed cake (Figure V.14, left). Overall, volatile species are grouped together per chemical family in the variables chart, except formic acid and syringol. The production of acetic acid and propionic acid is anti-correlated to the cellulose content, which might indicate that these compounds are released when the cellulose content diminishes. Phenols, furans and ketones production is grouped and not correlated to the cellulose and lignin content. Formaldehyde production is anti-correlated to the lignin content, as it is mainly produced by this macromolecular component. Concerning the biomasses from the family, grape seed cake presents a high lignin content and a low release of volatile species. Pine is not correlated to a release of a particular volatile species. Pine forest residues are correlated to most of phenols, furans and ketones and present a higher production of these compounds compared to other coniferous wood.

d) Agricultural biomasses and herbaceous crops

Finally, the PCA of the volatile species released in the torrefaction of agricultural biomasses and herbaceous crops was carried out. By selecting 2 principal components, the variability represented only achieves 75.7%, which already indicates a higher heterogeneity of the data compared to the two previous cases. A loss of accuracy is noticeable by the smaller size of the

observation points, as well as by their dispersion in observations chart (Figure V.15, left).



volatile species

- acid
- cyclic ketone
- furan
- alcohol
- phenol
- aldehyde
- linear ketone

biomasses

- deciduous wood
- herbaceous crops
- coniferous wood
- agricultural biomasses

Figure V.15. Variables chart (left) and observations chart (right) of the PCA on the total volatile species production in torrefaction for the agricultural and herbaceous biomasses

Concerning volatile species, the groups per chemical family seem less marked than in previous cases. Furans, some linear and cyclic ketones, formic acid and vanillin are particularly correlated to the hemicelluloses content and to the F1 axis. This is in agreement with the high hemicelluloses content and the important amount of volatile species released by corn cob. Lignin-base units, namely guaiacol and syringol, are again anti-correlated to the lignin content. Sunflower shells lead to a higher production of isoeugenol, eugenol, furan and methanol than the other agricultural biomasses. Grape seed cake is, again, strongly correlated to a low volatile species release and a high lignin content. Interestingly, the two species of wheat straw show dissimilarities in the volatile species release, which might be derived from differences in their macromolecular composition.

To conclude, the heterogeneity in agricultural biomasses results was again demonstrated in terms of volatile species production. The similarities between volatile species from the same chemical family are less marked, and the representation of the observations was less accurate than for deciduous and coniferous wood cases.

1.4. Conclusions of the PCA

PCA results highlight that macromolecular composition is a suitable tool to define variability in biomass characterization, while the elemental composition showed its limitations. The variability in biomass characterization can be correctly represented by the cellulose, hemicelluloses and lignin content per biomass. Extractives and ash content could be neglected by accepting a slight loss in the accuracy in the representation of data variability.

Concerning biomass samples, a similar macromolecular composition and solid transformation behavior through torrefaction were found for biomasses belonging to deciduous and coniferous woods families, respectively. Nevertheless, agricultural biomasses and herbaceous crops present a more heterogeneous behavior. As a result, one exemplar of each woody family could be sufficient, in a first approach, to model the kinetics behavior of the family, while several exemplars of agricultural biomasses would be required for the same objective.

By considering production profiles of the volatile species in function of the temperature, volatile species from the same chemical family exhibit different behaviors. This indicates that a representative per chemical family of volatile species would not be sufficient to model volatile species release in torrefaction. Interestingly, when considering the total production of each volatile species through the non-isothermal torrefaction, compounds from the same chemical family seem to be generally produced in a similar way. This observation supports the affirmation that biomass macromolecular composition in cellulose, hemicelluloses and lignin strongly impacts volatile species release in torrefaction. In the same biomass family, biomasses present a very different behavior in terms of total production of volatile species. Consequently, a single biomass per chemical family was shown not to be sufficient to represent the behavior of the family in terms of volatile species release.

In order to model the production of volatile species in biomass torrefaction, an enlarged biomass database of chemical compounds released and biomasses torrefied would be required, particularly but not exclusively for agricultural biomasses. As a result, the modelling of the volatile species production in biomass torrefaction should be foreseen in a future study. Meanwhile, a torrefaction model exclusively based on solid kinetics can be considered in a first step. It will be based on cellulose, hemicellulose and lignin composition as key parameters to describe biomass composition.

2. Torrefaction model

At this stage, a considerable amount of experimental data is now available, related both to solid compositions and to volatile species release during torrefaction, for a large variability of biomasses. The PCA approach allowed us to exhibit the role played by the macromolecular components and to emphasize some major trends. Nowadays, it seemed to be interesting to come back to a more mechanistic representation based on reaction kinetics modelling, inspired by the works previously undertaken. In this case, the called "Nocquet's model" will be enriched by data obtained in the present study from extracted macromolecular components. With this study, we just intend to lay the first bricks of the approach and to draw some prospects for the future. Besides, we are aware that the experimental uncertainties do not allow us to demand a strong accuracy in the comparison model-experiments. The objective is only to improve the understanding on the interest and the limitations of the modelling approach based on the additive behavior of biomass macromolecular components, in this case obtained by extraction from several biomasses. First of all, the previous torrefaction model based on commercial compounds to represent biomass macromolecular composition is analyzed. Secondly, a new version of the torrefaction model is proposed by considering an additive behavior in torrefaction of the extracted macromolecular components from the five reference biomasses (experimental data from IV.2). This approach is based on the key parameters determined through the PCA (see V.1).

2.1. Nocquet's model and commercial compounds

The additive model based on cellulose, hemicellulose and lignin composition suggested by Nocquet [6,7] was compared to experimental results for the 5 reference biomasses (Figure V.16a). The ratio between remaining solid mass estimated through Nocquet's model and obtained for raw biomass in TGA-GC/MS is also represented to facilitate the interpretation of the underestimation or overestimation by the model compared to the experimental results (Figure V.16b).

The Nocquet's model simulation achieves an acceptable fitting of the experimental data for the non-isothermal torrefaction part below 300°C, exhibiting a slight overestimation of the remaining solid mass. Nevertheless, as the model was built from experiments carried out on commercial compounds and beech, the fitting for other biomasses, such as pine and wheat straw is less good. In the case of pine, hemicelluloses are principally based on mannose sugars, which are less reactive than xylose-based sugars [22]. As hemicelluloses are represented in Nocquet's model by xylan, this explains the underestimation of the remaining solid mass in the case of pine. On the other hand, the use of commercial Avicel to represent celluloses seems to lead to a correct representation of solid kinetics at low torrefaction temperatures.

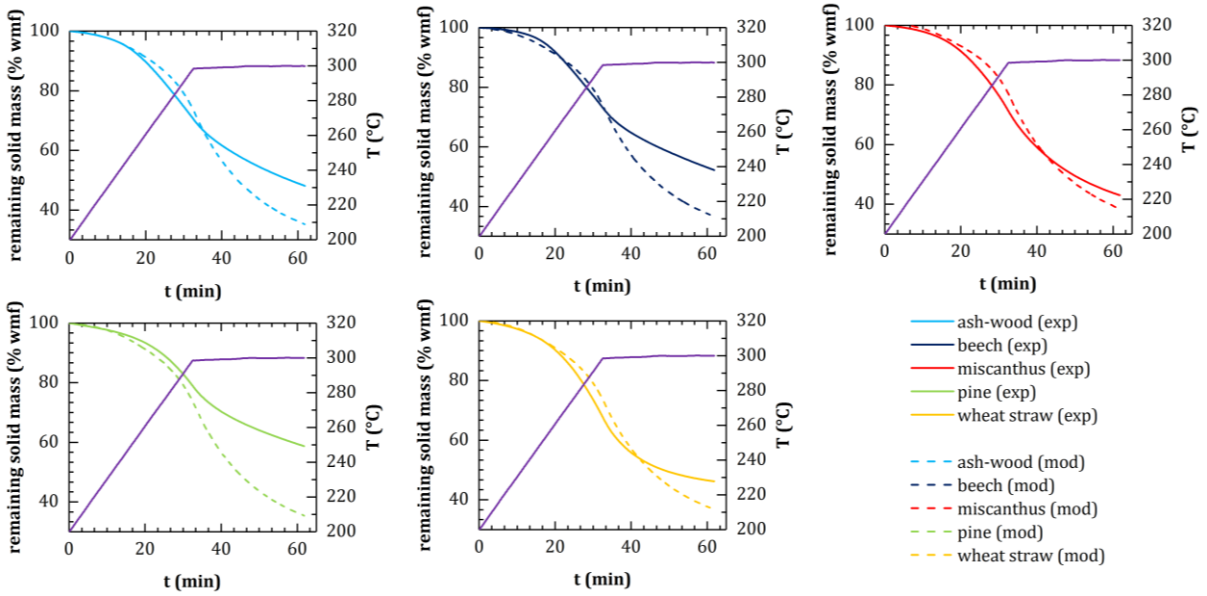


Figure V.16a. Remaining solid mass loss versus temperature and time in torrefaction modelled through Nocquet's model (dotted line) and obtained for raw biomass in TGA-GC/MS (line)

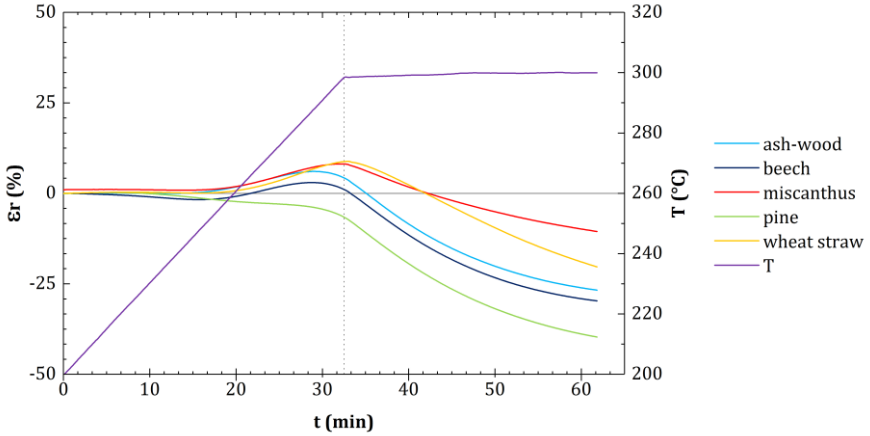


Figure V.16b. Relative error between remaining solid mass estimated through Nocquet's model and obtained for raw biomass in TGA-GC/MS in function of time and temperature

A strong underestimation of the remaining solid mass is observed in the isothermal step at 300°C. This might be a consequence of the enhanced degradation observed for commercial cellulose Avicel under these conditions (Figure IV.13). Finally, the extrapolation of the Nocquet's model for cellulose (Avicel), hemicelluloses (xylan) and beech dioxane lignin to other biomasses different from beech does not allow to take into account the particularities in the degradation of biomasses from different families. This is the case of the stabilization of the mass loss observed for agricultural biomasses in the isothermal step, compared to woody biomasses, which cannot be reproduced in this case. Other additive models based on commercial compounds were proposed in the literature, without distinguishing between biomass families [22,188].

2.2. First-level model

A new approach of the torrefaction additive model based on biomass macromolecular components was defined. The objective of predicting biomass behavior in torrefaction through its macromolecular composition in cellulose, hemicelluloses and lignin remains unchanged.

2.2.1. Representation of the first-level model

In a first approach, « cellulose II », « hemicelluloses 1 » and « lignin » were selected as the representative extracted fractions for each biomass. The model is called “additive model”, as it considers the weighted sum of the behavior of the extracted fractions in the proportions that the corresponding macromolecular components are present in raw biomass (Eq. 1).

$$m_{rb}(t_i, T_i) = x_{C,rb}\, m_{C^{II}}(t_i, T_i) + x_{H,rb}\, m_{H_1}(t_i, T_i) + x_{L,rb}\, m_L(t_i, T_i) \quad \text{Eq. 1}$$

$$T_i \in [200,300]°C$$

Where:

$m_{rb}(t_i, T_i)$: instantaneous remaining solid mass of raw biomass

$m_{C^{II}}(t_i, T_i)$: instantaneous remaining solid mass of « cellulose II » fraction

$m_{H_1}(t_i, T_i)$: instantaneous remaining solid mass of « hemicelluloses 1 » fraction

$m_L(t_i, T_i)$: instantaneous remaining solid mass of « lignin » fraction

$x_{C,rb}$: initial mass fraction of cellulose in raw biomass (at t = 0).

$x_{H,rb}$: initial mass fraction of hemicelluloses in raw biomass (at t = 0).

$x_{L,rb}$: initial mass fraction of lignin in raw biomass (at t = 0).

t_i, T_i: instantaneous values of time and temperature.

First of all, the kinetics of each extracted fraction were studied. The structure of the 2-succesive steps kinetic model of Di Blasi and Lanzetta was used in this work to describe solid conversion as shown on Figure 17.

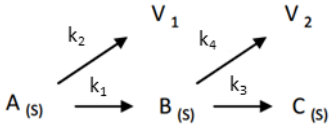


Figure V.17. Structure of the 2-succesive steps kinetic model of Di Blasi and Lanzetta [58].

In this model, A, B and C are solid species, V_1 and V_2 are gaseous species and k_1, k_2, k_3 and k_4 are the kinetic constants of each chemical reaction. The order of the chemical reactions was supposed to be 1, and the kinetics of the 4 reactions are supposed to follow the Arrhenius law.

$$k = k_0 \exp\left(\frac{-E}{R\,T}\right)$$ Eq. 2

k: kinetic constant (s^{-1}).

k_0: pre-exponential factor (s^{-1}).

E: activation energy (J/mol).

R: perfect gases constant (8.314 J mol^{-1} K^{-1}).

T: temperature (K).

The kinetic parameters of the kinetic model were calculated for each extracted fraction per biomass by least square fitting on absolute error between model and experimental data (Table V.2). The initialization was based on Nocquet's model parameters.

Table V.2. Kinetic parameters of 2-succesive steps kinetic model calculated for extracted fractions

« cellulose II »										
	ash-wood		**beech**		**miscanthus**		**pine**		**wheat straw**	
	k_0 (s^{-1})	**E (J/mol)**	**k_0 (s^{-1})**	**E (J/mol)**	**k_0 (s^{-1})**	**E (J/mol)**	**k_0 (s^{-1})**	**E (J/mol)**	**k_0 (s^{-1})**	**E (J/mol)**
r1	$1.32 \cdot 10^{12}$	$1.67 \cdot 10^{5}$	$1.32 \cdot 10^{12}$	$1.70 \cdot 10^{5}$	$1.32 \cdot 10^{12}$	$1.70 \cdot 10^{5}$	$1.32 \cdot 10^{12}$	$1.71 \cdot 10^{5}$	$1.32 \cdot 10^{12}$	$1.67 \cdot 10^{5}$
r2	$9.10 \cdot 10^{21}$	$2.76 \cdot 10^{5}$	$1.06 \cdot 10^{20}$	$2.90 \cdot 10^{5}$	$1.06 \cdot 10^{21}$	$2.78 \cdot 10^{5}$	$7.50 \cdot 10^{21}$	$2.78 \cdot 10^{5}$	$1.06 \cdot 10^{21}$	$2.74 \cdot 10^{5}$
r3	$9.30 \cdot 10^{30}$	$3.31 \cdot 10^{5}$	$2.10 \cdot 10^{30}$	$3.31 \cdot 10^{5}$	$2.10 \cdot 10^{30}$	$3.27 \cdot 10^{5}$	$9.30 \cdot 10^{30}$	$3.48 \cdot 10^{5}$	$2.10 \cdot 10^{30}$	$3.12 \cdot 10^{5}$
r4	$3.09 \cdot 10^{18}$	$3.33 \cdot 10^{5}$	$3.09 \cdot 10^{18}$	$1.97 \cdot 10^{5}$	$3.09 \cdot 10^{18}$	$1.95 \cdot 10^{5}$	$3.09 \cdot 10^{18}$	$3.33 \cdot 10^{5}$	$3.09 \cdot 10^{18}$	$1.85 \cdot 10^{5}$
Mean ε_a	0.318		0.039		0.020		0.116		0.062	
Mean ε_r	0.120%		0.015%		0.008%		0.038%		0.026%	
« hemicelluloses 1 »										
	ash-wood		**beech**		**miscanthus**		**pine**		**wheat straw**	
	k_0 (s^{-1})	**E (J/mol)**	**k_0 (s^{-1})**	**E (J/mol)**	**k_0 (s^{-1})**	**E (J/mol)**	**k_0 (s^{-1})**	**E (J/mol)**	**k_0 (s^{-1})**	**E (J/mol)**
r1	$7.02 \cdot 10^{5}$	$9.07 \cdot 10^{4}$	$7.09 \cdot 10^{5}$	$8.76 \cdot 10^{4}$	$1.15 \cdot 10^{6}$	$7.07 \cdot 10^{4}$	$1.21 \cdot 10^{6}$	$7.47 \cdot 10^{4}$	$6.36 \cdot 10^{5}$	$8.74 \cdot 10^{4}$
r2	$1.71 \cdot 10^{9}$	$1.23 \cdot 10^{5}$	$1.66 \cdot 10^{9}$	$1.21 \cdot 10^{5}$	$1.67 \cdot 10^{9}$	$1.21 \cdot 10^{5}$	$1.67 \cdot 10^{9}$	$1.21 \cdot 10^{5}$	$1.59 \cdot 10^{9}$	$1.24 \cdot 10^{5}$
r3	$6.83 \cdot 10^{8}$	$1.28 \cdot 10^{5}$	$7.09 \cdot 10^{8}$	$1.25 \cdot 10^{5}$	$7.21 \cdot 10^{8}$	$1.26 \cdot 10^{5}$	$7.20 \cdot 10^{8}$	$1.26 \cdot 10^{5}$	$6.63 \cdot 10^{8}$	$1.29 \cdot 10^{5}$
r4	$2.44 \cdot 10^{9}$	$1.39 \cdot 10^{5}$	$2.46 \cdot 10^{9}$	$1.33 \cdot 10^{5}$	$2.50 \cdot 10^{9}$	$1.27 \cdot 10^{5}$	$2.50 \cdot 10^{9}$	$1.28 \cdot 10^{5}$	$2.31 \cdot 10^{9}$	$1.37 \cdot 10^{5}$
Mean ε_a	0.012		0.016		0.101		0.057		0.010	
Mean ε_r	0.005%		0.025%		0.301%		0.123%		0.013%	
« lignin »										
	ash-wood		**beech**		**miscanthus**		**pine**		**wheat straw**	
	k_0 (s^{-1})	**E (J/mol)**	**k_0 (s^{-1})**	**E (J/mol)**	**k_0 (s^{-1})**	**E (J/mol)**	**k_0 (s^{-1})**	**E (J/mol)**	**k_0 (s^{-1})**	**E (J/mol)**
r1	$7.74 \cdot 10^{1}$	$5.35 \cdot 10^{4}$	$7.16 \cdot 10^{0}$	$4.34 \cdot 10^{4}$	$2.59 \cdot 10^{2}$	$5.38 \cdot 10^{4}$	$2.11 \cdot 10^{2}$	$6.31 \cdot 10^{4}$	$8.17 \cdot 10^{-1}$	$3.19 \cdot 10^{4}$
r2	$3.29 \cdot 10^{1}$	$5.35 \cdot 10^{4}$	$3.53 \cdot 10^{1}$	$5.39 \cdot 10^{4}$	$8.61 \cdot 10^{2}$	$6.54 \cdot 10^{4}$	$1.67 \cdot 10^{-4}$	$1.91 \cdot 10^{1}$	$1.13 \cdot 10^{2}$	$5.76 \cdot 10^{4}$
r3	$2.09 \cdot 10^{1}$	$3.62 \cdot 10^{4}$	$4.96 \cdot 10^{0}$	$3.64 \cdot 10^{4}$	$2.20 \cdot 10^{0}$	$3.79 \cdot 10^{4}$	$3.16 \cdot 10^{1}$	$3.64 \cdot 10^{4}$	$1.05 \cdot 10^{-1}$	$3.70 \cdot 10^{4}$
r4	$3.38 \cdot 10^{4}$	$1.11 \cdot 10^{5}$	$3.06 \cdot 10^{4}$	$1.31 \cdot 10^{5}$	$3.42 \cdot 10^{4}$	$9.00 \cdot 10^{4}$	$3.39 \cdot 10^{4}$	$9.30 \cdot 10^{4}$	$2.01 \cdot 10^{4}$	$1.20 \cdot 10^{5}$
Mean ε_a	0.004		0.001		<0.001		0.041		0.004	
Mean ε_r	0.001%		<0.001%		<0.001%		0.019%		0.002%	

A correct fitting of the model to the experimental data was achieved (Table V.2), which was slightly less accurate for:

- « Celluloses II » during the non-isothermal torrefaction: with the model, the degradation begins at a temperature close to 300°C, later than observed for the experimental data.
- « Hemicelluloses 1 » during the isothermal torrefaction: the model does not predict any solid degradation during this part, while experiments show a low solid mass loss.

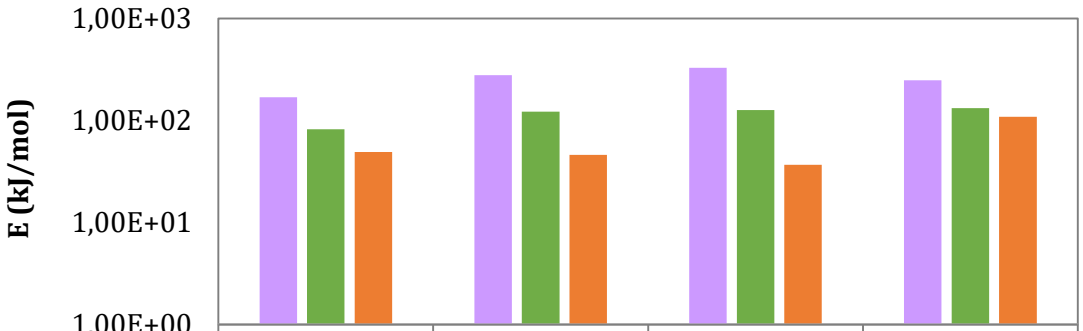
These parameters remain generally close to those proposed by Nocquet in the case of beech [7], except for lignin.

Similar values of activation energies were found for reactions 1, 2 and 3 in the case of extracted cellulose fractions. This might indicate that the mechanism of decomposition of cellulose in this step is independent of the biomass type. For the fourth reaction, activation energies for ash-wood and pine are sensibly higher to that of the other biomasses, which might indicate a higher resistance of the chemical bonds to be broken in this step for these biomasses.

The activation energies for the extracted hemicelluloses remain slightly lower for the first reaction, and the same order of magnitude for the other three reactions. Furthermore, the highest variability was found for the first reaction. This might indicate that the main difference in hemicellulose degradation, presumably derived from differences in their sugar composition in function of the biomass type, might correspond to the beginning of their transformation. However, this hypothesis needs to be confirmed by a more accurate determination of the sugar composition.

Lignin activation energies appear as heterogeneous for all reactions except for the third one. The low activation energy of the second reaction for pine lignin is noteworthy, which might indicate an easy devolatilization of this fraction from the beginning of its transformation.

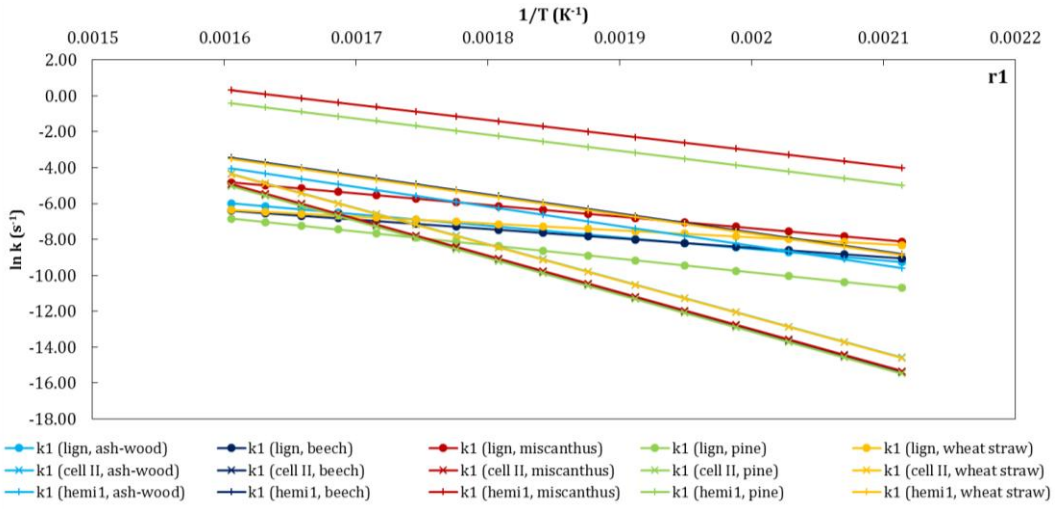
By comparing the average activation energy per chemical reaction for the three extracted fractions, it is revealed that this parameter is systematically higher for the « cellulose II » fraction, followed by « hemicelluloses 1» and « lignin » (Figure V.18). Interestingly, the highest difference in the activation energies for volatile species formation and solid transformation were observed for the intermediate steps (reactions 2 and 3).

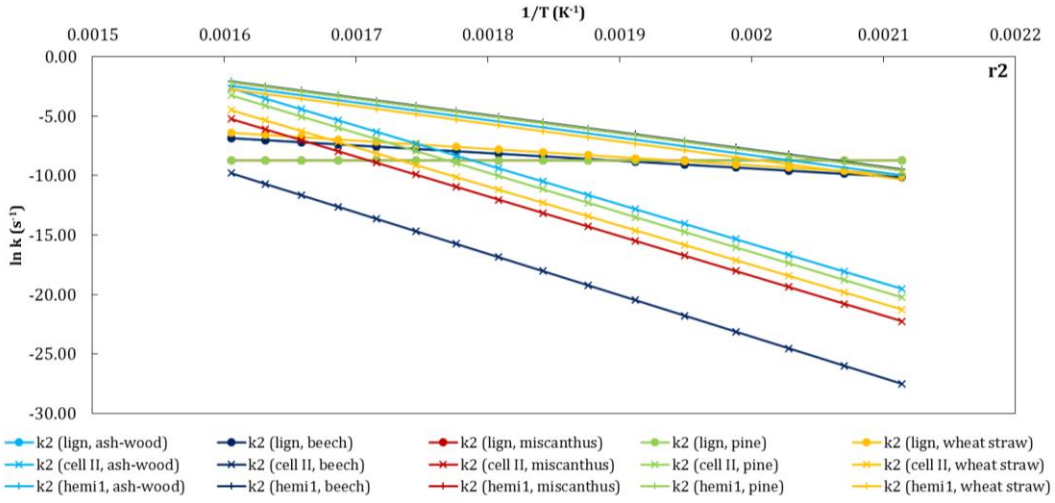


	r1	r2	r3	r4
Cellulose II	1,69E+02	2,79E+02	3,30E+02	2,49E+02
Hemicellulose	8,22E+01	1,22E+02	1,27E+02	1,33E+02
Lignine	4,91E+01	4,61E+01	3,68E+01	1,09E+02

Figure V.18. Average of the activation energy per chemical reaction for « cellulose II », « hemicelluloses 1 » and « lignin »

Kinetic constants for the four reactions of the torrefaction model were calculated per extracted macromolecular component for a typical torrefaction temperature range between 200 and 350 °C and represented as typically for a 1st order chemical reaction (ln k versus 1/T, Figure V.19).





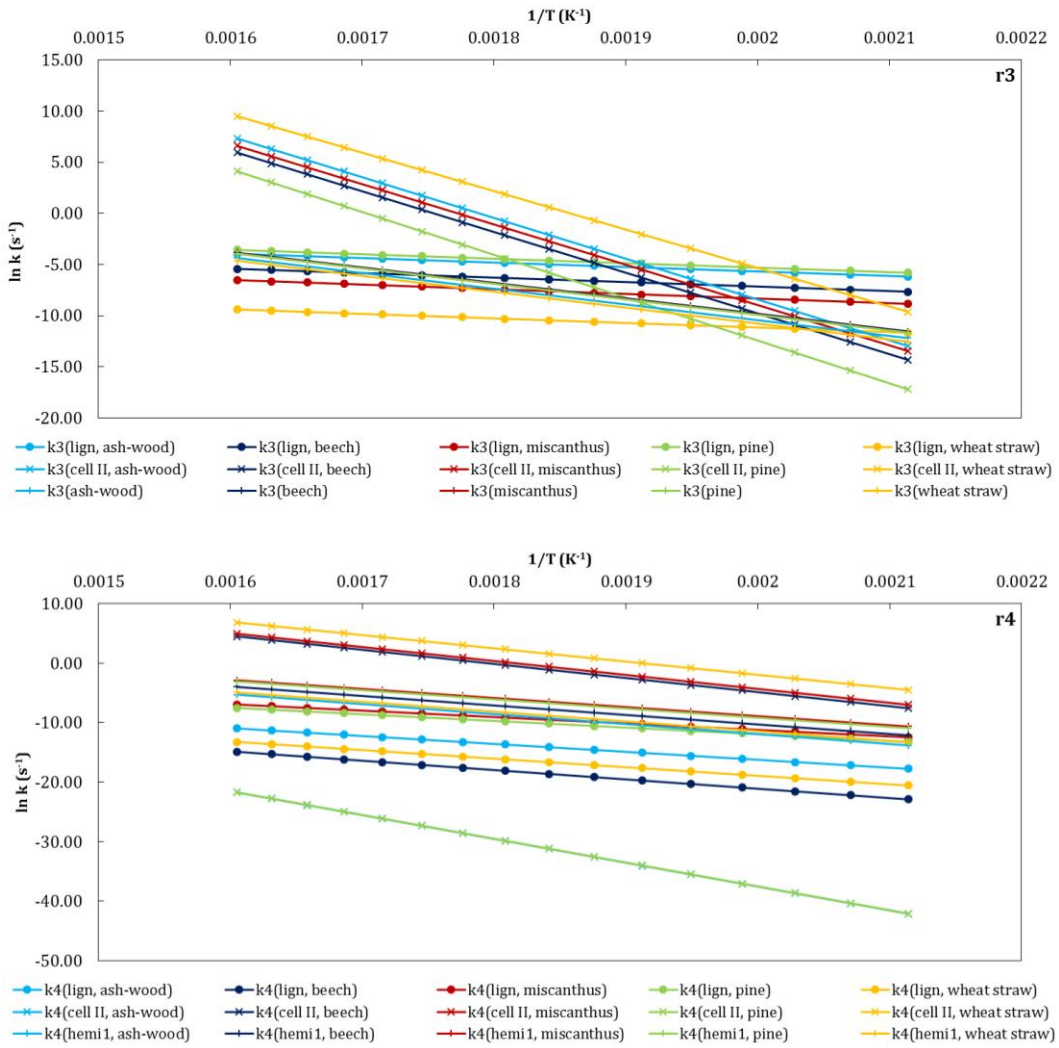


Figure V.19. Representation of the kinetic constant (ln) in function of the inverse of the temperature for the four chemical reactions (r1 to r4) of the torrefaction model based on « cellulose II », « hemicelluloses 1 » and « lignin » fractions

The kinetic constants of the four reactions concerning the « cellulose II » fraction present a stronger influence of the temperature than for « hemicelluloses 1» and « lignin » fractions. This is in agreement with its degradation enhanced at torrefaction temperatures close to 300 °C. Oppositely, the kinetic constants are little affected by the temperature for « lignin » fractions, except for the pine fraction, which is coherent with their slight degradation in the torrefaction temperature range. The main differences in the kinetic constant for the « hemicelluloses 1 » fractions are observed for the first reaction, which is consistent with its degradation in torrefaction depending on its sugar composition and from low torrefaction temperatures.

2.2.2. Comparison of the simplified additive model and the experimental data

2.2.2.1. Comparison of the torrefaction model and the raw biomass

The modelled behavior of each biomass in torrefaction was compared to the experimental results (Figure V.20a and V.20b). It is important to note that this approach is based on the

hypothesis that the initial macromolecular composition of biomass describes correctly the ratio between the extracted fractions to reconstruct raw biomass, which implies that:

- Extraction procedure is not supposed to modify the extracted fractions.
- « Cellulose II », « hemicelluloses 1 » and « lignin » extracted fractions are supposed to be representative of cellulose, hemicelluloses and lignin in biomass.
- Extractives are supposed not to participate in biomass torrefaction.
- Ashes are supposed to be inert in the torrefaction temperature range.

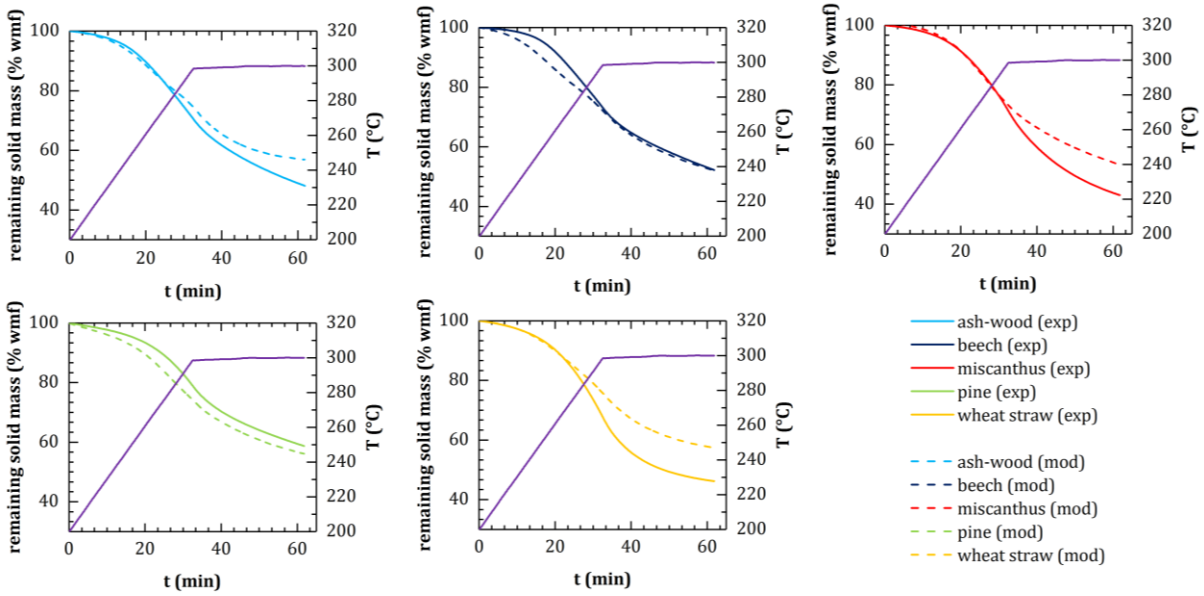


Figure V.20a. Remaining solid mass loss versus temperature and time during torrefaction first-level model (dotted line) and experimental data for raw biomasses in TGA-GC/MS (line)

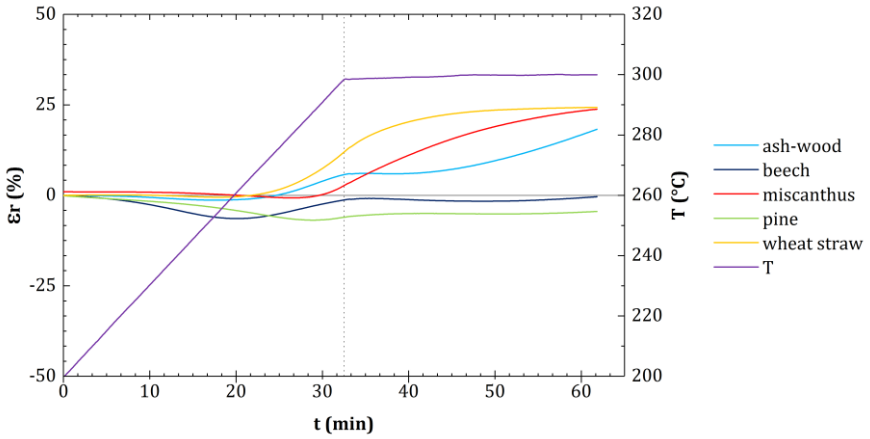


Figure V.20b. Relative error between remaining solid mass in torrefaction estimated through the first-level model and that obtained for raw biomass in TGA-GC/MS

The prediction by the model depends on the biomass and on the operating conditions. The model generally shows a slight underestimation of the remaining solid mass for pine, while it overestimates the remaining solid mass for ash-wood, miscanthus and wheat straw, particularly in the isothermal step. A correct prediction of the remaining solid in the non-isothermal

torrefaction was obtained for ash-wood, miscanthus and wheat straw, while the prediction in the subsequent isothermal step is better for beech. In the case of pine, the difference between the model curve and the experimental results is constant, around 5%, from intermediate torrefaction temperatures to the end of the isothermal step. This error can be considered as acceptable mainly due to uncertainties in sugar composition determination. In the case of biomasses from the same family, similarities can be remarked for the fitting obtained for miscanthus and wheat straw, but not for ash-wood and beech.

The dynamic prediction of the model according to time and temperature conditions was tested with beech under operating conditions different from those used for the fitting of kinetics parameters. The operating conditions of the torrefaction procedure were set as follows: the dynamic heating was carried out at 3°C/min, interrupted by two isothermal steps of 30 minutes at 280 and 300°C (Figure V.21). The model fits fairly well the solid kinetics, with a slight shift, but presumably in the range of experimental uncertainties, provided that the maximal relative error in the over-estimation of mass loss is inferior to 8%.

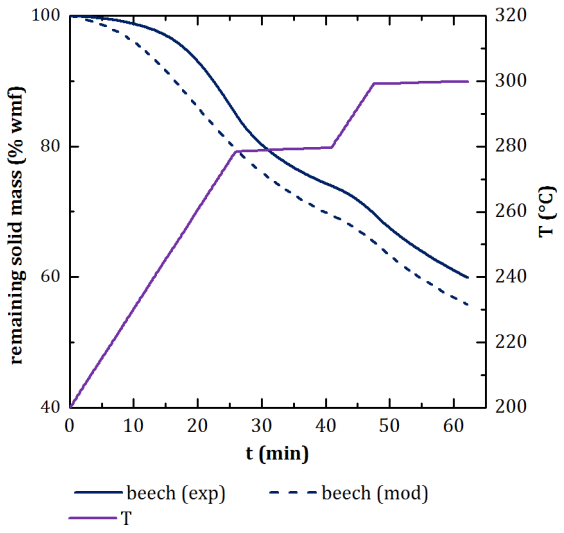


Figure V.21. Remaining solid mass loss versus temperature and time during torrefaction by the simplified additive model (dotted line) and the experimental data for beech in TGA-GC/MS (line)

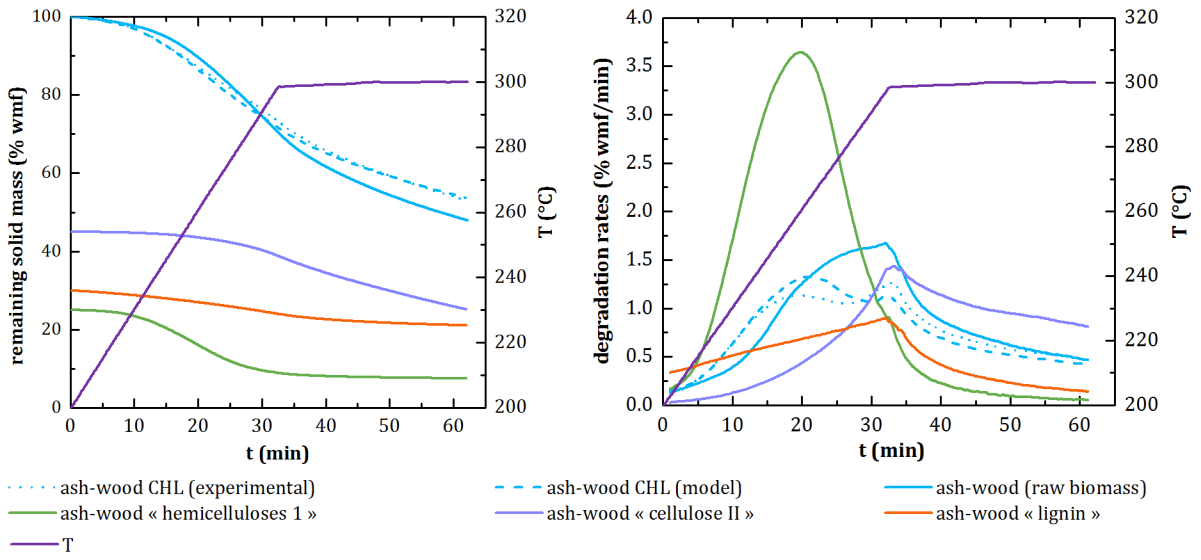
Besides, the difference between the model and the experimental results might also arise from elements that were not considered in its definition, which include:

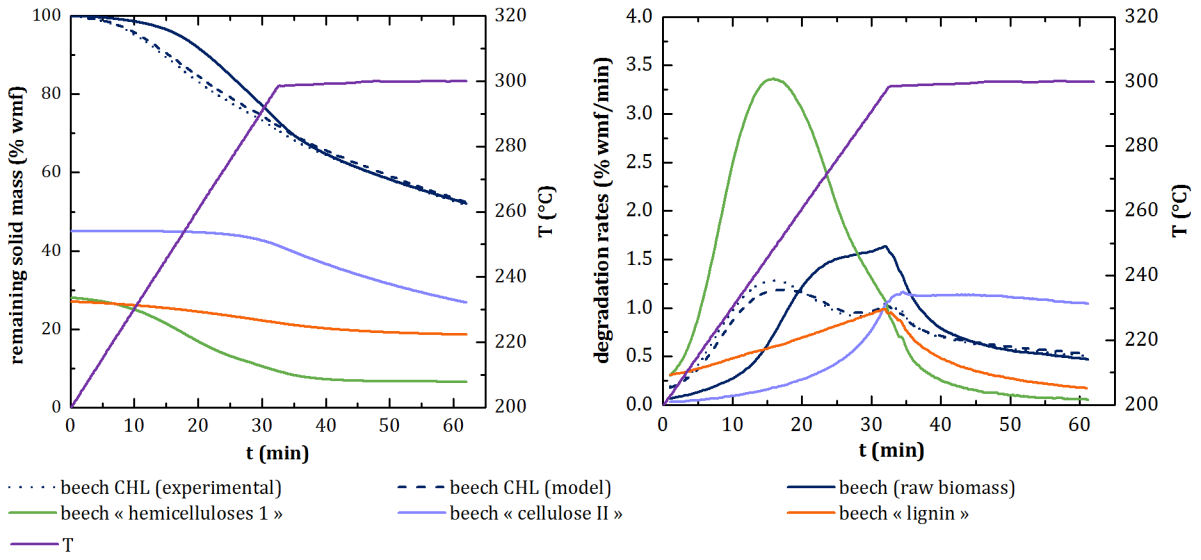
- Residual hemicelluloses («hemicelluloses 2» fraction).
- Change in the cellulose structure (type I to type II) and decrease in the polymerization degree.
- Ash and extractives, that were supposed inactive in the torrefaction temperature range.
- Interactions between macromolecular components, which were broken to separate the extracted fractions from biomass.

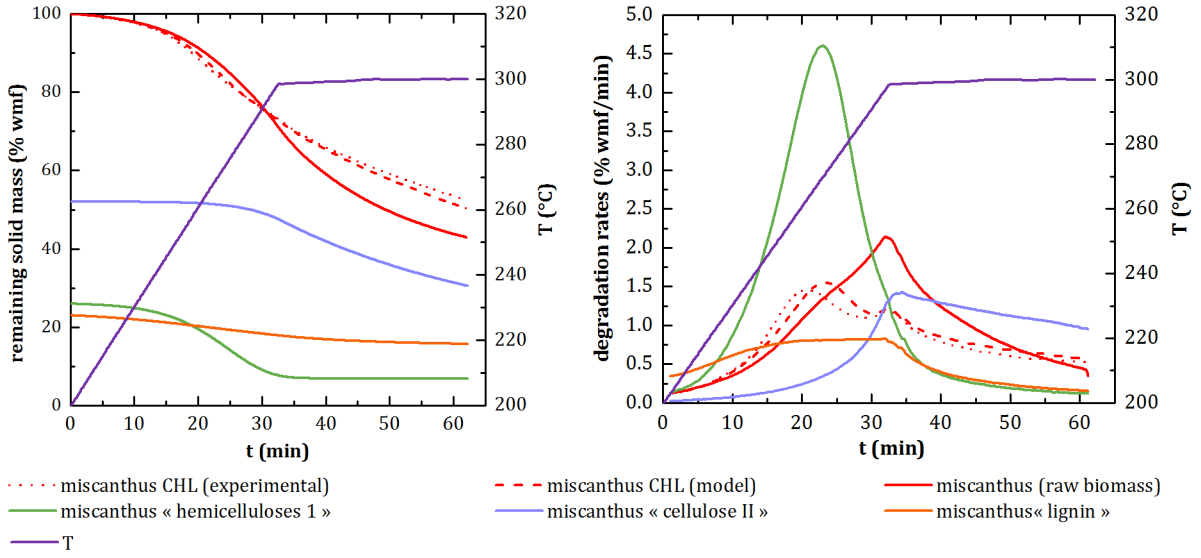
2.2.2.2. Comparison of the torrefaction model prediction, the ternary mixtures and the extracted fraction experiments

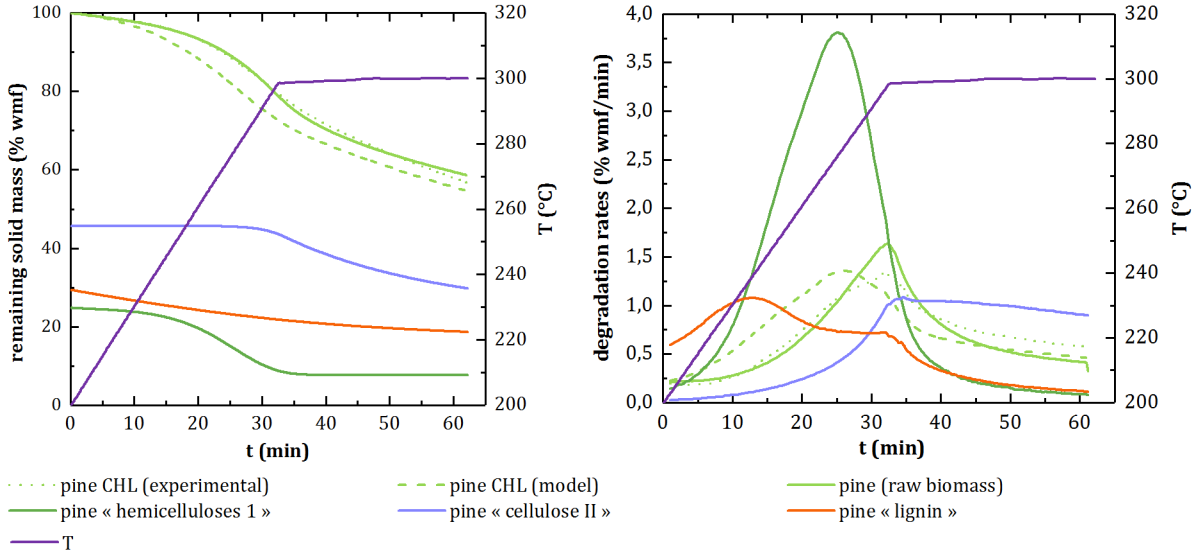
The result of the additive model was compared to the experimental data obtained on the raw biomass and on the ternary mixtures. The results with the ternary mixture (CHL experimental) and the prediction by the model are rather similar in terms of remaining solid mass profiles for all biomasses of study except for pine. In this last case, the remaining solid mass profile of the ternary mixture is similar to that of the raw biomass (Figure V.22, left). The comparison of the degradation rate profiles was added for a better identification of the differences between the solid kinetic profiles (Figure V.22, right). In the case of pine, the additive model fits to the raw biomass in terms of degradation rates profiles, while the ternary mixture clearly presents a translation of this behavior to earlier torrefaction temperatures. This might indicate the existence of interactions in solid phase for the pine ternary mixture which favored an earlier degradation of the components of the mixture.

The first maximum in the degradation rate profiles of the mixtures corresponds to the behavior of the «hemicelluloses 1» fractions, except for pine. The temperature of this maximum of degradation rate is in agreement to those obtained for the «hemicelluloses 1»; however, the absolute value of the degradation rate is lower in the case of the mixture, which is coherent with its composition. The second maximum, close to 300°C, principally corresponds to the behavior of the «cellulose II» fraction. This macromolecular compound is mostly degraded at temperatures close and above 300°C, so its degradation is interrupted by stopping the increasing temperature at 300°C. The impact of lignin on both maximums is low, as it is only slightly and progressively degraded in this temperature range (maximum degradation rates measured for the extracted fraction are around 1.0 %wmf/min). These maxima in the degradation rates profiles were reproduced in the additive model behavior.




remaining solid mass (% wmf)
T (°C)
t (min)
degradation rates (% wmf/min)
beech CHL (experimental)
beech CHL (model)
beech (raw biomass)
beech « hemicelluloses 1 »
beech « cellulose II »
beech « lignin »
T


remaining solid mass (% wmf)
T (°C)
t (min)
degradation rates (% wmf/min)
miscanthus CHL (experimental)
miscanthus CHL (model)
miscanthus (raw biomass)
miscanthus « hemicelluloses 1 »
miscanthus « cellulose II »
miscanthus« lignin »
T


remaining solid mass (% wmf)
T (°C)
t (min)
degradation rates (% wmf/min)
pine CHL (experimental)
pine CHL (model)
pine (raw biomass)
pine « hemicelluloses 1 »
pine « cellulose II »
pine « lignin »
T

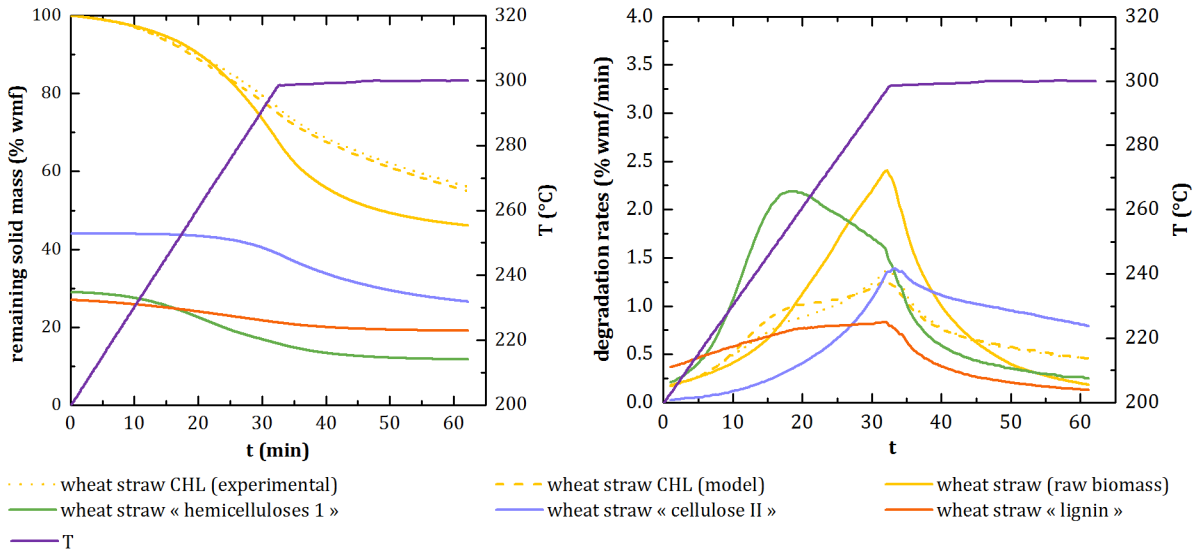


Figure V.22. Remaining solid mass (left) and degradation rates (right) versus time and temperature obtained in torrefaction in TGA-GC/MS of ternary mixtures, raw biomass and «cellulose II», «hemicelluloses 1» and «lignin» extracted fractions from 5 biomasses, compared to the simplified torrefaction model

According to the results, the additive model and the mixtures tend to describe solid kinetics in a similar way, which is consequence of the similitudes between the degradation patterns of the respective macromolecular components extracted from different biomasses. This observation might indicate that no interaction in solid phase happens during torrefaction of the physical mixture of the extracted fractions, except for pine. These results suggest that interactions between macromolecular components, which were broken during the extraction procedure, might influence biomass behavior in torrefaction.

2.2.1.3. Attempt of representation of interactions between macromolecular components

The behavior of the ternary mixtures (CHL exp) and of the simplified additive model (CHL mod, absolute value) is compared to the behavior of raw biomass (rawb) in Figure V.23 (absolute difference for each curve).

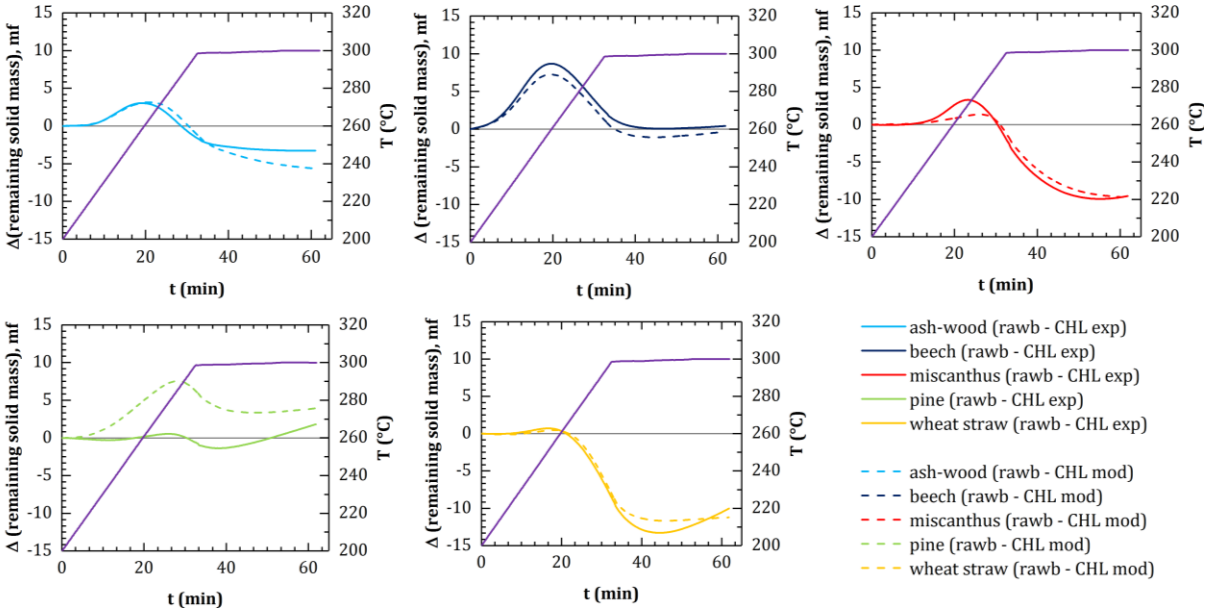


Figure V.23. Difference in remaining solid mass loss versus temperature and time in torrefaction between raw biomass (rawb) and either ternary mixtures (CHL exp) or additive model (CHL mod)

The differences observed are of course in agreement with the previous observations from Figures V.20 and 21. The difference between raw biomass and model behaviors in dynamic conditions is lower than that related to ternary mixtures, except for pine and wheat straw. This could be derived from the experimental uncertainties associated to the mixture of extracted fractions. The difference between raw biomass and the macromolecular components model might be mainly due to biomass inter-molecular interactions, as they are the main missing parameter in the additive model.

In conclusion, the first approach to model biomass torrefaction through the extracted macromolecular compounds was shown to be more successful than previous studies obtained with commercial compounds. The main advantage of this approach is the possibility of adapting the torrefaction model to the biomass type. However, results have shown some discrepancy between the additive model based on the main extracted fractions and the raw biomass. The difference between the experimental data and the additive model prediction might give an insight about the intra-macromolecular interactions in biomass.

2.3. Second-level model

At this stage, we aimed to consider new assumptions which could reduce the gaps between experiments and additive model predictions. These ones are as follows:

- replace « cellulose II » fraction kinetics by « cellulose I », as its crystalline structure is closer to that of the native cellulose in biomass;
- correct the hemicelluloses contribution by the weighted contribution of « hemicelluloses 1

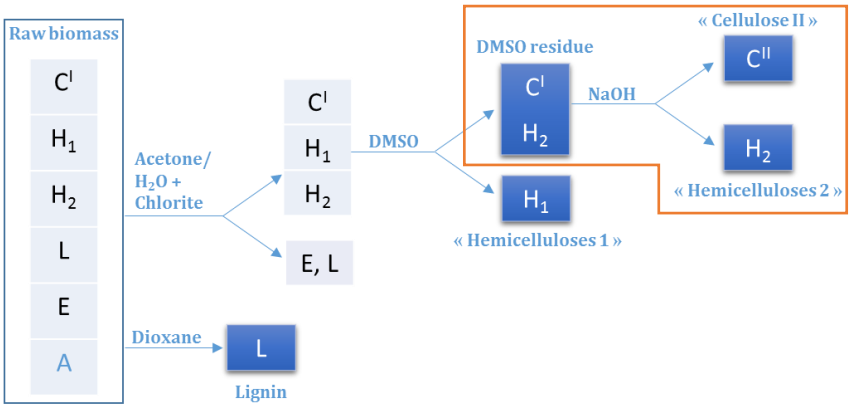
» and « hemicelluloses 2 » fractions.

To reach this goal, the « cellulose I » and « hemicelluloses 1 » fractions in the « DMSO residue » must be estimated as well as the ratio hemicellulose 1/ hemicellulose 2 in the biomass. This was performed thanks to sugar mass balances carried out on the extracted fractions containing polysaccharides.

2.3.1. Sugar mass balances

2.3.1.1. DMSO fraction composition

A sub-system was defined in the extraction procedure, including « DMSO residue », « cellulose II» and « hemicelluloses 2 » fractions (Figure V.24). The composition in the major sugars of each fraction, namely glucose and xylose, was considered. Minor sugars (mannose, arabinose and galactose) were discarded for sugar mass balances due to the higher uncertainty in their determination. Acetyl groups were also discarded since part of them is destroyed with the alkaline treatment, being also a minor entity in polysaccharide composition.



Macromolecular component	Abbreviation
Cellulose	C^I and C^{II}
Hemicelluloses	H_1
	H_2
Lignin	L
Extractives	E
Ash	A

Figure V.24. Detail of the sub-system for the sugar mass balance of the « DMSO residue » fraction

In a mass-fraction basis, the composition of the « DMSO residue » fraction is determined as follows:

$$1 = x_{C^{II},DMSO_r} + x_{H_2,DMSO_r} \quad \text{Eq. 3}$$

Where:

$x_{C^{II},DMSO_r}$: mass fraction of « cellulose II » in « DMSO residue ».

$x_{H_2,DMSO_r}$: mass fraction of « hemicelluloses 2 » in « DMSO residue ».

For an individual sugar (glucose, Glu, or xylose, Xyl) in « DMSO residue » fraction Eq. 4 can be written:

$$x_{Glu,DMSO_r} = x_{Glu,C^{II}}\, x_{C^{II},DMSO_r} + x_{Glu,H_2}\, x_{H_2,DMSO_r} \quad \text{Eq. 4}$$

$x_{Glu,DMSO_r}$: mass fraction of glucose in the « DMSO residue » fraction.

$x_{Glu,C^{II}}$: mass fraction of glucose in the « cellulose II » fraction.

x_{Glu,H_2}: mass fraction of glucose in the « hemicelluloses 2 » fraction.

Assuming that the only difference between both cellulose fractions is the structure arrangement, which affects the crystallinity type structure (I or II), « cellulose I » and « cellulose II » fractions are considered equivalent in terms of mass in « DMSO residue » and sugar composition (Eq. 5).

$$x_{C^I,DMSO_r} = x_{C^{II},DMSO_r} \quad \text{Eq. 5}$$

Knowing the sugar composition of the fractions (Tables III.3 and III.4), $x_{C^I,DMSO}$ and $x_{H_2,DMSO}$ can be calculated as:

$$x_{C^I,DMSO_r} = \frac{x_{Gl,DMSO\ r} - x_{Gl,H_2}}{x_{Gl,C^{II}} - x_{Gl,H_2}} \quad \text{Eq. 6}$$

$$x_{H_2,DMSO_r} = 1 - x_{C^I,DMSO_r} \quad \text{Eq. 7}$$

Values calculated for the two main sugars, xylose and glucose, are reported in Table V.3. The average of both results per biomass was used and the relative error between them is expressed. It is important to note that a considerable error margin should be admitted for these results, derived from the difficulties to accurately determine sugar composition.

Table V.3. Composition of the « DMSO residue » fraction in « cellulose I » and « hemicelluloses 2 » calculated by glucose and xylose sugar mass balances

	« cellulose I » mass fraction in DMSO residue (% wmf)				
	Ash-wood	**Beech**	**Miscanthus**	**Pine**	**Wheat straw**
Glucose	74.4	75.3	74.1	78.0	76.1
Xylose	80.3	79.7	86.2	79.8	88.4
Average	77.3	77.5	80.1	78.9	82.3
Absolute error	5.9	4.4	12.1	1.8	12.3
Relative error (%)	8.1%	5.9%	16.4%	2.3%	16.1%
	« hemicelluloses 2 » mass fraction in DMSO residue (% wmf)				
	Ash-wood	**Beech**	**Miscanthus**	**Pine**	**Wheat straw**
Glucose	25.6	24.7	25.9	22.0	23.9
Xylose	19.7	20.3	13.8	20.2	11.6
Average	22.7	22.5	19.9	21.1	17.7
Absolute error	5.9	4.4	12.1	1.8	12.3
Relative error (%)	23.3%	18.1%	46.9%	8.0%	51.4%

The difference in fraction ratios was more important for agricultural biomasses, namely miscanthus and wheat straw, which is coherent with the higher uncertainty associated with the determination of their sugar composition. The total polysaccharide content is measured for a given biomass; then, the distinction between cellulose composition, only based on glucose sugar,

and hemicelluloses composition, composed by glucose and other sugars, is carried out based on typical rations mannose/glucose in hemicelluloses from the literature. It is assumed that this ratio is 1.6 for deciduous wood and 1.0 for coniferous wood. This last ratio value is also supposed for agricultural biomasses and herbaceous crops, although the sugar distribution of their hemicelluloses is less well-known. Furthermore, the lower the sugar amount in biomass is, the higher is the uncertainty associated to its determination. However, the results stand on the average 0.8/0.2 ratio for « cellulose I » and « hemicelluloses 2 » in « DMSO residue ».

2.3.1.2. Hemicelluloses composition

The objective of this section is to determine the ratio of « hemicelluloses 1 » and « hemicelluloses 2 » fractions in the total « hemicelluloses » in biomass. This will allow to re-build the initial « hemicelluloses » kinetic behavior in torrefaction by weighting the kinetic behavior of both extracted fractions.

The sub-system to be defined would require a global polysaccharide balance, including cellulose and hemicellulose fractions. This is due to the presence of glucose in cellulose, while the other sugars are only present in hemicellulose fractions. However, this global balance would cumulate non-negligible errors in sugar determination for all fractions derived from the whole extraction procedure. In order to replace it, it is proposed to follow the previous reasoning about the « DMSO residue » fraction until the determination of the ratio between the hemicellulose fractions.

The mass of cellulose in the « DMSO residue » fraction is kept from that of the initial raw biomass, as it is extracted in a single fraction. Calculations based on mass-fractions are proposed.

The mass fraction of cellulose and hemicelluloses is firstly estimated, as results in Table III.3 are not normalized to 100%.

$$x_{C,rb} = \frac{m'_{C,rb}\,(as\ measured\ )}{mass\ \ balance\ \ (measured\ )} \qquad \text{Eq. 8}$$

$$x_{H,rb} = \frac{m'_{H,rb}\,(as\ measured\ )}{mass\ \ balance\ \ (measured\ )} \qquad \text{Eq. 9}$$

$x_{C,rb}$: mass fraction of cellulose in raw biomass (same as for « cellulose II »).

$x_{H,rb}$: mass fraction of hemicelluloses in raw biomass.

$m'_{C,rb}\,(as\ measured)$, $m'_{H,rb}\,(as\ measured)$ and $mass\ balance\ (measured)$ are values from the raw biomasses characterization (Table III.3).

As a result, the mass fraction of « DMSO residue » fraction derived from the extraction procedure can be calculated:

$$x_{DMSO_r,rb} = \frac{x_{C,rb}}{x_{C^{II},DMSO\ r}} \quad \text{Eq. 10}$$

$x_{DMSO_r,rb}$: mass fraction of « DMSO residue » in raw biomass.

The mass fraction of « hemicelluloses 2 » in raw biomass is, by difference:

$$x_{H_2,rb} = x_{DMSO_r,rb} - x_{C,rb} \quad \text{Eq. 11}$$

$x_{H_2,rb}$: mass fraction of « hemicelluloses 2 » in raw biomass.

The mass fraction of « hemicelluloses 1 » fraction can be derived as follows:

$$x_{H_1,rb} = x_{H,rb} - x_{H_2,rb} \quad \text{Eq. 12}$$

$x_{H_1,rb}$: mass fraction of « hemicelluloses 1 » fraction in raw biomass.

The composition of the total hemicelluloses in biomass is then calculated:

$$x_{H_1,H_T} = \frac{x_{H_1,rb}}{x_{H_1,rb} + x_{H_2,rb}} \quad \text{Eq. 13}$$

$$x_{H_2,H_T} = \frac{x_{H_2,rb}}{x_{H_1,rb} + x_{H_2,rb}} \quad \text{Eq. 14}$$

x_{H_1,H_T}: mass fraction of « hemicelluloses 1 » in total hemicelluloses from biomass.

x_{H_2,H_T}: mass fraction of « hemicelluloses 2 » in total hemicelluloses from biomass.

Finally, the ratio between the hemicellulose fractions is defined as:

$$\frac{x_{H_1,H_T}}{x_{H_2,H_T}} \quad \text{Eq. 15}$$

By using Eqs. 8 to 15, the composition of the hemicellulose fraction was calculated (Table V.4).

Table V.4. Composition of total hemicelluloses in raw biomass

	total « hemicelluloses » fraction composition, (% wmf)				
	Ash-wood	**Beech**	**Miscanthus**	**Pine**	**Wheat straw**
« hemicelluloses 1 »	47.4	34.9	53.5	33.9	47.4
« hemicelluloses 2 »	52.6	65.1	46.5	66.1	52.6

These results suggest that none of the hemicellulose fractions is negligible, which is coherent with their different sugar composition. As a result, it can be stated that « hemicelluloses 1 » and « hemicelluloses 2 » are complementary fractions to describe hemicelluloses in biomass, which is justified by their different sugar composition, and thus torrefaction behavior, for a given biomass.

In order to check these results of hemicelluloses composition, the mass balance on glucose was

estimated (Eq. 16), by using the calculated proportions of « hemicelluloses 1 » and « hemicelluloses 2 » in raw biomass (Table V.4).

$$x_{Glu,rb} = x_{Glu,H_1} x_{H_1,rb} + x_{Glu,H_2}\, x_{H_2,rb} + x_{Glu,C}\, x_{C,rb} \qquad \text{Eq. 16}$$

$x_{Glu,rb}$: mass fraction of glucose (Glu) in raw biomass.

x_{Glu,H_1}: mass fraction of glucose (Glu) in « hemicelluloses 1 ».

$x_{Gl,C}$: mass fraction of glucose (Glu) in « cellulose II ».

Then, the results were compared to the glucose composition measured in raw biomass, given by the sugar characterization (Table III.4).

Table V.5. Total glucose in raw biomass estimated by the composition of the extracted fractions

	Glucose (% wmf)				
	Ash-wood	**Beech**	**Miscanthus**	**Pine**	**Wheat straw**
Calculated Sugar mass balances	39.7	44.7	40.4	47.4	41.0
Measured Characterization tables	38.6	39.5	42.9	46.9	35.8
Absolute error	1.1	5.2	2.5	0.5	5.2
Relative error (%)	2.7%	13.2%	5.7%	1.1%	14.3%

By comparing calculated and measured values of glucose, they differ in function of the biomass type and the sugar considered. The acceptable relative error between the measured and the calculated values for glucose was considered around 15.0 % wmf, due to the uncertainty in sugar characterizations. While estimations carried out based on sugar mass balances for glucose is below this limit, results on the estimation of the total hemicelluloses composition can be considered as acceptable.

To sum up, the determination of hemicelluloses composition is validated by the sugar mass balances, with the limitations of the uncertainty associated to sugar composition determination in biomass and in the corresponding extracted fractions. The calculated composition is an approximation of the actual composition of hemicelluloses in biomass, which intends to improve hemicelluloses representation by considering both extracted fractions. Anyway, the results obtained justify that none of both extracted fractions can be neglected in the total hemicellulose description, at least in terms of solid kinetics.

.3.2. Reconstruction of the complementary fractions

2.3.2.1. « Cellulose I »

The « cellulose I » behavior in torrefaction was reconstructed from the composition of the « DMSO residue » fraction:

$$m_{DMSO_r}(t_i, T_i) = x_{C^I,DMSO_r}\, m_{C^I}(t_i, T_i) + x_{H_2,DMSO_r}\, m_{H_2}(t_i, T_i) \qquad \text{Eq. 17}$$

$$T_i \in [200,300]°C$$

Where:

$m_{DMSO_r}(t_i, T_i)$: instantaneous remaining solid mass of « DMSO residue »; t = 0, m($DMSO_r$) = 1.

$m_{C^I}(t_i, T_i)$: instantaneous remaining solid mass of « cellulose I »; t = 0, m(C^I) = 1.

$m_{C^{II}}(t_i, T_i)$: instantaneous remaining solid mass of « cellulose II »; t = 0, m(C^{II}) = 1.

$x_{C^I,DMSO_r}$: initial mass fraction of « cellulose I » in « DMSO residue » (at t = 0).

$x_{C^{II},DMSO_r}$: initial mass fraction of « cellulose II » in « DMSO residue » (at t = 0).

t_i, T_i: instantaneous values of time and temperature.

Then, the behavior of the « cellulose I » and the « cellulose II » fractions was compared (Figure V.25a). The relative error between these two fractions is also represented (Figure V.25b).

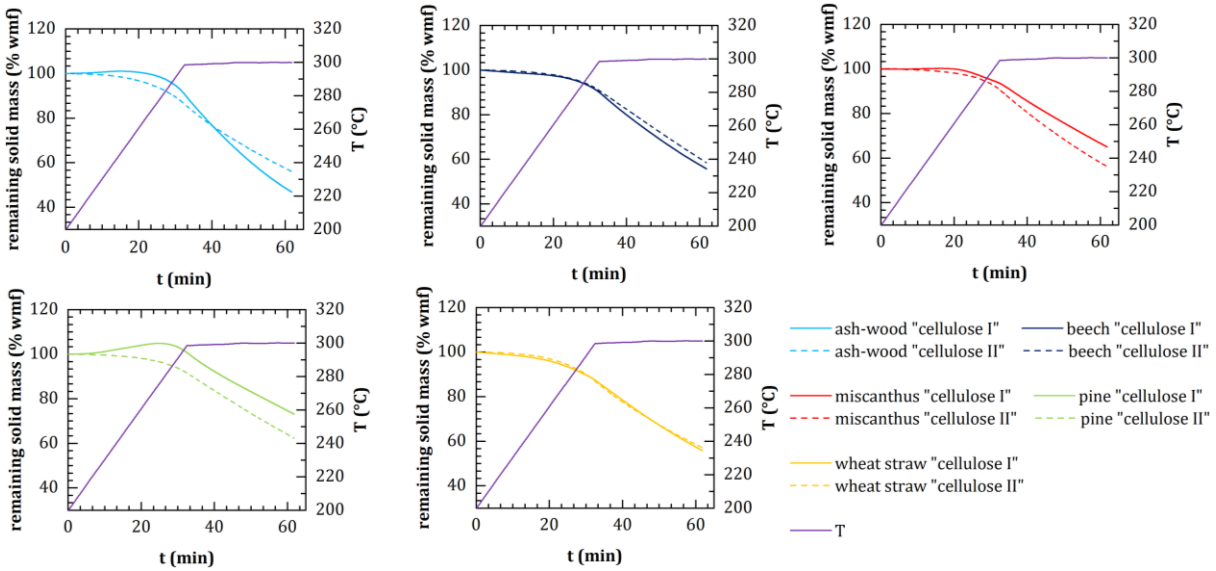


Figure V.25a. Remaining solid mass loss versus temperature and time in torrefaction for « cellulose I » and « cellulose II » fractions in TGA-GC/MS

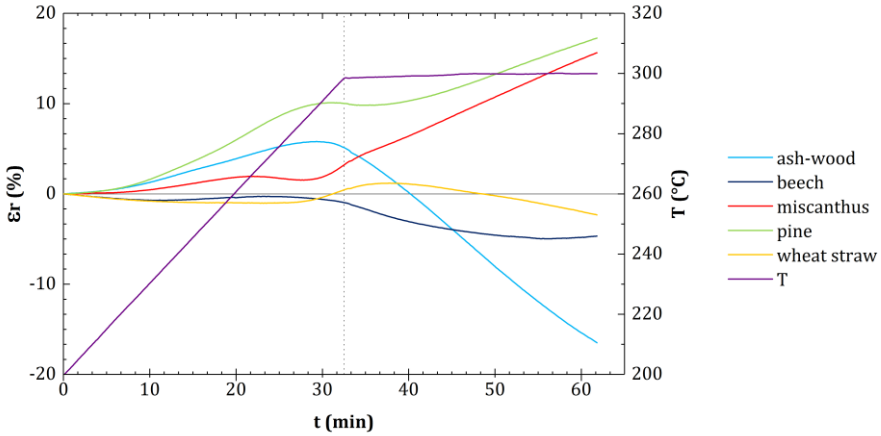


Figure V.25b. Relative error between remaining solid mass estimated through « cellulose I » and « cellulose II » fractions in TGA-GC/MS

The degradation of « cellulose I » is attenuated at the beginning of the isothermal torrefaction, compared to « cellulose II ». In the cases of miscanthus, pine and ash-wood, the reconstructed curves indicate a remaining solid mass higher than 100 %, which implies a slowing down of the solid mass loss compared to « cellulose II ». This might come from a slower degradation of « cellulose I » compared to « cellulose II ». It might also be derived from the subtraction of the « cellulose I » behavior of the « DMSO residue », which includes interactions between « cellulose I » and « hemicelluloses 2 ». Uncertainties in sugar characterization might also influence this behavior. The reconstructed curves, including interactions, were directly used in the second-level model.

2.3.2.2. Total « hemicelluloses »

The total « hemicelluloses » behavior in torrefaction was reconstructed for each biomass through a weighted sum of the contributions of the kinetic behavior of « hemicelluloses 1 » and « hemicelluloses 2 ». The remaining solid mass of total « hemicelluloses » at a given time and temperature is:

$$m_{H_T}(t_i, T_i) = x_{H_1,H_T}\, m_{H_1}(t_i, T_i) + x_{H_2,H_T}\, m_{H_2}(t_i, T_i) \qquad \text{Eq. 18}$$

$$T_i \in [200,300]°C$$

Where:

$m_{H_T}(t_i, T_i)$: instantaneous remaining solid mass of total hemicelluloses; t = 0, m(H_T) = 1.

$m_{H_1}(t_i, T_i)$: instantaneous remaining solid mass of « hemicelluloses 1 »; t = 0, m(H_1) = 1.

$m_{H_2}(t_i, T_i)$: instantaneous remaining solid mass of « hemicelluloses 2 »; t = 0, m(H_2) = 1.

x_{H_1,H_T} : initial mass fraction of « hemicelluloses 1 » in total hemicelluloses (at t = 0).

x_{H_2,H_T} : initial mass fraction of « hemicelluloses 2 » in total hemicelluloses (at t = 0).

t_i, T_i: instantaneous values of time and temperature.

The total hemicelluloses behavior in torrefaction was reconstructed per biomass (Figure V.26).

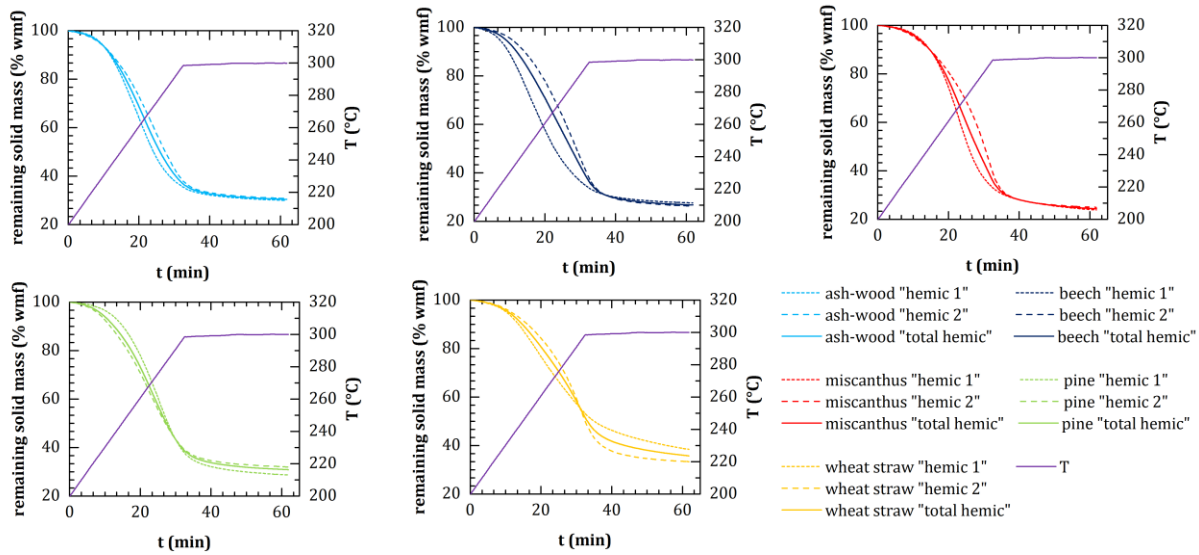


Figure V.26. Remaining solid mass loss versus temperature and time in torrefaction for hemicelluloses fractions in TGA-GC/MS

The behavior of both hemicelluloses fractions is different in the dynamic step, which concerns the major degradation of this fraction. The transformation depends on the sugar composition. Solid mass loss is faster in the case of all « hemicelluloses 1 » except for pine. This can be due to the higher composition in mannose of the pine « hemicelluloses 1 », which is known to be degraded slower than xylose, the major sugar of the other « hemicelluloses 1 » fractions. Oppositely, a considerable mannose content in wheat straw « hemicelluloses 2 » might be responsible of the slowest degradation of this fraction compared to « hemicelluloses 1 ».

During the isothermal step at 300°C, the behavior of both hemicelluloses fraction is nearly equivalent except in the case of the wheat straw « hemicelluloses 2 ». This fraction is mostly degraded and tends to the stabilization of the mass loss, while the « hemicelluloses 1 » fraction slowly continues its degradation. This might also be due to the high mannose content in wheat straw « hemicelluloses 2 » fraction.

2.3.3. Representation of the second-level model

The reconstructed fractions « cellulose I » and total « hemicelluloses » can be integrated in the additive model to improve the representation of biomass. Consequently, the model results in:

$$m'_{rb}(t_i, T_i) = x_{C,rb}\, m_{C^I}(t_i, T_i) + x_{H,rb}\, m_{H_T}(t_i, T_i) + x_{L,rb}\, m_L(t_i, T_i) \qquad \text{Eq. 24}$$

$$T_i \in [200,300]°C$$

Where:

$m'_{rb}(t_i, T_i)$: instantaneous remaining solid mass of raw biomass; t = 0, m(rb) = 1; 2nd level model.

The structure of the 2-succesive-step kinetic model of Di Blasi and Lanzetta was used again. The kinetic parameters were recalculated for the total « hemicelluloses » (Table V.7), while they were conserved for « lignin » and « cellulose I » fractions. Absolute error and relative error

expressed as the average of the square of relative errors are indicated. In this last case, it was not possible to adjust the new behavior of « cellulose I » (Figure V.25a,b) to the Di Blasi structure. The order of magnitude of the kinetic constants associated to cellulose and its low degradation in torrefaction allow to keep the calculated parameters for « cellulose II ».

Table V.7. Kinetic parameters of the 2-succesive steps kinetic model calculated for the new fractions

	total « hemicelluloses »									
	ash-wood		beech		miscanthus		pine		wheat straw	
	k_0 (s^{-1})	E (J/mol)	k_0 (s^{-1})	E (J/mol)	k_0 (s^{-1})	E (J/mol)	k_0 (s^{-1})	E (J/mol)	k_0 (s^{-1})	E (J/mol)
r1	$1.15 \cdot 10^{6}$	$6.89 \cdot 10^{4}$	$5.41 \cdot 10^{5}$	$7.14 \cdot 10^{4}$	$6.98 \cdot 10^{5}$	$8.15 \cdot 10^{4}$	$6.29 \cdot 10^{5}$	$7.31 \cdot 10^{4}$	$6.43 \cdot 10^{5}$	$8.65 \cdot 10^{4}$
r2	$1.67 \cdot 10^{9}$	$1.13 \cdot 10^{5}$	$1.67 \cdot 10^{9}$	$1.16 \cdot 10^{5}$	$1.17 \cdot 10^{9}$	$1.23 \cdot 10^{5}$	$1.67 \cdot 10^{9}$	$1.18 \cdot 10^{5}$	$1.59 \cdot 10^{9}$	$1.25 \cdot 10^{5}$
r3	$7.21 \cdot 10^{8}$	$1.24 \cdot 10^{5}$	$6.40 \cdot 10^{8}$	$1.25 \cdot 10^{5}$	$6.83 \cdot 10^{8}$	$1.27 \cdot 10^{5}$	$6.63 \cdot 10^{8}$	$1.24 \cdot 10^{5}$	$6.63 \cdot 10^{8}$	$1.28 \cdot 10^{5}$
r4	$2.50 \cdot 10^{9}$	$1.26 \cdot 10^{5}$	$2.46 \cdot 10^{9}$	$1.27 \cdot 10^{5}$	$2.44 \cdot 10^{9}$	$1.29 \cdot 10^{5}$	$2.47 \cdot 10^{9}$	$1.27 \cdot 10^{5}$	$2.31 \cdot 10^{9}$	$1.34 \cdot 10^{5}$
Mean Ea	0.131		0.218		0.067		0.104		0.010	
Mean Er	0.189%		0.294%		0.111%		0.157%		0.014%	

The main differences observed between the kinetic parameters calculated for the total « hemicelluloses » and the « hemicelluloses 1 » concern the pre-exponential factor of the first reaction (A →B, $k_{0,1}$). Both hemicellulose fractions are required to represent hemicellulose behavior in torrefaction, as their different sugar composition and, thus, different behavior in torrefaction, make them complementary for this aim. This supports correcting hemicelluloses behavior (Figure V.26).

2.3.3.1. Comparison with the first-level additive model and the raw biomass

The biomass behavior in torrefaction modelled by the second-level additive model was compared to the simulation based on the simplified first-level model and to the experimental results (Figure V.27).

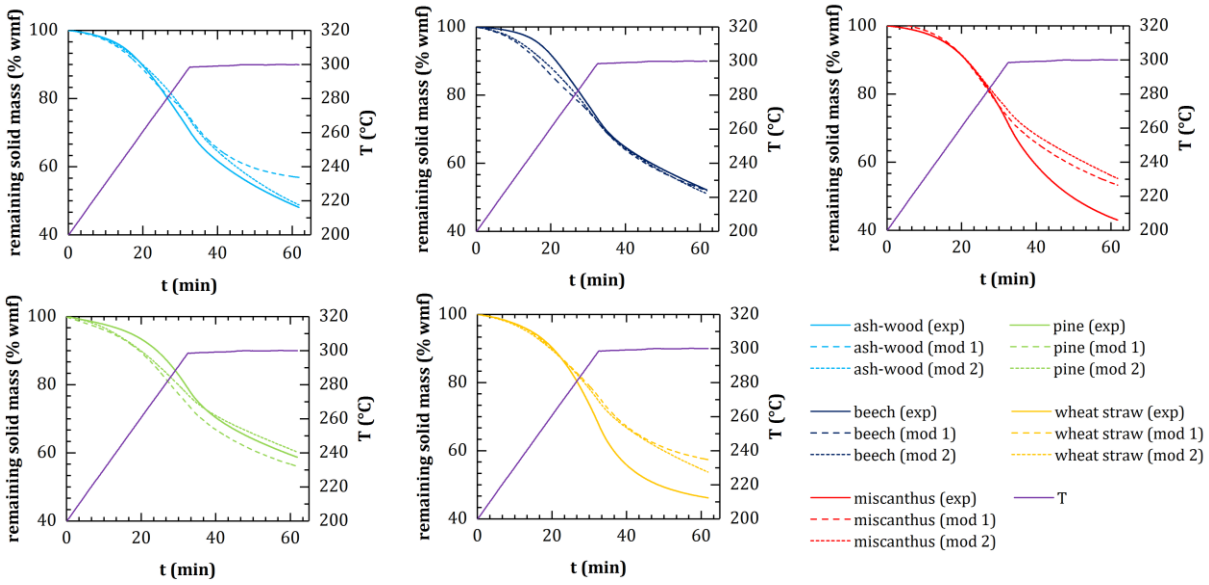


Figure V.27a. Remaining solid mass loss versus temperature and time in torrefaction for raw biomass in TGA-GC/MS (exp) and modelled through the first-level model (mod 1 curves) and the second-level model (mod 2)

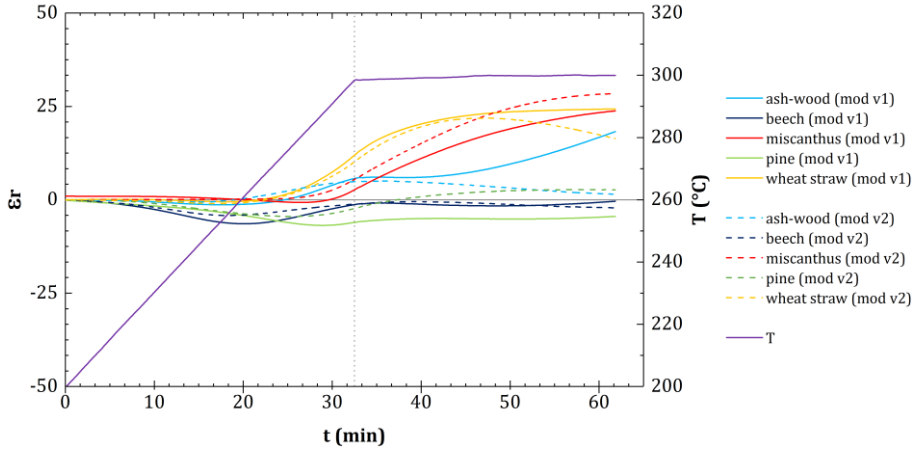


Figure V.27b. Relative error between remaining solid mass estimated through first-level model (line) and second-level model (dotted line) compared to that obtained for raw biomass in TGA-GC/MS

The prediction by the model in the non-isothermal torrefaction remains satisfactory and only slightly improved by the second-level model. However, the overestimation of the remaining solid mass by the first-level model in the non-isothermal torrefaction is improved for beech and sensibly for pine. The particular improvement of the representation in the dynamic step might be due to the consideration of the total « hemicelluloses » and in the isothermal step, to the « cellulose I ». However, no improvement was observed for wheat straw and miscanthus. This might correspond to the fact that their structure is poorly known, which leads to a higher uncertainty in their macromolecular and sugar characterization and, consequently, in their modelling.

2.3.3.2. Attempt of accounting with interactions between macromolecular components

Finally, differences between the behavior of the ternary mixture, the simulations of the first- and the second- level models, compared to raw biomass were exhibited in Figure V.28.

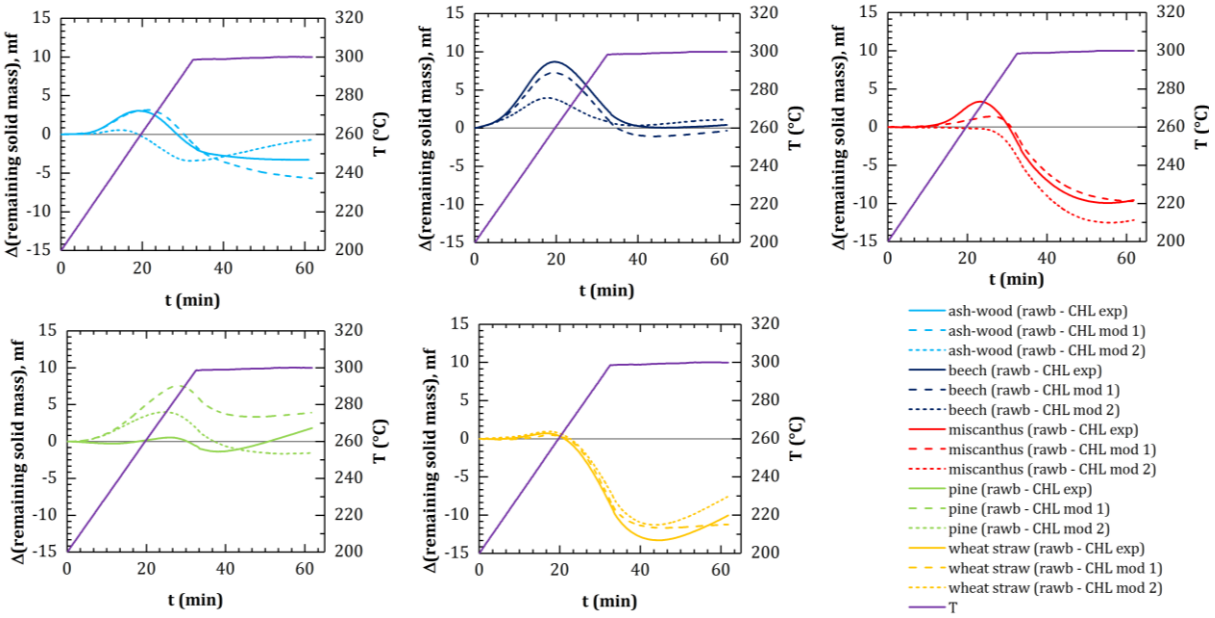


Figure V.28. Difference in the remaining solid mass loss versus temperature and time in torrefaction between the raw biomass (rawb) and either ternary mixtures (CHL exp) or the torrefaction model (mod, first-level: 1; second-level: 2)

The second-level model presents in general a better estimation of the remaining solid mass, compared to the first-level model and to the ternary mixtures, except for miscanthus.

Interactions between macromolecular components, supposed as being the cause of the difference between the experimental and the modelled behavior, are shown to present equivalent profiles for biomasses belonging to the same family (Figure V.28). This proportionality between the comparison curves per biomass might be derived from a lower degree of reticulation through inter-molecular bonds of the extracted fractions compared to the raw biomass.

A peak in the difference curves around 250°C corresponds to a higher underestimation and might indicate the scission of inter-molecular bonds between hemicelluloses and other macromolecular components, as they have been reported to be strongly degraded from this temperature (see chapter II). By considering the « cellulose I » curves in the construction of the improved model, a part of the interactions cellulose-hemicelluloses (II) are supposed to be taken into account. This is in agreement with the decrease of this peak for all biomasses. Surprisingly, the ternary mixture and the second-level model did not predict interactions in the same way in the isothermal step for pine and ash-wood, while the first-level model did it. No evidence was found to explain this behavior.

2.4. Extrapolation of the torrefaction model

The proposed torrefaction model was extrapolated to other biomasses investigated in the database, by considering the biomass family and the macromolecular composition in cellulose, hemicellulose and lignin for each biomass (Table V.8). The two versions of the model, (first- and second-level model) were considered, since the first one is based on more accurate experimental data and the second one, even if some uncertainty still remains in its construction, offers a better prediction of biomass behavior in torrefaction. The relative error in the prediction by both models is indicated per biomass family.

In the case of the deciduous wood, ash-wood and beech models were considered and applied to poplar and willow, as well as to beech in the first case and to ash-wood in the second case. A better prediction was achieved with the second-level model compared to the first-level one, in all cases except for willow, the maximum relative error being around 16 % and corresponding to the isothermal torrefaction. By comparing models from both deciduous woods, it is noticeable that they lead to equivalent results. As a result, one single model would be enough to represent deciduous wood.

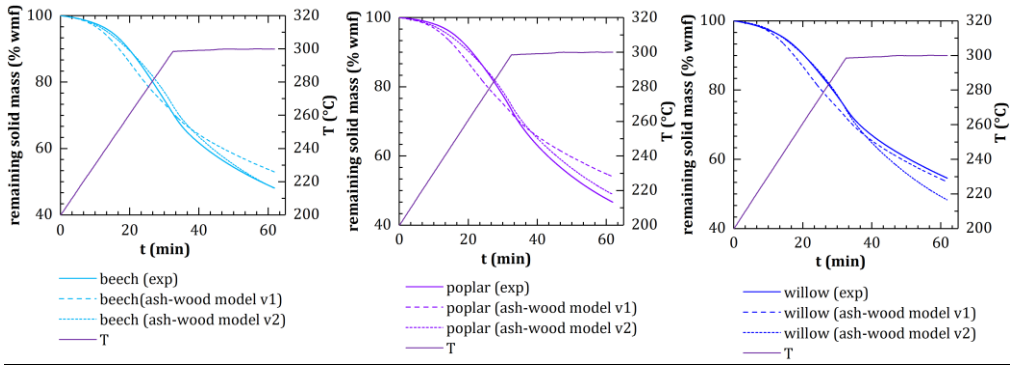
The prediction of the remaining solid mass for coniferous wood by the pine model is correct, both in non-isothermal and isothermal torrefaction steps. The maximum relative error corresponding to temperatures close to 300°C in the non-isothermal torrefaction was below 10 %. This model was also applied to grape seed cake, due to its high lignin content, as it is the case of coniferous wood. However, an overestimation of the remaining solid mass occurred in the whole torrefaction temperature range, including both thermal steps, until a relative error around 16 %. This might indicate that biomass family, namely woody or agricultural biomass, has a significant influence in the torrefaction behavior, as important as the macromolecular composition.

An accurate prediction of reed canary grass behavior is possible thanks to the herbaceous crops model built for miscanthus, with a relative error lower than 2 % for the second-level model.

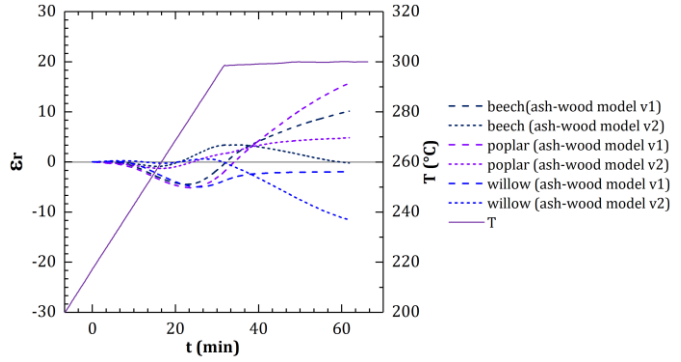
Both first and second level models lead to an underestimation of the remaining solid mass of agricultural biomasses, until a maximum relative error around 25 % for all biomasses. The exception is for grape seed cake, which is overestimated (relative error lower than for coniferous wood model, below 10 %). This might indicate a crucial role of interactions between macromolecular components in agricultural biomass, and the need of representing them in torrefaction models. The underestimation being similar for the three biomasses analyzed might indicate that interactions might be similar for agricultural biomasses, and thus one single biomass might be enough to represent the behavior of this family, by taking into account these interactions, at least for common agricultural biomasses such as cereal straws and other derivatives.

Table V.8. Prediction of remaining solid mass in function of time and temperature for raw biomasses from the database by the torrefaction model

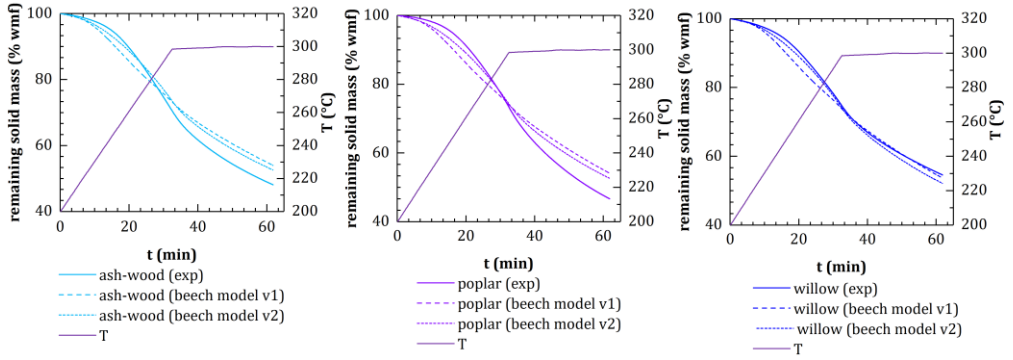
Deciduous wood (ash-wood model)



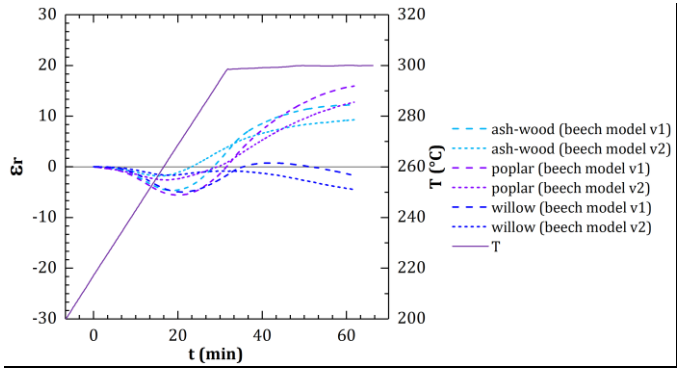
Relative error



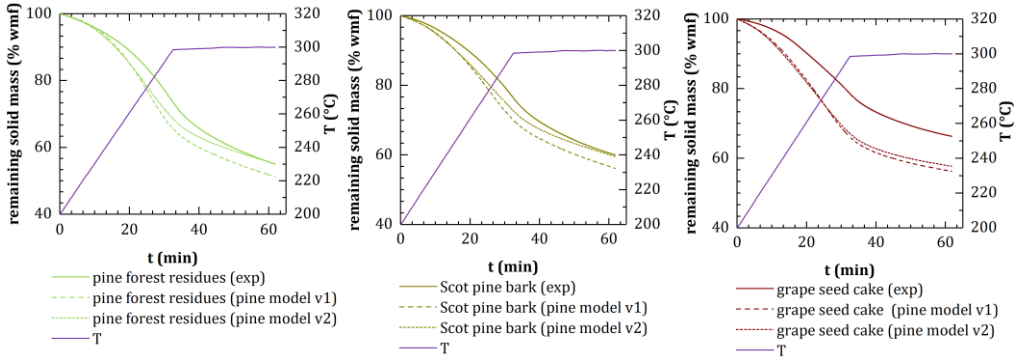
Deciduous wood (beech model)



Relative error



Coniferous wood (pine model)



Relative error

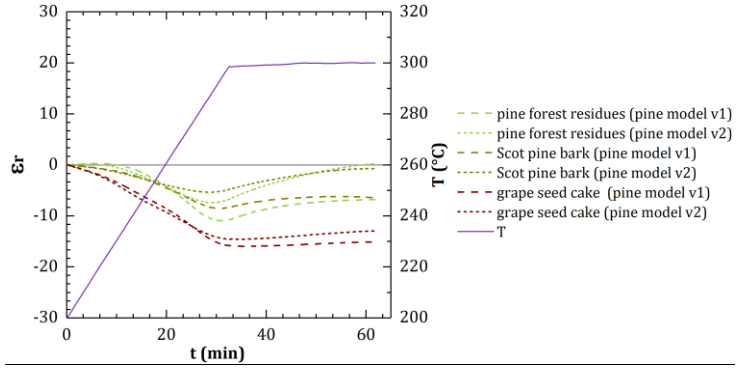
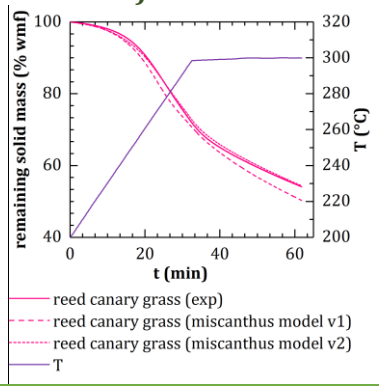
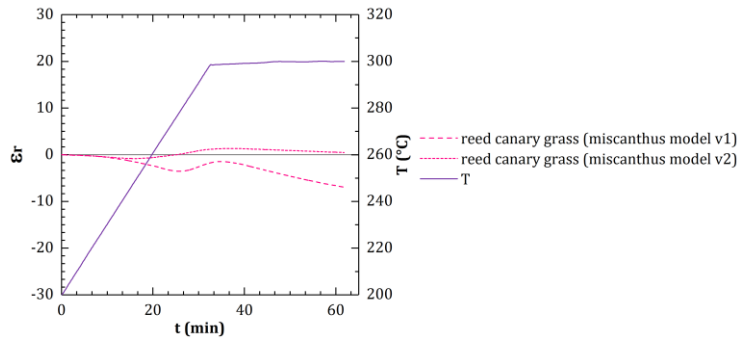


Table V.8. Prediction of remaining solid mass in function of time and temperature for raw biomasses from the database by the torrefaction model

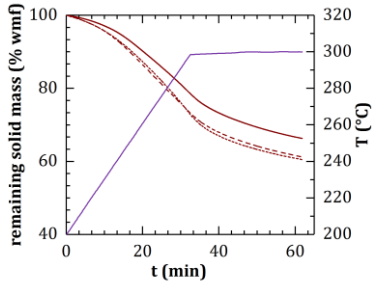
Herbaceous crops (miscanthus model)

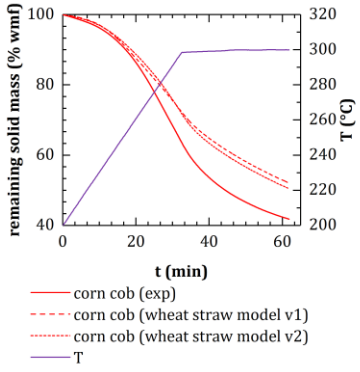


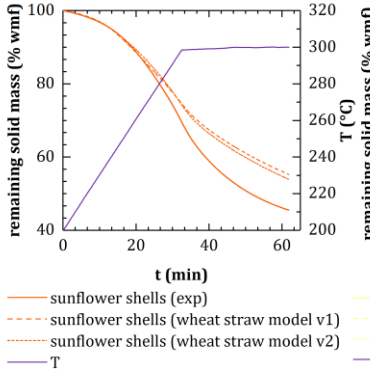
Relative error

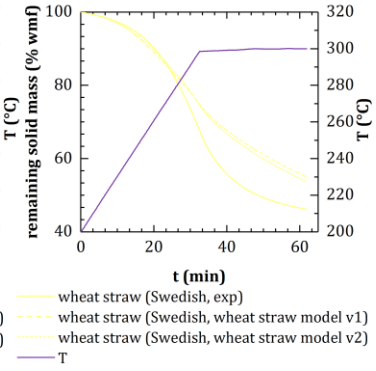


Agricultural by-products (wheat straw model)

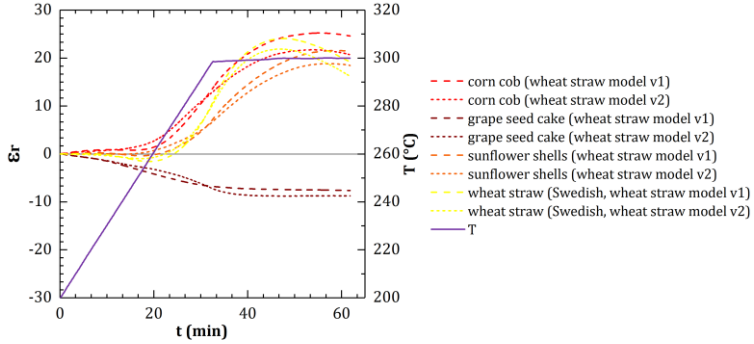








Relative error



2.5. Conclusion

An improved representation of the behavior of biomass in torrefaction was achieved with the additive model based on extracted macromolecular components from 5 different biomasses. This improvement is especially remarkable for deciduous (ash-wood and beech) and coniferous (pine) wood. The representation is less accurate for agricultural biomasses, represented by wheat straw. This might be due to the difficulty to produce hemicellulose fractions which preserve the complexity of the native hemicelluloses in biomass, and they are the determinant macromolecular component in biomass degradation during torrefaction. However, the uncertainty in sugar characterization also influences errors in biomass representation, especially for agricultural biomasses.

On the other hand, the consideration of different biomasses and of their extracted macromolecular components confirms that the specific behavior of biomass strongly depends on its biological origin. Interactions between macromolecular components seem to go in the same way for biomasses belonging to the same family, even for common agricultural biomasses such as cereal derivatives. This led us to suggest that one representative of each biomass family, namely deciduous wood, coniferous wood, herbaceous crops and agricultural by-products, is sufficient to describe the behavior of biomasses from the same family in torrefaction. A deeper assessment of biomass intra- and inter- molecular bonds, as well a more detailed lignin characterization, would help in the improvement of biomass description and modelling.

CONCLUSIONS AND OUTLOOK

Conclusions and outlook

Conclusions

The objective of this work was to assess the impact of biomass properties on its conversion in torrefaction, both in terms of solid mass loss and volatile species release, versus operating conditions. To do this, biomass was represented through its main macromolecular composition in cellulose, hemicelluloses and lignin. As a consequence of this analysis, the second objective was to propose a torrefaction additive model based on the behavior of these macromolecular components to describe biomass behavior in torrefaction.

Previous torrefaction studies typically considered only isothermal conditions, were carried out for a reduced number of biomasses and did not systematically check chemical regime. A deep description of volatile species released in torrefaction was not very frequent and usually focused on a reduced number of species, without assessing the impact of the operating conditions. The most recurrent modelling approach of biomass behavior in torrefaction was through the weighted sum of the individual behaviors of cellulose, hemicelluloses and lignin, typically represented by commercial compounds.

This work assessed the influence of biomass macromolecular composition for a large panel of woody and agricultural biomasses in torrefaction. Five biomasses representative of the main biomass families were selected and their cellulose, hemicelluloses and lignin components were extracted and analyzed in torrefaction. To do this, an experimental set-up coupling a thermogravimetric analyzer to a gas chromatography mass spectrometer device through a heated storage loop system was used (TGA-GC/MS). Solid degradation kinetics and production profiles of 23 volatile species released were followed during torrefaction experiments combining non-isothermal (200 to 300°C at 3°C/min) and isothermal (300°C, 30 min) conditions, ensuring the chemical regime thanks to the appropriate operating conditions. Data analysis was firstly carried out visually and secondly through Principal Component Analysis (PCA). The conclusions from this analysis led to propose an improved version of the additive model describing solid kinetics in torrefaction. This model was based on the macromolecular composition of biomass represented by extracted cellulose, hemicelluloses and lignin from different biomasses.

Raw biomass behavior in torrefaction was shown to be strongly dependent on the biomass family (deciduous and coniferous wood, agricultural by-products and herbaceous crops), as well as on its macromolecular composition. Two main categories could be observed in the non-isothermal part of the torrefaction experiment according to solid degradation profiles, with on the one hand deciduous wood and on the other hand all the other biomass types. In the subsequent isothermal step at 300 °C, the same solid degradation profile was observed for all biomasses, but with different rates. Regarding volatile species release, production profiles

versus temperature were found to be different among volatile species from the same chemical family. Finally, as first approach, a representative of each main wood family, namely deciduous and coniferous, seems to be sufficient to describe solid kinetics and volatile species release. One representative may be sufficient for herbaceous biomasses but seems to be insufficient for describing volatile species release from agricultural by-products. This seems to be derived from the heterogeneity of this group, which responds to the disparities in the macromolecular composition.

Five biomasses from the database were selected in order to deeply characterize their behavior in torrefaction through their extracted cellulose, hemicelluloses and lignin. These biomasses were ash-wood and beech for deciduous wood, pine for coniferous wood, miscanthus for herbaceous crops and French wheat straw for agricultural by-products. The main limitation in this selection was for agricultural by-products. The time required for obtaining the extracted fractions and the difficulties to select representative agricultural biomasses due to their heterogeneity led to select a cereal derivative, wheat straw, to represent the group.

Experimental results on extracted fractions from biomass, as well as their link with the sugar composition of the polysaccharide-based fractions, led to several conclusions, first of all in terms of solid mass loss behavior:

- Cellulose was represented through «cellulose II» in a first approach:
  - This fraction presents a higher polymerization degree, higher average molecular mass and preserved amorphous regions compared to commercial microcrystalline cellulose Avicel, a cellulose I type structure which was the typical model for cellulose in previous torrefaction studies.
  - Even if «cellulose II» properties are closer to those of native cellulose in biomass, they still remain far from it. However, «cellulose II» seems a more suitable model for cellulose behavior in torrefaction than commercial microcrystalline cellulose.
  - The degradation of cellulose was confirmed to be enhanced from 300°C. However, it was already detected from intermediate to high torrefaction temperatures, which might be derived from the lower polymerization degree of the «cellulose II» extracted fractions, compared to native cellulose in biomass.
  - The 5 «cellulose II» fractions presented similar behavior in torrefaction, so a single extracted cellulose fraction could be considered to represent cellulose behavior in torrefaction. This was confirmed by the similar kinetic parameters obtained for the «cellulose II» fractions in modelling.
- «DMSO residue» fractions, containing cellulose and residual hemicellulose, allowed to compare the behavior of cellulose I (in «DMSO residue») and the «cellulose II» fractions. The impact of this difference in the structure arrangement of the cellulose chains in

cellulose degradation in torrefaction cannot be experimentally assessed with the available fractions. However, it was estimated by extracting cellulose I behavior from the «DMSO residue» fractions. The obtained results suggest a low impact of the arrangement of cellulose chains on cellulose behavior in torrefaction.

- Hemicelluloses were represented by «hemicelluloses 1» and «hemicelluloses 2» fractions:
  - They were confirmed as the most degraded biomass macromolecular component in the torrefaction temperature range.
  - Different behaviors were observed for the ten extracted hemicellulose fractions, mainly due to their different sugar composition.
  - Xylose and mannose composition was shown to be the main factor conditioning the extent of hemicellulose mass loss, as well as the biomass family.
  - «Hemicelluloses 1», the first and main hemicellulose fraction with preserved acetyl groups, already gives a correct estimation of hemicellulose behavior in torrefaction.
  - Differences in sugar composition between hemicellulose fractions suggest that both of them are complementary to represent general hemicelluloses behavior in torrefaction.
- Lignin was represented through the «lignin» fraction:
  - Its degradation was confirmed to occur from the beginning of torrefaction and to be only partial in the torrefaction temperature range.
  - Differences were observed between the 5 «lignin» fractions.
  - Its degradation seems dependent on H (phenyl-), G (guaiacyl-) and S (syringyl-) composition.
  - 3 «lignin» fractions would be enough to represent lignin degradation in torrefaction:
    - pine lignin (principally G units),
    - deciduous wood lignin (G and S units) and
    - agricultural lignin (G, S, H units).
- The behavior of the ternary mixtures of extracted «cellulose II», «hemicelluloses 1» and «lignin» fractions in the proportions as they are present in biomass was compared in torrefaction to that of the corresponding raw biomasses:
  - Important differences between raw biomass and ternary mixtures were revealed.
  - These differences might correspond to interactions between macromolecular components, as the physical mixture was shown not to allow to reproduce them.
- The study of the binary mixtures of «cellulose II», «hemicelluloses 1» and «lignin» confirms that hemicellulose is the most degraded macromolecular component during torrefaction. This might indicate that a good knowledge of hemicellulose degradation and of its sugar composition would be a suitable approach for predicting biomass degradation

in torrefaction. However, the binary mixtures do not allow to reproduce interactions between macromolecular components in biomass either.

The main elemental composition of the solid through torrefaction changes substantially for raw biomasses and extracted hemicelluloses. This evolution is mainly reflected by the increase of the carbon content and the decrease of the oxygen content, while the hydrogen content remains low in all cases. Lignin and cellulose only present moderate changes in their composition, due to their limited degradation at the torrefaction temperatures. These results are in agreement with previous works and allow to define the evolution of the macromolecular formula of the raw materials, as well as of their extracted macromolecular components, in torrefaction.

Several conclusions were extracted from the experimental results on the production profiles of the volatile species released in torrefaction of the extracted fractions from the 5 reference biomass. First of all, in general:

- A lower amount of volatile species was detected and quantified for the extracted fractions compared to the raw biomasses, due to their specific nature.
- Some volatile species were released at lower temperatures for extracted macromolecular components than those indicated in the literature, typically determined for commercial compounds. This might confirm the lower representativeness of these latter for describing biomass behavior in torrefaction.
- Limitations of the experimental set-up lead to a less accurate quantification of the volatile species released for the extracted fractions and their mixtures, as they are produced in lower amounts than for raw biomasses. The representativeness of the results obtained was ensured by deeply contrasting these results with previous studies on the degradation mechanisms proposed for biomass torrefaction.
- Volatile species released by each extracted fraction were in agreement with the nature of each fraction and with the literature, excepted for minor compounds not included in previous studies.

Secondly, the volatile species detected per extracted fraction were detailed (Table IV.8) and compared to their proposed origin in the literature. The obtained results lead to conclude that:

- The production of volatile species quantified for the «cellulose II» fractions was higher than that of the commercial microcrystalline cellulose Avicel, due to their enhanced degradation.
  - Levoglucosenone was detected but could not be quantified.
  - The main quantified products were furans, mainly furans, ketones and acetic acid.
- Hemicelluloses lead to the highest variety and production of volatile species in

torrefaction, which is related to their degradation until a more important extent and their diverse sugar composition.

- Acetic acid, furfural and methanol were detected as the major compounds.

- Lignin leads to a low production of volatile species in torrefaction, whose nature is strongly conditioned by its composition in H, G and S units, due to its low degradation.
  - Phenols and formaldehyde are the main detected products from lignin.

- The ternary mixtures of «cellulose II», «hemicelluloses 1» and «lignin» in torrefaction:
  - They lead to a lower production of volatile species compared to that of raw biomasses. This might indicate that intra-molecular bonding between biomass macromolecular components, broken during extraction, implies a non-negligible release of volatile species, particularly small chemical compounds such as acetic acid.
  - Lignin losses in mixture preparation impacted phenols and formaldehyde production.
  - Interactions in gas phase of the released volatile species could not be highlighted by this method, due to the difference in the order of magnitude of the production profiles between the ternary mixtures and the corresponding raw biomasses.

- The binary mixtures of «cellulose II», «hemicelluloses 1» and «lignin» in torrefaction:
  - They contribute to elucidate the mechanisms of release of volatile species, especially when several pathways of formation occur in parallel (i.e. acetic acid, formaldehyde).
  - Similar experimental problems were encountered in lignin-based mixtures.
  - Interactions in gas phase between volatile species released could not be revealed.

PCA confirmed that macromolecular composition is a suitable tool to define variability in biomass characterization, while the elemental composition showed its limitations. The variability in biomass characterization can be correctly represented by the cellulose, hemicelluloses and lignin content per biomass. Extractives and ash content could be neglected, implying a slight loss in the accuracy of the representation of data variability.

Concerning biomass samples, a similar macromolecular composition and solid transformation behavior through torrefaction were found for biomasses belonging to deciduous and coniferous wood families, respectively. Nevertheless, agricultural biomasses and herbaceous crops present a more heterogeneous behavior. As a result, one exemplar of each wood family could be sufficient, in a first approach, to model the kinetics behavior of the family, while several exemplars of agricultural biomasses would be required for the same objective. These results were in agreement with direct observations from the experimental data.

By considering production profiles of the volatile species in function of the temperature, volatile species from the same chemical family exhibit different behaviors. This indicates that a representative per chemical family would not be sufficient to model volatile species release in torrefaction, which contradicts previous observations on the experimental results. Cellulose,

hemicelluloses and lignin content was shown to strongly impact volatile species release in torrefaction, due to similarities found in the total production of volatile species from a chemical family for biomasses with a close macromolecular composition. On the contrary, biomasses from the same family present a very different behavior in production profiles of the volatile species release. Consequently, a single biomass per chemical family was shown not to be sufficient to represent the behavior of the family in terms of volatile species release.

A torrefaction model exclusively based on solid kinetics was proposed, based on cellulose, hemicellulose and lignin composition as key parameters to describe biomass composition. PCA results confirmed the experimental observations about volatile species production in biomass torrefaction and suggested that their modelling would require a larger biomass database and a deeper study. Consequently, it should be foreseen in a future study. However, correspondences can be made between new biomasses and biomasses in the database, so as to estimate their volatile species production in torrefaction through the representative biomass from the same family in the database.

An improved representation of the behavior of biomass in torrefaction in terms of solid mass loss kinetics was achieved with the additive model based on extracted macromolecular components from 5 different biomasses. This improvement was especially remarkable for deciduous (ash-wood and beech) and coniferous (pine) wood. The representation is less accurate for agricultural biomasses, represented by wheat straw. This might be derived from the difficulty to produce hemicellulose fractions which preserve the complexity of the native hemicelluloses in biomass, are they are the determinant macromolecular component in biomass degradation through torrefaction. However, the uncertainty in sugar characterization also influences errors in biomass representation, especially for agricultural biomasses.

On the other hand, the consideration of different biomasses and of their extracted macromolecular components confirms that the specific behavior of biomass strongly depends on its biological origin. Interactions between macromolecular components seem to go in the same way for biomasses from the same family, even for typical agricultural biomasses such as cereal derivatives. This led us to confirm that one representative of each biomass family would be sufficient to describe the behavior of biomasses from the same family in torrefaction. However, a deeper assessment of biomass intra- and inter- molecular bonds, as well a more detailed lignin characterization, would help in the improvement of biomass description and modelling.

To sum up, biomass main macromolecular composition on cellulose, hemicelluloses and lignin, as well as biomass family, were shown to be critical factors influencing biomass behavior in torrefaction, both in terms of solid mass loss and volatile species release. As a result, an accurate and in-depth biomass characterization may contribute in the understanding and modelling of the mechanisms involved in biomass torrefaction.

Outlook

The present work limitations lead to propose the following perspectives for future work:

- Considering a larger biomass data base, especially concerning agricultural biomasses, which were shown as the more heterogeneous group, could lead to improve the representativeness of biomass diversity.
- Carrying out a deeper biomass characterization will help in explaining the obtained results and in correlating them to mechanisms proposed in the literature. This would be particularly useful for:
  - Lignin, in terms of its composition in phenyl- (H-), guaiacyl- (G-) and syringyl- (S-) units.
  - Extractives composition.
  - Minor biomass components, such as proteins, ferulic acids and hexuronic acids.
  - Interactions in biomass, both intramolecular and intermolecular, in terms of their nature and frequency.
- Improving the accuracy of the determination of the sugar composition, especially for agricultural biomasses. This implies a deeper knowledge of their structure and particularly of the ratio between hemicellulose sugars for each biomass. An exact determination of the error in this characterization would also be advisable.
- Optimizing the extraction procedure to obtain a higher representativeness of the fractions, as well as to increase their yield of production, especially for:
  - Cellulose, as for the moment no method allows to simultaneously preserve amorphous parts and cellulose I crystalline structure from native cellulose in biomass, together with acceptable polymerization degree and average molecular mass. The cellulose fraction obtained through the DMSO residue could be purified by an enzymatic treatment to obtain a more representative cellulose.
  - Hemicelluloses, as currently no extraction method allows to simultaneously extract total hemicelluloses from biomass, or at least a representative fraction of them in a single extraction step. Ionic solvents for hemicellulose extraction might be a solution to this problem.
  - Lignin, by using extraction methods leading to higher purity of lignin in enough quantity.
  - Extractives, to be recovered and analyzed in torrefaction.
  - Ash, to be recovered and analyzed in torrefaction. The current extraction methods modify the ash content of the initial biomass and the extracted fractions, due to the use of chemicals.

- The experimental set up TGA-GC/MS set up can be improved by:
  - Measuring water and permanent gases, presumably by on-line methods including a micro-GC or a FTIR adapted to the low amounts produced. This will allow to estimate the mass balance of the process.
  - Adapting the materials of the intermediate heated storage loop system and of the coupling conductions, with two objectives:
    - Allowing a higher temperature for transporting and storing volatile species. This will avoid condensation of heavy molecules that cannot be currently measured, such as sugars and pyrans, in cold points of the set-up.
    - Permitting torrefaction experiments until higher temperatures, around 370°C.
  - Increasing the sample mass guaranteeing the chemical regime, so as to produce a higher amount of the minor volatile species released, sufficient to their quantification.
  - In-situ measurements of solid evolution during torrefaction, for example through X-ray absorption spectroscopy (XAS) during heat treatment, coupled to the quantification of the volatile species release, would allow to correlate how chemical bonds are degraded in biomass and the mechanisms of production of the volatile species.

- The obtained results in the torrefaction of raw biomasses and of their extracted macromolecular components can contribute to:
  - Complete the proposed mechanisms involved in biomass torrefaction.
  - Improve the representation of biomass and of torrefaction products in recent torrefaction models (Anca-Couce, Dussan), because of the deep characterization of the raw materials and the detailed description of torrefaction products.
  - Build a larger database of biomass characterization and behavior in torrefaction for further PCA, as a larger amount of data could better represent biomass variability.

- The proposed torrefaction model might be improved by:
  - Considering real cellulose I and total hemicellulose fractions analyzed in TGA-GS/MS.
  - Improving the accuracy in sugar characterization, which impacts proportions in biomass macromolecular composition.
  - Assessing the impact of assuming a first order reaction and the selected kinetic scheme and proposing a more suitable one, especially for cellulose transformation.

- Particularly, the proposed methodology allowing to obtain the production profiles of the volatile species released in torrefaction in function of the temperature might contribute to explain the mechanisms involved in biomass transformation through torrefaction, in a similar way as Py-GC/MS was typically used for describing biomass degradation through fast pyrolysis. However, in this case, the influence of using a very slow (TGA-GC/MS) or very fast (Py-GC/MS) heating rate should be assessed.

BIBLIOGRAPHY

Bibliography

[1] Institute for Fuels and Renewable Energy, RENEW project - EC_BREC - Energy crops potential inventory - Country profiles, 2008. http://www.renew-fuel.com/download.php?dl=del_sp5_wp1_5-1-3-countries_08-01-15-ecbrec.pdf&kat=17 (accessed March 22, 2016).

[2] E. Ganko, RENEW Project - Final raport, 2008. http://www.renew-fuel.com/download.php?dl=renew-final-report-080627.pdf&kat=5 (accessed March 22, 2016).

[3] H.B. Goyal, D. Seal, R.C. Saxena, Bio-fuels from thermochemical conversion of renewable resources: A review, Renewable and Sustainable Energy Reviews. 12 (2008) 504–517. doi:10.1016/j.rser.2006.07.014.

[4] J.J. Harrington, R. Booker, Astley R.J., Modelling the elastic properties of softwood. Part I: The cell-wall lamellae, Holz Als Roh- Und Werkstoff. (1998) 37–41.

[5] S.V. Pisupati, A.H. Tchapda, Chapter 15: Thermochemical Processing of biomass, in: Advances in Bioprocess Technology, Pogaku Ravindra, Switzerland, 2015.

[6] T. Nocquet, C. Dupont, J.-M. Commandre, M. Grateau, S. Thiery, S. Salvador, Volatile species release during torrefaction of wood and its macromolecular constituents: Part 1 – Experimental study, Energy. 72 (2014) 180–187. doi:10.1016/j.energy.2014.02.061.

[7] T. Nocquet, C. Dupont, J.-M. Commandre, M. Grateau, S. Thiery, S. Salvador, Volatile species release during torrefaction of biomass and its macromolecular constituents: Part 2 – Modeling study, Energy. 72 (2014) 188–194. doi:10.1016/j.energy.2014.05.023.

[8] R. Pentananunt, A.N.M.M. Rahman, S.C. Bhattacharya, Upgrading of biomass by means of torrefaction, Energy. 15 (1990) 1175–1179. doi:10.1016/0360-5442(90)90109-F.

[9] W.-H. Chen, J. Peng, X.T. Bi, A state-of-the-art review of biomass torrefaction, densification and applications, Renewable and Sustainable Energy Reviews. 44 (2015) 847–866. doi:10.1016/j.rser.2014.12.039.

[10] E.M. Fisher, C. Dupont, L.I. Darvell, J.-M. Commandré, A. Saddawi, J.M. Jones, M. Grateau, T. Nocquet, S. Salvador, Combustion and gasification characteristics of chars from raw and torrefied biomass, Bioresource Technology. 119 (2012) 157–165. doi:10.1016/j.biortech.2012.05.109.

[11] M. Detcheberry, P. Destrac, S. Massebeuf, O. Baudouin, V. Gerbaud, J.-S. Condoret, X.-M. Meyer, Thermodynamic modeling of the condensable fraction of a gaseous effluent from lignocellulosic biomass torrefaction, Fluid Phase Equilibria. 409 (2016) 242–255. doi:10.1016/j.fluid.2015.09.025.

[12] K. Lê Thành, J.-M. Commandré, J. Valette, G. Volle, M. Meyer, Detailed identification and quantification of the condensable species released during torrefaction of lignocellulosic biomasses, Fuel Processing Technology. 139 (2015) 226–235. doi:10.1016/j.fuproc.2015.07.001.

[13] E. Rodriguez Alonso, C. Dupont, L. Heux, D. Da Silva Perez, J.-M. Commandre, C. Gourdon, Study of solid chemical evolution in torrefaction of different biomasses through solid-state 13C cross-polarization/magic angle spinning NMR (nuclear magnetic resonance) and TGA (thermogravimetric analysis), Energy. 97 (2016) 381–390. doi:10.1016/j.energy.2015.12.120.

[14] L.E. Arteaga-Pérez, C. Segura, V. Bustamante-García, O. Gómez Cápiro, R. Jiménez, Torrefaction of wood and bark from Eucalyptus globulus and Eucalyptus nitens: Focus on volatile evolution vs feasible temperatures, Energy. 93, Part 2 (2015) 1731–1741. doi:10.1016/j.energy.2015.10.007.

[15] A. Ohliger, M. Förster, R. Kneer, Torrefaction of beechwood: A parametric study including heat of reaction and grindability, Fuel. 104 (2013) 607–613. doi:10.1016/j.fuel.2012.06.112.

[16] L. Shang, J. Ahrenfeldt, J.K. Holm, S. Barsberg, R. Zhang, Y. Luo, H. Egsgaard, U.B. Henriksen, Intrinsic kinetics and devolatilization of wheat straw during torrefaction, Journal of Analytical and Applied Pyrolysis. 100 (2013) 145–152. doi:10.1016/j.jaap.2012.12.010.

[17] R.B. Bates, A.F. Ghoniem, Biomass torrefaction: Modeling of volatile and solid product

evolution kinetics, Bioresource Technology. 124 (2012) 460–469. doi:10.1016/j.biortech.2012.07.018.

[18] T. Nocquet, Torréfaction du bois et de ses constituants: Expériences et modélisation des rendements en matières volatiles., Université de Toulouse, 2012. http://ethesis.inp-toulouse.fr/archive/00002140/01/nocquet.pdf.

[19] M. Broström, A. Nordin, L. Pommer, C. Branca, C. Di Blasi, Influence of torrefaction on the devolatilization and oxidation kinetics of wood, Journal of Analytical and Applied Pyrolysis. 96 (2012) 100–109. doi:10.1016/j.jaap.2012.03.011.

[20] B. Arias, C. Pevida, J. Fermoso, M.G. Plaza, F. Rubiera, J.J. Pis, Influence of torrefaction on the grindability and reactivity of woody biomass, Fuel Processing Technology. 89 (2008) 169–175. doi:10.1016/j.fuproc.2007.09.002.

[21] T.G. Bridgeman, J.M. Jones, I. Shield, P.T. Williams, Torrefaction of reed canary grass, wheat straw and willow to enhance solid fuel qualities and combustion properties, Fuel. 87 (2008) 844–856. doi:10.1016/j.fuel.2007.05.041.

[22] M.J. Prins, K.J. Ptasinski, F.J.J.G. Janssen, Torrefaction of wood: Part 1. Weight loss kinetics, Journal of Analytical and Applied Pyrolysis. 77 (2006) 28–34. doi:10.1016/j.jaap.2006.01.002.

[23] T. Ferro, V. Vigouroux, A. Grimm, R. Zanzi, Torrefaction of agricultural and forest residues, in: Cubasolar 2004, Guantánamo, Cuba, 2004.

[24] Q.-V. Bach, W.-H. Chen, Y.-S. Chu, Ø. Skreiberg, Predictions of biochar yield and elemental composition during torrefaction of forest residues, Bioresource Technology. 215 (2016) 239–246. doi:10.1016/j.biortech.2016.04.009.

[25] J.H. Peng, X.T. Bi, S. Sokhansanj, C.J. Lim, Torrefaction and densification of different species of softwood residues, Fuel. 111 (2013) 411–421. doi:10.1016/j.fuel.2013.04.048.

[26] W.-H. Chen, K.-M. Lu, S.-H. Liu, C.-M. Tsai, W.-J. Lee, T.-C. Lin, Biomass torrefaction characteristics in inert and oxidative atmospheres at various superficial velocities, Bioresource Technology. 146 (2013) 152–160. doi:10.1016/j.biortech.2013.07.064.

[27] Y. Uemura, W.N. Omar, T. Tsutsui, S.B. Yusup, Torrefaction of oil palm wastes, Fuel. 90 (2011) 2585–2591. doi:10.1016/j.fuel.2011.03.021.

[28] W.-H. Chen, P.-C. Kuo, A study on torrefaction of various biomass materials and its impact on lignocellulosic structure simulated by a thermogravimetry, Energy. 35 (2010) 2580–2586. doi:10.1016/j.energy.2010.02.054.

[29] F.-X. Collard, J. Blin, A review on pyrolysis of biomass constituents: Mechanisms and composition of the products obtained from the conversion of cellulose, hemicelluloses and lignin, Renewable and Sustainable Energy Reviews. 38 (2014) 594–608. doi:10.1016/j.rser.2014.06.013.

[30] BEC, Glossary - Biomass, (2011). http://www.biomassenergycentre.org.uk/portal/page?_pageid=74,18700&_dad=portal&_schema=PORTAL#Biomass (accessed March 14, 2016).

[31] IEA, Good practice guidelines: Bioenergy Project Development and Biomass Supply, 2007. http://www.iea.org/publications/freepublications/publication/biomass.pdf (accessed March 15, 2016).

[32] P. McKendry, Energy production from biomass (part 1): overview of biomass, Bioresource Technology. (2002) 37–46.

[33] S.S. Amaral, J.A. de Carvalho Junior, M.A.M. Costa, T.G.S. Neto, R. Dellani, L.H.S. Leite, Comparative study for hardwood and softwood forest biomass: Chemical characterization, combustion phases and gas and particulate matter emissions, Bioresource Technology. 164 (2014) 55–63. doi:10.1016/j.biortech.2014.04.060.

[34] R.M. Rowell, Handbook of Wood Chemistry and Wood Composites, 2nd ed., CRC Press, 2013.

[35] FAO, Biofuels and the sustainability challenge, Food and Agriculture Organization of the United Nations, 2013. http://www.fao.org/publications/card/en/c/1f3e94cd-b985-59a8-8670-6c7e822d8bc0 (accessed March 16, 2016).

[36] FAO, Algae-based Biofuels: Applications and Co-products, Food and Agriculture Organization of the United Nations, 2010.

http://www.fao.org/publications/card/en/c/ab6ef06e-3c50-5a23-bfb9-38b51d2f01de (accessed March 16, 2016).
[37] S. Yokoyama, The Asian Biomass Handbook: A Guide for Biomass Production and Utilization, The Japan Institute of Energy, 2008.
[38] N. Rettenmaier, A. Schorb, S. Köppen, Status of biomass resource assessments version 3, 2010.
[39] FAO, Wood Fuels Handbook, Food and Agriculture Organization of the United Nations, Pristina, 2015. http://www.fao.org/3/a-i4441e.pdf (accessed March 16, 2016).
[40] AEBIOM, Bioenergy Europe Statistical Report 2017, 2017. http://www.aebiom.org/statistical-report-2017/statistical-report-2017-17-10-17/ (accessed September 13, 2018).
[41] AEBIOM, Bioenergy Europe Statistical Report – European Bioenergy Outlook, 2017. http://bioenergyeurope.org/statistical-report-2017/statistical-report-2017-17-10-17/.
[42] European Commission, State of play on the sustainability of solid and gaseous biomass used for electricity, heating and cooling in the EU, European Commission, 2014.
[43] P.J. Harris, Primary and secondary plant cell walls: A comparative overview, New Zealand Journal of Forestry Science. (2006) 36–53.
[44] E.M. Rubin, Genomics of cellulosic biofuels, Nature. 454 (2008) 841–845. doi:10.1038/nature07190.
[45] USDA, Wood handbook: wood as an engineering material - US Department of Agriculture, 2010.
[46] K. Werner, L. Pommer, M. Broström, Thermal decomposition of hemicelluloses, Journal of Analytical and Applied Pyrolysis. 110 (2014) 130–137. doi:10.1016/j.jaap.2014.08.013.
[47] J.M. Vargas-Moreno, A.J. Callejón-Ferre, J. Pérez-Alonso, B. Velázquez-Martí, A review of the mathematical models for predicting the heating value of biomass materials, Renewable and Sustainable Energy Reviews. 16 (2012) 3065–3083. doi:10.1016/j.rser.2012.02.054.
[48] P.F.H. Harmsen, W.J.J. Huijgen, L.M. Bermúdez López, R.R.C. Bakker, Literature Review of Physical and Chemical Pretreatment Processes for Lignocellulosic Biomass, Energy Research Centre of the Netherlands, 2010.
[49] S. Yen, J. Cheng, Hydrolysis of lignocellulosic materials for ethanol production: a review, Bioresource Technology. 83 (2002) 1–11.
[50] A. Dufresne, Les nanotechnologies dans l'industrie papetière, Techniques de l'Ingénieur. (2010).
[51] S.K. Guha, H. Kobayashi, A. Fukuoka, Chapter 13: Conversion of cellulose to sugar, in: Chapter 13:Conversion of Cellulose to Sugars, 2010. http://pubs.rsc.org/en/content/chapter/bk9781849730358-00344/978-1-84973-035-8 (accessed March 24, 2016).
[52] L.D. Gomez, C.G. Steele-King, S.J. McQueen-Mason, Sustainable liquid biofuels from biomass: the writing's on the walls, New Phytologist. 178 (2008) 473–485. doi:10.1111/j.1469-8137.2008.02422.x.
[53] H.A. Krässig, Cellulose, structure, accessibility and reactivity, Gordon and Breach Publishers, 1993. https://onlinelibrary.wiley.com/doi/abs/10.1002/pola.1994.080321221.
[54] H.V. Scheller, P. Ulvskov, Hemicelluloses, Annual Review of Plant Biology. 61 (2010) 263–289. doi:10.1146/annurev-arplant-042809-112315.
[55] A. Ebringerová, Z. Hromádková, T. Heinze, Hemicellulose, in: T. Heinze (Ed.), Polysaccharides I, Springer Berlin Heidelberg, 2005: pp. 1–67. doi:10.1007/b136816.
[56] W.-H. Chen, P.-C. Kuo, Isothermal torrefaction kinetics of hemicellulose, cellulose, lignin and xylan using thermogravimetric analysis, Energy. 36 (2011) 6451–6460. doi:10.1016/j.energy.2011.09.022.
[57] F. Shafizadeh, G.D. McGinnis, C.W. Philpot, Thermal degradation of xylan and related model compounds, Carbohydrate Research. 25 (1972) 23–33. doi:10.1016/S0008-6215(00)82742-1.
[58] C. Di Blasi, M. Lanzetta, Intrinsic kinetics of isothermal xylan degradation in inert atmosphere, Journal of Analytical and Applied Pyrolysis. 40–41 (1997) 287–303.

doi:10.1016/S0165-2370(97)00028-4.
[59] S. Wang, B. Ru, H. Lin, Z. Luo, Degradation mechanism of monosaccharides and xylan under pyrolytic conditions with theoretic modeling on the energy profiles, Bioresource Technology. 143 (2013) 378–383. doi:10.1016/j.biortech.2013.06.026.
[60] R. Sun, X. F. Sun, J. Tomkinson, Hemicelluloses and Their Derivatives, in: Hemicelluloses Sci Technol, 2003: pp. 2–22. doi:10.1021/bk-2004-0864.ch001.
[61] E. Sjöström, Wood chemistry: Fundamentals and Applications, 2nd ed., Academic Press, 1993.
[62] B. Monties, Les polymères végetaux: les lignines, 1980.
[63] Kirk-Othmer, Encyclopedia of Chemical Technology, Willey, 1999. http://onlinelibrary.wiley.com/book/10.1002/0471238961/homepage/EditorsContributors.html (accessed March 22, 2016).
[64] D. Fengel, G. Wegener, W. De Gruyer, Wood—chemistry, ultrastructure, reactions, Berlin and New York, 1984.
[65] X. Guo, S. Wang, K. Wang, Q. Liu, Z. Luo, Influence of extractives on mechanism of biomass pyrolysis, Journal of Fuel Chemistry and Technology. 38 (2010) 42–46. doi:10.1016/S1872-5813(10)60019-9.
[66] A. Kallioinen, A. Vaari, M. Rättö, J. Konn, M. Siika-aho, L. Viikari, Effects of bacterial treatments on wood extractives, Journal of Biotechnology. 103 (2003) 67–76. doi:10.1016/S0168-1656(03)00051-8.
[67] I. Volf, V.I. Popa, 4 - Integrated Processing of Biomass Resources for Fine Chemical Obtaining: Polyphenols, in: V. Popa, I. Volf (Eds.), Biomass as Renewable Raw Material to Obtain Bioproducts of High-Tech Value, Elsevier, 2018: pp. 113–160. doi:10.1016/B978-0-444-63774-1.00004-1.
[68] O.A. Simakova, E. Smolentseva, M. Estrada, E.V. Murzina, S. Beloshapkin, S.M. Willför, A.V. Simakov, D.Y. Murzin, From woody biomass extractives to health-promoting substances: Selective oxidation of the lignan hydroxymatairesinol to oxomatairesinol over Au, Pd, and Au–Pd heterogeneous catalysts, Journal of Catalysis. 291 (2012) 95–103. doi:10.1016/j.jcat.2012.04.012.
[69] L.H. Allen, Pitch control during the production of aspen kraft pulp, Pulp and Paper Canada. 89 (1988) 87–91.
[70] J.M. Leach, A.N. Thakore, Toxic constituents in mechanical pulping effluents, TAPPI. 59 (1976) 129–132.
[71] C. Dupont, S. Jacob, K.O. Marrakchy, C. Hognon, M. Grateau, F. Labalette, D. Da Silva Perez, How inorganic elements of biomass influence char steam gasification kinetics, Energy. 109 (2016) 430–435. doi:10.1016/j.energy.2016.04.094.
[72] G. Henriksson, J. Li, L. Zhang, M.E. Lindström, Chapter 9: Lignin Utilization, in: Thermochemical Conversion of Biomass to Liquid Fuels and Chemicals, 2010. http://pubs.rsc.org/en/content/chapter/bk9781849730358-00222/978-1-84973-035-8 (accessed March 24, 2016).
[73] S. Wang, B. Ru, H. Lin, W. Sun, Pyrolysis behaviors of four O-acetyl-preserved hemicelluloses isolated from hardwoods and softwoods, Fuel. 150 (2015) 243–251. doi:10.1016/j.fuel.2015.02.045.
[74] S. Wang, B. Ru, G. Dai, W. Sun, K. Qiu, J. Zhou, Pyrolysis mechanism study of minimally damaged hemicellulose polymers isolated from agricultural waste straw samples, Bioresource Technology. 190 (2015) 211–218. doi:10.1016/j.biortech.2015.04.098.
[75] R. Govett, T. Mace, S. Bowe, A practical guide for the determination of moisture content of woody biomass, University of Wisconsin, 2010. http://dnr.wi.gov/topic/ForestBusinesses/documents/BiomassMoistureContent.pdf (accessed March 22, 2016).
[76] ASTM International, ASTM D4442-15, Standard Test Methods for Direct Moisture Content Measurement of Wood and Wood-Based Materials, (2015). www.astm.org (accessed March 22, 2016).
[77] S.L. Brown, P. Schroeder, J.S. Kern, Spatial distribution of biomass in forests of the eastern USA, Forest Ecology and Management. (1999) 81–90.

[78] P.C.A. Bergman, A.R. Boersma, R.W.R. Zwart, J.H.A. Kiel, Torrefaction for biomass co-firing in existing coal-fired power stations "BIOCOAL," Energy research Centre of the Netherlands (ECN), 2015.
[79] W. Boie, Fuel technology calculations, Energietechnik. 3 (1953) 309–316.
[80] E. Peduzzi, G. Boissonnet, G. Haarlemmer, C. Dupont, F. Maréchal, Torrefaction modelling for lignocellulosic biomass conversion processes, Energy. 70 (2014) 58–67. doi:10.1016/j.energy.2014.03.086.
[81] C. Dupont, R. Chiriac, G. Gauthier, F. Toche, Heat capacity measurements of various biomass types and pyrolysis residues, Fuel. 115 (2014) 644–651. doi:10.1016/j.fuel.2013.07.086.
[82] T. Tamminen, Mobile Flip, Mobile Flip Project. (2016). http://www.mobileflip.eu/.
[83] M.J.C. van der Stelt, H. Gerhauser, J.H.A. Kiel, K.J. Ptasinski, Biomass upgrading by torrefaction for the production of biofuels: A review, Biomass and Bioenergy. 35 (2011) 3748–3762. doi:10.1016/j.biombioe.2011.06.023.
[84] D. Nhuchhen, P. Basu, B. Acharya, A Comprehensive Review on Biomass Torrefaction, International Journal of Renewable Energy & Biofuels. (2014) 1–56. doi:10.5171/2014.506376.
[85] P.R. Patwardhan, R.C. Brown, B.H. Shanks, Product Distribution from the Fast Pyrolysis of Hemicellulose, ChemSusChem. 4 (2011) 636–643. doi:10.1002/cssc.201000425.
[86] W.-H. Chen, W.-Y. Cheng, K.-M. Lu, Y.-P. Huang, An evaluation on improvement of pulverized biomass property for solid fuel through torrefaction, Applied Energy. 88 (2011) 3636–3644. doi:10.1016/j.apenergy.2011.03.040.
[87] J. Park, J. Meng, K.H. Lim, O.J. Rojas, S. Park, Transformation of lignocellulosic biomass during torrefaction, Journal of Analytical and Applied Pyrolysis. 100 (2013) 199–206. doi:10.1016/j.jaap.2012.12.024.
[88] Broström, Influence of torrefaction of the devolatilization and oxidation kinetics of wood, (2012).
[89] J. Wannapeera, B. Fungtammasan, N. Worasuwannarak, Effects of temperature and holding time during torrefaction on the pyrolysis behaviors of woody biomass, Journal of Analytical and Applied Pyrolysis. 92 (2011) 99–105. doi:10.1016/j.jaap.2011.04.010.
[90] W. Yan, T.C. Acharjee, C.J. Coronella, V.R. Vásquez, Thermal pretreatment of lignocellulosic biomass, Environ. Prog. Sustainable Energy. 28 (2009) 435–440. doi:10.1002/ep.10385.
[91] D. Ciolkosz, R. Wallace, A review of torrefaction for bioenergy feedstock production, Biofuels, Bioprod. Bioref. 5 (2011) 317–329. doi:10.1002/bbb.275.
[92] D. Güllü, A. Demirbaş, Biomass to methanol via pyrolysis process, Energy Conversion and Management. 42 (2001) 1349–1356. doi:10.1016/S0196-8904(00)00126-6.
[93] M. Phanphanich, S. Mani, Impact of torrefaction on the grindability and fuel characteristics of forest biomass, Bioresource Technology. 102 (2011) 1246–1253. doi:10.1016/j.biortech.2010.08.028.
[94] J. Klinger, E. Bar-Ziv, D. Shonnard, Kinetic study of aspen during torrefaction, Journal of Analytical and Applied Pyrolysis. 104 (2013) 146–152. doi:10.1016/j.jaap.2013.08.010.
[95] J.S. Tumuluru, S. Sokhansanj, J.R. Hess, C.T. Wright, R.D. Boardman, A review on biomass torrefaction process and product properties for energy applications, Industrial Biotechnology. 7 (2011) 384–401. doi:10.1089/ind.2011.7.384.
[96] V. Repellin, A. Govin, M. Rolland, R. Guyonnet, Energy requirement for fine grinding of torrefied wood, Biomass and Bioenergy. 34 (2010) 923–930. doi:10.1016/j.biombioe.2010.01.039.
[97] P. Basu, A.K. Sadhukhan, P. Gupta, S. Rao, A. Dhungana, B. Acharya, An experimental and theoretical investigation on torrefaction of a large wet wood particle, Bioresource Technology. 159 (2014) 215–222. doi:10.1016/j.biortech.2014.02.105.
[98] A. Anca-Couce, I. Obernberger, Application of a detailed biomass pyrolysis kinetic scheme to hardwood and softwood torrefaction, Fuel. 167 (2016) 158–167. doi:10.1016/j.fuel.2015.11.062.
[99] M.J. Prins, K.J. Ptasinski, F.J.J.G. Janssen, Torrefaction of wood. Part 2. Analysis of products, Journal of Analytical and Applied Pyrolysis. 77 (2006) 35–40. doi:10.1016/j.jaap.2006.01.001.

[100] J.-J. Lu, W.-H. Chen, Product Yields and Characteristics of Corncob Waste under Various Torrefaction Atmospheres, Energies. 7 (2013) 13–27. doi:10.3390/en7010013.

[101] A. Aho, N. Kumar, K. Eränen, B. Holmbom, M. Hupa, T. Salmi, D.Y. Murzin, Pyrolysis of Softwood Carbohydrates in a Fluidized Bed Reactor, International Journal of Molecular Sciences. 9 (2008) 1665–1675. doi:10.3390/ijms9091665.

[102] K.R. Hakeem, M. Jawaid, U. Rashid, Biomass and Bioenergy: Applications, Springer, 2014.

[103] M. Cremers, J. Koppejan, J. Middelkamp, J. Witkamp, S. Sokhansanj, S. Melin, S. Madrali, Status overview of torrefaction technologies - A review of the commercialisation status of biomass torrefaction, 2015. http://www.ieabcc.nl/publications/IEA_Bioenergy_T32_Torrefaction_update_2015b.pdf (accessed September 28, 2016).

[104] J. Miguel Carneiro Ribeiro, R. Godina, J. Matias, L. Nunes, Future Perspectives of Biomass Torrefaction: Review of the Current State-Of-The-Art and Research Development, Sustainability. 10 (2018). doi:10.3390/su10072323.

[105] D.R. Simbeck, Coal Gasification Guidebook: Status, Applications, and Technologies : TR-102034, Research Project 2221-39, Final Report, Electric Power Research Institute, 1993.

[106] E4tech, Review of Technologies for Gasification of Biomass and Wastes (Final raport) - NNFCC project 09/008, 2009. http://www.e4tech.com/wp-content/uploads/2016/01/gasification2009.pdf (accessed September 5, 2018).

[107] I. Pastorova, R.E. Botto, P.W. Arisz, J.J. Boon, Cellulose char structure: a combined analytical Py-GC-MS, FTIR, and NMR study, Carbohydrate Research. 262 (1994) 27–47. doi:10.1016/0008-6215(94)84003-2.

[108] J.B. Wooten, J.I. Seeman, M.R. Hajaligol, Observation and Characterization of Cellulose Pyrolysis Intermediates by 13C CPMAS NMR. A New Mechanistic Model, Energy Fuels. 18 (2004) 1–15. doi:10.1021/ef0300601.

[109] R. Fründ, H.-D. Lüdemann, 13C-NMR Spectroscopy of Lignins and Lignocellulosic Materials, in: A. Chesson, E.R. Ørskov (Eds.), Physico-Chemical Characterisation of Plant Residues for Industrial and Feed Use, Springer Netherlands, 1989: pp. 110–117. doi:10.1007/978-94-009-1131-4_10.

[110] T. Melkior, S. Jacob, G. Gerbaud, S. Hediger, L. Le Pape, L. Bonnefois, M. Bardet, NMR analysis of the transformation of wood constituents by torrefaction, Fuel. 92 (2012) 271–280. doi:10.1016/j.fuel.2011.06.042.

[111] T. Melkior, C. Barthomeuf, M. Bardet, Inputs of solid-state NMR to evaluate and compare thermal reactivity of pine and beech woods under torrefaction conditions and modified atmosphere, Fuel. 187 (2017) 250–260. doi:10.1016/j.fuel.2016.09.031.

[112] K. Wang, P.A. Johnston, R.C. Brown, Comparison of in-situ and ex-situ catalytic pyrolysis in a micro-reactor system, Bioresource Technology. 173 (2014) 124–131. doi:10.1016/j.biortech.2014.09.097.

[113] Z. Shi, Y. Zhou, H. Li, Y. Li, H. Hu, In-situ analysis of catalytic pyrolysis of Baiyinhua coal with pyrolysis time-of-flight mass spectrometry, Fuel. 227 (2018) 386–393. doi:10.1016/j.fuel.2018.04.109.

[114] C. Dupont, G. Boissonnet, J.-M. Seiler, P. Gauthier, D. Schweich, Study about the kinetic processes of biomass steam gasification, Fuel. 86 (2007) 32–40. doi:10.1016/j.fuel.2006.06.011.

[115] M. Pach, R. Zanzi, E. Björnbom, Torrefied Biomass a Substitue for Wood and Charcoal, in: Kuala Lumpur (Malaysia), 2002. http://hem.fyristorg.com/zanzi/paper/zanzi_apisceuVI.pdf (accessed March 31, 2016).

[116] P.T. Williams, S. Besler, The influence of temperature and heating rate on the slow pyrolysis of biomass, Renewable Energy. 7 (1996) 233–250. doi:10.1016/0960-1481(96)00006-7.

[117] J. Bourgois, R. Guyonnet, Characterization and analysis of torrefied wood, Wood Sci.Technol. 22 (1988) 143–155. doi:10.1007/BF00355850.

[118] W.-H. Chen, H.-C. Hsu, K.-M. Lu, W.-J. Lee, T.-C. Lin, Thermal pretreatment of wood (Lauan) block by torrefaction and its influence on the properties of the biomass, Energy. 36 (2011) 3012–3021. doi:10.1016/j.energy.2011.02.045.

[119] J. Mundike, F.-X. Collard, J.F. Görgens, Torrefaction of invasive alien plants: Influence of heating rate and other conversion parameters on mass yield and higher heating value, Bioresource Technology. 209 (2016) 90–99. doi:10.1016/j.biortech.2016.02.082.

[120] M.-F. Li, X. Li, J. Bian, C.-Z. Chen, Y.-T. Yu, R.-C. Sun, Effect of temperature and holding time on bamboo torrefaction, Biomass and Bioenergy. 83 (2015) 366–372. doi:10.1016/j.biombioe.2015.10.016.

[121] W.-H. Chen, P.-C. Kuo, Torrefaction and co-torrefaction characterization of hemicellulose, cellulose and lignin as well as torrefaction of some basic constituents in biomass, Energy. 36 (2011) 803–811. doi:10.1016/j.energy.2010.12.036.

[122] M.G. Grønli, G. Várhegyi, C. Di Blasi, Thermogravimetric Analysis and Devolatilization Kinetics of Wood, Ind. Eng. Chem. Res. 41 (2002) 4201–4208. doi:10.1021/ie0201157.

[123] G. Almeida, J.O. Brito, P. Perré, Alterations in energy properties of eucalyptus wood and bark subjected to torrefaction: The potential of mass loss as a synthetic indicator, Bioresource Technology. 101 (2010) 9778–9784. doi:10.1016/j.biortech.2010.07.026.

[124] K. Cheng, W.T. Winter, A.J. Stipanovic, A modulated-TGA approach to the kinetics of lignocellulosic biomass pyrolysis/combustion, Polymer Degradation and Stability. 97 (2012) 1606–1615. doi:10.1016/j.polymdegradstab.2012.06.027.

[125] P. Rousset, I. Turner, A. Donnot, P. Perré, Choix d'un modèle de pyrolyse ménagée du bois à l'échelle de la microparticule en vue de la modélisation macroscopique, Annals of Forest Science. 63 (2006) 17. doi:10.1051/forest:2005113.

[126] Y. Uemura, S. Saadon, N. Osman, N. Mansor, K. Tanoue, Torrefaction of oil palm kernel shell in the presence of oxygen and carbon dioxide, Fuel. 144 (2015) 171–179. doi:10.1016/j.fuel.2014.12.050.

[127] A. Chouchene, M. Jeguirim, B. Khiari, F. Zagrouba, G. Trouvé, Thermal degradation of olive solid waste: Influence of particle size and oxygen concentration, Resources, Conservation and Recycling. 54 (2010) 271–277. doi:10.1016/j.resconrec.2009.04.010.

[128] M.X. Fang, D.K. Shen, Y.X. Li, C.J. Yu, Z.Y. Luo, K.F. Cen, Kinetic study on pyrolysis and combustion of wood under different oxygen concentrations by using TG-FTIR analysis, Journal of Analytical and Applied Pyrolysis. 77 (2006) 22–27. doi:10.1016/j.jaap.2005.12.010.

[129] K.-M. Lu, W.-J. Lee, W.-H. Chen, S.-H. Liu, T.-C. Lin, Torrefaction and low temperature carbonization of oil palm fiber and eucalyptus in nitrogen and air atmospheres, Bioresource Technology. 123 (2012) 98–105. doi:10.1016/j.biortech.2012.07.096.

[130] P. Rousset, L. Macedo, J.-M. Commandré, A. Moreira, Biomass torrefaction under different oxygen concentrations and its effect on the composition of the solid by-product, Journal of Analytical and Applied Pyrolysis. 96 (2012) 86–91. doi:10.1016/j.jaap.2012.03.009.

[131] Y. Uemura, W. Omar, N.A. Othman, S. Yusup, T. Tsutsui, Torrefaction of oil palm EFB in the presence of oxygen, Fuel. 103 (2013) 156–160. doi:10.1016/j.fuel.2011.11.018.

[132] S. Saadon, Y. Uemura, N. Mansor, Torrefaction in the Presence of Oxygen and Carbon Dioxide: The Effect on Yield of Oil Palm Kernel Shell, Procedia Chemistry. 9 (2014) 194–201. doi:10.1016/j.proche.2014.05.023.

[133] S. Septien, High temperature gasification of millimetric wood particles between 800°C and 1400°C, 2011. http://ethesis.inp-toulouse.fr/archive/00001862/.

[134] M.J. Prins, K.J. Ptasinski, F.J.J.G. Janssen, More efficient biomass gasification via torrefaction, Energy. 31 (2006) 3458–3470. doi:10.1016/j.energy.2006.03.008.

[135] E. Biagini, F. Barontini, L. Tognotti, Devolatilization of Biomass Fuels and Biomass Components Studied by TG/FTIR Technique, Ind. Eng. Chem. Res. 45 (2006) 4486–4493. doi:10.1021/ie0514049.

[136] R. Moya, A. Rodríguez-Zúñiga, A. Puente-Urbina, J. Gaitán-Álvarez, Study of light, middle and severe torrefaction and effects of extractives and chemical compositions on torrefaction process by thermogravimetric analysis in five fast-growing plantations of Costa Rica, Energy. 149 (2018) 1–10. doi:10.1016/j.energy.2018.02.049.

[137] M. Lauberts, L. Lauberte, A. Arshanitsa, T. Dizhbite, G. Dobele, O. Bikovens, G. Telysheva, Structural transformations of wood and cereal biomass components induced by microwave assisted torrefaction with emphasis on extractable value chemicals obtaining, Journal of

Analytical and Applied Pyrolysis. (2018). doi:10.1016/j.jaap.2018.03.025.

[138] L.M. Romero Millán, F.E. Sierra Vargas, A. Nzihou, Steam gasification behavior of tropical agrowaste: A new modeling approach based on the inorganic composition, Fuel. 235 (2019) 45–53. doi:10.1016/j.fuel.2018.07.053.

[139] T. Khazraie Shoulaifar, N. DeMartini, O. Karlström, M. Hupa, Impact of organically bonded potassium on torrefaction: Part 1. Experimental, Fuel. 165 (2016) 544–552. doi:10.1016/j.fuel.2015.06.024.

[140] L.A. de Macedo, J.-M. Commandré, P. Rousset, J. Valette, M. Pétrissans, Influence of potassium carbonate addition on the condensable species released during wood torrefaction, Fuel Processing Technology. 169 (2018) 248–257. doi:10.1016/j.fuproc.2017.10.012.

[141] S. Zhang, Y. Su, K. Ding, S. Zhu, H. Zhang, X. Liu, Y. Xiong, Effect of inorganic species on torrefaction process and product properties of rice husk, Bioresource Technology. 265 (2018) 450–455. doi:10.1016/j.biortech.2018.06.042.

[142] A. Guerra, L.A. Lucia, D.S. Argyropoulos, Isolation and characterization of lignins from Eucalyptus grandis Hill ex Maiden and Eucalyptus globulus Labill. by enzymatic mild acidolysis (EMAL), Holzforschung. 62 (2008) 24–30. doi:10.1515/HF.2008.004.

[143] K. Katō, H. Komorita, Pyrolysis of Cellulose, Agricultural and Biological Chemistry. 32 (1968) 21–26. doi:10.1080/00021369.1968.10859016.

[144] M.V. Ramiah, Thermogravimetric and differential thermal analysis of cellulose, hemicellulose, and lignin, J. Appl. Polym. Sci. 14 (1970) 1323–1337. doi:10.1002/app.1970.070140518.

[145] D.F. Arseneau, Competitive Reactions in the Thermal Decomposition of Cellulose, Can. J. Chem. 49 (1971) 632–638. doi:10.1139/v71-101.

[146] A. Broido, M.A. Nelson, Char yield on pyrolysis of cellulose, Combustion and Flame. 24 (1975) 263–268. doi:10.1016/0010-2180(75)90156-X.

[147] A.G.W. Bradbury, Y. Sakai, F. Shafizadeh, A kinetic model for pyrolysis of cellulose, J. Appl. Polym. Sci. 23 (1979) 3271–3280. doi:10.1002/app.1979.070231112.

[148] R.K. Agrawal, Kinetics of reactions involved in pyrolysis of cellulose I. The three reaction model, Can. J. Chem. Eng. 66 (1988) 403–412. doi:10.1002/cjce.5450660309.

[149] R.K. Agrawal, Kinetics of reactions involved in pvrolvsis of cellulose II. The modified kilzer-bioid model, Can. J. Chem. Eng. 66 (1988) 413–418. doi:10.1002/cjce.5450660310.

[150] Luo, Wang, Liao, Cen, Mechanism Study of Cellulose Rapid Pyrolysis, Ind. Eng. Chem. Res. 43 (2004) 5605–5610. doi:10.1021/ie030774z.

[151] V. Mamleev, S. Bourbigot, J. Yvon, Kinetic analysis of the thermal decomposition of cellulose: The main step of mass loss, Journal of Analytical and Applied Pyrolysis. 80 (2007) 151–165. doi:10.1016/j.jaap.2007.01.013.

[152] D.K. Shen, S. Gu, The mechanism for thermal decomposition of cellulose and its main products, Bioresource Technology. 100 (2009) 6496–6504. doi:10.1016/j.biortech.2009.06.095.

[153] D.K. Shen, S. Gu, A.V. Bridgwater, The thermal performance of the polysaccharides extracted from hardwood: Cellulose and hemicellulose, Carbohydrate Polymers. 82 (2010) 39–45. doi:10.1016/j.carbpol.2010.04.018.

[154] S. Wang, X. Guo, T. Liang, Y. Zhou, Z. Luo, Mechanism research on cellulose pyrolysis by Py-GC/MS and subsequent density functional theory studies, Bioresource Technology. 104 (2012) 722–728. doi:10.1016/j.biortech.2011.10.078.

[155] A.D. Paulsen, M.S. Mettler, P.J. Dauenhauer, The Role of Sample Dimension and Temperature in Cellulose Pyrolysis, Energy Fuels. 27 (2013) 2126–2134. doi:10.1021/ef302117j.

[156] D. Chen, A. Gao, K. Cen, J. Zhang, X. Cao, Z. Ma, Investigation of biomass torrefaction based on three major components: Hemicellulose, cellulose, and lignin, Energy Conversion and Management. 169 (2018) 228–237. doi:10.1016/j.enconman.2018.05.063.

[157] J. Lédé, Cellulose pyrolysis kinetics: An historical review on the existence and role of intermediate active cellulose, Journal of Analytical and Applied Pyrolysis. 94 (2012) 17–32. doi:10.1016/j.jaap.2011.12.019.

[158] J. Piskorz, D. Radlein, D.S. Scott, On the mechanism of the rapid pyrolysis of cellulose, Journal of Analytical and Applied Pyrolysis. 9 (1986) 121–137. doi:10.1016/0165-2370(86)85003-3.

[159] J. Scheirs, G. Camino, W. Tumiatti, Overview of water evolution during the thermal degradation of cellulose, European Polymer Journal. 37 (2001) 933–942. doi:10.1016/S0014-3057(00)00211-1.

[160] N. Worasuwannarak, T. Sonobe, W. Tanthapanichakoon, Pyrolysis behaviors of rice straw, rice husk, and corncob by TG-MS technique, Journal of Analytical and Applied Pyrolysis. 78 (2007) 265–271. doi:10.1016/j.jaap.2006.08.002.

[161] H. Yang, R. Yan, H. Chen, D.H. Lee, C. Zheng, Characteristics of hemicellulose, cellulose and lignin pyrolysis, Fuel. 86 (2007) 1781–1788. doi:10.1016/j.fuel.2006.12.013.

[162] C. Branca, C.D. Blasi, C. Mango, I. Hrablay, Products and Kinetics of Glucomannan Pyrolysis, (2013). doi:10.1021/ie400155x.

[163] D.K. Shen, S. Gu, A.V. Bridgwater, Study on the pyrolytic behaviour of xylan-based hemicellulose using TG–FTIR and Py–GC–FTIR, Journal of Analytical and Applied Pyrolysis. 87 (2010) 199–206. doi:10.1016/j.jaap.2009.12.001.

[164] G.R. Ponder, G.N. Richards, Thermal synthesis and pyrolysis of a xylan, Carbohydrate Research. 218 (1991) 143–155. doi:10.1016/0008-6215(91)84093-T.

[165] Y. Peng, S. Wu, The structural and thermal characteristics of wheat straw hemicellulose, Journal of Analytical and Applied Pyrolysis. 88 (2010) 134–139. doi:10.1016/j.jaap.2010.03.006.

[166] T. Hosoya, H. Kawamoto, S. Saka, Cellulose–hemicellulose and cellulose–lignin interactions in wood pyrolysis at gasification temperature, Journal of Analytical and Applied Pyrolysis. 80 (2007) 118–125. doi:10.1016/j.jaap.2007.01.006.

[167] R. Alén, E. Kuoppala, P. Oesch, Formation of the main degradation compound groups from wood and its components during pyrolysis, Journal of Analytical and Applied Pyrolysis. 36 (1996) 137–148. doi:10.1016/0165-2370(96)00932-1.

[168] S. Wang, G. Dai, B. Ru, Y. Zhao, X. Wang, J. Zhou, Z. Luo, K. Cen, Effects of torrefaction on hemicellulose structural characteristics and pyrolysis behaviors, Bioresource Technology. 218 (2016) 1106–1114. doi:10.1016/j.biortech.2016.07.075.

[169] J.C. del Río, A. Gutiérrez, M. Hernando, P. Landín, J. Romero, Á.T. Martínez, Determining the influence of eucalypt lignin composition in paper pulp yield using Py-GC/MS, Journal of Analytical and Applied Pyrolysis. 74 (2005) 110–115. doi:10.1016/j.jaap.2004.10.010.

[170] J.C. del Río, A. Gutiérrez, I.M. Rodríguez, D. Ibarra, Á.T. Martínez, Composition of non-woody plant lignins and cinnamic acids by Py-GC/MS, Py/TMAH and FT-IR, Journal of Analytical and Applied Pyrolysis. 79 (2007) 39–46. doi:10.1016/j.jaap.2006.09.003.

[171] T. Ohra-aho, M. Tenkanen, T. Tamminen, Direct analysis of lignin and lignin-like components from softwood kraft pulp by Py-GC/MS techniques, Journal of Analytical and Applied Pyrolysis. 74 (2005) 123–128. doi:10.1016/j.jaap.2004.11.010.

[172] T. Ohra-aho, F.J.B. Gomes, J.L. Colodette, T. Tamminen, S/G ratio and lignin structure among Eucalyptus hybrids determined by Py-GC/MS and nitrobenzene oxidation, Journal of Analytical and Applied Pyrolysis. 101 (2013) 166–171. doi:10.1016/j.jaap.2013.01.015.

[173] J. Zhao, W. Xiuwen, J. Hu, Q. Liu, D. Shen, R. Xiao, Thermal degradation of softwood lignin and hardwood lignin by TG-FTIR and Py-GC/MS, Polymer Degradation and Stability. 108 (2014) 133–138. doi:10.1016/j.polymdegradstab.2014.06.006.

[174] H. Kawamoto, Lignin pyrolysis reactions, J Wood Sci. 63 (2017) 117–132. doi:10.1007/s10086-016-1606-z.

[175] K. Kuroda, A. Nakagawa-izumi, Analytical pyrolysis of lignin: Products stemming from β-5 substructures, Organic Geochemistry. 37 (2006) 665–673. doi:10.1016/j.orggeochem.2006.01.012.

[176] K.-I. Kuroda, T. Ashitani, K. Fujita, T. Hattori, Thermal behavior of beta-1 subunits in lignin: pyrolysis of 1,2-diarylpropane-1,3-diol-type lignin model compounds, J. Agric. Food Chem. 55 (2007) 2770–2778. doi:10.1021/jf0628126.

[177] Y. Huang, Z. Wei, Z. Qiu, X. Yin, C. Wu, Study on structure and pyrolysis behavior of lignin derived from corncob acid hydrolysis residue, Journal of Analytical and Applied Pyrolysis.

93 (2012) 153–159. doi:10.1016/j.jaap.2011.10.011.

[178] S. Zhou, B. Pecha, M. van Kuppevelt, A.G. McDonald, M. Garcia-Perez, Slow and fast pyrolysis of Douglas-fir lignin: Importance of liquid-intermediate formation on the distribution of products, Biomass and Bioenergy. 66 (2014) 398–409. doi:10.1016/j.biombioe.2014.03.064.

[179] D.K. Shen, S. Gu, K.H. Luo, S.R. Wang, M.X. Fang, The pyrolytic degradation of wood-derived lignin from pulping process, Bioresource Technology. 101 (2010) 6136–6146. doi:10.1016/j.biortech.2010.02.078.

[180] S. Septien, S. Valin, C. Dupont, M. Peyrot, S. Salvador, Effect of particle size and temperature on woody biomass fast pyrolysis at high temperature (1000–1400°C), Fuel. 97 (2012) 202–210. doi:10.1016/j.fuel.2012.01.049.

[181] G. Damköhler, Einflüsse der Strömung, Diffusion und des Wärmeüberganges auf die Leistung von Reaktionsöfen.: I. Allgemeine Gesichtspunkte für die Übertragung eines chemischen Prozesses aus dem Kleinen ins Große, Zeitschrift Für Elektrochemie Und Angewandte Physikalische Chemie. 42 (1936) 846–862. doi:10.1002/bbpc.19360421203.

[182] D.L. Pyle, C.A. Zaror, Heat transfer and kinetics in the low temperature pyrolysis of solids, Chemical Engineering Science. 39 (1984) 147–158. doi:10.1016/0009-2509(84)80140-2.

[183] C. Dupont, Vapogazéification de la biomasse : contribution à l'étude de la phénomenologie entre 800 et 1000°C, Université Claude Bernard - Lyon 1, 2006.

[184] C. Di Blasi, Modeling chemical and physical processes of wood and biomass pyrolysis, Progress in Energy and Combustion Science. 34 (2008) 47–90. doi:10.1016/j.pecs.2006.12.001.

[185] F. Shafizadeh, Introduction to pyrolysis of biomass, Journal of Analytical and Applied Pyrolysis. 3 (1982) 283–305. doi:10.1016/0165-2370(82)80017-X.

[186] A. Anca-Couce, Reaction mechanisms and multi-scale modelling of lignocellulosic biomass pyrolysis, Progress in Energy and Combustion Science. 53 (2016) 41–79. doi:10.1016/j.pecs.2015.10.002.

[187] M.S. Mettler, A.D. Paulsen, D.G. Vlachos, P.J. Dauenhauer, Pyrolytic conversion of cellulose to fuels: levoglucosan deoxygenation via elimination and cyclization within molten biomass, Energy Environ. Sci. 5 (2012) 7864–7868. doi:10.1039/C2EE21305B.

[188] C. Di Blasi, C. Branca, Kinetics of Primary Product Formation from Wood Pyrolysis, Ind. Eng. Chem. Res. 40 (2001) 5547–5556. doi:10.1021/ie000997e.

[189] C.A. Koufopanos, A. Lucchesi, G. Maschio, Kinetic modelling of the pyrolysis of biomass and biomass components, Can. J. Chem. Eng. 67 (1989) 75–84. doi:10.1002/cjce.5450670111.

[190] E. Ranzi, A. Cuoci, T. Faravelli, A. Frassoldati, G. Migliavacca, S. Pierucci, S. Sommariva, Chemical Kinetics of Biomass Pyrolysis, Energy Fuels. 22 (2008) 4292–4300. doi:10.1021/ef800551t.

[191] E. Ranzi, M. Corbetta, F. Manenti, S. Pierucci, Kinetic modeling of the thermal degradation and combustion of biomass, Chemical Engineering Science. 110 (2014) 2–12. doi:10.1016/j.ces.2013.08.014.

[192] M. Corbetta, A. Frassoldati, H. Bennadji, K. Smith, M.J. Serapiglia, G. Gauthier, T. Melkior, E. Ranzi, E.M. Fisher, Pyrolysis of Centimeter-Scale Woody Biomass Particles: Kinetic Modeling and Experimental Validation, Energy Fuels. 28 (2014) 3884–3898. doi:10.1021/ef500525v.

[193] A. Anca-Couce, R. Mehrabian, R. Scharler, I. Obernberger, Kinetic Scheme to Predict Product Composition of Biomass Torrefaction, Chemical Engineering Transactions. 37 (2014) 43–48. doi:10.3303/CET1437008.

[194] P.E.A. Debiagi, C. Pecchi, G. Gentile, A. Frassoldati, A. Cuoci, T. Faravelli, E. Ranzi, Extractives Extend the Applicability of Multistep Kinetic Scheme of Biomass Pyrolysis, Energy Fuels. 29 (2015) 6544–6555. doi:10.1021/acs.energyfuels.5b01753.

[195] K. Dussan, S. Dooley, R. Monaghan, Integrating compositional features in model compounds for a kinetic mechanism of hemicellulose pyrolysis, Chemical Engineering Journal. 328 (2017) 943–961. doi:10.1016/j.cej.2017.07.089.

[196] K. Dussan, S. Dooley, R.F.D. Monaghan, A model of the chemical composition and

pyrolysis kinetics of lignin, Proceedings of the Combustion Institute. (2018). doi:10.1016/j.proci.2018.05.149.

[197] A. Broido, A simple, sensitive graphical method of treating thermogravimetric analysis data, J. Polym. Sci. A-2 Polym. Phys. 7 (1969) 1761–1773. doi:10.1002/pol.1969.160071012.

[198] G. Várhegyi, E. Jakab, M.J. Antal, Is the Broido-Shafizadeh Model for Cellulose Pyrolysis True?, Energy Fuels. 8 (1994) 1345–1352. doi:10.1021/ef00048a025.

[199] F. Shafizadeh, P.P.S. Chin, Thermal Deterioration of Wood, in: Wood Technology: Chemical Aspects, American Chemical Society, 1977: pp. 57–81. http://dx.doi.org/10.1021/bk-1977-0043.ch005 (accessed April 29, 2016).

[200] F. Thurner, U. Mann, Kinetic investigation of wood pyrolysis, Ind. Eng. Chem. Proc. Des. Dev. 20 (1981) 482–488. doi:10.1021/i200014a015.

[201] W.-C.R. Chan, M. Kelbon, B.B. Krieger, Modelling and experimental verification of physical and chemical processes during pyrolysis of a large biomass particle, Fuel. 64 (1985) 1505–1513. doi:10.1016/0016-2361(85)90364-3.

[202] J. Ratte, F. Marias, J. Vaxelaire, P. Bernada, Mathematical modelling of slow pyrolysis of a particle of treated wood waste, Journal of Hazardous Materials. 170 (2009) 1023–1040. doi:10.1016/j.jhazmat.2009.05.077.

[203] J.L. Banyasz, S. Li, J.L. Lyons-Hart, K.H. Shafer, Cellulose pyrolysis: the kinetics of hydroxyacetaldehyde evolution, Journal of Analytical and Applied Pyrolysis. 57 (2001) 223–248. doi:10.1016/S0165-2370(00)00135-2.

[204] J. Klinger, E. Bar-Ziv, D. Shonnard, Unified kinetic model for torrefaction–pyrolysis, Fuel Processing Technology. 138 (2015) 175–183. doi:10.1016/j.fuproc.2015.05.010.

[205] D. da Silva Perez, C. Dupont, A. Guillemain, S. Jacob, F. Labalette, S. Briand, S. Marsac, O. Guerrini, F. Broust, J.-M. Commandre, Characterisation of the Most Representative Agricultural and Forestry Biomasses in France for Gasification, Waste Biomass Valor. 6 (2015) 515–526. doi:10.1007/s12649-015-9374-3.

[206] S.V. Vassilev, D. Baxter, L.K. Andersen, C.G. Vassileva, An overview of the chemical composition of biomass, Fuel. 89 (2010) 913–933. doi:10.1016/j.fuel.2009.10.022.

[207] S.V. Vassilev, D. Baxter, L.K. Andersen, C.G. Vassileva, T.J. Morgan, An overview of the organic and inorganic phase composition of biomass, Fuel. 94 (2012) 1–33. doi:10.1016/j.fuel.2011.09.030.

[208] R. Fahmi, A.V. Bridgwater, L.I. Darvell, J.M. Jones, N. Yates, S. Thain, I.S. Donnison, The effect of alkali metals on combustion and pyrolysis of Lolium and Festuca grasses, switchgrass and willow, Fuel. 86 (2007) 1560–1569. doi:10.1016/j.fuel.2006.11.030.

[209] G. Gellerstedt, J. Pranda, E.-L. Lindfors, Structural and Molecular Properties of Residual Birch Kraft Lignins, Journal of Wood Chemistry and Technology. 14 (1994) 467–482. doi:10.1080/02773819408003108.

[210] F.J. Kolpak, J. Blackwell, Determination of the Structure of Cellulose II, Macromolecules. 9 (1976) 273–278. doi:10.1021/ma60050a019.

[211] T. Stevanovic, Chemical Composition and Properties of Wood, in: Lignocellulosic Fibers and Wood Handbook, Wiley-Blackwell, 2016: pp. 49–106. doi:10.1002/9781118773727.ch3.

[212] E. Rodriguez Alonso, Contribution to the study of formation mechanisms of condensable by-products from torrefaction of various biomasses, Toulouse, INPT, 2015. http://www.theses.fr/2015INPT0148 (accessed February 27, 2018).

[213] M. González Martínez, C. Dupont, S. Thiery, X.M. Meyer, C. Gourdon, Characteristic Time Analysis of Biomass Torrefaction Phenomena - Application to Thermogravimetric Analysis Device, Chemical Engineering Transactions. 50 (2016) 61–66. doi:10.3303/CET1650011.

[214] J.F. Saldarriaga, R. Aguado, A. Pablos, M. Amutio, M. Olazar, J. Bilbao, Fast characterization of biomass fuels by thermogravimetric analysis (TGA), Fuel. 140 (2015) 744–751. doi:10.1016/j.fuel.2014.10.024.

[215] O. Faix, D. Meier, I. Fortlann, Thermal degradation products of wood. Gas chromatographic separation and mass spectrometric characterization of lignin derived products, Holz Als Roh- Und Werkstoff. (1990) 281–285.

[216] O. Faix, D. Meier, I. Fortlann, Thermal degradation products of wood. A collection of electron-impact (EI) mass spectra of monomeric lignin derived products, Holz Als Roh- Und Werkstoff. (1990) 351–354.

[217] O. Faix, I. Fortlann, J. Bremer, D. Meier, Thermal degradation products of wood. Gas chromatographic separation and mass spectrometric characterization of polysaccharide derived products, Holz Als Roh- Und Werkstoff. (1991) 213–219.

[218] O. Faix, D. Meier, I. Fortlann, J. Bremer, Thermal degradation products of wood. A collection of electron-impact (EI) mass spectra of monomeric polysaccharide derived products, Holz Als Roh- Und Werkstoff. (1991) 299–304.

[219] E. Borén, Off-gassing from thermally treated lignocellulosic biomass, 2017. https://umu.diva-portal.org/smash/get/diva2:1157529/FULLTEXT01.pdf.

[220] L. Eriksson, T. Byrne, E. Johansson, J. Trygg, C. Vikström, Multi-and Megavariate Data Analysis Part 1 Basic Principals and Applications, Unimetrics AB, 2001.

[221] M. Trauth, MATLAB® Recipes for Earth Sciences, 4th ed., Springer-Verlag, Berlin Heidelberg, 2015. //www.springer.com/us/book/9783662462430 (accessed August 22, 2018).

[222] A. Sequeiros, J. Labidi, Characterization and determination of the S/G ratio via Py-GC/MS of agricultural and industrial residues, Industrial Crops and Products. 97 (2017) 469–476. doi:10.1016/j.indcrop.2016.12.056.

[223] M. González Martínez, C. Dupont, S. Thiéry, X.-M. Meyer, C. Gourdon, Impact of biomass diversity on torrefaction: Study of solid conversion and volatile species formation through an innovative TGA-GC/MS apparatus, Biomass and Bioenergy. 119 (2018) 43–53. doi:10.1016/j.biombioe.2018.09.002.

[224] S. Fred, F.R. H, C.T. G, S.J. P, S. Yoshio, Production of levoglucosan and glucose from pyrolysis of cellulosic materials, Journal of Applied Polymer Science. 23 (1979) 3525–3539. doi:10.1002/app.1979.070231209.

[225] J. Zhang, J. Luo, D. Tong, L. Zhu, L. Dong, C. Hu, The dependence of pyrolysis behavior on the crystal state of cellulose, Carbohydrate Polymers. 79 (2010) 164–169. doi:10.1016/j.carbpol.2009.07.038.

[226] Z. Wang, A.G. McDonald, R.J.M. Westerhof, S.R.A. Kersten, C.M. Cuba-Torres, S. Ha, B. Pecha, M. Garcia-Perez, Effect of cellulose crystallinity on the formation of a liquid intermediate and on product distribution during pyrolysis, Journal of Analytical and Applied Pyrolysis. 100 (2013) 56–66. doi:10.1016/j.jaap.2012.11.017.

[227] S.D. Stefanidis, K.G. Kalogiannis, E.F. Iliopoulou, C.M. Michailof, P.A. Pilavachi, A.A. Lappas, A study of lignocellulosic biomass pyrolysis via the pyrolysis of cellulose, hemicellulose and lignin, Journal of Analytical and Applied Pyrolysis. 105 (2014) 143–150. doi:10.1016/j.jaap.2013.10.013.

[228] Y. Wu, Z. Zhao, H. Li, F. He, Low temperature pyrolysis characteristics of major components of biomass, Journal of Fuel Chemistry and Technology. 37 (2009) 427–432. doi:10.1016/S1872-5813(10)60002-3.

[229] E. Jakab, O. Faix, F. Till, T. Székely, Thermogravimetry/mass spectrometry study of six lignins within the scope of an international round robin test, Journal of Analytical and Applied Pyrolysis. 35 (1995) 167–179. doi:10.1016/0165-2370(95)00907-7.

[230] Q. Liu, S. Wang, Y. Zheng, Z. Luo, K. Cen, Mechanism study of wood lignin pyrolysis by using TG–FTIR analysis, Journal of Analytical and Applied Pyrolysis. 82 (2008) 170–177. doi:10.1016/j.jaap.2008.03.007.

[231] J. Kibet, L. Khachatryan, B. Dellinger, Molecular Products and Radicals from Pyrolysis of Lignin, Environ. Sci. Technol. 46 (2012) 12994–13001. doi:10.1021/es302942c.

[232] L. Chen, X. Wang, H. Yang, Q. Lu, D. Li, Q. Yang, H. Chen, Study on pyrolysis behaviors of non-woody lignins with TG-FTIR and Py-GC/MS, Journal of Analytical and Applied Pyrolysis. 113 (2015) 499–507. doi:10.1016/j.jaap.2015.03.018.

[233] J. San-Miguel-Ayanz, T. Durrant, R. Boca, G. Libertà, A. Branco, D. De Rigo, D. Ferrari, P. Maianti, T. Artés Vivancos, E. Schulte, P. Loffler, Forest Fires in Europe, Middle East and North Africa 2016, European Commision, Luxembourg, 2017. ISBN 978-92-79-71292-0, doi: 10.2760/17690 (accessed January 29, 2018).

[234] Centro de Coordinación de la Información Nacional sobre Incendios Forestales, Avance informativo de los incendios forestales del 1 de enero al 31 de diciembre de 2017, 2017. http://www.mapama.gob.es/es/desarrollo-rural/estadisticas/avanceinformativo1eneroa31dediciembrede2017_tcm7-358485.pdf (accessed January 29, 2018).

[235] A. Blanco Casal, A. García Arias, B. Valdês Paços, X. Carballido Presas, T. Paz Franco, O monte galego. Sermos Galiza., Santiago de Compostela, 2017.

[236] T. Tamminen, M. Campargue, D. Da Silva Perez, C. Dupont, F. Englund, P. Kotli, S. Larsson, E. Papadopoulou, K. Rasa, T. Raussi, P. Sajet, M. Wallin, Mobile and Flexible Processing of Biomass – EU project MOBILE FLIP, (2016).

[237] D. Woolf, J.E. Amonette, F.A. Street-Perrott, J. Lehmann, S. Joseph, Sustainable biochar to mitigate global climate change, Nature Communications. 1 (2010) 56. doi:10.1038/ncomms1053.

[238] L.J. Míguez Rodríguez, Chandrexa de Queixa, patrimonio natural, Deputación de Ourense, 2010.

[239] D.A. Agar, A comparative economic analysis of torrefied pellet production based on state-of-the-art pellets, Biomass and Bioenergy. 97 (2017) 155–161. doi:10.1016/j.biombioe.2016.12.019.

[240] R. García, M.P. González-Vázquez, C. Pevida, F. Rubiera, Pelletization properties of raw and torrefied pine sawdust: Effect of co-pelletization, temperature, moisture content and glycerol addition, Fuel. 215 (2018) 290–297. doi:10.1016/j.fuel.2017.11.027.

[241] G.J. Evans, R.R. Bellinder, R.R. Hahn, Integration of Vinegar for In-Row Weed Control in Transplanted Bell Pepper and Broccoli, Weed Technology. 25 (2011) 459–465. doi:10.1614/WT-D-10-00167.1.

[242] H. Fischer, Y. Kuzyakov, Sorption, microbial uptake and decomposition of acetate in soil: Transformations revealed by position-specific 14C labeling, Soil Biology and Biochemistry. 42 (2010) 186–192. doi:10.1016/j.soilbio.2009.10.015.

[243] R. Bados, L.S. Esteban, P. Pérez, R. Corredor, V. Zamora, I. Mediavilla, J.E. Carrasco, I. Blasco, R. Calero, H. Velasco, A. Carrascosa, Scrub harvesting trials for energy purposes, in: 2016: pp. 270–272.

[244] S. Pérez, C.J. Renedo, A. Ortiz, F. Delgado, I. Fernández, Energy potential of native shrub species in northern Spain, Renewable Energy. 62 (2014) 79–83. doi:10.1016/j.renene.2013.06.048.

[245] I. Mediavilla, E. Borjabad, M.J. Fernández, R. Ramos, P. Pérez, R. Bados, J.E. Carrasco, L.S. Esteban, Biofuels from broom clearings: Production and combustion in commercial boilers, Energy. 141 (2017) 1845–1856. doi:10.1016/j.energy.2017.11.112.

[246] H. Viana, D.J. Vega-Nieva, L. Ortiz Torres, J. Lousada, J. Aranha, Fuel characterization and biomass combustion properties of selected native woody shrub species from central Portugal and NW Spain, Fuel. 102 (2012) 737–745. doi:10.1016/j.fuel.2012.06.035.

[247] D.J. Vega-Nieva, L. Ortiz Torres, J.L. Míguez Tabares, J. Morán, Measuring and Predicting the Slagging of Woody and Herbaceous Mediterranean Biomass Fuels on a Domestic Pellet Boiler, Energy Fuels. 30 (2016) 1085–1095. doi:10.1021/acs.energyfuels.5b02495.

[248] B.D. González-González, H. Sixto, I. Alberdi, L. Esteban, S. Guerrero, M. Pasalodos, A. Vázquez, I. Cañellas, Estimation of shrub biomass availability along two geographical transects in the Iberian Peninsula for energy purposes, Biomass and Bioenergy. 105 (2017) 211–218. doi:10.1016/j.biombioe.2017.07.011.

[249] L. Núñez-Regueira, J. Proupín-Castiñeiras, J.A. Rodríguez-Añón, Energy evaluation of forest residues originated from shrub species in Galicia, Bioresource Technology. 91 (2004) 215–221. doi:10.1016/S0960-8524(03)00169-X.

[250] G. López González, Los árboles y arbustos de la península Ibérica e islas Baleares I, Mundi Prensa, Madrid, 2006.

[251] F. Bellot Rodríguez, La vegetación de Galicia, Consejo Superior de Investigaciones Científicas, Madrid, 1966.

[252] M.L. Meyer, P.R. Bloom, Lithium metaborate fusion for silicon, calcium, magnesium, and potassium analysis of wild rice, Plant and Soil. 153 (1993) 281–285.

[253] N.J. Walton, M.J. Mayer, A. Narbad, Vanillin, Phytochemistry. 63 (2003) 505–515. doi:10.1016/S0031-9422(03)00149-3.

[254] T. Koeduka, E. Fridman, D.R. Gang, D.G. Vassão, B.L. Jackson, C.M. Kish, I. Orlova, S.M. Spassova, N.G. Lewis, J.P. Noel, T.J. Baiga, N. Dudareva, E. Pichersky, Eugenol and isoeugenol, characteristic aromatic constituents of spices, are biosynthesized via reduction of a coniferyl alcohol ester, Proc. Natl. Acad. Sci. U.S.A. 103 (2006) 10128–10133. doi:10.1073/pnas.0603732103.

[255] R. Berggren, F. Berthold, E. Sjöholm, M. Lindström, Improved methods for evaluating the molar mass distributions of cellulose in kraft pulp, Journal of Applied Polymer Science. 88 (2003) 1170–1179. doi:10.1002/app.11767.

[256] M.G. Grønli, A theoretical and experimental study of the thermal degradation of biomass., Faculty of Mechanical Engineering, 1996.

[257] S. Whitaker, Forced convection heat transfer correlations for flow in pipes, past flat plates, single cylinders, single spheres, and for flow in packed beds and tube bundles, AIChE Journal. 18 (1972) 361–371. doi:10.1002/aic.690180219.

[258] R.H. Perry, Perry's Chemical Engineer Handbook, 7th ed., McGraw-Hill, 1997.

[259] B. Dalloz-Dubrujeaud, R. Faure, L. Tadrist, G. Giraud, Perte de pression et vitesse minimum de fluidisation dans un lit de particules 2D, C. R. Acad. Sci. Paris,. 328 (2000) 231–236.

[260] M. González Martínez, T. Ohra-aho, D. da Silva Perez, T. Tamminen, C. Dupont, Influence of step duration in fractionated Py-GC/MS of lignocellulosic biomass, Journal of Analytical and Applied Pyrolysis. Submitted (June 7th, 2018), under review (2018).

[261] European Commission, State of play on the sustainability of solid and gaseous biomass used for electricity, heating and cooling in the EU, 2014. https://ec.europa.eu/energy/sites/ener/files/2014_biomass_state_of_play_.pdf (accessed September 28, 2016).

[262] EEA Briefing 2/2005 - How much biomass can Europe use without harming the environment? — European Environment Agency, 2005. http://www.eea.europa.eu/publications/briefing_2005_2 (accessed March 14, 2016).

[263] J.-L. Wen, S.-L. Sun, B.-L. Xue, R.-C. Sun, Structural elucidation of inhomogeneous lignins from bamboo, International Journal of Biological Macromolecules. 77 (2015) 250–259. doi:10.1016/j.ijbiomac.2015.03.044.

[264] C. Yan, M. Yin, N. Zhang, Q. Jin, Z. Fang, Y. Lin, Y. Cai, Stone cell distribution and lignin structure in various pear varieties, Scientia Horticulturae. 174 (2014) 142–150. doi:10.1016/j.scienta.2014.05.018.

[265] J. Ponomarenko, T. Dizhbite, M. Lauberts, A. Volperts, G. Dobele, G. Telysheva, Analytical pyrolysis – A tool for revealing of lignin structure-antioxidant activity relationship, Journal of Analytical and Applied Pyrolysis. 113 (2015) 360–369. doi:10.1016/j.jaap.2015.02.027.

[266] Á.T. Martínez, J. Rencoret, G. Marques, A. Gutiérrez, D. Ibarra, J. Jiménez-Barbero, J.C. del Río, Monolignol acylation and lignin structure in some nonwoody plants: A 2D NMR study, Phytochemistry. 69 (2008) 2831–2843. doi:10.1016/j.phytochem.2008.09.005.

[267] C. Crestini, F. Melone, M. Sette, R. Saladino, Milled Wood Lignin: A Linear Oligomer, Biomacromolecules. 12 (2011) 3928–3935. doi:10.1021/bm200948r.

[268] M. Mattonai, D. Licursi, C. Antonetti, A.M. Raspolli Galletti, E. Ribechini, Py-GC/MS and HPLC-DAD characterization of hazelnut shell and cuticle: Insights into possible re-evaluation of waste biomass, Journal of Analytical and Applied Pyrolysis. (2017). doi:10.1016/j.jaap.2017.07.019.

[269] J. Rencoret, J.C. del Río, K.G.J. Nierop, A. Gutiérrez, J. Ralph, Rapid Py-GC/MS assessment of the structural alterations of lignins in genetically modified plants, Journal of Analytical and Applied Pyrolysis. 121 (2016) 155–164. doi:10.1016/j.jaap.2016.07.016.

[270] I. Ericsson, P. Almén, Kinetic and quantitative studies of the formation of SO2 from iron(II) and calcium sulfates by sequential and fractionated pyrolysis, Journal of Analytical and Applied Pyrolysis. 36 (1996) 37–49. doi:10.1016/0165-2370(95)00922-1.

[271] P. Selsbo, I. Ericsson, M. Kleen, Characterization of sulfur in wood pulps using pyrolysis-gas chromatography with sulfur-selective detection: Part 1. Fractionated pyrolysis, Journal

of Analytical and Applied Pyrolysis. 43 (1997) 1–14. doi:10.1016/S0165-2370(97)00055-7.

[272] M. Kleen, T. Ohra-aho, T. Tamminen, On the interaction of HBT with pulp lignin during mediated laccase delignification—a study using fractionated pyrolysis-GC/MS, Journal of Analytical and Applied Pyrolysis. 70 (2003) 589–600. doi:10.1016/S0165-2370(03)00028-7.

[273] L.C.A. Barbosa, C.R.A. Maltha, V.L. Silva, J.L. Colodette, Determination of the siringyl/guaiacyl ratio in eucalyptus wood by pyrolysis-gas chroma-tography/mass spectrometry (PY-GC/MS), Química Nova. 31 (2008) 2035–2041. doi:10.1590/S0100-40422008000800023.

[274] C.F. Lima, L.C.A. Barbosa, C.R. Marcelo, F.O. Silvério, J.L. Colodette, Comparison between analytical pyrolysis and nitrobenzene oxidation for determination of syringyl/guaiacyl ratio in Eucalyptus spp. lignin, BioResources. 3 (2008) 701–712. doi:10.15376/biores.3.3.701-712.

[275] M. Chemin, A.-L. Wirotius, F. Ham-Pichavant, G. Chollet, D. Da Silva Perez, M. Petit-Conil, H. Cramail, S. Grelier, Well-defined oligosaccharides by mild acidic hydrolysis of hemicelluloses, European Polymer Journal. 66 (2015) 190–197. doi:10.1016/j.eurpolymj.2015.02.008.

[276] J. Ralph, R.D. Hatfield, Pyrolysis-GC-MS characterization of forage materials, J. Agric. Food Chem. 39 (1991) 1426–1437. doi:10.1021/jf00008a014.

[277] A. Demirbas, The influence of temperature on the yields of compounds existing in bio-oils obtained from biomass samples via pyrolysis, Fuel Processing Technology. 88 (2007) 591–597. doi:10.1016/j.fuproc.2007.01.010.

[278] A.D. Pouwels, A. Tom, G.B. Eijkel, J.J. Boon, Characterisation of beech wood and its holocellulose and xylan fractions by pyrolysis-gas chromatography-mass spectrometry, Journal of Analytical and Applied Pyrolysis. 11 (1987) 417–436. doi:10.1016/0165-2370(87)85045-3.

[279] X. Bai, K.H. Kim, R.C. Brown, E. Dalluge, C. Hutchinson, Y.J. Lee, D. Dalluge, Formation of phenolic oligomers during fast pyrolysis of lignin, Fuel. 128 (2014) 170–179. doi:10.1016/j.fuel.2014.03.013.

[280] A. Nakagawa-Izumi, Y.Y. H'ng, L.T. Mulyantara, R. Maryana, V.T. Do, H. Ohi, Characterization of syringyl and guaiacyl lignins in thermomechanical pulp from oil palm empty fruit bunch by pyrolysis-gas chromatography-mass spectrometry using ion intensity calibration, Industrial Crops and Products. 95 (2017) 615–620. doi:10.1016/j.indcrop.2016.11.030.

[281] H. Yokoi, T. Nakase, Y. Ishida, H. Ohtani, S. Tsuge, T. Sonoda, T. Ona, Discriminative analysis of Eucalyptus camaldulensis grown from seeds of various origins based on lignin components measured by pyrolysis-gas chromatography, Journal of Analytical and Applied Pyrolysis. 57 (2001) 145–152. doi:10.1016/S0165-2370(00)00137-6.

[282] A. Alves, M. Schwanninger, H. Pereira, J. Rodrigues, Analytical pyrolysis as a direct method to determine the lignin content in wood: Part 1: Comparison of pyrolysis lignin with Klason lignin, Journal of Analytical and Applied Pyrolysis. 76 (2006) 209–213. doi:10.1016/j.jaap.2005.11.004.

[283] T. Ohra-aho, F.J.B. Gomes, J.L. Colodette, T. Tamminen, Carbohydrate composition in Eucalyptus wood and pulps – Comparison between Py-GC/MS and acid hydrolysis, Journal of Analytical and Applied Pyrolysis. 129 (2018) 215–220. doi:10.1016/j.jaap.2017.11.010.

[284] Q. Lu, X. Yang, C. Dong, Z. Zhang, X. Zhang, X. Zhu, Influence of pyrolysis temperature and time on the cellulose fast pyrolysis products: Analytical Py-GC/MS study, Journal of Analytical and Applied Pyrolysis. 92 (2011) 430–438. doi:10.1016/j.jaap.2011.08.006.

[285] M. Kleen, G. Gellerstedt, Characterization of chemical and mechanical pulps by pyrolysis—gas chromatography/mass spectrometry, Journal of Analytical and Applied Pyrolysis. 19 (1991) 139–152. doi:10.1016/0165-2370(91)80040-F.

[286] H. Nimz, Beech Lignin—Proposal of a Constitutional Scheme, Angewandte Chemie International Edition in English. 13 (1974) 313–321. doi:10.1002/anie.197403131.

[287] A. Antonović, V. Jambreković, J. Franjić, N. Španić, S. Pervan, J. Ištvanić, A. Bublić, Influence of sampling location on content and chemical composition of the beech native

lignin (Fagus sylvatica L.), Periodicum Biologorum. 112 (2010) 327–332.
[288] J. Ralph, Hydroxycinnamates in lignification, Phytochem Rev. 9 (2010) 65–83. doi:10.1007/s11101-009-9141-9.
[289] J.-L. Faulon, G.A. Carlson, P.G. Hatcher, A three-dimensional model for lignocellulose from gymnospermous wood, Organic Geochemistry. 21 (1994) 1169–1179. doi:10.1016/0146-6380(94)90161-9.
[290] J. Vogel, Unique aspects of the grass cell wall, Current Opinion in Plant Biology. 11 (2008) 301–307. doi:10.1016/j.pbi.2008.03.002.
[291] C. Crestini, D.S. Argyropoulos, Structural Analysis of Wheat Straw Lignin by Quantitative 31P and 2D NMR Spectroscopy. The Occurrence of Ester Bonds and α-O-4 Substructures, J. Agric. Food Chem. 45 (1997) 1212–1219. doi:10.1021/jf960568k.
[292] G.C. Galletti, P. Bocchini, Pyrolysis/gas chromatography/mass spectrometry of lignocellulose, Rapid Commun. Mass Spectrom. 9 (1995) 815–826. doi:10.1002/rcm.1290090920.
[293] T.B.T. Lam, K. Kadoya, K. Iiyama, Bonding of hydroxycinnamic acids to lignin: ferulic and p-coumaric acids are predominantly linked at the benzyl position of lignin, not the β-position, in grass cell walls, Phytochemistry. 57 (2001) 987–992. doi:10.1016/S0031-9422(01)00052-8.
[294] M. S. Mettler, S. H. Mushrif, A. D. Paulsen, A. D. Javadekar, D. G. Vlachos, P. J. Dauenhauer, Revealing pyrolysis chemistry for biofuels production: Conversion of cellulose to furans and small oxygenates, Energy & Environmental Science. 5 (2012) 5414–5424. doi:10.1039/C1EE02743C.
[295] J. Rencoret, P. Prinsen, A. Gutiérrez, Á.T. Martínez, J.C. del Río, Isolation and Structural Characterization of the Milled Wood Lignin, Dioxane Lignin, and Cellulolytic Lignin Preparations from Brewer's Spent Grain, J. Agric. Food Chem. 63 (2015) 603–613. doi:10.1021/jf505808c.

ANNEX

Annex

I. Complementary raw biomasses

1. Introduction

Forest fires have devastated increasing surfaces in Europe in the last years, especially in the Mediterranean countries. The extreme climate conditions such as extended heat waves, droughts or storms, combined with the abandon of part of the land area previously dedicated to the primary sector, strongly contribute to increase the risk of wildfires [233].

In Spain, nearly 180,000 hectares of forest burnt in 2017, mainly because of the dry climatic conditions in the second half of the year, which represents about twice the average of the previous 10 years. 37.5 % of this forest surface corresponded to woody areas, 56.1% to shrubs and open woodland and the rest to grazing lands. Geographically, 73.8 % of the total burnt forest area corresponds to the Northwest region, in particular the region of Galicia [234]. This could be explained by the fact that Galicia is the Spanish region with the highest annual increase of its biomass volume [235].

Diverse solutions and preventive plans have been proposed to fight against forest fires, such as allowing controlled fires to reduce forest fuel and create discontinuities in the vegetation. This practice is also positive to improve pastures, favor the settlement of various species, and improve accessibility to the forest [233]. However, the carbon footprint of controlled fires is not negligible, especially if it is applied at a large scale.

Biomass valorization may contribute to dispose the excess of forestry resources, particularly from areas presenting a high fire hazard. Consequently, the accessibility of these areas may be improved and shepherding activities can be restored, as they have traditionally regulated biomass in the rural environment, protecting it from fires. Nevertheless, the technology required for this biowaste valorization needs to face with the dispersion, the seasonality and the irregularity of biomass production. A mobile treatment technology was identified as helpful to deal with these characteristics of biomass waste production, avoiding transportation costs and logistics, as well as to provide a valorization solution with a direct impact at local scale [236].

Torrefaction consists of a mild thermochemical conversion process, suitable for dry biomasses, that is, below around 60 % moisture before harvesting. It typically occurs between 200 and 300 °C during a few tens of minutes in a default-oxygen atmosphere [78]. The mild conditions of the process, as well as its robustness proved at industrial scale [103–106], suggest torrefaction as a suitable process for biomass waste conversion through mobile units.

The torrefied solid produced has properties closer to coal in terms of heating value, carbon content, hydrophobicity, grindability as well as flowability [21]. Some studies have pointed out the role of the torrefied solid and pyrolysis biochar in dealing with climate change, as it is

suitable for carbon sequestering, while it can simultaneously provide energy and increasing crop yields [237]. Even if the torrefied product has been traditionally used for energetic purposes such as combustion, co-combustion and gasification [10,21,78,115], it can contribute to soil regeneration and amendment, due to its hydrophobic capacity and mineral content. This use would be related to the traditional clearing of these shrub areas through controlled fires which kept the burnt material on the soil, which was known to improve the quality of the growing pasture [238]. Finally, the torrefied product can be pelletized to be easier transported and easier to handle [239,240]. In all these cases, a local use of the torrefied product obtained from the shrub biowaste valorization is possible.

During torrefaction, condensable coproducts are released, which can damage the installation but may also be source of green chemicals [6,12]. However, it is noteworthy that the diverse chemical composition of the condensable fraction released in torrefaction constitutes an analytical challenge to separate its constituents. The study of this fraction by chemical families allows identifying possible uses of the mixture, generally instead of considering the extraction of one single component [11]. For example, acetic acid has been pointed out as a green herbicide [241] that does not persist in the environment [242].

Previous studies and projects have characterized biomasses susceptible to be involved in forest fires in the South of Europe, in terms of availability and of energetic potential [243,244]. In some cases, the suitability of these biomasses was directly tested in combustion boilers [245,246]. In other cases, the production of pellets for energy purposes was also considered as an alternative [247]. The results of these studies have pointed out that this shrub biowaste appears as a promising resource for energetic valorization, due to its acceptable and stable high heating value as raw material (HHV,~20 MJ kg^{-1}) and its high availability [248,249]. However, up to now, the suitability of transforming shrub biowaste through thermochemical conversion has only been briefly studied in the literature for brooms (*Cytisus multiflorus, Pterospartum tridentatum*) and for fern (*Pteridium aquilinum*) [214].

The objective of this work is to assess the possibility of valorizing through torrefaction six biomasses with a high risk of being involved in forest fires in the South of Europe. To do this, biomasses are deeply characterized at lab-scale in terms of macromolecular and elemental composition, solid transformation kinetics and gaseous species release in torrefaction, including the mass balance of the torrefaction products. The behavior in torrefaction of the biomasses of study is linked to their macromolecular composition, so as to explain how their transformation happens and to estimate the yield of the solid product and the volatile species released in function of the operating conditions.

2. Geographical context

The selected case study corresponds to the Serra de Queixa, a mountainous area included in the Central Massif in Ourense (Galicia), in the North-West of Spain.

2.1. Description of the vegetal cover

The vegetal cover of the Serra de Queixa is non-uniform and distributed in altitudinal strips. It presents remarkable variations due to the anthropic action and to its geographical situation, between the Eurosiberian and the Mediterranean regions [238].

At low altitudes, from 700 to 1200 meters, the vegetation is mainly characterized by deciduous forests, principally including birch (*Betula alba*) and Pyrenean oak (*Quercus pyrenaica*). These forests usually alternate with mowing pastures. Small riparian forests of maples (*Acer pseudoplatanus*) and hazel trees (*Corylus avellana*) can also be found, as well as scattered and sparse patches of relict holly trees (*Ilex aquifolium*) in high valleys with a difficult access. The development of the Pyrenean oak forests is favorable due to the siliceous soils, which acceptably resist frost and drought, and was typically used by its capacity of abundantly supply good quality wood [250]. However, as this activity is decreasing, deciduous wood forests in the area are becoming impenetrable, which increases their propensity to burn.

By ascending in altitude, above 1200 meters, the area is cleared and currently deforested of the oak forest. The traditional clearing of the mountain allowed converting the area into pasture land, enhancing the natural forage grasses (*Nardus stricta*) and obtaining arable land for the cultivation of rye (*Secale cereale*) for livestock and human consumption. The clearing of the mountains let the place to Mediterranean high mountain scrubland, mainly composed of heather and broom. The surface affected by this practice is of approximately 9 000 hectares in the area of study and is estimated to be around 25% of the total vegetal cover in the region [238]. The most abundant heather species are Mediterranean heathlands, especially the association *Pterosparto-Ericetum australis* [251]. This heathland type grows in very poor and shallow soils, acting in soil retention and preventing erosion. Brooms are quickly developed in the places without competition with other species. They are *Fabaceae* or *Papilionoideae* species of the genus *Cytisus* and *Genista*, which includes *Cytisus multiflorus*, *Cytisus striatus* and *Cytisus scoparius*. At higher altitudes, they are replaced by *Genista florida* and on the peaks by *Genista obtusirramea*. Fern (*Pteridium aquilinum*) and gorse (*Ulex minor*) also appear mixed to these plants in variable ratios.

The top of the mountains are characterized by a succession of gentle slopes, where the abundant precipitation facilitates the appearance of well-drained wet surfaces suitable for natural pastures growing.

2.2. Incurrence in forest fires

Three main groups can be established between the species involved in forest fires:

- The first group includes herbaceous species such as fern (*Pteridium aquilinum)*. It is characterized by a high water content, due to its development mainly in wet areas, and a high flammability. These species can be involved in the beginning of fires, especially in dry weather conditions, but usually it does not contribute to maintain them, due to its low biomass content. As a result, its risk of being involved in forest fires is considered low.

- The second group concerns shrublands, including brooms (*Cistus spp*), heather (*Erica spp*) and gorse (*Ulex europaeus*). These species are characterized by a high combustible mass content, while their water content is low. Their high flammability is propitious to start fires in dry weather conditions. Furthermore, the combustion can be maintained for a long time thanks to their compact woody structure, which also favors a quickly propagation of the fire. Their risk of being involved in forest fires is high, as well as their occurrence in the area of study.

- The third group includes wood, being oak (*Quercus pyrenaica*) the most abundant species. They usually suffer a partial and superficial burn in forest fires, including bark and superficial tissue layers. They can survive after a non-prolonged exposition to fire, by quickly recovering from the root to the carbonized branches.

3. Biomass characterization

6 biomasses were selected in order to cover the diversity of lignocellulosic biomass of the region of study (Table A.I.1). The large availability of these biomasses and their high risk of causing fires in the warm season are, in a first approach, interesting arguments for studying their potential in thermochemical valorization.

The selected biomasses include five underexploited solid biofuels from shrublands (white broom, yellow broom, heather, fern and gorse). The knowledge in the literature about these biomasses in terms of thermochemical conversion is very limited [214]. A deciduous wood, Pyrenean oak, was also included in this study, because of its high mismanaged production and low quality for furnishing or construction (thin and twisted trunk). For the 6 biomasses, the whole plant is considered (trunks, branches, leaves, flowers), as they represent an important volume of these biomass resources.

Concerning the preparation of the biomasses, they were harvested in the North-West of Spain (Chandrexa de Queixa, Ourense) in the summer 2016. Then, biomasses were shredded to 2-3 mm particle size and let drying at ambient temperature for 14 days. Then, they were dried at 105°C for 24h. Two successive shredding operations were carried out on the dry biomass: a first grinding step with a 1.5 mm-grid with an Universal cutting mill Retsch (Retsch GmbH, Haan, Germany) and a second grinding step to a particle size inferior to 500 µm with an Universal

cutting mill Fritsch Pulverisette 14 (Fritsch GmbH, Idar-Oberstein, Germany). All particle size fractions resulting from this last grinding were considered (no screening was made).

Table A.I.1. Biomass samples (raw and after preparation, < 500µm)

	Fern	Gorse	Heather	Oak	White broom	Yellow broom
Raw						
< 500 µm						

Moisture was evaluated by comparing biomass before and after the convective drying (Table A.I.2). Moisture content was low, due to the 14-days drying. The original moisture content of biomass, after harvesting and before natural drying, would be much higher, around 50 %, except for oak, around 30 % [45].

Table A.I.2. Biomass characterization

Composition	*Method*	**Fern**	**Gorse**	**Heather**	**Oak**	**White broom**	**Yellow broom**
Physical properties				*% w*			
Moisture content	*NF EN 14774*	11.8	9.0	13.3	14.8	11 .3	17.3
Macromolecular composition				*% wmf*			
Polysaccharides	*TAPPI T249 cm-85*	45.4	47.1	41.1	50.7	60.2	67.8
Lignin	*TAPPIT222om-83/ T222 om-84*	30.1	30.0	35.9	25.3	25.0	22.1
Extractives	[205]	15.1	14.5	18.3	14.0	11.8	7.4
Ash	*XP CEN/TS 14775*	4.5	1.4	1.3	3.6	1.2	1.3
Mass balance		*95.0*	*93.0*	*96.6*	*93.7*	*98.2*	*98.5*
Neutral sugars composition of polysaccharides *(normalized to 100 %)*				*%*			
Glucose	*TAPPI T249 cm-85*	65.3	64.3	58.6	60.5	60.8	65.1
Xylose		16.5	24.8	33.1	28.8	30.5	30.7
Mannose		13.8	0.0	0.0	0.0	0.0	0.0
Galactose		2.7	4.2	4.8	4.9	3.1	1.7
Arabinose		1.7	6.7	3.6	5.7	5.6	2.5
Functional groups				*% wmf*			
Acetyl	[205]	3.7	4.8	5.8	5.5	5.9	6.7

%w: mass percentage; % wmf: weight-moisture-free; % of the total monosugars

Biomass chemical organic and inorganic composition was measured as described by [205] (Tables A.I.2 and A.I.3). However, cellulose and hemicellulose content was not calculated, but only reported as "Polysaccharides content" in Table 1. Indeed, part of glucose content measured could belong to hemicelluloses, especially xyloglucans and galactoglucomannas. To our knowledge, no detailed information exists about the chemical composition of hemicelluloses for most of the biomasses studied in this work, which prevents us from estimating cellulose and hemicelluloses content.

Biomass macromolecular composition is within the range of variation observed for other biomasses studied in the literature [205–207,223].

Lignin content values are in the typical range of other biomasses, except for heather (around 36 %). Polysaccharides content of fern and gorse is similar to that obtained for oak. Contrary, quite high values were measured for the two *Genista* species, especially for yellow broom (around 68 %). On the other hand, due to high lignin and extractive content, the polysaccharide content of heather is considerably lower than that of the other biomasses.

The extractives content of the 6 biomasses is quite high, which is typically a characteristic of agricultural and tannin-containing biomasses, such as oak [205,223]. The valorization of the molecules contained in the extractives fraction could be the object of a more thorough study, considering its composition and the suitable extraction method from biomass.

The sugar composition present in the polysaccharides of the different biomasses is similar for glucose (58 to 65 %), but presents some differences when the other sugars content is analyzed. Xylose is present in high proportions for all biomasses (24 to 35 %), except for fern, which presents similar proportions of xylose and mannose. This latter is completely absent in other biomasses. Galactose and arabinose content is lower than glucose and xylose content, and present some variation between the biomasses. The acetyl group content is similar for all biomasses, although fern presents smaller values. As a consequence of these observations, fern hemicelluloses seem to be a mixture of xylans and (galacto)glucomannans, similarly to agricultural biomasses. The other biomasses seem to contain predominantly xylans (eventually glucoxylans for the shrub biomasses). The presence of arabinose and galactose could be explained by the presence of arabinogalactans type II, generally found in herbal plants [55].

Ash content is very low for all biomasses except for fern which is similar to the agricultural biomasses (Table A.I.2). Biomass elemental composition was measured following typical standards (Table A.I.3). Ash composition was measured through Inductively Coupled Plasma Atomic Emission Spectroscopy (ICP–AES) after mineralization for all inorganic species except for silicon, which was measured after alkaline melting, as proposed by [252].

Table A.I.3. Biomass main inorganic composition

Element	*Method*	Fern	Gorse	Heather	Oak	White broom	Yellow broom
Main elemental composition				*% w*			
C	*XP CEN/TS15104*	47.5	50.0	52.3	47.2	47.8	49.2
H	*XP CEN/TS15105*	5.8	6.4	6.4	5.9	6.4	6.3
N	*XP CEN/TS15107*	0.6	1.1	0.7	0.7	0.9	1.0
O	*By difference*	42.4	41.7	40.0	44.2	43.9	43.2
Main inorganic ash composition				*g / Kg (biomass)*			
Al	*XP CEN/TS 15290*	2.9	10.3	14.4	2.1	4.3	10.6
Ca		63.0	136.5	98.7	239.3	121.1	118.5
Cu		0.2	0.5	0.1	0.1	0.4	0.1
Fe		2.4	10.2	10.8	2.5	6.3	10.8
K		289.3	132.9	213.8	101.7	279.2	229.9
Mg		24.5	55.4	52.1	18.6	66.8	80.7
Mn		2.2	9.4	24.2	4.4	5.0	10.5
Na		50.2	91.9	21.7	3.9	3.8	14.4
Ni		0.2	< 0.1	0.1	< 0.1	0.1	0.1
P		27.2	39.7	41.1	19.7	34.8	36.3
Si		79.4	39.3	74.6	11.0	10.4	32.9
Zn		0.5	2.3	1.0	0.9	1.2	1.2

%w: mass percentage

A similar main elemental composition was found for the biomasses of study, which remains in the same order of magnitude of that reported in previous studies [71,205,207]. Differences were observed in the main inorganics content, slightly lower for the two broom species. Potassium content was lower for gorse and oak, while the calcium content was higher for these biomasses compared to the other biomasses of study.

As a result, the macromolecular composition of the biomasses of study seems close to that of deciduous wood for all biomasses except for fern, whose composition seems closer to that of agricultural biomasses. The main elemental composition of these biomasses is similar, with small differences between the species.

4. Behavior in torrefaction

4.1. Solid kinetics

TGA experiments were carried out to compare the kinetic behavior of the 6 biomasses (Figure A.I.1) to that of the biomasses in the database (Figure IV.1). A general mass loss between 24.4 and 30.8% was achieved at the end of the dynamic torrefaction (200-300°C, 3°C/min), while it was between 42.1 and 52.7% for the overall torrefaction, after the isothermal step (300°C, 30 min).

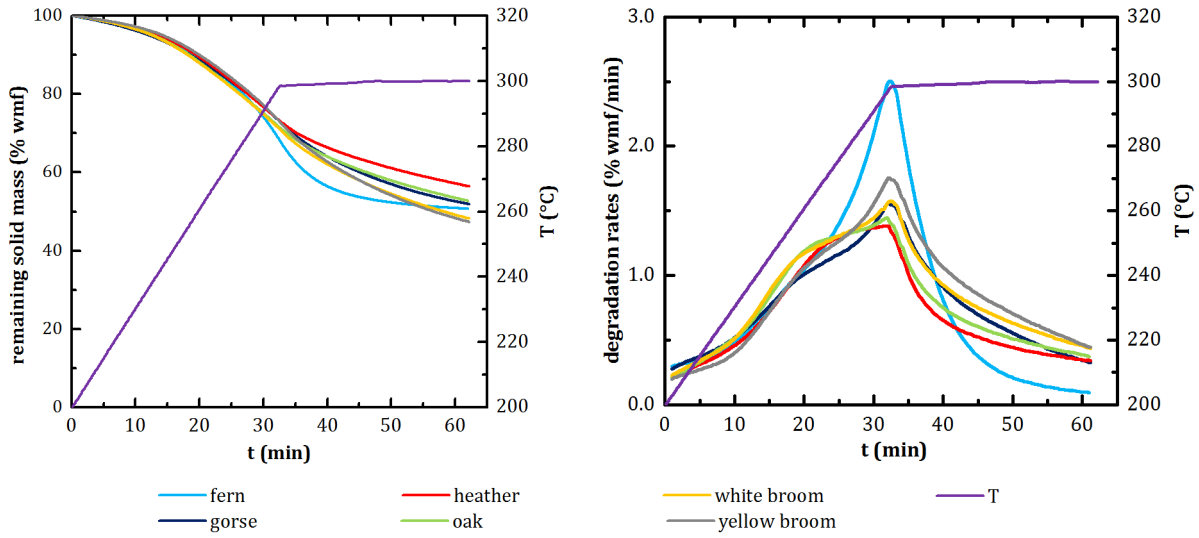


Figure A.I.1. Remaining solid mass (left) and degradation rates (right) versus time and temperature obtained during torrefaction of the complementary biomasses in TGA-GC/MS

Concerning the kinetics of the solid transformation, similar profiles were found for the investigated biomasses, except for fern, both in terms of solid mass loss and degradation rates (Figure A.I.1). In the dynamic torrefaction, the solid degradation is characterized by an acceleration of the mass loss until around 250°C, followed by a slower acceleration until the end of the dynamic torrefaction. In the isothermal step, the mass loss is progressively decelerated. In the case of fern, the change in mass loss acceleration at intermediate torrefaction temperatures is less remarkable, reaching higher values of the degradation rate around 300°C (2.5% compared to 1.4 -1.7% for the other biomasses). Furthermore, the deceleration in the isothermal step is more accentuated, nearly tending to zero after 30 minutes at 300°C.

The solid degradation profile of fern seems closer to that of a coniferous wood or a wheat straw, whereas the kinetic behavior of the 5 other biomasses is rather similar to that of a deciduous wood. This could be explained by the particular composition of fern, with a high ash content, typical of agricultural biomasses, and a ratio xylan/glucomannan in its hemicellulose sugars close to 1 as for annual plants, this latter sugar being typical of coniferous wood.

The quality of the solid product after torrefaction was evaluated in terms of the evolution of its elemental composition in C, H and O (Figure A.I.2). The results show an increase of the carbon content from 19.6% for heather to 42.6% for fern. This can be explained by the higher percentage of permanent gases (CO, CO_2) produced in fern torrefaction compared to heather torrefaction (experiments not shown here). The composition in O was consequently diminished of 45.0% for fern and 23.5% for heather. The composition in H was barely affected after torrefaction, except for yellow broom, for which it decreased by about 11.8 %. These results are in agreement with those from the biomasses in the database.

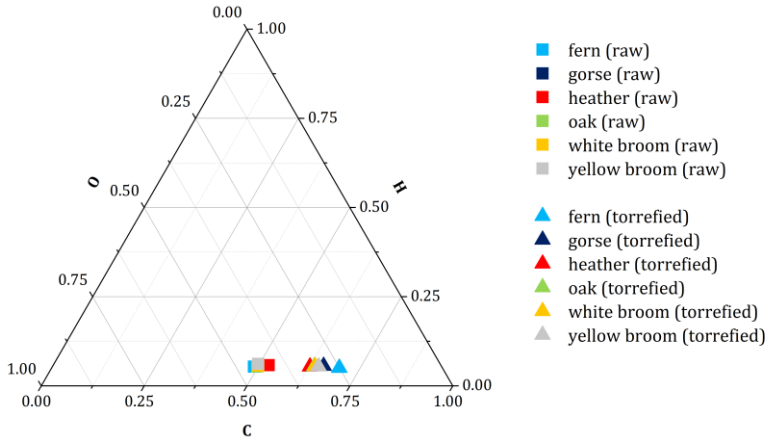


Figure A.I.2. Ternary diagram of CHO elemental composition of raw and torrefied biomasses in TGA-GC/MS

In a process view-point, considering the results, brooms, gorse, heather and oak present a similar behavior in torrefaction in terms of solid kinetics. This behavior, which can be predicted from the deciduous wood in the database, implies that any mixture of these materials, which is more often the case in practice, is expected to behave similarly in torrefaction. As a result, the valorization through mobile torrefaction units of these individual biomasses or of their mixture, even in variable proportions, is expected to be easy to handle and the result predictable through the database. Fern presents a behavior in torrefaction closer to that of herbaceous crops and agricultural biomasses. However, it often grows separated from these species, in wetter and darker areas typical of the caducifolius forest rather than in the shrubland areas susceptible to suffer forest fires. As a result of this natural separation, it can be excluded of the study. Its native high moisture content (> 50%) makes it more suitable for direct composting. However, it can sometimes grow in deforested areas, mixed with shrublands; this is the reason why it has also been considered in this study.

Finally, the natural drying of these biomasses by leaving them several days in the field after harvesting and before collecting them makes their moisture content uniform for all biomasses, including for fern (Table A.I.2). As a result, they can be transformed together, even if the kinetic solid yield is more difficult to be predicted because of the different behavior of fern compared to brooms, heather, gorse and oak.

These results on complementary raw biomasses confirm the suitability of the raw materials included in biomass database to represent biomass diversity, especially in the case of woody biomasses. Consequently, the solid kinetic behavior in torrefaction can be estimated by identifying the biomass family in the database to which a biomass of study belongs. This estimation can be considered acceptable for woody biomasses in terms of solid degradation profile and final mass loss, if biomass macromolecular composition remains similar to that of the biomasses in the same family in the database. However, in the case of agricultural biomasses, including herbaceous crops, the heterogeneity in their macromolecular composition complicates

an accurate estimation of their behavior in torrefaction. In this case, the estimation can be approximated by the agricultural or herbaceous biomass in the database with the closest macromolecular composition.

4.2. Volatile species release

23 chemical compounds were quantified in GC/MS for the dynamic torrefaction from 200 to 300°C at 3°C/min. The quantified chemical compounds include acids, furans, phenols, ketones, alcohols and aldehydes and are in agreement with biomasses from the database and with previous studies [7,12,29].

The total quantified volatile species production goes from 2.5 mg for heather to 1.5 mg for oak, released by a mass of biomass transformed from 265 mg for heather to 308 mg for oak (all experiments were normalized to 1g of initial biomass for comparison). This quantified fraction can be considered acceptable as only a part of the volatile species could be identified in the gaseous mixture released in biomass torrefaction, which is in accord with previous studies in the literature [7,12].

By analyzing the total production per chemical family and per biomass (Figure A.I.3), acids appear as the major chemical compounds quantified, followed by alcohols and aldehydes. Furans, phenols and ketones are detected in minor amounts. The non-identified volatile fraction is expected to contain also these categories of chemical species, as well as sugar molecules, which could not be identified with our chromatographic column. However, it is noteworthy that the diverse chemical composition of the condensable fraction released in torrefaction constitutes an analytical challenge to separate its constituents [11]. The study of this fraction by chemical families allows identifying possible uses of the mixture, generally instead of considering the extraction of one single component [11]. For example, acetic acid has been pointed out as a green herbicide [241] that does not persist in the environment [242].

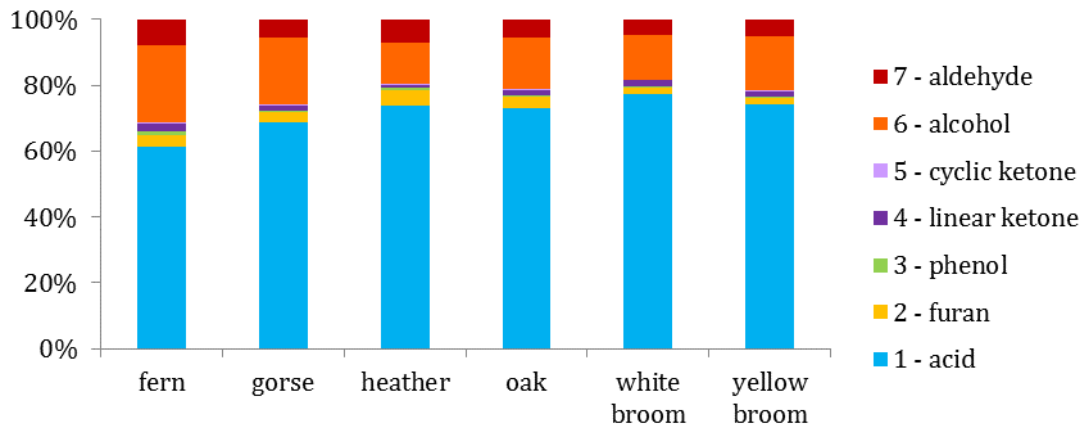


Figure A.I.3. Distribution of the total production of volatile species per chemical family in biomass torrefaction of the complementary biomasses in TGA-GC/MS (200-300°C, 3°C/min)

The major volatile species detected are acetic acid (from 60.7 to 77.1 % of the total volatile species quantified), methanol (12.6 to 23.6 %), formaldehyde (4.8 to 7.7 %), furfural (1.6 to 4.3 %) and hydroxyacetone (0.3 to 1.2 %). Minor amounts of chemical compounds that can present an interesting added-value as green chemicals are produced, such as vanillin [253] and eugenol/isoeugenol [254].

Secondly, the study of the profile of formation of each volatile species in function of the torrefaction temperature was carried out. Results are presented here for the major volatile species detected (Figures A.I.4 to A.I.9).

Acetic acid production is higher for heather and brooms, compared to that of fern (Figure A.I.4, left), which can be explained by the slightly lower acetyl content of fern (5.2 % compared to 6.0 to 6.8 %). Its maximum of production is around 270°C, which corresponds to the degradation of hemicellulose sugars, containing acetyl groups in terminal positions [13,73]. No other volatile species presented a profile of production close to that of acetic acid. Other acids detected were formic acid and propionic acid. In the first case, only small amounts were detected at 270 to 300°C for heather and fern, below 1 mg (formic acid produced at a given T) per g (biomass transformed). This compound is supposed to be formed from the breaking of carboxylic acid function of the hexuronic acids in hemicelluloses [163]. Propionic acid presents an increasing production with increasing torrefaction temperature (Figure A.I.4, right).

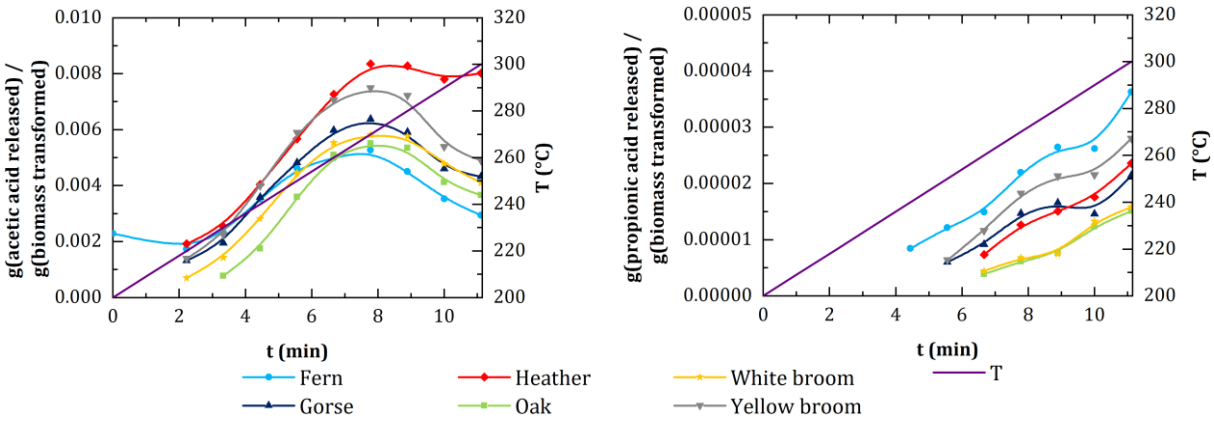


Figure A.I.4. Production profiles of acetic acid (left) and propionic acid (right) in biomass torrefaction in TGA-GC/MS (200-300°C, 3°C/min)

Methanol presents also a particular profile of production, with the maximum of its production profile at low torrefaction temperatures (Figure A.I.5). This chemical species is expected to be mainly produced by hemicelluloses, from the fragmentation of the methoxy group of the 4-O-methyl-α-D glucuronic acid [99,163]. Even it is mainly produced by fern, the highest hemicellulose content was found for brooms, which could indicate that it would be necessary to go more into detail in the hemicellulose composition in biomass to explain its production, as it was done with acetyl groups for acetic acid.

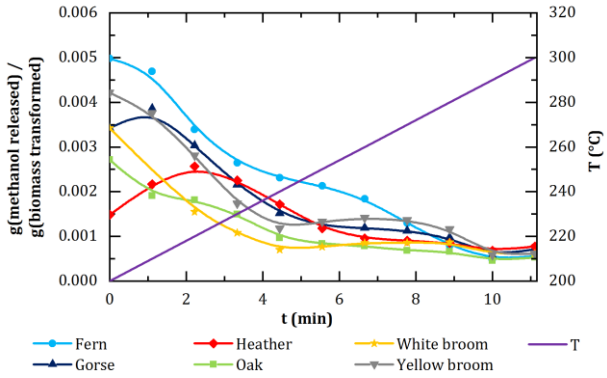


Figure A.I.5. Production profiles of methanol in biomass torrefaction in TGA-GC/MS (200-300°C, 3°C/min)

Formaldehyde is characterized by a rather constant profile of production in function of temperature (Figure A.I.6). It has been reported in the literature to be released in lignin decomposition, more precisely from the fragmentation between Cβ and Cγ in lignin structure, when the hydroxyl group is linked to the Cγ [229,230]. The results show a higher production for heather and fern, while brooms, oak and gorse present a lower production. This is consistent with the higher lignin content of heather (37.1 %), the lower for oak (27.0 %) and for brooms (25.5 % for white broom, 22.4 % for yellow broom). However, gorse and fern have similar lignin content (32.2 % and 31.7 %, respectively) and the formaldehyde production is different at lower temperatures (below 260°C). This could indicate a difference in lignin structure between fern, whose macromolecular composition and thermochemical behavior seem close to agricultural biomasses, and gorse, which seems closer to deciduous wood. Indeed, lignin from deciduous wood lignin is composed by G- (guaiacyl-) and S- (syringyl-) units [63], while lignin from herbaceous plants also contains H- (phenyl-) units [222]. These results are in accord with the observations on biomasses from the database (Figure A.I.11).

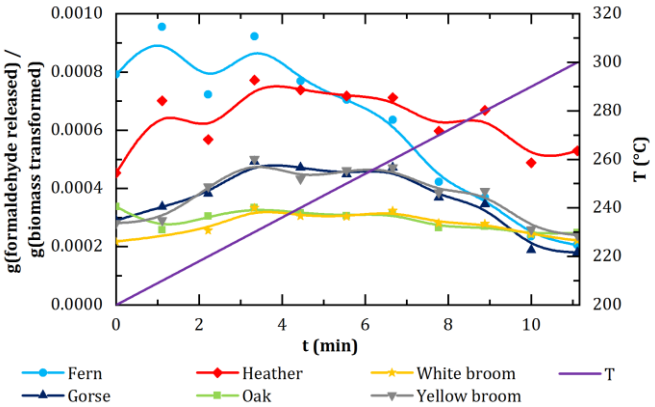


Figure A.I.6. Production profiles of formaldehyde in biomass torrefaction in TGA-GC/MS (200-300°C, 3°C/min)

The profile of production of hydroxyacetone starts at intermediate torrefaction temperatures and presents two local minima at 270 and 290°C, followed by an increase in the production at 300°C (Figure A.I.7, left). This chemical compound is expected to be produced by hemicelluloses

[29], which explains its release at intermediate torrefaction temperatures, and by cellulose, which could contribute to the rise in the production at 300°C [152]. On the other hand linear ketones, such as 2,3-pentanedione and 2-propanone,1-(acetyloxy)-, present profiles with a production that increases with temperature in an equivalent order of magnitude for the 6 biomasses, below 1 mg (compound produced at a given T) per g (biomass transformed) (Figure A.I.7, right). They would rather come from the defragmentation of hemicelluloses.

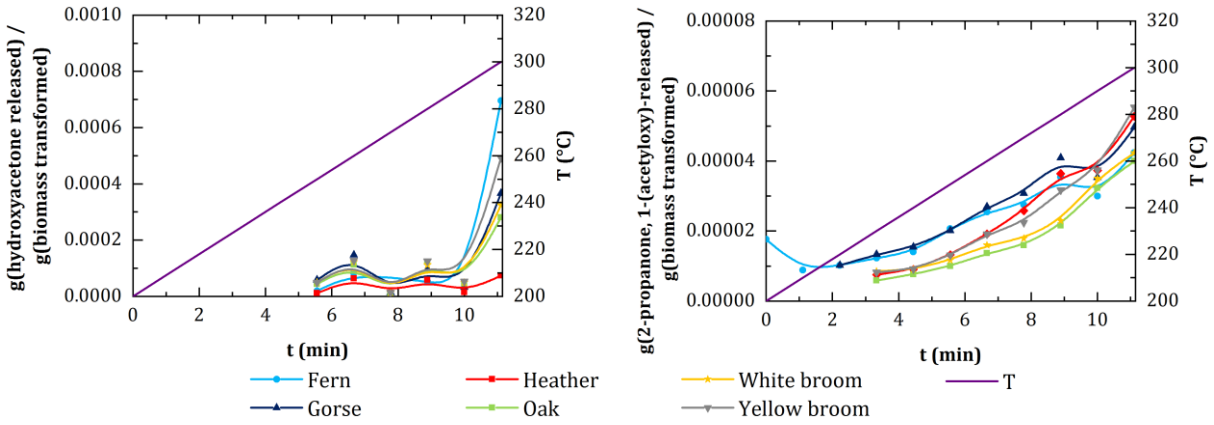


Figure A.I.7. Production profiles of hydroxyacetone (left) and 2-propanone,1-(acetyloxy)- (right) in biomass torrefaction in TGA-GC/MS (200-300°C, 3°C/min)

Furfural is the main furan detected. These compounds are mostly glucan-derived compounds from cellulose [152], but they can also come from hemicelluloses depolymerization [165]. However, the profile of formation of the furans detected is characterized by an increase in the production with the increasing torrefaction temperatures (Figure A.I.8, right), except for furfural, whose production is only slightly increasing with temperature (Figure A.I.8, left). This is in accord with previous studies, which have detected furfural at low temperatures [163]. As for all the furans detected, the highest furfural production was quantified for heather and fern, which contrasts with the fact that these are the biomass with the lower carbohydrate content (cellulose + hemicellulose).

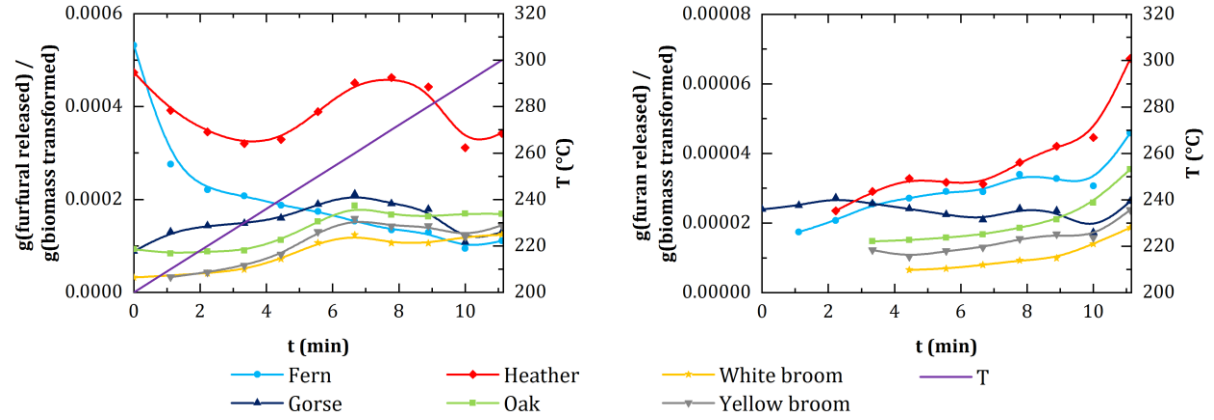


Figure A.I.8. Production profiles of furfural (left) and furan (right) in biomass torrefaction in TGA-GC/MS (200-300°C, 3°C/min)

The profile of production of phenol starts at intermediate torrefaction temperatures around

250°C and shows an increasing production until 300°C (Figure A.I.9, left). Phenol was the major phenolic compound detected, followed by guaiacol (about half of the phenol production, Figure A.I.9, right). Other phenolic compounds, such as isoeugenol, syringol and vanillin were detected in minor amounts between 280 and 300°C. Cathecol, eugenol and 2-methoxy-4-vinylphenol did not enable to represent a profile of formation, as they were only detected in small amounts at 300°C, and were not considered in this analysis. Phenolic compounds are produced from defragmentation of lignin. The maximum production of phenol was measured for heather and fern, as in the case of formaldehyde.

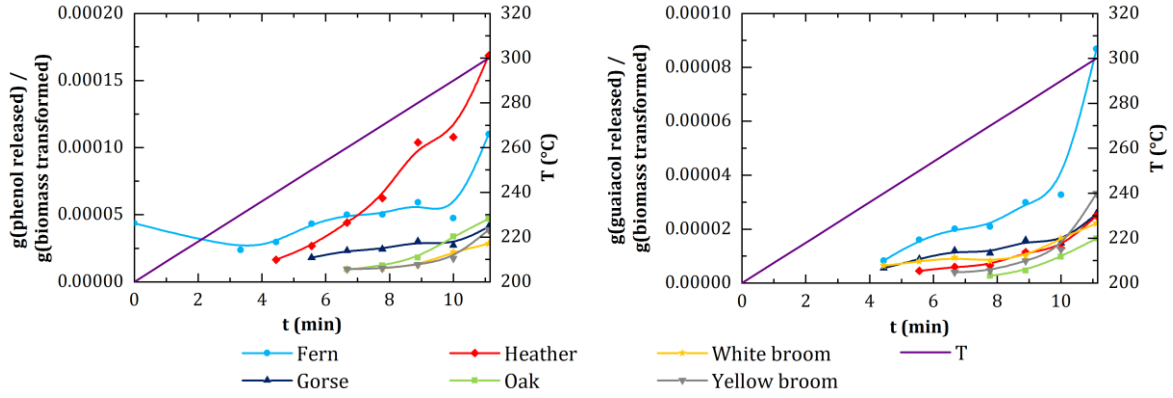


Figure A.I.9. Production profiles of phenol (left) and guaiacol (right) in biomass torrefaction in TGA-GC/MS (200-300°C, 3°C/min)

In a process view-point, the composition of the volatile fraction of the 6 biomasses in torrefaction is similar, which indicates that the condensable fraction would have a similar composition by torrefying a mixture of these biomasses, as they are present in the nature. At the same time, the profile of formation and the temperature of the maximum production can suggest the origin of the volatile species. The production profiles of the volatile species are a useful tool to set the optimum operating temperature which enhances the proportion of a given volatile species in the condensable fraction obtained from torrefaction.

5. Conclusions

According to these results, it seems challenging to accurately predict the behavior of a new biomass in terms of volatile species production just by comparison to biomasses in the database. However, the results show general tendencies of production of the volatile species which are related to their macromolecular composition. These observations are in agreement with previous studies in the literature and complement them by suggesting the evolution of the production of each volatile species in function of the biomass type and of the torrefaction temperature. As a result, production profiles of volatiles species released from biomasses in the database can be considered as a tool to roughly estimate the proportions of volatile species produced for a given biomass. The main criterion for this comparison is suggested to be biomass macromolecular composition, together with biomass family (woody, herbaceous or agricultural biomass).

II. Characterization methods

Table A.II.1. Characterization methods for determining biomass macromolecular and elemental composition

Component	Standard method	Description of the method
Extractives	Internal method	ASE (Accelerated Solvent Extractor) type extraction with two cycles at 1500 psi, firstly with water at 110 °C then with acetone at 95 °C. Solvents were evaporated under reduced pressure, and then the residues were weighed and reported as the extractive content.
Lignin		Measured on the extracted samples. Determined by the sum of Klason and soluble lignin.
Klason lignin	TAPPI standard T222 om-83	Residue after double acidic hydrolysis and ionic chromatography analysis.
Soluble lignin	TAPPI standard T222 om-84	Residue after double acidic hydrolysis and ionic chromatography analysis.
Cellulose, hemicellulose	TAPPI T249 cm-85	Ion chromatography after a two-step hydrolysis of delignified extracted samples in sulfuric acid.
Neutral monosugars	ASTM E1758	Ion chromatography: Dionex DX5000 system equipped with GP50 gradient pumps using NaOH 150 mM and water as eluents, a CarboPac PA-10 column and an ED50 electrometric detector (amperometric cell).
Acetyl groups	Internal method	Ion chromatography: IonPac AS11-HC column and an electrometric detector in conductometric mode with an eluant gradient NaOH 60 mM and water.
Ash content	XP 199 CEN/ TS 14775	Residue after total combustion at 550°C.
Carbon (C) content	XP CEN/ TS 15104	Total combustion and measurement of gases.
Hydrogen (H) content	XPCEN/ TS 15105	Total combustion and measurement of gases.
Nitrogen (N) content	XPCEN/ TS 15107	Total combustion and measurement of gases.
Oxygen (O) content	-	By difference.

III. Cellulose size-exclusion chromatography characterizations

The « cellulose II » extracted fractions were characterized in terms of molar mass distribution (MMD) by means of a derivatization procedure using cellulose tricarbanilates (CTC's). It consists of a non-polar cellulose derivative that is fully soluble in THF, the chromatographic solvent used for the analysis of MMD by size-exclusion chromatography (SEC). Cellulose reaction with phenylisocyanate allows full derivatization of the OH groups of the cellulosic chains, i.e. a degree of substitution of three, and the molar mass of the substituted monomers becomes 519 g/mol. In the case of the commercial microcrystalline cellulose Avicel, the derivatization was carried out by using pyridine as derivatization solvent.

Derivatization to form CTC's followed a procedure adapted from Berggren et al. (2003) [255]. Solvent exchange with pure/dry dimethylacetamide (DMAC) was applied on the wet pulp sample (50 mg dry basis). DMAC-LiCl (6% LiCl) and phenylisocyanate were added simultaneously onto cellulose and the reaction was carried out in closed stirred flasks at 40°C under mild stirring. It was stopped after 5 days by adding an excess of methanol. Dilution in DMAC and final dilution in THF allowed reaching a CTC concentration of about 0.35 mg mL-1 for SEC injection. The chromatographic system included a Malvern GPC-max system equipped with DRI, UV, LALS, RALS and viscometer detectors, three PL-GEL mixed-B columns, one PL-GEL guard column, all kept in an oven at 35°C. The system was eluted with THF at a flow rate of 1 mL min-1. Data were treated with the OMNISEC 4.5TM software from Malvern Corporation.

For molar mass quantification, a SEC-multidetection system was applied, which coupled differential refractometer (DRI), UV spectrophotometry detector, dual-angle light-scattering (LALS/RALS) detectors and viscometer. The coupling of DRI and LS allows quantifying the molar mass of each eluent fraction. Coupling DRI and viscometer signals leads to the intrinsic viscosity, which in turn results in data of hydrodynamic radius. The gyration radius will be calculated from the Zimm plot based on the two-angle LS detector signal.

The molar mass distribution from each « cellulose II» fraction and from the commercial microcrystalline cellulose Avicel were firstly analyzed (Figure A.III.1). It is important to note that all molar mass values given here are those of tricarbanilate cellulose from the cellulosic samples, with a monomer molar mass of 519 g/mol. Thus, to obtain the data for the actual underivatized cellulose, one should divide by 519 and multiply by 162, which is the molar mass of the anhydroglucose monomer ($C_6H_{10}0_5$).

Strong similarities were found for the « cellulose II» fractions from ash-wood, miscanthus, pine and wheat straw, which exhibit a relatively narrow molar mass distribution (MMD) centered around 5.3 (Log M_n, ~ 200 000 Da). However in the case of beech « cellulose », this distribution is considerably wider. Comparatively, Avicel cellulose (commercial microcrystalline cellulose) exhibits a molar mass distribution more shifted towards lower mass values. Typically also, one

can notice in this sample a significant fraction of low mass molecules, represented by the second maximum of the curve (around Log M = 4.2, ~ 15 000 Da, Figure III.4). This fraction corresponds to small chains of degraded cellulose and residues of hemicelluloses which can generally be measured as xylose and mannose sugars in the commercial Avicel cellulose, which is issued from bleached wood pulp submitted to acid hydrolysis.

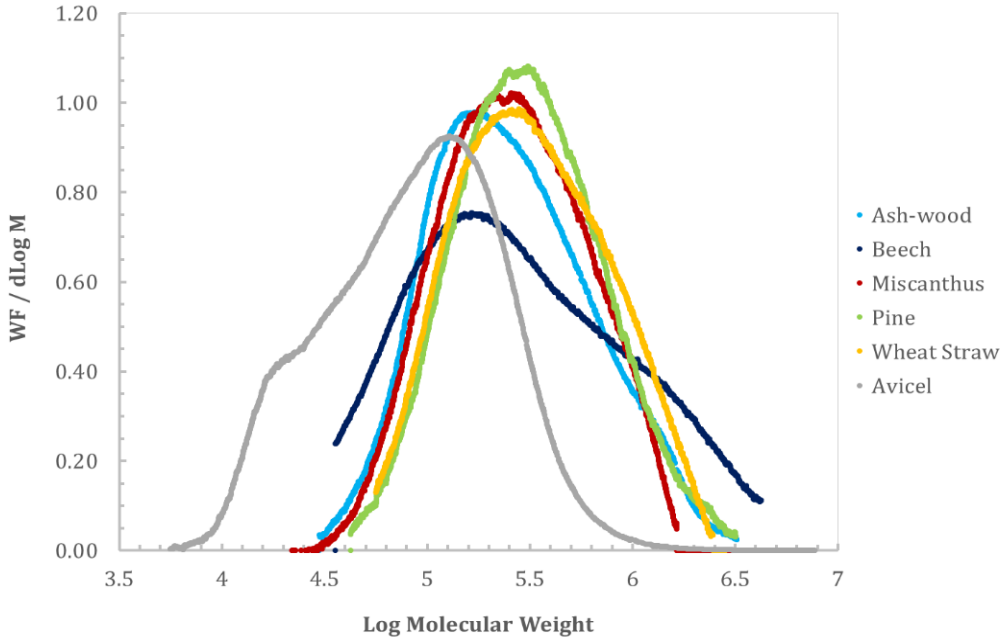


Figure A.III.1. Molar mass distribution of the « cellulose II» fractions and the commercial microcrystalline cellulose Avicel (relative abundance curves or differential curves)

The tendencies represented by the MMD curves are in accordance with the mean molar mass values reported in Table A.III.1

Table A.I.III.1. Average molar mass and polymerization degree of the « cellulose II » fractions from reference biomasses and of the commercial microcrystalline cellulose Avicel

		« cellulose II » extracted fractions					Commercial microcrystalline cellulose
Parameters	**Units**	**Ash-wood**	**Beech**	**Miscanthus**	**Pine**	**Wheat straw**	
DPn	-	341	320	368	441	453	103
DPw	-	744	1084	688	849	883	254
Dp at peak	-	375	440	498	590	544	249
Dispersity = DPw/DPn	-	2.18	3.39	1.87	1.92	1.95	2.46
Sample Recovery	%	115.1	92.5	80.7	84.6	80.3	83.7

The average degrees of polymerization (DP) of the « cellulose II» fractions were in the range of 300 to 450 for the number-average DP (DPn) and 700 to 1100 for the weigh-average DP (DPw) (Table A.III.1). For Avicel it was found 100 and 250, respectively, which thus appears to be four

and five times lower. Similar values were found for deciduous woods, different from those for coniferous wood, which is in agreement with the literature [211]. All these values are in accordance with the peak DP values, slightly smaller for the hardwoods than for pine, miscanthus and wheat straw, but significantly higher than for the Avicel cellulose.

In both cases, extracted cellulose fractions can be compared to native cellulose, whose DPn is higher than 10 000 for an average molecular weight up to 2 000 000 [9,10] (see section II.1.3). This confirms that the extracted fractions remain more fragmented than the native material but less than commercial cellulose.

The dispersity $Đ_M$ of the cellulose polymer, represented by the ratio DPw/DPn, leads to the distinction of two families of cellulose fractions: on the one hand, ash-wood and beech « cellulose » fractions; on the other hand, miscanthus, pine and wheat straw « cellulose II » fractions (Table A.III.1). The dispersity of the microcrystalline cellulose is between both families. Beech and ash-wood were put in the same group since they are both hardwoods and exhibit a lower DPn, although their dispersity differs because of the wider MMD of beech. Dispersity around 1.9 for miscanthus, pine and wheat straw celluloses is an indicator of a narrow MMD. This might also indicate a high degree of purity of these « cellulose II » fractions, with a few number of small chains and a small amount of hemicelluloses cross-links, which block the mobility of the polymer chains and prevent their volume expansion in the solvent. On the contrary, in the case of hardwoods, a higher dispersity was found even if polymer chains DP's were slightly smaller (also confirmed by the DP at peak values). This might suggest the presence of small chains and/or of reticulations in the polymer, which will also be reflected in the hydrodynamic parameters. Finally, the commercial microcrystalline cellulose Avicel exhibits a higher dispersity, principally caused by a MMD including two populations (lower and higher molar mass), one of them containing very degraded cellulose and hemicelluloses chains.

Thanks to the multi-detection coupled to the SEC analyzer, hydrodynamic parameters can also be evaluated (Table A.III.2). They contribute in the assessment of the flexibility of the cellulose chains, conditioned by their degree of reticulation and their flexibility.

Intrinsic viscosity (η) gives an indication of the molar volume of the solvated polymer, and its variation with chain length gives an idea of the freeness and flexibility of the polymer chains, also related to the existence of cross-links (or not). The latter behavior is resumed by calculating the Mark-Houwink-Sakurada (MHS) parameters derived from the MHS curves, representing the relationship between log η and log M (Figure A.III.2), as given by the equation:

$$[\eta] = K + \alpha M \qquad \text{Eq. 1}$$

The weight-average hydrodynamic radius (R_h) is derived from intrinsic viscosity and molar mass M, and it corresponds to the hydrodynamic polymer volume following Einstein's theory of

flow (the radius of the equivalent sphere flowing in the solvent).

The intrinsic viscosity and the R_h are close for the 5 extracted celluloses and much higher than the equivalent values for the microcrystalline cellulose (Table A.III.2). The higher R_h for the beech « cellulose II » is derived from the presence of small and long chains due to the high dispersity of the polymer. In the case of Avicel, the lower R_h is in accordance with the shorter length of the cellulose chains.

Table A.III.2. Hydrodynamic parameters of the « cellulose II » fractions from 5 biomasses and of the commercial microcrystalline cellulose Avicel

		« cellulose II » extracted fractions					Commercial microcrystalline cellulose
Parameters	**Units**	**Ash-wood**	**Beech**	**Miscanthus**	**Pine**	**Wheat straw**	
η	mL/g	167.2	270.8	258.3	284.9	254.6	93.4
Rh	nm	20.07	26.47	23.55	26.50	25.93	11.50
Mark-Houwink-Sakurada parameters							
a	-	0.748	0.798	0.917	0.961	1.082	0.909
Log K	-	-3.899	-4.088	-4.668	-4.951	-5.724	-4.657

The slope of the Mark-Houwink curves (a, Table A.III.2) leads to the distinction of two families of behavior, as in the case of the mass-related parameters. Firstly, ash-wood and beech exhibit values between 0.7 and 0.8, taking into account the higher dispersity of beech cellulose. Secondly, miscanthus, pine and wheat straw values are close to 1. The commercial microcrystalline cellulose presents a similar behavior, around 0.9. In the first case, the extracted celluloses from pine and beech are characterized by a higher dispersity, which indicates the higher presence of diverse polymer chain lengths. In particular, the presence of small chains limits the flexibility of the polymer and impacts its ability to be volumetrically expanded. In the second case, higher values of the slope of the Mark-Houwink equation (a), close to 1 (Figure A.III.2), might be derived from an effective extraction procedure which removed small chains and reticulations, including hemicellulose residues, leading to a homogeneous length of the polymer chains. The extraction procedure seems to be less effective for deciduous wood, whose structure is stronger. It might conserve at least partially some small chains and cellulose reticulations in the primitive biomass structure. In the case of Avicel, the short length of the polymer chains should lead to a correct volumetric expansion of the polymer. However, the presence of hemicellulose residues and the mixture of different chain lengths rigidify the structure and limit, in a certain extent, the flexibility of the chains.

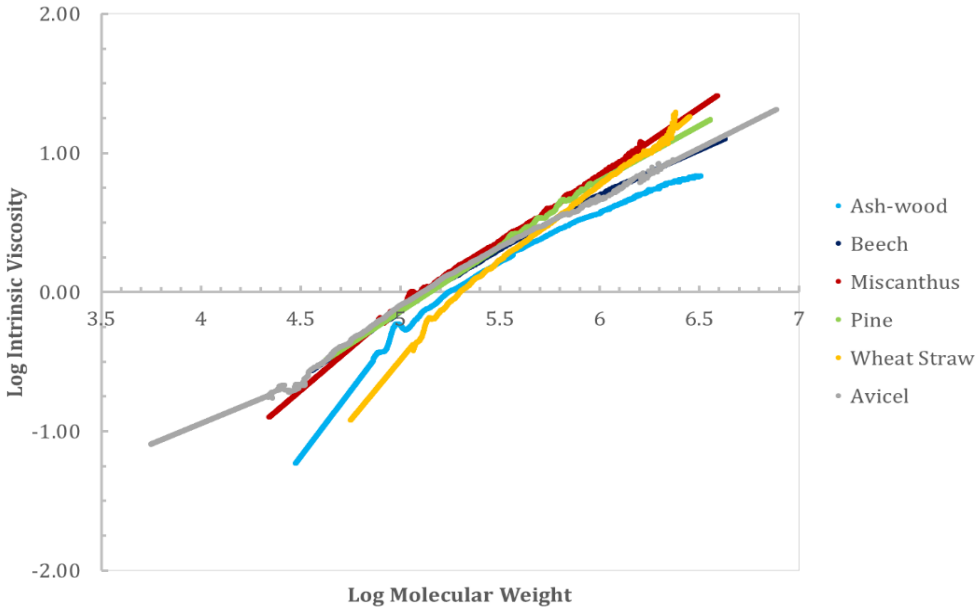


Figure A.III.2. Mark-Houwink-Sakurada curves (MHS) for of « cellulose II» fractions and the commercial microcrystalline cellulose Avicel (relative abundance curves or differential curves)

To sum up, the characterization of « cellulose II» extracted fractions and of the commercial microcrystalline cellulose revealed that this last compound is not representative of the native cellulose in biomass. The main reasons of this affirmation are its low average molar mass, a wide molar mass distribution and a high dispersity, which constrain the cellulose chains in their hydrodynamic behavior. This behavior is derived from the acidic hydrolysis treatment utilized in its extraction. Indeed, this treatment is especially effective in removing hemicellulose residues and amorphous cellulose areas. That is the reason why this treatment leads to a highly crystalline cellulose, which does not reproduce neither the natural amorphous areas of native cellulose nor the typical cellulose chain length in biomass. On the contrary, the alkaline treatment in the extraction procedure selected for this study was shown to lead to higher molar mass values and narrower molar mass distributions, with a low proportion of small chains, and hemicellulose residues. These characteristics of « cellulose II» fractions seem closer to those of native cellulose in biomass, except the cellulose II allomorphic structure. As a result, these fractions are considered as more representative of cellulose in biomass compared to the commercial microcrystalline cellulose traditionally selected in the literature.

IV. Calculations for the characteristic time analysis in torrefaction

1. Bed-scale analysis

The bed of particles is considered as a continuous medium, whose properties are a linear combination of properties of wood and of the torrefaction inert atmosphere, normally nitrogen or helium, pondered by the bed porosity (ε ≈ 0.5, assumed as constant during torrefaction). In characteristic time analysis, wood concerned properties for estimating bed properties are thermal conductivity, mass heat capacity and volumetric weight. These properties are obtained from literature, as indicated in Table A.IV.1.

Table A.IV.1. Physical properties of wood

Properties	Symbol	Unit	Biomass value	Source
Volumetric weight	ρ	Kg/m3	710	[183]
Mass heat capacity	cp	KJ/(Kg K)	cp = 0.103.1 + 0.003.867 T	[45]
Thermal conductivity	λ	W/(m K)	0.11	
Emissivity	ω	-	0.9	[256]
Porosity	ε	-	0.5	[18]

Characteristic time definitions for torrefaction, as well as for heat transfer processes involved in torrefaction experiments, are indicated in Table A.IV.2.

Table A.IV.2. Characteristic time definition for torrefaction of wood applied to bed-size analysis

Phenomena	Characteristic time definition	Eq.	Source
Torrefaction (considered as 1st order reaction)	$t_{torref} = \frac{1}{k_{torref}}$;	(1)	[22]
	$k_{torref} = 2{,}48.10^4 exp\left(\frac{-76000}{RT}\right)$	(2)	
Heat transfer by external radiation	$t_{rad} = \frac{\rho_{bed} Cp_{bed} L_C}{\omega\sigma(T_g + T_{bed})(T_g^2 + T_{bed}^2)}$	(3)	-
Heat transfer by internal conduction	$t_{cond} = \frac{\rho_{bed} Cp_{bed} L_C^2}{\lambda_{bed}}$	(4)	-
Heat transfer by external convection	$t_{conv} = \frac{\rho_{bed} Cp_{bed} L_C}{h_t}$	(5)	-
Heat exchange coefficient	$Nu = \frac{h_t L_C}{\lambda_g}$	(6)	-
Nusselt number	$Nu = 2 + 0.6 Re^{1/2} Pr^{1/3}$	(7)	[257]
Prandlt number	$Pr = \frac{\mu_g Cp_g}{\lambda_g}$	(8)	-
Reynolds number	$Re = \frac{\rho_g v_g L_C}{\mu_g}$	(9)	-

The properties of the gas atmosphere (helium) required for these calculations stem from the literature [258]. Concerning gas speed in each device, this parameter is calculated by the gas flow previously indicated and the internal section of the TGA oven (20 mm). Besides, gas is considered at the torrefaction temperature, while wood, and thus particle bed and particle surface, are at the ambient temperature of 298 K. A characteristic length is required in several of these equations (Eqs. 3-6, 9). At bed-scale, this dimension is defined as the ratio between the volume of the cylinder formed by the bed of particles and the surface of its two bases, which is equivalent to half of the thickness of the particle bed.

Non-dimensional numbers defined in the literature for torrefaction and pyrolysis (Damkhöler, Pyro, Biot) will be indicated when characteristic time analysis will be presented. It is important to note that characteristic times are considered to be in the same order of magnitude if their ratio is inferior to a factor of 10.

2. Particle-scale analysis

Characteristic times were also calculated for an isolated particle situated inside the bed of particles. In this case, it can be considered that the particle is only heated by external convection in the bed and internal conduction inside the particle, while external heating by radiation is so slow that it can be neglected. At the same time, heat transfer coefficient for convection was evaluated by assuming a null gas flow around the particle inside the bed, so that Nusselt number is equal to 2 [18]. Regarding internal mass diffusion, its characteristic time was also calculated at this scale of the analysis by the equations 10 to 12 indicated in Table A.IV.3. It was supposed that water is the main product going out of the particle, so diffusion coefficient was estimated by the method of Fuller, Schettler and Giddings [258] considering water in equilibrium with the gaseous atmosphere composed by helium.

Table A.IV.3. Characteristic time of internal mass diffusion at particle-scale

Phenomena	Characteristic time definition		Source
Internal mass diffusion time	$t_{int\ diff} = \frac{L_C^2}{D_{eff}}$	(10)	[22]
Effective diffusion coefficient	$D_{eff} = \left(\frac{\varepsilon}{\tau}\right) D$	(11)	-
Diffusion coefficient	$D = \frac{0.001 T^{1.75} \left(\frac{1}{M_{H_2O}} + \frac{1}{M_{He}}\right)^{1/2}}{P^g \left((\sum \nu)_{H_2O}^{1/3} + (\sum \nu)_{He}^{1/3}\right)^2}$	(12)	Method of Fuller, Schettler, and Giddings [258]

Equations for characteristic time calculations at particle-scale analysis are the same as for bed-scale, by replacing bed properties in equations 1 to 9 with particle properties. In this case, particle properties are considered as equivalent to wood properties indicated in Table A.IV.1. Characteristic length corresponds to the ratio between the volume and the surface of the

particle, which is equivalent to $d_p/6$ considering wood particles as spherical. In internal mass diffusion calculations, tortuosity of a bed composed by spherical particles is $\pi/2$ [259].

3. Calculations and discussion

Both characteristic time analysis at bed and particle-scale were carried out from 200 to 300 °C, every 10 °C, in order to plot the evolution of characteristic times of torrefaction and thermal transfer with the temperature during the experiments. Results for **bed-scale analysis** are shown in Figure A.IV.1, where y-axis is in a logarithmic scale. In Table A.VI.5, numeric results for non-dimensional numbers are given.

Table A.VI.5. Non-dimensional numbers for characteristic time analysis (bed-scale, TGA-GC/MS)

		T (°C)										
	definition	**200**	**210**	**220**	**230**	**240**	**250**	**260**	**270**	**280**	**290**	**300**
Bi_T	t_{cond}/t_{conv}	7.5	7.6	7.7	7.9	8.0	8.1	8.2	8.3	8.5	8.6	8.7
Da	t_{torref}/t_{conv}	7809	5250	3588	2489	1751	1249	902	660	488	365	275
Py	t_{torref}/t_{cond}	1042	690	464	317	220	154	110	79	58	42	32
t_{rad}/t_{conv}		33.6	32.7	31.8	31.0	30.2	29.4	28.7	27.9	27.2	26.5	25.9

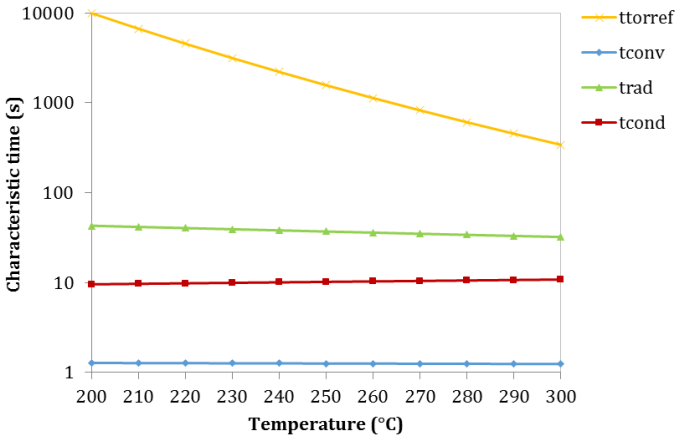


Figure A.IV.1. Characteristic times for TGA-GCMS system (bed-scale analysis)

The results show that torrefaction time is significantly higher than characteristic times concerning heat transfer in the temperature range from 200°C to 300°C. Even if the difference decreases with temperature, torrefaction time still remains more important. As a result, torrefaction is governed by chemical regime in this range of temperatures at the defined operating conditions, for a particle size of 200 µm and a bed thickness of 2 mm. Concerning external heat transfer, radiation is slower than convection, so we can assume that external heating is operated by external convection. On the other hand, internal conduction can be considered comparable to external convection. Consequently, heat transfer mainly occurs by external convection and internal conduction, and the influence of internal conduction increases with increasing temperature.

TGA-experiments were carried out in a helium atmosphere, while usually torrefaction experiments at lab-scale are performed in a nitrogen atmosphere. Thermodynamic properties of

these gases are different: volumetric weight of nitrogen is about 7 times higher than for helium, dynamic viscosity of helium is about 10 times higher than for nitrogen and thermal conductivity of helium is about 6 times higher than for nitrogen. This affects Reynolds, Prandtl and Nusselt numbers calculations in heat transfer coefficient for convection.

Regarding **particle-scale analysis**, results are presented in Figure A.IV.2, and non-dimensional numbers obtained from characteristic times calculations are indicated in Table A.VI.6.

Table A.VI.6. Non-dimensional numbers for characteristic time analysis (particle-scale, TGA-GC/MS)

		T (°C)										
	definition	**200**	**210**	**220**	**230**	**240**	**250**	**260**	**270**	**280**	**290**	**300**
$\mathbf{Bi_T}$	t_{cond}/t_{conv}	0.62	0.94	1.28	1.63	1.98	2.35	2.72	3.11	3.50	3.91	4.33
Da	t_{torref}/t_{conv}	$4.5{\cdot}10^5$	$4.5{\cdot}10^5$	$4.0{\cdot}10^5$	$3.5{\cdot}10^5$	$2.9{\cdot}10^5$	$2.4{\cdot}10^5$	$2.0{\cdot}10^5$	$1.6{\cdot}10^5$	$1.3{\cdot}10^5$	$1.1{\cdot}10^5$	$0.9{\cdot}10^5$
Py	t_{torref}/t_{cond}	$7.2{\cdot}10^5$	$4.7{\cdot}10^5$	$3.2{\cdot}10^5$	$2.1{\cdot}10^5$	$1.5{\cdot}10^5$	$1.0{\cdot}10^5$	$7.0{\cdot}10^4$	$5.0{\cdot}10^4$	$4.0{\cdot}10^4$	$3.0{\cdot}10^4$	$2.0{\cdot}10^4$
t_{rad}/t_{conv}		166	243	315	384	449	510	568	623	675	724	770

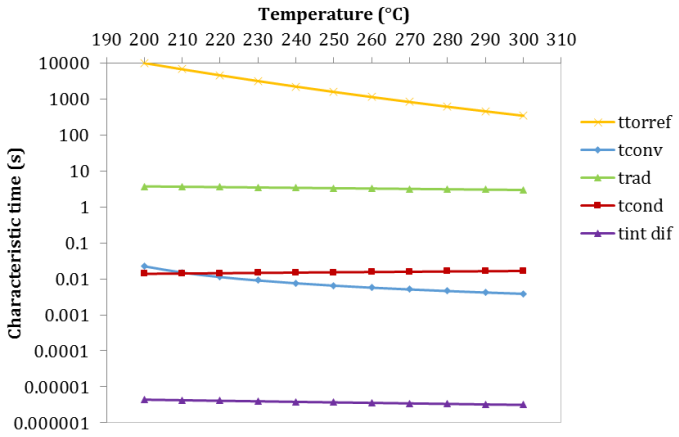


Figure A.IV.2. Characteristic times for TGA-GC/MS system (particle-scale analysis)

Characteristic time analysis indicates that torrefaction is much slower than heat transfer. In fact, the heating time of an isolated particle can be considered as instantaneous regarding to torrefaction. This is also proved by non-dimensional Da and Py numbers, which is in agreement with the literature [18]. External heat transfer is assumed to occur by convection.

Internal diffusion of the volatile species produced during torrefaction must be considered as it might be an obstacle for the reaction. In this case, maximal internal diffusion time is inferior to 0.01s. The order of magnitude of this characteristic time is lower than heat transfer and torrefaction times.

To conclude, heat transfer at bed scale occurs by external convection and internal conduction, but the chemical regime is predominant in the torrefaction experiments under the cited conditions. At the particle scale, heating of the particle is instantaneous compared to reaction, as well as evacuation of the volatile products. These results are in concordance with the literature [18], and with some authors who consider directly the chemical regime in torrefaction and its time as the characteristic time of the process [94].

4. Sensitivity analysis of parameters involved

Characteristic time studies on the literature point out that only the consideration of a magnitude order in characteristic times is acceptable, due to the uncertainty in the determination of solid properties and kinetic laws [114]. In this context, an analysis of the sensitivity of these not-well-known properties provides a critical regard more accurate about the results that are obtained.

The properties for a xylan particle were assumed to be similar to average wood properties, while bed properties were estimated from xylan ones, using porosity as the ponderation factor. Affected parameters are porosity, volumetric weight, mass heat capacity and thermal conductivity, both at particle and at bed-scale. Thermal conductivity is reported to present only slight variations with biomass moisture content and temperature, thus the considered value is representative. Concerning mass heat capacity, a correlation was proposed for dry wood, while moisture content above fiber saturation contributes to heat capacity according to the simple rule of mixtures [45]. The sensitivity analysis was applied to porosity and volumetric weight of wood at bed-scale (Figure A.IV.3), because of their more significant influence on characteristic time analysis.

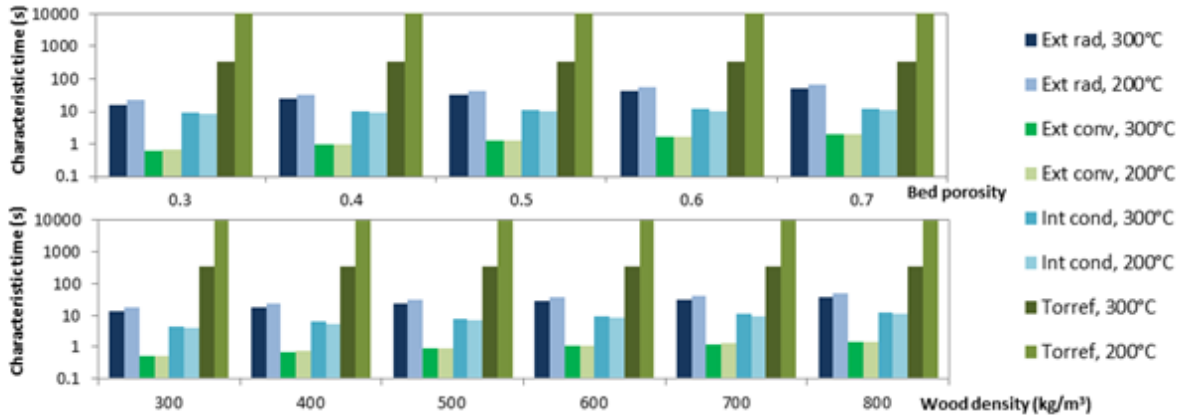


Figure A.IV.3. Analysis of sensibility of porosity of the bed and wood density applied characteristic time calculations for torrefaction in the TGA at bed-scale

The results show that both porosity of the bed and wood density increase notably external radiation, which remains in all cases the slowest phenomenon and can be neglected compared to external convection, which is instantaneous and comparable to internal conduction. Even if torrefaction is still the limiting phenomenon in all cases, it can be appreciated that thermal phenomena acquire more importance at higher temperatures, when torrefaction is quicker, so they can become comparable in function of the operating conditions and an intermediate regime would be reached. In this context, mapping the variations in the main operating conditions in function of temperature allows to control that torrefaction remains governed by the chemical regime. In this way, maximum heating rate in TGA tolerated for the chemical regime can be estimated from heat transfer characteristic time results.

V. Leakage tests of the storage loops

In order to test the performances of the heated storage loop system, a mixture of gases type BTEX (benzene, toluene, ethylbenzene and xylene) was directly injected in the loops at a constant flow rate (not measured). While the gas was circulating, loops were controlled by the pilot software and filled with the mixture (the time of circulation of the gas at each loop was identical). Once the loops filled, the gaseous content of each loop was analyzed in GC/MS, as usually. The detected peak area was compared in all loops for each of the four gas components (Figure A.V.1), and compared to the corresponding average peak area.

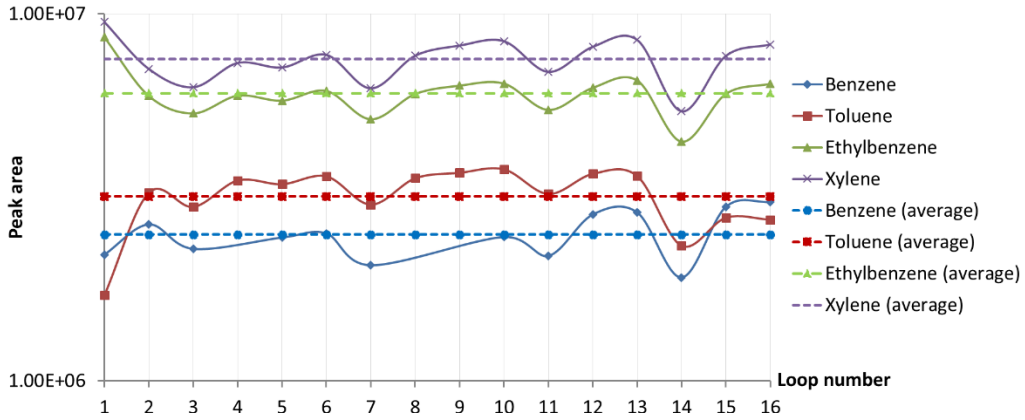


Figure A.V.1. Leaking test of the 16 heated storage loops with a BTEX mixture; GC/MS peak area detected for each loop (average of peak for comparison)

Some of the loops showed a negative deviation regarding the average peak area, which may indicate that they are losing a part of their gaseous content by leaking. The small positive and negative deviations are in the uncertainty range of the determination of the peak area (15-20%). This behavior concerns specially loops 3, 7, 11 and 14, which were discarded for the next experiments (Figure A.V.2). Loop 1 was also discarded because of a technical problem (double peaks in chromatograms because of bad-rinsing at the beginning of the experiments, which cannot be corrected).

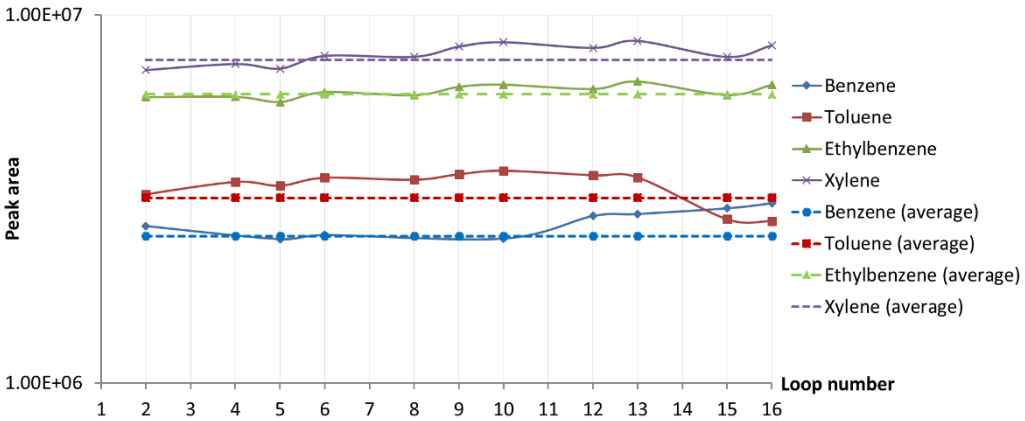


Figure A.V.2. Leaking test of the 16 heated storage loops with a BTEX; leaking loops (1, 3, 7, 11, 14) were removed (average of peak area is represented for comparison)

VI. Uncertainty estimation

The objective of this section is to define the error associated to the measurements of the solid mass and the peak area of the volatile species. As a result, it can be checked if the reproducibility of the experiments is acceptable and thus if one single experiment can be used to represent solid or volatile species behavior.

1. Uncertainty in solid degradation

In the literature, thermogravimetric measurements have been associated to a very low uncertainty [124,214]. This one, which mainly concerns the mass of the sample weighted, was estimated by the reproducibility of the experiments (Table A.VI.1). The error in solid mass determination is less than 0.5%, which is lower than the differences in remaining solid mass between biomasses. As a result, a single experiment can be considered to represent a given biomass. On the other hand, the uncertainty in the measurement of the sample temperature during torrefaction is considered as a systematic error that can be neglected.

Table A.VI.1. Comparison of remaining solid mass at the end of non-isothermal torrefaction (300°C, 0 min) and of isothermal torrefaction (final 300°C, 30min); repeatability between experiments for 9 biomasses

	remaining solid mass (%)		**error (standard deviation)**	
Experiment	**300°C/0 min**	**300°C/30min**	**300°C/0 min**	**300°C/30min**
	End dynamic stage	**End isothermal stage**	**End dynamic stage**	**End isothermal stage**
Salix 01	25.02%	45.58%	0.08%	0.19%
Salix 02	24.91%	45.32%		
Wheat straw 01	29.07%	54.40%	0.34%	0.29%
Wheat straw 02	28.59%	53.99%		
Forest residues 01	26.20%	45.16%	0.30%	0.28%
Forest residues 02	25.78%	44.76%		
Grape seed cake 01	21.28%	33.79%	0.22%	0.30%
Grape seed cake 01	20.97%	33.37%		
Corn cob cake 01	36.08%	58.32%	0.03%	0.14%
Corn cob cake 02	36.12%	58.52%		
Sunflower seed shells 01	30.09%	54.60%	0.01%	0.03%
Sunflower seed shells 02	30.08%	54.64%		
Reed canary grass 01	27.82%	46.07%	0.14%	0.07%
Reed canary grass 01	27.63%	45.96%		
Scots pine bark 01	23.43%	40.12%	0.10%	0.21%
Scots pine bark 01	23.29%	39.82%		
Poplar 01	26.35%	53.50%	0.00%	0.08%
Poplar 02	26.34%	53.62%		

2. Uncertainty in volatile species detection and quantification

Errors associated to peak area semi-quantification in GC/MS can be summarized as:

- Uncertainty in the measure of the carrier gas flow (dilution of the volatile species released), before and after heated storage loop system.
- Condensation of the volatile species during transport and/or storage, forming fouling in the system.
- Errors in the quantification of the volatile species in GC/MS analysis (peak area).

Errors associated to the retention time in peak detection are considered as negligible. Semi-quantification methods were programmed in the GC/MS chromatogram analysis software in order to quickly detect volatiles after each experiment. The retention times indicated in these methods for each chemical compound are set for varying about 0.2 minutes, which is enough in most cases. When retention times vary more, they are adjusted manually for an optimized detection of the concerned compound. Besides, each chemical compound peak is considered at its characteristic m/z rapport, which minimizes the error with other peaks nearby.

Finally, there is an error associated to the sampling temperature of each storage loop. In fact, this temperature is automatically ordered by the software of the storage loop system. When torrefaction is launched in the thermobalance, at about 80°C, the loop system software is also launched. Thermobalance heats the biomass sample at 3°C/min and volatile samples are stored at the selected temperatures, as indicated in section III.2.

A maximum error of 1°C in the sampling temperature is reported with this sampling system. This does not include neither the error associated to the measure of the temperature by the thermocouple (unknown) nor the difference between the measure of the thermocouple (gaseous atmosphere in TGA) and the biomass particle/bed temperature (chemical regime is supposed, as discussed in section III.3.1).

The quantification of the errors mentioned is complicated and not accurate because of the configuration of the TGA-GC/MS system. That is the reason why three alternative methods were initially proposed for the description of the errors involved in volatile semi-quantification. As a result, for estimating the error associated to the semi-quantification of a given volatile species, the production of a given volatile species was described as the average of the two curves corresponding to the two repetitions of the experiment. The error associated to the curve was described as the standard deviation calculated for a set of a defined number of torrefaction experiments of a reference biomass or compound (for example, commercial xylan or a given biomass like ash wood). To validate this choice, the standard deviation was calculated for each detected chemical compound (at its 11 points of temperature) considering 3 repetitions for a single biomass (example for acetic acid in Figure A.VI.1). In total, this validating procedure was applied to 4 biomasses (ash wood, pine, miscanthus, wheat straw, Table A.VI.2), in order to

compare the differences between the calculated errors per temperature point.

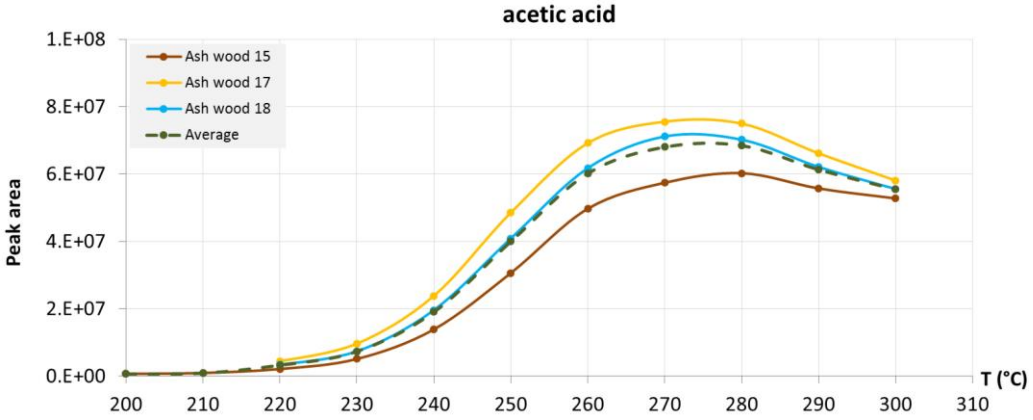


Figure A.VI.1. Example of the peak area semi-quantified for the production of acetic acid in 3 torrefaction experiments with ash wood in TGA-GC/MS (11 temperature points)

The results show that the error at each temperature point obtained by comparing 3 experiments per biomass varies in function of the biomass and of the temperature. However, it can be generally defined as a maximum of 34.9 % and an average error of 19.2 % (Table A.VI.2). The overall error was defined for the chemical compound and assumed to be in the same order of magnitude for the other biomasses.

Table A.VI.2. Example of error comparison for 3 experiments per biomass in the semi-quantification of the acetic acid (11 temperature points)

	T (°C)										
	200	**210**	**220**	**230**	**240**	**250**	**260**	**270**	**280**	**290**	**300**
Experimentations	**Relative error** (in %)										
Ash-wood	nd	nd	34.9	30.8	26.2	22.5	16.3	13.9	11.0	8.6	4.8
Miscanthus	nd	nd	0.8	19.7	24.3	19.7	12.3	13.6	15.1	20.7	20.2
Wheat Straw (French)	12.1	11.1	14.3	7.8	18.0	20.3	22.3	24.7	28.4	27.5	16.6
Pine	nd	nd	14.0	19.2	18.2	18.7	26.9	25.1	26.7	32.1	31.7
Average error	19.2 %				**Maximum error**			34.9 %			

The errors in the determination of the detected volatile species are approximately in the same order of magnitude for all quantified volatile species (calculations not supplied). The representation for acetic acid confirms that the shape of the profile and the order of magnitude of the production for the volatile species are kept (Figure A.VI.1).

As a result, a single experiment can be considered as acceptable for the representation of a given volatile species, the overall error in volatile species being estimated between 20 and 35%. This result can be considered as acceptable because of the complexity of the detection of the volatile species produced in torrefaction in the TGA-GC/MS.

VII. Calibration of volatile species in GC/MS

A calibration rate was calculated with an identical procedure for each volatile species in Table A.VII.1, by assuming a linearity of the results. For each chemical compound, first of all, a solution of the analytical standard was prepared at a given concentration and injected in the GC/MS. The determination of the corresponding peak area at the m/z defined as characteristic for the volatile allowed to derive the maximum and minimum of concentration required in the calibration range. Secondly, a series of 7 solutions were prepared from the standard by successive dilutions, and injected for peak area determination in GC/MS. The calibration rate was obtained by representing peak area in function of the concentration of the solution. Calibration rates directly indicate by their slope the proportionality factor between peak area and concentration, as they were forced to (0,0) point. The coefficient of determination of each calibration rate (R^2) was also indicated. The linearity assumed for the proportionality calculations was confirmed by the high coefficient of determination (R^2) obtained for all the calibration rates (>0.9, in most of the cases > 0.99) (Table A.VII.1).

Each solution of the calibration range was analyzed 5 times in GC/MS in order to take into account the experimental deviations in the GC/MS measurements (a maximum of 5% of standard deviation was determined).

Table A.VII.1. Calibration rates for the quantification of 23 volatile species from TGA-GC/MS torrefaction experiments

	Production			Calibration Rate								
Chemical compound	**purity of the standard**	**Max peak area**	**min peak area**	**Max peak area**	**min peak area**	**Max conc g/L**	**min conc g/L**	**curve slope Peak A = f(g/L)**	**Max m µg**	**min m µg**	**curve slope Peak A = f(µg)**	**R^2**
formic acid	**99%**	1862453	35730	61609416	182951	9.963	0.100	5657385	0.9963	0.0100	565739	0.9924
acetic acid	**100%**	75532568	671872	88360104	27077	2.411	0.005	35099207	0.2411	0.0005	3509921	0.9979
hydroxyacetone	**90%**	88524504	32158	121605176	51929	1.843	0.002	62922748	0.1843	0.0002	6292275	0.9985
propionic acid	**99%**	4301582	32645	169419024	49724	2.250	0.009	75709549	0.2250	0.0009	7570955	0.9936
furfural (2-furaldehyde)	**99%**	12591075	164651	77211680	53301	1.066	0.002	71445232	0.1066	0.0002	7144523	0.9996
2-furanmethanol	**99%**	5738132	32204	14479360	31530	0.462	0.005	29730990	0.0462	0.0005	2973099	0.9918
phenol	**100%**	2608364	31372	14287177	17965	0.460	0.002	29678035	0.0460	0.0002	2967803	0.9921
phenol, 2-methoxy (guaiacol)	**100%**	4966202	30384	51782596	3733	0.460	0.001	109083195	0.0460	0.0001	10908319	0.9987
phenol, 2,6-dimethoxy (syringol)	**99%**	7229040	33627	134544304	33012	1.793	0.003	74177433	0.1793	0.0003	7417743	0.9987
furan	**99%**	1760434	31395	34043940	27339	0.510	0.001	64008652	0.0510	0.0001	6400865	0.9987
acetylfuran	**99%**	1710164	31165	43275228	9745	0.456	0.001	92622116	0.0456	0.0001	9262212	0.9994
2(5H)-furanone	**96%**	9878666	32278	12084307	16747	0.217	0.001	54624792	0.0217	0.0001	5462479	0.9908
2-methoxy-4-vinylphenol	**97%**	7609884	30304	16174215	31298	0.292	0.004	53803862	0.0292	0.0004	5380386	0.9962
cathecol	**99%**	1957343	35922	21985136	112074	0.476	0.048	38341949	0.0476	0.0048	3834195	0.9193
vanillin	**99%**	1721061	31715	29616222	10584	0.452	0.005	60931819	0.0452	0.0005	6093182	0.9879
2-propanone,1-(acetyloxy)-	**97%**	6352081	30253	106743248	47517	0.920	0.001	112578677	0.0920	0.0001	11257868	0.9991
formaldehyde	**37%**	14016522	84111	21772476	93240	0.878	0.005	24530290	0.0878	0.0005	2453029	0.9982
methanol	**100%**	20601246	545585	29205620	180369	0.665	0.008	41443030	0.0665	0.0008	4144303	0.9934
3-furaldehyde	**97%**	2035828	30521	35972376	3347	0.387	0.000	91506860	0.0387	0.0000	9150686	0.9997
2,3-pentanedione	**100%**	1558480	32398	1755345	12590	0.065	0.000	27130594	0.0065	0.0000	2713059	0.9853
4-cyclopentene-1,3-dione	**95%**	1245099	47461	3583506	669	0.091	0.000	35646635	0.0091	0.0000	3564663	0.9937
isoeugenol (cis+trans)	**98%**	7610149	63156	23571270	6240	0.474	0.009	44129220	0.0474	0.0009	4412922	0.9676
cis-isoeugenol	**-**	777220	32720	595128	6240		-	-				-
trans-isoeugenol	**-**	6832929	30436	23037952	25463	-	-	-				-
eugenol	**99%**	1247648	31382	19115946	9915	0.512	0.005	34820207	0.0512	0.0005	3482021	0.9845

VIII. Py-GC/MS

1. Influence of step duration in fractionated Py-GC/MS of lignocellulosic biomass

M. González Martínez, T. Ohra-aho, D da Silva Perez, T. Tamminen, C. Dupont

This work was submitted to the Journal of Analytical and Applied Pyrolysis (June 2018, currently under revision)[260].

Abstract

Fractionated pyrolysis coupled to gas chromatography and mass spectrometry (Py-GC/MS) appears as an interesting analytical tool for elucidating lignocellulosic biomass structure, as it allows the progressive release of chemical fragments representative of biomass macromolecular composition. This paper highlights the importance of optimizing temperature and time parameters in fractionated Py-GC/MS for a clear separation of the chemical compounds released at each pyrolysis step using beech wood as raw material. Fractionated Py-GC/MS between 250 °C and 500 °C showed that the release temperature of the volatile degradation products varied between the volatile species detected and in some cases showed multiple temperature optima. This behavior may be due to differences in the macromolecular structures and linkage types giving rise to the degradation products. Therefore, fractionated Py-GC/MS is suggested to be a potential biomass characterization method.

Highlights

- Effect of fractionated pyrolysis time on degradation behavior of beech was studied.
- Pyrolysis time at different temperatures was optimized.
- Time optimization increased the yield of the volatile degradation products of beech.
- Time optimization separated pyrolysis products released according to their origin from biomass.

Keywords: beech; Py-GC/MS; fractionated pyrolysis; lignin; hemicelluloses; cellulose

1. Introduction

There is a general agreement on the need to increase the use of renewable energetic sources, among which biomass [261]. Lignocellulosic biomass designates various resources, which include agricultural and forest residues, both from hardwood and softwood species, as well as energy crops [32]. A large part of these resources remains underused at the moment [262].

Lignocellulosic biomass is mainly constituted of three types of organic polymers, namely i) cellulose, ii) hemicelluloses and iii) lignin, these two latter constituents forming matrix around

cellulosic fibers. These constituents appear to be strongly different in terms of composition, location and amount among plants and plant tissues themselves [61,205,206]. Cellulose, which accounts for around 40 to 50 % water-mass-free (wmf) of biomass, is a linear semi-crystalline homopolysaccharide formed of several thousands of glucopyranose units linked together through β1-4 glycosydic linkages. Hemicelluloses, which represent about 20 to 25 %wmf of biomass, are branched heteropolysaccharides mainly formed of several types of C5 sugar units (xylose and to a less extent arabinose) and C6 sugar units (glucose, mannose and to a less extent galactose). Hemicellulose units are linked with some other units, in particular 4-*O*-methyl-α-*D* glucuronic acids and acetyl groups. Contrary to cellulose, hemicelluloses are amorphous and their degree of polymerization is limited to a few hundreds. Lignin, which usually accounts for around 20 to 30 %wmf of biomass, is amorphous but its structure is totally different than carbohydrates. In fact, lignin structure is much more complex and still subject of research [263–266]. Lignin is mainly made up of phenylpropane units of three types according to their number of methoxy substituents on ring – 0 for H unit (hydroxyphenyl), 1 for G unit (guaiacyl) and 2 for S unit (syringyl). These units are known to be linked together with ether and carbon-carbon bonds, β-*O*-4 bonds being the most abundant bond type. Noteworthy is the existence of linkages between the different constituents [48]. Although lignin has been traditionally described as a tridimensional polymer whose linkages between the phenylpropane units are randomly formed by radical polymerization, the most accept idea nowadays is that, at least *in-situ*, wood lignin is rather formed by linear oligomers [267].

To get deeper understanding of biomass complex structure, analytical pyrolysis coupled to gas chromatography and mass spectrometry (Py-GC/MS) device has largely been used during the last decades [172,173,222,268,269]. In such device, flash heating – typically of more than 10000 $°C \cdot s^{-1}$ – is applied to a very small sample of biomass, usually of about 100 µg, up to classical temperatures of pyrolysis, namely 400 to 600 °C. Under these conditions, biomass is largely converted into volatile species, which are directly led to Gas Chromatography Mass Spectrometry (GC/MS) for their determination and quantification. The obtained spectra enable to get detailed information on formed degradation products and then indirectly on biomass structure. The limitation in isothermal pyrolysis done under constant conditions is that a degradation product released from different mechanisms cannot be separated. In the fractionated pyrolysis the sample is not directly heated to the maximum temperature but heated to successive steps of increasing temperatures [270,271]. This procedure favors the release of volatile species at different temperatures and thus gives a better indication of their origin in terms of thermal stability of the related linkages. Up to now, fractionated pyrolysis has been used to determine interactions of pulping chemicals with lignin, residues of sulphur as well as lignin structure from chemical pulps [171,271,272]. Previous studies observed the influence of the pyrolysis temperature on the composition of lignin derived products formed [273,274]. In

these studies, the duration selected at each temperature was fixed to avoid the possible secondary reactions in each pyrolysis step. However, the influence of duration step on biomass degradation behavior, particularly for hemicellulose, cellulose and lignin, has never been systematically assessed by fractionated pyrolysis.

The aim of this work is to identify the duration/temperature conditions in fractionated pyrolysis that provide the most informative data regarding the macromolecular components of biomass. To achieve this goal, tests were performed on one typical hardwood sample under different programs of duration/temperature steps. Finally, the nature of the volatile compounds (carbohydrate derivatives and phenolic compounds) allowed to estimate the contribution from the degradation behavior of cellulose, hemicellulose and lignin to the torrefaction of beech wood.

2. Material and methods

2.1. Biomass description

Experiments were carried out on beech wood harvested on the South of France. Firstly, beech was dried by blowing heated air (40–60 °C) through a perforated floor, until all the material reaches about 5% moisture content. The dried beech was then shredded with a Lindner Micromat 2000 (Linder-Recylingtech GmbH, Spittal, Austria) with 15 mm screen size and then milled to 0.5 mm with a Universal cutting mill Fritsch Pulverisette 19 (Fritsch GmbH, Idar-Oberstein, Germany). Beech was then sampled following standard XP CENT/TS 14780. This procedure ensures sample homogeneity and representativeness in experiments [213].

Beech composition in main organic constituents as well as in ash is given in Table A.VIII.1. The extractive content was measured using an ASE (Accelerated Solvent Extractor) extraction with two cycles at 1500 psi, firstly with water at 110 °C then with acetone at 95 °C. Solvents were evaporated under reduced pressure, and then the residues were weighed and reported as the extractive content. The lignin and polysaccharides contents were measured using the extracted samples. The lignin content was determined by the sum of Klason and soluble lignin as described in TAPPI standard T222 om-83. Polysaccharides content was measured by ion chromatography after a two-step hydrolysis of samples in sulfuric acid (TAPPI standard T249 cm-85). The neutral monosugars obtained were quantified by ion chromatography using a Dionex DX5000 system equipped with GP50 gradient pumps using 150 m*M* NaOH and water as eluents, a CarboPac PA-10 column and an ED50 electrometric detector using an amperometric cell (ASTM E1758 standard method). Acetyl group content was also quantified from the same hydrolysate by ion chromatography but using different conditions: IonPac AS11-HC column and an electrometric detector in conductometric mode using an eluent gradient 60 m*M* NaOH and water. Ash content was measured using the XP CEN/TS 14775 standard. Methylglucuronic acid

(MeGlcA) content was estimated using a ratio 12 xylose units / 1 MeGlcA units according to Chemin et al. [275].

Table A.VIII.1. Beech macromolecular composition

Chemical composition	**%wmf ***
Cellulose	41.7
Hemicelluloses	27.7
Lignin	26.5
Ash	0.8
Extractives	1.8
Functional groups	**%wmf ***
Acetyl	8.3
Methylglucuronic acid	2.4
Neutral monosugars distribution	**% ****
Xylose	29.1
Mannose	3.0
Galactose	2.0
Arabinose	2.0
Glucose	63.9

** water-mass-free* *** % of total monosugars*

Values measured were in agreement with those from literature on hardwood [205,206]. As expected, ash content was very low, lignin content was relatively high and hemicellulose was mainly constituted of xylan.

2.2. Py-GC/MS experiments

Py-GC/MS tests were carried out in a filament pulse pyrolyzer (Pyrola2000, PyroLab, Sweden). Degradation products released during pyrolysis were analyzed through a Gas Chromatography (Agilent 7890B) coupled to a Mass Spectrometer (Agilent 5977A).

About 100 µg of beech was accurately weighed on an automatic ultramicro balance (CHAN 29 Instruments Inc. Cerritos. USA) and then immediately put in a small cavity at the center of a platinum filament in the pyrolyzer sample holder. Each sample was pyrolyzed according to a different fractionated pyrolysis program of time and temperature, covering the pyrolysis temperature range, as detailed in Table A.VIII.2. A heating time of 8 ms was set to go from chamber temperature of 150 °C to each pyrolysis temperature, which corresponds to a heating rate higher than 2000 °C·s^{-1}. After each temperature step, volatile products were sent to the Gas Chromatography (GC) injector with an Ultra inert split liner (Agilent) using a pulsed injection mode (pressure 25 psi for 0.8 minutes) in a 24.2 mL·min^{-1} flow of helium. After the injection, the flow of helium was set to 14 mL·min^{-1}. The injector was maintained at 250 °C, using a split ratio of 1:10. During each GC/MS analysis, the sample was kept in the pyrolysis chamber at 150 °C. In GC/MS analysis, helium was used as carrier gas (constant flow rate of 1.0 mL/L) and pyrolysis

products were separated using a capillary column (J&W DB-1701: 30 m × 0.25 mm, film 1 μm). The GC temperature program was set as follows: the initial temperature of 100 °C was held 1 min, then the column was heated to 265 °C at 6 °C·min^{-1}, kept at this temperature during 5.75 min and finally heated to 280 °C at 6 °C·min^{-1} and kept at this temperature for 3.25 min. The total time of GC/MS analysis was therefore 40 min. Ion trap mass spectrometer was used for compound detection with mass scan range of m/z between 29 and 300 (EI 70 eV). Temperature of ion source and quadrupole were set at 230 °C and 150 °C respectively.

Table A.VIII.2. Duration at each temperature step for the different profiles used

	1	2	3	4
Temperature (°C)	**Duration of step (s)**			
250	5	40	300	40
300	5	40	300	30
350	5	40	300	25
370	5	40	300	20
400	5	40	300	15
450	5	40	300	10
500	5	40	300	5

The peak areas of the pyrolysis products were integrated using total ion chromatogram (TIC) for each compound. Noise height in GC/MS chromatograms (~ 10^3) was fixed as detection limit for peaks. Peak areas were normalized considering sample mass. Normalized peak areas were used to determine the total yield of the volatile species released in fractionated pyrolysis (sum of volatile species, Table A.VIII.3). Moreover, each pyrolysis product was represented as the percentage of production corresponding to each temperature/time step normalized by the total production during the whole pyrolysis experiment. For each point, the average of two parallel measurements was calculated. Pyrolysis products identification was based on data from literature [215–218,276] as well as on commercial NIST 2011 MS library. The degradation products including their origin are presented in Table A.I.3.

3. Results and discussion

3.1. Effect of residence time on volatile species formation

Four profiles of temperature/time steps were considered (Table A.VIII.2). Temperatures were chosen to cover the typical degradation range of biomass between 250 and 500 °C, with successive increase of 50 °C, and an additional point at 370 °C in the zone of maximum production of volatile species. Duration of steps was defined according to different criteria in order to determine the influence of this parameter in fractionated pyrolysis. For profiles 1, 2 and 3 the same duration was selected for all temperature steps of the experiment. The profile 1 corresponds to a very short pyrolysis time (5 s), the profile 3, to a long time (300 s), and the profile 2, to an intermediate time (40 s). In profile 4, duration times were set up progressively,

that is, at a given pyrolysis temperature, some seconds were added successively until any volatile specie was detected in GC/MS analysis, similarly to previous studies [171,272]. This procedure corresponds to the optimal duration/temperature program for fractionated pyrolysis.

The detected volatile species are indicated in Table A.I.3. The degradation products were separated into carbohydrate derivatives (Ch) and lignin derivatives (Lg). The effect of residence time on the volatile formation was evaluated by calculating the total yield of volatile species released at the selected temperature range (Figure A.VIII.1). The result shows that the highest yield of volatile species was obtained at optimized conditions (profile 4). That is probably because optimization prevents secondary reactions [270,271]. Shorter pyrolysis time gave lower yields. The yield was increased when the residence time was changed to intermediate pyrolysis time whereas extension of time after 40 s did not enhance the yield. Concerning the lignin and carbohydrate derivatives distribution in the detected products, the Lg/Ch ratio varied between 0.4 for the fastest profile (beech 1) and 0.6 for the slowest one (beech 3). A deeper discussion on these compounds will be done in next sub-section.

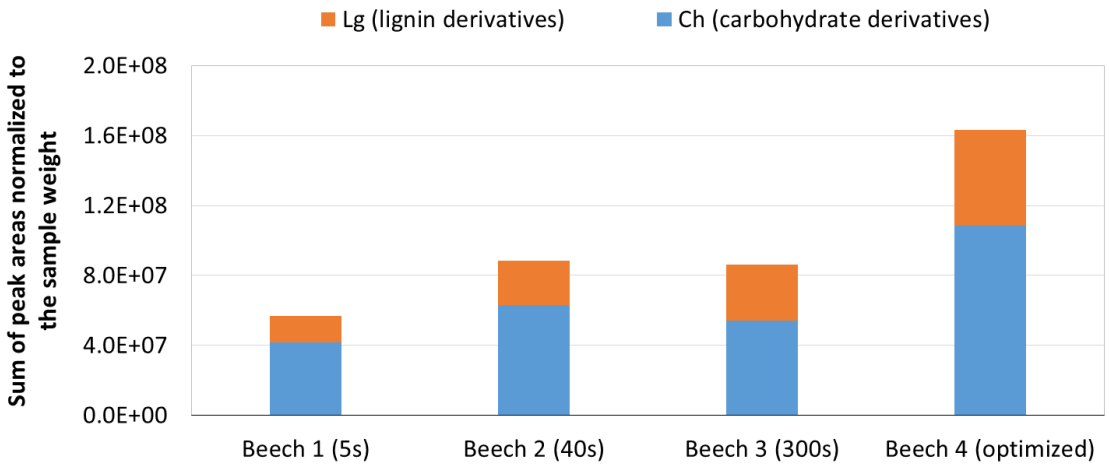


Figure A.VIII.1. Total yield of volatile species formed at different residence times in fractionated pyrolysis experiments

Table A.VIII.3. Chemical compounds detected in GC/MS analysis of the volatile species released in the fractionated pyrolysis of beech

Phenolic compounds	**MW**	**Origin**	
Phenol	94	Lg	lignin H-type
2-Methylphenol	108	Lg	lignin H-type
4-Methylphenol	108	Lg	lignin H-type
Guaiacol	124	Lg	lignin G-type
3-Methylguaiacol	138	Lg	lignin G-type
4-Methylguaiacol	138	Lg	lignin G-type
4-Vinylguaiacol	150	Lg	lignin G-type
4-Ethylguaiacol	152	Lg	lignin G-type
Vanillin	152	Lg	lignin G-type
Eugenol	164	Lg	lignin G-type
cis-Isoeugenol	164	Lg	lignin G-type
trans-Isoeugenol	164	Lg	lignin G-type
Homovanillin	166	Lg	lignin G-type
Acetoguaiacone	166	Lg	lignin G-type
4-(1-hydroxy-prop-2-enyl)guaiacol	180	Lg	lignin G-type
trans-Coniferyl alcohol	180	Lg	lignin G-type
Syringol	154	Lg	lignin S-type
4-Methylsyringol	168	Lg	lignin S-type
4-Vinylsyringol	180	Lg	lignin S-type
Syrignaldehyde	182	Lg	lignin S-type
4-Ethylsyringol	182	Lg	lignin S-type
4-Allylsyringol	194	Lg	lignin S-type
trans-Propenylsyringol	194	Lg	lignin S-type
Homosyringaldehyde	196	Lg	lignin S-type
Acetosyringone	196	Lg	lignin S-type
Syringylacetone	210	Lg	lignin S-type
Carbohydrate derivatives	**MW**	**Origin**	
Acetic acid	60	Ch/Lg	acetyl groups in hemicelluloses
Hydroxyacetone	74	Ch	cellulose/hemicelluloses
2(5*H*)-Furanone	84	Ch	cellulose/hemicelluloses
Furfural	96	Ch	cellulose/hemicelluloses
2-Furanmethanol	98	Ch	cellulose/hemicelluloses
1,2-Cyclopentanedione	98	Ch	hemicelluloses
2-Hydroxy-3-methyl-2-cyclopenten-1-one	112	Ch	hemicelluloses
5-Hydroxymethyldihydrofuran-2-one	116	Ch	cellulose/hemicelluloses
1,5-Anhydro-4-deoxypent-1-en-3-ulose	114	Ch	xylan
5-Hydroxymethylfurfural	126	Ch	hexoses - mainly cellulose
1,4-Anhydroxylopyranose	132	Ch	xylan
1,5-Anhydroarabinofuranose	132	Ch	arabinose
1,4-Anhydrogalactopyranose	162	Ch	galactose
1,4-Dideoxy-D-glycero-hex-1-enopyranos-3-ulose	144	Ch	hexoses - mainly cellulose
1,6-Anhydroglucopyranose (levoglucosan)	162	Ch	cellulose

Lg: lignin; Ch: carbohydrates

The degradation behavior of beech clearly varied among the different residence times (profiles 1, 2, 3 and 4) at the studied temperature range (Figure A.VIII.2). Shortening the residence time shifted the maximum weight loss to the higher temperature region. The longer the residence time was, the higher the amount of volatile species was released at low temperature region. Release of volatile species at low temperature region was negligible at short residence time, which indicated that short time in the low temperature region is not sufficient to degrade bonds among lignocellulose components. Optimization of time produced a profile looking more like a sum of long and short residence times. Fractionated pyrolysis carried out at intermediate time was close to optimized conditions. At low temperatures, the time for the degradation of sample components needs to be longer than that at higher temperatures. However, keeping a sample for a relative long time at the same temperature ends in deoxygenation followed by secondary reactions and higher char formation. That kind of reactions is favored for example in biomass torrefaction processes [9]. It appears that progressive heating of the sample from low temperature to high temperature regions at short times (5 s) globally decreases volatile species formation (Figure A.VIII.1). Generally, under fast pyrolysis conditions, an increase in temperature from 350 to 550 °C should enhance the volatile species formation [155,277].

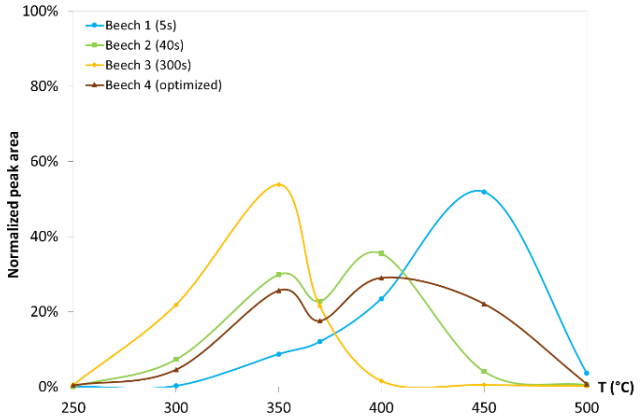


Figure A.VIII.2. Release of volatile species from beech in fractionated Py-GC/MS at different residence times

3.2. Volatile species identified

Detailed analysis of the data of the thermal behavior of beech during fractionated pyrolysis was performed. The volatile species detected are listed in Table A.VIII.3. They are derivatives originated from cellulose, hemicellulose sugars and lignin, in accord with those classically found in Py-GC/MS studies [107,173,276,278]. The degradation products were separated into carbohydrate derivatives (section 3.2.1) and phenolic compounds (3.2.2).

Main carbohydrate derivatives were levoglucosan and 1,5-anhydro-4-deoxypent-1-en-3-ulose from cellulose and xylan, respectively. A high yield of acetic acid was detected as well, in agreement with the high number of acetyl groups measured (Table A.VIII.1). Acetic acid can originate from xylan, cellulose and lignin, however elimination of acetyl groups linked to xylan in

hemicelluloses are expected to be its major source in beech wood pyrolysis. The presence of acetic acid and levoglucosan in a large amount was in accordance with previous studies [147,153]. Other carbohydrate derivatives are 1,5-anhydroarabinofuranose, 1,4-anhydroxylopyranose, 1,4-anhydrogalactopyranose, various furans, hydroxyacetone and 1,2-cyclopentanedione, which were also released in significant amounts.

Several lignin-derived compounds originated from guaiacyl and syringyl type substructures could also be identified, in agreement with previous pyrolysis studies from literature [172,173,177,178,222,273,274,279–282]. Hardwood main lignin derivatives were guaiacyl and syringyl type, but also small amounts of *p*-hydroxyphenyl type degradation products were detected. The main syringyl-derivatives were 4-vinylsyringol, syringol, 4-methylsyringol and trans-propenylsyringol, while the major guaiacyl-derivatives were 4-vinylguaiacol, 4-methylguaiacol and guaiacol. Other lignin derivatives were mainly degradation products containing carbonyl groups and guaiacyl type derivatives with hydroxyl groups (Table A.VIII.3). *p*-Hydroxyphenyl type structures detected were phenol and 4-methylphenol.

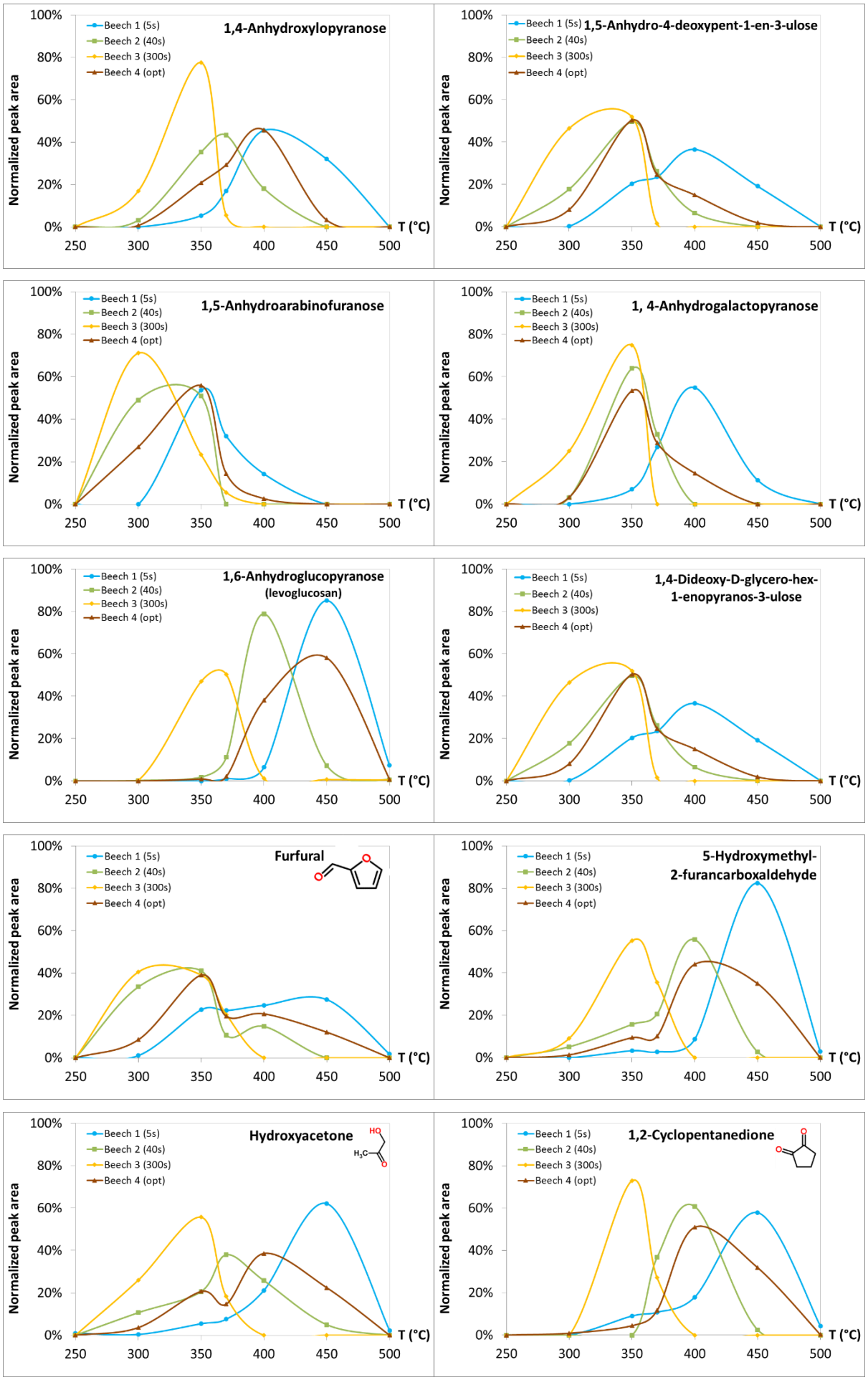
3.2.1. Carbohydrate derivatives

As shown in Figure A.VIII.3, there is a clear influence of step duration at each temperature on the profile of carbohydrate-derived volatile species release versus temperature. Indeed, when the duration of each temperature step was very long (300 s, profile 3), products were mostly formed at lower temperatures. On the contrary, when the duration of each temperature step was very short (5 s, profile 1), products were mainly released at higher temperatures, from 300 °C to 500 °C, with a different maximum depending on the product studied. In the case of an intermediate pyrolysis duration identical for all temperature steps (40 s, profile 2), products were almost only formed at intermediate pyrolysis temperatures (350 to 400°C). Eventually, in the case of variable step durations (profile 4), products were formed over the whole range of temperatures. Interestingly, other degradation products such as hydroxyacetone generated two relative maxima at optimized conditions (profile 4), which could correspond to two different pathways of formation/origin of these chemical compounds. 1,5-anhydro-4-deoxypent-1-en-3-ulose and 1,4-anhydroxylopyranose degradation products from xylan presented slightly different profiles with a different maximum at 350 and 400 °C, respectively. At low temperature region, the formation of acetic acid was closely followed by the formation of 1,5-anhydro-4-deoxypent-1-en-3-ulose, both with a maximum at 350 °C. That presumably indicated a common origin from the acetylated xylan units known to be present in beech wood [153]. These observations are in perfect agreement with the hemicelluloses composition (essentially xylans) and the acetyl groups concentration measured for the sample used in this work (Table A.I.1). However, other mechanisms for the acetic acid formation have also been proposed, as the decomposition of glucuronic acid units in hemicellulose and through the complex reaction of ring-opened glucose

units [59,73]. That could explain the second maximum of acetic acid at higher temperature. The ratio xylose/glucuronic acids for wood beach is 12 according to Chemin et al [275]. Release of 1,4-anhydroxylopyranose at higher temperature indicates that it is formed from non-acetylated xylan units that are thermally more stable [283]. The thermal stability of arabinose was shown to be lower, which is in accord with the release of 1,5-anhydroarabinofuranose at lower temperatures in comparison with the formation of other hemicellulose derived anhydrosugars. This observation is also supported by the very low concentration of arabinose units (only 2 % of neutral monosugars) in beech hemicelluloses (Table A.VIII.1). The formation of 1,4-anhydrogalactopyranose was closely followed by the formation of 1,5-anhydro-4-deoxypent-1-en-3-ulose.

Levoglucosan was clearly released at temperatures higher than the other anhydrosugars (profile 4), proving the higher thermal stability of cellulose compared to hemicelluloses, as reported in the literature [161]. The formation of 1,4-dideoxy-D-*glycero*-hex-1-enopyranos-3-ulose and 5-hydroxymethylfurfural closely followed the degradation of levoglucosan, however including a maximum at lower temperature (400 °C) in comparison with levoglucosan (450 °C). The formation of furans, such as 5-hydroxymethylfurfural and furfural, directly from cellulose instead of from anhydrosugars secondary reactions, supports this result [155,284]. It has been supposed that pyrans (such as 1,4-dideoxy-D-*glycero*-hex-1-enopyranos-3-ulose) can be formed via primary reactions and via levoglucosan intermediate, which can undergo condensed-phase secondary depolymerization [187]. Based on the results of this study, these two formation reactions of pyrans cannot be distinguished. 1,4-dideoxy-D-*glycero*-hex-1-enopyranos-3-ulose and 5-hydroxymethylfurfural had also a minor maximum at 350 °C, a temperature for which the formation of levoglucosan had not started yet (profile 4). This supports the theory defending that some compounds are also originated from hexose sugars other than cellulose, such as galactoglucomannan or glucomannan, as previously reported [285], despite the low concentration of these monosugars in beech hemicelluloses (Table A.VIII.1).

Furfural, hydroxyacetone, and 1,2-cyclopentanedione were also released in significant amounts. These compounds have all been reported to be formed from cellulose as a result of ring opening reaction of levoglucosan [155], but also from hemicelluloses [29,165]. All these compounds showed two maxima at 350 and 400 °C, except 1,2-cyclopentanedione [165].


1,4-Anhydroxylopyranose
1,5-Anhydro-4-deoxypent-1-en-3-ulose
1,5-Anhydroarabinofuranose
1, 4-Anhydrogalactopyranose
1,6-Anhydroglucopyranose (levoglucosan)
1,4-Dideoxy-D-glycero-hex-1-enopyranos-3-ulose
Furfural
5-Hydroxymethyl-2-furancarboxaldehyde
Hydroxyacetone
1,2-Cyclopentanedione
Beech 1 (5s)
Beech 2 (40s)
Beech 3 (300s)
Beech 4 (opt)
Normalized peak area
T (°C)

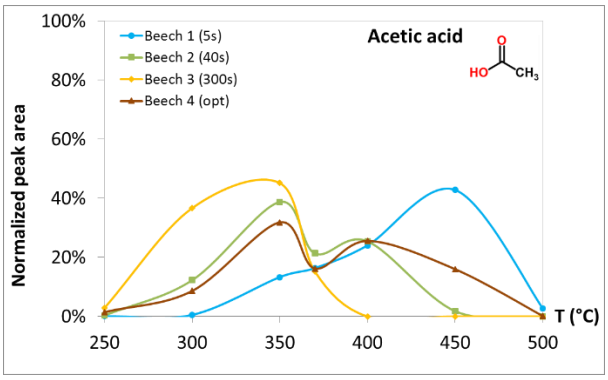


Figure A.VIII.3. Production profiles of carbohydrate degradation products in fractionated Py-GC/MS of beech

3.2.2. Phenolic compounds

As shown in Figure A.VIII.4, chemical compounds based on G (guaiacyl) - and S (syringyl) - type structures were released in a similar way during fractionated pyrolysis. This is slightly in accordance with the S/G ratio units of beech lignin reported in the literature [286,287]. However, the maximum production temperature varied with step duration and compound type released. When the duration of each temperature step was very long (300 s, profile 3), all compounds were mostly formed at lower temperatures with a maximum at 300 to 350 °C, with non-detectable production from 400 °C. On the contrary, for a very short pyrolysis time (5 s, profile 1), phenolic species were all released mainly at higher temperatures. In the case of an intermediate duration identical for all temperature steps (40 s, profile 2), these compounds were almost only formed at intermediate pyrolysis temperatures. In profile 4, in which duration was adjusted to allow the release of all possible volatile species in each pyrolysis temperature step, G- and S- derivatives were released at increasing temperatures with the length decrease of their side-chain-substituent. For example, for guaiacyl compounds, eugenol is mainly produced at 350 °C, ethylguaiacol at 370 °C, methylguaiacol at 400 °C and guaiacol at 450 °C. As a result, fractionated pyrolysis carried out under optimized time conditions enables to distinguish the long-side-chain-derivatives, such as eugenol and 4-allylsyringol, and the short-side-chain-lignin-derivatives, such as guaiacol and syringol. The result follows primary and secondary pyrolysis reactions that have been explained to occur at temperatures between 200 and 600 °C [174]. This also confirms that in optimized conditions compounds from different origin can be distinguished from each other, but not when very short or long residence time are used.

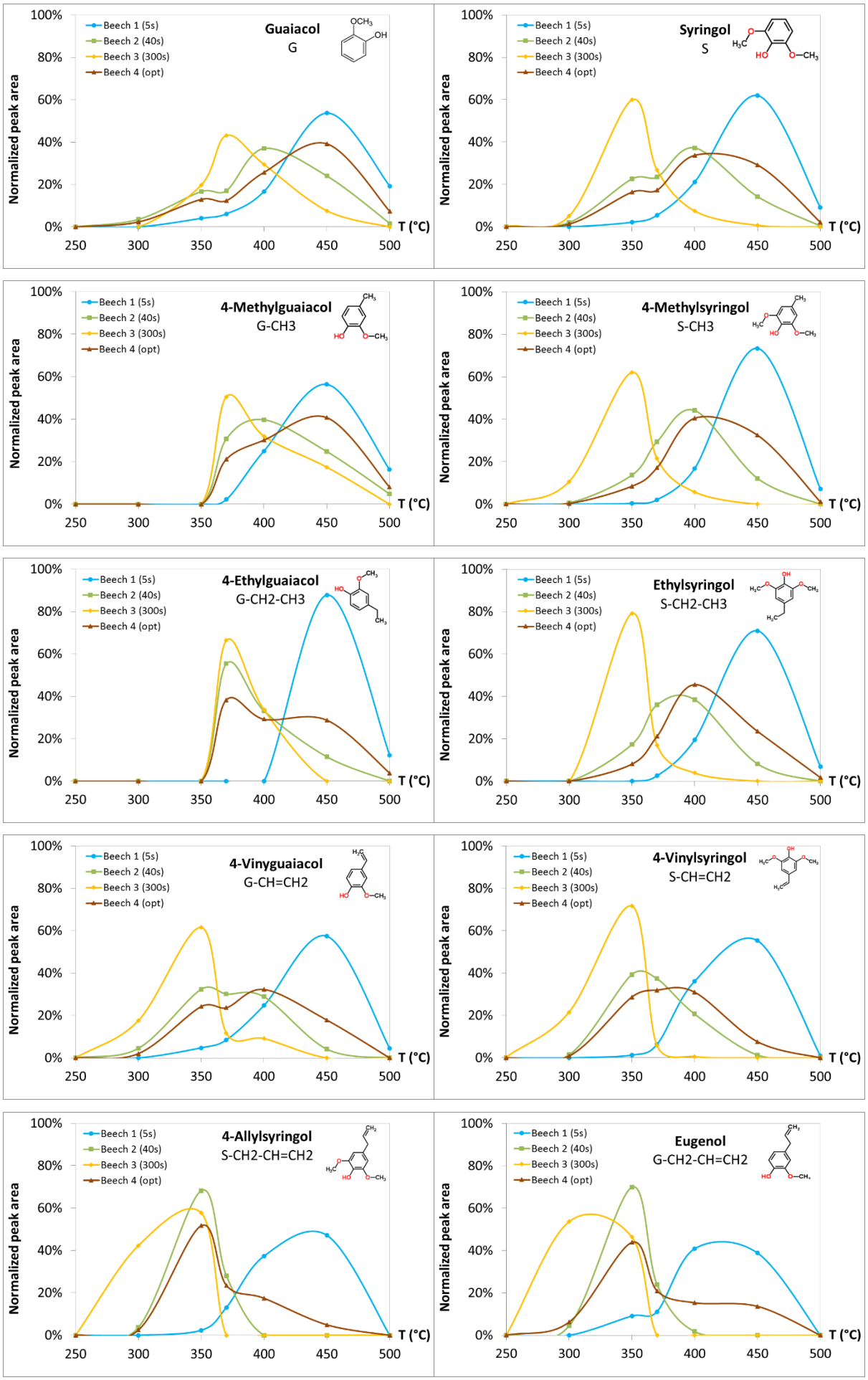
When the optimized duration step profile was selected, eugenol and 4-allylsyringol (3-C, 3 carbon atoms) were mostly released at moderate pyrolysis temperature (350 °C). Other phenolic compounds released at that temperature were G- and S- derivatives containing O in a 1, 2 or 3-C-atom-side chain, as aldehydes, ketones or alcohol substituents (Figure A.VIII.4). These compounds were vanillin, homovanillin, acetoguaiacone and 4-(1-hydroxy-prop-2-enyl)guaiacol for the G-derivatives and *trans*-propenylsyringol, syringaldehyde, homosyringaldehyde and

syringylacetone and for the S-type compounds. These types of compounds having C=C and C=O structures in side chain were reported to be formed in a primary pyrolysis stage in the temperature range of 200–400 °C, in which β-ether bond is degraded. The degradation of β-*O*-4 bond is linked to the release of functional groups (hydroxyl group, polysaccharide, lignin unit) present in the α-carbon in propyl side chain together with free or non-phenolic structure [174]. In beech wood it can be expected that first maxima obtained for phenolic compounds (350 °C) is a result of the cleavage of β-ether bonds in lignin. But also carbohydrate derived products degraded at the same maximum might be partly formed as a result of ether bond cleavage among lignin and polysaccharides.

The formation of the G- and S-type derivatives with a double bond in the side-chain, namely 4-vinylguaiacol and 4-vinylsyringol, tended to occur at lower pyrolysis temperatures compared to the formation of the saturated 2-C-side-chain derivatives, namely 4-ethylguaiacol and ethylsyringol. These results are in agreement with literature [29]. At the same time, it can be suggested that vinyl-derivatives are from two different origins of lignin, as two relative maxima can be distinguished in the corresponding production curves at 350 and 400 °C.

The short side-chain derivatives (1-C) such as 4-methylguaiacol and 4-methylsyringol, exhibited a maximum of production at around 400 to 450 °C. This transformation is explained in the literature by secondary pyrolysis cracking reactions of the side-chain C–C bonds, which increases the yields of monomers and implies the transition of the products from unsaturated to saturated alkyls side chains [174]. However, these degradation products could also be formed because of the cleavage of condensed linkages of lignin such a β-1 and β-5, which has been reported to form higher yields of guaiacol and 4-methylguaiacol, respectively. Other monomers can be detected as well, but with a lower yield [175,176]. Higher dissociation energy is needed for the degradation of carbon-carbon than carbon-oxygen bonds among lignin units [174]. That may explain the second maximum in lignin degradation products.

Finally, at higher fractionated pyrolysis temperatures, the basic lignin structures were released, namely guaiacol and syringol compounds. This corresponds to the basic-non-substituted-structure of lignin, and thus explains their more difficult removal from biomass structure. It has been explained that they could come from secondary pyrolysis reactions involving the rupture of ramifications between aromatic rings [47]. Some authors have pointed out that this moment corresponds to the highest decomposition rate of lignin and the maximum production of phenols [177,178]. However, these products can also be formed from the condensed lignin substructures similar as methyl derivatives [175,176].


Guaiacol
G
Syringol
S
4-Methylguaiacol
G-CH3
4-Methylsyringol
S-CH3
4-Ethylguaiacol
G-CH2-CH3
Ethylsyringol
S-CH2-CH3
4-Vinyguaiacol
G-CH=CH2
4-Vinylsyringol
S-CH=CH2
4-Allylsyringol
S-CH2-CH=CH2
Eugenol
G-CH2-CH=CH2
Beech 1 (5s)
Beech 2 (40s)
Beech 3 (300s)
Beech 4 (opt)
Normalized peak area
T (°C)

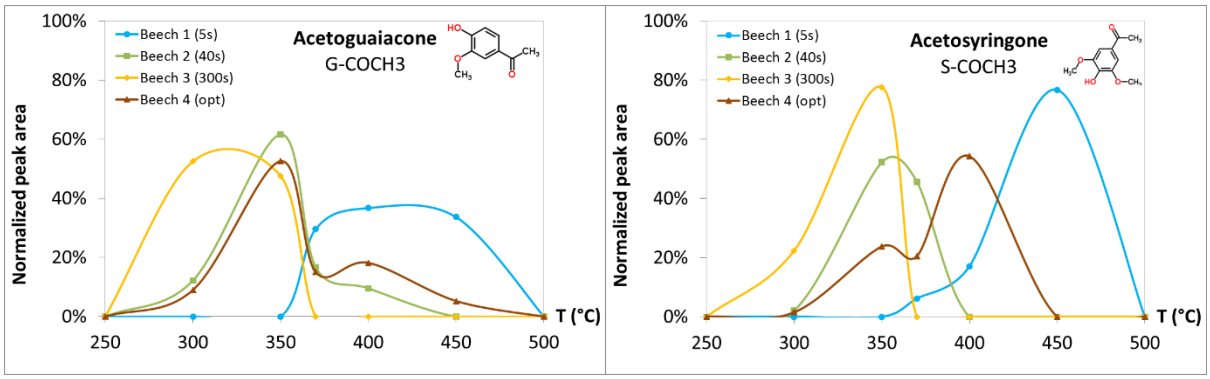


Figure A.VIII.4. Production profiles of the main G- and S-type phenolic compounds in fractionated Py-GC/MS of beech

Among H-type chemical compounds, only phenol and methyl phenol were detected (Table A.VIII.3, Figure A.VIII.5). These compounds were released at significantly higher temperatures, with a maximum of production at 450 °C for phenol and between 400 and 450 °C for methylphenol. Similar result has been reported earlier [171].

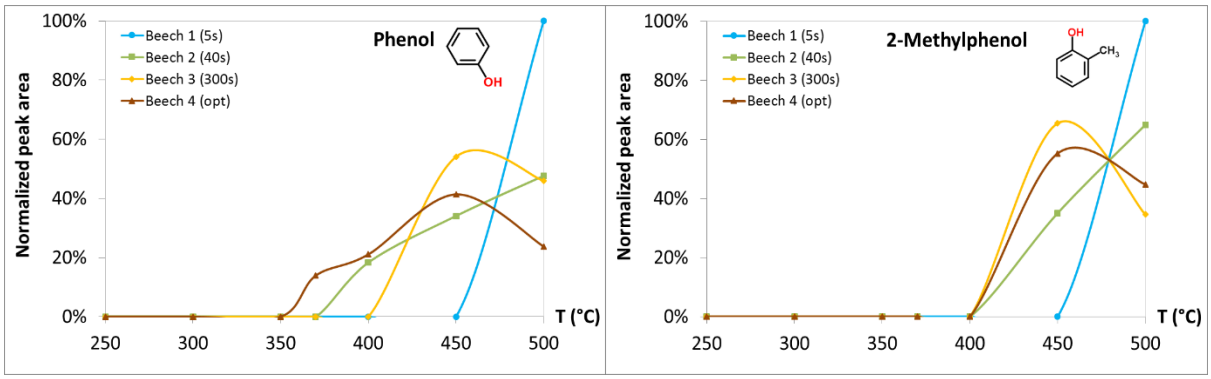


Figure A.VIII.5. Production profiles of the main H- type phenolic compounds (non-derived from lignin) in fractionated Py-GC/MS of beech

4. Conclusions

The influence of step duration at each temperature in fractionated pyrolysis Py-GC/MS experiments on biomass was demonstrated. A Py-GC/MS program using the same time for each step of the fractionated pyrolysis does not allow to appreciate any difference in pyrolysis products formation. However, when optimized temperature and time configuration is used, pyrolysis products can be released at different pyrolysis progression degrees according to their origin. At the same time, this operating procedure enables to distinguish several relative maximum production peaks for some compounds, which could indicate different pathways of formation and origins in biomass structure. Such fractionated pyrolysis experiments can therefore be a useful tool to dissociate the phenomena involved in biomass thermal degradation and the origin of products associated, as well as to characterize biomass structure.

2. Detailed structural elucidation of different lignocellulosic biomass types using optimized temperature and time profiles in Py-GC/MS

M. González Martínez, T. Ohra-aho, T. Tamminen, D. da Silva Perez, M. Campargue, C. Dupont

This work is ready for submission to the Journal of Analytical and Applied Pyrolysis (October, 2018).

Abstract

Fractionated pyrolysis experiments coupled to gas chromatography and mass spectrometry experiments (Py-GC/MS) were carried out on eight woody and agricultural biomasses, including beech, poplar, pine forest residues, Scot Pine bark, reed canary grass, corn cob, grape seed cake and wheat straw. The selected temperature and duration for each fractionated pyrolysis step allowed separating the volatile pyrolysis products in function of their origin from biomass. As a result, carbohydrate derivatives from hemicelluloses were released at earlier fractionated pyrolysis steps, compared to those produced from cellulose degradation. Phenolic derivatives, mainly produced by lignin, were stepwise produced in function of the length and the nature of their side-chain substituents. Protein derivatives were also released in the whole Py-GC/MS temperature range. On the other hand, macromolecular composition and biomass family were shown to play a crucial role in the thermal degradation of the biomasses of study. Production profiles exhibited resemblances per chemical species between deciduous and coniferous woods, while they appear to be more heterogeneous for agricultural biomasses. Herbaceous crops presented an intermediate behaviour between wood and agricultural biomasses.

Highlights

- Degradation behaviour of eight different biomasses was evaluated by fractionated Py-GC/MS.
- Fractionated Py-GC/MS helps in revealing biomass structure through volatile product profiles.
- Biomass family and macromolecular composition drastically affect biomass thermal degradation.
- Carbohydrate derivative origin impacts the maximum temperature of their production profile.
- Length of the side-chain of phenolic derivatives indicates their order of release in Py-GC/MS.

Keywords: Py-GC/MS; fractionated pyrolysis; lignocellulosic biomass; lignin degradation; carbohydrate degradation

1. Introduction

Lignocellulosic biomass, including woody, agricultural and herbaceous resources, has been shown to play a strategic role in the current transformation of the energetic production [261]. Its macromolecular composition consists mainly of cellulose, hemicelluloses and lignin, with

water, minor amounts of proteins, pectins, minerals and other trace components [48]. While cellulose and hemicelluloses are based on various monosaccharides, lignin is an oxygenated polymer based on phenylpropane units [5]. The proportions and distribution of these macromolecular components in biomass physical structure is complex and depends on the biomass type. Interactions between cellulose, hemicelluloses and lignin in biomass have been demonstrated to play a role in its thermochemical conversion [166].

Cellulose is a major structural component of cell walls, which provides mechanical strength and chemical stability to lignocellulosic biomass. It is present in biomass under the shape of microfibrils consisting of a semi-crystalline macromolecular structure formed by a long straight chain of (1,4)-D-glucopyranose units linked by β-1,4 glycosidic bond [48,50,51]. Glucan chains composing cellulose are linked together through extensive hydrogen bonding, forming linear organized arrays of chains. The order in the glucan chains in the microfibrils is sometimes altered, leading to disordered areas along the length of microfibrils. These more likely-amorphous regions are suspected to be more propitious to the association of hemicelluloses with cellulose microfibrils [52].

Hemicelluloses are heteropolysaccharides formed by several types of sugar molecules composed either by five or six carbon atoms. In the first case, pentose sugars are the base of the structure (arabinose, xylose), while in the second case hexose sugars constitute hemicelluloses (galactose, glucose and mannose). Hexuronic acids (e.g. glucuronic acid) can also be present in the structure, as well as acetyl groups connected to the chain, usually to xylans and arabinoxylans [52]. The function of hemicelluloses is to contribute to the formation of a resistant and cohesive network of cellulose microfibrils. The structure of hemicelluloses is conditioned by the main sugar involved in the polymer construction, the frequency and the nature of the ramifications and the degree of polymerization [54].

Lignin structural units are represented by *p*-hydroxypenyl (H), guaiacyl (G) and syringyl (S) units, derived from the copolymerization of *p*-coumaryl alcohol, coniferyl alcohol and sinapyl alcohol, respectively [62]. Important differences exist between lignin structure from wood, distinguishing hardwood (angiosperm) and softwood (gymnosperm). Lignin from softwood is mostly formed by G units and some H units, mainly, while lignin constituting hardwood contains varying ratios of G and S units [63]. On the other hand, lignin from herbaceous plants present three types of units (H, S and G) [222]. The analysis of agricultural biomasses implies a more complex lignin structure containing G- and H- units, respectively. In addition, these biomasses often contain *p*-hydroxycinnamic acids (*p*-coumaric and ferulic acids) [170]. The role of *p*-hydroxycinnamic acids in herbaceous biomasses was described as a bridge between lignin and carbohydrates through LCC (lignin-carbohydrates complexes) [288]. As a result, these acids were not considered as part of the lignin structure. In addition, some proteins are present in agricultural biomasses.

Structurally, significant differences exist between hardwood and softwood in cell structure, concerning complexity and cell types. More precisely, softwoods present a simpler structure with only two cell types mainly invariable. Hardwoods are characterized by a higher degree of variability within a higher number of cell types, presenting also a characteristic type of cell (vessel element or pore), which is absent in softwoods [45,289]. In both cases, tissues of woody biomasses contain the main part of lignin in the secondary cell wall layers [46]. Even if the cell structure of agricultural biomasses and herbaceous crops is close to that of hardwood, the main differences concern the macromolecular components forming the cell walls, how they are linked together, and the abundance and nature of pectins, proteins and phenolic compounds [290].

The objective of this work is the broadening of the use of fractionated Py-GC/MS to the elucidation of the structure of woody and agricultural biomasses. All together eight biomasses were studied. The distribution of the volatile pyrolysis products grouped per chemical family and through the seven steps of the fractionated pyrolysis experiments was firstly studied. In a second step, the formation of volatile pyrolysis products was analysed in function of their repartition in each step of the fractionated Py-GC/MS and in function of the biomass type. Pyrolysis products derived from carbohydrates, lignin and proteins were monitored. Special attention was paid to the correct identification of the source of some degradation products that may be derived from several components, such as *p*-hydroxyphenyl derivatives (protein/lignin/*p*-hydroxybenzoic acid) and vinyl derivatives (cinnamic acids/lignin). The role of inorganic components was not studied as the aim was to simulate the reactions in practical thermal processing. Therefore the samples were studied as such without washing.

2. Material and methods

2.1. Biomass description

Eight biomasses, representative of the European diversity, were selected for fractionated Py-GC/MS experiments. This includes two deciduous woods (beech, poplar), two coniferous woods (pine forest residues, Scots pine bark), three agricultural by-products (corn cob, grape seed cake and wheat straw (Swedish)) and one herbaceous crop (reed canary grass). Biomass characterization and preparation was described in section III.1.1. Comments on this characterization are already reported in [223].

2.2. Py-GC/MS experiments

Py-GC/MS measurements were performed as described in section Annex VIII.1.2.2, using the fractionated pyrolysis program of temperatures and times indicated in Table A.VIII.4. The most suitable time at each temperature was set in preliminary experiments with beech, by checking that all volatile species are released at each pyrolysis step [260].

Table A.VIII.4 Time set at each step of fractionated pyrolysis experiments (Py-GC/MS) for the selected temperatures

step	temperature (°C)	time (s)
1	250	40
2	300	30
3	350	25
4	370	20
5	400	15
6	450	10
7	500	5

Table A.VIII.5 includes volatile species released in fractionated pyrolysis of the eight selected biomasses and detected in GC/MS analysis. Pyrolysis products could be identified thanks to data from the literature [215–218], as well as to the commercial NIST 2011 MS library.

Table A.VIII.5. Chemical compounds followed in GC/MS analysis of the volatile species released in the fractionated pyrolysis of different biomasses

Chemical compound	MW	Chemical compound	MW
Guaiacyls		**Anhydrosugars (and dihydropyranoses)**	
3-methylguaiacol	123	1,4-anhydroxylopyranose	57
guaiacol	124	1,5-anhydroarabinofuranose	57
homovanillin	137	1,6-anhydroglucopyranose (levoglucosan)	60
4-ethylguaiacol	137	1,4-anhydrogalactopyranose	73
4-(1-hydroxy-prop-2-enyl)guaiacol	137	1,5-anhydro-4-deoxypent-1-en-3-ulose	114
4-methylguaiacol	138	1,4-dideoxy-D-glycero-hex-1-enopyranos-3-ulose	144
vanillin	151	**Acids**	
acetoguaiacone	151	acetic acid	60
eugenol	164	**Furans**	
cis-isoeugenol	164	2(5H)-furanone	55
trans-isoeugenol	164	5-hydroxymethyldihydrofuran-2-one	85
dihydroconiferyl alcohol	137	furfural	96
trans-coniferyl alcohol	180	5-hydroxymethylfurfural	97
Syringyls		2-furanmethanol	98
syringol	154	**Ketones**	
syringylacetone	167	hydroxyacetone	43
4-ethylsyringol	167	1,2-cyclopentanedione	98
homosyringaldehyde	167	2-hydroxy-3-methyl-2-cyclopenten-1-one	112
4-methylsyringol	168		
acetosyringone	181	**Protein derivatives**	
syrignaldehyde	182	indole	117
4-allylsyringol	194	methylindole	130
4-propenylsyringol	194		
***p*-hydroxyphenyls**		**Vinyl derivatives**	
phenol	94	4-vinylphenol	120
4-methylphenol	107	4-vinylguaiacol	150
2-methylphenol	108	4-vinylsyringol	180

Peak areas of pyrolysis products were integrated using extracted-ion chromatogram (EIC) with the selected ion for each compound (Table A.VIII.5). Then, peak areas were normalized considering the weight of the sample. The average of two parallel measurements was calculated for each point. Peak area in the chromatogram was the selected magnitude for the data analysis, due to the impossibility of calibrating all detected chemical species.

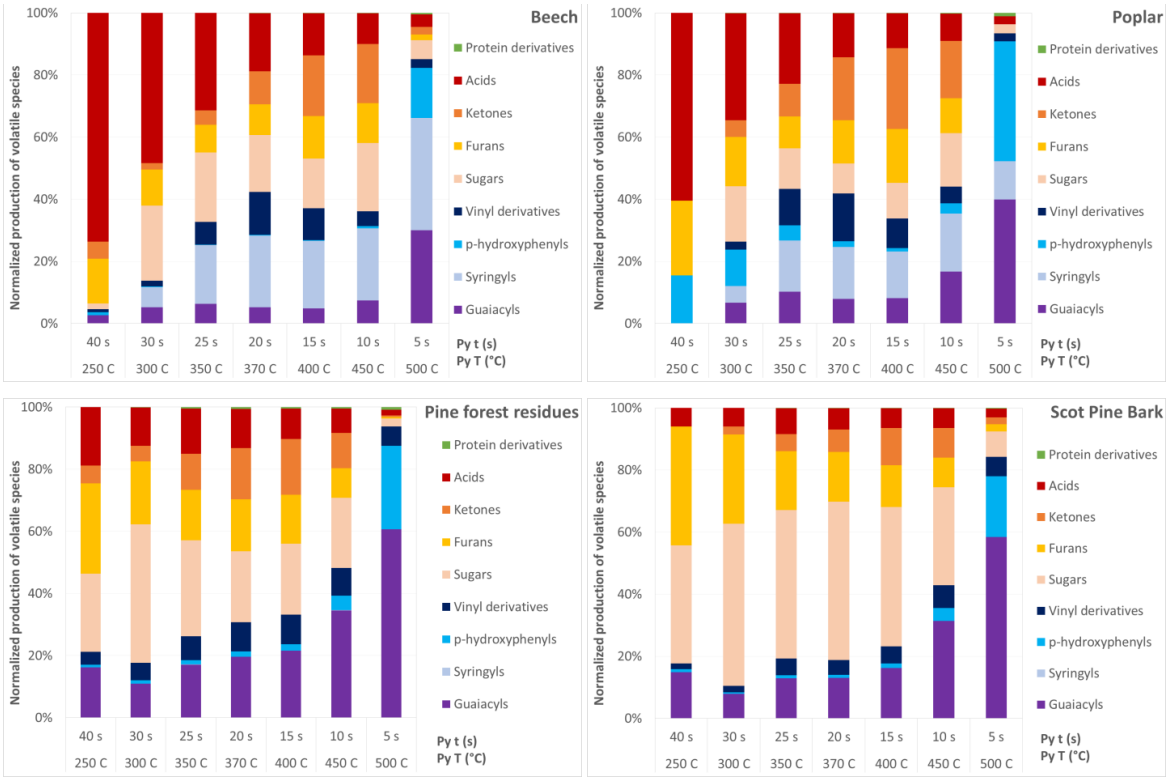
In a first step, pyrolysis products were grouped per chemical family and their peak areas were added. The production ratio per chemical family at each fractionated pyrolysis step was calculated as a ratio of the total production of volatile species of the given step (Figure A.VIII.6).The addition of peak areas of different volatile species belonging to the same chemical family can only be considered for comparing trends between families and/or biomasses.

Secondly, the production profile of each pyrolysis product was represented in function of temperature and step duration. To do this, the production of the pyrolysis product was calculated for each step of the fractionated pyrolysis as the percentage of the total production of the given species in the seven steps of fractionated pyrolysis (Figures A.VIII.7 to A.VIII.15).

3. Results and discussion

3.1. Analysis of the volatile species released per biomass

The production of volatile species per chemical family released in the Py-GC/MS experiments with different biomasses was compared (Figure A.VIII.6Figure). Biomasses were grouped by families: deciduous wood (beech, poplar), coniferous wood (pine forest residues, Scot pine bark) and agricultural by-products, including herbaceous crops (corn cob, grape seed, cake, reed canary grass, wheat straw).



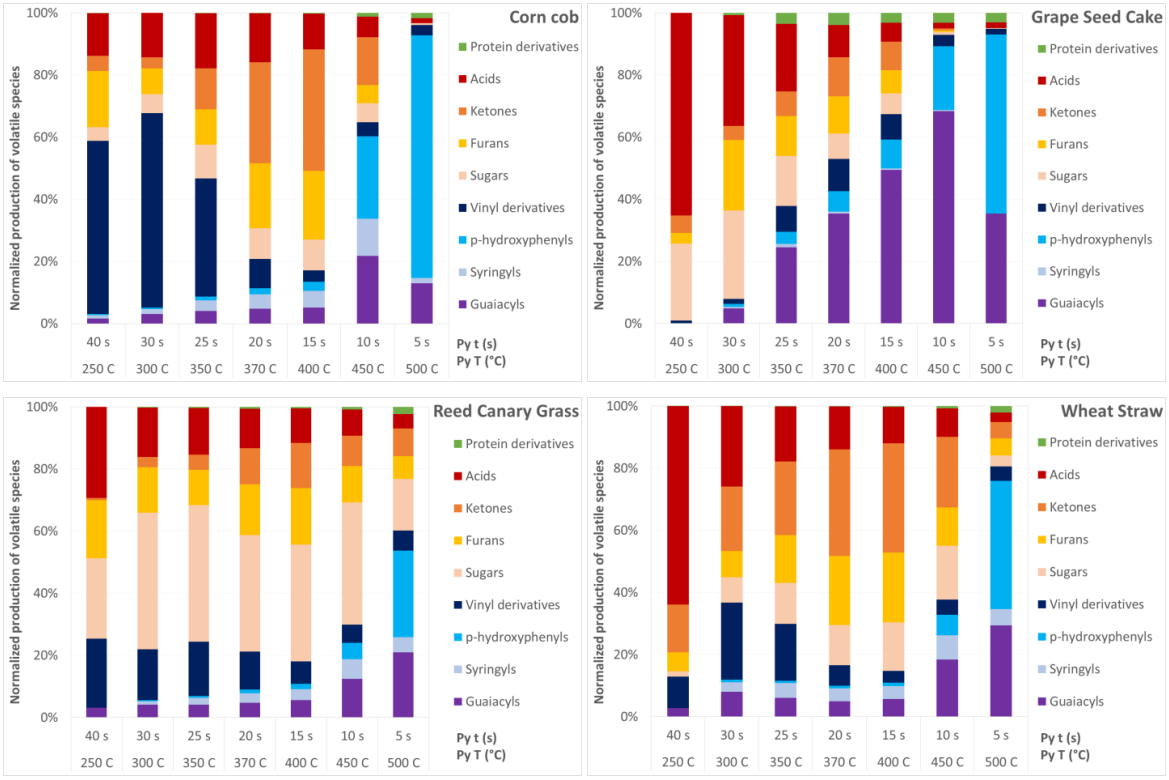


Figure A.VIII.6. Total production of volatile species classified in chemical families and normalized per temperature in the fractionated fast pyrolysis of the eight selected biomasses in Py-GC/MS

The percentages of the pyrolysis products from the chemical families considered were variable in function of the biomass type and the fractionated pyrolysis step. Similar distribution of the pyrolysis products was shown per duration/temperature step for biomasses from the same family, particularly for deciduous and coniferous wood, respectively. This distribution is more heterogeneous for agricultural biomasses, including herbaceous crops, presumably because of their more heterogeneous macromolecular composition compared to woods (Table III.4).

However, wheat straw, corn cob and reed canary grass showed similarities in product distribution, which is probably due to their rather similar macromolecular structure. These biomasses differed from the woody biomasses and grape seed cake releasing a high proportion of vinyl derivatives in the low temperature region (250-350 °C). The result indicated the presence of hydroxycinnamates, in which *p*-coumaric acid has been reported to acylate the γ-carbon in lignin side chain and ferulic acids polysaccharides. The ferulic acid has been found to be cross linker forming ether and ester bonds among lignin and carbohydrates, respectively [288,291]. The release of carbohydrate derivatives (ketones, furans and sugars) slightly varied among agricultural biomasses, indicating differences among macromolecular components. The production of volatile species from grape seed cake is distinct from that of the other agricultural biomasses, which might be due to its noticeably high lignin content, as well as because of differences in lignin units. However, similarities were found among coniferous wood, which are enriched with guiacyl-type lignin, the lignin type also predominant in grape seed cake.

3.2. Detailed analysis of volatile species per detected chemical compound

Volatile species detected in each fractionated Py-GC/MS experiment were classified in chemical families in function of their nature into phenolic, carbohydrate and protein derivatives. The production profiles of each volatile species, represented by the normalized peak area in function of the step of the fractionated pyrolysis, were compared for the 8 biomasses considered (Figures A.VIII.7 to A.VIII.15).

3.2.1. Phenolic derivatives

Phenol production (Figure A.VIII.7) occurs in the whole fractionated pyrolysis range and is characterized by two relative maxima, except for poplar, with a single maximum at 350 °C, representing half of its phenol production. No evidence was found in the literature to justify this particular behaviour of poplar. Methylphenols are characterized by an enhanced production with pyrolysis temperature, with a minor maximum at 350 °C. It has been reported in the literature that phenols released in the temperature range of 400-600 °C might be produced in secondary reactions from lignin, via demethoxylation of guaicyl-type lignin derivatives [174]. Phenolic derivatives were released at significantly higher temperatures compared to the corresponding guaiacyl and syringyl counterparts, which might explain the secondary reaction phenomenon. However, in fractionated pyrolysis, it is expected that secondary reaction are mainly avoided. Therefore the origin of these *p*-hydroxyphenyl derivatives is expected to be mainly from H-type lignin units. Other minor routes of formation have been reported in the literature, as for phenol, 2-methylphenol and 4-methylphenol, which can be produced from lignin or the aminoacid tyrosine in protein [292].

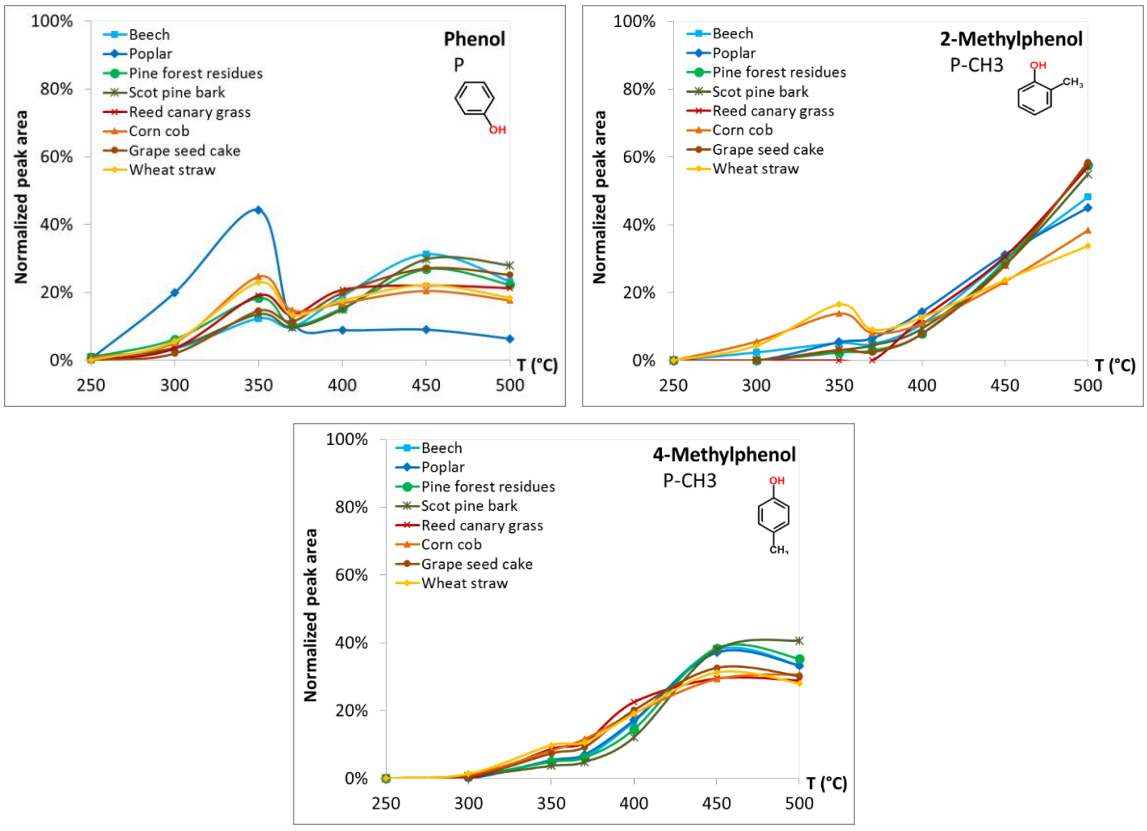
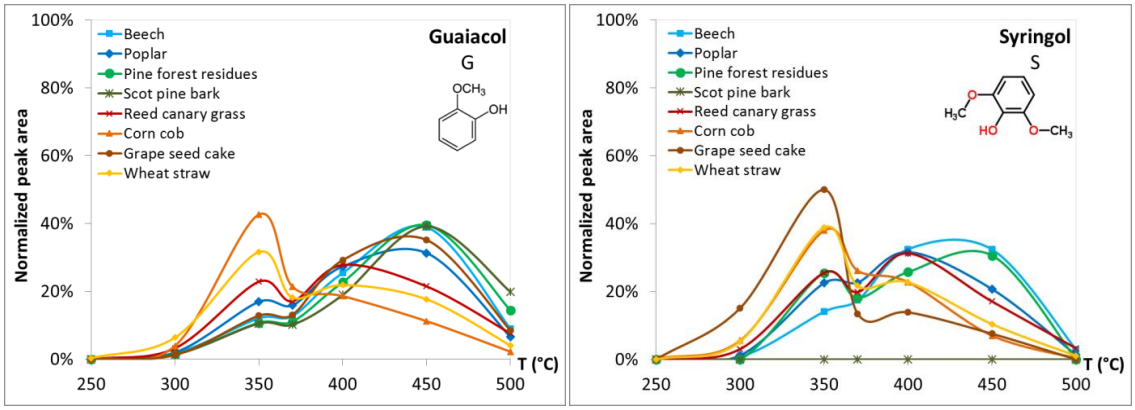


Figure A.VIII.7. Production profiles of phenyl- derivatives in fractionated Py-GC/MS

As proposed in [260], equivalent guaiacyl- and syringyl- derived structures with the same side chain length are compared (Figure A.VIII.8 and Figure A.VIII.9).

For guaiacyl- and syringyl- compounds with short side chains (Figure A.VIII.8), the maximum of production is between 350 and 370°C for agricultural biomasses (wheat straw and corn cob) and around 400 °C for woody biomasses (beech, poplar, forest residues, pine bark). The exception of this behaviour is for 4-methylguaiacol and 4-methylsyringol, which present the maximum of production for all biomasses at around 400 to 450 °C. Different lignin origin might explain the exceptional formation of 4-methylguaiacol and 4-methylsyringol in comparison to the other linear saturated side chain structures [175]. The appearance of several maxima in the production profile indicates that the degradation product might be formed from different routes.

By comparing biomass behaviour per families, resemblances are observed for woody biomasses, which principally present the maximum of the production profiles at 400 to 450 °C (Figure A.VIII.8). On the contrary, the production of these compounds by corn cob and wheat straw occurs in the whole fractionated pyrolysis, the maximum of the production being located between 300 and 400 °C in function of the product. Reed canary grass exhibits an intermediate behaviour between woody and agricultural biomasses. Grape seed cake presents a particular behaviour which does not correspond between equivalent guaiacyl- and syringyl- derivatives. While the maximum of its guaiacol production profile is around 450 °C, the corresponding maximum for the syringol production is around 350 °C. Concerning methyl- and ethyl- guaiacyl-derivatives, its behaviour is closer to that of woods, which is not the case for the equivalent syringyl derivatives. Furthermore, only few syringyl-type degradation products were detected, whose thermal behaviour was different in comparison to the corresponding guaiacyl derivatives.



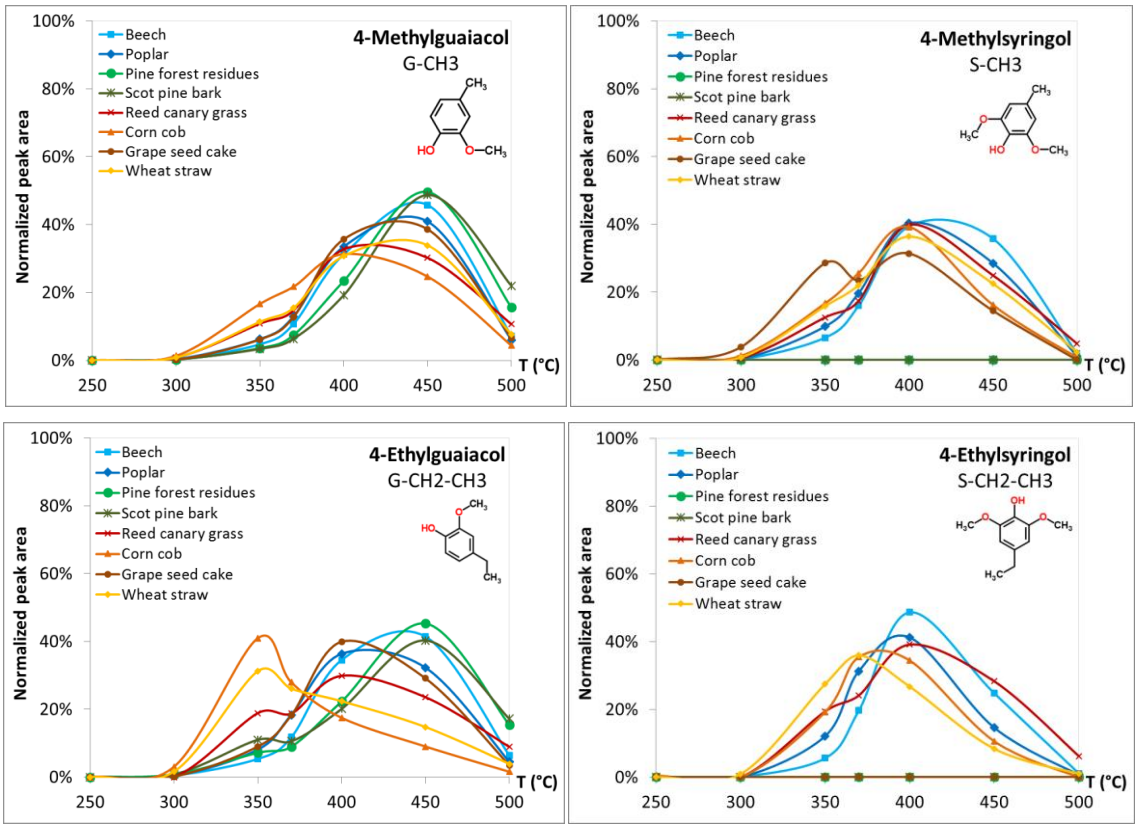
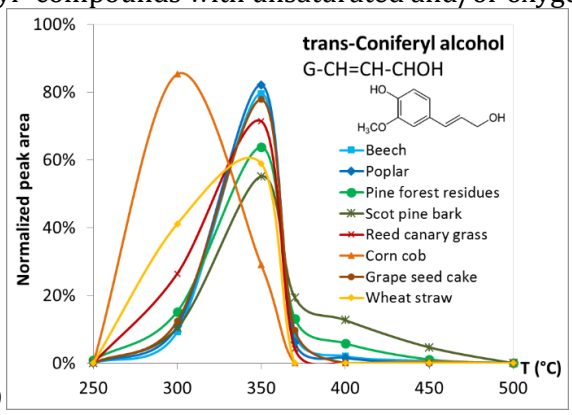


Figure A.VIII.8. Production profiles of analogous short chain guaiacyl- (left) and syringyl- (right) derivatives in fractionated Py-GC/MS

In the case of guaiacyl- and syringyl- compounds with unsaturated and/or oxygenated side-chains (Figure A.VIII.9



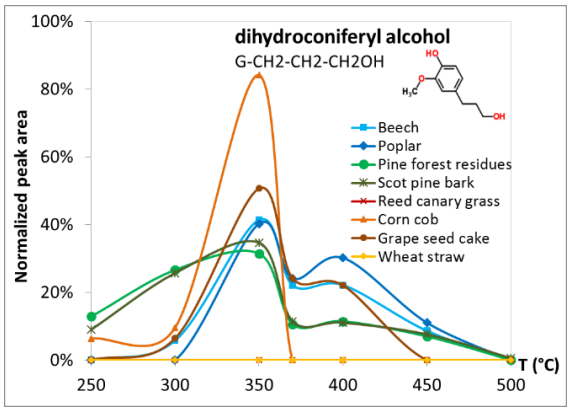
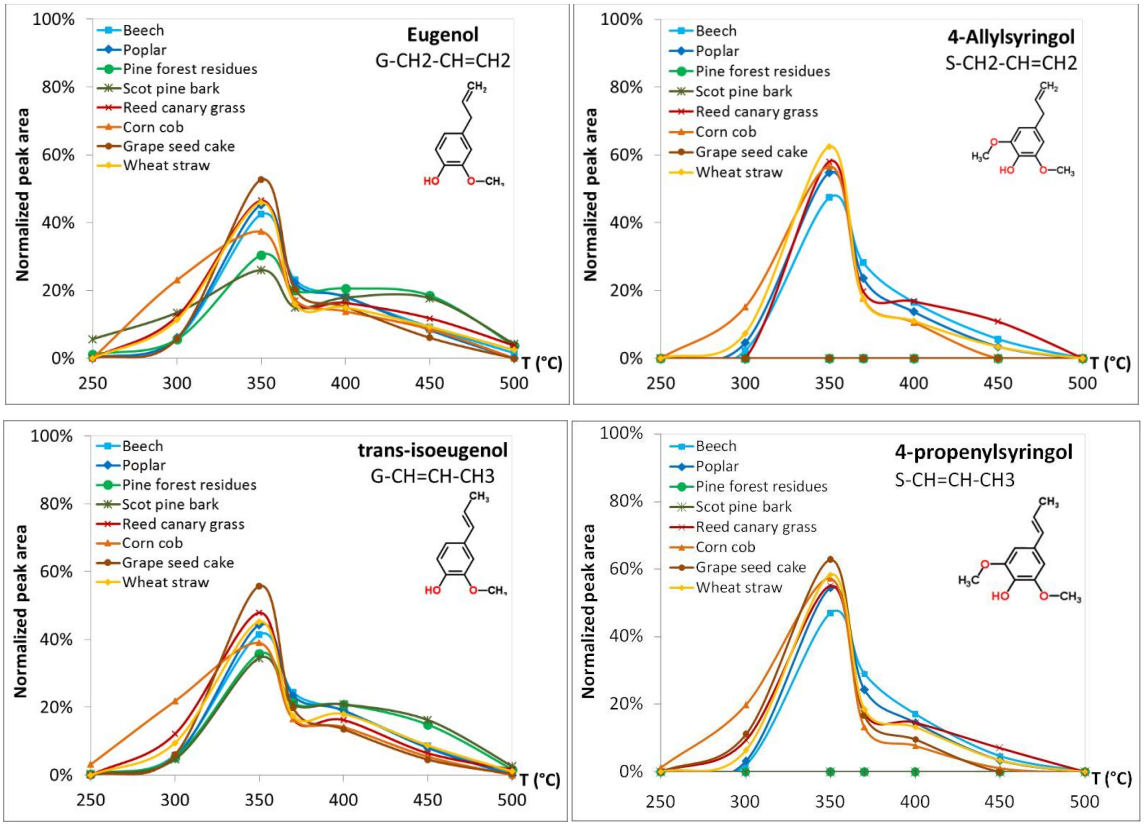


Figure), the maximum of their production is generally at lower temperatures, around 350 °C, for all biomasses. This maximum is especially marked for grape seed cake, which presents a high lignin content, and reed canary grass. The formation of all of these compounds continues at

higher temperatures, but with a much lower yield. A second local maximum at higher temperatures (around 400 °C) can be observed for the production of both guaiacyl- and syringyl compounds from all biomasses, indicating a probable different origin for the same degradation products.

The patterns observed for the formation of most of the degradation products in Figure A.VIII.9 are very similar for all biomasses, for both the G and S series. This probably indicates that the origin of these products is normal G/S-type lignin, and that they are formed mainly as a result of the cleavage of β-O-4 linkage of lignin [174]. Anomalous behaviour is seen in the case of vanillin, acetoguaiacone and transconiferyl alcohol (only in the G series) for corn cob, reed canary grass and wheat straw, which is probably caused by some unknown parallel degradation route. Dihydroconiferyl alcohol was released in a significant high amount already at 250 °C from pine forest residue and scot pine bark. The formation of this compound at low temperatures might be related to the high extractive content of these biomasses. This hypothesis is supported by the fact that this alcohol has been detected in the monomer form in coniferous wood extractives [64].



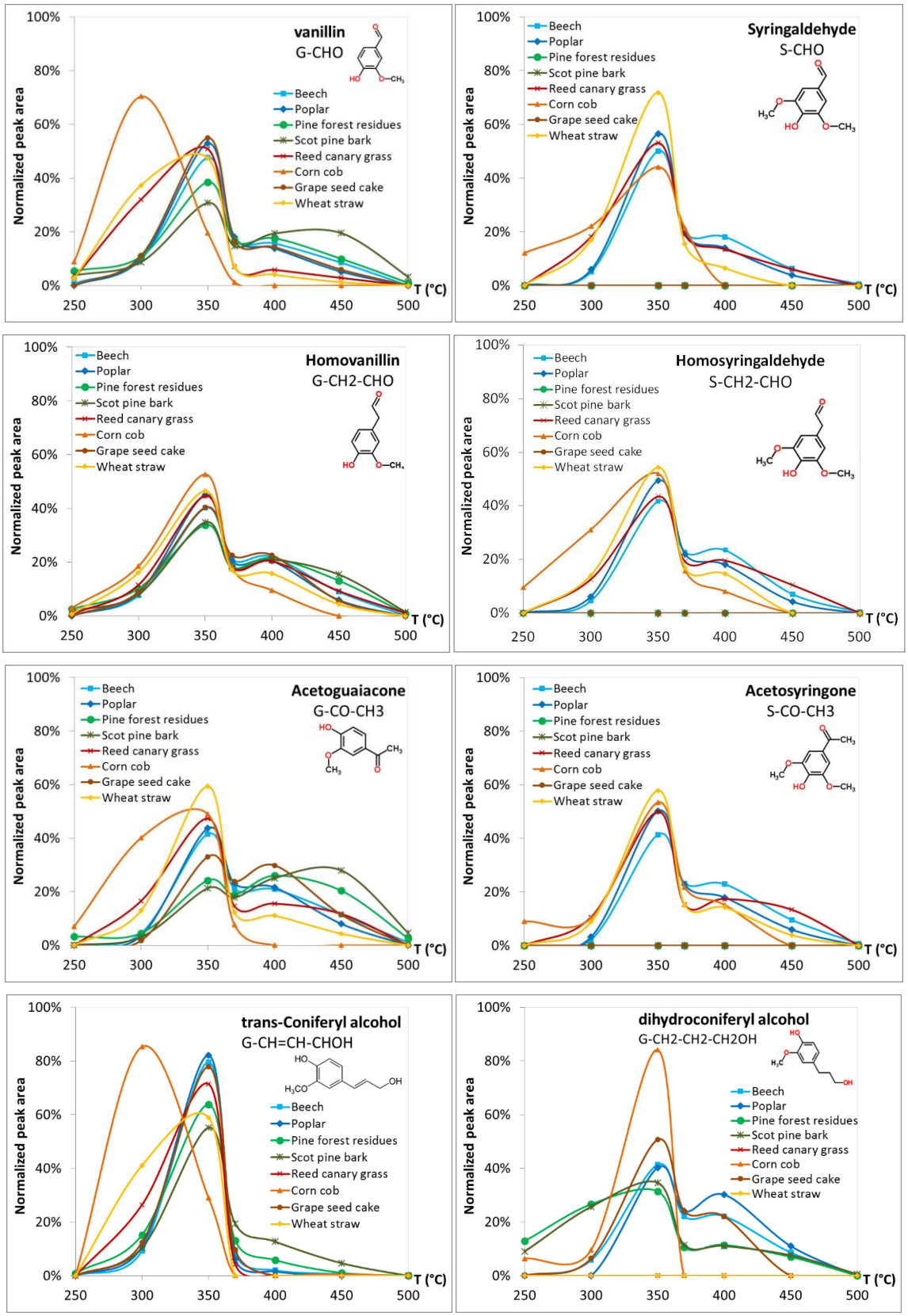


Figure A.VIII.9. Production profiles of unsaturated and oxygenated guaiacyl- (left) and syringyl- (right) derivatives in fractionated Py-GC/MS

For herbaceous and agricultural biomasses, vinylphenol and vinylguaiacol can be also formed from *p*-hydroxycinnamic acids (*p*-coumarylic and ferulic acids) in addition to lignin [170,293]. According to [260], the first maximum of production of these compounds could correspond to the production from p-hydroxycinnamic acids, while the maximum at higher temperatures could

represent the formation of this compound from lignin. In the case of wheat straw, corn cob and reed canary grass, the maximum of the production for 4-vinylguaiacol is around 350 °C, which could indicate that the major part of the production of this compound is derived from *p*-hydroxycinnamic acids. In the case of woody biomasses, the maximum is at intermediate and higher temperatures. For grape seed cake (high content in lignin) and reed canary grass (herbaceous crop), the behaviour is intermediate (Figure A.VIII.10).

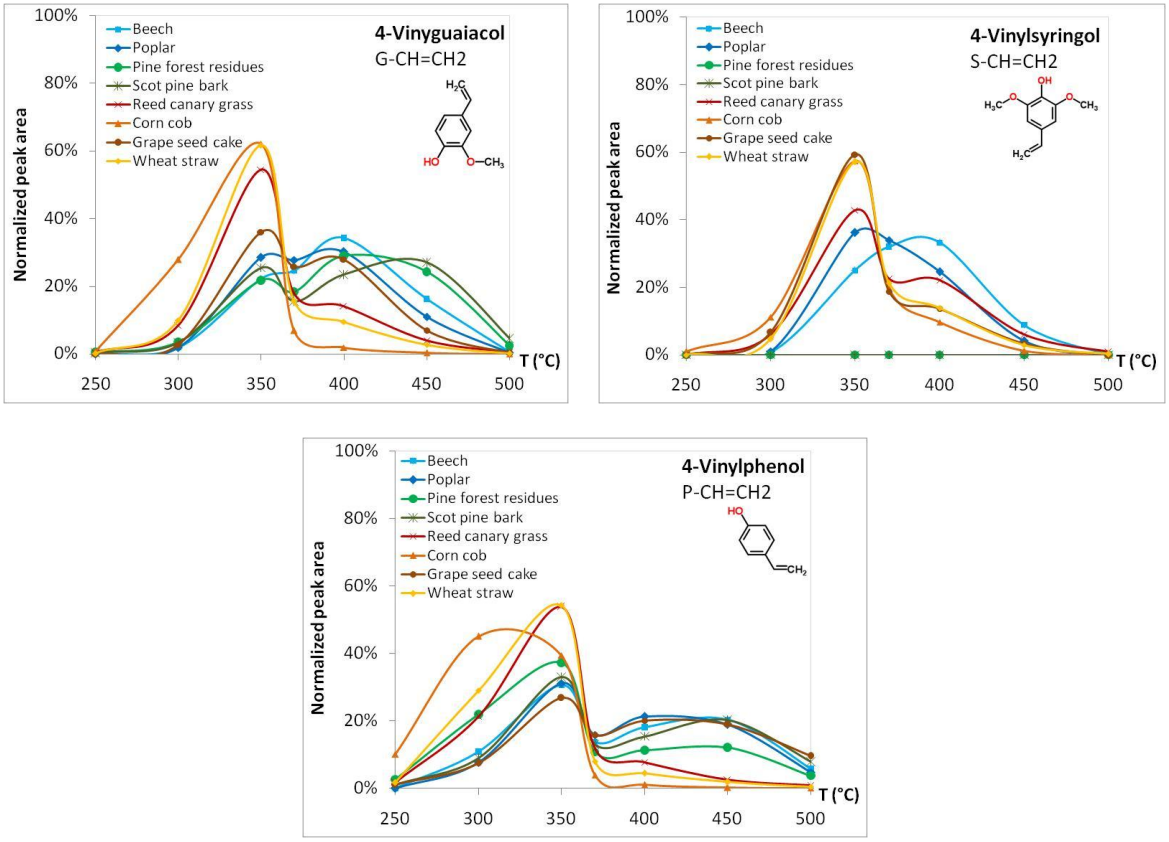


Figure A.VIII.10. Production profiles of vinyl derivatives in fractionated Py-GC/MS

3.2.2. Carbohydrate derivatives

Six carbohydrate-derived molecules were identified in the volatile mixture resulting from the Py-GC/MS experiments of 8 biomasses (Figure A.VIII.11). The production of these molecules is reported to be directly related to the thermal decomposition of cellulose and hemicelluloses in biomass [292]. Hemicelluloses are an amorphous heteropolymer, which is thermally decomposed at early temperatures in classical thermochemical conversion processes (250 to 320 °C) [22,116]. On the other hand, cellulose is a more crystalline polymer that degrades at slightly higher temperatures (around 280 to 400 °C) [9,116,135]. According to this, the sugar molecules released can be associated to their origin in function of their maximum temperature of production. As a result, hemicelluloses derivatives would be 1,4-anhydroxylopyranose and 1,5-anhydro-4-deoxypent-1-en-ulose (derived from xylan), 1,5-anhydroarabinofuranose (derived from arabinan) [46], 1,4-anhydrogalactopyranose (derived from galactan). The maximum temperature of the production profile of these three carbohydrates is between 300

and 350 °C, which corresponds to the temperature range of hemicelluloses degradation. On the contrary, 1,6-anhydroglucopyranose (levoglucosan) would be derived from cellulose, as its maximum of production is around 400 °C. Finally, the production profile of 1,4-dideoxy-d-glycero-hex-1-enopyranos-3-ulose occurs at lower temperatures for grape seed cake and softwood (350 °C), and at higher temperatures for agricultural biomass, herbaceous crops and hardwood. This compound is formed from cellulose- and hexose-sugar-based hemicelluloses, such as galactoglucomannan and glucomannan. Its formation follows both those of 1,4-galactopyranose and 1,6-anhydroglucopyranose suggesting that the first maximum would mainly correspond to the degradation of these hexose-sugar-based hemicelluloses (high amount in softwood and crops), and the second maximum from cellulose.

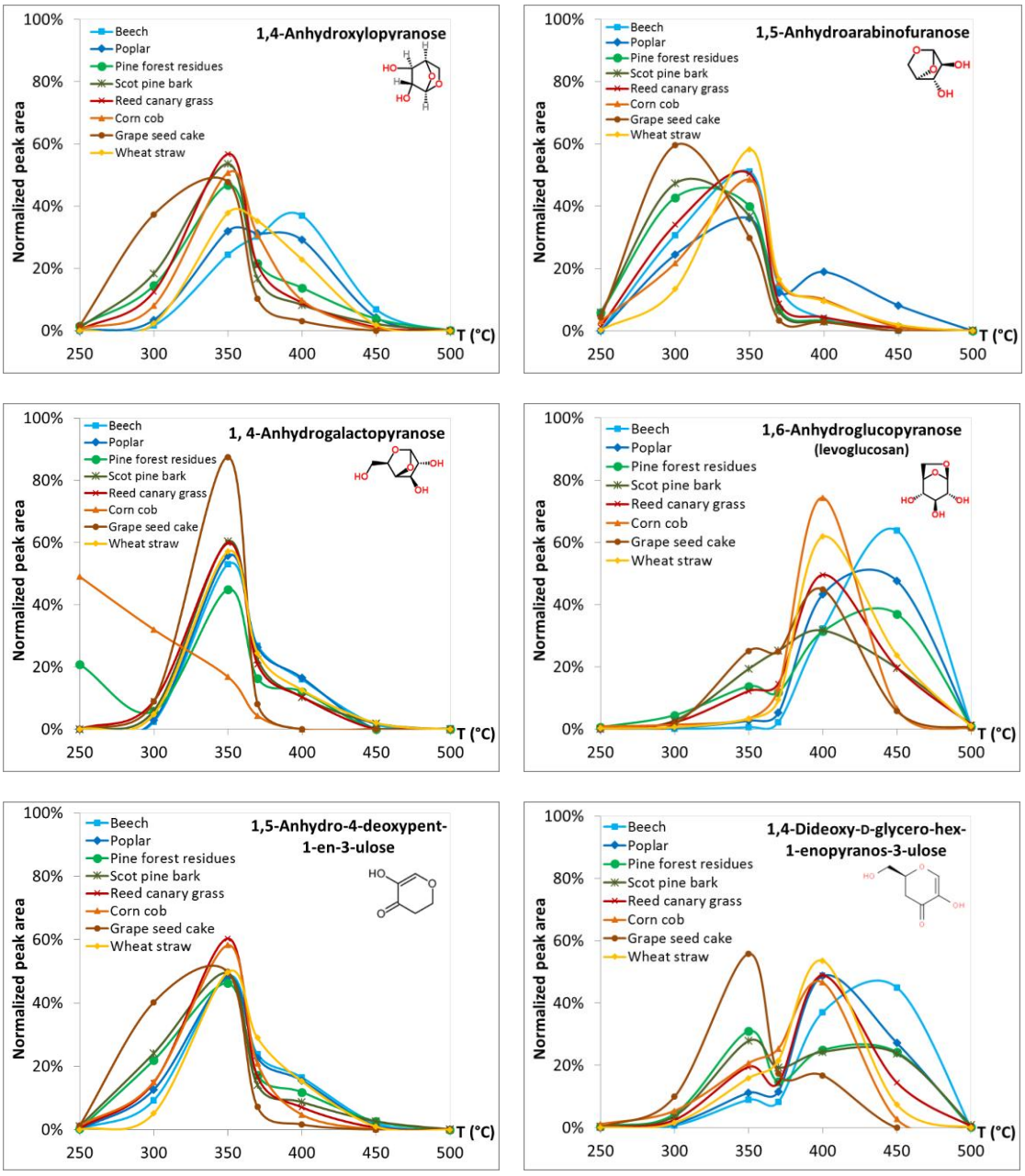


Figure A.VIII.11. Production profiles of sugar molecules in fractionated Py-GC/MS

Small molecules, including acids, ketones and furans, are principally carbohydrate derivatives. Acetic acid is one of the major detected compounds in fractionated Py-GC/MS of biomass (Figure A.VIII.12). Its profile of formation, similar for all the biomasses in this study, is characterized by a maximum of production at 350 °C, followed by a regular production until 450 °C. The main mechanism of formation of acetic acid is from the scission of acetyl groups in hemicelluloses [153], which is accordance with the maximum of the production profile at lower temperatures in Py-GC/MS. In addition to hemicelluloses, in some herbaceous plans the γ-carbon in lignin side chain has been reported to be acetylated and is susceptible to release acetic acid [170]. However, this release of acetic acid from lignin side chain is expected to occur in the same temperature region as from hemicelluloses, due to the ester linkage, but in a lower amount. Other mechanisms have been proposed, as the decomposition of uronic acid unit in hemicelluloses and through the complex reaction of ring-opened sugar units [59,73], which could correspond to the regular production at intermediate temperatures in Py-GC/MS. The differences in acetyl content in the biomasses studied (from 1.6 to 8.3 %) do not allow distinguishing a higher production of acetic acid in Figure A.VIII.12, as the percentages of the total production per pyrolysis step are represented.

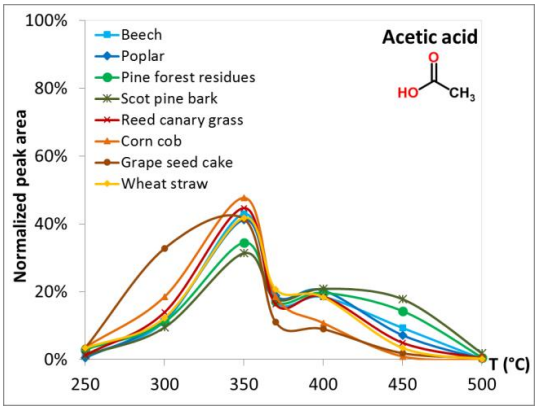


Figure A.VIII.12. Production profiles of acetic acid in fractionated Py-GC/MS

One linear ketone (hydroxyacetone) and two cyclic ketones (1,2-cyclopentanedione and 2-cyclopenten-1-one, 2-hydroxy-3-methyl-) were identified in biomass Py-GC/MS experiments (Figure A.VIII.13). Ketones and other small compounds were reported to be released in the rapid depolymerization of hemicelluloses, but also from cellulose [187], directly or through unstable intermediaries which go through dehydration, fragmentation and secondary reactions [29]. Cyclic ketones are produced in hemicelluloses depolymerization [162,163,227], derived from pyran or furan rings [29], but also in cellulose pyrolysis at high temperatures [187,228,294]. These pathways of formation might be in accordance with the highest percentage of the production at the intermediate steps of the fractionated pyrolysis, without a maximum temperature clearly distinguished. An interesting exception is beech, exhibiting increasing profiles with a maximum at 400 °C, suggesting the presence of some parallel formation route of this degradation product in this biomass.

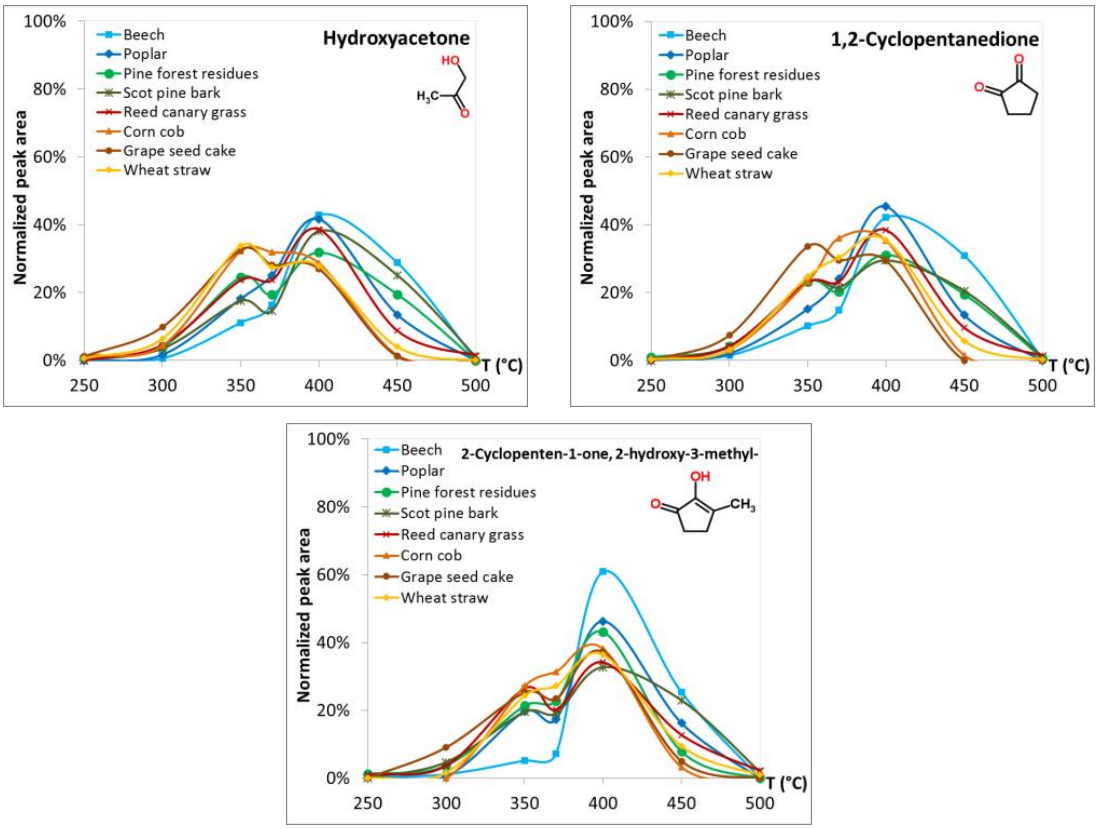


Figure A.VIII.13. Production profiles of ketones of in fractionated Py-GC/MS

Furans are in general produced at intermediate to high temperatures under the established Py-GC/MS operating conditions (Figure A.VIII.14). The exception is for furfural, which is produced mainly around 350 °C, with a small peak at 400 °C. The origin of furans in the thermal decomposition of cellulose was pointed out as depolymerization reactions. They consist in a contraction of the pyran ring of levoglucosan through the elimination of oxygenated groups and the formation of double bonds C=C. Then, weak bonds might break and liberate furan compounds such as furfural [154]. The release of furfural from hemicelluloses is attributed to the ring-open and rearrangement reactions of the xylan unit [163], which might occur at lower temperatures than the formation of this product from cellulose. In general, furan production from hemicelluloses is related to depolymerization reactions occurring by cleavage of glycosidic linkages between sugar units. This formation typically happens at temperatures slightly higher for glucomannan-based hemicelluloses, compared to xylan-based hemicelluloses [162], as pyran rings derived from glucomannan (6 C-atoms) can change into more stable furan rings (5 C-atoms) [29]. The two relative maxima observed in the production curves of furans might contribute to explain the percentage of the production of each pyrolysis compound that might be derived from hemicelluloses or from cellulose, respectively, as hemicelluloses thermal degradation starts at lower temperatures. Most of the furfural production might be derived from hemicelluloses, as the maximum of the curve is around 350 °C, or even lower for grape seed cake and coniferous wood. Deciduous wood and reed canary grass present a maximum of the production profiles around 400 °C for the other furans detected, which might indicate an origin from cellulose. They might also come from hemicelluloses either less accessible or linked to

cellulose.

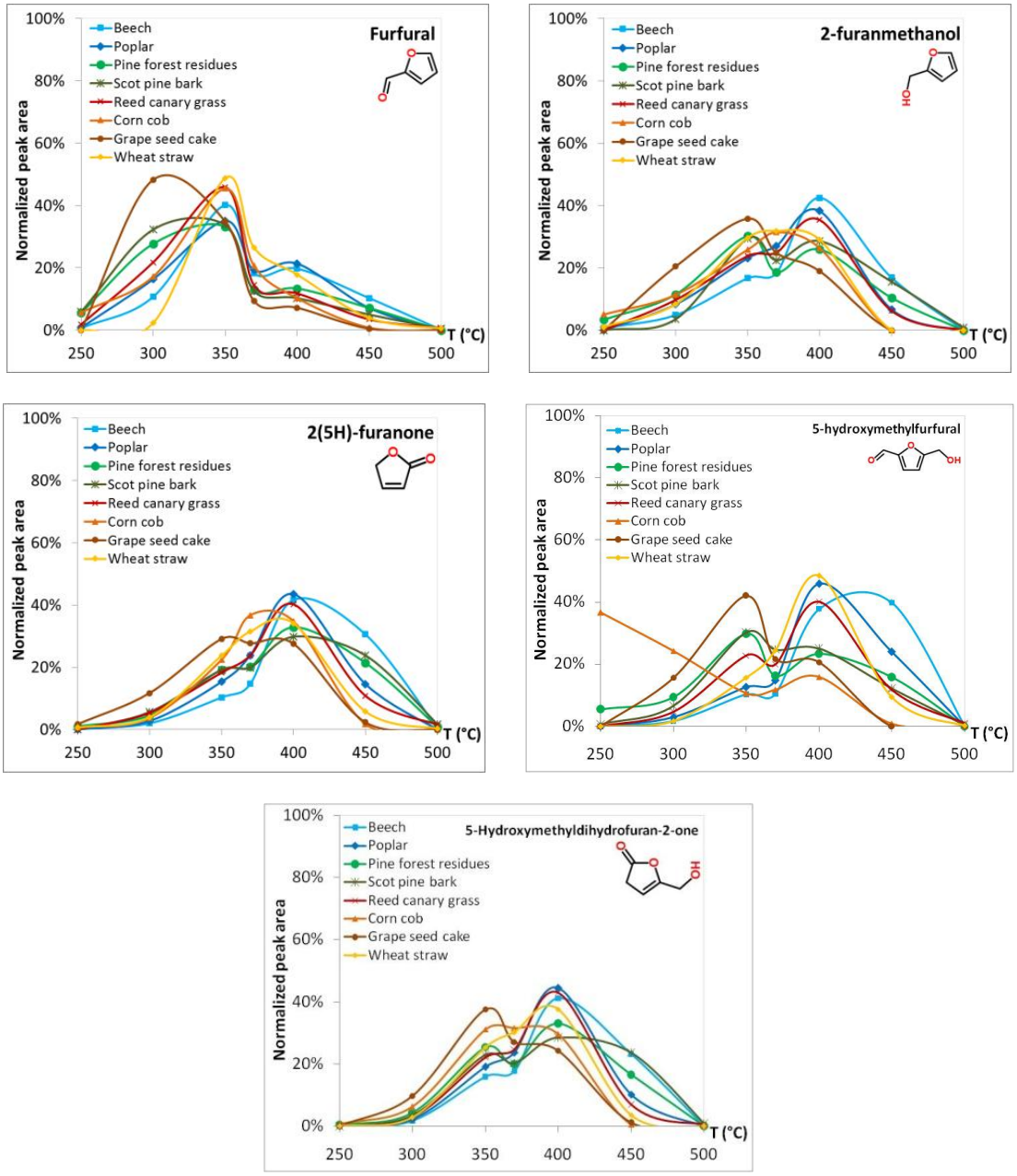


Figure A.VIII.14. Production profiles of furans in fractionated Py-GC/MS

3.2.3. Protein derivatives

Indole and methylindole, which were reported to be derived from protein thermal degradation [272,295] are produced in the whole range of fractionated pyrolysis (Figure A.VIII.15). Their production profiles are different from those of phenol, 2-methylphenol and 4-methylphenol, which were reported to be partially produced by proteins [292]. This confirms that these phenol derivatives have also other sources than proteins.

The fact that the specific marker compounds (the indoles) for protein were detected in all biomasses is an indication of the sensitivity of the applied analysis method, as the protein contents especially in the woody biomasses are extremely low.

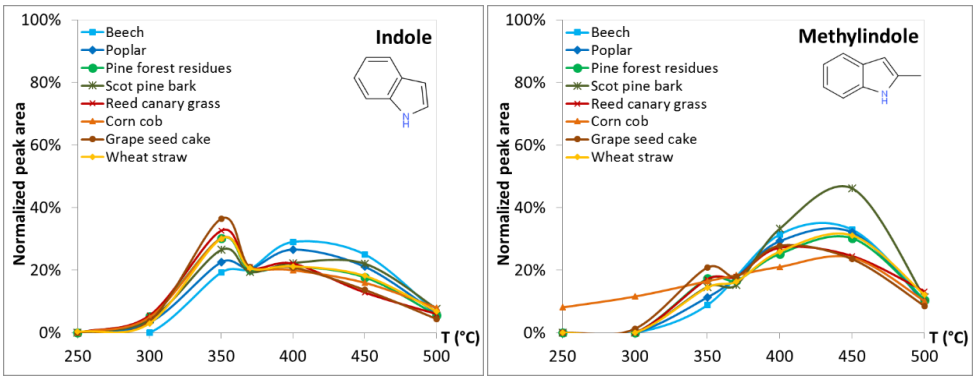


Figure A.VIII.15. Production profiles of protein derivatives in fractionated Py-GC/MS

Conclusions

Fractionated pyrolysis coupled to GC/MS was shown as a useful tool to distinguish the origin of the pyrolysis volatile products from the macromolecular components of biomass, namely cellulose, hemicelluloses and lignin. Important differences were observed in the distribution of the pyrolysis volatile products in function of the biomass type. In particular, deciduous wood, represented by beech and poplar, exhibited similar behaviours in terms of volatile species release. This was also showed for coniferous wood, represented by pine forest residues and Scot pine bark. On the contrary, agricultural biomasses presented important differences in the distribution of the pyrolysis products along the temperature/duration pyrolysis program. These differences may be derived from the more heterogeneous macromolecular composition of agricultural biomasses, particularly noticeable between corn cob, which presents a high polysaccharide content, and grape seed cake, with a high lignin content.

The representation of the percentages of each pyrolysis product produced per temperature/duration step of the pyrolysis program, regarding the total production of the volatile species, was proposed to contribute to the distinction of the origin of the pyrolysis products from cellulose, hemicelluloses and lignin. This normalization discards the differences in the absolute production of the pyrolysis products due to the biomass type. In the case of phenyl derivatives, guaiacyls and syringyls with longer side chain substituents are produced at lower pyrolysis temperatures, while phenolic compounds without side chain, such as guaiacol and syringol, are released at higher temperatures. This indicates a more difficult removal of these last compounds from the biomass structure in thermal degradation, compared to the long-chain phenolic compounds that are expected to be released from easily cleaved aryl ether structures. Furthermore, the structure of hardwood and softwood might be more resistant to thermal degradation, compared to agricultural biomasses, according to the production profiles of lignin derivatives. In the case of the polysaccharides, pyrolysis products exhibiting a maximum in the production profile at low to intermediate pyrolysis temperatures (around 350 °C) might be mainly derived from hemicelluloses. On the contrary, those presenting a maximum at intermediate to high pyrolysis temperatures (around 400 °C) would be derived from cellulose or from less accessible hemicelluloses.

IX. Influence of the polymerization degree in the starting degradation temperature of cellulose in torrefaction

Cotton linter samples, which constitutes a crystalline cellulose with a high purity, were prepared at different viscosimetric polymerization degrees (DPv = 25, 691, 755, 831 and raw, 1628) through a patented procedure based on ClO_2 and NaOH. Afterwards, the prepared samples were torrefied in TGA-GC/MS under two temperature and time programs:

- Non-isothermal torrefaction (200 to 300°C at 3°C/min) followed by isothermal torrefaction (300°C, 30 min).
- Non-isothermal torrefaction (200 to 300°C at 3°C/min) followed by isothermal torrefaction (350°C, 30 min).

Solid degradation kinetics for cotton linters were followed during torrefaction experiments. Results are presented in Figure A.IX.1 (until 300 °C) and Figure A.IX.2 (until 350°C). Volatile species released could not be quantified in this case.

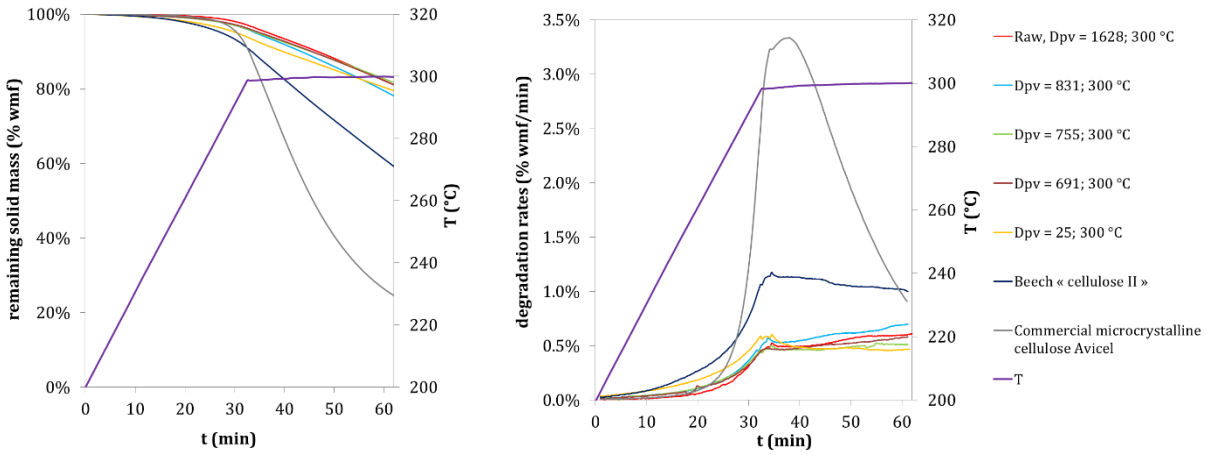


Figure A.IX.1. Remaining solid mass loss versus temperature and time obtained for the cotton linters with different degrees of polymerization in torrefaction in TGA-GC/MS until 300°C

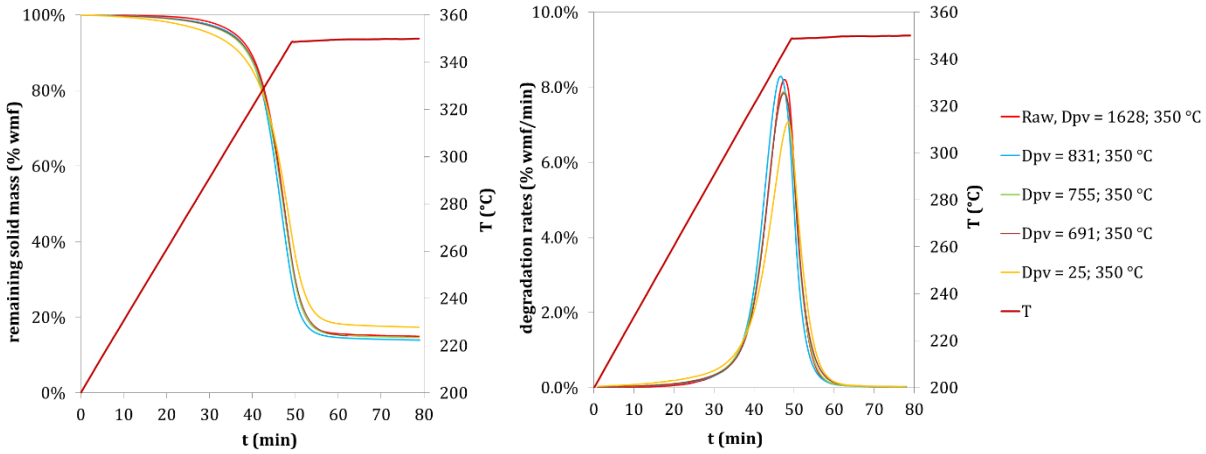


Figure A.IX.2. Remaining solid mass loss versus temperature and time obtained for the cotton linters with different degrees of polymerization in torrefaction in TGA-GC/MS until 350°C

Cotton linters started to be degraded at slightly lower temperatures for samples with a lower polymerization degree. This was observed under both torrefaction conditions. However, significant differences were observed in the starting temperature in function of the polymerization degree, that is, for samples of low (DPv = 25), intermediate (DPv = 691, 755, 831) and high (DPv = 1628) polymerization degrees.

In torrefaction experiments until 300°C, cotton linters degradation is enhanced from temperatures close to 300°C and is progressive under the isothermal step. This acceleration is also observed in torrefaction experiments until 350°C. However, in this case, the increase of the temperature from 300 to 350°C results in a strong acceleration of the degradation, going until maximum degradation rates between 7 to 8.5 % wmf/min at around 310 to 330°C, respectively. Cotton linter samples with a higher polymerization degree suffer a higher acceleration of the degradation at this temperature. Mass loss starts to decelerate below 350°C, which indicates that the main degradation of cotton linters happens between 300 and 350°C.

To sum up, a significant difference is required in the polymerization degree to observe an earlier degradation of cellulose in torrefaction. This corresponds to differences upper to 20 times in polymerization degrees. By comparing these results with extracted « cellulose II » fractions, the preservation of amorphous cellulose from native biomass seems to have a stronger influence in lowering the starting degradation temperature of cellulose than its polymerization degree.